SOVIET PHYSICS

JETP

A translation of the Journal of Experimental and Theoretical Physics of the USSR.

SOVIET PHYSICS JETP VOL. 37(10), NO. 2, pp. 235-416 FEBRUARY, 1960

ACADEMICIAN NIKOLAĬ NIKOLAEVICH BOGOLYUBOV

(On the occasion of his fiftieth birthday)

J. Exptl. Theoret. Phys. (U.S.S.R.) **37**, 333-335 (August, 1959)

ON August 21, 1959 Nikolai Nikolaevich Bogolyubov, one of our most prominent mathematicians and theoretical physicists, attains the age of fifty.

N. N. Bogolyubov was born in the city of Gor'kiĭ. His exceptional gift for mathematics was noted very early. Already in 1923 he took part in the seminar of Academician N. M. Krylov. In 1924 he wrote his first scientific paper, and next year, at the age of sixteen he became a graduate student in the faculty of mathematical physics of the Academy of Sciences of the Ukrainian S.S.R. In 1928 he defended his candidate's dissertation, and in 1930 he was awarded the degree of Doctor of Mathematics honoris causa.

At first Bogolyubov's scientific and pedagogic activities took place in Kiev. There he worked in the Academy of Sciences of the Ukrainian S.S.R. and taught at Kiev University, where from 1936 he held a chair, while between 1946 and 1949 he was the dean of the Mechanical and Mathematical Faculty. After his transfer to Moscow Bogolyubov became the head of the division of theoretical physics of the V. A. Steklov Mathematics Institute of the U.S.S.R. Academy of Sciences and became (beginning in 1956) the head of the Theoretical Physics Laboratory of the Joint Institute for Nuclear Research. His pedagogic activity is continued at Moscow University where he holds the chair of Statistical Physics and Mechanics.

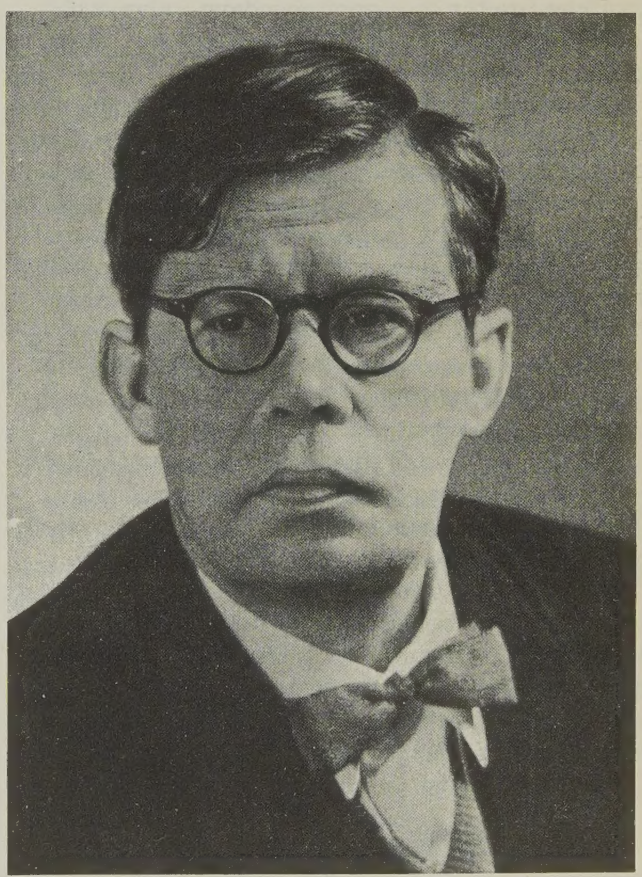

Bogolyubov is the author of approximately 200 scientific publications on various problems of mathematics and theoretical physics. His important contributions to science are recognized not only in the Soviet Union but also abroad. His books have been translated into many languages; his appearances at international conferences are invariably greeted with interest.

In 1947 Bogolyubov was elected corresponding

member of the U.S.S.R. Academy of Sciences, in 1948 he was elected an active member of the Academy of Sciences of the Ukrainian S.S.R., and in 1953 he became an academician of the U.S.S.R. Academy of Sciences. He has also been awarded a doctor's degree honoris causa by the Hyderabad University (India).

Bogolyubov's scientific and social activities have received high recognition by the Party and the Government. He was awarded a Stalin prize, and in 1958 he was honored with a Lenin prize. He was also awarded six decorations, among them two orders of Lenin.

The first papers which gained Bogolyubov wide recognition were of a purely mathematical nature. Thus, a series of his early investigations had for its aim the study of the direct methods of the calculus of variations. One of the papers of this series[1] received the distinction of being awarded a prize by the Bologna Academy of Sciences (The Merlani prize). We should also note his important contributions to the theory of nearly-periodic functions,[2] to the theory of boundary-value equations,[3] and to the theory of dynamic systems[4] (together with N. M. Krylov).

During the period from 1932 to 1943 Bogolyubov, together with Academician N. M. Krylov, developed the theory of nonlinear oscillations ("nonlinear mechanics"). Nonlinear mechanics, which at the present time forms a division of mathematical physics, has been to a large extent created by the papers of Bogolyubov and Krylov,[4-9] among which we should especially note the basic monograph[9] which has received wide recognition in the leading countries of the world. These investigations have important technical applications. The methods of solving problems in the theory of nonlinear oscillations, developed by Bogolyubov and his pupils, have been described in a book[10] written by him together with Yu. A. Mitropol'skiĭ.

Bogolyubov's intensive scientific activity in the field of physics began in the postwar years. In his first papers on physics he applied the asymptotic methods developed by him earlier to problems in statistical mechanics. In particular, he investigated in these papers the establishment of statistical equilibrium in a system in contact with a heat bath.[3]

The name of Bogolyubov is associated with methods of constructing distribution functions and kinetic equations in statistical physics.[11] These methods are the most general ones of all those in existence. For these investigations and also for his monograph,[3] Bogolyubov was awarded the distinction of being named a laureate of the Stalin prize, first class. He later generalized his derivation of the kinetic distribution functions to include quantum statistics.[12]

Bogolyubov proposed a method of approximate second quantization.[12] In particular, this method (in an article together with S. V. Tyablikov[13]) made it possible to give a consistent formulation of the polar model of metals due to S. Shubin and S. V. Vonsovskiĭ.

Bogolyubov is responsible for an important method in the theory of superconductivity. Already in 1947, in an article on the microscopic theory of superfluidity,[14] he showed that an imperfect Bose gas may possess the properties of superfluidity. In the course of this research, he developed the method of canonical transformations, which played an essential role in the development of the theory of superconductivity. In 1957 after the appearance of the note by Bardeen, Cooper and Schrieffer (which communicated certain results of calculations carried out on the basis of the idea of the essential role played by paired interactions between electrons) Bogolyubov developed a consistent theory of superconductivity, using for this purpose the method of canonical transformations. He confirmed the point of view that superconductivity may be treated as superfluidity of the electron gas.[15]

This method was later developed in detail by Bogolyubov together with his pupils, and has been described in the monograph written together with V. V. Tolmachev and D. V. Shirkov.[16] The new method turned out to be useful also for the investigation of the properties of nuclear matter.[17] The development of this method has led to the formulation of a variational principle which is a generalization of the well known Fock method in atomic physics.[18]

Bogolyubov has also made a fundamental contribution to quantum field theory. In an extensive series of papers he investigated, together with his pupils, the mathematical structure and the principles of causality and unitarity in quantum field theory. He developed (together with O. S. Parasyuk) a general theory of the multiplication of causal functions as applied to the regularization of the scattering matrix.[19] Building upon these rules and upon a clearly formulated principle of causality, he gave a mathematically rigorous formulation of quantum field theory on the basis of perturbation theory. This work has been described in an original monograph written by him together with D. V. Shirkov.[20] One can also include

among the same series of papers the articles on the renormalization group (also together with D. V. Shirkov[21]).

A second extensive series of papers by Bogolyubov on quantum field theory is devoted to the theory of dispersion relations. In this field, which is considered to be the most promising one in contemporary quantum field theory, he is associated with the method of formulating dispersion relations and with the first rigorous proof of the dispersion relation for the scattering of π mesons by nucleons. In the course of these proofs Bogolyubov investigated a number of subtle questions relating to the theory of generalized functions and to the theory of functions of many complex variables. The method of dispersion relations is described in his monograph written together with B. V. Medvedev and M. K. Polivanov.[22] This monograph is the only book in the world literature devoted to dispersion relations. His work on the theory of generalized functions and on the theory of dispersion relations has led to the creation of a new direction of research in contemporary quantum field theory. It is specifically for his work on superconductivity and on quantum field theory that Bogolyubov was awarded a Lenin prize in 1958.

Bogolyubov devotes much effort to the education of young scientists. He responds in a lively fashion and with great enthusiasm to each new interesting paper, to each new physical idea. He has brought into being schools of nonlinear mechanics (in Kiev) and of theoretical physics (in Moscow).

The editorial board of this journal expresses their hearty greetings to Nikolaĭ Nikolaevich Bogolyubov and wishes him many years of health, happiness and significant creative attainments for the benefit of Soviet science.

---

[1] Certain New Methods in the Calculus of Variations, Ann. di Mat. **7**, 243-272 (1930).

[2] On Trigonometric Approximation of Functions over an Infinite Interval, Izv. Akad. Nauk SSSR (Division of Math. and Nat. Sci.) **23**, 149 (1931). Certain Arithmetic Properties of Quasi-periods, Зап. каф. матем. физики АН УССР (Publ. of the Division of Math. Phys. Acad. Sci. Ukr. S.S.R.), Kiev, **4**, 185 (1939).

[3] О некоторых статистических методах в математической физике (Certain Statistical Methods in Mathematical Physics) L'vov, Acad. Sci. Ukr. S.S.R., 1945.

[4] General Measure Theory in Nonlinear Mechanics, Сб. трудов по нелинейной механике (Collected Works on Nonlinear Mechanics), Kiev, Acad. Sci. Ukr. S.S.R., 1937, pp. 55-112; Ann. of Math. **38**, 65 (1937).

[5] Новые методы нелинейной механики в их применении к изучению работы электронных генераторов (New Methods of Nonlinear Mechanics and their Application to the Study of the Operation of Electronic Generators). ONTI, 1934.

[6] Символические методы нелинейной механики в их приложении к исследованию резонанса в электронном генераторе (Symbolic Methods of Nonlinear Mechanics and their Application to the Study of Resonance in Electronic Generators), Acad. Sci. Ukr. S.S.R., 1934.

[7] Основные проблемы нелинейной механики (Fundamental Problems of Nonlinear Mechanics), Acad. Sci. Ukr. S.S.R. 1934.

[8] Приложение методов нелинейной механики к теории стационарных колебаний (Application of Methods of Nonlinear Mechanics to the Theory of Stationary Oscillations), Acad. Sci. Ukr. S.S.R., 1934.

[9] Введение в нелинейную механику (Introduction to Nonlinear Mechanics), Acad. Sci. Ukr. S.S.R., 1937.

[10] Асимптотические методы в теории нелинейных колебаний (Asymptotic Methods in the Theory of Nonlinear Oscillations), 2nd ed. Fizmatgiz, 1958.

[11] Проблемы динамической теории в статистической физике (Problems of Dynamic Theory in Statistical Physics), Gostekhizdat, 1946.

[12] Лекции по квантовой статистике (Lectures on Quantum Statistics), Kiev, 1949.

[13] Application of Perturbation Theory to the Polar Model of a Metal, J. Exptl. Theoret. Phys. (U.S.S.R.) **19**, 251 (1949); An Approximate Method of Finding the Lowest Energy Levels in Metals, J. Exptl. Theoret. Phys. (U.S.S.R.) **19**, 256 (1949).

[14] On the Theory of Superfluidity, J. Phys. (U.S.S.R.) **11**, 23 (1947); Вестник МГУ (Bull. Moscow State Univ.) **7**, 43 (1947).

[15] On a New Method in the Theory of Superconductivity, J. Exptl. Theoret. Phys. (U.S.S.R.) **34**, 58 and 73 (1958), Soviet Phys. JETP **7**, 41 and 51 (1958); Доклады высшей школы (Trans. of the Higher Schools) No. 1 (1958).

[16] Новый метод в теории сверхпроводимости (A New Method in the Theory of Superconductivity), Acad. Sci. U.S.S.R., 1958.

[17] On the Condition for Superfluidity of Nuclear Matter. Dokl. Akad. Nauk SSSR **119**, 52 (1958), Soviet Phys.–Doklady **3**, 279 (1958).

[18] A Generalized Variational Principle, Dokl. Akad. Nauk SSSR **119**, 244 (1958), Soviet Phys.–Doklady **3**, 292 (1958). On the Compensation

Principle in the Method of the Self-consistent Field, Usp. Fiz. Nauk **67**, 549 (1959), Soviet Phys.–Uspekhi **2**, 236 (1959).

[19] On the Theory of Multiplication of Causal Singular Functions, Dokl. Akad. Nauk SSSR **100**, 25 (1955); A Calculation Formalism for the Multiplication of Causal Singular Functions, Dokl. Akad. Nauk SSSR **100**, 429 (1955); A Calculation Formalism for the Multiplication of Causal Functions, Izv. Akad. Nauk SSSR, Ser. Mat. **20**, 585 (1956); Acta Math. **97**, 227 (1957).

[20] Введение в теорию квантованных полей (Introduction to the Theory of Quantized Fields), Fizmatgiz (1957); [Transl. publ. by Interscience, New York (1959)].

[21] The Multiplicative Renormalization Group in Quantum Field Theory, J. Exptl. Theoret. Phys. (U.S.S.R.) **30**, 77 (1956), Soviet Phys. JETP **3**, 57 (1956).

[22] Вопросы теории дисперсионных соотношений. (Problems in the Theory of Dispersion Relations), Fizmatgiz, 1958.

Translated by G. Volkoff
65

ON THE MECHANISM OF SURFACE IONIZATION OF ATOMS OF THE ALKALI EARTH METALS

Yu. K. SZHENOV

Submitted to JETP editor January 14, 1959

J. Exptl. Theoret. Phys. (U.S.S.R.) **37**, 336-339 (August, 1959)

The concurrent surface ionization of the alkali earth metals (barium, strontium, calcium, and magnesium) and an alkali metal (sodium) on incandescent tungsten was investigated with a mass spectrometer. The ionization coefficients were found to be significantly higher when oxygen was circulated over the tungsten. The results obtained are explained on the basis of the Saha-Langmuir theory. The specific character of the ionization of alkali-earth metals when the tungsten is oxidized is related to the evaporation of molecules of the oxides of these metals from the surface.

POSITIVE surface ionization was investigated thoroughly only for alkali metals. The experimental data agree in this case satisfactorily with the Saha-Langmuir theory.[1-4] The results of the relatively small number of investigations with the alkali-earth metals, which furthermore were not carried out under identical conditions, cannot be interpreted unambiguously.

It was established by Starodubtsev and Timokhina,[5] who used a mass-spectrometric procedure to investigate concurrent surface ionization of magnesium and sodium, that the temperature variation of the ion currents from pure tungsten corresponds approximately to the Saha-Langmuir theory. However, the estimated ionization coefficients for magnesium were found to be considerably higher than the theoretical ones. Morozov[6] in his experiments on barium observed no great deviations from the theory in the high-temperature region, while at low temperatures the results were affected by inadequate vacuum conditions. Along with this, Dobretsov, Starodubtsev, and Timokhina[7] have observed, in an investigation of the ionization of calcium and magnesium on tungsten coated with a thin layer of oxides of these elements, unique phenomena which do not lend themselves to a simple interpretation.

In our own paper[8] we cited several results of a mass-spectrometric investigation of the surface ionization of strontium, calcium, and manganese, results that found use in the measurement of the magnetic moments of nuclei by means of magnetic resonance in molecular beams.[9] Further experiments have supplemented and refined these results and have made it possible to explain the mechanism of the phenomenon. The experiments were carried out with a mass-spectrometric detector of molecular beams.[10] The measurement procedure is analogous to that described in reference 5.

Typical temperature characteristics of concurrent surface ionization of Ba, Sr, Ca, Mg, and the alkali metal Na, used for comparison, on a highly-incandescent tungsten filament, upon simultaneous evaporation of the metals from various furnaces, are shown in Fig. 1. At filament temperatures ranging from 1600 to 2200°K, the logarithms of the ion currents of the investigated elements are approximately linear in 1/T, while the values of the effective work function of tungsten, calculated by the Saha-Langmuir formula from the slopes of the lines, had a spread ranging from 4.6 to 4.8 volts for different elements and in different experiments. The coefficients of surface ionization, estimated from the values of the ion current, from the temperature of the calibrated-slit furnace temperature, and from the geometry of the instrument are of the same order of magnitude as the theoretical ones. Taking into account the "spotty" structure of the surface of the metallic filament, the results obtained can be explained on the basis of the Saha-Langmuir theory.

As is well known, a considerable increase in the coefficient of surface ionization for alkali metals can be attained upon oxidation of the tung-

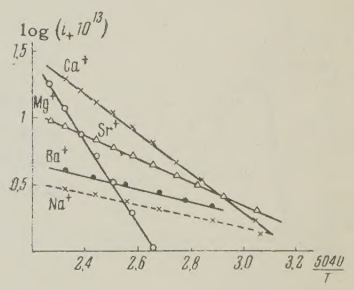

FIG. 1. Temperature characteristics of ion currents from pure tungsten (i_+ amperes).

sten by increasing the work function. However, at temperatures above 1600° K, necessary for the evaporation of the adsorbed atoms of the alkali-earth metals, the oxygen film on the tungsten becomes unstable.

A considerable and stable increase in the effectiveness of the ionization in the high-temperature range is observed during continuous oxidation of tungsten in a stream of oxygen.[8] However, this method does not make it possible to compensate fully for the desorption of oxygen from the surface, owing to the partial destruction of the oxygen film by the oxygen molecules formed when the volatile tungsten oxide WO_3 interacts with this film.[11] One can therefore expect that under increased oxygen pressure, the oxygen film on the tungsten and accordingly the work function will tend to limiting values, determined by the filament temperature.

The dependence of the Na and Sr ion currents on the oxygen pressure in a system operating at constant filament temperature (Fig. 2) confirms,

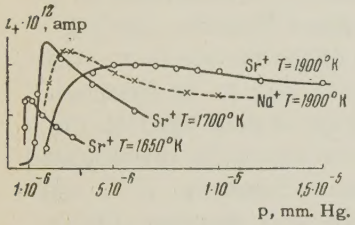

FIG. 2. Dependence of the ion currents of Sr and Na on the oxygen pressure.

in general outline, this hypothesis. Certain reductions in the Na and Sr ion currents at T = 1900° K in the high-pressure region can be naturally attributed to scattering of the atomic and ion beams by the oxygen. It is interesting that as the temperature of the filament drops, the curves for Sr, unlike those for Na, drop ever more rapidly with increasing pressure. This effect is particularly pronounced in the case of Ba.

At a constant inflow of oxygen, the ion current of Na monotonically increases with diminishing temperature, reaching saturation at T < 1600° (Fig. 3). Thanks to the stability of the oxygen film on the tungsten at such temperatures, the cessation of oxygen flow no longer causes a reduction in the sodium ion current. The strontium ion current at T > 1800° K behaves similar to sodium in a qualitative way, but it drops sharply at lower temperatures. An analogous situation is observed for the other alkali-earth metals (Fig. 4).

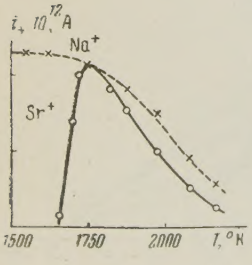

FIG. 3. Temperature dependence of the ion currents of Sr and Na from oxidized tungsten. Oxygen pressure p = 3.5 × 10^{-6} mm. Hg.

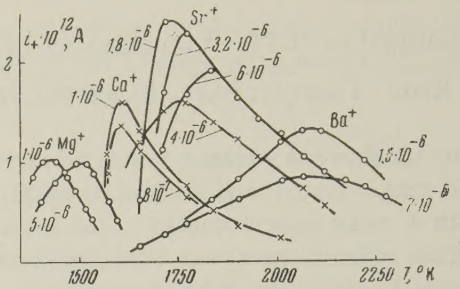

FIG. 4. Temperature dependence of the ion currents of Ba, Sr, Ca, and Mg from oxidized tungsten. The oxygen pressure in mm. Hg. is indicated on the diagram.

For an identical inflow of oxygen, the positions of the maxima of the ion currents are arranged in order of increasing atomic numbers of the elements. As the oxygen pressure is increased, the maxima shift towards the higher temperatures. In the high-temperature region, beyond the maximum of the ion current vs. temperature curve, the ionization coefficients increase with inflow of oxygen to an equal degree for all of the investigated elements.

The foregoing results have a natural explanation, if it is assumed that the Saha-Langmuir theory is applicable in the foregoing region of high temperatures. As the temperature is reduced from the maximum, the ion-current exhibits considerable inertia, as manifest by rapid variations of filament temperature or rapid variations of the intensity of the atomic beam. This inertia is due to the long lifetime of the atoms on the film. Figure 5 shows curves of the logarithm of the time (in seconds), during which the ion current is reduced by $\frac{1}{2}$ after a sudden blocking of the atomic beam, vs. 1/T. Under these conditions, the surface ionization of alkali-earth metals assumes a clearly pronounced specific character. The sharp reduction in the ion current with decreasing tem-

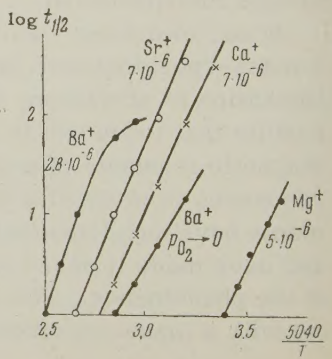

FIG. 5. Temperature characteristics of the lifetimes of the atoms on the filament. The oxygen pressure P_{O_2} is indicated on the curves in mm. Hg.

perature (Figs. 3 and 4) and with increasing pressure of oxygen (Fig. 2), not observed for sodium, cannot be attributed to a reduction in the work function by the adsorbed atoms of the alkali-earth metals, for example, because an analogous situation is observed at a very weak atomic-beam intensity and correspondingly at negligibly small equilibrium covering of the surface by the adsorbed atoms. Nor can we accept an explanation that brings into play the surface diffusion of the adsorbed atoms. If the coefficients of diffusion over the surface of the tungsten are taken into account,[12] the time necessary to go beyond the limits of the effective section of the ionizer filament is several orders of magnitude greater than the mean lifetimes of the atoms on the filament.

The most probable premise is that the peculiarities of surface ionization of alkali-earth metals are due to a possible formation of molecules of the oxides of these metals on the surface, followed by evaporation of these molecules. Similar phenomena take place in surface ionization of rare-earth elements and actinides, where ions of the oxides are observed directly along with the atomic ions.[13-16] In our experiments, the ions BaO^+ and SrO^+ were observed when the ion source of the detector operated in a mode wherein volume ionization of the gas molecules was produced by the electrons emitted by the filament. The formation and evaporation of oxides should play an increasing role with increasing oxygen pressure and with decreasing filament temperature, leading to a decrease in the yield of atoms from the surface. Retaining the premises of the Saha-Langmuir theory as regards the surface ionization of the atoms, we can explain qualitatively the anomalous drop in the ion currents observed under these conditions for alkali-earth metals.

In conclusion, I express my deep gratitude to Prof. V. Hartman for guidance in the initial stage of the investigation, to A. G. Kucheryaev and Sh. M. Gogichaĭshvili for help with the work, and to A. M. Romanov for valuable critical comments.

[1] L. N. Dobretsov, Электронная и ионная эмиссия (Electron and Ion Emission), Gostekhizdat, 1952, pp. 245-268.

[2] A. M. Romanov and S. V. Starodubtsev, J. Tech. Phys. (U.S.S.R.) **27**, 722 (1957), Soviet Phys.-Tech. Phys. **2**, 652 (1958).

[3] A. M. Romanov, J. Tech. Phys. (U.S.S.R.) **27**, 1233 (1957), Soviet Phys.-Tech. Phys. **2**, 1125 (1958).

[4] S. Datz and H. Taylor, J. Chem. Phys. **25**, 389 (1956).

[5] S. V. Starodubtsev and Yu. I. Timokhina, Сб., посвящ. 70-летию акад. А. Ф. Иоффе (Collection in Honor of the 70th Birthday of Acad. A. F. Ioffe), 1950, p. 117.

[6] G. A. Morozov, J. Tech. Phys. (U.S.S.R.) **17**, 1143 (1947).

[7] Dobretsov, Starodubtsev, and Timokhina, Dokl. Akad. Nauk SSSR **55**, 307 (1947).

[8] Yu. K. Szhenov, J. Exptl. Theoret. Phys. (U.S.S.R.) **29**, 901 (1955), Soviet Phys. JETP **2**, 775 (1956).

[9] Kucheryaev, Szhenov, Gogichaĭshvili, Leont'eva, and Vasil'ev, J. Exptl. Theoret. Phys. (U.S.S.R.) **34**, 774 (1958), Soviet Phys. JETP **7**, 533 (1958).

[10] Kucheryaev, Szhenov, Gogichaĭshvili, Leont'eva, and Vasil'ev, Приборы и техника эксперимента (Instruments and Measurement Engg.), in press.

[11] E. W. Müller, Z. Elektrochem. **59**, 372 (1955).

[12] G. F. Mityanskiĭ, Радиотехника и электроника (Radio Engineering and Electronics) **2**, 1493 (1957).

[13] Hin Lew, Phys. Rev. **91**, 619 (1953).

[14] M. J. Inghram and W. A. Chupka, Rev. Sci. Instrum. **24**, 518 (1953).

[15] R. N. Ivanov and G. M. Kukavatze, Приборы и техника эксперимента (Instruments and Measurement Engg.) **1**, 106 (1957).

[16] G. R. Hall and A. J. Walter, Can. J. Chem. **34**, 246 (1956).

Translated by J. G. Adashko
66

DISCRETE ELECTRON ENERGY LOSSES AND SECONDARY EMISSION FROM CdO

N. B. GORNYĬ

Leningrad Electrotechnical Communications Institute

Submitted to JETP editor February 14, 1959

J. Exptl. Theoret. Phys. (U.S.S.R.) **37**, 340-348 (August, 1959)

It is shown that the discrete energy losses of the electrons reflected from a CdO surface are determined by the CdO crystal structure. The spectra of the discrete losses in CdO and MgO, which have identical crystal lattices (face-centered cubic), are similar and their differences are due to differences in the lattice constants. The groups of genuine secondary electrons with discrete energies are produced in CdO by a single type of mechanism, which yields the aforementioned discrete electron energy losses. The maximum value of the secondary electron emission coefficient for CdO is only $\delta_{max} = 1.25$. The small magnitude of this quantity confirms an earlier suggestion regarding the dependence of δ_{max} on the relation between the minimum discrete energy loss and the electron work function.

INTRODUCTION

MANY investigations of the discrete electron energy losses lead to the conclusion that these losses are connected with the crystal structure of the given substance.[1-6] Of all the substances investigated, the least definite results were obtained for MgO. As the energy V_p of the primary electrons is increased, the peaks of the discrete electron energy losses in MgO become "smeared" and consequently less and less distinguishable.[6] For MgO with a face-centered cubic lattice the structural factor for the (210) and (211) [also (110)] planes is zero, and no discrete losses with the corresponding energy values should be observed. However, we did observe energies close to these values.[6] It was therefore of interest to investigate the discrete electron energy losses in a substance analogous to MgO and having the same crystal structure. CdO was chosen for this purpose.

It was also deemed interesting to verify with CdO the correctness of the relation, established for several substances, between the ratios of the values of the discrete electron energy losses to the work function, on the one hand, and to the yield of secondary electrons on the other.[7] We investigated therefore the secondary electron emission of CdO.

As far as we know, neither the discrete electron energy losses nor the yield of secondary electrons from the surface of CdO have been investigated heretofore.

EXPERIMENTAL DATA

A round plate was made of a piece* of CdO approximately 0.5 mm thick. After treatment with acid and alkali and subsequent washing in distilled water and pure alcohol, the plate was placed in the instrument. The construction of the vacuum instrument was similar to that used in reference 8. After prolonged training and degassing of the instrument, the pressure (measured with an ionization manometer) prior to the sputtering of the getter and sealing of the instrument was less than 3×10^{-7} mm mercury.

In the measurements of the electron energy distribution, the magnetic field of the earth was compensated for by two coils 1 m in diameter. The corresponding measurements were carried out at night, when the noise level was a minimum.

Electrical differentiation in a spherical-capacitor circuit[1] was employed to investigate the discrete energy losses of the electrons reflected from the surface of the CdO. Figure 1 shows the distribution of inelastically-scattered electrons, at several values of energy of the incident electrons, V_p, and at 250°C. All curves of Fig. 1 show distinct peaks of discrete energy losses. An analysis of the experimental curves displays more clearly the positions of the individual discrete-loss peaks. The dotted curves next to the experimental curves (Fig. 1) characterize the continuous background due to inelastic losses.

*The CdO was graciously supplied by V. P. Zhuze, to whom we are most grateful.

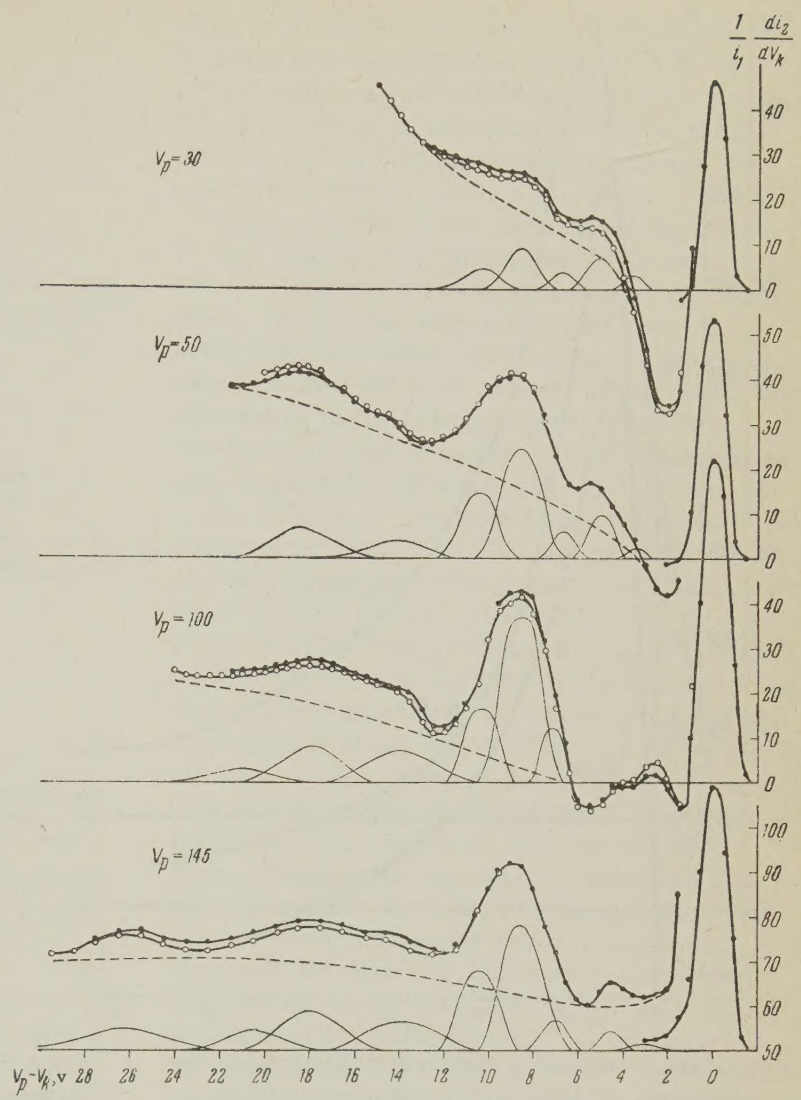

FIG. 1. Energy distribution of inelastically scattered electrons, obtained for CdO at several values of V_p and at t = 250°C. The peaks of elastically-rebounding electrons are drawn on a smaller scale.

The first four rows of the table list the values of the discrete-energy losses, $V_p - V_k$, which we obtained at the corresponding values of V_p. Line 5 shows the Miller indices h, k, and *l*, for which the values of the energy W were calculated with the following formula[6]

$$W = h^2 (h^2 + k^2 + l^2) / 8ma^2, \qquad (1)$$

where m is the electron mass, a is the lattice constant of CdO, and h is Planck's constant. These values are listed in line 6 of the table.

It can be seen from the table that the corresponding experimentally-determined peaks of $V_p - V_k$ are the same, within experimental accuracy, for all energies of the incident electrons investigated. The experimental values of the discrete electron energy losses, $V_p - V_k$, are in good agreement with the values of W, calculated with Eq. (1).

To verify that the discrete losses obtained were due to electron transitions between bands,[1,6] we investigated the energy distribution of the true

Values of discrete energy losses in CdO

No.	V_p, v	$V_p - V_k$, v								
1	30	3.5	5	6.8	8.6	10.3				
2	50	3.5	5	6.6	8.6	10.5	14.2	18.5		
3	100	2.8	4.5	7.0	8.5	10.3	13.8	18	21	
4	145	3	4.6	7.0	8.5	10.4	14	18	20.5	26.5
5	*hkl*	110	111	200	210	211	220	311	222	400
6	*W*	3.4	5.1	6.8	8.6	10.3	13.7	18.8	20.5	27.4
7	$(V_p - V_k)_{MgO}$	4	5.2	6.8	8	10	14.8	20		27.4

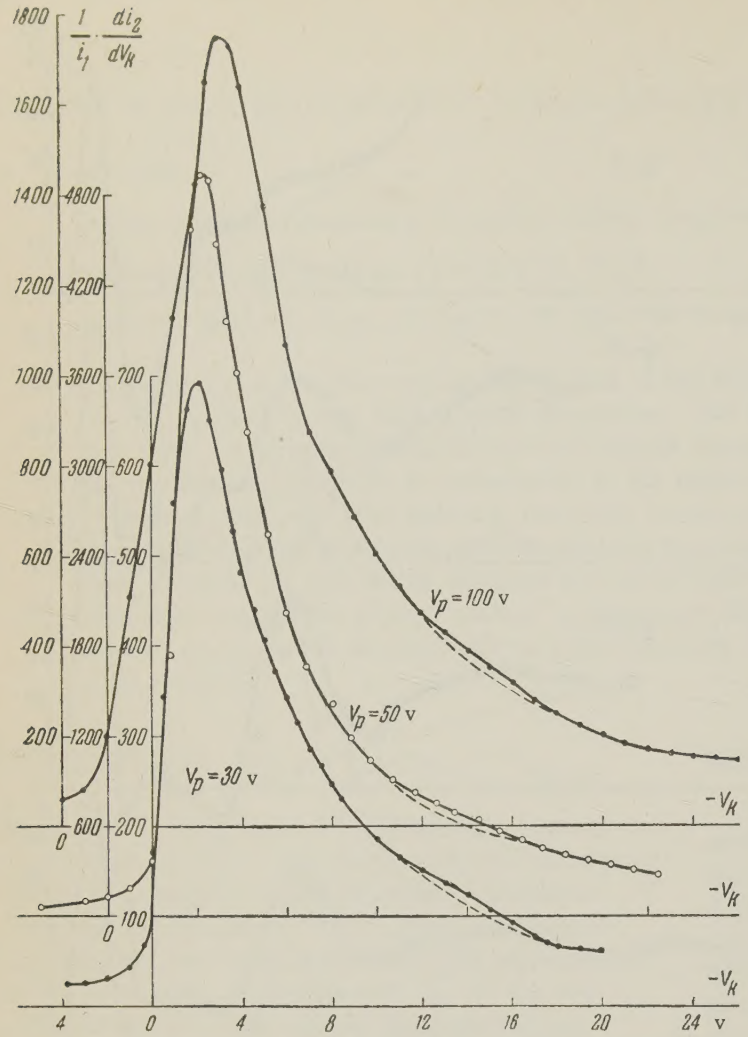

FIG. 2. Curves showing the energy distribution of the genuine secondary electrons, obtained for CdO at several values of V_p and at t = 250°C (lower set of coordinates – for the curve at V_p = 30 v; middle set – for V_p = 50 v; upper set – for V_p = 100 v).

secondary electrons. Figure 2 shows the energy distribution, obtained for the genuine secondary electrons by the method of electric differentiation, at several values of V_p. In all curves of Fig. 2, we see, apart from the principal maximum, also a bend that indicates the presence of a discrete group of genuine secondary electrons with an approximate energy of 14 ev.

The secondary electron emission from CdO was investigated with the same vacuum instrument as used to determine the discrete energy losses.

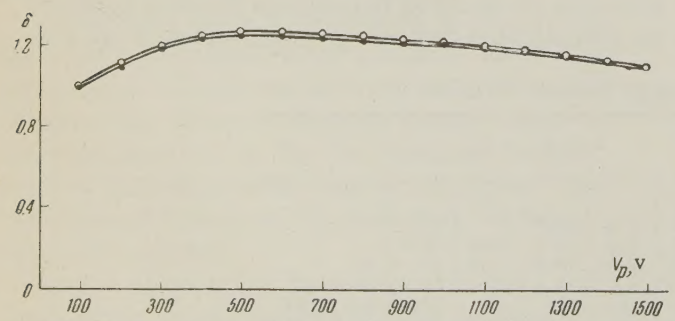

FIG. 3. Curves $\delta = f(V_p)$, obtained from the surface of CdO at t = 20°C (open circles) and t = 400°C (full circles).

Since our sample of CdO had a relatively low resistance (ρ = 0.027 ohm-cm at room temperature), the secondary emission was investigated in the static mode.

Figure 3 shows the curves $\delta = f(V_p)$, which characterize the dependence of the secondary-emission coefficient δ on the energy of the incident electrons V_p at 20° and 400°C. For CdO, the maximum value of δ was found to be 1.25 at V_p = 500 volts. In the entire measured range of V_p, δ varied very little with the temperature.

To determine the character of the variation of the energy distribution of the secondary electrons with V_p, we plotted delay curves, $I_2/I_1 = f(V_k)$ for several values of V_p, at room temperature and at t = 400°C. The curves obtained for equal values of V_p but different temperatures were found to be identical. Figure 4a shows delay curves obtained for V_p = 150 volts (curve 1) and V_p = 500 volts (curve 2) at 400°C, while Fig. 4b shows the secondary-electron energy distribution curves obtained by numerical differentiation of the delay curves of Fig. 4a.

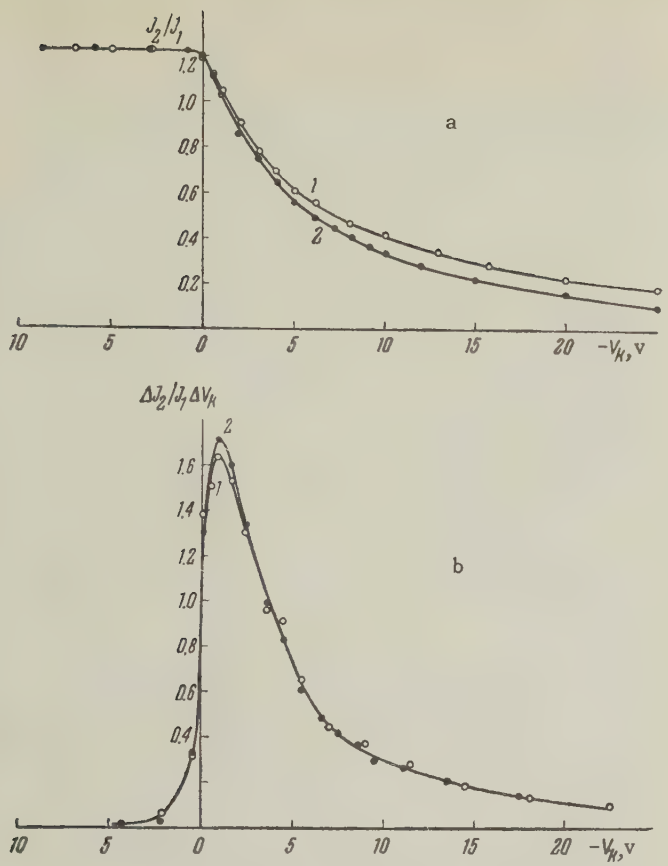

FIG. 4. a – delay curves, b – energy distribution of the secondary electrons (both for t = 400°C). Curves 1 – V_p = 150 v, curves 2 – V_p = 500 v.

Curve 1 (Fig. 4a) is normalized so that its points in the range of positive V_k coincide with the points of curve 2.

It can be seen from Fig. 4b that the distributions obtained at V_p = 150 and 500 v are practically the same; the values of the most probable electron energies are also the same.

DISCUSSION OF THE EXPERIMENTAL DATA

The distributions of the inelastically-scattered electrons, obtained for CdO (Fig. 1), are similar in external appearance to the distributions obtained for MgO (reference 6), at lower incident-electron energies (V_p ranging from 30 to 40 v). Only the peaks of discrete losses on the CdO curve are shifted towards the region of lower values of $V_p - V_k$ compared with the MgO curve, because CdO has a greater lattice constant than MgO.

To compare the data obtained for MgO with those obtained for CdO it is necessary to reconcile the values of the discrete losses $V_p - V_k$ for MgO (reference 6) with the lattice constant of CdO. For this purpose, values of $V_p - V_k$ [see Eq. (1)] must be multiplied by $(4.21/4.70)^2$, where 4.21 and 4.70 are the lattice constants of MgO and CdO respectively. All the discrete losses we obtained for MgO (line 7 of the table), reduced in this manner, are in very good agreement with the discrete losses for CdO.

Comparing the Miller indices corresponding to the values of discrete losses W in CdO (see table) with those previously obtained[6] for W in MgO, we note that they are in complete agreement with each other. Furthermore, two peaks were obtained for CdO, exactly as for MgO, corresponding to the indices* (210) and (211), for which the structural factor is zero and the corresponding values, W = 8.6 and 10.3 ev, should not be observed. The only values not noted in reference 6 for MgO are W = 4.3 ev and W = 34.2 ev, corresponding to the indices (110) and (400) respectively. However, the value $V_p - V_k$ = 5v, listed in Table 3 of reference 6, does correspond to W = 4.3 ev, and the peak of the discrete losses, W = 34.2 ev, is seen on the curves obtained for V_p values of 50 and 100 v (Fig. 3 of reference 6), although it is not noted in the table. It is possible thus to assume that all the discrete losses obtained for CdO were also obtained for MgO. Leder, Mendlowitz, and Marton[4] established a correspondence between discrete energy losses and crystal structure for several substances. We observed the same correspondence between the discrete losses of GeO_2 and MoO_2, which have an identical crystal structure.[5] Comparison of the data obtained for CdO and MgO confirms the connection between the foregoing discrete electron energy losses and the crystal structure of the given substance.

It must be noted that the smoothing of the peaks of discrete losses with increasing energy of the incident electrons, which we observed for MgO, were not noted for CdO. As V_p increases the peak at $V_p - V_k$ = 12 v of the MgO distribution curves becomes smoothed out, but the corresponding CdO peak at 9 volts, to the contrary, becomes even more pronounced. As already pointed out in reference 6, the primary and secondary electrons lose their energy to phonon excitation as they are displaced in MgO. This leads to an ever increasing smoothing of the MgO peaks with increasing energy of incident electrons. The fact that the curves $\delta = f(V_p)$ for CdO do not change with the temperature (Fig. 3) indicates the absence of losses to phonon excitation. Therefore

*Table 3 of reference 6 contains an erroneous value (411). in column 6 instead of (211).

the peaks of CdO, unlike those of MgO, remain pronounced (unsmeared) with increasing V_p.

We already noted that the energy distribution curves of the genuine secondary electrons (Fig. 2) have, in addition to the principal maximum, also an inflection point due to the peak of the ~14-ev genuine secondary electrons. It is natural to assume that groups of genuine secondary electrons with discrete energies appear in the substance during acts of inelastic interaction between the incident electrons and the lattice electrons of the solid, which lead to discrete energy losses of the incident electrons.[1,6] The curves showing the distribution of the inelastically-rebounding electrons (Fig. 1) contain two most intense groups, for which the mean values of the discrete losses are 8.5 — 9 and 18 — 18.5 ev. Apparently the second group of discrete losses causes the appearance of the aforementioned group of 14-ev genuine secondary electrons. The work function for CdO is found here to be approximately 4 — 4.5 ev. The first group of discrete losses (8.5 — 9 ev) should cause the appearance of a group of genuine secondary electrons with energies 4 — 4.5 ev. The peak due to a group of electrons with such energies would be located on the curve (Fig. 2) at the principal maximum, in the steepest portion of the distribution curve, where it is most difficult to detect. From the distribution curves for the inelastically-rebounding electrons (Fig. 1) it is seen that as the energy V_p of the incident electrons increases from 30 to 100 ev, the intensity of the peak at $V_p - V_k = 9$ v increases. Consequently, the peak of the group of genuine secondary electrons, caused by this discrete loss, should also increase with increasing V_p within the indicated limits. This should lead to a corresponding increase in the ordinates of the distribution curves of the genuine secondary electrons with increasing V_p in the region of $V_k = 4 - 4.5$ v. Figure 2 shows the shift of the principal peak of the true secondary electrons towards higher energies as V_p increases from 30 to 100 v, in agreement with the foregoing considerations.

Thus, the presence of a group of genuine secondary electrons with the indicated energy values shows that the discrete losses in CdO are produced by excitation of electron transitions between bands.

Proceeding now to a discussion of the CdO curves of the secondary-electron yield [$\delta = f(V_p)$ (Fig. 3)], the delay curves, and the distribution curves obtained at considerably differing values of V_p (Fig. 4), we note that they differ considerably from the corresponding curves obtained for MgO. Whereas the $\delta = f(V_p)$ curves obtained for CdO (Fig. 3) hardly vary as the temperature changes from 20 to 400°C, the curves for MgO drop considerably with increasing temperature.[9,10] This means that the energy lost by electrons to phonon excitation is quite small in CdO and relatively large in MgO.

The fact that the relative number of low-energy secondary electrons (Fig. 4b) fails to increase with increasing V_p up to $V_p = 500$ v, at which the $\delta = f(V_p)$ curve has a maximum, shows that in practice the energy lost by the secondary electrons does not increase with increasing V_p, in contrast with what takes place for MgO.[11] These two features of CdO, and also the small value of $\delta_{max} = 1.25$ and the negligible variation of δ with V_p, indicate that the secondary electrons are emitted from a smaller effective depth than from MgO, and that this depth varies little with V_p.

It was shown in several investigations that for a given substance the effective depth of emission of secondary electrons is independent of or hardly dependent on the energy of the primary electrons V_p, and remains constant over a wide range of the latter.[12-15] The research of Morgulis and Nakhodkin[14] indicates here that: 1) at a given V_p, δ increases more rapidly with increasing film thickness for a more effective emitter (Sb — Cs, $\delta_{max} = 10$) than for a less effective emitter (Ge, $\delta_{max} = 1.2$), and 2) the effective depth is greater than 100 mμ for Sb — Cs and 70 mμ for Ge.

Let us try and determine the cause of the low value of the coefficient of secondary emission of CdO. It is known that the secondary electron emission is a complicated phenomenon, consisting of several processes. The principal processes are:

1. Displacement of the primary electrons in the solid, accompanied by an energy loss to the excitation of the internal secondary electrons.

2. Energy lost by the secondary electrons as they move in the solid, accompanied by possible formation of tertiary electrons.

3. Emission of the secondary and tertiary electrons from the solid.

Since CdO and MgO have an identical crystal structure and an identical mechanism of discrete losses, and have consequently an identical mechanism of secondary-electron excitation, the first two of the above processes should not differ greatly for these substances. Obviously, the third process is very important in this case. The considerable difference in the coefficients of secondary emission of CdO and MgO is apparently due to the difference in the probability of the emission of secondary

and tertiary electrons through the outer surfaces of these substances.

This difference in the electron-emission probabilities can be explained by starting with the criterion that determines the secondary-emission probability as a function of the ratio of the least discrete-energy loss, $(V_p - V_k)_{min}$, to the work function $e\varphi$ of a given substance.[7] The secondary electrons which have energies E greater than $(V_p - V_k)_{min}$ while inside the substance, will expend their energy on phonon excitation as they move (losing an insignificant amount of energy, $\sim kT$, during each act of excitation and on the excitation of the lattice electrons losing thereby an energy not less than $(V_p - V_k)_{min}$ during each such process. The second energy-loss process experienced by the secondary electron will continue until its energy is reduced to a value at which the loss probability becomes close to zero. This occurs when $E \leq (V_p - V_k)_{min}$. Thus, the overwhelming majority of secondary and tertiary electrons that move towards the surface reach it at an energy close to $(V_p - V_k)_{min}$. If $(V_p - V_k)_{min}$ of a given substance is greater than the work function $e\varphi$, then most of the excited electrons of the crystal lattice, moving towards the surface and having an energy $(V_p - V_k)_{min}$, may still have an energy greater than $e\varphi$ as they reach the surface, enough to escape outside. This can be true for electrons which arrive even from a relatively large distance and which have lost a certain portion of their energy to phonon excitation. For such a substance, the effective depth of emission will be comparatively greater, the yield of secondary electrons will be considerable, and phonon losses should cause a noticeable dependence of the yield of electrons on the temperature.

On the other hand, if $(V_p - V_k)_{min}$ of a given substance is less than $e\varphi$, then the overwhelming majority of these electrons with energy close to $(V_p - V_k)_{min}$ cannot escape outside, with the exception of a small group of secondary electrons which are produced on the surface and which do not have a chance to expend their energy to a value close to $(V_p - V_k)_{min}$ as they move on toward the surface. Consequently, the effective depth of emission of secondary electrons for such a substance is small, the yield of secondary electrons is insignificant, and no temperature dependence should be observed for the yield of secondary electrons, owing to the insignificant energy expended for phonon losses at the small emission depth.

For MgO, $(V_p - V_k)_{min} = 5$ ev and exceeds the work function. For CdO, $(V_p - V_k)_{min} = 3 - 3.5$ ev (see table) and is less than $e\varphi$. Therefore MgO belongs to the first group of substances, with a large yield of secondary electrons, while CdO belongs to the second group, with a small yield of secondary electrons.[7]

In conclusion I express my gratitude for M. M. Kozlovskiĭ and A. G. Podgaĭskiĭ for help in the measurements.

[1] N. B. Gornyĭ, J. Exptl. Theoret. Phys. (U.S.S.R.) **27**, 649 (1955); **30**, 160 (1956), Soviet Phys. JETP **3**, 175 (1956).

[2] A. R. Shul'man and I. I. Farbshteĭn, Dokl. Akad. Nauk SSSR **104**, 56 (1955).

[3] N. B. Gornyĭ, J. Exptl. Theoret. Phys. (U.S.S.R.) **31**, 132 (1956), Soviet Phys. JETP **4**, 132 (1957).

[4] Leder, Mendlowitz, and Marton, Phys. Rev. **101**, 1460 (1956).

[5] N. B. Gornyĭ and A. V. Reĭtsakas, J. Exptl. Theoret. Phys. (U.S.S.R.) **33**, 571 (1957), Soviet Phys. JETP **6**, 443 (1958).

[6] N. B. Gornyĭ, Izv. Akad. Nauk SSSR, Ser. Fiz. **22**, 475 (1958), Columbia Tech. Transl. p. 481.

[7] N. B. Gornyĭ, J. Exptl. Theoret. Phys. (U.S.S.R.) **35**, 281 (1958), Soviet Phys. JETP **8**, 193 (1959).

[8] N. B. Gornyĭ, J. Exptl. Theoret. Phys. (U.S.S.R.) **26**, 88 (1954).

[9] J. B. Johnson and K. G. McKay, Phys. Rev. **91**, 582 (1953).

[10] N. B. Gornyĭ and A. V. Reĭtsakas, Сб. трудов ЛЭИС (Collected Papers of the Leningr. Electrotechnical Communications Inst.) **5** (38), (1958).

[11] N. R. Whetten and A. B. Laponsky, Phys. Rev. **107**, 1521 (1957).

[12] B. I. Dyatlovitskaya, Dokl. Akad. Nauk SSSR **63**, 641 (1948).

[13] I. M. Bronshteĭn and T. A. Smorodina, J. Exptl. Theoret. Phys. (U.S.S.R.) **27**, 215 (1954).

[14] N. D. Morgulis and N. G. Nakhodkin, Dokl. Akad. Nauk SSSR **94**, 1029 (1954).

[15] N. G. Nakhodkin and V. A. Romanovskiĭ, Izv. Akad. Nauk SSSR, Ser. Fiz. **22**, 454 (1958), Columbia Tech. Transl. p. 457.

Translated by J. G. Adashko
67

SHORTWAVE RADIATION FROM A VACUUM SPARK

S. V. LEBEDEV, S. L. MANDEL'SHTAM, and G. M. RODIN

P. N. Lebedev Physics Institute Academy of Sciences, U.S.S.R.

Submitted to JETP editor March 3, 1959

J. Exptl. Theoret. Phys. (U.S.S.R.) **37**, 349-354 (August, 1959)

It has been established that a spectroscopic light source — a vacuum "hot" spark — emits soft x-ray radiation (wavelengths shorter than 6 A). The radiation intensity remains quite high in the arc stage of the discharge, in which case the potential difference across the electrodes is less than 100 volts. A spectroscopic measurement of the electron temperature (Al VII line) indicates $T_e = 200{,}000°$.

INTRODUCTION

IT is well known that in the so-called "hot" vacuum spark, spectra due to highly ionized atoms are excited; in many cases these atoms lose half or more of their electrons, for example Fe XVII, Al XII, or C V. The radiation from these atoms lies in the vacuum ultraviolet and the soft x-ray regions of the spectrum. The spectra of these sparks have been investigated to 6 A.[1] These emission spectra require energies of the order of 2000 ev in order to be excited.* Although the vacuum spark has been used for a long time in spectroscopic investigations to produce spectra of multiply charged ions the excitation mechanism is not yet understood. A first step toward this goal is the correlation of the time behavior of this radiation with the electrical characteristics of the discharge.

The present paper describes the results of an investigation of this problem in the harder radiation region with wavelengths shorter than 6 A.

It is also of interest to estimate the temperature of the discharge by a spectroscopic method. Temperature measurements of this kind have recently been reported by Akimov and Malkov.[2]

METHOD

The spark was excited between two iron electrodes: one was a plate 2 mm thick with an aperture 5 mm in diameter while the other was a cylinder 4 mm in diameter. The distance from the base of the cylinder to the plate was 4 mm. The spark was observed through the aperture in the plane electrode. The pressure in the working volume before the discharge was 1×10^{-5} mm Hg. Breakdown in the interelectrode space was realized by means of a triggering device. The current source was a 3.3-μfd capacitor charged to 40 kv, the inductance of the circuit was 1.5 μh, the damping resistance was 0.2 Ω, and the maximum current i was 4.8×10^4 amp. During the first half-cycle the cylindrical electrode was the anode.

The radiation from the spark was passed through a beryllium filter which absorbed completely the longwave part of the spectrum (to 6 or 7 A). A scintillator wavelength shifter placed directly behind the filter was used to shift the radiation to the ultraviolet and visible; this converted radiation was detected by a system consisting of a FEU-25 photomultiplier and a cathode-ray oscilloscope. The photocurrent I(t) was compared with the current i(t) recorded by the other beam of the oscilloscope. The rated integrated sensitivity of the photomultiplier is 10 amp/lumen. The thickness of the beryllium filter was 0.25 mm, the diameter was 18 mm, the distance between the filter and the spark was 15 cm, and the distance to the input window of the photomultiplier was 10 cm. Two scintillators were used; A, tetraphenyl-butadiene in polystyrene 3 mm thick and B, a CsI(Tl) scintillator 5 mm thick.

RESULTS OF THE EXPERIMENTS

The first group of experiments was carried out with scintillator A. The photomultiplier was oriented in such a way that only the luminescent radiation from the scintillator reached it. Since this scintillator passes radiation shorter than approximately 1 A (which did not strike the photomultiplier) without noticeable absorption, the radiation of the scintillator detected by the

*For example, in Fe XVII and Al XII the ionization potentials are 1266 and 2085 volts respectively.

photomultiplier consisted of the softer part of the radiation (1 to 6 A). Examples of the photocurrent oscillograms obtained in this way are shown in Figs. 1a and 1b. It is apparent from these oscillograms that when the discharge is excited the radiation intensity remains sizeable for 5 to 7 microseconds.

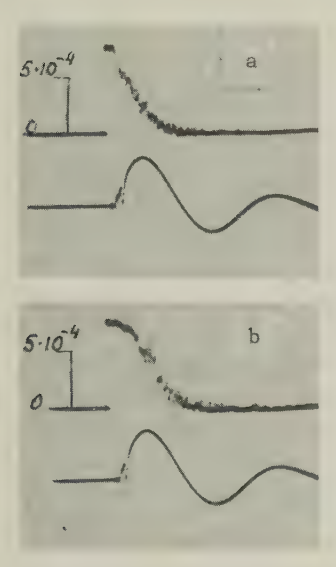

FIG. 1. Upper oscillogram: photocurrent as a function of time; this photocurrent characterizes the radiation of the vacuum spark; the lower oscillogram is the current in the spark gap. The photomultiplier is excited by the luminescence radiation of scintillator A which absorbs radiation from the spark in the region between 6 and approximately 1.5 A. The dip at the beginning of the current curve is due to the exposure marker in the photography of the spark.

The second group of experiments was carried out with scintillator B, which absorbs completely all radiation passing through the beryllium filter. Examples of the photocurrent oscillograms obtained in this case are shown in Figs. 2a, 2b, and 2c. In the oscillograms in Figs. 2a and 2b the scintillator radiation was attenuated by six sheets of writing paper; in the oscillogram in Fig. 2c two sheets were used. In the last case the photomultiplier was operated almost at saturation, since the light flux incident upon it was very large. Hence, at the beginning of the oscillogram in Fig. 2c the sensitivity of the photomultiplier is much smaller than in the other experiments. These measurements also indicate that the radiation lasts for a significant interval of time after breakdown — approximately 10 microseconds. The change in the radiation intensity as a function of time has a characteristic form: at a definite instant of time the radiation falls off sharply; then, near the point at which the current passes through zero, the radiation again increases, reaching a maximum at $i = 0$, then falling off and again rising, exhibiting a second maximum. In Figs. 2a, 2c, and 3b the positions of the maxima are denoted by arrows.

In a third group of experiments the photomultiplier was placed directly in the path of the beam, which passed through scintillator A; the emission of the scintillator was stopped by a filter made from black paper. The photomultiplier was excited directly by the hard radiation ($\lambda < 1$ to 1.5 A), which was not registered in the first group of experiments and which was not separated from the

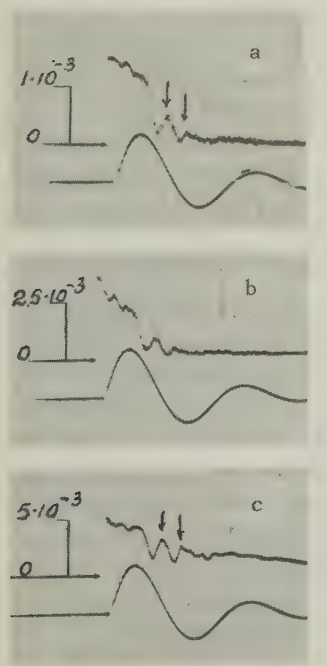

FIG. 2. The same as Fig. 1 for scintillator B, which absorbs all radiation from the spark at wavelengths shorter than 6 A. The scintillator radiation is attenuated by six (Fig. a, b) and two (Fig. c) sheets of paper. In the last case the photomultiplier operates close to saturation. The photocurrent curves are displaced along the time axis with respect to the current curves (in Figs. 1 and 3 this displacement is much smaller).

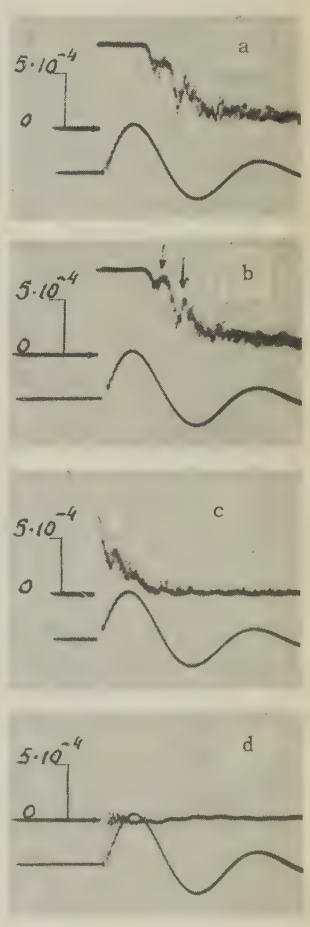

FIG. 3. The same as Fig. 1 for direct irradiation of the photomultiplier by shortwave radiation from the spark; a and b) wavelengths shorter than 1.5 A; c) shorter than 0.6 A; d) results of a control experiment in which a photomultiplier was covered by a copper shield 0.5 mm thick.

total radiation in the second group of experiments. The photocurrent oscillograms shown in Figs. 3a and 3b have the same characteristic features as the oscillograms of Fig. 2. The use of a supplementary filter made from nickel, 0.1 mm thick (Fig. 3c) and 0.2 mm thick leads us to the conclusion that this radiation continues to exhibit a significant intensity at least up to $\lambda = 0.6$ A.

The scales for Figs. 1, 2, and 3 are apparent from the maximum value of the current, which is 4.8×10^4 amp, and from its half-wavelength, which corresponds to a time of 7×10^{-6} sec. The photocurrent scale is given in amperes and applies only in the oscillogram limits which have been indicated.

The results of these experiments indicate that the radiation at wavelengths between 0.6 and 6 A has a "post-starting" characteristic, i.e., it appears after breakdown of the gap. The results which have been observed cannot be explained by the "stretching" of the scintillator radiation. In the first group of experiments the scintillator was characterized by an emission time of less than 10^{-8} sec. However the rate of decay of the photocurrent on the oscillograms in Figs. 1a and b is considerably smaller — a reduction of the photocurrent by a factor of e (in the linear region of amplifier operation) corresponds to a time of approximately 1×10^{-6} sec. Scintillator B, used in the second group of experiments, had an emission time of 1×10^{-6} sec; however the shape of the photocurrent curve observed in these experiments (the existence of two maxima) again indicates that the effect cannot be explained by "stretching" of the scintillator radiation.

In all experiments the time delay in the oscilloscope amplifer and cable was less than 7×10^{-8} sec. Consequently no element in the detection system could delay the signal by a time of the order of a microsecond.

To insure that the results were not due to spurious effects, the photomultiplier was shielded by black paper in the first and second groups of experiments; in the third group a copper foil was used. The photocurrent oscillograms obtained under these conditions are shown in Fig. 3d. It should be noted that each experiment was repeated at least 10 times and that the characteristic features were reproduced in all cases (Figs. 3a and 3b). The maximum spread in the photocurrent can be ascertained by a comparison of Figs. 1a and 1b. This spread is due to the fact that the luminous spot on the electrodes does not remain fixed; this was verified by photographing the electrodes in the visible region of the spectrum with an exposure time of 0.3 microseconds. Thus, the presence of soft x-rays, which continues in the post-breakdown stage of the discharge, has been established rather reliably.

Measurements were also made to enable us to estimate the voltage drop across the interelectrode space in the stage of the discharge being discussed here. The discharge circuit described above was used for this purpose but the initial condenser voltage was reduced to 22 kv and the length of the spark gap was reduced to 2 mm. The electrodes in this case were iron and copper rods 5 mm in diameter. A lead-out section was sealed to the system at a distance of 0.5 mm from the ends of the electrodes and connected to the oscilloscope through a voltage divider (the resistance of the divider was $1 \times 10^4\ \Omega$, the input capacity of the oscilloscope was $3 \times 10^{-5}\ \mu$fd.). The oscilloscope records the sum $U = U_d + U_d^{ind} + U_0^{ind}$ where $U_d + U_d^{ind}$ is the voltage across the discharge channel (averaged over the cross section) and U_0^{ind} is the voltage across the output section and divider induced by the current i. The U(t) oscillogram is shown in Fig. 4. The $U'(t) \sim di/dt$ patterns were obtained by moving the electrodes

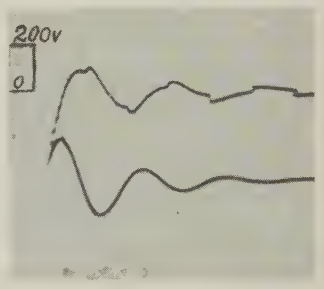

FIG. 4. The upper oscillogram is the total voltage along the inter-electrode gap and the measurement circuit, U(t). The maximum current value in the spark (lower oscillogram) is 2.5×10^4 amp and the half-wavelength corresponds to a time of 7×10^{-6} sec.

together until contact was made; these differ from U(t) by the absence of discontinuities at the point at which the current (i) passes through zero (the difference in the corresponding values of U and U′ is close to the value of the discontinuity. From this it is apparent that the part of the detected total voltage U(t) proportional to di/dt is determined basically by the voltage U_0^{ind} and that U_d^{ind} has almost no effect on the shape of the oscillogram. Consequently U_d^{ind} is much smaller than U_0^{ind}. According to Fig. 4 the maximum value of U(t) is approximately 100 volts; hence the factor U_d^{ind} is not more than several tens of volts. The other part of the voltage drop in the interelectrode space U_d is not due to the inductance and is clearly expressed at the end of the U(t) oscillogram where $U_d^{ind} + U_0^{ind}$ become small because the current i is reduced. $U_d(t)$ exhibits approximately the same nature and magnitude (approximately 20 volts) as the voltage drop across a gap in air, which has been studied in detail at lower currents.

Wavelength A	Transition	Energy of the upper level, ev	AiGi, sec^{-1}
240.77	$2p^3\ ^2D^0_{5/2} - 2p^4\ ^2P_{3/2}$	59	$1.14 \cdot 10^{11}$
356.885	$2p^3\ ^4S^0_{3/2} - 2p^4\ ^4P_{5/2}$	35	$0.63 \cdot 10^{11}$

Thus, the total voltage drop in the vacuum spark $U_d + U_d^{ind}$ amounts to tens of volts and, in any case, is never greater than 100 volts. However we may note that at higher currents and frequencies U_d^{ind} increases in proportion to di/dt.

In principle the connection between the first maximum on the photocurrent oscillograms in Fig. 2 and the possible significant increase in the voltage between the electrodes at the moment the current in the spark passes through zero is not unusual; this phenomenon is well known for air discharges. However we do not see the voltage discontinuities in our oscillograms; hence if they appear in the vacuum spark their duration is less than 3×10^{-7} sec. It should also be noted that voltage discontinuities cannot explain the second maximum in the photocurrent oscillograms.

ESTIMATE OF THE TEMPERATURE OF A VACUUM SPARK

The temperature of a vacuum spark was determined by the Ornshteĭn technique, using the intensities of the Al VII lines. The transition probabilities for these lines were computed in the Coulomb approximation using the Bates and Damgaard technique. The wavelengths, spectroscopic notation, upper level energies, and transition probabilities (AiGi) are given in the table.

In these measurements the maximum current in the spark was 1.3×10^4 amp and the circuit inductance was 2.6 μh. The spark was produced by a 1-μfd capacitor charged to 24 kv. These spectra were obtained with a vacuum spectrograph (DFS-6) with a diffraction grating in the oblique incidence unit. The spectrum was photographed on a film which was sensitized by a solution of sodium salicylate in methyl alcohol. The measurements of the relative intensities of the spectral lines were carried out in the first and second order spectra under the assumption that the quantum yield of the luminescent radiation of the sodium salicylate is constant. Intensity markers were obtained by means of a stepped quartz absorber at a wavelength close to the maximum of the radiation of the sensitizer.

The value of the electron temperature in the vacuum spark was found to be of the order of 2×10^5 °K.

It should be noted that although the heterochromatic photometry technique which we have used is standard in the vacuum region of the spectrum[3] the constancy of the quantum yield of the sensitizer used by us has been checked only up to 700 A.[4,5] Hence it is possible that the use of this method in the shorter wavelength region may lead to errors which we are not able to evaluate at the present time.

The measured value of the temperature is in good agreement with an estimate made from the general form of the spectrum. An analysis of the spectrogram indicates that for the conditions at hand the Al VI and Al VII lines are intense, the Al VIII line is weak and the Al IX and Al X lines are invisible. In Fig. 5 is shown the line intensity for these ions, as a function of temperature, computed from the Saha-Boltzmann formula for the lines with the highest intensities with excitation potentials of 30 — 40 volts for electron concentrations* $n_e = 10^{18}$ electrons/cm^3.

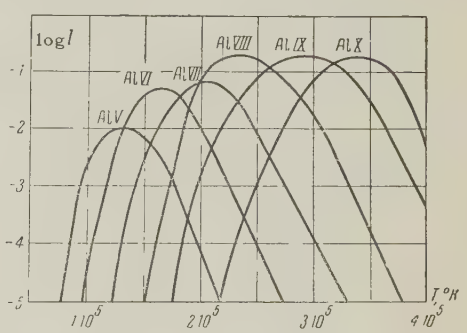

FIG. 5. Intensity of the lines of multiply charged ions as a function of temperature computed from the Saha-Boltzmann formula for $n_e = 10^{18}$ electron/cm^3.

It is apparent from this figure that the observed shape of the spectrum corresponds to a temperature $T = 1.8 \times 10^5$ °K. When $n_e = 10^{17}$ and $n_e = 10^{19}$ electrons/cm^3 the intensities of the Al VI and Al VII lines become equal to $T = 1.5 \times 10^5$ and $T = 2.1 \times 10^5$ °K; all of these values are in good

*The quantity n_e is estimated from the conductivity of the discharge on the basis of the current measurements, the measurements of the voltage drops between electrodes, and the diameter of the discharge channel (the channel was photographed in the visible region with a Kerr cell). Values of n_e between 10^{17} and 10^{19} electrons/cm^3 were obtained.

agreement with the results of the present temperature measurements $T_e = 2 \times 10^5$ °K and are much higher than the value $T \approx 4.6 \times 10^4$ °K obtained by Akimov and Malkov[2] using the Al III lines. As has been noted by these authors, the temperature values they report correspond to the instant at which the ions are excited. It is probable that this given temperature characterizes the peripheral (colder) portions or later stages of the discharge.

CONCLUSION

We have observed shortwave radiation which, to a considerable degree, is not "starting" radiation and which is to be associated with the later stages of the discharge; it is probable that this radiation is due to the radiation of the plasma itself — the ion line and continuous spectra. However the possibility is not excluded that the radiation is due to electron bremsstrahlung at the electrodes. Before this problem can be solved the radiation will have to be examined by means of spectral analyses.

The energy of the corresponding photons is 2×10^3 to 2×10^4 ev; thus, this radiation cannot be attributed to electrons which are directly accelerated by the voltage between the electrodes since this voltage is less than 100 volts. Moreover, the observed radiation cannot be explained by "thermal" electrons because at a temperature of 20 ev the number of electrons with energies between 2×10^3 and 2×10^4 ev is clearly not sufficient to produce the sizeable intensity which is observed. Thus we are forced to assume that the mechanism by which this radiation is produced is analogous to the mechanism responsible for the hard radiation in high-intensity pulsed discharges, such as those which have been observed in recent years;[6,7] this mechanism is still not fully understood. The problem will require further investigation and is under study at the present time. It seems to us that one of the probable origins for this effect may be the production, in localized regions of the plasma, of high-intensity electric fields, which are induced as a consequence of its deformation.[8]

[1] B. Edlen, Physica, **13**, 545 (1947).

[2] E. M. Akimov and I. P. Malkov, Оптика и спектроскопия (Optics and Spectroscopy) **6**, 96 (1959).

[3] H. Greiner, Z. Naturforsch. **12**, 735 (1957).

[4] Herman-Montagne, Lewi, and Ricard, Compt. rend, **202**, 1668 (1936).

[5] Johnson, Watanabe, and Tousey, J. Opt. Soc. Am. **41**, 702 (1951).

[6] S. Yu. Luk'yanov and I. M. Podgornyĭ, Атомная энергия (Atomic Energy) **3**, 97 (1956).

[7] Podgornyĭ, Kovalevskiĭ, and Pal'chikov, Dokl. Akad. Nauk SSSR **123**, 825 (1958), Soviet Phys. Doklady **3**, 1208 (1959).

[8] B. A. Trubnikov, Физика плазмы и проблема управляемых термоядерных реакций (Plasma Physics and the Problem of a Controlled Thermonuclear Reaction) U.S.S.R. Acad. Sci. 1958, Vol. 4, p. 87.

Translated by H. Lashinsky
68

ON DIRECT PRODUCTION OF ELECTRON-POSITRON PAIRS BY HIGH-ENERGY ELECTRONS

V. A. TUMANYAN, G. S. STOLYAROVA, and A. P. MISHAKOVA

Submitted to JETP editor February 21, 1959

J. Exptl. Theoret. Phys. (U.S.S.R.) 37, 355-365 (August, 1959)

The absolute number of spurious tridents for 10^{10}, 10^{11}, and 10^{12} ev primary electrons is computed by the Monte Carlo method for two types of the bremsstrahlung spectrum: for the one given by the Bethe-Heitler formula and for that described by the Migdal formulae, which take into account the Landau-Pomeranchuk and the Ter-Mikaelyan effects. It is shown that it is feasible to measure the energy of fast electrons by determining the energy dependence of the mean transverse distance between the vertices of electron-positron pairs produced by bremsstrahlung γ quanta. The value of the cross section for the direct production of electron-positron pairs calculated by Bhabba is confirmed experimentally.

1. INTRODUCTION

MANY investigations[1-13] have been devoted to the determination of the cross section for the direct pair production by high-energy electrons in the energy range 0.5 — 100 Bev. Different authors obtained different cross sections for direct pair production. The cross sections measured in references 1, 3, 6, 7, and 8, are several times larger than the value calculated by Bhabha,[14] while, in the other experiments, no such discrepancy is observed.

The basic difficulty in an experimental determination of the cross section for direct production of electron-positron pairs by high-energy electrons lies in the necessity of excluding the so-called spurious tridents.*

In the majority of the experiments mentioned above, a correction for the number of spurious tridents, calculated by Kaplon and Koshiba,[1] has been used. However, this correction for the number of spurious tridents represents only a rough approximation, since a number of factors, which substantially influence the number of the spurious tridents, have been neglected. In the calculations of Kaplon and Koshiba, the change in the energy of the electron due to the emission of bremsstrahlung quanta had been neglected. This energy decrease, however, has a direct bearing on the electron scattering, which determines essentially the number of spurious tridents. In addition, the decrease in the electron energy softens the energy spectrum of the emitted photons and leads to an increase of the angles at which they are emitted. The conversion mean free path was assumed to be the same for γ quanta of all energies, and to be equal to its minimum value, i.e., $^9/_7$ radiation lengths, although, for photons of comparatively small energies (≤ 1 Bev), its marked increase should be taken into account. The angular distribution of photons was assumed to be Gaussian, which also is an insufficiently accurate approximation.

Finally, the results of the calculation are given as a ratio of the number of spurious tridents to the total number of pairs produced in the conversion of γ quanta of the electron bremsstrahlung. The use of a correction of such a form for the number of spurious tridents can lead to ambiguity, since the pairs produced by electron bremsstrahlung at sufficiently large distances from the track of the electron have a rather low detection efficiency in contrast to the pairs near the track, and spurious tridents are detected with an efficiency of almost 100%. On the other hand, the presence of secondary pairs of the electromagnetic cascade is always possible near the electron track, and a suitable procedure of distinguishing these pairs from those produced by the bremsstrahlung radiation of the primary electron does not exist. It should still be noted that the number of pairs of high-energy electrons produced by the

*We shall use the following terminology: trident — an event of a direct production of an electron-positron pair by an electron; spurious trident — an electron-positron pair produced in the conversion of a γ quantum of the bremsstrahlung radiation of an electron at a very small distance from its track. The tracks of the electron and of the pair produced by the γ quantum cannot be distinguished in experiments from the event of a direct production of an electron-positron pair by an electron; an observed trident is either a trident or a spurious trident.

bremsstrahlung is subject to marked fluctuations even for a strictly fixed value of the electron energy.

The difficulty in applying the correction was partially avoided in the experiment of Fay,[2] who calculated the average number of bremsstrahlung pairs for the energy range of the measurements of the cross section for the production of tridents by electrons.

In addition to Kaplon and Koshiba,[1] the correction for the spurious tridents has also been calculated by Block and King,[3] but their work is also not free from the above-mentioned errors, and, in addition, they assumed that the bremsstrahlung quanta are emitted only at the beginning of the electron trajectory, which is not the actual case.

In connection with the above, a calculation of the number of spurious tridents has been carried out in reference 4 by means of the Monte Carlo method. The calculation has been carried out, as in reference 1, for nuclear emulsions. After reference 4 had already gone to press, the authors had the occasion to get acquainted with the work of Weill, Gailloud, and Rosselet,[5] who calculated the number of spurious tridents by numerical integration.

In the present article, a new, improved calculation by the Monte Carlo method is presented. A detailed comparison (where this is possible) with the calculations of Weill et al.[5] is carried out. The absolute number of spurious tridents obtained is used in a calculation, based on our experimental data, of the cross section for direct pair production by electrons.

2. CALCULATION OF THE ABSOLUTE NUMBER OF SPURIOUS TRIDENTS BY THE MONTE CARLO METHOD

The calculation was carried out for electrons of three primary energies: 10^{10}, 10^{11}, and 10^{12} ev. A total of 105 case histories of the passage of an electron through one radiation length, assumed to equal to 2.9 cm in the emulsion, were traced for each of these energies.

It was assumed that the electron, with a given initial energy, is produced at the point $x = y = z = 0$ (Fig. 1) and moves along the x axis. Its passage through matter was followed up to $x = 2.9$ cm. This limitation was dictated by the fact that, for $x > 2.9$ cm, a cascade initiated by the primary high-energy electron develops intensely, which makes it difficult to follow the electron track in the emulsion. Apart from this, a marked degradation of the energy of the initial electron occurs at such distances.

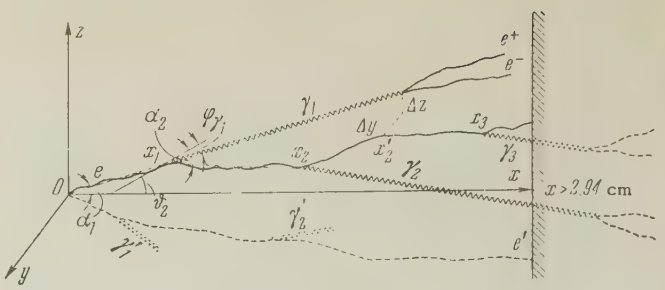

FIG. 1. The Monte Carlo case history.

The coordinates x_i of the points where γ quanta were emitted by an electron of energy E_i were found by using the value of the total cross section for the bremsstrahlung, according to Bethe and Heitler. This cross section was obtained by integrating the differential energy spectrum, for the case of complete screening, from the electron energy $2mc^2$ to E_i.[15a] The choice of the lower energy limit is due to the fact that the only γ quanta of interest are those with energies sufficient to produce electron-positron pairs. The bremsstrahlung cross section, as well as all the cross sections used in the calculations for the elementary processes were computed for the NIKFI-R nuclear emulsion. However, the results are equally correct for the Ilford G-5 emulsion, since the composition of both types is almost identical.

The energy of the emitted γ quantum was determined from the differential energy spectrum of Bethe and Heitler.[15a] Two projections of the angle $\overline{\varphi}$, at which the bremsstrahlung γ quantum was emitted, were found by using the expression for the angular distribution in the ultrarelativistic case.[16] For each emitted energy quantum $E_{\gamma i}$, the decrease in the electron energy beyond the point x_i was taken into account: the energy of the electron beyond the point x_i was taken as $E_{i+1} = E_i - E_{\gamma i}$. In general, it was assumed that, in the interval $x_i \le x \le x_{i+1}$, the electron energy was $E_{i+1} = E_0 - \sum_1^i E_{\gamma k}$, E_0 being the initial electron energy. All elementary processes along the path $x_i \le x \le x_{i+1}$ were found for an electron energy equal to E_{i+1}.

The x coordinates of the conversion points x'_m were found by means of the equations of reference 15b for the pair production cross section (the formulae were integrated numerically) for γ quanta emitted at points $x_1, x_2 \ldots, x_i$. Electron pairs with $x' > 2.9$ cm were not considered any further. The electron coordinates y_i, z_i, y'_m, z'_m due to the multiple scattering were then found. In the multiple scattering process, two angles

were taken into account: the angle of the chord $\bar{\alpha}$, and the angle of the tangent $\bar{\vartheta}$. The distribution of the projection of the angle $\bar{\alpha}$, was obtained from the Gaussian distribution for y and z ($\alpha_y = y/x$, $\alpha_z = y/z$). However, for fixed y and z, the distribution of the projection of the angles of the tangent is no longer Gaussian. In such a case, it is necessary to use the Fermi distribution[15c] which, for the projection on y and for a given y, is given by the formula

$$P(x, y, \vartheta_y)\, dy d\vartheta_y = \frac{2\sqrt{3}}{\pi\theta_s^2 x^2} \exp\left[-\frac{4}{\theta_s^2 x}\left(\vartheta_y^2 - \frac{3y}{x}\vartheta_y + \frac{3y^2}{x^2}\right)\right].$$

However, it can be shown that the distribution for the projection of the angle $\vartheta'_y = \vartheta_y - {}^3/_2\,\alpha_y$ is Gaussian. In view of this fact, we first found the angles ϑ', and then the projections of the true angle of the tangent were found from the relation $\vartheta_1 = \vartheta'_1 + {}^3/_2\,\alpha_{i-1}$. (See Fig. 1; ϑ_1 was always assumed to be equal to zero).

Each of the coordinates of the electron y_n and z_n at any point x_n is expressed as:

$$y_n = \sum_1^n x_i \left(\sum_1^n \vartheta_{iy} + \alpha_{ny}\right);$$

$$z_n = \sum_1^n x_i \left(\sum_1^n \vartheta_{iz} + \alpha_{nz}\right).$$

where x_i denotes the distance between x_i and x_{i-1}. Coordinates of the conversion points of the γ quanta and the vertices of the electron pairs are equal to

$$y'_k = \sum_1^l x_i \left(\sum_1^l \vartheta_{iy} + \alpha_{ly}\right) + s\left(\sum_1^{l+1} \vartheta_{iy} + \varphi_{ly}\right),$$

$$z'_k = \sum_1^l x_i \left(\sum_1^l \vartheta_{iz} + \alpha_{lz}\right) + s\left(\sum_1^{l+1} \vartheta_{iz} + \varphi_{lz}\right),$$

where s is the path traversed by the γ quantum before conversion, and l is the index denoting the point at which it was emitted. In this notation, the projections of the distance between the electron and the vertex of the pair are equal to

$$\Delta y = y_n - y'_k, \qquad \Delta z = z_n - z'_k.$$

To be able to compare the results of the present calculation with those of Weill et al.,[5] a value of 32 Mev-deg $\times (100\mu)^{-1/2}$ was used for the multiple-scattering constant, which also takes into account inelastic scattering. In addition, to explain the influence of the multiple scattering constant on the number of spurious tridents, the calculations were carried out also with the value 26.2 Mev-deg $\times (100\mu)^{-1/2}$.

As in reference 4, the calculations were carried out for two forms of the bremsstrahlung spectrum of the electron. However, instead of the bremsstrahlung spectrum of Ter-Mikaelyan, which was used in reference 4, we used the spectrum given by the formulae of Migdal[17] (the numerical calculations of reference 18 were actually used), since the latter takes into account both the Landau-Pomeranchuk[19] and Ter-Mikaelyan[20] effects.

To ascertain the contribution of the process (in which the vertices of the pairs produced by bremsstrahlung γ quanta of one of the electrons of a high-energy pair are found near the track of the other electron, so that the corresponding Δy and Δz satisfy the criteria of spurious trident production) to the number of the spurious tridents, the case history of an additional electron, shown dotted in Fig. 1 was followed. It is assumed that the additional electron is emitted only at an angle $\bar{\omega}$ with respect to the direction of the main electron, given by the formula of Stearns[21]

$$\bar{\omega} = (2mc^2/E)\ln(E/mc^2),$$

where E denotes the total energy of both electrons. For the additional electron, the radiation energy loss was taken into account. The projections of the distances between the additional electron and the vertices of the pairs produced by the main electron were calculated.

The ionization loss, Compton scattering and nuclear photoeffect were neglected in the calculation, because of their small role in the energy range under consideration. The small energy losses of the electron in the production of tridents and the increase of the length of the electron due to multiple scattering were also neglected.

3. RESULTS OF THE CALCULATION

In reference 1, the pairs produced in the conversion of the bremsstrahlung γ quanta, with vertices at a distance $\rho = (\Delta y^2 + \Delta z^2)^{1/2} \leq 0.2\,\mu$ from the primary electron, were considered as spurious tridents. In reference 4, three different criteria were considered: $\rho \leq 0.2$, 0.3, and $0.4\,\mu$. In reference 5, the following criterion of a spurious trident is introduced: $\Delta y \leq 0.2\,\mu$, $\Delta z \leq 0.44\,\mu$. The difference between the projections on y and z is due to the shrinking of the emulsion along z.

To work out a single criterion for the production of a spurious trident, and for the convenience of comparison with the work of Weill et al.,[5] the results of the present calculations are carried out for the criterion $\Delta y \leq 0.2\,\mu$, $\Delta z \leq 0.44\,\mu$. Results will be given below also for the criterion $\Delta y \leq 0.3\,\mu$, $\Delta z \leq 0.66\,\mu$, which can be useful for the determination of spurious tridents in especially unfavorable conditions of observation and, in

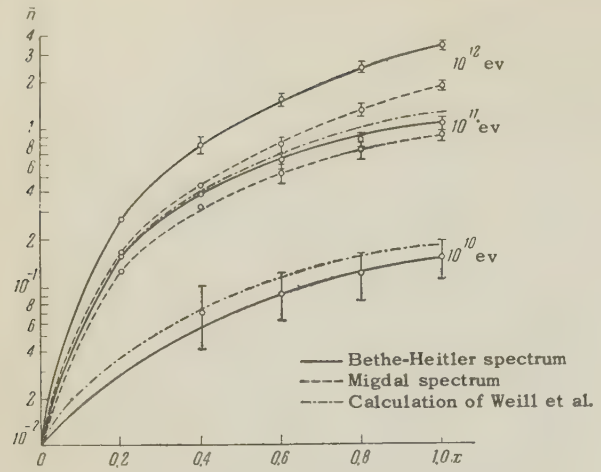

FIG. 2. Dependence of the average number of spurious tridents $\bar{n}$ on the transverse distance $\bar{x}$ (in radiation units) for various electron energies.

addition, show the dependence of the number of spurious tridents on the criterion used.

The dependence of the mean number of spurious tridents $\bar{n}$ on the distance from the point $x = y = z = 0$ where the primary electron was produced is shown in Fig. 2. The errors shown represent the standard deviations from the average calculated from the data of the Monte Carlo method.

The comparison of the present data with the results of Weill et al.[5] should essentially be carried out only for the case of the Bethe-Heitler bremsstrahlung spectrum and for an electron energy of 10^{10} and 10^{11} ev, since neither the 10^{12} ev energy nor the possible Migdal spectrum were considered in reference 5. For an energy of 10^{10} ev, the results of both calculations coincide within the limit of errors; for 10^{11} ev, our curve calculated by the Monte Carlo method lies somewhat lower. This can be explained by the fact that, in our calculation, the radiation energy loss was taken into account, which leads to an increase in the average angle of multiple scattering, and one should therefore expect a corresponding decrease in the number of spurious tridents. The results of both calculations can, therefore, be regarded as being fully in agreement. It should be noted that, although at 10^{11} ev the number of spurious tridents for the Bethe-Heitler and Migdal spectra are in agreement within the limits of errors, a marked discrepancy is obtained for 10^{12} ev electrons (see Fig. 3), Therefore, at energies $\approx 10^{12}$ ev, the question whether the bremsstrahlung spectrum according to Migdal[17] is correct or not is of primary importance in explaining the number of spurious tridents.

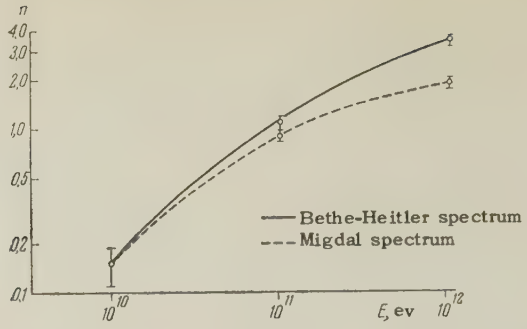

FIG. 3. Dependence of the number of spurious tridents $\bar{n}$ on electron energy.

Using the weaker criterion $\Delta y \leq 0.3\mu$, $\Delta z \leq 0.66\mu$, the number of spurious tridents per radiation length increased on the average by $\sim 20\%$ for 10^{10} and 10^{11} ev, and by 3% for 10^{12} ev as compared with the data in Fig. 2. For the normal criterion, $\Delta y \leq 0.2\mu$, $\Delta z \leq 0.44\mu$, using a multiple scattering constant equal to 26.2 Mev-deg $\times (100\mu)^{-1/2}$ instead of the 32 Mev-deg $\times (100\mu)^{-1/2}$ used in the present calculation, the number of spurious tridents increases, on the average, by 23% for 10^{10} and 10^{11} ev and by 5% for 10^{12} ev.

This increase in the number of spurious tridents upon changing the criterion and the multiple scattering constant can be explained by the transverse distribution of the pairs shown in Fig. 4, from which it follows that the number of pairs does not vary greatly if r is changed, for all pairs, by a factor of $1.2 - 1.5$ from the value $r \approx 0.2\mu$. The picture, however, is greatly different for electron energies of $\approx 5 \times 10^{11}$ ev, where the maximum of the transverse distribution of pairs shifts to the region $\rho \approx 0.2 - 0.3\mu$. In the reduction of experimental data on electrons of such energies, a detailed analysis of the selection criteria for spuri-

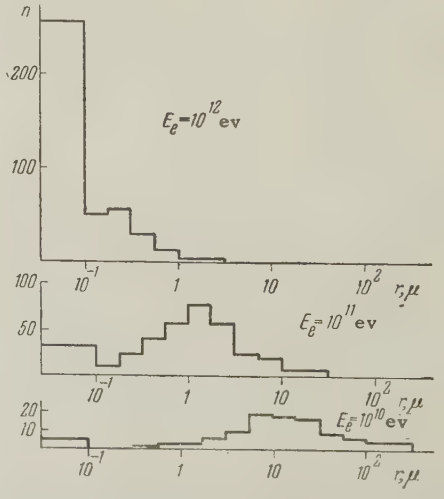

FIG. 4. Differential transverse distribution of pairs; n – number of pairs, r – distance of the pair vertices from the axis.

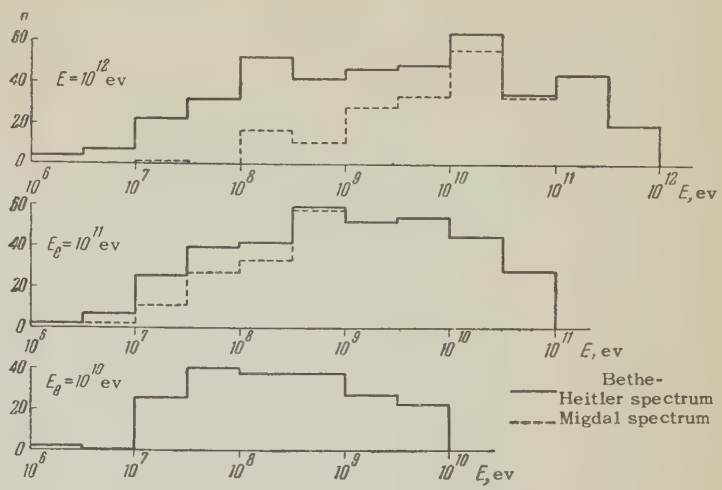

FIG. 6. Differential energy spectrum of electron-positron pair; solid line – according to Bethe-Heitler; dotted line – according to Migdal; n – number of pairs.

ous tridents should therefore be carried out.

A possible source of the increased number of spurious tridents, in the case where electron pairs are radiated, is the conversion of γ quanta bremsstrahlung of a single electron of the pair just next to the track of another electron, i.e., the production of a spurious trident involving the second electron. Such a cause of increase in the number of spurious tridents can be especially important for such values of the pair energy at which its components diverge to a small extent at distances comparable to one radiation length.

The information obtained by means of 105 additional electrons showed only one additional production of a spurious trident. From this fact one can conclude that the mutual production of spurious tridents (taking possible fluctuations into account) increases the number of spurious tridents on each electron of the pair in not more than a few percent of the cases.

The integral energy spectrum of primary electrons after their passage through one radiation length in the emulsion is shown in Fig. 5.

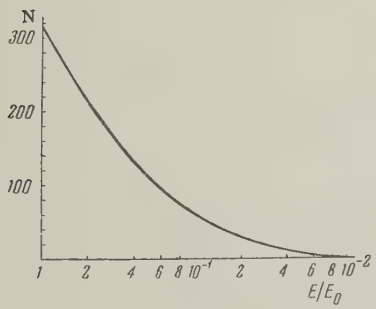

FIG. 5. Integral energy spectrum of primary electrons after traversing one radiation length; N – number of electrons, $\Sigma N = 315$.

It should be noted that, in the limits of standard deviations, a decrease of the energy by a factor of E was obtained for electrons traversing one radiation length, which is in agreement with the results of the cascade shower theory in approximation A.

The differential energy spectrum of electron pairs produced in the conversion of bremsstrahlung radiation γ quanta of primary electrons is shown in Fig. 6. The energy spectra of spurious tridents can be useful in accumulating a large amount of data for good statistical accuracy and may help explain the distribution of the transverse momenta with which the spurious tridents are produced.

The differential transverse distribution of pairs, the dependence of the average transverse distance of the pairs from the axis, and the average number of pairs produced by electrons per radiation length are shown in Figs. 4 and 7. In view of the fact that a possible new method of electron energy measurement in the range $10^{10} - 10^{12}$ ev follows from Fig. 7, we shall discuss briefly the problem of energy measurement.

In the study of the isolated electron-photon and photon components of explosion showers in nuclear emulsions, one encounters the important problem

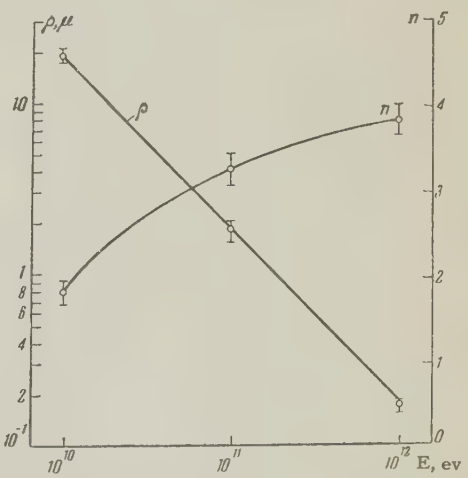

FIG. 7. Dependence of the average transverse distance of pairs from the axis, ρ, and of the average number of pairs n produced per radiation length on the electron energy.

of measuring the energy of an electron-positron pair above 10^{10} ev. The most accurate method is the measurement of the primary electron energy from the characteristics of the electromagnetic cascade initiated by it. In that case one usually measures the energy spectrum of the cascade electrons at a certain distance from its origin. Then, from the known values of $N(E_0, E > E_k, x)$ (number of electrons at a distance x with energy $> E_k$), the energy of the electron or of the pair producing the cascade is determined from theoretical cascade curves. This method becomes the more accurate the bigger the x that can be used to study the distribution of electrons of the cascade. However, the emulsion layers have limited dimensions and, therefore, it is impossible to use the optimal x for the energy measurement. In addition, events in which only the initial part of the cascade is recorded in the emulsion ($x \leq 1.5-2$ radiation lengths) are very frequent. In these cases, because of large fluctuations in the number of secondary electrons, the energy cannot be determined at all from the cascade development. Finally, the energy measurements by the above method are very difficult for the photon component of explosion showers, where it is very often impossible to distinguish between separate cascades.

Another method of energy measurement is through a measurement of the relative multiple scattering. By such a method, however, it is possible to carry out measurements only up to $\approx 10^{11}$ ev, and it is necessary to have close, almost parallel, tracks of high-energy particles.

A unique method is that of energy measurements from the magnitude of the decreased ionization at the initial portion of the track of very energetic pairs ($E_0 \approx 10^{12}$ ev) (the Chudakov-Perkins effect). However, the accuracy of this method is not high, because, in final analysis it is the angle of emission of the pair components, which has a rather large distribution, which is really measured. In addition, marked fluctuations of ionization are also always present.

The possibility of the measurement of the energy of primary electrons on the basis of the transverse distribution of vertices of secondary pairs is very attractive. It should be expected that the characteristics of the transverse development should depend strongly on the initial electron energy. Unfortunately, calculations of such a type are almost completely lacking in the literature, apart from a few qualitative considerations, which is clearly due to the difficulties connected with an analytical solution of such problems.

The dependence of the average transverse distance of the vertices of the pairs (produced in the conversion of bremsstrahlung γ quanta of the primary electron) from the original axis, which coincides with the direction of motion of the electron in the very beginning of its trajectory, has been calculated. This axis (the x axis in Fig. 1) clearly coincides with the axis of the developing cascade. For the calculation of the average r, only the pairs whose vertices were at $x \leq 2.9$ cm were used. The dependence of the average number of pairs on the electron energy was also obtained. The result, however, is shown only for orientation purposes, since the average number of pairs produced in the conversion of bremsstrahlung γ quanta depends only weakly on the energy of the radiating electron. The number of these pairs has a Poisson distribution for the electron energies used in the present calculation. It is evident that this result will not be correct for the total number of pairs, since the additional cascade pairs markedly increase the fluctuations in the number of pairs. The errors shown in Fig. 7 are standard deviations from the average, and were computed from the data of the Monte Carlo calculations.

The straight line obtained for the energy dependence of the mean transverse distance of pair vertices from the axis, makes it possible to carry out an estimate of the energy of the primary electron, provided we have data on pairs produced by γ quanta of the primary electron or on a pair at a distance $x = 2.9$ cm from the point of origin. For the x axis, one should naturally take the center of mass of all possible trajectories. The proposed method makes it possible to measure the energy of the primary electron pair (events most often found in the experiment) with standard deviation of 64% for the energy of 10^{10} ev, 44% for 10^{11} ev, and 39% for 10^{12} ev. One should bear in mind that the accuracy of the energy estimate depends on the number of pairs produced in the conversion of γ quanta bremsstrahlung radiation of the primary electron. The shown errors are calculated for the average number of pairs for each energy.

The accuracy of the method decreases for measurements of the energy of a single electron, owing to the decrease of the average number of pairs by a factor of two. In that case, however, the energy cannot be measured, in general, from the decrease of ionization in the beginning of the pair trajectories, nor can the method of the relative multiple scattering measurement be used as a rule (the second energy trace is missing). Therefore, one should think that the proposed

method will be useful in that case, too.

The electron pairs of the second generation may represent an additional source of error. These pairs can be produced in the conversion of bremsstrahlung γ quanta of all these electron pairs which, in turn, have been produced in the conversion of bremsstrahlung γ quanta of the primary electron. Such cascade pairs may lead to an underestimate of the energy of the primary electron.

From the results of the present calculation, we tried to estimate the approximate number of cascade pairs. For a primary electron of 10^{12} ev, one should expect about three cascade pairs for 8 pairs produced by bremsstrahlung γ quanta (for $x < 2.9$ cm). The average distance of cascade pairs from the axis is larger, by about a factor of ten, than the average distances shown in Fig. 7. The mean longitudinal distance x at which cascade pairs are produced amounts to ≈ 2.6 cm, while the average x for the bremsstrahlung pairs is ≈ 2 cm.

The probability of a cascade pair production up to $x = 2$ cm is small, and can, in practice, be neglected. From the pairs observed in experiments up to $x = 2$ cm, one can calculate their average transverse distance $\bar{r}_2$. It should then be taken into account that $\bar{r}_2$ will be increased to $x = 2.9$ cm. If we assume that r increases as $x^{3/2}$ (in fact, after the emission of a γ quantum, its distance from the axis increases only linearly), then $\bar{r}$ at a given point x should be $r_x = \bar{r}_2 x^{3/2}/2\sqrt{2}$. Furthermore, we can introduce the condition that all pairs for $r > 4r_x$ be excluded, since they are due to cascade development. This rule is analogous to the exclusion of the deviations larger than 4 times the average value in the multiple-scattering measurement.

Since the cascade pairs have, on the average, a smaller energy than the pairs produced by bremsstrahlung γ quanta of the primary electron, we can introduce an additional condition $E \ll \bar{E}_2$, where E is the energy of the pair studied and $\bar{E}_2$ is the average energy of the pairs. $\bar{E}_2$ can also be estimated from Fig. 5.

We note, finally, that beyond $x = 2$ cm the number of cascade pairs increases as the square of x, in contrast to bremsstrahlung pairs, which are roughly linearly distributed with respect to x. For an energy of 10^{11} ev, one should expect one such pair per 6.5 pairs of bremsstrahlung radiation. The same exclusion procedure can be applied here. For 10^{10} ev, one can neglect the contribution of cascade pairs.

Thus, one can hope that the procedure of the exclusion of cascade pairs will make it possible to avoid an underestimate of the electron energy. A small fraction of the electron pairs near the axis, with a comparatively large energy, will be difficult to exclude by the above procedure. However, because of the small transverse distances from the axis, this fraction of cascade pairs will not introduce a large error.

4. EXPERIMENTAL RESULTS

We recorded a high-energy nuclear interaction* of the type $2+31\alpha$ in a stack of stripped nuclear emulsions irradiated in the stratosphere. The energy (measured against the value of the angle containing half of all the shower tracks) was found to be 9×10^{13} ev. High-energy electron-positron pairs ($E_0 \gtrsim 10$ Bev) produced in the photon component of the star were used for the experimental measurements of the mean free path λ_{exp} of trident production by electrons. The electron-positron pairs traversed ≈ 1.5 cm in single emulsion layers, and the shower traversed about 8.5 cm in the whole stack.

Tracks of shower particles of the narrow cone and the photon component of the nuclear interaction were followed up to their exit from the stack. In scanning, the coordinates of the vertices of the electron-positron pairs were found and recorded. For further measurements, only the electron-positron pairs sharply distinguishable from the main mass of tracks were chosen, a procedure necessary for a reliable identification of visible tridents.

The measurements of the relative multiple scattering were used mainly to estimate the energy of the electron-positron pairs. The measurements were carried out using a Koristka MS-2 microscope. In calculating the electron energy from the average values of the second differences of relative multiple scattering, the results of reference 22 were used. It is shown there that the usual procedure of energy determination, by measurement of the relative scattering of the components of high-energy electron-positron pairs, leads to a serious underestimate.

For two electron-positron pairs, the average second differences of the relative multiple scattering were not larger than the noise level ($0.15 \pm 0.02\mu$) even for maximum cell length (4500μ). For such pairs, the ionization near their vertices was measured by the grain counting method. The Perkins-Chudakov effect was not detected for these pairs, probably because the energy was less than 1000 Bev. In addition, the method described in Sec. 3 was used for the measurements of the energy in these two cases. The energies of the

*The interaction has been found by A. Ya. Burtsev.

electron-positron pairs estimated in such a way were found to be (1 to 3) $\times 10^{11}$ ev, which did not contradict the estimates obtained by scattering and ionization measurements.

Since a large number of high-energy electrons is present in the photon component of a nuclear interaction, an increase in the number of spurious tridents over the calculated value is possible, owing to the process discussed in Sec. 3. This increase can occur in the conversion of γ quanta near the track of the investigated electron. For an estimate of the probability of such an event, 24 cm of shower-particle tracks of the narrow cone in the region of intensive development of the photon component were studied, and no electron pairs satisfying the spurious trident criterion were observed on this length.

As a result of an experimental study of the photon-component of the nuclear shower, 25 events of production of apparent tridents were observed. The total length of the investigated track, for electrons with an average energy of 20 Bev, equals 42.1 radiation lengths. After excluding the spurious tridents along each electron track, according to the results of the Monte Carlo calculations (Fig. 2), it was found that 9.3 ± 5.5 tridents were produced on the given total length of 42.1 radiation lengths, which corresponded to a mean free path $\lambda_{exp} = 4.5^{+6.5}_{-1.6}$ radiation lengths. The standard deviation in the determination of the number of tridents is $\Delta N_t = \sqrt{(\Delta N_{VT})^2 + (\Delta p)^2}$, where ΔN_{VT} is the standard deviation in the number of apparent tridents. The tridents were assumed to be distributed according to the Poisson law, which was confirmed by the data of the Monte Carlo calculation. Δp is the error in the calculated Monte Carlo curves for the number of spurious tridents, and it is usually small as compared with ΔN_{VT}.

Since the mean free path for trident production at 20 Bev equals, according to the Bhabha theory, $\lambda_{theor} = 7$ radiation lengths, one can consider that the measured λ_{exp} is in agreement with that value. These results contradict to a certain degree the results of Weill et al.,[5] according to which λ_{exp}, outside the limit of errors, is substantially smaller than the corresponding theoretical value. However, in reference 5, the error of ΔN_T was clearly underestimated, since, from the data presented there, it follows that $\Delta N_T < \Delta N_{VT}$.

The obtained data on the production of tridents by electrons of an average energy of 20 Bev are not in contradiction with the predictions of quantum electrodynamics.

In conclusion, the authors wish to express their gratitude to Prof. I. I. Gurevich for his constant interest and useful discussion during the course of the research, and also would like to thank deeply Profs. A. I. Alikhanyan, K. A. Ter-Martirosyan, and M. L. Ter-Mikaelyan for interesting and helpful discussions, A. A. Varfolomeev and B. A. Nikol'skiĭ for useful advice, and V. A. Zharkov for considerable help in carrying out the calculations.

[1] M. F. Kaplon and M. Koshiba, Phys. Rev. **97**, 193 (1955).

[2] H. Fay, Nuovo cimento **5**, 293 (1957).

[3] M. M. Block and D. T. King, Phys. Rev. **95**, 171 (1954).

[4] Tumanyan, Zharkov, and Stolyarova, Dokl. Akad. Nauk SSSR **122**, 208 (1958), Soviet Phys.–Doklady **3**, 953 (1959).

[5] Weill, Gailloud, and Rosselet, Nuovo cimento **4**, 1436 (1957).3 (1957).

[6] M. Koshiba and M. F. Kaplon, Phys. Rev. **100**, 327 (1955).

[7] E. Lohrmann, Nuovo cimento **5**, 1074 (1957).

[8] J. E. Naugle and P. S. Freier, Phys. Rev. **92**, 1086 (1955).

[9] Block, King, and Wada, Phys. Rev. **96**, 1627 (1954).

[10] Debenedetti, Garelli, Tallone, and Vigone, Nuovo cimento **4**, 1151 (1956).

[11] F. J. Loeffler, Phys. Rev. **108**, 1058 (1957).

[12] Debenedetti, Garelli, Tallone, and Vidone, Nuovo cimento **4**, 1142 (1956).

[13] S. L. Leonard, Bull. Am. Phys. Soc. **1**, 167 (1956).

[14] H. J. Bhabha, Proc. Roy. Soc. **A152**, 559 (1935).

[15] B. Rossi, High-Energy Particles (Prentice-Hall, New York, 1955), a) p. 49, Eq. (5); b) p. 81, Eqs. (5-10); c) p. 71, Eq. (6).

[16] W. Heitler, Quantum Theory of Radiation (Oxford University Press, 1953), 3rd edition.

[17] A. B. Migdal, J. Exptl. Theoret. Phys. (U.S.S.R.) **32**, 633 (1957), Soviet Phys. JETP **5**, 527 (1957).

[18] Varfolomeev, Gerasimova, Gurevich, Makar'ina, Romantseva, Svetlolobov, and Chueva, Proc. of the 1958 Annual Rochester Conference of High-Energy Physics, CERN, 1958, p. 297.

[19] L. D. Landau and I. Ya. Pomeranchuk, Dokl. Akad. Nauk SSSR **92**, 535 (1953).

[20] M. L. Ter-Mikaelyan, Dokl. Akad. Nauk SSSR **94**, 1033 (1954).

[21] M. Stearns, Phys. Rev. **76**, 836 (1957).

[22] A. P. Mishakova and V. A. Tumanyan, Приборы и техника эксперимента (Instruments and Measurement Engg.) in press.

Translated by H. Kasha
69

RECOIL NUCLEI FROM THE DISINTEGRATION OF SILVER BY FAST PROTONS

N. I. BORISOVA, M. Ya. KUZNETSOVA, L. N. KURCHATOVA, V. N. MEKHEDOV, and L. V. CHISTYAKOV

Joint Institute for Nuclear Research

Submitted to JETP editor March 4, 1959

J. Exptl. Theoret. Phys. (U.S.S.R.) **37**, 366-373 (August, 1959)

We have studied the angular and energy distributions of the recoil nuclei Ag^{106}, $Ag^{103,104}$ Nb^{90}, Zr^{89}, $Rb^{81,82}$ and Se^{73} produced when silver is bombarded by 480-Mev protons. These isotopes were separated from the reaction products radiochemically. The energy distribution of the recoil nuclei is shown to be exponential, and the parameters of the distribution are determined at an angle of 90°. We give a qualitative explanation of the observed distribution. The results confirm that Se^{73}, $Rb^{81,82}$, Zr^{89}, and Nb^{90} are formed by evaporation of α particles, protons, and neutrons.

INTRODUCTION

A number of recent papers[1-6] deal with recoil nuclei produced in reactions where high energy particles interact with complex nuclei. These papers give data on the kinetic energies of the reaction products, on their angular distributions, and on the excitation energy of the initial nucleus. The fundamental method used has been to determine an effective range in the target material for nuclei recoiling in the forward, backward, and perpendicular directions relative to the bombarding particles. Conclusions about the mechanisms of the reactions are made on the basis of the values obtained for these effective ranges. However, in our view there is a fundamental drawback to a study of the disintegration process through such experiments; that is, the effective range in the target material gives no information about the distribution of ranges of the recoil nuclei.

In the following we describe briefly some experiments to measure directly the ranges and angular distributions of some of the recoil nuclei from a thin silver target. The experiments were carried out in 1951-52, and are described in detail in reference 7. Particular attention was paid to reaction products appearing when many nucleons leave the initial nucleus. The statistical theory is, to some extent, suitable for describing the production of such reaction products, and, as will be shown below, these nuclei are formed by the evaporation of neutrons, protons and α particles. Our results on reaction products where only a few nucleons leave the initial nucleus (i.e., the radioactive isotopes of silver) are only preliminary.

METHOD

The problem reduced to determining the activity of a given isotope captured on a thin organic film placed near the silver target. Polystyrene was used to make the films. These were fitted into special containers, as shown in Fig. 1. The containers were made of very pure graphite and had thick walls (1 cm) to attenuate the protons bombarding the films. Container a was used to study the recoil nuclei at 90°, while container b was used to measure angular distributions. The target was a silver foil 0.5 mg/cm^2 thick. Spectral analysis of the foil showed admixtures of Mg, Si, Fe, Al, and traces of Pb ($< 10^{-3}$%) and Au ($< 10^{-3}$%).

The target was irradiated in the internal proton beam for an hour at a current of $\sim 0.1\,\mu$a. After the bombardment, the reaction products of interest were extracted chemically from the films and the foil.

The following isotopes were studied: Ag^{103}+

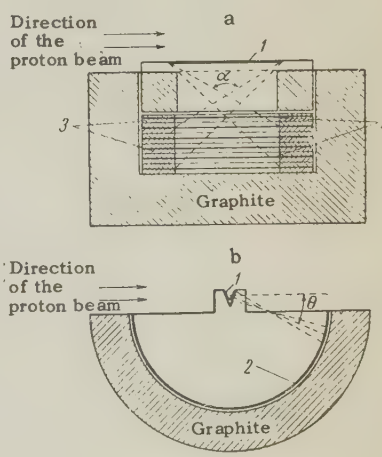

FIG. 1. Diagrams of the foil holders used to study the energy distribution of recoil nuclei (a) and their angular distribution (b). 1 – silver target; 2 – polystyrene films; 3 – celluloid frames.

Ag^{104} (β^+, K) T = 70 min; Ag^{106} (K), T = 8 days; Zr^{89} (β^+, K), T = 80 hrs; Nb^{90} (β^+, K), T = 16 hrs; $Rb^{81} + Rb^{82}$ (β^+, K), T = 6 hrs; and Se^{73} (β^+, K), T = 6.7 hrs. Zr and Nb were not separated chemically. Zr^{89} and Nb^{90} could easily be distinguished by their decay curves.

In the chemical separation of these isotopes, the films were either burned in a muffle furnace and the ash then dissolved (the films having been first wrapped in filter paper), or dissolved in sulfuric acid with a suitable carrier. The latter was the method used with selenium. The chemical method used in the separation and purification was standard,[8] except for minor details connected with the method for getting the active isotopes caught on the film into solution. The isotopes were identified by their half-lives. An electromagnet was used to determine the sign of the particle radiation. Half-lives measured in weak activities sometimes differed from accepted values (by not more than 20 or 25%).

The yield of an isotope was calculated with allowance for the time of irradiation, the length of time after cessation of the irradiation, the chemical yield, and corrections for the geometry of the experiment. The geometrical factors were necessary because the first and last films did not subtend the same solid angles α. The geometrical factors were calculated only roughly, assuming an isotropic angular distribution for the nuclei emitted. For the films on the ends, the correction factor for solid angle at the foil varied from 1.5 to 3.5.

Since the measurements were all relative, it was not necessary to introduce corrections for absorption of particle radiation in the counter walls, to take into account K capture, or to correct the results for self-absorption.

ANGULAR DISTRIBUTION OF THE REACTION PRODUCTS

For the recoil nuclei Ag^{106}, $Ag^{103,104}$, Nb^{90}, Zr^{89}, and $Rb^{81,82}$, the angular distributions were determined in three directions: forward, 90° to the proton beam, and backward. The target was a strip of foil 5 mm wide and bent into a semicylinder 40 mm long. Table I shows the angular distribution obtained. The same table shows the intervals of angle θ covered at the three directions. The total measured activity associated with a given isotope (i.e., the number of nuclei emitted forward, backward and at 90°, plus half the activity remaining in the foil) was taken to be 100%. This sum, of course, underestimates the total number of nuclei (some intermediate parts of the film are discarded, some of the nuclei do not hit the detector after leaving the target, etc.). It was not possible to estimate the number of nuclei lost in these ways, and this reflected on the accuracy of the results. The accuracies of the data in Table I are not greater than 50%. The ratio of the number of nuclei emitted forward to those emitted backward is 2 or 3 times greater for all the products than it is for Ag^{106}.

TABLE I

Isotope	Number of nuclei, %			
	Foil	forward ($5° \leqslant \theta \leqslant 58°$)	perpendicular ($63° \leqslant \theta \leqslant 117°$)	backward ($122° \leqslant \theta \leqslant 175°$)
Ag^{106}	90	6.0	2.0	2.0
$Ag^{103+104}$	90	6.0	3.0	1.0
Nb^{90}	70	21	7	2
Zr^{89}	66	24	7.5	2.5
Rb^{81+82}	≈30	≈40	~20	~5.0

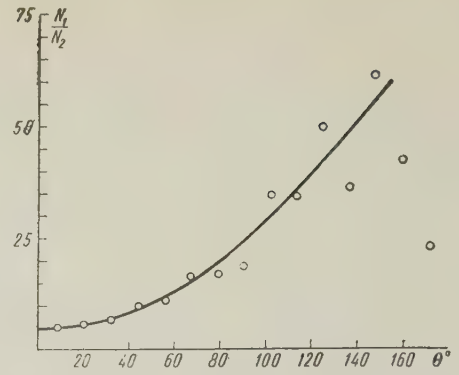

FIG. 2. Ratio of the activity in the first foil to that in the second as a function of the angle θ with the direction of the proton beam.

We measured the kinetic energies of nuclei emitted at various angles θ to the proton beam. This was done by exposing two films in container b simultaneously and determining the ratio of the activities at the corresponding places. The first foil was 0.48 mg/cm^2 thick, while the second one had a thickness of 0.59 mg/cm^2. The ratios of activities at corresponding places on the two foils are shown in Fig. 2. From the figure it is clear that nuclei emitted at small angles θ have relatively large kinetic energies.

A special experiment was carried out in another geometry to study the anisotropy of the emitted nuclei. In this experiment, a 1.7 × 4 cm strip of foil was oriented perpendicular to the proton beam. Aluminum collecting foils were fastened in special graphite holders on each side of the foil and parallel to it. These foils were 25 μ thick and had an area 2.5 times greater than that of the radiator. The distances between the aluminum and silver foils were 2 — 3 mm; they were arranged to minimize the number of nuclei

TABLE II

Isotope	Observed activity, %			forward / backward ratio	Yield* relative to $Ag^{103+104}$	Relative thick-sample yield*
	forward	foil	backward			
Ag^{106}	13.0	84.7	2.3	5.6	74.0	~70.0
$Ag^{103+104}$	17.0	81.0	2.0	8.5	100.0	100.0
Nb^{90}	49.0	45.0	6.0	8.2	93.0	80.0
Zr^{89}	49.0	46.0	5.0	8.7	42.0	38
Se^{73}	67.0	21.0	12.0	5.6	1.5	~2

*The relative yields are calculated without reference to the absolute number of counts

missing the aluminum foils. In such a geometry, experimental errors were held to a minimum. The whole package was irradiated with protons having a mean energy 400 Mev. In this experiment, we looked for selenium rather than rubidium. The results are shown in Table II. For comparison, the table also gives the yields of the various nuclei studied in this experiment relative to yields found with thick silver samples.[9]

It is clear that the thick-target yields agree with those found here, to within 25%. As in the previous experiment, the fraction of nuclei emitted from the foil increases as the number of nucleons knocked out of the target nucleus increases. However, for Se^{73}, about 20% of the nuclei remain in the foil, i.e., their energies are insufficient to penetrate a layer of Ag 0.5 μ thick. It is difficult to make a definite conclusion about the dependence of the anisotropy on Z.

This experiment confirms that the forward/backward ratio for Ag^{106} is less by a factor of almost two than it is for $Ag^{103+104}$.

ENERGY DISTRIBUTION OF THE REACTION PRODUCTS

Using the geometry of Fig. 1a, the energy distribution of the recoil nuclei was studied for the same isotopes as those above, and also for Se^{73} at an angle 90° ± 40°. For each element, the results of direct measurements of the fraction of nuclei having various ranges is shown in Fig. 3. The error bars shown are due to the thicknesses of the polystyrene films. The first point is half the activity remaining in the silver foil. As is evident from the figure, for each element the number of recoil nuclei decreases with increasing range. The range increases with decreasing Z of the product nucleus. In the region of small ranges and for light nuclei, the rate at which the curve drops decreases somewhat, the effect being more marked for smaller Z. In selenium, there is an irregularity in the distribution near a range 0.25 mg/cm^2. This irregularity is probably an experimental error and upon changing to an energy scale one can see that it is within the assigned limits of error. The largest range shown corresponds to an activity equal to or less than the counter background, i.e., 16 counts/min. Some indications of activities with longer ranges were found, but these are not shown on the graph because the counting rate was so slow the half life could not be determined. This made it difficult to find the longest range nuclei emitted.

The reaction products considered appear also as light fragments in the fission of uranium. This makes it possible to go from ranges to energies in our experiment by using the experimental range-energy curve for light uranium fission fragments.[10] The curve used is shown in Fig. 4, which also shows the range-energy relation for fission fragments in silver.[10] The curve for polystyrene was obtained using the atomic stopping power of polystyrene (the mean atomic number

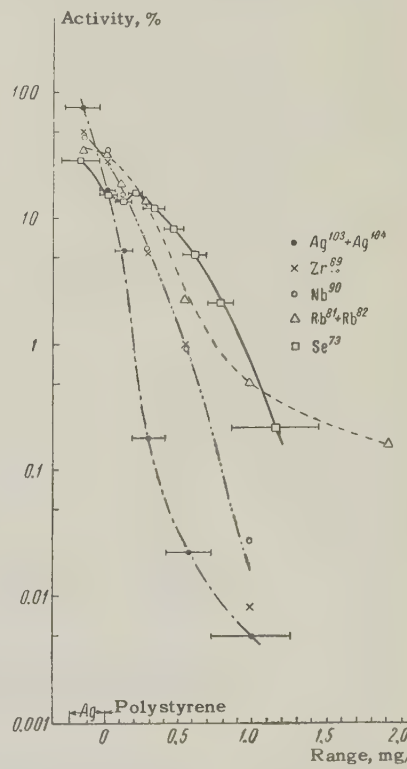

FIG. 3. Range distribution of nuclei recoiling at an angle 90° ± 40°.

FIG. 4. Range-energy relation for the reaction products of interest.

being taken to be 3).

The masses of the isotopes studied differ from those of the light fission fragments of uranium by 7 to 10 units. This difference might lead to a slightly greater range (at a given energy) for the isotopes we are considering. However, this effect could not be taken into account and was neglected.

Figure 5 shows the energy distribution of the recoil nuclei. In going from ranges to energies, we also made corrections for geometrical factors. For all the curves, the first points correspond to half the activity remaining in the foil. They correspond to a range of 0.25 mg/cm^2 in silver, or an energy loss of 2.0 Mev. Although such a determination of the energy loss is somewhat artificial, the first points agree well with the remaining experimental points.

Figure 5 shows that, for all the reaction products, the number of nuclei decreases linearly with increasing logarithm of their energy. The slopes of the straight lines differ, the slope being steepest for silver and flattest for selenium.

DISCUSSION OF THE EXPERIMENTAL RESULTS

Energy can be imparted to a product nucleus either through a direct interaction, or after the formation of a compound nucleus. The energy and angular distributions of the recoil nuclei are obtained by combining the momenta obtained directly from the bombarding particle with the mean momentum possessed by the recoil nucleus after all particles have been emitted.

The momentum given a nucleus by the bombarding particle usually lies in the direction of motion of the protons, while the momentum transferred in evaporation has an isotropic distribution. The sum of these two momenta, one from direct interaction and one from evaporation, will be a minimum in the backward direction. Hence nuclei emitted backward must have less energy than

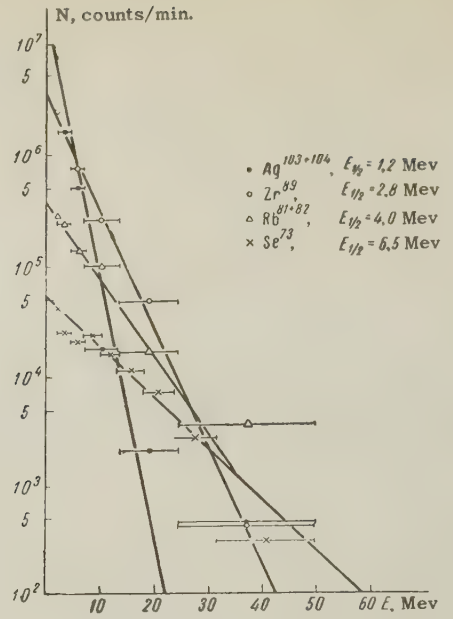

FIG. 5. Energy distribution of nuclei recoiling at an angle of 90° ± 40°.

those emitted at 90° or forward. This conclusion is supported by Fig. 2, which shows the ratio of activities in the first and second foils grows with increasing θ. From this it follows also that the energy distribution of the reaction products at 90° to the proton beam should be essentially determined by the mean energy transferred to the emitted particles. We note that in our case we can neglect cascade particles since they will have little effect on the distribution at 90°. Strictly speaking, one should take into account not only cascade processes, but also interactions where the momentum transferred by the bombarding particle does not lie in the direction of motion of the bombarding particle. The existence of high energy tails is presumably due to these two processes. The curve for $Ag^{103+104}$ in Fig. 5 shows that such events are rare, but do take place (about $1:10^4$). We neglect such details because of the computational difficulties involved.

Let us look at the average momentum a recoil nucleus has after all particles have evaporated. The problem of finding the mean momentum after a number of nucleons have been ejected independently and isotropically is analogous to the problem of finding the mean angle of multiple scattering when a fast particle traverses a layer of thickness d.* In multiple scattering,[11,12] the mean-square angle of scattering is given by

*The method described below was proposed by B. T. Geĭlikman. We obtained similar results by considering the statistical equilibrium between the product nucleus and the emitted particles.[7]

TABLE III

Isotope	$\bar{E}$, Mev, experimental	$\bar{E}$, Mev, (n, p)	$\bar{E}$, Mev, (n, p, α)	Mean number of particles α : p : n	Mean energy carried off			Total energy carried off (α, p, n)
					α	p	n	
$Ag^{103+104}$	2,6	0,4	0,4	0 : 0 : 4—5 (0 : 1 : 4—5)	—	—	—	—
Nb^{90}	6	1,7	3,8	1,1 : 3,8 : 9,8	21	63	108	192 (200—210)
Zr^{89}	6	1,9	4,1	1,3 : 4,4 : 9,4	24	73	103	200 (200—210)
Rb^{81+82}	9	2,6	6,4	1,8 : 6,4 : :12,4—13,4	33	106	136—147	275—286 (230—250)
Se^{73}	14	4,3	9,7	2,5 : 9 : 16	46	148	176	370

$$\overline{\varphi^2} = (\bar{\psi})^2 d/\lambda, \qquad (1)$$

where λ is the mean free path, $(\bar{\psi})^2$ is the mean-square angle of scattering in one collision, and $d/\lambda = n$ is the number of collisions. In our case, this is the number of nucleons evaporated. The size of the angle corresponds to momentum. Assuming, then, that when a definite kind of particle is emitted, the recoil nucleus gets a momentum of a certain fixed magnitude, the mean-square momentum of the recoil nucleus can be written

$$\sqrt{\overline{p^2}} = \bar{p}_{el}\sqrt{n}. \qquad (2)$$

The momentum distribution of the nuclei must be Gaussian, i.e.,

$$w(p^2) = w_0 e^{-\beta p^2}. \qquad (3)$$

The constants β and w_0 are determined by normalization and evaluation of the mean, so that

$$\int_{-\infty}^{\infty} w(p^2)\, d\omega = 1, \qquad \int_{-\infty}^{\infty} w(p^2)\, p^2\, d\omega = \overline{p^2}, \qquad (4)$$

where $d\omega = 4\pi p^2 dp$ is the volume element in momentum space. Finally, the momentum distribution can be written

$$w(p^2) = 0.165\,(\overline{p^2})^{-3/2} \exp\{-1.5\, p^2/\overline{p^2}\}. \qquad (5)$$

Upon changing from momentum to energy, one can compare this distribution with the experimental one. The comparison was made in the following way. For each element in Fig. 5, we found the value $E_{1/2}$ at which the number of nuclei in the distribution decreased by a factor 2. From the value of $E_{1/2}$ we found the mean energy $\bar{E} = 1.5\, E_{1/2}/0.693$. On the other hand, $\bar{E}$ can be obtained from the mean momentum $\bar{R} = \sqrt{\overline{p_\alpha^2}} + \sqrt{\overline{p_p^2}} + \sqrt{\overline{p_n^2}}$ given a nucleus when it ejects a known number of particles. The calculation was made on the following assumptions: a) the nucleus evaporated only neutrons and protons (n, p); b) the nucleus evaporated alpha particles, neutrons, and protons (α, n, p). The mean energies carried away by alpha particles and protons, as obtained from experiments with photoemulsions, are 14 and 8 Mev respectively.[13-16] The numbers of alpha particles and protons were chosen to satisfy the relation* $\alpha/p = 0.3$;[16,17] the mean energy of the evaporating neutrons was taken to be 2.5 Mev.[18] The experimental and calculated quantities are shown in Table III.

The table shows that for four nuclei (Nb, Zr, Rb, and Se) the agreement between experimental and calculated values of $\bar{E}$ is improved by taking into account the evaporation of α particles. Even in these cases, however, the calculated values of $\bar{E}$ are 30 or 40% less than the experimental ones. The difference is presumably due to our neglect of cascade processes, though it is also possible that errors in the range-energy relation and approximation in the calculations played a role. Rough estimates show, for example, that if one were to assume that in the formation of Nb^{90} there is emitted one cascade particle with an energy of ~ 30 Mev and travelling at 90° to the proton beam, then the discrepancy between the values of $\bar{E}$ is decreased to almost one-half. Unfortunately, lack of experimental data precludes a more exact treatment of cascade processes. We propose to fill in this gap in subsequent work.

For $Ag^{103+104}$ the value of $\bar{E}$ calculated assuming that 4 to 6 nucleons evaporate is about 6 times smaller than the experimental one. Such a discrepancy can be removed only if we assume that each neutron emitted carries off an energy ~ 30 Mev. In this case most of the ejected neutrons must be formed in cascade processes, the observed radioactive silver isotope remaining after a sequence of knock-on events.

In spite of the limitations mentioned above, the energy spectrum of the recoil nuclei gives some information on the numbers of α particles, protons, and neutrons emitted and on their energies.

*The values of $\bar{E}$ calculated under the assumptions $\alpha/p = 0.5$ and 0.4 differed but little from the value calculated with $\alpha/p = 0.3$.

One can then compute the excitation energy and what fractions of it are due to the various particles. In computing the excitation energy of the compound nucleus, one must take into account the binding energies of the particles ejected. The binding energy of an α particle was taken to be 4.5 Mev, while that of neutrons and protons was taken to be 8.5 Mev.[19-21] The results of such calculations are shown in the last columns of Table III. The numbers in parentheses are the excitation energies calculated from the momentum given the compound nucleus by the incident proton.[7] These excitation energies were obtained from the angular distributions of the corresponding reaction products, as shown in Table I. It is clear that the excitation energies agree satisfactorily with one another. The energy used to evaporate neutrons is almost one half of the total excitation energy.

We should like to express our sincere thanks to B. V. Kurchatov and to Prof. B. T. Geĭlikman for their help and valuable suggestions.

[1] Si-Chang Fung and I. Perlman, Phys. Rev. **87**, 623 (1952).

[2] R. E. Batzel and G. T. Seaborg, Phys. Rev. **82**, 607 (1951).

[3] Sugarman, Campos, and Wielgoz, Phys. Rev. **101**, 388 (1956).

[4] N. T. Porile, Phys. Rev. **108**, 1526 (1957).

[5] F. P. Denisov and P. A. Cerenkov, J. Exptl. Theoret. Phys. (U.S.S.R.) **35**, 544 (1958); Soviet Phys. JETP **8**, 376 (1959).

[6] L. V. Volkova and F. P. Denisov, J. Exptl. Theoret. Phys. (U.S.S.R.) **35**, 538 (1958); Soviet Phys. JETP **8**, 372 (1959).

[7] V. N. Mekhedov, Dissertation, Inst. Nuc. Prob. U.S.S.R. Acad. Sci., 1954.

[8] Kurchatov, Mekhedov, Borisova, Kuznetsova, Kurchatova, and Chistyakov, Сессия АН СССР по мирному использованию атомной энергии (Session of the Academy of Sciences of the USSR on the Peaceful Uses of Atomic Energy), 1955 [Engl. Transl. by U. S. Dept. of Commerce].

[9] Kurchatov, Mekhedov, Kuznetsova and Kurchatova, Сводный отчет ИЯП АН СССР (Summary Report of the Institute for Nuclear Problems Academy of Sciences, U.S.S.R.) 1951.

[10] C. B. Fulmer, Phys. Rev. **108**, 1113 (1957).

[11] B. Rossi and K. Greisen, Interaction of Cosmic Rays with Matter (Russ. Translation) IIL, 1950

[12] E. Fermi, Nuclear Physics (Russ. Translation) IIL, 1951.

[13] Harding, Lattimore, and Perkins, Proc. Roy. Soc. (London) **196A**, 325 (1949).

[14] N. Page, Proc. Phys. Soc. (London) **63A**, 250 (1950).

[15] R. W. Deutsch, Phys. Rev. **92**, 515 (1953).

[16] E. L. Grigor'ev and L. P. Solov'eva, J. Exptl. Theoret. Phys. (U.S.S.R.) **31**, 932 (1956); Soviet Phys. JETP **4**, 801 (1957).

[17] P. E. Hodgson, Phil. Mag. **42**, 82 (1951).

[18] Goldanski, Ignatenko, Mukhin, Pen'kina and Skoda-Ulyanov, Phys. Rev. **109**, 1762 (1958).

[19] W. Heisenberg, Vorträge über Kosmische Strahlung, Berlin 1953.

[20] Y. Fujimoto and Y. Yamaguchi, Progr. Theoret. Phys. **5**, 787 (1950).

[21] K. J. Le Couteur, Proc. Phys. Soc. **63A**, 498 (1950).

Translated by R. Krotkov
70

SPECTRUM OF PHOTO PROTONS PRODUCED BY γ RAYS IN THE NARROW 82-89 Mev ENERGY RANGE

E. B. BAZHANOV

Leningrad Physico-Technical Institute, Academy of Sciences, U.S.S.R.

Submitted to JETP editor March 3, 1959

J. Exptl. Theoret. Phys. (U.S.S.R.) **37**, 374-379 (August, 1959)

Energy spectra were investigated for protons ejected from C^{12} and Al^{27} by γ rays from bremsstrahlung spectra possessing peak energies of 82 and 89 Mev. The experimental data are compared with curves based on Dedrick's data. Although the agreement is not very good it may nevertheless be possible that the quasi-deuteron mechanism contributes significantly to the interaction of γ rays with the nuclei considered.

1. INTRODUCTION

THERE is considerable interest at the present time in the interaction of high energy γ rays with nuclei. From work with γ rays having energies greater than 150 Mev, it can be concluded that at such energies the most important mechanism is the quasi-deuteron one. The results of Odian et al.[1] and of Barton and Smith[2] show that this mechanism can explain almost all the yield of protons having energies greater than 60 Mev. For γ ray energies less than 150 Mev, the picture is not so clear. The work of Gorbunov and Spiridonov[3] on the photodisintegration of He^4 shows that for γ rays having energies in the interval 70 — 170 Mev, the quasi-deuteron interaction amounts to about 30%, and becomes less important at lower energies. Qualitative results obtained by Chuvilo and Shevchenko[4] and also by us[5] indicate that the two-nucleon mechanism can be important at energies less than 100 Mev. Whitehead et al.[7] have recently made a quantitative comparison with the calculations of Dedrick,[6] which were carried out for C^{12} on the basis of the quasi-deuteron interaction. Using γ rays in a narrow energy range (~ 20 Mev) centered on $\bar{E}_\gamma = 96$ Mev, both the excitation function obtained for 37-Mev protons and the energy and angular distribution of the protons agree satisfactorily with Dedrick's calculations.

In the following we present some energy spectra for photo-protons from C^{12} and Al^{27}. They were obtained by a difference method, using γ rays in the narrow energy range bounded by the maximal energies of two bremsstrahlung spectra, the bounds being $E_{\gamma\,max} = 82$ and 89 Mev. The spectra are compared with Dedrick's calculations for the same energy range.

2. BRIEF DESCRIPTION OF THE EXPERIMENT

The method used for getting the energy spectrum of those protons arising from γ rays having energies lying in a certain narrow region of a continuous spectrum depends on the fact that two bremsstrahlung spectra having maximal energies E_1 and E_2 ($E_2 > E_1$) which differ but little from each other (the spectra being normalized to the same number of effective quanta) will then practically coincide at energies less than E_1. Figure 1 shows two spectra with maximal energies $E_{\gamma\,max} = 82$ Mev and $E_{\gamma\,max} = 89$ Mev. The cross-hatched area is their difference.

The proton energy spectra obtained with these two bremsstrahlung spectra were then subtracted, having first been normalized to a γ ray dose corresponding to the passage of one effective quantum through the target. The difference spectrum so

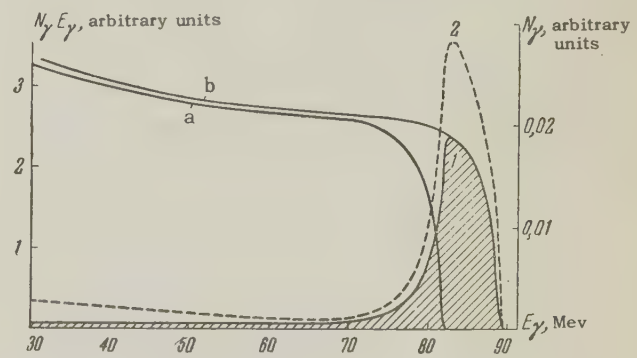

FIG. 1. Bremsstrahlung spectra of γ rays having maximal energies: a) 82 mev, b) 89 Mev. The spectra are normalized to the same total number of effective quanta. Cross hatched area bounded by curve 1 is their difference in units $E_\gamma N_\gamma$. Curve 2 — difference of spectra in units of N_γ, the number of quanta. Scale along ordinate at left is for curves a, b, and 1; along the right, for curve 2.

obtained corresponds to the γ ray spectrum shown by the cross-hatched area in Fig. 1.

The protons were detected by a scintillation telescope, which was described previously.[5] The protons were detected at 90° relative to the γ-ray beam. The targets were oriented at 45° to the direction of the beam. The target thicknesses were C^{12} — 150 mg/cm^2, Al^{27} — 40.5 mg/cm^2. The solid angle of the telescope was 1.08×10^{-2} sterad; its angular resolution function was almost a triangle having a base ±6.0°. Each telescope consisted of two counters. The thickness of the crystal in the back counter NaI(Tl) was 1.8 cm, while the thickness of the crystal in the front counter CsI(Tl) was 0.025 cm. Lead diaphragms defining the telescope solid angle did not allow protons to pass through without traversing the full thickness of the crystal in the back counter. In order to decrease the background, which was due chiefly to the layer of air near the target, the target was placed in an evacuated chamber. As a result, the proton counting rate without the target was less than 1% of the counting rate with the target. Accidental coincidences, as measured by introducing a delay line in one of the telescope channels, accounted for less than 0.1% of the total count.

Since the proton spectrum was obtained by taking the difference between two large almost equal numbers, it was important that the telescopes operate stably. Since the equipment was on round the clock for long periods of time, temperature drifts in the electronics were not important. The gain of each channel was controlled using a Po^{210} source. Measurements at different γ ray energies were continuously alternated. Constant monitoring showed that the stability of the whole setup was satisfactory. More than 80% of the results in all series of measurements lay within the limits of statistical error.

The dose of γ rays passing through the target was measured by the same method as described previously.[5]

With the telescopes it was easy to discriminate between electrons and heavy charged particles. There were few enough deuterons so that these could not have introduced any distortions.[8]

3. RESULTS AND DISCUSSION

The table shows the proton energy spectra from C^{12} and Al^{27}, taken with the continuous bremsstrahlung spectra having maximal energies 82 and 89 Mev. For carbon, our data at $E_{\gamma\,max}$ = 89 Mev can be compared with the results of Whitehead et al.[7] at $E_{\gamma\,max}$ = 90 Mev. These spectra are shown in Fig. 2. The yields of protons having energy E_p = 37 Mev agree well (the errors shown are, in both cases, statistical). The cross shows the proton yield quoted in reference 4, and obtained with a bremsstrahlung spectrum having a maximum energy 84 Mev. The energy spectra shown in Fig. 2 disagree somewhat in their decreasing portions. The discrepancy does not disappear completely if one takes into account the finite resolution of the second counter in the telescope and errors in the telescope's energy calibration. The error bars parallel to the abscissa take these two effects into account. Errors connected with corrections for finite target thickness are small at such high proton energies and cannot change the positions of the experimental points very much.

Figures 3 and 4 show the energy distribution of protons from C^{12} and Al^{27} obtained in the manner described above for a narrow range of γ ray energies. Only statistical errors are shown. On both figures, curve 1 is calculated from Dedrick's data. The experimental results represent the difference in proton yields per effective quantum, so in comparing with Dedrick's data it is convenient to place it on the same footing, especially as this takes into account the contribution of low energy quanta (see Fig. 1) almost completely. Dedrick's calculations were for only four γ-ray energies in the interval 50 — 125 Mev, so the theoretical yields were calculated by first interpolating the cross section to intermediate γ-ray energies, then subtracting the results for the two energy intervals:

Target	Mean proton energy E_p, Mev	Proton yield, $\frac{cm^2 10^{-30}}{sterad \cdot Mev \cdot Q}$ $E_{\gamma\,max}$=82 Mev	Proton yield, $\frac{cm^2 10^{-30}}{sterad \cdot Mev \cdot Q}$ $E_{\gamma\,max}$ = 89 Mev
C^{12}	17.8	4.028±0.040	4.120±0.042
	21.4	2.841±0.052	3.134±0.055
	26.0	1.882±0.034	2.044±0.036
	31.4	0.961±0.028	1.127±0.030
	36.8	0.443±0.010	0.573±0.011
	44.0	0.113±0.004	0.196±0.005
	52.2	0.003±0.0005	0.020±0.002
Al^{27}	15.4	18.63 ±0.18	18.98 ±0.19
	19.1	11.01 ±0.22	11.90 ±0.28
	24.0	5.71 ±0.13	6.38 ±0.16
	27.7	4.07 ±0.12	4.70 ±0.12
	29.8	2.59 ±0.08	3.01 ±0.11
	33.6	1.85 ±0.08	2.06 ±0.08
	36.7	0.82 ±0.40	1.06 ±0.06
	41.0	0.523±0.035	0.764±0.038
	49.9	0.078±0.013	0.127±0.016

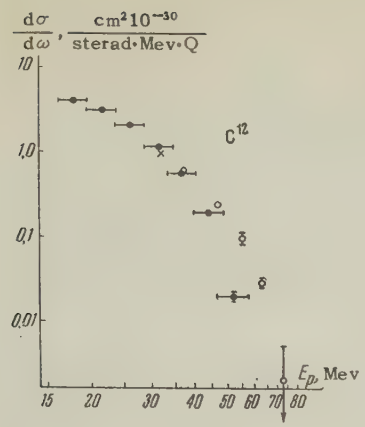

FIG. 2. Energy spectrum of protons ejected from C^{12} when this nucleus is irradiated by the full bremsstrahlung spectrum having $E_{\gamma\,max} = 89$ Mev. Protons observed at 90°. ● – our data, ○ – data of Whitehead et al.,[7] × – data of Chuvilo and Shevchenko.[4] Errors shown are statistical.

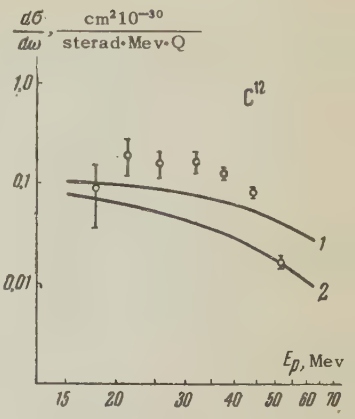

FIG. 3. Energy spectrum for protons from C^{12} for rays in a narrow energy range; $\theta = 90°$. Curves calculated from data of Dedrick;[6] 1 – without taking into account scattering of protons in the nucleus, 2 – taking scattering into account. The errors shown are statistical.

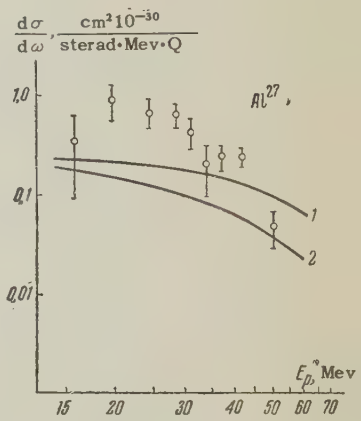

FIG. 4. Same as Fig. 3, but for protons from Al^{27}.

50 – 89 Mev and 50 – 82 Mev in units $cm^2 \cdot 10^{-30}$/sterad-Mev-Q. The contribution of quanta having energies less than 50 Mev is not included, but taking reaction thresholds into account it can be shown that for protons with energy $E_p = 15$ Mev coming from the nucleus C^{12}, this contribution to the theoretically calculated yield is less than 10%. This estimate also holds essentially for Al^{27}.

Curve 1 neglects barrier penetration effects, since at these high proton energies such effects are small. On the other hand, an exact treatment of barrier effects is difficult because the distribution of the orbital angular momenta l of the emitted protons is not known.

In the following we make an approximate estimate of the effect of nucleon scattering in the nucleus. If we assume that nucleon scattering inside the nucleus can be considered as a direct interaction with individual nucleons in the nucleus (which assumption is supported by a number of investigations on the inelastic scattering of nucleons from nuclei), we can expect the total number of protons leaving the nucleus to decrease, and the relative number of low energy protons to increase. This will make the spectrum drop off more sharply. Calculations on the mean free path λ[9] show that for light nuclei this is comparable with nuclear dimensions. For C^{12}, $R = 2.3 \times 10^{-13}$ cm, while $\lambda = 3.4 \times 10^{-13}$ cm for $r_0 = 1.4 \times 10^{-13}$ cm. Hence one need consider only protons which are not scattered at all or only once; it is further assumed that all singly scattered protons having an energy greater than 10 Mev leave the nucleus without experiencing another collision. It is interesting to consider protons traveling at an angle θ with the direction of the γ-ray beam, but leaving the nucleus after scattering at an angle 90°. To simplify the integration, it was assumed that the angular distribution of the scattered protons was a straight line, falling to zero at an angle of 90° with the direction of travel before the collision. This agrees in its general features with the angular distribution of protons scattered from nuclei.[10] The energy distribution of the scattered protons was taken to be isotropic between the limits $E_{p\,min} = E_F$ and $E_{p\,max} = E_p - \frac{2}{5} E_F$ (E_F being the Fermi energy and E_p the proton energy before the collision relative to the bottom of the potential well). Such an energy distribution does not differ too much from the experimentally observed one, especially at large scattering angles.[10,11]

Curves 2 in Figs. 3 and 4 show the energy spectrum calculated from Dedrick's data but taking into account scattering inside the nucleus. The particle yield decreases about the same for both nuclei by ~40%. All calculations were carried out for $r_0 = 1.4 \times 10^{-13}$ cm and a potential well of depth 40 Mev.

Comparison of the calculated curves with the experimental data shows that for both elements more protons are observed experimentally than calculated. For carbon, the experimental proton yield in the energy range 15 – 50 Mev is about double the calculated quantity (curve 1). It is not possible to make a more precise statement because the statistical errors of the experimental points are too large.

Whitehead et al.[7] note that for γ-ray energies

in the region bounded by the maxima of bremsstrahlung spectra lying at 90 Mev and 110 Mev ($\bar{E}_\gamma = 96$ Mev), and for protons having energies $E_p \geq 37$ Mev, the number of protons at 90° with the direction of the incident beam agrees satisfactorily with Dedrick's calculations, the value of r_0 being taken to be 1.4×10^{-13} cm. In our case most of the protons observed have energies in the range 15 — 40 Mev and are ejected by γ rays of somewhat lower energy ($E_{\gamma\,max} = 82 - 89$ Mev). The discrepancy with Dedrick's calculations can be due to several reasons: in the first place, it is possible that with decreasing γ ray energies the relative importance of various mechanisms for the interaction can change and the quasi-deuteron mechanism becomes inadequate, and in the second place it may be that the accuracy of the calculations changes. Simplifying assumptions, defining the model for the interaction, have been made, and the interaction between the emitted nucleons and the nucleus in its final state neglected, so that only approximate agreement with experiment can be expected. Changing r_0 to 1.2×10^{-13} cm increases the theoretical yield by a factor 1.6 and considerably improves agreement with our data. Hence a detailed comparison between the forms of the calculated and experimental spectra is not justified.

For Al^{27}, the experimental yield for protons in the energy interval 15 — 50 Mev is about three times greater than that predicted by Dedrick; however, it is quite likely that the Gaussian distribution of momenta about $E_0 = 16$ Mev, which he has assumed, is not justified for Al^{27}. A distribution corresponding to a smaller value of E_0 could lead to a higher yield of low energy protons and hence to a steeper fall-off in the spectrum, since the total number of protons taking part in the interaction remains the same.

On the whole, however, it cannot be denied that for both of the elements investigated the quasi-deuteron mechanism for the interaction can make a significant contribution.

In conclusion, the author would like to thank Prof. A. P. Komar, his colleagues L. A. Kul'chitskiĭ, V. P. Chizhov, Yu. M. Volkov, A. V. Kulikov and G. M. Shklyarevskiĭ, and the synchrotron group at the Institute of Physics and Technology of the Academy of Sciences of the U.S.S.R. for discussions of results obtained and for their interest in this work.

[1] Odian, Stein, Wattenberg, Feld, and Weinstein, Phys. Rev. **102**, 837 (1956).

[2] M. Q. Barton and J. H. Smith, Phys. Rev. **110**, 1143 (1958).

[3] A. N. Gorbunov and V. M. Spiridonov, J. Exptl. Theoret. Phys. (U.S.S.R.) **34**, 866 (1958); Soviet Phys. JETP **7**, 600 (1958).

[4] N. V. Chuvilo and V. G. Shevchenko, Труды Всесоюзной конференции по ядерным реакциям при малых и средних энергиях (Trans. All-Union Conference on Nuclear Reactions at Low and Intermediate Energies) Acad. Sci. U.S.S.R. 1958, p. 435.

[5] Bazhanov, Volkov, and Kul'chitskiĭ, J. Exptl. Theoret. Phys. (U.S.S.R.) **35**, 322 (1958), Soviet Phys. JETP **8**, 224 (1959).

[6] K. G. Dedrick, Phys. Rev. **100**, 58 (1955).

[7] Whitehead, McMurray, Aitken, Middlemas, and Collie, Phys. Rev. **110**, 941 (1958).

[8] V. P. Chizhov and L. A. Kul'chitskiĭ, J. Exptl. Theoret. Phys. (U.S.S.R.) **36**, 345 (1959), Soviet Phys. JETP **9**, 239 (1959).

[9] Hayakawa, Kawai, and Kikuchi, Progr. Theoret. Phys. **13**, 415 (1955).

[10] R. M. Eisberg and G. F. Igo, Phys. Rev. **93**, 1039 (1954).

[11] J. W. Weil and B. D. McDaniel, Phys. Rev. **92**, 391 (1953).

Translated by R. Krotkov
71

HEAVY NUCLEI FLUX IN THE PRIMARY COSMIC RADIATION AT A GEOMAGNETIC LATITUDE OF 31°N

K. I. ALEKSEEVA and N. L. GRIGOROV

Moscow State University

Submitted to JETP editor March 7, 1959

J. Exptl. Theoret. Phys. (U.S.S.R.) **37**, 380-388 (August, 1959)

The flux of primary heavy particles in the stratosphere was measured with apparatus consisting of a telescope surrounded by hodoscope counters and of two pulse ionization chambers placed between the trays of the telescope counters. The ionization produced in each of the chambers by single particles with a charge $Z \geq 1$ traversing the telescope was measured. The flux of primary α particles at the top of the atmosphere at a geomagnetic latitude of 31° N was found to be equal to 0.335 ± 0.035 particles $cm^{-2}min^{-1}sterad^{-1}$, which is $(16 \pm 2)\%$ of the total particle flux. The flux of primary particles with $Z > 2$ under similar conditions was found to be equal to 0.019 ± 0.006 particles $cm^{-2}min^{-1}sterad^{-1}$, which is $\sim 6\%$ of the number of α particles and about 1% of the total particle flux at the top of the atmosphere at a geomagnetic latitude of 31° N.

INTRODUCTION

THE discovery of atomic nuclei of heavy elements in primary cosmic radiation in addition to protons[1,2] has aroused great interest in the study of the composition of primary cosmic rays. As has been determined since, in spite of the small fraction of heavy nuclei in the total flux of primary particles, these heavy nuclei amount to 30 — 35% of all nucleons reaching the top of the atmosphere and carry about 30% of the total energy of the cosmic radiation, and produce about 50% of the ionization in the upper layers of the atmosphere. An accurate knowledge of the composition of the multi-charged primary component is necessary also for a solution of the problem of the origin of the cosmic radiation and the distribution of its sources. A wide range of problems connected with the composition of the heavy primary component of cosmic rays has led to a number of experimental investigations. In addition to the fundamental experiments on the determination of the spectrum of heavy nuclei, as carried out by Bradt and Peters et al. with nuclear photo-emulsions,[3-5] a series of experiments with low-pressure Geiger counters,[1,2] proportional counters,[6] and scintillation counters[7] have been carried out.

A study of the charge spectrum of cosmic-ray primaries in the stratosphere was carried out in our laboratory using pulse ionization chambers and a hodoscope. By means of a telescope and hodoscope, the vertical beam of single particles traversing the apparatus was selected. By measuring the ionization produced by these particles in two pulse ionization chambers placed inside the telescope, we were able to determine the charge spectrum and, consequently, the mass spectrum of the heavy nuclei of the primary cosmic radiation. On September 18, 1954, the apparatus constructed for this purpose was lifted by probing balloons to the stratosphere at 31° N geomagnetic latitude, and, for a period of several hours, stayed at an altitude of 25 — 27 km (an average atmospheric depth of 24 g/cm^2). The measurements of the ionization chambers and of the hodoscope were transmitted to the earth by radio.

APPARATUS

A schematic diagram of the position of the counters and ionization chambers in the apparatus, and a block diagram of the electronic circuitry, using miniature directly-heated tubes, are shown in Fig. 1.

The telescope, which selected a vertical beam of single particles, consisted of three trays A, B, C, of self-quenched Geiger-Müller counters, three counters in each tray,* connected to a triple-coincidence circuit (see Fig. 1). Two identical cylin-

*The dimensions of the counters were: internal diameter, 2 cm; geometrical length, 30; thickness of the glass walls, 1-1.5 mm. The counters were filled with a mixture of argon and ethylene. A thin graphite layer spread on the internal surface of the glass wall served as the cathode.

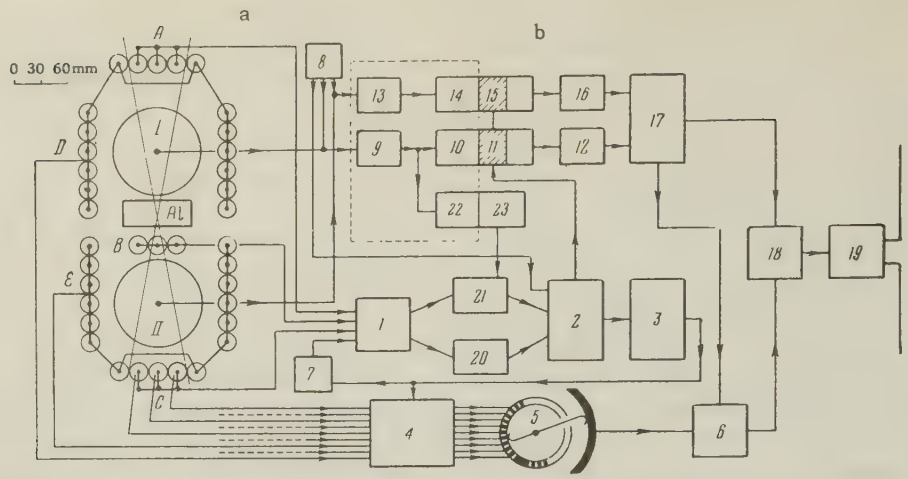

FIG. 1. a – diagram of the position of the counters and ionization chambers in the apparatus; b – block diagram of the electronic circuits of the apparatus: 1 – triple coincidence circuit; 2 – gating univibrator; 3 – hodoscope master pulse shaping circuit; 4 – hodoscope; 5 – rotary switch; 6 – hodoscope pulse tube; 7 – triple coincidence gating circuit; 8 – generator of calibration pulses; 9 to 10, 13 to 14, and 9 to 22 – channels of linear amplification; 11 and 15 – gating circuits; 12 and 16 – pulse stretching circuits; 17 – circuit for simultaneous transmission of pulses of both chambers; 18 – modulator of the transmitter; 19 – transmitter; 20 – scaling circuit 1:4; 21 – "four-fold" coincidence circuit; 23 – univibrator with trigger level set for the pulse produced in the ionization chamber by two to three relativistic particles.

drical pulse ionization chambers,* I and II, were placed inside the telescope for the measurement of the specific ionization of particles traversing the telescope. The chambers were connected to linear amplifiers 9 — 10, 13, 14, and 9 — 22. The ionization chambers and the telescope were surrounded by two groups of counters D and E. The counters D and E, and also each of the telescope counters, were connected to a hodoscope. The passage of several particles (nonlocal showers) through the instrument, and also the production of electron-nuclear showers in the material of the telescope by the particles traversing it were, as a rule, accompanied by a discharge of the counter groups D, E, or the discharge of more than one counter in the telescope trays. Such showers were excluded from consideration since, in the majority of cases, they were nonlocal. Only these cases where one counter was discharged in each of the telescope trays A, B, and C, owing to single particles traversing the telescope without interaction, were subject to further analysis. In order to minimize the loss in the number of single particles due to the production of δ-showers and electron-nuclear showers in the material inside the telescope, it was necessary to reduce the amount of matter in the telescope to a minimum. Nevertheless, an aluminum absorber of 3.0 cm thickness was placed between the trays A and B of the telescope counters under the upper ionization chamber I. This was done in order to exclude the secondary low-energy protons, with an initial ionization greater than three times the minimum ionization, from the flux of single particles, and thus to lower the background in the ionization range of α particles. In the following, in the calculation of the flux of multiply-charged particles, a correction was applied for the exclusion of single particles from the beam due to the production of showers in the matter inside the telescope.

The instrument was triggered by a triple coincidence ($\tau = 5 \times 10^{-6}$ sec) of discharges in the counter trays A, B, C of the telescope (block 1). To increase the statistical accuracy of the measured flux of multi-charged particles, we constructed an instrument with a rather large geometrical factor $S\Omega = 22.7$. To avoid overloading of the electronic circuits by a large number of pulses from single particles, all pulses from the triple coincidence circuit (block 1) were fed through 20 with a scaling factor of 1:4. However, to prevent a decrease in the number of the recorded multiply-charged particles, "four-fold coincidences" between the total number of triple coincidences without scaling and the pulses due to particles which, in chamber I, produced two to three times the ionization of a singly-charged relativistic particle, were analyzed by circuit 21.

*The dimensions of the cylindrical pulse ionization chambers were: diameter, 10 cm; length, 30 cm; wall thickness, 0.5 mm brass. The diameter of the internal electrode consisting of a steel rod placed along the cylinder axis was equal to 3 mm. The chambers were filled with spectrally pure argon at a pressure of 5 atmos. The working voltage was 1000 v.

The ionization pulses were fed to a "four-fold" coincidence circuit through a parallel amplification channel 9 — 22 and a univibrator 23 with a triggering level corresponding to a pulse produced in the ionization chamber by two to three singly-charged particles. The "four-fold" coincidences were analyzed by circuit 21. A marker circuit containing a neon lamp MTKh-90 was connected to the common anode of the tubes of this circuit. Whenever a "four-fold" coincidence occurred, the neon lamp was ignited and a voltage pulse appeared on the switch blade connected to its cathode. The marker circuit was also connected to the output of scaler 20. Pulses from circuit 21 ("four-fold" coincidences) as well as the pulses from circuit 20 (triple coincidences scaled down in the ratio 1:4) were fed to a univibrator 2 generating square pulses of 2×10^{-4} sec duration. The pulses from the gate univibrator were used to trigger the amplifying channel of the chambers and to start a short powerful pulse for triggering the hodoscope, which was produced by a short-duration ($\tau = 5 \times 10^{-6}$ sec) univibrator with consecutive power amplification by means of a cathode follower (block 3). The shaped master pulse from block 3 was fed to the screen grids (connected in parallel) of the tubes of the hodoscope 4. The hodoscope was similar to the one used in the experiments of Vernov and Charakhch'yan.[8] Pulses from the hodoscope were fed to a mechanical rotary switch 5,[8] the blades of which were connected to the cathodes of the neon lamps MTKh-90 placed in the anode circuit of the hodoscope tubes, and which were used as the indicators of discharge of the given hodoscope counters. The central connection of the switch contacted, in turn, all the blades and passed the voltage pulses from the neon lamps to a cut-off tube of the hodoscope 6, which was gated a short time after the passage of the stretched pulses from the two chambers. The resolving time of the hodoscope was 2×10^{-5} sec. To avoid the superposition of hodoscope pulses corresponding to various master pulses, a special circuit 7 blocked the coincidence circuit during the recording of the pulses of the chambers and of the hodoscope.

Electron pulses produced in chambers I and II during the passage of charged particles were fed to low-noise linear amplifiers 9, 10, 13, and 14.* Since we were not interested in the continuous recording of all pulses from the chambers, but only of those pulses produced in the chamber during the passage of a particle through the telescope, it was necessary to trigger the amplification channel of the chamber, i.e., to gate the channel in points 11 and 15 for a passage of a particle through the telescope. The opening of the closed gates 11 and 15 was done by a square pulse produced by the gate univibrator 2. The time during which the amplification channel was open was equal to 2×10^{-4} sec, the width of the transmitted pulse being $\sim 1 \times 10^{-4}$ sec.

For radio transmission of the chamber pulses, the amplitude of the pulse V was, after the amplification of the pulses and their passage through the gating lamps, transformed into the pulse length T by means of stretching circuits 12 and 16. The linearity between V and T was insured in a sufficiently wide range.

In the construction of the instrument, we were faced with the problem of a simultaneous radio transmission of the pulses from the two chambers and the pulses from the hodoscope. For a simultaneous recording of the pulses from the two chambers, a special three-tube multivibrator was designed (block 17). This multivibrator, upon a simultaneous arrival of the stretched pulses from both chambers, produced pulses with a frequency of the order of 300 kcs. After the pulse in one of the chambers had ended, the multivibrator frequency was changed to ~ 1000 kcs. A special marking circuit made it possible to determine whether the larger of the pulses belonged to the upper or to the lower chamber, according to the discharge (or the lack of it) of the neon lamp incorporated in this circuit. The pulses modulated in such a way were fed to modulator 18 of the transmitter and then to the transmitter 19. A short time after the pulses from the chambers were transmitted, the pulses from the hodoscopes also arrived through the tube 6. After the hodoscope pulses had been automatically recorded a few times by means of a relay, the voltage was taken off the neon lamps of the hodoscope and of the neon tube of circuit 7 which blocked the coincidence circuit and, after that, the instrument was ready for recording the next pulse.

The signals received on earth were recorded by photographing, on moving film, the electron beam of an oscillograph connected to the output of the receiver. An example of such a film record of the pulses from the two chambers and from the hodoscope made during the flight is given in Fig. 2.

To convert the length of the stretched pulse into multiplicity of ionization (in terms of the probable ionization due to a single-charged relativistic particle) the instrument was calibrated

*The circuit diagram of the low-noise linear amplifier was taken from reference 9.

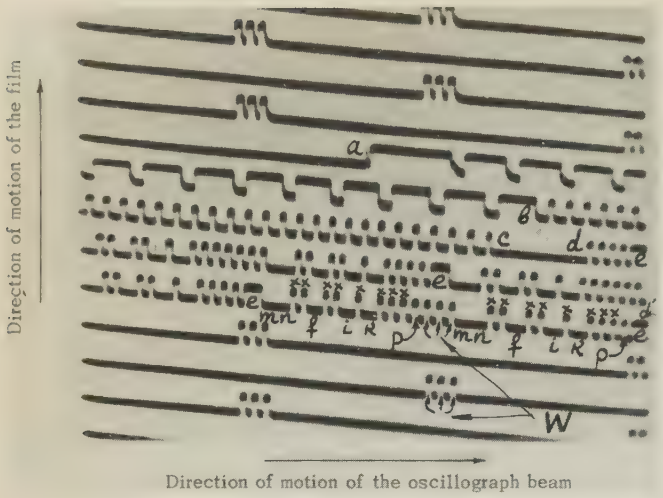

FIG. 2. A picture of the recorded pulses from the chambers and the hodoscope on film during flight: ab – pulse from an α particle in the top chamber; multiplicity of ionization equal to 4.0-4.25; ab + bc – pulse from the same α particle in the lower chamber; multiplicity of ionization equal to 4.75-5.0; dd′ – pulses from the hodoscope; e – marker of the master pulse; f, i, k – discharge counters; pulses on the blades of the switch for nondischarging counters are denoted by x; m – marker of the pulse amplitude from chambers; n – marker of triple coincidences with scaling factor; p – marker of "four-fold" coincidences; w – barograph signals.

by measuring (before the flight) the dependence of the length of the signal at the amplifier output on the amplitude of the signal at the input. For use in the stratosphere, the calibration curves obtained were corrected using the singly-ionizing particles which give a well defined maximum in the particle-ionization spectrum in the atmosphere, and using the fixed calibration signals in the region of 15-fold ionization produced by a special internal generator 8 built for this purpose. Signals from the generator during the time of flight were fed, a few times per minute, to the amplifier input and, correspondingly, to the gating univibrator 2. The range of linearly amplified pulses from the chambers was 10 to ~400 μv at the amplifier input. This permitted a good measurement of the ionization produced by singly-charged relativistic particles (the probable ionization due to a singly-charged relativistic particle produces a pulse equal to 18 μv at the amplifier input) and by multiply-charged particles with $Z = 2$, 3, and 4. Heavy nuclei with $Z \gtrsim 4$, causing saturation of the last tubes of the linear amplifier, could not be distinguished one from another.

As an illustration of the resolving power of the instrument in the ionization range $J/J_0 = 1 - 4$ (J_0 is the probable ionization produced in the chamber by a relativistic singly-charged particle; J is the ionization produced in the chamber by the given particle), the spectrum of ionization pulses from single particles obtained in measurements at the surface of the earth (H = 1 km) is shown in Fig. 3. The half-width of the distribution obtained is determined by: a) fluctuations in the ionization produced by relativistic particles in the gas of the chamber, and b) by the superposition of noise. (The rms value of the noise at the amplifier input was equal to $\sim 10 \times 10^{-6}$ v for the probable pulse from a singly-charged particle equal to 1.8×10^{-5} v.)

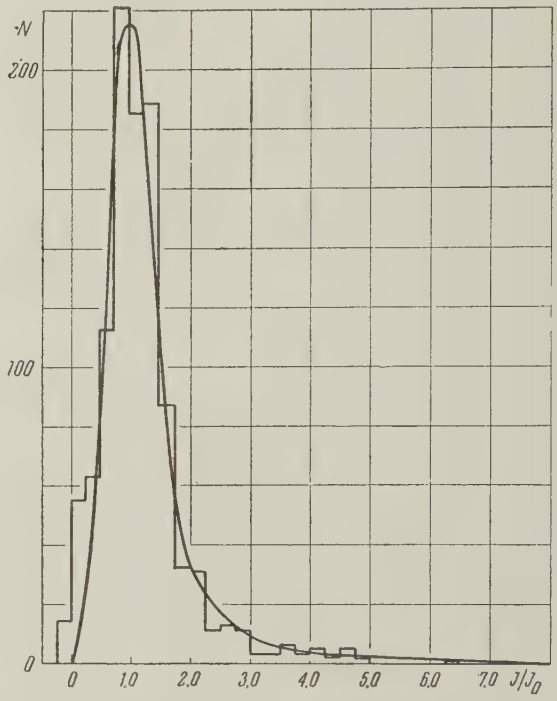

FIG. 3. Spectrum of ionization pulses from single cosmic ray particles at an altitude H = 1 km. N – number of particles; J/J_0 – ionization in relative units.

REDUCTION OF EXPERIMENTAL DATA

In view of the presence of a large background from slow singly-charged particles in the stratosphere in the ionization range $J/J_0 = 1 - 4$, and also because of the presence within that range of a certain number of singly-charged relativistic particles (see Fig. 3), it was not possible to find, for α particles, a sharp maximum at the point $J/J_0 = 4.0$ in the ionization spectrum of particles in the stratosphere. The experimental material obtained was reduced therefore in the following manner:

Distributions were plotted in the (x, y) plane (see, e.g., Fig. 4) of simultaneous pulses produced by single particles in the upper and lower chambers. Each particle had a definite place in such a diagram, depending on the ionization produced in chamber I (x axis) and chamber II (y axis).

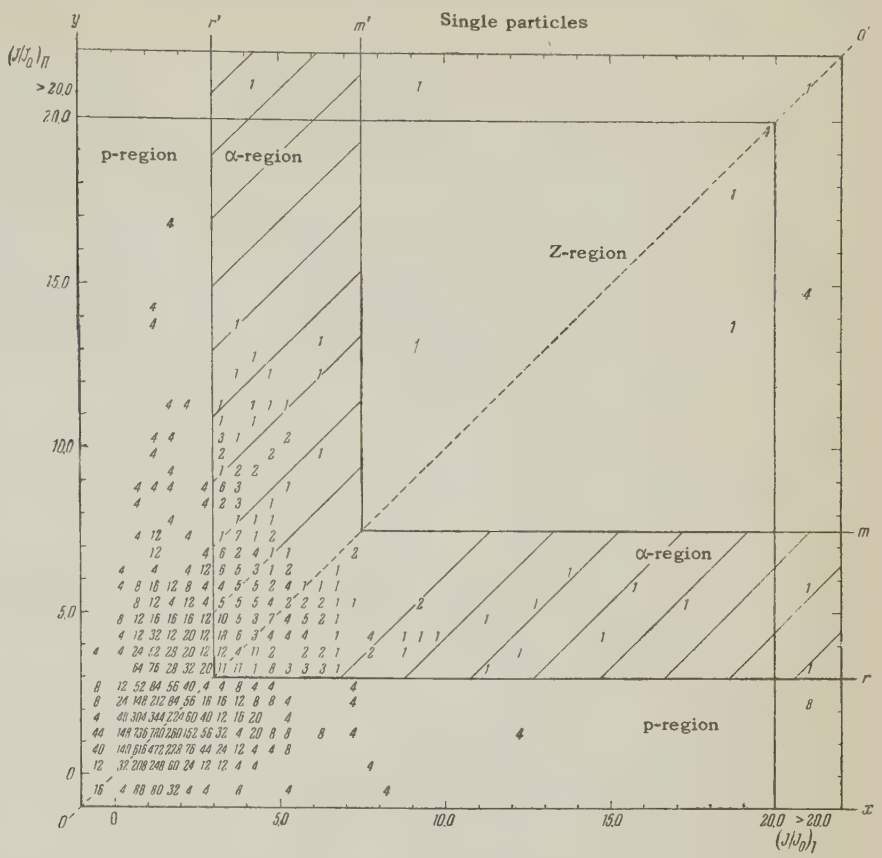

FIG. 4. Distribution of single particles traversing the instrument at an altitude H = 25-27 km with respect to the ionization produced by them in the two chambers. The value of the pulse in the top chamber $(J/J_0)_I$ is given on the x axis, and the value of the simultaneous pulse in the lower chamber $(J/J_0)_{II}$ on the y axis.

(The value of ionization is expressed in units equal to the probable ionization due to a relativistic singly-charged particle.) In the absence of fluctuations in the ionization, the nuclei of H, He, Li, etc., on this plane would be grouped along the straight line OO′ running from the origin of coordinates O at an angle of 45°, around points with coordinates 1:1, 4:4, 9:9, etc. In the presence of fluctuations, the particles with a given value of Z will fall into a certain ionization range, with the most probable value at the above points. For the determination of the flux of α particles, it was necessary to determine the actual limits of the ionization range of α particles and the value of the background from singly-charged particles in that range. In practice, we followed the following procedure: Ionization diagrams of single particles were constructed for three altitudes, H = 1 — 11 km, H = 11 — 15 km, and H = 25 — 27 (plateau of the flight, Fig. 4). It could be assumed with certainty that, at altitudes below 15 km, there was no considerable amount of primary α particles in the composition of cosmic rays. This means that all particles detected in the range of ionization due to α particles at altitudes below 15 km are background pulses of singly-charged particles. The upper limit of the α particle region accepted by us which roughly coincided with the lower limit of the region of particles with $Z > 2$ (Z region), is denoted in the diagram by two perpendicular lines m and m′ (see Fig. 4) parallel to the coordinate axes x and y, with the point of intersection on the straight line OO′ going through the origin of coordinates at an angle of 45° with the coordinate axes. The lower limit of the α region is denoted on the diagram by the lines r and r′. This limit, and also the background of singly-charged particles in the α region (in the region between the lines r — r′, and m — m′, dashed on the drawing) were determined by us experimentally.

To evaluate the background magnitude in the α region, we moved the point of intersection of the lines r and r′ in the ionization diagrams along the straight line OO′, giving it a sequence of values $(J/J_0)_I = (J/J_0)_{II} = 4.0$, 3.5, 3.0, 2.5, and 2.0. For all these positions of the limit, we counted the number of pulses in the α-particle region and in the p region (the region of singly-charged particles) for altitudes H = 1 — 11 km and H = 11 — 15 km, using the total geometrical factor of the apparatus. The ratio of the number of particles in the α region to the number of particles in the p region gives the background due to singly-charged particles in the α region. The value of the background in the α region, ex-

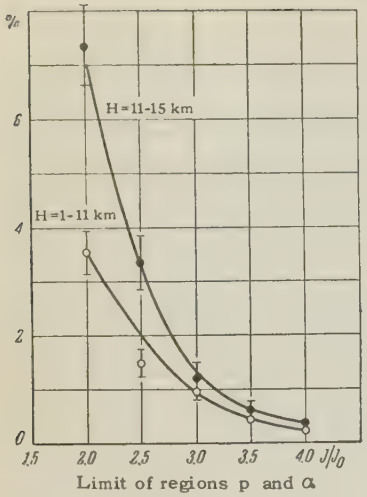

FIG. 5. Value of the background from singly-charged particles in the α region at the altitudes H = 1-11 km, and H = 11-15 km as a function of the choice of the lower limit of this region (top limit of α region $J/J_0 = 7.5$). Value of the background is given in percent of the number of singly-charged particles in the p region.

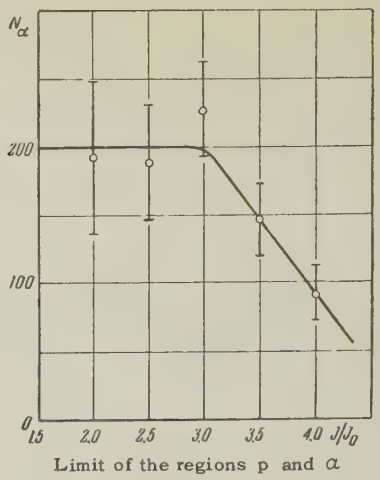

FIG. 6. Number of single α particles N_α recorded on the plateau (H = 25-27 km, t = 78 min) as a function of the choice of the lower limit of the α particle region. Correction for the background of singly-charged particles has been introduced.

pressed as a fraction (in %) of the number of singly-charged particles in the p region, as a function of the chosen limits of the regions p and α for altitudes H = 1 — 11 km and H = 11 — 15 km, is given in Fig. 5.

The number of α particles recorded at the plateau (H = 25 — 27 km, t = 78 min) is given in Fig. 6 as a function of the position of the limit r — r′ between the proton and the α-particle region obtained from the data of Fig. 4.* The background due to singly-charged particles, according to the data of Fig. 5, for the altitude H = 11 — 15 km has been subtracted from each point of the curve in Fig. 6. The curve in Fig. 6 shows that when the point of intersection of the straight lines r and r′ moves from the value $(J/J_0)_I = (J/J_0)_{II} = 4.0$ towards smaller values, the number of α particles first increases and then, beginning with the value $(J/J_0)_I = (J/J_0)_{II} = 3.0$, remains constant. Thus, by passing the lower limit of the α region through the point $(J/J_0)_I = (J/J_0)_{II} = 3.0$, as shown in Fig. 4, we practically take all α particles into account.

EXPERIMENTAL RESULTS

The results of the measurement of the flux of primary α particles and heavy primary nuclei with Z > 2 in the stratosphere at 31° N geomagnetic latitude are given in the table. The first row of the table lists the number of single particles in the α region (Z = 2) and in the Z region (Z > 2) which did not produce nuclear interactions recorded at the depth of 24 g/cm². To the recorded number of particles in the region Z = 2, we applied a correction for the background from single-charged particles and for α particles producing δ stars in the matter of the telescope, and which, therefore, were excluded from the category of singly-charged particles.* After introducing the corrections, we obtained the number of primary α particles at the depth of 24 g/cm² which did not produce nuclear interactions in the matter of the telescope (4th and 5th rows of the table). Also presented here is the number of primary heavy nuclei with Z > 2, in the calculation of which we introduced no correction for δ showers, in view of the arbitrariness of its introduction, and no correction for the background, in view of the small statistical accuracy of its determination at low altitudes.

For the determination of the flux of α particles and heavy nuclei with Z > 2 at the top of the atmosphere, it is necessary to take into account the absorption of the flux due to nuclear in-

*The numbers in Fig. 4 denote the number of particles in the given ionization range recorded during the stay of the instrument at the altitude of 25-27 km. In the proton region these numbers were obtained as a result of multiplication by four of the recorded number of triple coincidences with a scaling factor 1:4, accompanied or not accompanied by a "four-fold" coincidence. In the α-particle region and in the region of particles with Z > 2 these numbers were obtained as the result of adding the scaled-down number of triple coincidences multiplied by four, not accompanied by "four-fold" coincidences to the total number of "four-fold" coincidences (accompanied and not accompanied by a scaled-down triple coincidence).

*The correction for δ showers was introduced on the basis of measurements carried out in the laboratory with other instruments without absorbers consisting of a small-sized telescope surrounded by hodoscoped counters. These instruments, in view of their small dimensions, practically did not record nonlocal showers. Therefore, all showers recorded by these instruments at sea level could have been regarded as δ showers. From data obtained by means of this instrument, δ showers are produced by singly-charged particles which amount to ~5% of the number of single particles traversing the instrument. Since the ionization is proportional to the square of the charge of the ionizing particle, we assumed the percentage of δ showers produced by α particles to be equal to 20% of the number of single α particles.

Results of the measurement* of the flux of heavy primary particles in the stratosphere at 31° N geomagnetic latitude

Charge of the heavy primary nucleus	$Z = 2$	$Z > 2$
Number of single particles recorded at the depth of 24 g/cm² in the ionization regions	317±18	10±3.2
Correction for the background due to singly charged particles	−90±22	not introduced
Correction for the number of nuclei producing δ showers	+45±6	not introduced
Number of primary heavy nuclei at the depth of 24 g/cm² not producing nuclear interactions	272±29	10±3.2
The same in $cm^{-2}min^{-1}sterad^{-1}$	0.154±0.016	0.0056±0.0018
Absorption coefficient of heavy nuclei due to nuclear interactions in the matter of the apparatus, exp (−x/L)	0.815	0.740
The same in the layer of air above the instrument	0.565	0.400
The flux of heavy nuclei I^0_Z at the limit of the atmosphere at 31° N geomagnetic latitude in $cm^{-2}min^{-1}sterad^{-1}$	0.335±0.035	0.019 ±0.006
I^0_Z/I_0, %	16±2	~1

*Duration of measurements t = 78.0 min; geometrical factor of the instrument $S_\Omega = 22.7$; the number of single particles in the $Z = 1$ ionization range recorded at the depth of 24 g/cm² equals 7512 ± 87; amount of matter in the telescope of the setup − 8.1 g/cm²Al + 1.7 g/cm²Cu + 2.0 g/cm²glass.

teractions in the matter of the instrument and in the layer above it. The values of the absorption coefficient exp (−x/L) in the matter of the absorber and in the layer of air above it are given in the table for α particles and heavy nuclei with $Z > 2$ (x denotes the thickness of the absorber, and L the mean free path for inelastic interactions). In the calculation of these coefficients, we used the geometrical cross section of the inelastic interaction of α particles and nuclei* with $Z = 7$ with Al, Cu, and N nuclei of the medium. After taking the nuclear interactions into account, the flux of α particles at the limit of the atmosphere at 31° N geomagnetic latitude was found to be equal to 0.335 ± 0.035 particles $cm^{-2}min^{-1}sterad^{-1}$, which amounts to (16 ± 2)% of the total flux I_0 of primary particles.[10,11] For the flux of heavy nuclei with $Z > 2$, the value obtained was 0.019 ± 0.006 particle $cm^{-2}min^{-1}sterad^{-1}$, i.e., ~6% of the number of primary α particles and ~1% of the total particle flux..

V. F. Grushin took part in the experiment.

*The average value of the atomic number for the flux of heavy nuclei with $Z > 2$ was assumed to be equal to 7.

[1] M. A. Pomerantz and F. L. Hereford, Phys. Rev. **76**, 997 (1949).

[2] S. F. Singer, Phys. Rev. **76**, 701 (1949); **80**, 47 (1950).

[3] H. L. Bradt and B. Peters, Phys. Rev. **77**, 54 (1950); **80**, 943 (1950).

[4] Freier, Anderson, Naugle, and Ney, Phys. Rev. **84**, 322 (1951).

[5] Dainton, Fowler, and Kent, Phil. Mag. **43**, 729 (1952).

[6] Perlow, Davies, Kissinger, and Shipman, Phys. Rev. **88**, 321 (1952).

[7] E. P. Ney and D. M. Thon, Phys. Rev. **81**, 1068 (1951).

[8] S. N. Vernov and A. N. Charakhch'yan, Dokl. Akad. Nauk SSSR **62**, 319 (1948).

[9] I. D. Rapoport, Izv. Akad. Nauk SSSR, Ser. Fiz. **19**, 519 (1955), Columbia Tech. Transl. p. 466.

[10] Alekseeva, Brikker, Grigorov, Savin, and Shcherbakov, Dokl. Akad. Nauk SSSR **115**, 71 (1957), Soviet Phys.–Doklady **2**, 303 (1958).

[11] K. I. Alekseeva and N. L. Grigorov, J. Exptl. Theoret. Phys. (U.S.S.R.) **35**, 599 (1958), Soviet Phys. JETP **8**, 416 (1959).

Translated by H. Kasha
72

EFFECT OF UNIAXIAL COMPRESSION ON THE QUANTUM OSCILLATIONS OF THE MAGNETIC SUSCEPTIBILITY OF BISMUTH

N. B. BRANDT and G. A. RYABENKO

Moscow State University

Submitted to JETP editor March 13, 1959

J. Exptl. Theoret. Phys. (U.S.S.R.) **37**, 389-391 (August, 1959)

The effect of uniaxial compression along the trigonal axis, using pressures up to 340 kg/cm^2, on the frequency and amplitude of the quantum oscillations of the magnetic susceptibility of bismuth was investigated for temperatures between 1.6 and 4.2° K. The results obtained are discussed on the basis of the semi-phenomenological theory of Kosevich.

DURING a study of the effect of hydraulic pressure on the magnetic susceptibility oscillations in bismuth, it was found that the deformation of the Fermi surface due to pressure was strongly anisotropic;[1,2] such an anisotropy was not found in zinc.[3,4*] From the standpoint of Kosevich's theory[5] a deformation of this type, associated with a change in the dispersion relationship, shows that the basic cause of the deformation is not a change in the Fermi energy E_0 (without a significant change in the dispersion law, as occurs in zinc), but is a change in the crystal lattice angles and an associated change in the dispersion law. In this connection one can expect the effect of uniaxial compression on the oscillation frequency, E_0/β, of the magnetic susceptibility of bismuth to be anomalously large compared with that to be expected if only E_0 changed; here β is the effective Bohr magneton — see the Landau formulae quoted by Shoenberg.

The apparatus for producing the uniaxial compression is shown in Fig. 1. The housing 1, the piston 2, which transmits pressure to the specimen 3, the threaded bushing 4 and the specimen enclosure 6 were made from very pure aluminum bronze; the spring 5 was made from 4% beryllium bronze. The calibration of the spring was performed in a special apparatus and the result was recalculated in terms of the pitch of the compression bushing thread 4. The elastic constant of the spring was 15 kg/mm. The whole apparatus, with the help of the adjusting device 9, was fixed on the glass rod of a torsion balance suspension system.

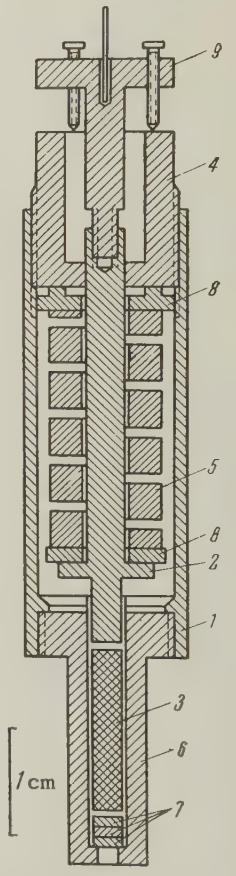

FIG. 1. Apparatus for studying the magnetic anisotropy of single crystals under uniaxial compression. 1 – housing, 2 – piston transmitting pressure to the specimen, 3 – specimen, 4 – threaded bushing, 5 – spring, 6 – specimen enclosure, 7, 8 – washers, 9 – adjusting device.

The measurements were performed on three single-crystal specimens made from "Hilger" bismuth after it had been recrystallized 30 times; the specimens were strictly cylindrical, 3 mm in diameter and 10 mm long. The trigonal axis of the specimens coincided with the longitudinal axis to within 0.5°. To avoid possible bending of the specimen during compression a sliding support was used; this consisted of a layer of graphitic lubricant 50 μ thick completely filling the space between the specimen 3 and the enclosure 6.[7] The small error in the orientation of the trigonal axis of the specimen relative to the axis of the suspen-

*The effect of uniaxial deformation on the magnetic susceptibility oscillations in zinc has also been studied.[4]

sion was corrected by means of the adjusting apparatus 9. When the orientation is correct there is no couple for any direction in a magnetic field of 12,000 oersteds at room temperature. The complicated variation of the couple[2,8] observed in the basal plane at helium temperatures is, apparently, a consequence of the phase shifts and different amplitudes of the oscillations associated with each of the three ellipsoids of the Fermi surface; this destroys the mutual compensation of the magnetic moments which takes place at high temperatures.

The magnetic susceptibility anisotropy was measured on specimens at zero stress, at stresses of 35, 70, 200, and 340 kg/cm^2, and after removing the stress, for temperatures between 1.6 and 4.2° K. If the load did not exceed 250 kg/cm^2 the amplitude of the oscillations was almost completely restored on removing the stress. For large loads there was noticeable hysteresis. For every value of the load the values of E_0/β (proportional to the area S_m of the extremal section of the Fermi surface by a plane perpendicular to the magnetic field[9]) were determined for angles Ψ between the vector **H** and the twofold axis of the specimen of 0, +2, −2 (or +3, −3), +28, +30, +32, +15, +45°. The dependence of $E_0/\beta \sim S_m$ on Ψ which was obtained is shown in Fig. 2. As is seen from the

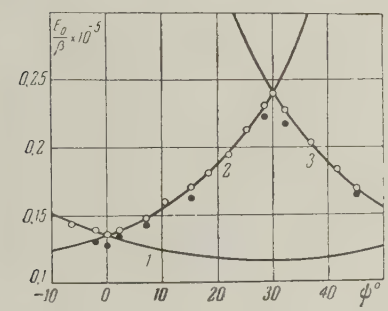

FIG. 2. Variation of oscillation frequency with the angle Ψ between the magnetic field direction and the diad axis. 1, 2, 3 – theoretical curves derived from Landau's formulae. Experimental data: o – unstressed, • – with a stress of 340 kg/cm^2.

figure, the values E_0/β for uncompressed specimens agree very well with the theoretical curves (continuous lines) derived from Landau's formulae using the tensor-effective masses determined by Shoenberg.[6] On applying uniaxial compression the frequency of oscillation falls. Since the relative frequency change should be the same for all values of Ψ, the changes of E_0/β obtained for the same stress but for different angles Ψ were averaged; this was done to decrease the effect of errors in the relative determination of the twofold axis orientation in experiments with different loads. The variation of $\Delta(E_0/\beta)/(E_0/\beta)$ with stress is shown in Fig. 3.

The change of E_0/β on compressing bismuth along the trigonal axis is anomalously large. For a stress of 350 kg/cm^2 the reduction of E_0/β cor-

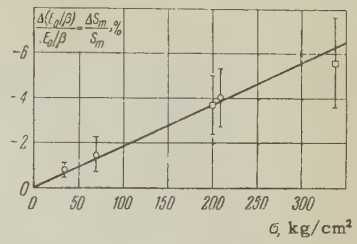

FIG. 3. Variation of relative oscillation frequency change with applied stress: o – specimen Bi-1, □ – specimen Bi-2.

responds to that which occurs for the same orientation at a hydrostatic pressure of about 1000 atmos.[2]

Thus, for bismuth, which has no groups of electrons with greatly differing concentrations and in which the Fermi surface deformation corresponding to a change in the bounding energy E_0 cannot, therefore, be a determining effect, the main cause of the Fermi surface deformation is the change of the crystal lattice angles. It is very possible that a similar deformation mechanism will be observed also in metals similar to bismuth.

We express gratitude to Prof. A. I. Shal'nikov for his interest in the work.

[1] Verkin, Dmitrienko, and Lazarev, J. Exptl. Theoret. Phys. (U.S.S.R.) **31**, 538 (1956), Soviet Phys. JETP **4**, 432 (1957).

[2] N. B. Brandt and V. A. Venttsel', J. Exptl. Theoret. Phys. (U.S.S.R.) **35**, 1083 (1958), Soviet Phys. JETP **8**, 757 (1959).

[3] Dmitrienko, Verkin, and Lazarev, J. Exptl. Theoret. Phys. (U.S.S.R.) **35**, 328 (1958), Soviet Phys. JETP **8**, 229 (1959).

[4] B. I. Verkin and I. M. Dmitrienko, J. Exptl. Theoret. Phys. (U.S.S.R.) **35**, 291 (1958), Soviet Phys. JETP **8**, 200 (1959).

[5] A. M. Kosevich, J. Exptl. Theoret. Phys. (U.S.S.R.) **35**, 249 (1958), Soviet Phys. JETP **8**, 171 (1959).

[6] D. Shoenberg, Phil. Trans. Roy. Soc. **245**, 1 (1952).

[7] N. B. Brandt, Приборы и техника эксперимента (Instrum. and Meas. Engg.), in press.

[8] Verkin, Lazarev, and Rudenko, Сб. Памяти Вавилова (Vavilov Memorial Coll.), Acad. Sci. U.S.S.R., 1952, p. 344.

[9] I. M. Lifshitz and A. M. Kosevich, Dokl. Akad. Nauk SSSR **96**, 963 (1954). J. Exptl. Theoret. Phys. (U.S.S.R.) **29**, 730 (1955), Soviet Phys. JETP **2**, 636 (1956).

Translated by K. F. Hulme
73

RESULTS OF A STUDY OF THE DISINTEGRATION OF CARBON NUCLEI BY 660-Mev PROTONS

A. P. ZHDANOV and P. I. FEDOTOV

Radium Institute, Academy of Sciences, U.S.S.R.

Submitted to JETP editor March 21, 1959

J. Exptl. Theoret. Phys. (U.S.S.R.) **37**, 392-398 (August, 1959)

The disintegration of the carbon nuclei in a suspension of diamond particles introduced into nuclear emulsion was investigated. The cross sections for the various reactions have been obtained. An analysis of the angular and energy distributions of the disintegration has been carried out under the assumption of a two-stage interaction between high-energy particles and light nuclei.

INTRODUCTION

THE last five years have brought a marked increase in the number of experiments devoted to the study of the interaction of high-energy particles with light nuclei, especially the nuclei of C, N, and O which are contained in nuclear photoemulsions. These investigations are of interest, on one hand, as an attempt at a better understanding of the mechanism of nuclear interactions and, on the other, because of the possibility of obtaining data valuable for the study of the influence of high-energy ionizing radiation on the cells of living tissues.

One of the main difficulties in the interpretation of the physical processes that occur in the emulsion is that it contains several elements. The interactions of different particles with the complex nuclei of the emulsion are divided into two main groups: interactions with the light nuclei (C, N, O) and interactions with the heavy ones (Ag, Br). The separation of these interactions is based on a potential-barrier criterion. By this criterion the stars containing a track with length smaller than 50μ (this range corresponds to an α particle with energy of 9 Mev and to a proton of 2.3 Mev) are classified as disintegrations involving light nuclei. The emission of particles with such a range from heavy nuclei is considered as very improbable, because of a much higher Coulomb barrier than in light nuclei.

This selection criterion, correct for low excitation energies of the nucleus,[1,2] is under serious doubt for high excitation energies which arise in the interaction between a nucleus and an incident particle having an energy of several hundred Mev and more. When a heavy nucleus is strongly excited, the deformation of the nuclear surface can lead to a lowering of the potential barrier. On the other hand, an emission of unstable fragments, which disintegrate in a way similar to the disintegration of light nuclei, i.e., with the emission of low-energy α particles, is possible. Even if we assume that the potential-barrier criterion is correct, the correctness of experimental results obtained for light nuclei is in doubt. In fact, as was shown by McKeague[3] and by the authors, about half of the light nuclei disintegrate without emitting particles with ranges smaller than 50μ, and such disintegrations will evidently be more probable the larger the energy of the incident particle.

In view of the considerable difficulties in separating the interactions involving heavy and light nuclei of the emulsion in many experiments devoted to the study of interactions involving light nuclei, the methods of diluted emulsions[2] and "emulsion sandwiches"[4] were used.

The method of diluted emulsions is based on a comparison of the experimental data obtained on emulsions with various concentrations of gelatine. The drawback of this method is that it enables us to obtain only a limited amount of data with respect to the class of interactions studied. In addition, the lowering of the content of silver halides in diluted emulsions markedly increases the difficulty of finding and measuring the investigated stars.

In the emulsion-sandwich method, disintegrations of the light elements C, N, O, produced in a gelatine layer placed between two emulsion layers, are studied. This method makes it possible to pick out disintegrations of light elements with greater accuracy. However, admixtures from disintegrations of Ag and Br nuclei are present

here, too, because of the diffusion of these nuclei into the gelatine layer during the production of the emulsion sandwiches, especially when thin gelatine layers are used. Increasing the thickness of the gelatine layer leads to considerable losses of tracks in the gelatine and makes it much more difficult to find the disintegration.

Apart from these drawbacks, there is an additional one, common to both types of experiments. Both methods provide only data averaged over several elements. For the study of light nuclei, this is clearly insufficient, since it is possible that each nucleus has its own individual features.

To study disintegrations involving the nuclei of a specific element, it has been proposed[5] to introduce this element into the emulsion in the form of a suspension. However, this method also is not free from drawbacks, the most important of which is the presence of "indeterminacy zones." These zones are due to the opacity of the introduced particles so that some of the disintegrations involving the emulsion nuclei near the particles can be regarded as disintegrations involving the investigated element itself. The admixture of such events, due to the "indeterminacy zones," in the case when light-element suspensions are used, is considerable and can completely distort the experimental results.

In the study of the interaction between protons and carbon nuclei, we used a suspension of diamond powder.[6] The diamond particles, $5-7\mu$ in diameter, are well transparent, which makes it possible to eliminate the "indeterminacy zones." Doubts that may be raised as to the nature of certain disintegrations in the lower parts of the introduced suspension particles are dispelled by scanning the disintegrations from the side of the glass of the plate, using a long-focus immersion objective 31×0.6.

EXPERIMENTAL METHOD

Sandwich emulsions were used in the experiment. The middle layer, $15-20\mu$ thick, contained the diamond particles. Two types of emulsions were used: emulsions recording protons with energies up to 16 — 20 Mev (type D), and relativistic emulsions (type S). Emulsions of the D type permit a good identification of α particles and protons in the study of the low-energy fraction of secondary particles for ranges up to 30μ, and also make it possible to increase considerably the yield of the studied reactions, owing to the increased time of emulsion irradiation. Emulsions of the S type contain a considerably smaller number of stars, but make it possible to observe the total picture of the investigated disintegrations on carbon.

The plates were irradiated by a 660-Mev proton beam of the proton synchrotron of the Joint Institute for Nuclear Research parallel to the emulsion plane. Tracks of α particles and protons in the D emulsion were identified independently by two persons, both visually and by grain counting. Practically identical results were obtained. The tracks in the S emulsion were identified by measuring the gaps in the particle tracks with a range greater than 50μ, using a special eyepiece for gap measurement.[7]

The nature of particles with a range insufficient for a good identification by the grain-counting method or by the measurement of the gaps, could, in the majority of cases, be established from the charge conservation in the disintegration. This condition, in any case, is the main criterion of checking the obtained nuclear decay scheme.

EXPERIMENTAL RESULTS

In scanning the plates, 540 disintegrations on carbon were found and measured, 190 of which were in the S emulsion and 350 in the D emulsion. The average number of secondary tracks per star in the disintegration of the C^{12} nucleus, found from the analysis of stars in the S emulsion, was found to be equal to three. This value was found taking into account the correction for the absorption of short tracks, mainly α particles, by the diamond particles with average radius 3μ. This correction was calculated according to the formula

$$N / N_t = (3l / 4\bar{R}^3)(\bar{R}^2 - \tfrac{1}{12} l^2), \qquad (1)$$

where N is the observed number of tracks with range l, N_t is the true number of tracks with range l $(0 \leq l \leq 2\bar{R})$, and $\bar{R}$ is the average radius of diamond particle. Taking the difference in the stopping powers of the diamond and the emulsion into account, the correction for the absorption of α particles amounted to 2% of the total number of α particles.

For disintegrations of carbon in the S emulsion the ratio of the number of α particles to the number of protons, n_α / n_p, equals 0.76. From a comparison of the mean number of tracks per disintegration of C_6^{12} in the S and D emulsions, it is found that, on the average, 0.84 protons per star were lost in the emulsion. A ratio $n_\alpha / n_p = 0.77$ was obtained by taking the proton losses for stars in the D emulsions into account. This value was obtained taking the admixture of Li among the α particles in the D emulsion into

account. The number of Li tracks and their range distribution was obtained from the study of disintegrations of carbon in the S emulsion. The good agreement between the ratio n_α/n_p for two emulsions with different sensitivities served as a confirmation of the good identification of tracks.

1. Distribution of the disintegrations with respect to the number of prongs and the reaction type. The distributions were obtained from the results of the analysis of disintegrations in the S emulsion. The distribution of disintegrations of carbon with respect to the number of tracks is given in Table I. The track of the incident proton is included in the number of tracks given in the table.

TABLE I

Number of tracks	Percent of the total number of decays	Cross section, mb
1	13.0	31±2*
2	12.0	28±2
3	9.2	17±4
4	15.0	34±5.5
5	34.0	78±8
6	14.0	32±5.5
7	2.2	5.5±2.2
8	0.6	1.5±1

*The cross section is taken from reference 8.

In view of the fact that only stars with $n \geq 2$ prongs were recorded, the cross section for the production of single-prong stars in the reactions $C_6^{12}(p, pn)C_6^{11}$ and $C_6^{12}(p, p2n)C_6^{10}$ for 648-Mev incident protons was taken from the work of Symonds, Warren, and Young.[8] The cross section for the production of two-prong stars in the reactions $C_6^{12}(p, 2pn)B_5^{10}$ and $C_6^{12}(p, 2p)B_5^{11}$ was also obtained in an indirect way, since omissions of stars with too fast protons were possible. Taking into account the fact that nuclei C_6^{11} and B_5^{11}, C_6^{10} and B_5^{10} are mirror nuclei, and also knowing the cross sections for p-p and p-n collisions, we obtained the cross section for the production of two-prong stars equal to 28 mb.

The distribution of stars according to the type of reaction and the cross sections for these reactions are given in Table II. The absorption cross section $\sigma_a = 227 \pm 12$ mb for carbon, for 650 Mev protons, was taken from the work of Moskalev and Gavrilovskiĭ.[9]

As can be seen from Table II, the most probable type of disintegration is the disintegration of C_6^{12} into two protons and two α particles. The explanation of this fact and a detailed discussion of the results of Table II will be given separately.

2. Particles with $Z \geq 3$. In addition to α particles and protons, we observed, in a number of cases, the emission of a particle with charge 3 or 4. The estimated cross sections of the fragmentation of Li and Be with ranges greater than 20 μ amounts to 6.5 ± 2.5 mb and 3 ± 1.5 mb respectively. These cross sections are in agreement, within the limits of errors, with the data of Ostroumov and Yakovlev,[10] obtained for the same proton energy.

The cross section for the production of Be given in Table II equals 15 ± 4 mb. The cross section for the production of Be_4^7 from carbon, obtained by Rowland and Wolfgang[11] for protons in the range 0.34 — 3 Bev, amounts to about 11 mb. Thus, the reaction $C_6^{12}(p, 3pxn)$ Be produces mainly the isotope Be_4^7. This result, strange at first glance, is clearly due to the strong dependence of the cross section on the energy of the first excited state of the decaying residual nucleus. For Be_4^9, this level is sufficiently low (2.43 Mev) so that, even for a small excitation energy, it decays into α particles and a neutron. The transition probability between this level and the ground state through an emission of a γ quantum is not greater than 0.01.[12] For Be_4^7, the level leading to the decay of the nucleus lies considerably higher (7.1 Mev),[13] which leads to a more pronounced yield of Be_4^7 as compared with Be_4^9.

It is interesting to calculate the fraction of decays in which the interaction of a 660-Mev proton with C^{12} leads to a total disintegration of the

TABLE II

Type of decay	Percent of the total number of decays	Cross section, mb	Type of decay	Percent of the total number of decays	Cross section, mb
$C_6^{12}\left(p, \begin{matrix} pn \\ p2n \end{matrix}\right)C_6^{11, 10}$	13.4	31±2	$p\alpha$Li	7.0	16±4
$C_6^{12}\left(p, \begin{matrix} 2p \\ 2pn \end{matrix}\right)B_5^{11, 10}$	12.2	28±2	$2p$Be	6.5	15±4
			$6p$	2.35	6±2.5
$2p2\alpha$	32.6	74±8	$2p2\alpha\pi^+$	1.75	4±1.5
$4p\alpha$	12.2	28±5	$3p$Li	1.75	4±1.5
3α	7.0	16±4	$5p\alpha\pi^-$	0.56	1.3±0.8

nucleus into p, d, t, and α. From Table II, we find that this fraction amounts to 0.59 of the total number of disintegrations of light nuclei of the emulsion produced by 660-Mev and 1000-Mev protons. Serebrennikov[14] and Philbert[15] found the probability of a total disintegration of the nuclei into particles with $Z < 3$ to be 0.67 for $E_p = 660$ Mev and to 0.7 for $E_p = 1000$ Mev. The small discrepancy between the data of our experiments and those of references 14 and 15 is due partly to the unique features of the decay of C^{12}, and partly to the approximate character of the estimate of this probability in references 14 and 15.

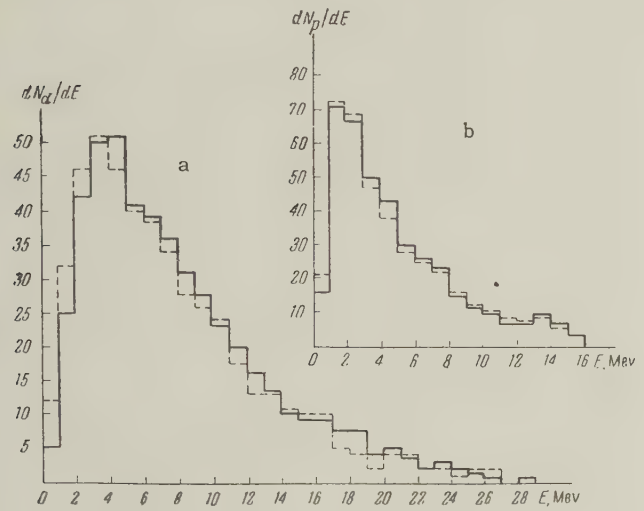

FIG. 1. Energy distribution; a – α particles; b – protons. Solid curve – in the laboratory system of coordinates; dashed – in the coordinate system affixed to the nucleus.

3. Energy and angular distribution of secondary particles. The energy distribution of α particles and protons in disintegrations recorded in the D emulsion is shown in Figs. 1a and b. The energy distribution of the protons is, at the high-energy end, limited by the sensitivity of the D emulsion. Such a limitation is absent for the energy distribution of α particles, and we can observe α particles from the decays of C^{12} up to 72 Mev. The energy distributions are corrected for the particles which escape into the air and into the glass of the plate, and the energy distribution for α particles is corrected for an admixture of tracks of Li, which has already been mentioned above.

Angular distributions of α particles and protons are given in Figs. 2a and b. The forward-backward ratios are 1.77 ± 0.2 and 1.55 ± 0.2 for α particles and protons respectively. The anisotropy in the angular distributions is due to two causes, if we assume a two-stage reaction mechanism: a) The particles knocked out of the nucleus in the first stage of the reaction in n-n collisions and in collisions between a nucleon and a group of nucleons of the nucleus (the knocked-out particles in light nuclei are, by an absolute majority, emitted into the forward hemisphere), and b) the excess of particles in the forward hemisphere due to the fact that the residual nucleus decaying in the second stage of the reaction is not at rest but moves with a certain average velocity v in the direction of the primary proton beam.

These two effects can be separated if the velocity v of the residual nucleus is known. We shall assume that, for any energy range of secondary particles, the anisotropy is due only to the motion of the nucleus. Then, knowing the velocity distribution of particles in the coordinate system affixed to the residual nucleus, which can easily be obtained from the velocity distribution in the laboratory system, one can calculate v from the expression that connects v with the fraction of particles emitted into the forward hemisphere.

In the calculation of v, we used the energy spectrum of the α particles. For α particle energies from 0 to 4 Mev in the system of coordinates of the moving nucleus, one can neglect the admixture of α particles knocked out of the

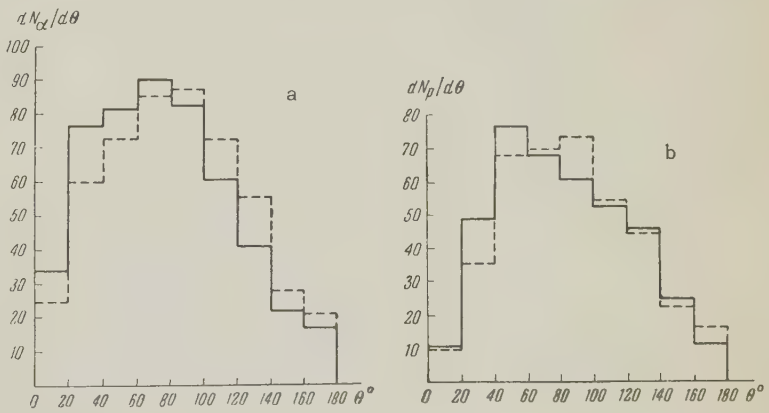

FIG. 2. Angular distribution: a – α particles; b – protons. Solid line – in the laboratory system of coordinates; dashed – in the system affixed to the moving nucleus. θ – space angle between the decay track and the proton beam from the accelerator.

nucleus, in view of the presence of a Coulomb barrier in the C^{12} nucleus. The value obtained is $v = (2.7 \pm 0.6) \times 10^8$ cm/sec.

Using the calculated value of v, we plotted the energy and angular distributions in the coordinate system affixed to the moving nucleus. These distributions are shown dotted in Figs. 1 and 2.

Assuming that all knocked-out particles are emitted into the forward hemisphere, one can determine, from the angular distributions, the number of α particles and protons knocked out from the nucleus. Calculation carried out by the Monte Carlo method confirms the correctness of the assumption with respect to the angles of emission of the knocked-out particles. According to the calculations, 94% of the protons knocked out of the nucleus move into the forward hemisphere. If we assume that all protons not recorded in the D emulsion, i.e., having an energy larger than 16 Mev, are also knocked-out protons, we obtain the result that 46% of the protons and 11% of the α particles are knocked out. This amounts to 0.97 protons and 0.18 α particles knocked out per star.

A calculation by the Monte Carlo method yields 0.75 knocked-out protons per star. The discrepancy between the experimental and calculated values is due, on one hand, to the fact that inelastic p-p, n-p, and nucleon-nucleon group collisions were neglected in the calculations, which leads to a decrease of the number of knocked-out protons. On the other hand, a small part of the protons with energies above 16 Mev are protons due to the decay of the residual nucleus, so that the obtained experimental value of the number of knocked-out protons is somewhat overestimated.

Results of the studies of the high-energy part of the decay products of carbon will be discussed elsewhere.

In conclusion, the authors would like to express their gratitude to M. G. Meshcheryakov and V. P. Dzhelepov for providing the facilities to carry out the experiment, to G. M. Subbotina for help in the reduction of the experimental data, and to I. M. Kuks for taking part in the discussion of the results.

[1] Menon, Muirhead, and Rochat, Phil. Mag. **41**, 583 (1950).

[2] Lees, Morrison, Muirhead, and Rosser, Phil. Mag. **44**, 304 (1953).

[3] R. McKeague, Proc. Roy. Soc. **236**, 104 (1956).

[4] Blau, Oliver, and Smith, Phys. Rev. **91**, 949 (1953).

[5] A. P. Zhdanov and K. I. Ermakova, Dokl. Akad. Nauk SSSR **70**, 211 (1950).

[6] A. P. Zhdanov and P. I. Fedotov, Приборы и техника эксперимента (Instruments and Measurement Engg.), in press.

[7] Zhdanov, Kolpakov, Kuz'min, Raguzin, and Fedotov, Приборы и техника эксперимента (Instruments and Measurement Engg.) **1**, 46 (1958).

[8] Symonds, Warren, and Young, Proc. Phys. Soc. **A70**, 824 (1957).

[9] V. I. Moskalev and B. V. Gavrilovskiĭ, Dokl. Akad. Nauk SSSR **110**, 972 (1956), Soviet Phys.–Doklady **1**, 607 (1956).

[10] V. I. Ostroumov and Yu. P. Yakovlev, J. Exptl. Theoret. Phys. (U.S.S.R.) **35**, 1358 (1958), Soviet Phys. JETP **8**, 949 (1959).

[11] F. S. Rowland and S. F. Wolfgang, Phys. Rev. **110**, 175 (1958).

[12] Bodansky, Eccles, and Halpern, Phys. Rev. **108**, 1019 (1957).

[13] Bashkin, Ajzenberg, Browne, Goldhaber, Laubenstein, and Richards, Phys. Rev. **79**, 238 (1950).

[14] Yu. I. Serebrennikov, Candidate Dissertation, Leningrad Polytechnical Institute 1959.

[15] G. Philbert, J. phys. et radium **18**, 656 (1957).

Translated by H. Kasha
74

DESTRUCTION OF SUPERCONDUCTIVITY IN THIN FILMS BY FIELD AND CURRENT

N. I. GINZBURG and A. I. SHAL' NIKOV

Moscow State University

Submitted to JETP editor March 18, 1959

J. Exptl. Theoret. Phys. (U.S.S.R.) **37**, 399-405 (August, 1959)

Measurements were made on the critical magnetic fields and currents required to destroy superconductivity in thin cylindrical tin films. Qualitative agreement with the Ginzburg-Landau theory was obtained. The structure of the films studied is discussed.

EXPERIMENTAL data on the properties of superconductors with small dimensions, whilst at the time substantially assisting the development of the London and Ginzburg-Landau theories, have not lost their significance in the new microscopic theory.

The aim of the present work was to try to establish the conditions for the destruction of superconductivity in thin tin films by magnetic fields and currents. Although a large number of works on thin films have appeared, we know of no attempts to study systematically a series of identical specimens fabricated simultaneously under identical conditions.

We studied films of various thicknesses which were made in the form of thin cylinders with a large ratio of length to diameter. As is known, when superconductivity in thin films is destroyed by a current, there must be no edges, since the magnetic fields at them attain the critical values for very small currents. The intermediate state arising at the film edges causes Joule heating, which increases avalanche-like and leads to a rapid transition into the normal state for the entire film. The only specimen geometries for which there are no edges are discs and cylinders. Disc specimens were used by Alekseevskiĭ and Mikheeva;[1] however, during their fabrication a number of difficulties arose which from our point of view make work with them rather inconvenient. An attempt to use cylindrical films was made some years ago[2] and gave encouraging results. Now we have greatly improved this method.

Although, as will be seen from what follows, we did not succeed in completely avoiding the region of anomalously small destructive currents as occurred also when studying discs, nevertheless the method we chose was certainly suitable for solving the problem posed.

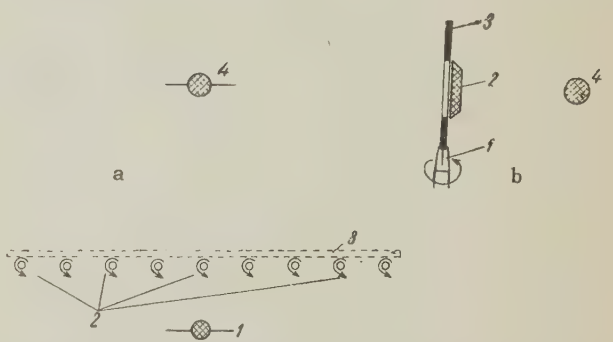

FIG. 1. a) 1 – specimen evaporator, 2 – specimens, 3 – copper screen, 4 – evaporator for contacts. b) 1 – holder, 2 – copper screen, 3 – specimen, 4 – evaporator for contacts.

EXPERIMENTAL METHOD

The tin films studied (purity of the original tin 99.998%) were deposited on glass rods measured to an accuracy of 0.01 mm which were 0.6 to 0.8 mm in diameter and 24 mm long. The carefully washed rods (nine at a time) were fixed in vertical holders on a special revolving apparatus under a vacuum bell-jar and were continuously rotated at a rate of 8 rpm while the films and contacts were condensed. The process of making the films lasted 5 to 8 minutes and the subsequent deposition of contacts approximately 30 minutes. The disposition of evaporators and substrates is clear from Fig. 1a.; the fixing of the glass rods and the position of the cooled copper screen are shown in Fig. 1b. The screen cross section chosen ensured an adequately sharp transition in thickness from the contact layer to the specimen layer, and also minimized the chance of depositing on to the specimen layer any additional material during contact evaporation. During evaporation (from a previously used tungsten evaporator) the pressure was less than 10^{-6} mm of mercury, and the mean surface temperature of the glass rods while the

specimen layer was being deposited did not apparently exceed 40 — 60° C. The tungsten wire crucible for depositing the contact layers was repeatedly fed with tin wire, so that the amount of tin evaporated from it exceeded the amount of tin used to make the specimen layer by a large factor (50 to 100). The amount of substance evaporated on to the specimen was calculated originally from the change in weight of the evaporator and the geometry. To check this calculation we made experiments to determine directly the amount of substance deposited on the specimen, using radioactive tracers.* To do this, strips of thin high-purity aluminum foil were fixed on the screen behind the specimens, alternating with the series of films; the strips, together with a quantity of the original tin were irradiated in a pile and then allowed to stand for several days. After standing one could take the measured activity, after allowing for the background from the foil, to be determined only by the gamma radiation from the Sn^{117} isotope. From several similar experiments, it was found that the relative distribution on the specimens agreed very satisfactorily with the distribution calculated from purely geometrical considerations, but that quantitatively from experiment to experiment the amount exceeded that calculated by a factor of 1.5 to 2. Such a discrepancy destroys the validity of the method and was caused by uneven evaporation of the tin from the surface of the tungsten crucible. Our results were referred to the quantity of substance deposited on the specimen as determined from the experiments with active tin.

In what follows we provisionally describe the separate specimens not by the amounts of substance deposited on them, but by the thicknesses (the density of the condensate was taken to be 7.0 g/cc). Special attention was paid to mounting the finished films in the apparatus and to making reliable current and potential contacts to them.

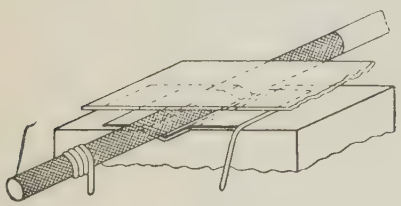

FIG. 2

The specimen mounting and the method of attaching contacts are shown in Fig. 2. The potential contacts were mechanical springs of thin tin foil pressed between the jaws of the holder and the

*We thank I. S. Shapiro and I. A. Antonova for help with these measurements.

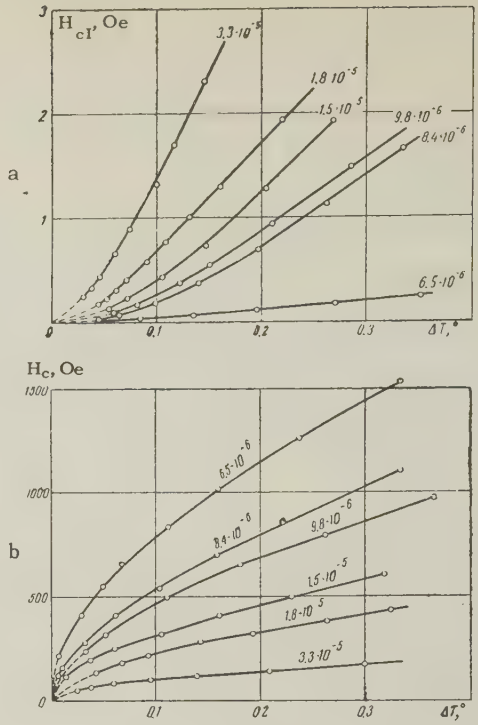

FIG. 3

thick contact layer of tin on the specimen. The current leads were made from three or four close turns of soft tinned copper wire (dia. 50 μ) — previously soldered over with a tin-lead solder (melting point 140° C) on a glass rod of the same diameter as the specimen. The short cylinders thus made were tightly put on to the mounted specimen and soldered to it without the use of flux. Several specimens with films of different thickness were mounted parallel to one another in the bottom of a Dewar filled with liquid helium and placed between the poles of an electromagnet. The Dewar was accurately set up relative to the direction of the electromagnet field, using screws and a turning device. The resistance measurements on the films were made using a potentiometer system; to determine the critical currents the ballast resistance in the film circuit was smoothly changed, and with the aid of a high resistance millivoltmeter the instant at which resistance appears was determined.

The temperature range in which the measurements were made was determined at one extreme, by the fact that when measuring the currents needed to destroy superconductivity, I_c, it was impossible to approach closer to the critical temperature than two or three hundredths of a degree, owing to the inadequate sensitivity of the measuring circuit; at the other extreme it was determined by the fact that for large departures from the critical temperature ($\Delta T \approx 0.4$) the Joule heat

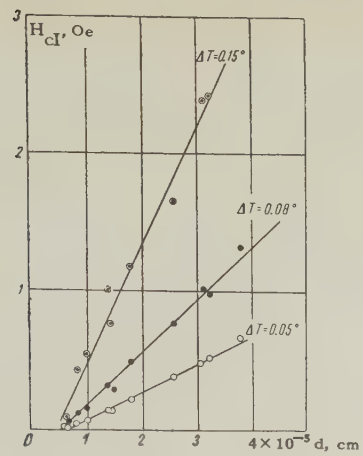

FIG. 4

evolved during the transition increases substantially, causing irreversible changes in the film. The critical magnetic fields (for which these limitations did not apply) were determined in the same temperature interval.

The axes of the films were set parallel to the field by turning the apparatus relative to the electromagnet and finding the minimum resistance of the films for a sub-critical temperature (the setting accuracy was a fraction of a degree).

The results of simultaneous measurements on the critical currents and fields are given for one of the series of films on Figs. 3a and b. Figures 4 and 5 show the variation of critical field with effective film thickness for various departures from the critical temperature.

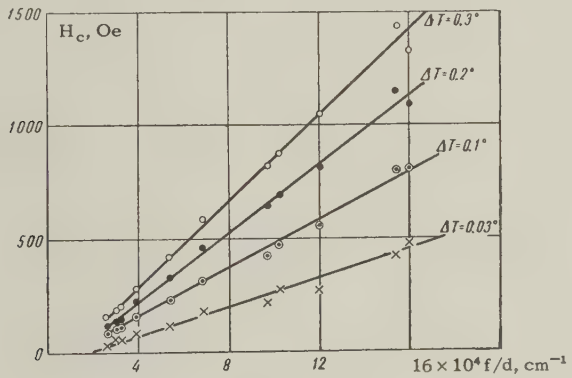

FIG. 5

DISCUSSION OF RESULTS

To treat the experimental results obtained, Ginzburg's work[3] on the critical currents in thin films was used; formulae are given there which are applicable when the film thickness is smaller than the penetration depth of the magnetic field, but greater than the parameter, ξ, in the theories of Pippard[4] and Bardeen, Cooper, and Schrieffer.[5] The value of the critical field in this case is given as

$$H_c = \frac{\sqrt{6}\,\delta_{00}\sqrt{T_c}}{d}\left|\frac{dH_{cm}}{dT}\right|(\Delta T)^{1/2}, \qquad (1)$$

and the size of the critical field of a current H_{cI} as

$$H_{cI} = \frac{4\sqrt{2}\,d}{3\sqrt{3}\,\delta_{00}\sqrt{T_c}}\left|\frac{dH_{cm}}{dT}\right|(\Delta T)^{3/2}, \qquad (2)$$

where d is the film thickness and δ_{00} is the penetration depth at 0°K (for tin $|dH_{cm}/dT| = 151$ oe/deg.).

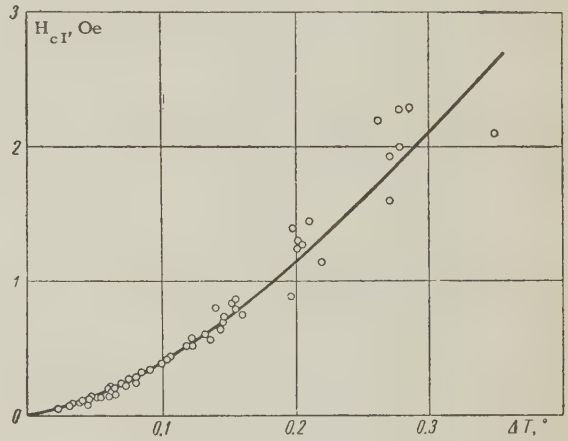

FIG. 6

In Figs. 6 and 7 the variations of H_{cI} and H_c are given for two series of films; it is seen that the experimental points lie satisfactorily on the appropriate curves $A\Delta T^{3/2}$ and $B\Delta T^{1/2}$, fitted to our data at $\Delta T = 0.1°K$ (the scale on the ordinate axis corresponds to a film of 1.5×10^{-5} cm; for other films the scale is appropriately altered).

The ratio of $H_c H_{cI}/{}^8/_3 H_{cm}^2$, which, according

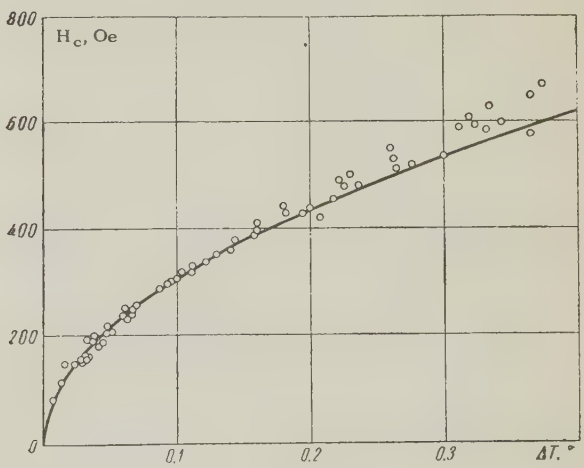

FIG. 7

to reference 3, ought to be constant and numerically equal to unity, was much smaller in our experiments and was 0.22 ± 0.03; the penetration depths* δ_{00}^{H} and δ_{00}^{I} were, respectively, $1.9 \pm 0.3 \times 10^{-5}$ cm and $9.3 \pm 1.5 \times 10^{-5}$ cm, which are much greater than the value δ_{00} for bulk tin of 5×10^{-6} cm. The small value of the ratio $H_c H_{cI} / {}^{8}/_{3} H_{cm}^{2}$ may be connected with the fact that the critical currents measured in the experiment are greatly reduced by the inevitable presence in the specimens of uncontrolled "weak" spots, which also determine the current which destroys superconductivity.

The data presented in Figs. 4 and 5 show that the inverse and direct proportionalities of the critical field on the film thickness expected from Eqs. (1) and (2) are on the whole obeyed.

The substantial difference (about a factor of three) in the penetration depth δ_{00}^{H} we have found from the value obtained by Zavaritskiĭ[6] for thin films can perhaps be explained by the fact that Zavaritskiĭ determined penetration depths which varied systematically with thickness only for the very thickest films he studied. Also an important factor here is the inaccuracy in our determinations of the true thickness of the films. The penetration depths determined from the current data are much bigger because anomalously small currents destroy superconductivity, and these results cannot serve as material for comparison with the theory. In comparatively finely dispersed films Pippard's parameter ξ (see reference 4) is much smaller than in sufficiently good massive specimens. Therefore, it is understandable that our value of δ_{00}^{H} is substantially larger than δ_{00} for the bulk metal.

In principle, there are two possible variants of experiments with thin layers obtained under clean conditions by condensation in vacuum (we ignore all other methods of producing thin layers). The first of these variants consists in the successive manufacture of separate films with a known quantity of substance deposited on unit area under conditions in which one is easily able to vary within wide limits the temperature of the dielectric substrate on which the condensation is carried out. The drawback of this method is the difficulty of accurately repeating the conditions when making the series of specimens required, and also the limitation in the choice of geometrical shape.

The second possibility (used in our work) consists of the simultaneous fabrication of a series of specimens with different masses (which had been chosen beforehand) deposited on separate substrates. However, this method can be realized in practice only if the temperature of the substrate is close to room temperature.

Of course, the structure of films obtained by condensation depends very much on the temperature of the condensation surface and even the speed of condensation.

The lower the temperature of the substrate relative to room temperature, the denser and more highly dispersed is the deposit. Close to helium temperatures all deposited metals without exception are very homogeneous and are apparently completely amorphous deposits (not possessing a defined crystalline structure) with densities only slightly reduced relative to that of the bulk metal.*

The speed of condensation in these conditions is not important and can affect the structure of the deposited films only if the heat produced by radiation from the evaporator and by the heat of condensation causes the substrate temperature to rise.

On increasing the substrate temperature the conditions under which the deposit is formed are different for different metals. Here one can state the following qualitative considerations.

Refractory and high melting-point metals form deposits, the structure of which is not greatly affected by the substrate temperature.† The deposits are homogeneous and highly dispersed — electrical conductivity appears in them at very small effective thicknesses (of the order of atomic). Relatively fusible and low melting-point metals‡ (which include tin) form, under these condensation conditions, films whose structure depends markedly on the amount of substance deposited on unit area of substrate. In the very first stage of condensation on a clean substrate separate centers grow isolated from one another; this causes metallic conductivity to appear only at effective thicknesses of many hundreds of atomic layers. The density in this "sub-layer" is significantly smaller than the bulk density of the condensed metal. The formation of a comparatively dense layer during further condensation proceeds on the "sub-layer" already created,

*In these calculations the data for the very thin films were not used.

*We leave aside the possibility of transformation polymorphs in the film.

†If this temperature is sufficiently far from the melting point of the metal.

‡The specific behavior of alkaline metal films is not considered.

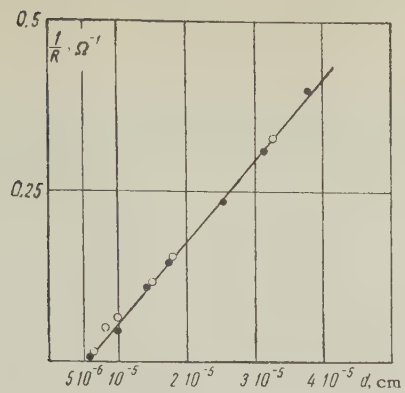

FIG. 8

a fact which is well illustrated by Fig. 8, which shows the variation of the electrical conductivity of tin films on their effective thickness.*

As is seen from this graph, the normal variation of conductivity with thickness starts only after the formation of the "sub-layer" has finished.

Thus, it must be borne in mind that the series of films we made are quite far from ideal, since in the thickest the "sub-layer" can amount to 10% of their thickness. Some compensation for the depth inhomogeneity of films obtained at room temperature is provided by their comparatively highly dispersed state — the crystallite dimensions apparently approach their effective film thicknesses in magnitude. In this sense they are quite different from the highly dispersed "amorphous" films obtained by condensation at low temperatures.

However, all the drawbacks of the method we chose for making the films are balanced by the possibility of making a series of specimens simultaneously and of obtaining these specimens in an ideal shape for the problem posed, i.e., the study of the destruction of superconductivity by current.

We are grateful to V. L. Ginzburg for his interest in the work and valuable discussion and to D. I. Vasil'ev for help with the experiment.

*On cooling to 4.2° the resistance of our films fell by a factor of ten for the thinnest films and by a factor of 30 for the thickest ones.

[1] N. E. Alekseevskiĭ and M. N. Mikheeva, J. Exptl. Theoret. Phys. (U.S.S.R.) **31**, 951 (1956), Soviet Phys. JETP **4**, 810 (1957).

[2] L. A. Feĭgin and A. I. Shal'nikov, Dokl. Akad. Nauk SSR **108**, 823 (1956).

[3] V. L. Ginzburg, Dokl. Akad. Nauk SSSR **118**, 464 (1958), Soviet Phys.–Doklady **3**, 102 (1958).

[4] A. B. Pippard, Proc. Roy. Soc. **216**, 547 (1953).

[5] Bardeen, Cooper, and Schrieffer, Phys. Rev. **108**, 1175 (1957).

[6] N. V. Zavaritskiĭ, Dokl. Akad. Nauk SSSR **78**, 665 (1951).

Translated by K. F. Hulme
75

SOME FEATURES OF THE SPONTANEOUS FISSION OF U^{238}

B. D. KUZ'MINOV, L. S. KUTSAEVA, V. G. NESTEROV, L. I. PROKHOROVA, and G. P. SMIRENKIN

Submitted to JETP editor March 25, 1959

J. Exptl. Theoret. Phys. (U.S.S.R.) 37, 406-412 (August, 1959)

The average number of neutrons emitted per event of spontaneous U^{238} fission, $\bar{\nu} = 2.1 \pm 0.1$, and the quantity $\Delta = (\bar{\nu}^2 - \bar{\nu})/\bar{\nu}^2 = 0.95 \pm 0.05$, which characterizes the neutron distribution, were measured by a double-coincidence technique. These values, as well as the results of previous studies of neutron emission from spontaneous U^{238} fission do not agree with the semi-empirical laws valid for most investigated nuclei. The number of neutrons emitted was determined to be 64.5 ± 2.0 per gram-hour. The decay constant and spontaneous fission half-life computed from the data obtained in the present investigation are 31 ± 1.5 fissions per gram-hour and $(6.5 \pm 0.3) \times 10^{15}$ years, respectively.

INTRODUCTION

THOROUGH investigations of prompt neutrons from fission have clarified many details of the process of neutron emission by excited fragments. A number of experiments[1,2] and calculations[3] have shown that the average number $\bar{\nu}$ of neutrons emitted per fission event increases approximately linearly with the excitation energy E_X of the fissioning nucleus. A comparison of the data on $\bar{\nu}$ for the spontaneous fission[2] of Pu^{240} and Pu^{242} and the neutron-induced fission of Pu^{239} and Pu^{241} shows that the linear dependence of $\bar{\nu}$ on E_X can evidently be extended into the sub-threshold region of excitation energies as far as the spontaneous fission of an unexcited compound nucleus.

The excitation energies E_X of fragments from neutron-induced fission and from spontaneous fission differ by the amount $E_{inc} + E_{comp}$ where E_{inc} is the kinetic energy of the incident neutron and E_{comp} is its binding energy in the compound nucleus. It is assumed that the average kinetic energy of fragments is independent of the excitation energy of the fissioning nucleus.[3] Therefore the linear dependence of $\bar{\nu}$ on E_X can be applied to experimental data on neutron-induced fission to obtain $\bar{\nu}$ for the spontaneous fission of a number of nuclides for which the direct measurement of this quantity is practically impossible.

In references 4 and 1 an attempt was made to calculate the dependence of $\bar{\nu}$ on the number of nucleons A and charge Z of a spontaneously fissioning nucleus. The results of these calculations are in satisfactory agreement with both the experimental values of $\bar{\nu}$ for spontaneous fission and with the values obtained by extrapolating data on induced fission. An exception is provided by the values of $\bar{\nu}$ for the spontaneous fission of U^{238}, 2.26 ± 0.16 and 2.4 ± 0.2, which do not agree with the calculation and appreciably exceed the extrapolated values of $\bar{\nu}$ for neighboring uranium isotopes. Extrapolation of the experimental values of $\bar{\nu}$ for photofission of U^{238} yields a result which is considerably lower than the two values given above.[5]

In addition to this discrepancy an anomaly in the distribution of the number of neutrons is observed in the spontaneous fission of U^{238}. The probability $P(\nu)$ of emitting a given number ν of neutrons in one fission event is represented satisfactorily for the great majority of the investigated nuclei by the binomial law[6]

$$P(\nu) = \frac{\nu_m!}{\nu!\,(\nu_m - \nu)!} \left(\frac{\bar{\nu}}{\nu_m}\right)^{\nu} \left(1 - \frac{\bar{\nu}}{\nu_m}\right)^{\nu_m - \nu}, \qquad (1)$$

where ν_m is the maximum possible number of emitted neutrons. From (1) we obtain the relation

$$\Delta = (\bar{\nu}^2 - \bar{\nu})/\bar{\nu}^2 = 1 - 1/\nu_m. \qquad (2)$$

An experimental study of the distribution $P(\nu)$[6] determined that Δ for both spontaneous and neutron-induced fission of nuclides from U^{233} to Cf^{252} is given approximately by the semi-empirical expression

$$\Delta = 0{,}714 \pm 0{,}035\,\bar{\nu} \qquad (3)$$

and thus depends only slightly on $\bar{\nu}$; its values for the aforementioned nuclides lie in the interval $0.79 - 0.85$.

Geiger and Rose[7] have measured the ratios of the first three moments of the distribution $P(\nu)$ for spontaneous fission of U^{238} ($\bar{\nu}^2/\bar{\nu} = 3.26$, $\bar{\nu}^3/\bar{\nu} = 12.73$), the relation between which is better represented by the Poisson distribution

$$P(\nu) = \bar{\nu}^{\nu} e^{-\bar{\nu}} / \nu!, \qquad (4)$$

than by the binomial law (1). From these results it follows that for spontaneous fission of U^{238} we have $\Delta = 1$, whereas from (3) for $\bar{\nu} = 2.3$ we obtain $\Delta = 0.79$.

Since the experimental values of $\bar{\nu}$ and Δ for spontaneous fission of U^{238} were obtained by indirect methods[7,8] and do not obey the same relations as for a number of other nuclides, the direct experimental measurement of these quantities was of definite interest.

MEASUREMENT OF $\bar{\nu}$

$\bar{\nu}$ was determined by relative measurements of the number of coincidences between detectors of prompt neutrons and of spontaneous fissions of U^{238} and Pu^{240}. Two multilayer ionization chambers in parallel (Fig. 1) were used to detect spontaneous fissions of U^{238}. 12 g of uranium depleted of U^{235} were deposited in layers 2 mg/cm^2 thick on both sides of aluminum foils. An identical chamber contained 2.5 mg of Pu^{240} (92% Pu^{240} and 8% Pu^{239}) on platinum foil. The chamber containing U^{238} was filled with argon to a pressure of 5 atm, while the chamber containing plutonium was filled with a mixture, 90% Ar + 10% CO_2, to 35 mm Hg. The lower pressure of this mixture considerably improved the discrimination between fission fragments and piled-up α particles. The operating point on the characteristic of the fission chambers was selected by extrapolating the counting rate for α particles to 0.1% of the spontaneous fission intensity.

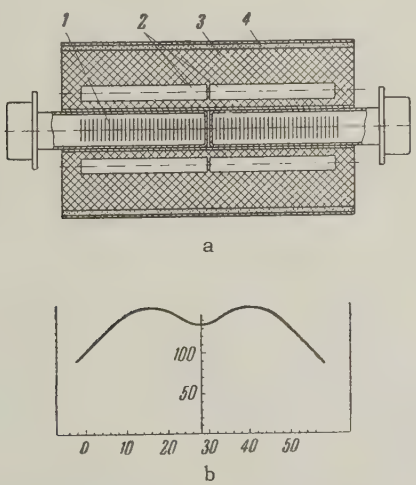

FIG. 1. a) Diagram of apparatus for measurement of $\bar{\nu}$ (U^{238}). 1 – layers of U^{238}, 2 – $B^{10}F_3$ counters, 3 – paraffin, 4 – shielding layer; b) efficiency of neutron registration along the detector: The vertical axis represents the number of counts per unit time, while the horizontal axis represents the distance from the edge of the detector in cm.

The fission chambers were surrounded by 24 proportional $B^{10}F_3$ counters in paraffin, as shown in Fig. 1, which were connected in parallel. The efficiency of registering prompt fission neutrons was ~4%. The electronic equipment registered pulses from the chambers, counters and coincidence circuits, which had a resolving time of $\sim 6 \times 10^{-4}$ sec. Accidental coincidences during measurements with Pu^{240} amounted to less than 0.2%, and ~0.01% with U^{238}, and were therefore not taken into account.

The total number of registered coincidences was ~2400 for U^{238} and ~12,000 for Pu^{240}; as a result of these measurements a correction was introduced for nonuniform efficiency along the neutron detector. Three experimental runs were in satisfactory agreement and yielded the ratio $\bar{\nu}(U^{238})/\bar{\nu}(Pu^{240}) = 0.92 \pm 0.03$. Using $\bar{\nu}(Pu^{240}) = 2.26 \pm 0.05$,[2] we obtain $\bar{\nu}(U^{238}) = 2.1 \pm 0.1$.

MEASUREMENT OF Δ

The measurement of Δ was based on double coincidences between neutrons from a single fission event. These methods have been described in detail by Geiger and Rose.[7] Samples of uranium and plutonium were placed inside a paraffin block together with two six-counter groups of $B^{10}F_3$ counters connected for coincidences (Fig. 2). Eight disks, each consisting of 200 g of depleted uranium, were spaced uniformly along the length of the neutron detector. Calibration was performed by means of a thin spherical plutonium sphere containing about 2% Pu^{240}. With a shell thickness of 1.5 mm the multiplication constant was 1.05. For Pu^{240} Δ is known to have the value 0.807 ± 0.008.[6]

The pulse counting rate of each channel was

$$N_i = \bar{\nu} F \varepsilon_i, \qquad i = 1.\ 2. \qquad (5)$$

The double coincidence counting rate was

$$N_c = (\bar{\nu}^2 - \bar{\nu}) F \varepsilon_1 \varepsilon_2 \eta, \qquad (6)$$

where F is the number of spontaneous fissions

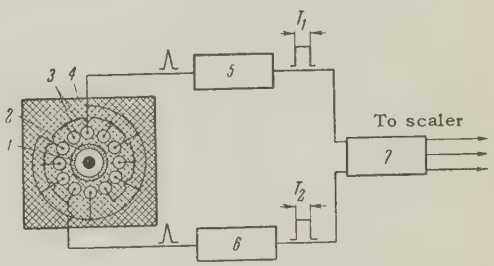

FIG. 2. Diagram of apparatus for measurement of Δ: 1 – U^{238}, 2 – shielding layer of B_4C, 3 – $B^{10}F_3$ counters, 4 – paraffin, 5 and 6 – amplifiers, 7 – coincidence circuit.

per unit time in the sample: ϵ_1, ϵ_2 are the efficiencies of the counting channels; η is the double-coincidence selection factor which takes into account the finite resolving time of the coincidence circuit.

For U^{238} and Pu^{240} (5) and (6) with the notation $\delta = (\bar{\nu}^2 - \bar{\nu})/\bar{\nu}$ give

$$\frac{\delta_U}{\delta_{Pu}} = \frac{N_c(U)}{N_c(Pu)} \frac{(N_1+N_2)_{Pu}}{(N_1+N_2)_U} \frac{\epsilon_{Pu}}{\epsilon_U} \frac{\overline{\epsilon_U^2}}{\overline{\epsilon_U}^2}. \quad (7)$$

Our experimental ratio was $\delta_U/\delta_{Pu} = 1.085 \pm 0.02$.

Using the known values of $\bar{\nu}$ and Δ for Pu^{240} and the measured value of $\bar{\nu}$ for U^{238}, we obtain

$$\Delta_U = 0.95 \pm 0.05.$$

This result includes a correction for the multiplication of spontaneous fission neutrons in the samples and geometric factors ϵ_{Pu}/ϵ_U and $\overline{\epsilon_U^2}/\overline{\epsilon_U}^2$ accounting for the difference in the arrangements of the uranium and plutonium samples.

MEASUREMENT OF THE SPONTANEOUS FISSION HALF-LIFE

In addition to giving the values of $\bar{\nu}_U$ and Δ_U, (5) and (6) can be used to determine the number of neutrons $Q = \bar{\nu}F/M$ emitted in unit time by a gram of uranium. Q was measured in three ways.

(a) Comparison of the channel counts for the uranium and plutonium samples gives

$$\frac{(N_1+N_2)_U}{(N_1+N_2)_{Pu}} = \frac{(\bar{\nu}F)_U}{(\bar{\nu}F)_{Pu}} \frac{\epsilon_U}{\epsilon_{Pu}}. \quad (8)$$

The determination of $(\bar{\nu}F)_U$ from this equation required knowledge of F_{Pu}, which can be calculated if the concentration of Pu^{240} in the spherical shell is known. This concentration was measured by comparing the emitted neutron intensity from the sphere and from a standard plutonium disk of known concentration and weight. From (8) we then obtained $Q = 60.3 \pm 3.6$ neutrons/g-hr.

b) Using the value of F_{Pu} measured above, it is easy to determine $(\bar{\nu}F)_U$ and therefore Q from the relation

$$\frac{(N_c/N_1N_2)_U}{(N_c/N_1N_2)_{Pu}} = \frac{(F\bar{\nu})_{Pu}}{(F\nu)_U} \frac{\overline{\epsilon_U^2}}{\overline{\epsilon_U}^2} \frac{\delta_U}{\delta_{Pu}}. \quad (9)$$

In this way we obtain $Q = 67.5 \pm 3.7$ neutrons/g-hr.

c) Q can be determined by measuring the selection factor η, independently of F_{Pu}, using

$$\left(\frac{N_c}{N_1N_2}\right)_U = \frac{\eta}{(F\bar{\nu})_U} \frac{\overline{\epsilon_U^2}}{\overline{\epsilon_U}^2} \delta_U. \quad (10)$$

The selection factor was determined by studying the dependence of the number of true coincidences on the resolving time of the coincidence circuit. With τ as the mean life of slowed-down neutrons in the detector the time distribution of registered neutrons obeys the law $\tau^{-1}e^{-t/\tau}$. The probability of registering the coincidence of two neutrons can be obtained from the relation

$$\eta = \int_0^\infty e^{-t/\tau}\frac{dt}{\tau}\int_t^{t+T_1} e^{-t'/\tau}\frac{dt'}{\tau} \Big/ \int_0^\infty e^{-t/\tau}\frac{dt}{\tau}\int_t^{t+T_2} e^{-t'/\tau}\frac{dt'}{\tau}$$
$$= 1 - (e^{-T_1/\tau} + e^{-T_2/\tau})/2, \quad (11)$$

where T_1 and T_2 are the durations of pulses reaching the coincidence circuit from the first and second channels, respectively.

In the present experiment we have

$$\eta \approx 1 - e^{-T/\tau}, \quad (12)$$

since the pulse durations in both channels were selected to be approximately equal: $T_1 \approx T_2 = T$. T also becomes the resolving time of the coincidence circuit. The mean neutron lifetime τ was determined by bringing the experimental relation between the number of coincidences and the resolving time T into best agreement with (11).

From all of the foregoing data we obtained

$$\tau = 1.44 \cdot 10^{-4} \text{ sec}, \qquad \eta = 0.82 \pm 0.02$$

for $T = 2.38 \cdot 10^{-4}$ sec.

A calculation by means of (10) gives $Q = 65.0 \pm 2.3$ neutrons/g-hr. The number of neutrons emitted by a gram of uranium per hour, which was obtained by averaging the values of Q determined by the methods described above, is

$$Q = (64.5 \pm 2) \text{ neutrons/g-hr.}$$

Hence the decay constant $\lambda = Q/\bar{\nu}$ and the spontaneous fission half-life $T_{1/2}$ become

$$\lambda = (31 \pm 1.5) \text{ fissions/g-hr,}$$

$$T_{1/2} = (6.5 \pm 0.3) \cdot 10^{15} \text{ years}$$

DISCUSSION OF RESULTS

Our measured result $\Delta = 0.95 \pm 0.05$ agrees with the measurements of Geiger and Rose. However, we cannot conclude on the basis of these experiments that the number of neutrons emitted per spontaneous fission of U^{238} obeys a Poisson distribution. Neither a binomial distribution nor a Poisson distribution for $P(\nu)$ can apparently be justified theoretically, since the probability for the emission of a given number ν of neutrons is determined by the distribution of the excitation energy. Nevertheless, the Poisson law is a worse

TABLE I

Authors	Q neutrons/g-hr	Authors	Q neutrons/g-hr
Fermi[11]	54		
Scharff-Goldhaber and Klaiber[12]	63	Hanson[6]	57.5±3.6
		Rotblat[6]	53 ±13
Pose[13]	55.5	Littler[8]	59.5±3.3
		Present authors	64.5±2.0

approximation than the binomial law to the real distribution $P(\nu)$, since with the former $\nu_m = \infty$ and $\Delta \equiv 1$, independently of the excitation energy of the fissioning nucleus, and this conflicts with experimental results.

The binomial distribution is also insufficiently accurate since, for example, Eqs. (2) and (3) now give $\nu_m = 1/(0.286 - 0.035)$, which is smaller than the observed maximum number of neutrons per fission, at least for the spontaneous fission of Cm^{244} and Cf^{252}.[6,9] The real distribution $P(\nu)$ is evidently somewhere between the two distributions mentioned.

The deviation of the experimental value of Δ from (3) clearly indicates that the width of the excitation energy distribution in the spontaneous fission of U^{238} is greater than for other nuclides with the same mean excitation energy. Leachman calculated $\overline{\nu}^2/\nu = 2.70$, which is closer to our value (2.98 ± 0.05) than to the result obtained by Geiger and Rose (3.26 ± 0.16).

Our result, $\overline{\nu} = 2.08 \pm 0.08$, for the spontaneous fission of U^{238} agrees within experimental error with the value obtained by Geiger and Rose (2.26 ± 0.16) but is smaller than Littler's result (2.4 ± 0.2). The data indicate, as previously, that $\overline{\nu}$ for the spontaneous fission of U^{238} is ~ 0.4 above the results calculated in references 1 and 4. In these papers it was assumed that the kinetic energy of fragments depends linearly on $Z^2/A^{1/3}$, which is only slightly different for close isotopes, so that the computed kinetic energy of fragments is almost identical for neighboring uranium isotopes. However, Kovrigin and Petrzhak have shown in a recent paper[10] that the mean kinetic energy of fragments from the spontaneous fission of U^{238} is 3 or 4 Mev lower than in the fission of U^{235} induced by thermal neutrons. This indicates that the actual excitation energy of fragments in the spontaneous fission of U^{238} is 3 or 4 Mev higher than that calculated in references 1 and 4; $\overline{\nu}$ is thus increased by 0.4 or 0.5.

It is interesting to compare $\overline{\nu}$ for the spontaneous fission and photofission of U^{238}. Reference 5 gives $\overline{\nu} = 1.6 \pm 0.5$ for U^{238} fission induced by γ rays with about 5 Mev. Assuming that with rising excitation energy $\overline{\nu}$ increases linearly and $d\overline{\nu}/dE = 0.13$ Mev^{-1},[1] we would expect $\overline{\nu} \approx 2.8$ in photofission induced by 5-Mev γ rays.

The features of U^{238} fission discussed in the present paper show the inadequacy of semi-empirical laws which ignore the characteristics of individual nuclides.

Tables I and II compare the values of Q and λ obtained in the present work and by other investigators.

TABLE II

Authors	λ, fissions/g-hr
Segrè[11]	24.8±0.9
Whitehouse and Galbraith[14]	24.2±1.5
Flerov et al.[15]	19.8±2.9
Present authors	31.0±1.5

The authors are grateful to Professor A. I. Leĭpunskiĭ for his interest and are indebted to I. I. Bondarenko and V. S. Stavinskiĭ for valuable discussions.

[1] Bondarenko, Kuz'minov, Kutsaeva, Prokhorova, and Smirenkin, Proc. of the Second International Conference on the Peaceful Uses of Atomic Energy, Geneva, 1958, Report No. 2187.

[2] R. B. Leachman, Proc. of the Second International Conference on the Peaceful Uses of Atomic Energy, Geneva, 1958, Report No. 2467.

[3] R. B. Leachman, Phys. Rev. **101**, 1005 (1956).

[4] B. D. Kuz'minov and G. N. Smirenkin, J. Exptl. Theoret. Phys. (U.S.S.R.) **34**, 503 (1958), Soviet Phys. JETP **7**, 346 (1958).

[5] Lazareva, Gavrilov, Valuev, Zatsepina, and Stavinskiĭ, Conference of the Academy of Sciences of the U.S.S.R. on the Peaceful Uses of Atomic Energy, Session of the Division of Physico-Mathematical Sciences, Acad. Sci. Press, 1955, p. 306, Engl. Transl., Consultants Bureau, New York, 1955, p. 217.

[6] Diven, Martin, Taschek, and Terrell, Phys. Rev. **101**, 1012 (1956).

[7] K. W. Geiger and D. C. Rose, Can. J. Phys. **32**, 498 (1954).

[8] D. J. Littler, Proc. Phys. Soc. (London) **A65**, 203 (1952).

[9] J. Terrell, Phys. Rev. **108**, 783 (1957).

[10] B. S. Kovrigin and K. A. Petrzhak, Атомная энергия (Atomic Energy) **4**, 547 (1958).

[11] E. Segre, Phys. Rev. **86**, 21 (1952).

[12] G. Scharff-Goldhaber and G. S. Klaiber, Phys. Rev. **70**, 229 (1946).

[13] H. Pose, Z. Physik **121**, 293 (1943).

[14] W. J. Whitehouse and W. Galbraith, Phil. Mag. **41**, 429 (1950).

[15] Podgurskaya, Kalashnikova, Stolyarov, Vorob'ev, and Flerov, J. Exptl. Theoret. Phys. (U.S.S.R.) **28**, 503 (1955), Soviet Phys. JETP **1**, 392 (1955).

Translated by I. Emin
76

POLARIZATION OF RECOIL PROTONS PRODUCED IN ELASTIC SCATTERING AT 307 Mev

E. L. GRIGOR' EV and N. A. MITIN

Joint Institute for Nuclear Research

Submitted to JETP editor April 1, 1959

J. Exptl. Theoret. Phys. (U.S.S.R.) **37**, 413-421 (August, 1959)

Results are presented of an investigation of the polarization of recoil protons appearing in elastic π^+-p scattering through an angle of $140 \pm 8°$ in the c.m.s. at an energy of 307 ± 5 Mev. A polarization value $P_i = -0.19 \pm 0.17$ has been derived from the data on the magnitude of the left-right asymmetry in elastic scattering of recoil protons on photographic emulsion nuclei. Phase shifts satisfying the indicated polarization value and consistent with the differential cross section for elastic scattering of π^+-mesons by protons are given by Eq. (1).

Problems connected with the use of various phase shift sets for analysis of the experimental data are discussed.

INTRODUCTION

PHASE-SHIFT analysis of the differential cross sections for the elastic scattering of π mesons by protons leads, in general, to a whole sequence of solutions which agree equally well with the experimental results. By means of additional considerations, based on a great number of experimental and theoretical investigations of the interaction between π mesons and nucleons, it is possible to eliminate several ambiguities and to reject some of the solutions, i.e., to reduce the number of possible solutions to a minimum. As an example of this, we recall the application of the dispersion relations to meson-nucleon scattering.

There exists a direct method for a unique choice of the solution, based on phase-shift analysis of a whole set of experimental data on elastic scattering of mesons by protons, involving the differential cross sections and the polarization of the recoil protons. The polarization of recoil protons, as was shown first by Fermi,[1] is very sensitive to the values of phase shifts, and its measurement can therefore serve as a good method of uniquely choosing from among different sets of phase shifts the one compatible with the differential cross sections as well as with the polarization data.

The basic condition for the measurement of the polarization of recoil protons is the availability of an intense beam of π mesons of high energy. In this case, by scattering the π mesons at large angles, it is possible to create a sufficiently intense polarized beam of recoil protons with energy greater than 100 Mev. For this beam the effect of polarization in elastic scattering by the analyzer nuclei is great and, consequently, the magnitude of the asymmetry in scattering can be considerable.

A beam of π^+ mesons emitted from the synchrocyclotron of the Joint Institute for Nuclear Research, with an intensity of about 1,000 mesons per cm^2-sec at an energy of 307 Mev, created sufficiently favorable conditions for performing an experiment to measure the polarization of the recoil protons. The recoil protons from the π^+-p scattering, coming out at an angle of 20° in the laboratory system, had in this case an energy of 170 Mev, which was very convenient for conducting these measurements.

On the basis of the results of the phase-shift analysis previously performed by Mukhin and Pontecorvo[2] for π-meson energies of 240, 270, and 307 Mev, the expected values of polarization were calculated for the case where only the contribution of the SP-states is taken into account, as well as for the case when the contribution of the D-state is also considered. In Fig. 1 are shown the results of the calculations, made in accordance with the solutions obtained, in which the phase δ_{33} is positive and δ_{35} is negative. On the same figure are shown the results of calculations of the polarization for 307 Mev in the case when the opposite choice of signs for δ_{33}

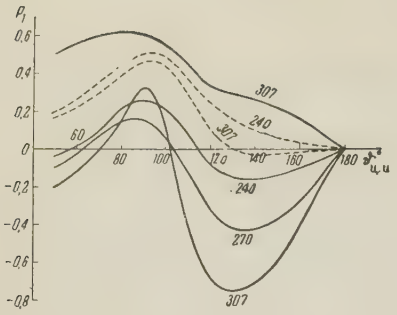

FIG. 1. Polarization of recoil protons as a function of π^+-meson scattering angle in the c.m.s. The dotted curves are for SP-analysis, the solid curves are for the SPD-analysis. The calculations were made on the basis of phase-shift sets from reference 2 for 240, 270, and 307 Mev. The upper solid curve corresponds to the set $\alpha_3 = -30°$; $\alpha_{33} = 140°$; $\alpha_{31} = -15°$; $\delta_{33} = -10°$; and $\delta_{35} = 10°$.

and δ_{35} is made. As can be seen from the figure, an important feature of the calculated curves is that relatively small values of phase shifts in the D-state significantly influence the polarization. This is especially noticeable for angles from 130° to 150°. Here the value of polarization, in the case of SPD analysis, firstly increased sharply compared to SP analysis, and secondly, changes its sign when the opposite choice of the signs of δ_{33} and δ_{35} is made. Therefore it is completely natural that the main goal of the experiment (which is to measure the polarization of the recoil protons for the angles of scattering of mesons in the interval 130° to 150° in the center of mass system) should be, first, a determination of the value of the contribution of the D state to the scattering, that is, of the values of δ_{33} and δ_{35}, and second, a determination of the signs of these phases.

There is practically no information on the contribution of the D-state to the scattering, although this question has been considered in several papers.[3] This is due to the fact that the measurements of the differential cross sections, owing to the limited precision of the results, are not sensitive enough to small values of phase shifts in the D-state. Therefore, the "optimal" sets of phase shifts in the case of SPD analysis do not permit one to draw reliable conclusions about the values of phase shifts in the D-state. Up to the present time, no polarization experiments have been made at such energies where the D-state can give a considerable effect. To determine the most favorable conditions for an experiment to measure the polarization of the recoil protons, corresponding estimates were made for π^+ mesons with energies from 200 to 307 Mev. These estimates were made by taking into account the intensities of the meson beams, the energies of the recoil protons, and the expected value of the polarization for these energies, and also by taking into account the information about the values of the differential cross sections and accuracy of their measurements. These estimates have shown that the most favorable conditions for the experiment occur at a π^+-meson energy of 307 Mev. At this energy, for a meson scattering angle of 140° in the c.m.s., (the corresponding value of the energy of the recoil proton is 170 Mev), the polarization calculated for the "optimal" set of phase shifts in the case of SPD analysis ($\alpha_3 = -13.0°$; $\alpha_{31} = -4.0°$; $\alpha_{33} = +133.7°$; $\delta_{33} = 9.5°$; $\delta_{35} = -10.0°$) was found by Mukhin and Pontecorvo to be $P_1 = -0.71$. In this case, in elastic scattering of the recoil protons by the photoemulsion nuclei, a considerable left-right asymmetry was expected, reaching a value of 0.3 or 0.4 for the scattering angles 6° and greater.

At the present time the results of only one experiment measuring the polarization of recoil protons are known.[4] In this experiment, at a π^--meson energy of 220 Mev, the polarization of recoil protons was measured for 15° and 30° in the laboratory system. Owing to major experimental difficulties, the statistical accuracy of the measurements was not good. However, based only on experimental results, an analysis of these results permits one to reject, directly, two solutions out of four and to determine precisely the sign of the phase α_1.

CONDITIONS OF THE EXPERIMENT

The setup of the experiment is shown in Fig. 2. The method of obtaining the π^+-meson beam was already described several times (see, e.g., reference 5). Mesons with energies of 307 ± 5 Mev passed through a collimator 5 cm in diameter and hit a liquid hydrogen target. The working part of the target consisted of a metallic vessel 30 cm long and 8 by 8 cm in cross section. This vessel was covered with a thick layer of foam plastic. The front and back walls of the target, through which the beam of mesons and recoil protons passed, had a rounded shape and were made of

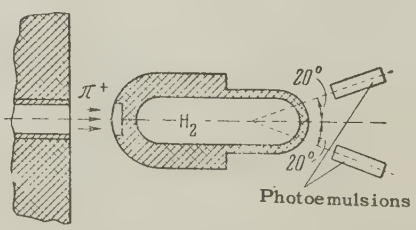

FIG. 2. Experimental setup.

brass foil 0.4 mm thick. These parts of the target were covered by a thinner layer of foam plastic, 3 cm thick. The target was placed on a special table in such a way that the axis of the target coincided very accurately with the axis of the meson beam.

The recoil protons, emitted from the target at an angle of 20°, struck photoplates placed in holders held on bars at the same angle to the left and to the right of the axis of the meson beam. The initial energy of the recoil protons was 170 Mev, but an average of 10 Mev was lost in the passage through the liquid hydrogen, the walls of the target, and in the emulsion. The emulsion played a double role, as a detector of particles and as a target for the elastic scattering of the recoil protons, that is, an analyzer of their polarization.

An investigation of background conditions showed that there were two sources of background, and it was necessary to take them into serious consideration. First was the background from the walls of the liquid hydrogen target. An estimate of this background, made by irradiating the empty target with a beam of π^+ mesons, showed it to be small, less than 1%, because in our case the working part of the target had a great length and a large cross section, and also because there was a small angular divergence of the mesons in the beam. The second background was due to the liquid hydrogen, which filled the working part of the target. This background was caused by the fact that the beam of π^+ mesons used in this experiment contained apart from a large number of protons with a momentum equal to the momentum of the mesons (the corresponding energy of the protons was $E_p = 92$ Mev), an additional number of protons with greater energy ($E_p > 150$ Mev), i.e., protons with momenta much greater than that of the mesons. The scattering of the latter protons by the hydrogen in the target produced recoil protons which could not be separated in the emulsion from the recoil protons due to π^+-p scattering. The number of high-energy protons was estimated with photoplates, irradiated in the beam of 307-Mev π^+ mesons by counting the grain density in the tracks of protons travelling along with the mesons. The measurements showed that the number of protons in the beam, with energies of 150 to 200 Mev, was not more than 2% of the number of mesons. Since the differential cross sections for emission of recoil protons (at an angle of 20° in the laboratory system) in p-p scattering are approximately equal in our case to those of the π^+-p scattering, the total background was not greater than 3%.

We searched, in this experiment, for events of elastic scattering of the recoil protons by the nuclei of the photoemulsion, in order to determine the value of the left-right asymmetry in this scattering. The search for the cases of elastic scattering was made by the method of scanning along the tracks. We chose proton tracks satisfying the following conditions: 1) The deviation of the proton tracks from the principal 20° beam direction should not be greater than ±4°, meaning a choice of recoil-proton tracks corresponding to meson scattering angles of $\vartheta = 140 \pm 8°$ in the c.m.s. 2) The dip angle of the tracks relative to the plane of the emulsion did not exceed 12°. 3) The grain density in the investigated tracks corresponded to the grain density in the tracks of 160-Mev protons. The latter density was measured in special control photoplates, irradiated by a beam of 160-Mev protons and developed each time together with the photoplates on which the search for the elastic scattering events took place. Because of the geometry of the experiment, the fulfillment of the first two conditions implied the choice of the tracks of the recoil protons which arose in a small bounded region of the liquid hydrogen target, the cross section of which was determined by the cross section of the meson beam.

Electron-sensitive emulsions of the NIKFI-R type with 400-μ emulsions were used. The scattering cases found during the scanning along the tracks were identified as elastic if the grain density in the track was the same before and after the scattering, and if there were no tracks of recoil nuclei or of electrons at the point of scattering. In each identified case of elastic scattering, the angle of scattering ϑ_p, the azimuthal angle φ, and the grain density on the sections of the tracks before and after scattering were measured. All cases of elastic scattering of recoil protons at an angle $\geq 3°$ in the plane of the emulsion were recorded; in this case, even during a brief examination of the track, the kink is very easy to see, thus disclosing the existence of scattering.

RESULTS OF MEASUREMENTS

On the photoplates, situated to the left and to the right of the axis of the π-meson beam there were found 545 cases of elastic scattering of the recoil protons by the nuclei of the photoemulsion within a scattering angle $\vartheta_p = 3.5$ to 27°, with azimuth angles $0° \leq \varphi \leq 60°$. The results of the measurements for the right and the left photoplates were correspondingly added in order to

TABLE I. Experimental results for different intervals of recoil-proton scattering angles ϑ_p and azimuth angles φ

ϑ_p, deg	$\varphi = 0$—30°		$\varphi = 30$—60°		The value of assymetry ε
	left	right	left	right	
3.5— 6	88	93	24	25	0.03±0.07
6 — 9	52	63	24	25	0.08±0.08
9 —13	28	32	11	15	0.12±0.12
13 —27	15	22	12	16	0.20±0.20

increase the statistical material. Table I lists the results, summed in such a way that all cases of scattering are considered to have taken place in the right photoplate. All cases of scattering are divided into four intervals of the scattering angle ϑ_p, each interval being in turn subdivided into two intervals of the azimuth angle φ. The asymmetry was determined for each interval of scattering angle.

It is known that in the experiments on the elastic double scattering of protons by nuclei the asymmetry ϵ is connected with the polarizations that arise in the first and second scattering through the relationship $\epsilon = P_1 \cdot P_2$. In our case P_1 is the polarization of the recoil protons from π^+-p scattering, and P_2 arises in the elastic scattering of these protons by the nuclei of the photoemulsion. It is therefore possible to determine the polarization of the recoil protons, provided the experimental values of asymmetry and of P_2 are known. The polarization of 135-Mev protons in elastic scattering by the nuclei of the photoemulsion was investigated by Feld and Maglic.[6] The results of this work were used by us to analyze our experimental results obtained in order to determine P_1.

The polarization of the recoil protons, calculated according to the data of Table I and the results of Feld and Maglic, averaged over the four angular intervals, was found to be $P_1 = -0.19 \pm 0.17$. The sign of the polarization momentum was chosen relative to the direction $\mathbf{n}$ determined by the vector product $\mathbf{n} = [\mathbf{k}_p \times \mathbf{k}_\pi]$, where $\mathbf{k}_p$ is the momentum of the recoil proton and $\mathbf{k}_\pi$ is the momentum of the π meson before scattering. The error indicated in this result is the standard deviation.

As pointed out previously, the polarization expected in our experiment, calculated on the basis on the "optimal" set of phase shifts in an SPD analysis in which the phases are $\delta_{33} = 9.5°$ and $\delta_{35} = -10°$, is $P_1 = -0.71$. The value $P_1 = -0.19 \pm 0.17$ obtained in the experiment is a great deal smaller than expected.

The most natural way to explain this discrepancy is to assume that the phase shifts of the D-states δ_{33} and δ_{35}, which determine in our case the large value of the expected polarization, are much smaller than 10°. Table II lists sets of phase shifts, which satisfy, within the limits of errors, the experimental value of polarization and are consistent with the differential cross sections of the meson-nucleon scattering. The phase shift sets are listed in the table in decreasing order of δ_{33}.

TABLE II. Phase shift sets satisfying the experimental value of the polarization

δ_{33}, deg	δ_{35}, deg	α_3, deg	α_{33}, deg	α_{31}, deg	Computed polarization	M
5	—5	—19	133.5	— 6	—0.39	5.0
5	—2	—22	132	— 8	—0.33	5.4
5	0	—21	132	— 8	—0.27	14.9
3	—3	—23	133.2	— 8	—0.27	12.7
3	—3	—25	132	—10	—0.30	11.9
2	—5	—22	132	— 8	—0.27	12.6
2	—3	—23	133.2	— 8	—0.22	11.4
2	—2	—24	133	—10	—0.23	11.7
2	—2	—23.2	133.2	— 8.4	—0.19	8.8
0	—5	—22	132	— 8	—0.16	11.8
0	0	23.2	133.2	— 8.4	—0.04	12.0

In the last column the table gives the value of

$$M = \sum_i \left[\frac{f(\alpha, \delta, \vartheta_i) - \sigma(\vartheta_i)}{\Delta\sigma(\vartheta_i)} \right]^2,$$

which characterizes the degree of deviation of the differential cross section, $f(\alpha, \delta, \vartheta_i)$, computed by phase-shift analysis from the experimental values of the differential cross section $\sigma(\vartheta_i)$. The table enables us to choose the set of phase shifts which corresponds in the best possible way to experimental polarization and differential scattering cross section data. The following set of phase shifts satisfies this condition:

$$\alpha_3 = -23{,}2°; \quad \alpha_{33} = 133{,}2°; \quad \alpha_{31} = -8{,}4°;$$
$$\delta_{33} = (2^{+3}_{-2})° \quad \delta_{35} = (-2^{+2}_{-3})°, \qquad (1)$$

where the first three phase shifts coincide with the SP set, and δ_{33} and δ_{35} are significantly smaller than the values given by Mukhin and Pontecorvo for SPD analysis.

It is quite natural to expect the contribution of the D-states to increase rapidly for higher energies. The phase-shift analysis of experimental results[7] of elastic scattering of 500-Mev π^+ mesons has led to the conclusion that phase shifts in D-states do not exceed 10°. If we suppose, according to the results of our work, that the phase shifts of the D-states are equal to 2° at 307 Mev, and extrapolate the obtained value to high energies using the law $\delta \sim \eta^5$, where η is the relative momentum of the meson in the c.m.s., then we

TABLE III. Values of polarization P_1 corresponding to phase shifts with different signs of δ_{33} and δ_{35} phases

δ_{33}, deg	δ_{35}, deg	α_3, deg	α_{31}, deg	α_{33}, deg	P_1	M
−10	10	−30	−15	140	0.25	3.0
− 2	2	−23,2	− 8.4	133.2	0.11	12.0
− 3	− 3	−23	− 8	133.2	0.17	7.2
3	3	−23	− 8	133.2	−0.08	48.1

obtain for an energy of 500 Mev a value of 8° for the phase shifts of the D-states. This fact serves as a confirmation (though a far from sufficient one), of the correctness of the estimated values obtained in the present work for δ_{33} and δ_{35}.

The results obtained in the present work permit us to make a definite choice of the signs of D-state phases, whereby δ_{33} is positive and δ_{35} negative. As can be seen from Table III, an opposite choice of signs contradicts the experimental polarization data, since this choice would give a positive sign for the P_1. In the table this is illustrated only by two examples, but the calculations show that not one of the phase-shift sets in which δ_{33} is negative and δ_{35} positive can give a negative value of polarization and thus satisfy the experimental results. This conclusion is correct also for the case when δ_{33} and δ_{35} are both negative; one such example is given as an illustration in the third row of the table. The last case given in the table is one when both δ_{33} and δ_{35} are positive and the polarization is negative. From calculations for this case it follows that phase-shift sets in which δ_{33} and δ_{35} are both positive always give a negative polarization, whose absolute value increases with an increase of these phases. However, such phase-shift sets are incompatible in practice with the differential scattering cross section. This fact is shown by a large value of M even for the relatively small values of phase shifts for the D-states.

It has already been pointed out that the polarization determined in the experiment is significantly smaller than the expected value, calculated on the basis of the "optimum" SPD phase-shift set found by Mukhin and Pontecorvo. A possible reason for the obtained discrepancy may be the influence of inelastic processes, connected with the production of mesons by mesons, on the value of the polarization of the recoil protons in the elastic π^+-p scattering. A quantitative estimate of such an influence can be easily made by making the assumption (which is quite valid[8] up to 500 Mev) that the contribution of the inelastic processes is small and, consequently, the imaginary parts of the phase shifts are small. In this case the introduction of the imaginary parts cannot cause a noticeable change in the real parts, which already have been determined from the phase analysis. In deducing a polarization equation that takes into account the influence of inelastic processes (under the above assumption), the expansion was made only to terms linear in the imaginary part of the phase shifts. The corresponding expression for the polarization* was of the form $P = P_1 + \Delta P_1$, where P_1 was expressed only in terms of the real parts of the phase shifts and ΔP_1 contained terms linear in the imaginary parts and determined the additional polarization due to the inelastic processes. The calculation was made under the assumption that together with the main real parts $\alpha_3 = -13.0°$, $\alpha_{31} = -4.0°$, $\alpha_{33} = 133.7°$, $\delta_{33} = 9.5°$, and $\delta_{35} = -10°$, which determine the value of expected polarization, the phase shifts contain also small imaginary increments

$$\beta_3 = \beta_{31} = \beta_{33} = \gamma_{33} = \gamma_{35} = 0.02 \text{ rad.}$$

where β and γ are the corresponding imaginary parts of the phase shifts. Below are given the results of calculations for the case when only the additional polarization ΔP_1 due to the imaginary increments is computed:

The imaginary parts of the phase shifts taken into account	All phases	SP-phases only	D-phases only
The additional part of polarization ΔP_1	0.05	0.016	0.034

Therefore, when the imaginary part is equal to 0.02, the absolute value of polarization is decreased by merely 0.05, that is, instead of -0.71 it is equal to -0.66. To decrease the absolute value of polarization to 0.19 and thus agree with the mean value of the experimental result obtained under the condition that the real part of the phase remains unchanged, it is necessary that the imaginary part of all phases should be ~ 0.2. Such a large value is incompatible with the total cross section of the inelastic processes, which cannot, apparently, be greater than[8] 2 mb for 300 Mev, while in the case of a phase-shift with an imaginary part equal to 0.2, the cross section of the inelastic processes is significantly higher than 2 mb for each separate state that participates in the scattering. It appears therefore that it is impossible to explain the discrepancy between the expected and experimental values of polarization by a reasonable account of the influence of the inelastic processes.

*The equations for the polarization in terms of the scattering phase shifts are not given here, since they are cumbersome.

The small value of the phase shifts of the D-states for 307 Mev permits some conclusions concerning the variations of α_3 and α_{31} with the meson momentum. Assuming that the absolute values of the phases of the D-states increase rapidly with the energy, we can consider that at meson energies lower than 300 Mev allowances for the D-states have practically no influence on the values of α_3 and α_{31}. For higher energies the contribution of the D-states and their influence on the values of α_3 and α_{31} are taken into the account by assuming that δ_{33} and δ_{35} are proportional to η^5. Figure 3 shows the values of α_3 as a function of η with all these facts taken into consideration. The linear formula $\alpha_3 = -0.11\eta$ was proposed by Orear[9] holds up to 200 Mev, but for higher energies the experimental values of α_3, do not fit this formula even if we take into consideration large inaccuracies in the determination of α_3. It follows from the figure that at energies higher than 200 Mev $|\alpha_3|$ increases more rapidly with the meson momentum than is indicated by the relationship $\alpha_3 = -0.11\eta$ which, as was already stated, describes satisfactorily the experimental values of α_3 for energies below 200 Mev. In connection with this, it is interesting to remark that, in this same energy range, changes take place also in the dependence[3] of α_{33} on the meson energy. These changes consist of the fact that the experimental values of α_{33}, for meson energies greater than 200 Mev, do not fit the plot of Chew and Low, as they do for smaller energies.

The small value of α_{31} and the large relative error in its determination did not lead up to the present time to any conclusion about the variation α_{31} with the meson energy. In the work of Mukhin and Pontecorvo it was pointed out that at energies higher than 220 Mev α_{31} behaves regularly, meaning that it has a negative sign and its absolute value does not exceed 10° up to 310 Mev. It has been pointed out also that taking into the account the D-state leads to a systematic decrease of α_{31}, for example a two-fold decrease for 307 Mev. Chiu and Lomon[10] have found that the dependence of α_{31} on the momentum at energies up to 307 Mev can be satisfactorily described by the relationship $\alpha_3 = -0.91\eta^3$ (degrees). The phase-shift analysis in this work was done by assuming that only the SP-states participate in the scattering. This is apparently justifiable for the energies up to 307 Mev, as follows from the present work. The value of $\alpha_{31} = -8.4°$ indicated in our work also agrees satisfactorily with this relationship.

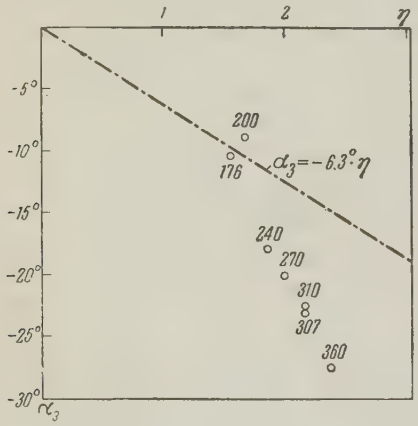

FIG. 3. Variation of α_3 with meson momentum in the c. m. s. The experimental values of α_3 are taken from the SP analysis,[3] with allowance for the corrected values of the D-state phases, obtained in the present work. The numbers denote meson energies in Mev.

All the previous discussions were concerned with the case when only phase solutions of the Fermi type are taken into account in the calculations. It is interesting to discuss the question whether or not it is possible, on the basis of the obtained experimental results, to disregard the Yang type phase shifts. Although the results of investigations[11] based on the use of dispersion relationships definitely permit the exclusion of solutions of the Yang type, one task of experimental research on polarization is to confirm this fact directly.

Table IV lists the computed values of the polarization* of recoil protons for a set of Yang type phase shifts. It can be seen in the example of the first three sets of phase shifts that whereas for the SP and SPD sets with $\delta_{33} = -\delta_{35} = 2°$ the polarization is positive, the sign of the polarization is reversed for the set in which the phase shifts of the D-state have been increased in absolute value to 10°. Estimates, on the assumption that the absolute value of δ_{33} is approximately

TABLE IV. Values of polarization computed on the basis of Yang type phase shift sets

δ_{33}, deg	δ_{35}, deg	α_3, deg	α_{31}, deg	α_{33}, deg	P_1
0	0	—23.3	298.3	156.7	0.41
2	—2	—23.2	298	157	0.27
9.5	—10	—13	297	159	—0.24
—14	5.5	—13	297	159	0.91

*In these calculations the purpose was to obtain purely qualitative results about the values and the signs of polarization, which are in a definite way determined by the values and the signs of δ_{33} and δ_{35}. Therefore, some of the phase-shift sets in Table IV may give a relatively high value of M.

equal to that of δ_{35}, show that the polarization goes through zero when δ_{33} and δ_{35} equal $\sim 5°$. The last set of the phase shifts given in the table is one for which δ_{33} and δ_{35} have respectively negative and positive signs; the polarization corresponding to this set has a large positive value. From the calculations it follows that all phase shifts of the Yang type in which δ_{33} is negative and δ_{35} is positive give a high positive value of polarization.

Thus, on the basis of experimental data on the magnitude of the polarization, the following phase shift sets of the Yang type are definitely excluded: 1) the set corresponding to the SP analysis; 2) sets corresponding to SPD analysis in which the D-state phase shifts δ_{33} and δ_{35} have respectively negative and positive signs; 3) phase shift sets in which δ_{33} and δ_{35} have respectively positive and negative signs and do not exceed 5° in absolute value. In the last case, for sets in which δ_{33} and δ_{35} have absolute values higher than 5°, the computed value of polarization may be in agreement with the experimental value.

We express our deep thanks to L. I. Lapidus for his valuable comments and numerous discussions, to A. I. Mukhin for helping in performing the experiment, to S. B. Nurushev for the discussion of results, and also to L. Mal'tseva, T. Rybakova and R. Khristova, who did much work in scanning the photo-emulsions.

We are deeply indebted to Professors V. P. Dzhelepov and B. M. Pontecorvo for constant interest and attention to our work.

[1] E. Fermi, Phys. Rev. **91**, 947 (1953).

[2] A. I. Mukhin and B. M. Pontecorvo, J. Exptl. Theoret. Phys. (U.S.S.R.) **31**, 550 (1956), Soviet Phys. JETP **4**, 373 (1957).

[3] Mukhin, Ozerov, Pontecorvo, Grigoriev, and Mitin. CERN Symposium, Geneva (1956). N. A. Mitin and E. L. Grigoriev, J. Exptl. Theoret. Phys. (U.S.S.R.) **32**, 445 (1957), Soviet Phys. JETP **5**, 378 (1957).

[4] Ashkin, Blaser, Burger, and Romanowski. Proc. 1958 Ann. Intern. Conf. on High Energy Physics at CERN (1958).

[5] Meshcheryakov, Zrelov, Neganov, Vzorov, and Shabudin, J. Exptl. Theoret. Phys. (U.S.S.R.) **31**, 45 (1956), Soviet Phys. JETP **4**, 60 (1957).

[6] B. T. Feld, and B. C. Maglic, Phys. Rev. Lett. No. **10**, 375 (1958).

[7] W. J. Willis. Proc. 1958 Ann. Intern. Conf. on High Energy Physics at CERN, Geneva (1958).

[8] Blevins, Block and Leitner, Phys. Rev. **112**, 1287 (1958).

[9] J. Orear, Phys. Rev. **96**, 176 (1954).

[10] H. Y. Chiu and E. L. Lomon, Ann. Phys. **6**, 50 (1959).

[11] W. Gilbert and G. R. Screaton, Phys. Rev. **104**, 1758 (1956).

Translated by S. Kotz
77

ION OSCILLATIONS IN A PLASMA

T. F. VOLKOV

Submitted to JETP editor March 11, 1959

J. Exptl. Theoret. Phys. (U.S.S.R.) 37, 422-426 (August, 1959)

The effect of a high-frequency electromagnetic field on ion oscillations in a plasma is considered. It is shown that the frequencies of the quasi-acoustic longitudinal plasma oscillations are functions of the field amplitude. Possible instability mechanisms are discussed.

1. The effect of a high-frequency electromagnetic field on plasma oscillations has been considered by us in the hydrodynamic approximation in an earlier paper.[1] In the present paper we develop a kinetic approach to this problem. It is assumed that the plasma density is low so that collisions can be neglected.

The problem may be formulated as follows. A monochromatic plane electromagnetic wave of arbitrary amplitude is propagated through a uniform plasma. If the density of the plasma is perturbed by any external effect the electromagnetic field is partially reflected from points at which the plasma density is high and is increased at points of reduced density. This process can be of interest if the characteristic dimensions of the perturbation are of the order of the electromagnetic wavelength. The increased intensity of the electromagnetic field leads to an interaction with the plasma oscillations in which the phase velocity of the plasma waves are functions of the amplitude of the electromagnetic field. Under certain conditions this mechanism can result in an instability, that is to say, in perturbations which increase in time.

2. We consider the one-dimensional problem, assuming that all quantities depend on the single spatial coordinate z. The motion of the ions and electrons is described by the kinetic equations (collisions are neglected):

$$\frac{\partial f_\alpha}{\partial t} + v_z' \frac{\partial f_\alpha}{\partial z'} + \frac{e_\alpha}{m_\alpha}\left(E_x - \frac{v_z'}{c} H_y\right)\frac{\partial f_\alpha}{\partial v_x'} + \left(E_z + \frac{v_x'}{c} H_y\right)\frac{\partial f_\alpha}{\partial v_z'} = 0. \quad (1)$$

Here $\alpha = i$ or e, for ions or electrons respectively.

The electromagnetic field satisfies Maxwell's equations

$$\frac{\partial^2 E_x}{\partial z^2} = \frac{4\pi}{c^2}\frac{\partial}{\partial t}\sum_\alpha e_\alpha \int v_x' f_\alpha \, d\mathbf{v}' + \frac{1}{c^2}\frac{\partial^2 E_x}{\partial t^2}, \quad (2)$$

$$\frac{\partial E_z}{\partial z} = 4\pi \sum_\alpha e_\alpha \int f_\alpha \, d\mathbf{v}', \quad (3)$$

$$\frac{\partial E_x}{\partial z} = -\frac{1}{c}\frac{\partial H_y}{\partial t}. \quad (4)$$

It is well known[2,3] that in an inhomogeneous high-frequency electromagnetic field the particles execute rapid oscillations in the direction of the electric field and drift slowly along the field gradient. We separate the field into high-frequency components and low-frequency components. It will be assumed that the E_x is created by external sources and is characterized by a frequency Ω which is higher than the Langmuir frequency $\omega_0 = (4\pi N_0 e^2/m_e)^{1/2}$. In this field the particles execute rapid oscillations along the x axis. On the other hand, E_z results from the separation of charges in the slow drift motion of the particles in the z direction. The frequency of this field is of the same order as that of the plasma oscillations which, hereinafter, will be assumed to be much smaller than Ω. Introducing the following notation in the equations of motion

$$v_j' = v_j + \tilde{v}_j, \qquad j = x, y, z \quad (5)$$

(where v_j corresponds to the slow motion and $\tilde{v}_j$ to the fast oscillations) and assuming that in one oscillation period the particle is displaced by a distance much smaller than the characteristic distance in which the external field changes, we have

$$m_\alpha \frac{d\tilde{v}_x}{dt} = e_\alpha E_x(z, t), \qquad m_\alpha \frac{dv_z}{dt} = \frac{e_\alpha}{c}\overline{\tilde{v}_x H_y} + e_\alpha E_z \quad (6)$$

(the bar denotes averaging over the fast oscillation period).

Introducing the substitution of variables (5) in the kinetic equations (1), after averaging we obtain

$$\frac{\partial \bar{f}_\alpha}{\partial t} + v_z \frac{\partial \bar{f}_\alpha}{\partial z} + \frac{e_\alpha}{m_\alpha} E_z \frac{\partial \bar{f}_\alpha}{\partial v_z} + \frac{e_\alpha}{m_\alpha c}\overline{\tilde{v}_x H_y \frac{\partial f_\alpha}{\partial v_z}} = 0. \quad (7)$$

From Eqs. (2) and (3) we have

$$\frac{\partial^2 E_x}{\partial z^2} = \frac{4\pi}{c^2}\frac{\partial}{\partial t}\sum_\alpha e_\alpha \int \tilde{v}_x \bar{f}_\alpha \, d\mathbf{v} + \frac{1}{c^2}\frac{\partial^2 E_x}{\partial t^2},$$

$$\frac{dE_z}{dz} = 4\pi \sum_\alpha e_\alpha \int \bar{f}_\alpha \, d\mathbf{v} \qquad (8)$$

(hereinafter we will omit the bar over the averaged distribution function).

We seek a solution of the system (4), (7), and (8) by successive approximations, assuming that

$$f_\alpha = f_\alpha^{(0)} + f_\alpha^{(1)} + \ldots, \quad E = E^{(0)} + E^{(1)} + \ldots,$$
$$E_z = E_z^{(1)} + \ldots . \qquad (9)$$

The field $E_Z^{(0)}$ will be assumed to be zero because the plasma is quasi-neutral. The quantity $f_\alpha^{(0)}$ is the Maxwell distribution function:

$$f_\alpha^{(0)} = (m_\alpha / 8\pi T_\alpha)^{3/2} N_0 \exp(-m_\alpha v^2 / 2T_\alpha). \qquad (10)$$

In the zeroth approximation Eq. (8) assumes the form

$$d^2 E^{(0)} / dz^2 + \varkappa^2 E^{(0)} = 0$$

($\kappa^2 = \Omega^2\epsilon/c^2$, $\epsilon = 1 - \omega_0^2/\Omega^2$ and the motion of the ions in the high-frequency field is neglected). Whence

$$E^{(0)} = E_0 e^{i\varkappa z + i\Omega t}. \qquad (11)$$

As a first approximation, in Eq. (8) we write

$$E^{(1)} = E(z, t)\, e^{i\Omega t}.$$

It is assumed that the time dependence of the amplitude is slow since it is determined by the change in E_x due to the plasma oscillations. In solving Eq. (8), in general we can neglect the dependence of $E^{(1)}$ on time, taking t as a parameter.

In the first approximation we have from Eq. (8)

$$\frac{d^2 E^{(1)}}{dz^2} + \varkappa^2 E^{(1)} = \frac{4\pi}{c^2} E^{(0)} \sum_\alpha \frac{e_\alpha^2}{m_\alpha} \int f_\alpha^{(1)} d\mathbf{v}. \qquad (12)$$

Whence*

$$E^{(1)} = \frac{4\pi}{c^2 \varkappa} \int_\infty^z E^{(0)} \left(\sum_\alpha \frac{e_\alpha^2}{m_\alpha} \int f_\alpha^{(1)} d\mathbf{v} \right) \sin \varkappa (z - \zeta)\, d\zeta. \qquad (13)$$

Using Eqs. (11) and (13), we can find H_y from Eq. (4). Substituting in the kinetic equations (7) and averaging, we have

$$\frac{\partial \varphi_\alpha^{(1)}}{\partial t} + v_z \frac{\partial \varphi_\alpha^{(1)}}{\partial z} + \frac{e_\alpha}{m_\alpha} E_z \frac{\partial f_\alpha^{(0)}}{\partial v_z} - \frac{2\pi e_\alpha^2 E_0^2}{m_\alpha^2 c^2 \Omega^2} \frac{\partial \varphi_\alpha^{(0)}}{\partial v_z}$$
$$\times \int_\infty^z \left(\sum_\alpha \frac{e_\alpha^2}{m_\alpha} \int_{-\infty}^{\infty} \varphi_\alpha^{(1)} dv_z \right) \cos 2\varkappa (z - \zeta)\, d\zeta = 0. \qquad (14)$$

In order to obtain the complete system it is necessary to add the first-approximation equation for

$$\frac{\partial E_z}{\partial z} = 4\pi \sum_\alpha e_\alpha \int_{-\infty}^{\infty} \varphi_\alpha^{(1)} dv_z, \qquad \varphi_\alpha \equiv \int f_\alpha dv_x dv_y. \qquad (15)$$

We seek a solution of the system (14) and (15) which is proportional to $\exp(ist + ikz)$. The quantity s is assumed to be complex with a positive real part, corresponding to the Laplace transform.[4] The condition which must be satisfied to solve the system of homogeneous algebraic equations which we have obtained is given by the dispersion equation

$$1 + (\theta k^{*-2} - p\theta m_e^2 / m_i^2)\psi_i + (k^{*-2} - p)\psi_e - p\theta k^{*-2}\psi_e\psi_i = 0. \qquad (16)$$

where we have introduced the following notation:

$$k^* = kD, \quad \varkappa^* = \varkappa D, \quad D = (T_e / 4\pi N_0 e^2)^{1/2}, \quad \theta = T_e / T_i,$$
$$\xi = v_e / v_i, \quad v_e = (T_e / m_e)^{1/2}, \quad v_i = (T_i / m_i)^{1/2},$$

$$p = \omega_0^2 E_0^2 / 8\pi m_e c^2 N_0 \Omega^2 (k^{*2} - 4\varkappa^{*2}), \quad \psi_e = \frac{1}{\sqrt{2\pi}} \int \frac{te^{-t^2/2} dt}{t + Z},$$

$$\psi_i = \frac{1}{\sqrt{2\pi}} \int \frac{te^{-t^2/2} dt}{t + \xi Z}, \quad Z = \frac{s^*}{k^*}, \quad s^* = \frac{s}{\omega_0}.$$

Following Landau,[4] the integration in the expressions for ψ_e and ψ_j is carried out along a contour which is parallel to the real axis and which passes the singular points $t = -Z$ and $t = -\xi Z$ from below. We then obtain (cf. reference 5)

$$\psi_e = F(Z) + i\sqrt{\pi/2}\, Z e^{-Z^2/2},$$
$$\psi_i = F(\xi Z) + i\sqrt{\pi/2}\, Z\xi e^{-Z^2\xi^2/2}, \qquad (17)$$

where

$$F(Z) = 1 - Ze^{-Z^2/2} \int_0^Z e^{-\tau^2/2} d\tau.$$

3. We now investigate the dispersion equation. Consider the case in which $k^{*2} \ll 1$ and $k^{*2}p \ll 1$. In practice this means that we are considering perturbations characterized by wavelengths considerably longer than the Debye radius but not as large as a half-wavelength of the electromagnetic wave, because when $k \to 2\kappa$, p approaches ∞. Equation (16) assumes the form

$$\theta\psi_i + \psi_e = p\theta\psi_e\psi_i. \qquad (18)$$

Suppose further that $Z = \alpha + i\beta$ ($\alpha = \omega/kv_e$ is the dimensionless frequency and $\beta = \gamma/kv_e$ is the decay factor). We seek a solution for which $\alpha \gg \beta$. Expanding in powers of β/α, we have from Eq. (18)

$$\theta F(\xi\alpha) + F(\alpha) = p\theta F(\xi\alpha) F(\alpha), \qquad (19)$$

$$\beta = \sqrt{\frac{\pi}{2}}\, \alpha \frac{p\theta [F(\xi\alpha) e^{-\alpha^2/2} + \xi F(\alpha) e^{-\xi^2\alpha^2/2}] - \theta\xi e^{-\xi^2\alpha^2/2} - e^{-\alpha^2/2}}{F'(\alpha) + \theta F'(\xi\alpha) - p\theta [F(\alpha) F(\xi\alpha)]'} \qquad (19a)$$

*The field $E^{(1)}$ is bounded at infinity.

(the primes denote differentiation with respect to α).

Equation (19) can be used to determine α. Once α is known we can use Eq. (19a) to determine β. We make the assumption (which is justified by the results) that $\alpha \ll 1$ and $\xi\alpha \gg 1$; thus, using the expansion of the function $F(x)$ for small and large values of the argument (cf. reference 5), we have when $\theta \gg 1$

$$\alpha^2 = (m_e/m_i)(1-p) \tag{20}$$

or, in the usual units,

$$\left(\frac{\omega}{ka}\right)^2 = 1 - \frac{1}{\gamma(k^2/\varkappa^2 - 4)}, \quad a^2 = \frac{T_e}{m_i}, \quad \gamma = \frac{\varepsilon}{1-\varepsilon}\frac{T_e}{\Phi}, \tag{21}$$

where Φ is the effective potential, which is

$$\Phi = e^2E_0^2/m_e\Omega^2 \approx 4.8 \cdot 10^{-8}E_v\lambda^2, \qquad \lambda = c/\Omega.$$

The ion mass is taken as 3.3×10^{-24} g and E_V is the amplitude of the electric field in volts per centimeters.

Computing the damping factor we have

$$\beta = \sqrt{\frac{\pi}{8}\frac{m_e}{m_i}\frac{1+p}{1-p}}. \tag{22}$$

Equation (21) coincides with the corresponding hydrodynamic formula which has been obtained earlier.[1] In contrast with the hydrodynamic case, the oscillations characterized by the dispersion relation in Eq. (20) exist, as is shown by an investigation of Eq. (19), if θ is larger than some number of order unity (an estimate shows that the relation $\theta \gtrsim 3.5$ must be satisfied). When $\theta \sim 1$, $1-p > 0$, and $p \sim 1$ these oscillations are highly damped. If $p = 0$, we have $\omega = (T_e/m_i)^{1/2}k$, i.e., these oscillations become quasi-acoustic ion oscillations such as those which have been considered by a number of authors.[6-8*] While these oscillations take place the electrons move, without collisions, in the potential well which is formed because the ions are shifted from their equilibrium positions. The electrons and the electromagnetic field produce an effective pressure and the effective density is determined by the ions. The ions move slowly; in one period they traverse a path which is $1/\xi$ of the wavelength, i.e., the ions do not leave the region of the perturbation. When these oscillations are produced long-range electric forces arise in the plasma. As is well known, in a gas consisting of neutral particles the production of acoustic oscillations without collisions is impossible. The oscillations characterized by the dispersion relation in Eq. (21) are analogous to magneto-acoustic oscillations but the role of the magnetic pressure is played by the average pressure of the high-frequency electromagnetic field. When $p > 1$, we have $\mathrm{Re}\, s < 0$, i.e., there is an instability which, as in the hydrodynamic case, arises by virtue of a resonance if the wavelength of the perturbation is equal to half the wavelength of the electromagnetic wave. Since the Fourier spatial spectrum of any localized perturbation contains the harmonic with $k = 2\kappa$, it may be assumed that a uniform plasma in the field of a high-frequency traveling electromagnetic wave becomes unstable when $p > 1$ ($\theta \gg 1$) regardless of the amplitude of the electromagnetic field.

In the present paper we have considered the linearized equations. Hence we cannot determine the final results of the appearance of an instability within the framework of the present analysis. However, it may be assumed that if the pressure of the electromagnetic field $E_0^2/8\pi$ is much smaller than the plasma pressure the instability will only lead to small oscillations.

The author wishes to thank Academician M. A. Leontovich for discussion of this work.

*This problem has also been considered in the author's Diploma paper, Moscow Engineering Physics Institute, 1953.

[1] T. F. Volkov, Сб. Физика плазмы и проблема управляемых термоядерных реакций (Plasma Physics and the Problem of a Controlled Thermonuclear Reaction), **4**, Acad. Sci. U.S.S.R., Moscow, 1958, p. 98.

[2] R. Z. Sagdeev, ibid., vol. III, 346 (1958).

[3] A. V. Gaponov and M. A. Miller, J. Exptl. Theoret. Phys. (U.S.S.R.) **34**, 242 (1958), Soviet Phys. JETP **7**, 168 (1958).

[4] L. D. Landau, J. Exptl. Theoret. Phys. (U.S.S.R.) **16**, 574 (1936).

[5] V. N. Faddeeva and N. M. Terent'ev, Таблицы значений интеграла вероятностей от комплексного аргумента (Tables of Values of the Probability Integral for Complex Arguments), Gostekhizdat, Moscow, 1954.

[6] J. B. Bernstein, Phys. Rev., **109**, 10 (1958).

[7] S. I. Braginskiĭ and A. P. Kazantsev, Физика плазмы и проблема управляемых термоядерных реакций (Plasma Physics and the Problem of a Controlled Thermonuclear Reaction) **4**, Acad. Sci. U.S.S.R., Moscow, 1958, p. 24.

[8] K. N. Stepanov, J. Exptl. Theoret. Phys. (U.S.S.R.) **34**, 1292 (1958), Soviet Phys. JETP **7**, 892 (1958).

Translated by H. Lashinsky
78

ON THE SOLUTION OF THE KINETIC EQUATION FOR A PLASMA IN A VARIABLE MAGNETIC FIELD

Yu. N. BARABANENKOV

Moscow State University

Submitted to JETP editor September 17, 1958

J. Exptl. Theoret. Phys. (U.S.S.R.) **37**, 427-429 (August, 1959)

The motion of a completely ionized plasma (collisions being neglected) along a narrow magnetic tube of an axially symmetrical magnetic field is considered by means of the kinetic equation. The equation is solved under the assumption of sufficiently slow variation of the magnetic field. Canonical variables are chosen as the independent variables of the distribution function.

We consider a completely ionized plasma without collisions, contained in a narrow magnetic tube of an axially magnetic field (the axis of the tube coincides with the axis of symmetry of the field). The motion of the charge along the tube is described by the following equations[1] (in the Hamiltonian form)

$$\dot{V}_\parallel = -\partial\mathcal{H}/\partial x, \qquad \dot{x} = \partial\mathcal{H}/\partial V_\parallel,$$

$$\mathcal{H}(J_\perp, V_\parallel, x, t) = {}^1/_2 [V_\parallel^2 + J_\perp H(x, \mu)],$$

$$J_\perp \equiv V_\perp^2 / H(x, \mu) = \text{const}. \tag{1}$$

Here $V_\parallel$ and $V_\perp$ are the components of the velocity of the charge along and perpendicular to the magnetic tube, and μ is a time dependent parameter.

We carry out a canonical transformation of the variables x, $V_\parallel$ to the angle variable φ and the action variable $J_\parallel$:

$$V_\parallel = \partial S(J_\perp, J_\parallel, x, t)/\partial x, \qquad \varphi = \partial S(J_\perp, J_\parallel, x, t)/\partial J_\parallel,$$

$$\mathcal{H}' = \mathcal{H}(J_\perp, J_\parallel, t) + \partial S(J_\perp, J_\parallel, x, t)/\partial t. \tag{2}$$

The generating function* S and the action variable $J_\parallel$ are defined by the equations

$$S = \int [2\mathcal{H} - J_\perp H(x, \mu)]^{1/2} dx,$$

$$J_\parallel = \frac{1}{2\pi} \oint [2\mathcal{H} - J_\perp H(x, \mu)]^{1/2} dx, \tag{3}$$

where the integration is carried out along the trajectory of the charge for a fixed value of the parameter μ. In the variables φ and $J_\parallel$, the system (1) takes the form

$$\dot{J}_\parallel = \partial h/\partial\varphi, \qquad \dot{\varphi} = \omega - \partial h/\partial J_\parallel,$$
$$h \equiv -\partial S/\partial t, \qquad \omega \equiv \partial\mathcal{H}/\partial J_\parallel. \tag{4}$$

The system (4) corresponds to the Liouville equation for the distribution function* F

$$\frac{\partial F}{\partial t} + \frac{\partial h}{\partial\varphi}\frac{\partial F}{\partial J_\parallel} + \left(\omega - \frac{\partial h}{\partial J_\parallel}\right)\frac{\partial F}{\partial\varphi} = 0. \tag{5}$$

We assume that the magnetic field changes slowly with time

$$H^{-1}\partial H/\partial t \ll \langle V_\perp^2 \rangle^{1/2}/a, \tag{6}$$

where a is a distance of the order of the size of the inhomogeneity of the magnetic field along the magnetic tube. In this case we can look for a solution of Eq. (5) in the form of an expansion in powers of the small quantity $1/\omega$:

$$F = F^{(0)} + \lambda^{-1}F^{(1)} + \ldots,$$
$$\langle F^{(1)} \rangle_\varphi = \ldots = 0, \qquad \omega \equiv \lambda\omega_1, \tag{7}$$

where the index φ next to the averaging symbol denotes averaging over the angle variable φ. Substitution of (7) in (5) gives

$$\frac{\partial F^{(0)}}{\partial\varphi} = 0, \qquad \frac{\partial F^{(0)}}{\partial t} = 0,$$

$$F^{(1)} = -\frac{1}{\omega_1}\frac{\partial F^{(0)}}{\partial J_\parallel}(h - \langle h \rangle_\varphi). \tag{8}$$

Thus, limiting ourselves to terms proportional to

*Generally speaking, in the case of an arbitrary dependence of μ on the time, the generating function is equal to $S + S_1(J_\perp, J_\parallel, \mu)$, where S_1 is a certain function (see reference 2). However, in our approximation, S_1 can be omitted.

*As is explained below, in our case no sufficiently slow change of the magnetic field of the space charge is produced by the motion of the plasma. Therefore there is no necessity of making a distinction between the distribution functions of the electrons and ions.

$1/\omega$, we obtain the following solution of Eq. (5):

$$F(J_\perp, J_\parallel, \varphi, t) = F^{(0)}(J_\perp, J_\parallel) - \frac{1}{\omega}\frac{\partial F^{(0)}}{\partial J_\parallel}(h - \langle h\rangle_\varphi). \quad (9)$$

We shall give another derivation of Eq. (9). For this purpose we note that under conditions (6), the system (4) is a system with a rapidly changing phase.[3] Its approximate solution has the form

$$J_\parallel = \bar{J}_\parallel + (h - \langle h\rangle_\varphi)/\omega, \qquad d\bar{J}_\parallel/dt = 0. \quad (10)$$

If at the initial moment the distribution function is equal to $F^{(0)}(J_\perp, J_\parallel)$, then at the instant t we have

$$F(J_\perp, J_\parallel, \varphi, t) = F^{(0)}(J_\perp, \bar{J}_\parallel) \approx F^{(0)}(J_\perp, J_\parallel) - \omega^{-1}(\partial F^{(0)}/\partial J_\parallel)(h - \langle h\rangle_\varphi). \quad (11)$$

According to (10), the action variable itself, $J_\parallel$ is not adiabatically invariant, but its average value $\bar{J}_\parallel$ over the period of the unperturbed motion of the system (4) is (i.e., for $\mu = \text{const.}$). As is evident from (11), the function $F^{(0)}$ in (9) can be set equal to the distribution function at the initial instant.

Let us consider a specific example. We describe the magnetic field in the form

$$H(x, t) = \bar{H}(t)(1 + x^2/a^2), \quad (12)$$

and the distribution function at the initial instant as a Maxwell distribution

$$F^{(0)} = N_0(\pi\Theta)^{-3/2}\exp[-(V_\perp^2 + V_\parallel^2)/\Theta]. \quad (13)$$

According to Eq. (9), we get

$$F(x, V_\parallel, t) = N_0(\pi\Theta)^{-3/2}\left[1 - \frac{1}{2\Theta}\frac{\dot{\bar{H}}}{\bar{H}}\left(\frac{\bar{H}_0}{\bar{H}}\right)^{1/2} V_\parallel x\right] \times \exp\left\{-\frac{1}{\Theta}\left(\frac{\bar{H}_0}{\bar{H}}\right)^{1/2}\left[\left(\frac{\bar{H}_0}{\bar{H}}\right)^{1/2}\frac{V_\perp^2}{\Phi(x, t)} + V_\parallel^2\right]\right\}, \quad (14)$$

where

$$\Phi(x, t) = (a^2 + x^2)/[a^2 + (\bar{H}/\bar{H}_0)^{1/2}x^2]. \quad (15)$$

Calculations of the moments from zeroth to third order in the velocity relative to (14) leads to the following relations:

$$\frac{n}{n_0} \equiv \frac{N}{N_0}\frac{\bar{H}_0}{\bar{H}} = \left(\frac{\bar{H}}{\bar{H}_0}\right)^{1/4}\Phi = \begin{cases}(\bar{H}/\bar{H}_0)^{1/4} & \text{for } x \to 0,\\ (\bar{H}/\bar{H}_0)^{-1/4} & \text{for } x \to \pm\infty,\end{cases}$$

$$\langle V_\perp^2\rangle/\langle V_\perp^2\rangle_0 = (\bar{H}/\bar{H}_0)\Phi, \qquad \langle V_\parallel^2\rangle/\langle V_\parallel^2\rangle_0 = (\bar{H}/\bar{H}_0)^{1/2},$$
$$\langle V_\perp^2\rangle/2\langle V_\parallel^2\rangle = (\bar{H}/\bar{H}_0)^{1/2}\Phi \geqslant 1 \qquad \langle V_\parallel\rangle = -(\dot{\bar{H}}/4\bar{H})x,$$
$$\langle V_\perp^2 V_\parallel\rangle = \langle V_\perp^2\rangle\langle V_\parallel\rangle, \qquad \langle V_\parallel^3\rangle = 3\langle V_\parallel^2\rangle\langle V_\parallel\rangle. \quad (16)$$

According to (16), as the magnetic field is increased the plasma is compressed to the region of its minimum value. The kinetic temperatures of the plasma increase. In this case the velocity distribution becomes anisotropic: the transverse temperature is greater than the longitudinal. The heat flow is equal to 0 and the compression of the plasma is adiabatic.

In conclusion I take this opportunity to thank Professor Ya. P. Terletskiĭ for the discussion of the research.

[1] H. Alfvén, Cosmical Electrodynamics, Oxford, 1950 (Russian translation, IIL, 1952).

[2] V. N. Volosov, Dokl. Akad. Nauk SSSR **123**, 587 (1958).

[3] N. N. Bogolyubov, and Yu. A. Mitropol'skiĭ, Асимптотические методы в теории нелинейных колебаний (Asymptotic Methods in the Theory of Nonlinear Oscillations) Fizmatizdat, 2nd ed., 1958.

Translated by R. T. Beyer
79

DISPERSION OF ELECTROMAGNETIC WAVES IN CRYSTALS

V. M. AGRANOVICH

Submitted to JETP editor January 7, 1959

J. Exptl. Theoret. Phys. (U.S.S.R.) 37, 430-441 (August, 1959)

A microscopic quantum theory of dispersion of electromagnetic waves in molecular crystals is developed. An expression is derived for the index of refraction due to the contribution of the excited states of the electrons. Interaction between exciton states and the field is considered without the use of perturbation theory.

INTRODUCTION

A microscopic quantum theory of dispersion of electromagnetic waves in isotropic, condensed media was developed by Fano.[1] In contrast to earlier work,[2] the oscillator strengths of electromagnetic transitions were not considered to be small in the work of Fano. Certain interest attaches to a generalization of the results obtained by Fano and to an analysis of the dispersion of electromagnetic waves in crystals of arbitrary symmetry.

A microscopic theory of dispersion, within the framework of classical physics, was developed by Born and Ewald.[3]

In the present paper we develop a microscopic quantum theory of the dispersion of electromagnetic waves for a specific model of a molecular crystal. However, the method of consideration can be used for any crystal.

The vibrations of the nucleus were not taken into account in this analysis. Consequently, the problem of the complex index of refraction should be considered separately.

1. TRANSITION TO THE REPRESENTATION OF SECOND QUANTIZATION

In the problem considered here of the interaction of the electromagnetic field with the electrons of a crystal, it is useful to employ a Coulomb gauge for the vector potential and thus assume that the vector potential of the microscopic field satisfies the condition (see reference 3):

$$\operatorname{div} \mathbf{A} = 0. \tag{1}$$

In this case, as is well known, the complete Hamiltonian of the system of the electrons and the field can be written in the form[4]

$$\hat{H} = \hat{H}_1 + \hat{H}_2 + \hat{H}_{\text{int}}, \tag{2}$$

where the Coulomb interaction of all charges making up the crystal are included in $\hat{H}_1$, $\hat{H}_2$ is the Hamiltonian corresponding to the free electromagnetic field of the transverse photons, $\hat{H}_{\text{int}}$ is the operator of interaction between all charges and the transverse field of the photons. In a molecular crystal, the operator $\hat{H}_1$ can best be represented in the following form

$$\hat{H}_1 = \sum_{\mathbf{n}\alpha} \hat{H}_{\mathbf{n}\alpha} + \frac{1}{2} \sum_{\mathbf{n}\alpha,\, \mathbf{n}\beta}{}' \hat{V}_{\mathbf{n}\alpha,\, \mathbf{m}\beta}. \tag{3}$$

In this expression $H_{\mathbf{n}\alpha}$ represents the Hamiltonian of an isolated molecule located at the position $\mathbf{n}\alpha$ ($\mathbf{n}$ is the unit lattice vector and α is the number of the molecule in the cell, $\alpha = 1, 2, \ldots, \sigma$), $\hat{V}_{\mathbf{n}\alpha,\mathbf{m}\beta}$ is the operator of Coulomb interaction between the charges of the molecules $\mathbf{n}\alpha$ and $\mathbf{m}\beta$.

We proceed to the representation of second quantization. For this purpose we choose as the set of basic functions the wave functions describing the stationary states of the isolated molecule.

Let $\varphi^{\mathrm{f}}_{\mathbf{n}\alpha}$ be the wave function of the $\mathbf{n}\alpha$ molecule in a state f and not interacting with its surroundings. The value $\mathrm{f} = 0$ corresponds to the ground state of the molecule. The function $\varphi^{\mathrm{f}}_{\mathbf{n}\alpha}$ satisfies the equation

$$H_{\mathbf{n}\alpha}\varphi^{f}_{\mathbf{n}\alpha}(\tau_{\mathbf{n}\alpha}) = E^{f}_{\mathbf{n}\alpha}\varphi^{f}_{\mathbf{n}\alpha}(\tau_{\mathbf{n}\alpha}), \tag{4}$$

where $\tau_{\mathbf{n}\alpha}$ is the set of coordinates of the electrons of the molecule $\mathbf{n}\alpha$. To abbreviate the notation, we denote the set of indices by the single index $\mathrm{s} \equiv (\mathbf{n}\alpha)$.

We now introduce normalized and antisymmetrized products (neglecting the overlap integrals):

$$\Psi_{\ldots N_s(f_s)\ldots}(\tau_1, \ldots, \tau_{N\sigma}) = [(N\sigma S)!]^{-1/2} \sum_P (-1)^P P \prod_{s,\, f_s}{}' \varphi^{f_s}_s(\tau_s), \tag{5}$$

where S is the number of electrons in a molecule. Each occupation number $\mathrm{N_S}(\mathrm{f_S})$ is equal to zero or unity and indicates the state of the s-th mole-

cule. Therefore,

$$\sum_{f_s} N_s(f_s) = 1, \qquad \sum_{s,\, f_s} N_s(f_s) = N\sigma. \tag{6}$$

Here N is the number of elementary cells in the basic volume and σ is the number of molecules in the elementary cell. We can represent the wave function, which depends on the variables $\{\tau_S\}$, in the following form:

$$\Psi(\tau_1, \ldots, \tau_{N\sigma}) = \sum_{\ldots N_s(f_s)\ldots} C(\ldots N_s(f_s)\ldots) \times \Psi_{\ldots N_s(f_s)\ldots}(\tau_1, \ldots, \tau_{N\sigma}). \tag{7}$$

Here $C(\ldots N_S(f_S)\ldots)$ is the wave function of the electrons in the second-quantization representation. Let the additive operator

$$\hat{U}_1 = \sum_s \hat{U}_s(\tau_s) \tag{8}$$

and each of the operators $\hat{U}_S$ act only on the variable τ_S. Then, if we neglect the exchange of electrons which belong to different molecules, the matrix element is

$$\{\hat{U}_1\}_{\ldots N_s(f_s)\ldots N'_s(f_s)\ldots} = \sum_{p,\, f_p,\, f'_p} \langle \varphi_{f_p}, \hat{U}_p \varphi_{f'_p} \rangle \{a_{f'_p f_p}\}_{\ldots N_s(f_s)\ldots \ldots N'_s(f_s)\ldots} \tag{9}$$

where

$$\{a_{f'_p f_p}\}_{\ldots N_s(f_s)\ldots \ldots N'_s(f_s)\ldots} = N_p(f_p)\, N'_p(f'_p) \prod_{f_{s_1},\, s_1 \neq p} \delta[N_{s_1}(f_{s_1}) - N'_{s_1}(f_{s_1})].$$

Since we shall be interested below in the excited states of a crystal, which correspond to a completely determined — say the f-th — excited state in the isolated molecule, we shall assume that f_S takes on only two values, $f_S = 0$ or f. Then, if $f_p \neq f'_p$,

$$N_p(f_p)\, N'_p(f'_p) = N_p(f_p)\, N'_p(f'_p)\, \delta[N'_p(f'_p) - N_p(f'_p) - 1] \times \delta[N'_p(f_p) - N_p(f_p) + 1],$$

where $\delta(x) = 1$ if $x = 0$, and $\delta(x) = 0$ if $x \neq 0$. Now if $f_p \neq f'_p$,

$$N_p(f_p)\, N'_p(f_p) = N_p(f_p)\, N'_p(f_p) \times \delta[N'_p(f_p) - N_p(f_p)]\, \delta[N'_p(f'_p) - N_p(f'_p)].$$

Therefore, for arbitrary f_p and f'_p,

$$\{a_{f'_p f_p}\}_{\ldots N_s(f_s)\ldots N'_s(f_s)\ldots} = N_p(f_p)\, N'_p(f'_p) \prod_{s,\, f_s} \delta[N'_s(f_s) - N_s(f_s) + \delta(f_s - f_p) - \delta(f_s - f'_p)].$$

Moreover, since

$$N_p(f_p) = \delta[N_p(f_p) - 1], \qquad N'_p(f'_p) = \delta[N'_p(f'_p) - 1],$$

we conclude that

$$\{a_{f'_p f_p}\}_{\ldots N_s(f_s)\ldots, N'_s(f_s)\ldots} = \delta[N_p(f_p) - 1]\, \delta[N_p(f'_p) - \delta(f_p - f'_p)] \prod_{s,\, f_s} \delta[N'_s(f_s) - N_s(f_s) + \delta(f_s - f_p) - \delta(f_s - f'_p)].$$

Thus the operator $a_{f'_p f_p}$ can be represented as the product of two operators

$$a_{f'_p f_p} = b^+_{f_p} b_{f'_p}, \tag{10}$$

which are defined as follows:

$$b_{f_p} C(\ldots N_s(f_s)\ldots) = \delta[N_p(f_p)]\, C(\ldots N_s(f_s) + \delta(f_s - f_p)\ldots),$$

$$b^+_{f_p} C(\ldots N_s(f_s)\ldots) = \delta[N_p(f_p) - 1]\, C(\ldots N_s(f_s) - \delta(f_s - f_p)\ldots). \tag{11}$$

It is easy to show that

$$a_{f_p f_p} C(\ldots N_s(f_s)\ldots) = N_p(f_p)\, C(\ldots N_s(f_s)\ldots),$$

i.e., that

$$b^+_{f_p} b_{f_p} = N_p(f_p).$$

On the other hand,

$$b_{f_p} b^+_{f_p} = 1 - N_p(f_p).$$

Thus,

$$b_{f_p} b^+_{f_p} + b^+_{f_p} b_{f_p} = 1.$$

Since the operators b_{f_p}, $b^+_{f_p}$ and $b_{f'_p}$, $b^+_{f'_p}$ act on different variables for $f_p \neq f'_p$, the following commutation rules hold:

$$b_{f_p} b_{f'_p} - b_{f'_p} b_{f_p} = 0, \qquad b^+_{f_p} b^+_{f'_p} - b^+_{f'_p} b^+_{f_p} = 0,$$

$$b_{f_p} b^+_{f'_p} - b^+_{f'_p} b_{f_p} = 0.$$

The operators with different p commute in all combinations.

Thus the operators b_{f_p} are neither Fermi nor Bose operators (they are the so-called Pauli operators). Making use of (9) and (10) we find that

$$U_1 = \sum_{p,\, f_p,\, f'_p} \langle \varphi_{f_p}, \hat{U}_p \varphi_{f'_p} \rangle b^+_{f_p} b_{f'_p}. \tag{12}$$

For an operator of the binary type

$$\hat{U}_2 = \sum_{p \neq p_1} U_{pp_1}(\tau_p, \tau_{p_1})$$

we can in similar fashion establish the following

expression in the second-quantization representation:

$$\hat{U}_2 = \sum_{\substack{p \neq p_1 \\ (f_p f'_p f_{p_1} f'_{p_1})}} U_{pp_1}(f_p f_{p_1};\ f'_p f'_{p_1}) b^+_{f_p} b^+_{f_{p_1}} b_{f'_p} b_{f'_{p_1}}. \qquad (13)$$

Here

$$U_{pp_1}(f_p f_{p_1};\ f'_p f'_{p_1}) = \int \varphi_p^{f_p *} \varphi_{p_1}^{f_{p_1} *} U_{pp_1} \varphi_p^{f_p} \varphi_{p_1}^{f_{p_1}} d\tau_p d\tau_{p_1}$$

— exchange terms (14)

We now write down (in the second-quantization representation) the operator $\hat{H}_1$. Making use of Eqs. (12) and (13), we find that

$$\hat{H}_1 = \sum_{s, f_s} E_s^{f_s} N_s(f_s) + \frac{1}{2} \sum_{\substack{s \neq s_1 \\ (f_s, f_{s_1}, f'_s, f'_{s_1})}} V_{ss'}(f_s f_{s_1};\ f'_s f'_{s_1}) b^+_{f_s} b_{f'_s} b^+_{f_{s_1}} b_{f'_{s_1}}$$

$$\equiv \hat{H}_1^{(0)} + \hat{H}_1^{(1)} + \hat{H}_1^{(2)},$$

where

$$\hat{H}_1^{(0)} = \sum_{s, f_s} E_s^{f_s} N_s(f_s) + \frac{1}{2} \sum_{\substack{s \neq s_1 \\ (f_s, f_{s_1})}} V_{ss_1}(f_s f_{s_1};\ f_s f_{s_1}) N_s(f_s) N_{s_1}(f_{s_1}),$$

$$\hat{H}_1^{(1)} = \frac{1}{2} \sum_{s \neq s_1} V_{ss_1}(0f;\ f0) [b^+_{s0} b_{sf} b^+_{s_1 f} b_{s_1 0} + b^+_{s_1 0} b_{s_1 f} b^+_{sf} b_{s0}],$$

$$\hat{H}_1^{(2)} = \frac{1}{2} \sum_{s \neq s_1} V_{ss_1}(00;\ ff) [b^+_{s0} b^+_{s_1 0} b_{sf} b_{s_1 f} + b^+_{sf} b^+_{s_1 f} b_{s0} b_{s_1 0}]. \qquad (15)$$

We shall consider in what follows such excited states of the crystal which, for $V_{ss_1} \to 0$, correspond to a number of excited molecules which is small in comparison with the number N. Therefore, we shall neglect in the Hamiltonian $\hat{H}_1^{(0)}$ the components that are quadratic relative to $N_s(f)$.

In this approximation (neglecting the interaction of the excitons),

$$\hat{H}_1^{(0)} = E_0 + \sum_s N_s(f) \Big\{ (E_s^f - E_s^0) + \sum_{s_1}{}' [V_{ss_1}(0f,\ 0f) - V_{ss_1}(00,\ 00)] \Big\},$$

where

$$E_0 = \sum_s E_s^0 + \frac{1}{2} \sum_{s \neq s_1} V_{ss_1}(00,\ 00).$$

We now introduce the operators

$$B_{sf} = b^+_{s0} b^+_{sf}, \qquad B_{sf} = b^+_{sf} b_{s0}. \qquad (16)$$

Then

$$B^+_{sf} B_{sf} = b^+_{s0} b_{sf} b^+_{sf} b_{s0} = N_s(f)[1 - N_s(0)]$$

$$= N_s(f) - N_s(0) N_s(f) = N_s(f),$$

since

$$N_s(0) + N_s(f) = 1.$$

Further,

$$B_{sf} B^+_{sf} - B^+_{sf} B_{sf} = N_s(0)[1 - N_s(f)]$$

$$- N_s(f)[1 - N_s(0)] = 1 - 2N_s(f).$$

In the states under examination, the mean value is $\overline{N_s(f)} \ll 1$. Therefore, we can assume approximately that

$$B_{sf} B^+_{sf} - B^+_{sf} B_{sf} = 1. \qquad (17)$$

Since, for $s \neq s_1$, the operators B_{sf}, B^+_{sf} and $B_{s_1 f}$, $B^+_{s_1 f}$ commute with one another, we conclude that these operators are approximately operators of the Bose type. Thus, using (15) and (16), we obtain the following expression for the operator $\hat{H}_1$:

$$\hat{H}_1 = E_0 + \sum_s \Big\{ (E_s^f - E_s^0) + \sum_{s_1}{}' [V_{ss_1}(0f,\ 0f) - V_{ss_1}(00,\ 00)] \Big\} B^+_{sf} B_{sf} + \sum_{s \neq s_1} V_{ss_1}(0f,\ 0f) B^+_{sf} B_{s_1 f}$$

$$+ \frac{1}{2} \sum_{s \neq s_1} V_{ss_1}(00,\ ff)[B_{sf} B_{s_1 f} + B^+_{sf} B^+_{s_1 f}]. \qquad (18)$$

To determine the elementary excitations corresponding to the Hamiltonian $\hat{H}_1$, it is necessary to diagonalize the quadratic form (18). As Tyablikov has shown, a quadratic form of the type (18) is diagonalized as the result of a transformation to the new Bose-operators B_ρ and B^+_ρ (the method of Tyablikov is given in detail in the book of Bogolyubov[5]):

$$B_{sf} = \sum_\rho (B_\rho u_{s\rho} + B^+_\rho v^*_{s\rho}), \qquad B^+_{sf} = \sum_\rho (B^+_\rho u^*_{s\rho} + B_\rho v_{s\rho}), \qquad (19)$$

where the quantities $u_{s\rho}$ and $v_{s\rho}$ entering into Eq. (19) are determined as the solutions of the equations

$$E u_s = \sum_{s_1} [\delta_{ss_1} \Delta + (1 - \delta_{ss_1}) V_{ss_1}(0f,\ 0f)] u_{s_1} + \sum_s (1 - \delta_{ss_1}) V_{ss_1}(00,\ ff) v_{s_1},$$

$$- E v_s = \sum_{s_1} [\delta_{ss_1} \Delta + (1 - \delta_{ss_1}) V_{ss_1}(0f,\ 0f)] v_{s_1} + \sum_{s_1} (1 - \delta_{ss_1}) V_{ss_1}(00, ff) u_{s_1}. \qquad (20)$$

The possible values of E are determined from the condition of the existence of nontrivial solutions for the set of equations (20), where

$$\Delta \equiv (E_s^f - E_s^0) + \sum_{s_1}{}' [V_{ss_1}(0f, 0f) - V_{ss_1}(00, 00)].$$

The solutions of Eq. (20) should be chosen to satisfy the following normalization conditions (see reference 5):

$$\sum_s (|u_s|^2 - |v_s|^2) = 1. \quad (21)$$

Recalling now that $s = (n\alpha)$, we shall seek solutions of the system (20) in the following form:

$$u_{n\alpha} = N^{-1/2} u_\alpha e^{ikr_{n\alpha}}, \qquad v_{n\alpha} = N^{-1/2} v_\alpha e^{ikr_{n\alpha}}. \quad (22)$$

Substituting (22) in (20), we conclude that u_α and v_α satisfy a set of 2σ equations

$$(E - \Delta) u_\alpha = \sum_\beta \Gamma^{(1)}_{\alpha\beta}(k) u_\beta + \sum_\beta \Gamma^{(2)}_{\alpha\beta}(k) v_\beta,$$

$$-(E + \Delta) v_\alpha = \sum_\beta \Gamma^{(1)}_{\alpha\beta}(k) v_\beta + \sum_\beta \Gamma^{(2)}_{\alpha\beta}(k) u_\beta, \quad (23)$$

where

$$\Gamma^{(1)}_{\alpha\beta}(k) = \sum_m V_{n\alpha,\, m\beta}(0f,\ 0f) \exp\{ik(r_{m\beta} - r_{n\alpha})\},$$

$$\Gamma^{(2)}_{\alpha\beta}(k) = \sum_m V_{n\alpha,\, m\beta}(00,\ ff) \exp\{ik(r_{m\beta} - r_{n\alpha})\}. \quad (23a)$$

Equating the determinant of the set of equations (22) to zero, we obtain an equation for E. In the general case, for arbitrary k, an equation of order σ is obtained for the quantity E^2. This equation determines σ positive roots of $E_\mu(k)$ ($\mu = 1, 2, \ldots, \sigma$).

We consider, as an example, a crystal with a single molecule in the elementary cell ($\sigma = 1$). In this case, we find that

$$E(k) = \{[\Delta + \Gamma^{(1)}(k)]^2 - [\Gamma^{(2)}(k)]^2\}^{1/2}.$$

In those cases in which $\Delta \gg \Gamma^{(2)}(k)$,

$$E(k) \approx \Delta + \Gamma^{(1)}(k) - [\Gamma^{(2)}(k)]^2/2\Delta. \quad (24)$$

In the theory, where the Heitler-London method is used (which is equivalent to carrying out the diagonalization of the quadratic form (18) under the additional condition

$$\sum_s B^+_{sf} B_{sf} = 1,$$

see reference 6), the last term in (24) is absent. The value of the energy (24), as expected, turns out to be smaller than the value obtained with the use of the additional condition. However, this decrease is unimportant, since the ratio $|\Gamma^{(2)}(k)|/\Delta$ in molecular crystals, where Δ is of the order of several electron volts, is at most less than 0.1.* The operator $\hat{H}_1$ is represented by the new Bose-operators in the following form (see reference 5):

$$\hat{H}_1 = E_0 - \sum_{\alpha, k\mu} E_\mu(k) |v_\alpha(k, \mu)|^2 + \sum_{k\mu} E_\mu(k) B^+_{k\mu} B_{k\mu}. \quad (25)$$

*The difference between the expression E(k) and the corresponding value obtained by the Heitler-London method can become substantial when the width of the forbidden zone is of the same order as that of the allowed zone.

Thus $E_\mu(k)$ is the energy of the elementary excitation (μ, k). The second term in (25), which is absent when the Heitler-London method is used, is readily shown to be a small correction to the energy $E_0 \sim [\Gamma^{(2)}]^2/\Delta$.

2. DISPERSION OF ELECTROMAGNETIC WAVES IN MOLECULAR CRYSTALS

The Hamiltonian of transverse photons[4] has the form

$$\hat{H}_2 = \sum_{(qj)} \hbar q c\, a^+_{qj} a_{qj}. \quad (26)$$

In this expression, q is the wave vector, j (= 1 or 2) is the number of the transverse polarization, a^+_{qj} and a_{qj} are the Bose operators of annihilation and creation of transverse photons (qj). The interaction operator in the nonrelativistic approximation can be represented in the following form:

$$\hat{H}_{int} = -\sum_{(n\alpha)} \frac{e}{mc} \hat{A}(r_{n\alpha}) \hat{J}_{n\alpha} + \frac{e^2 S}{2mc^2} \sum_{(n\alpha)} \hat{A}^2(r_{n\alpha}) \equiv H^{I}_{int} + H^{II}_{int}, \quad (27)$$

where $\hat{J}_{n\alpha}$ is the operator of the total momentum of the electrons of the molecule $(n\alpha)$.

According to reference 4, the vector potential operator is

$$\hat{A}(r) = \sum_{(qj)} \sqrt{2\pi c^2 \hbar / Vqc}\, l_{qj} (a_{qj} e^{iqr} + a^+_{qj} e^{-iqr}). \quad (28)$$

We choose the wave functions of the isolated molecules to be real and assume that the isolated molecules are not in any of the stationary states and do not possess dipole moments.

Substituting Eq. (28) in (27), we get

$$\hat{H}^{I}_{int} = -\sum_{qj} \frac{e}{m} \sqrt{2\pi\hbar/Vqc} \left\{ a_{qj} \left[\sum_{n\alpha} l^{iqr_{n\alpha}} (l_{qj} \hat{J}_{n\alpha}) \right] + a^+_{qj} \left[\sum_{n\alpha} e^{-iqr_{n\alpha}} (l_{qj} \hat{J}_{n\alpha}) \right] \right\}. \quad (29)$$

Let us consider the operator

$$\hat{R}_\pm = \sum_{n\alpha} e^{\pm iqr_{n\alpha}} (l_{qj} \hat{P}_{n\alpha}),$$

where $\hat{P}_{n\alpha}$ is the dipole-moment operator of the molecule $(n\alpha)$. In the second-quantization representation,

$$\hat{R}_\pm = \sum_{n\alpha} e^{\pm iqr_{n\alpha}} (l_{qj} P^{0f}_{n\alpha}) (b^+_{n\alpha,0} b_{n\alpha,f} + b_{n\alpha,0} b^+_{n\alpha,f}),$$

or, transforming to the Bose operators $B_{q\mu}$, and neglecting transfer processes, we conclude that the operator $\hat{R}_\pm$ is given by

$$\hat{R}_{\pm} = \sqrt{N}\sum_{\mu}\left\{\sum_{\alpha}(\mathbf{l}_{qj}\mathbf{P}^{0f}_{\alpha})\,[u_{\alpha}(\mathbf{q}\mu) + v_{\alpha}(\mathbf{q}\mu)]\right\}(B_{\mp q\mu} + B^{+}_{\pm q\mu}).$$

We introduce the operator

$$\hat{\mathbf{J}}_{\pm} = \sum_{n\alpha} e^{\pm i\mathbf{q}\mathbf{r}_{n\alpha}}(\mathbf{l}_{qj}\mathbf{J}_{n\alpha}).$$

This operator is defined in the following way:

$$\hat{J}_{\pm} = (im/\hbar e)(\hat{H}_1\hat{R}_{\pm} - \hat{R}_{\pm}\hat{H}_1).$$

Therefore, making use of Eq. (25), we find that

$$\hat{\mathbf{J}}_{\pm} = \frac{im}{\hbar e}\sum_{\mu}E_{\mu}(\mathbf{q})\left\{\sum_{\alpha}(\mathbf{l}_{qj}\mathbf{P}^{0f}_{\alpha})\,[u_{\alpha}(\mathbf{q}\mu) + v_{\alpha}(\mathbf{q}\mu)]\right\}(B_{\mp q\mu} - B^{+}_{\pm q\mu}).$$

Thus, we finally obtain the following expression for the operator H^{I}_{int}:

$$H^{I}_{int} = \sum_{\mu, q, j} T(j, \mathbf{q}, \mu)\,[a_{qj}(B_{-q,\mu} - B^{+}_{q,\mu}) + a^{+}_{qj}(B_{q\mu} - B^{+}_{-q\mu})], \tag{30}$$

where

$$T(j, \mathbf{q}, \mu) = i\sqrt{2\pi N/qcV\hbar}\sum_{\alpha}(l_{q,j}\mathbf{P}^{0f}_{\alpha}) \times [u_{\alpha}(\mathbf{q},\mu) + v_{\alpha}(\mathbf{q}, \mu)]\,E_{\mu}(\mathbf{q}). \tag{30a}$$

Equations (30) and (30a) were obtained for crystals possessing a center of inversion. In such crystals the values of u_{α} and v_{α} can be chosen such that the conditions

$$u_{\alpha}(\mathbf{q}, \mu) = u_{\alpha}(-\mathbf{q}, \mu) = u^{*}_{\alpha}(\mathbf{q}, \mu),$$
$$v_{\alpha}(\mathbf{q}, \mu) = v_{\alpha}(-\mathbf{q}, \mu) = v^{*}_{\alpha}(\mathbf{q}, \mu).$$

are satisfied. In a similar way, we find that, with accuracy to within an unimportant constant term:

$$H^{II}_{int} = \frac{\hbar\omega_0^2}{4}\sum_{qj}\frac{1}{qc}(2a^{+}_{qj}a_{qj} + a_{qj}a_{-qj} + a_{qj} + a^{+}_{qj}a^{+}_{-qj}). \tag{31}$$

Here ω_0 is the frequency of the plasma oscillations

$$\omega_0^2 = 4\pi e^2 N_1 \sigma S/m,$$

where $N_1 = N/V$.

Combining Eqs. (30), (31), (26), and (25), and returning to the Hamiltonian of the entire system (2), we conclude that this Hamiltonian is given by

$$\hat{H} = E_0 - \sum_{\alpha,\mu,\mathbf{q}} E_{\mu}(\mathbf{q}, \mu)\,|v_{\alpha}(\mathbf{q}, \mu)|^2 + \sum_{\mathbf{q},\mu} E_{\mu}(\mathbf{q})\,B^{+}_{q\mu}B_{q\mu} + \sum_{qj}\hbar qc a^{+}_{qj}a_{qj} - \sum_{\mu,q,j} T(j, \mathbf{q}, \mu)\,[a_{qj}(B_{-q\mu} - B^{+}_{q\mu}) + a^{+}_{qj}(B_{q\mu} - B^{+}_{-q\mu})] + \frac{\hbar\omega_0^2}{4}\sum_{qj}\frac{1}{qc}(2a^{+}_{qj}a_{qj} + a_{qj}a_{-qj} + a^{+}_{qj}a^{+}_{-qj}). \tag{32}$$

The problem of the determination of the elementary excitations that characterize the entire system of electrons and the field is equivalent to the problem of the diagonalization of the Hamiltonian (32). From these considerations it follows that the only Bose operators involved are those which correspond to the wave vectors $\mathbf{q}$ and $-\mathbf{q}$. Therefore, for the diagonalization of Eq. (32), it is sufficient to examine the quadratic form

$$H_q = \sum_{\mu}E_{\mu}(\mathbf{q})(B^{+}_{q\mu}B_{q\mu} + B^{+}_{-q\mu}B_{-q\mu}) + \sum_{j}\hbar qc\,(a^{+}_{qj}a_{qj} + a^{+}_{-qj}a_{-qj}) \times\left(1 + \frac{\omega_0^2}{2q^2c^2}\right) + \frac{\hbar\omega_0^2}{2}\sum_{j}\frac{1}{qc}(a_{qj}a_{-qj} + a^{+}_{qj}a_{-qj}) - \sum_{\mu j}T(j, \mathbf{q}, \mu)\,[(a_{qj} + a^{+}_{-qj})(B_{-q\mu} - B^{+}_{q\mu}) + (a_{-qj} + a^{+}_{qj})(B_{q\mu} - B^{+}_{-q\mu})]. \tag{33}$$

The quadratic form (33) can be diagonalized with the aid of the method of Tyablikov, already used in Sec. 1. Following this method, we transform to new Bose operators ξ_{ρ} and ξ^{+}_{ρ}:

$$B_{q\mu} = \sum_{\rho}[\xi_{\rho}u_{q\mu}(\rho) + \xi^{+}_{\rho}v^{*}_{q\mu}(\rho)],$$
$$a_{qj} = \sum_{\rho}[\xi_{\rho}u_{qj}(\rho) + \xi^{+}_{\rho}v^{*}_{qj}(\rho)], \tag{34}$$

where the quantities u and v satisfy the following set of equations:

$$[E_{\mu}(\mathbf{q}) - \mathscr{E}]\,u_{q\mu} + \sum_{j}T(j, \mathbf{q}, \mu)(u_{qj} + v_{-qj}) = 0,$$
$$[E_{\mu}(\mathbf{q}) + \mathscr{E}]\,v_{-q\mu} - \sum_{j}T(j, \mathbf{q}, \mu)(u_{qj} + v_{-qj}) = 0, \tag{35}$$

$$(\hbar qc - \mathscr{E})\,u_{qj} - \sum_{\mu}T(j, \mathbf{q}, \mu)(u_{q\mu} - v_{-q\mu}) + \frac{\hbar\omega_0^2}{2qc}(u_{qj} + v_{-qj}) = 0,$$
$$(\hbar qc + \mathscr{E})\,v_{-qj} - \sum_{\mu}T(j, \mathbf{q}, \mu)(u_{q\mu} - v_{-q\mu}) + \frac{\hbar\omega_0^2}{2qc}(u_{qj} + v_{-qj}) = 0.$$

Comparing the first equation in this set with the second, and the third with the fourth, we find that

$$v_{-q\mu} = -\frac{E_{\mu}(\mathbf{q}) - \mathscr{E}}{E_{\mu}(\mathbf{q}) + \mathscr{E}}u_{q\mu}, \qquad v_{-qj} = \frac{\hbar qc - \mathscr{E}}{\hbar qc + \mathscr{E}}u_{qj}.$$

Up to now we have considered only one of the excited states of the molecules. However, it is possible to take all the excited states into consideration. For this purpose, it suffices to consider the index μ as a compound index characterizing not only the number of exciton zones, but also the

excitation level of the molecule corresponding to this zone. In this approximation, u and v are determined as before from the set of equations (35). However, the index μ now runs over an infinite set of values.

Such consideration of all the excited states of the molecules of the crystal is carried out in the spirit of the correspondence principle, according to which, in the dipole approximation, the optical behavior of the molecule is equivalent to the behavior of a corresponding set of oscillators. It should be noted that an account of all the excited states of the molecule is necessary only for obtaining the correct asymptotic behavior of $n^2(\omega)$ when $\omega \to 0$ and $\omega \to \infty$. No such account is necessary if the study is limited to the dependence of $n^2(\omega)$ in the region of frequencies close to one of the absorption bands in the molecule.

It follows from the system of equations (35) that the only states that interact with the transverse electromagnetic field are those for which $T(j, \mathbf{q}, \mu) \neq 0$. Expressing the quantity $u_{\mathbf{q}\mu}$ for these states in terms of $u_{\mathbf{q}j}$ with the help of the first of Eqs. (35), and substituting the resultant expression in the third of Eqs. (35), we get a system of two linear equations for the quantities $u_{\mathbf{q}j}$. Setting the determinant of this equation equal to zero, we obtain an involved equation for the energy of the elementary excitation $\mathscr{E}$ in the system of electron plus field. This equation has the following form:

$$(\hbar^2q^2c^2+\hbar^2\omega_0^2-\mathscr{E}^2)^2-(\hbar^2q^2c^2+\hbar^2\omega_0^2-\mathscr{E}^2)(\Sigma_{11}+\Sigma_{22}) +\Sigma_{11}\Sigma_{22}-\Sigma_{12}\Sigma_{21}=0, \tag{36}$$

where

$$\Sigma_{ij}=\Sigma_{ji}=\sum_{\mu} T(i, \mathbf{q}, \mu)\, T(j, \mathbf{q}, \mu)\frac{4\hbar qcE_{\mu}(\mathbf{q})}{\mathscr{E}^2-E_{\mu}^2(\mathbf{q})}. \tag{37}$$

Equation (36) does not determine the energy of elementary excitations without dipole moments [for which $\mathscr{E} = E_{\mu}(\mathbf{q})$]. Moreover, Eq. (36) does not determine the longitudinal elementary excitations. For consideration of the latter, it is necessary to set the determinant of the system of equations for the quantities $u_{\mathbf{q}\mu}$ and $u_{\mathbf{q}j}$ equal to zero. This set of equations is obtained from (32) after elimination of the quantities $v_{-\mathbf{q}\mu}$ and $v_{-\mathbf{q}j}$.

The index of refraction of light waves $n^2 \equiv \hbar^2q^2c^2/\mathscr{E}^2$ can be obtained from Eq. (33):

$$n_{12}^2(\mathbf{s}, \omega)=1-\frac{\omega_0^2}{\omega^2}+\frac{1}{2\mathscr{E}^2}(\Sigma_{11}+\Sigma_{22}) \pm\frac{1}{2}\left[\left(\frac{\Sigma_{11}-\Sigma_{22}}{\mathscr{E}^2}\right)^2+4\left(\frac{\Sigma_{12}}{\mathscr{E}^2}\right)^2\right]^{1/2}. \tag{38}$$

In this equation and in what follows, the notation

$$\omega \equiv \mathscr{E}/\hbar, \qquad \mathbf{s} \equiv \mathbf{q}/q$$

is employed.

Equation (38) appears to have a pole at $\omega = 0$. We shall show that the components $\sim \mathscr{E}^{-2}$ in Eq. (38) vanish identically. Actually, let us consider the two operators

$$\hat{\Pi} = \sum_{n\alpha} \hat{\mathbf{P}}_{n\alpha}, \qquad \dot{\hat{\Pi}} = \sum_{n\alpha} \dot{\hat{\mathbf{P}}}_{n\alpha},$$

where $\hat{\mathbf{P}}_{n\alpha}$ is the operator of the dipole moment of the $n\alpha$-th molecule. We introduce $\mathbf{x}$ and $\mathbf{y}$ as two orthogonal coordinates. The operators $\dot{\Pi}_x$ and Π_y satisfy the following commutation relations:

$$\dot{\Pi}_x\Pi_y-\Pi_y\dot{\Pi}_x=-i\hbar\frac{e^2}{m}N\sigma S\delta_{xy}. \tag{39}$$

In the second-quantization representation

$$\Pi_y=\sum_{n\alpha} P_{\alpha y}^{0f}(b_{n\alpha,0}^{+}b_{n\alpha,f}+b_{n\alpha,0}b_{n\alpha,f}^{+})$$

or, transforming to the Bose operators $B_{\mathbf{q}\mu}$ ($B_{\mathbf{q}\mu}|_{q=0} \equiv B_{\mathbf{s}\mu}$),

$$\Pi_y=\sqrt{N}\sum_{\mu\alpha}\left\{P_{\alpha y}^{0f}[u_{\alpha}(\mathbf{s}\mu)+v_{\alpha}(\mathbf{s}\mu)]\right\}(B_{\mathbf{s}\mu}+B_{\mathbf{s}\mu}^{+}). \tag{40}$$

The operator $\dot{\Pi}_x$ is determined in the following fashion:

$$-i\hbar\dot{\Pi}_x=\hat{H}_1\Pi_x-\Pi_x\hat{H}_1.$$

Inserting Eq. (25) in this relation, we find that

$$\dot{\Pi}_x=\frac{i\sqrt{N}}{\hbar}\sum_{\mu}E_{\mu}(\mathbf{s}) \times\left\{\sum_{\alpha}P_{\alpha y}^{0f}[u_{\alpha}(\mathbf{s}\mu)+v_{\alpha}(\mathbf{s}\mu)]\right\}(B_{\mathbf{s}\mu}-B_{\mathbf{s}\mu}^{+}). \tag{41}$$

Making use of Eqs. (39), (40), and (41) we obtain the desired summation rule:

$$2\sum_{\mu}E_{\mu}(\mathbf{s})\left\{\sum_{\alpha}P_{\alpha x}^{0f}[u_{\alpha}(\mathbf{s}\mu)+v_{\alpha}(\mathbf{s}\mu)]\right\} \times\left\{\sum_{\beta}P_{\beta y}^{0f}[u_{\beta}(\mathbf{s}\mu)+v_{\beta}(\mathbf{s}\mu)]\right\}=\hbar^2\frac{e^2}{m}\sigma S\delta_{xy}. \tag{42}$$

If we introduce the notation

$$\mathbf{P}_{0\mu}(\mathbf{s}) \equiv \sum_{\alpha} P_{\alpha}^{0f}[u_{\alpha}(\mathbf{s}\mu)+v_{\alpha}(\mathbf{s}\mu)],$$

we can rewrite Eq. (42) somewhat differently:

$$2\sum_{\mu}E_{\mu}(\mathbf{s})|\mathbf{P}_{0\mu}(\mathbf{s})|^2\cos\varphi_y(\mu\mathbf{s})\cos\varphi_x(\mu\mathbf{s})=\hbar^2\frac{e^2}{m}\sigma S\delta_{xy}. \tag{43}$$

Since

$$E_{\mu}^2(\mathbf{q})/\mathscr{E}^2(\mathscr{E}^2-E_{\mu}^2(\mathbf{q})) \equiv 1/[\mathscr{E}^2-E_{\mu}^2(\mathbf{q})]-1/\mathscr{E}^2,$$

$$\frac{1}{\mathscr{E}^2}\Sigma_{jj_1}=-\frac{8\pi N_1}{\mathscr{E}^2}\sum_{\mu}E_{\mu}(\mathbf{q})|P_{0\mu}(\mathbf{q})|^2\cos\varphi_j(\mu\mathbf{q})\cos\varphi_{j_1}(\mu\mathbf{q}) -8\pi N_1\sum_{\mu}\frac{E_{\mu}(\mathbf{q})|\mathbf{P}_{0\mu}(\mathbf{q})|^2\cos\varphi_j(\mu\mathbf{q})\cos\varphi_{j_1}(\mu\mathbf{q})}{\mathscr{E}^2-E_{\mu}^2(\mathbf{q})}.$$

Here j, $j_1 = 1, 2$, and $\varphi_j(\mu q)$ is the angle between the vectors $\mathbf{P}_{0\mu}(\mathbf{q})$ and l_{qj}.

Making use of the summation rule (43), we find that the substitution of the resultant expression for Σ_{jj_1} in Eq. (38) eliminates the terms proportional to $\mathcal{S}^{-2}$. We can write the following as the final equation for the quantities $n_{1,2}(\omega)$, with accuracy to small terms $\sim (d/\lambda)^2$:

$$n_{1,2}^2(\omega, \mathbf{s}) = 1 - \frac{1}{2}\sum_{\mu}\frac{\omega_0^2 F_\mu(\mathbf{s})\sin^2\varphi(\mu s)}{\omega^2 - \Omega_\mu^2(\mathbf{q})} \pm \frac{1}{2}\left\{\left[\sum_{\mu}\frac{\omega_0^2 F_\mu(\mathbf{s})(\cos^2\varphi_1(\mu q) - \cos^2\varphi_2(\mu q))}{\omega^2 - \Omega_\mu^2(\mathbf{q})}\right]^2 + 4\left[\sum_{\mu}\frac{\omega_0^2 F_\mu(\mathbf{s})\cos\varphi_1(\mu q)\cos\varphi_2(\mu q)}{\omega^2 - \Omega_\mu^2(\mathbf{q})}\right]^2\right\}^{1/2}, \quad (44)$$

where

$$F_\mu(\mathbf{s}) \equiv \frac{2m}{\sigma S e^2 \hbar^2}|\mathbf{P}_{0\mu}(\mathbf{s})|^2 E_\mu(\mathbf{s}),\ \Omega_\mu(\mathbf{q}) \equiv E_\mu(\mathbf{q})/\hbar,$$

F_μ is the oscillator strength corresponding to the level μ. This quantity is essentially independent of $\mathbf{s}$.

It is easy to show that as $\omega \to \infty$,

$$n_{1,2}^2(\omega, \mathbf{s}) \to 1 - \omega_0^2/\omega^2.$$

If $\omega \approx \Omega_f$, i.e., if the frequency is close to one of the absorption bands in the isolated molecule, one can separate in the sums over μ the resonance components that play the dominant role.

Let us consider some special cases.

1. The elementary cell of the crystal contains a single molecule ($\sigma = 1$). In this case,

$$n_1^2(\omega, \mathbf{s}) = \varepsilon(\omega, \mathbf{s}) - \frac{\omega_0^2 F(\mathbf{s})}{\omega^2 - \Omega^2(\mathbf{q})}\sin^2\varphi(\mathbf{s}),$$

$$n_2^2(\omega, \mathbf{s}) = \varepsilon(\omega, \mathbf{s}),$$

where the function $\epsilon(\omega, \mathbf{s})$ depends weakly on the frequency ω and the direction $\mathbf{s}$.

2. The crystal possesses cubic symmetry. In this case, the f-th molecular term corresponds to a twofold degenerate exciton band of transverse waves ($\mu = 1, 2$; $\mathbf{P}_{0\mu}(\mathbf{s}) \perp \mathbf{s}$, $|\mathbf{P}_{01}| = |\mathbf{P}_{02}|$, $\mathbf{P}_{01} \perp \mathbf{P}_{02}$) and to an exciton band of longitudinal waves, $\mu = 3$, $\mathbf{P}_{03} \parallel \mathbf{s}$. In this case, E_μ depends only on the absolute value q of the vector $\mathbf{q}$ and, consequently,

$$n_1^2(\omega, \mathbf{s}) = n_2^2(\omega, \mathbf{s}) = 1 - \frac{1}{2}\sum_{\mu}[\omega_0^2 F_\mu/(\omega^2 - \Omega_\mu^2(q))].$$

The factor $\frac{1}{2}$ stands before the sum because each component appears twice in the sum over μ owing to the twofold degeneracy of the terms. Close to one of the resonances,

$$n_1^2 = n_2^2 = \varepsilon(\omega) - \omega_0^2 F_2/[\omega^2 - \Omega^2(q)],$$

where the function $\epsilon(\omega)$ dependes weakly on the frequency.

3. Let us now consider a crystal containing two molecules in the elementary cell. Molecular crystals of this group are naphthalene, anthracene and a number of others. In such crystals, each allowed molecular term corresponds to two allowed crystalline terms ($\mu = 1, 2$), for which the vectors $\mathbf{P}_{0\mu}$ are orthogonal (see reference 5). If the wave vector $\mathbf{q}$ is orthogonal to the plane of the vectors $\mathbf{P}_{0\mu}$, the general expression for the indices of refraction is materially simplified in the frequency region close to the frequencies of the doublet.

In this case we find from the general expression (44) that

$$n_1^2(\omega) = \varepsilon(\omega) - \omega_0^2 F_1/[\omega^2 - \Omega_1^2(\mathbf{q})],$$

$$n_2^2(\omega) = \varepsilon(\omega) - \omega_0^2 F_2/[\omega^2 - \Omega_2^2(\mathbf{q})].$$

Account of the spatial dispersion in the expressions obtained above can be carried out similarly to what was done in references 7 — 9. However, it must be noted that in inactive crystals the role of new effects, which arise upon consideration of spatial dispersion, is evidently small (in spite of the estimates given in reference 8).

In conclusion, the author thanks V. L. Ginzburg for his valuable advice and discussion of the work, and also A. S. Davydov and V. P. Silin for useful discussions.

[1] U. Fano, Phys. Rev. **103**, 1202 (1956).

[2] S. M. Neamtan, Phys. Rev. **92**, 1362 (1953); **94**, 327 (1954).

[3] M. Born and Kun Huang, Dynamical Theory of Crystal Lattices, Clarendon Press, Oxford, 1954; Russ. transl. IIL, 1958.

[4] W. Heitler, Quantum Theory of Radiation, Oxford, 1953; Russ. transl. IIL, 1956.

[5] N. N. Bogolyubov, Лекции по квантовой статистике (Lectures on Quantum Statistics) Kiev, 1949.

[6] A. S. Davydov, Теория поглощения света в молекулярных кристаллах (Theory of Light Absorption in Molecular Crystals), Kiev, 1951.

[7] S. I. Pekar, J. Exptl. Theoret. Phys. (U.S.S.R.) **33**, 1022 (1957); Soviet Phys. JETP **6**, 785 (1958).

[8] V. L. Ginzburg, J. Exptl. Theoret. Phys. (U.S.S.R.) **34**, 1593 (1958); Soviet Phys. JETP **7**, 1096 (1958).

[9] V. M. Agranovich and A. A. Rukhadze, J. Exptl. Theoret. Phys. (U.S.S.R.) **35**, 982 (1958), Soviet Phys. JETP **8**, 685 (1959).

Translated by R. T. Beyer
80

THE ELECTROMAGNETIC INTERACTION IN THE HEISENBERG THEORY

Ya. I. GRANOVSKIĬ

Institute of Nuclear Physics, Academy of Sciences, Kazakh S.S.R.

Submitted to JETP editor February 6, 1959

J. Exptl. Theoret. Phys. (U.S.S.R.) 37, 442-451 (August, 1959)

The interaction of nucleons at large distances is considered on the basis of a nonlinear Lagrangian of general form. By means of the Heisenberg commutation function it is shown that there are forces with the Coulomb dependence on the distance and with a fine-structure constant equal to 1/138 (scalar theory). The causes of the absence of electromagnetic forces in the vector, tensor, and axial-vector theories are analyzed. Deviations from the Coulomb law and their effects on renormalization are discussed.

THE quantization of the wave equation

$$\gamma_\mu \partial\psi / \partial x_\mu - l^2 \psi(\bar{\psi}\psi) = 0 \qquad (1)$$

by means of the commutation function

$$S(x) = (2\pi)^{-4} \int e^{iqx} \frac{\varkappa^3}{q^2(q^2+\varkappa^2)} \left[\frac{\varkappa \gamma_\nu q_\nu}{q^2} - i \right] d^4q \qquad (2)$$

has made it possible to show[1] that a theory based on these two propositions contains forces with the Coulomb dependence on distance and with the fine-structure constant[2,3]

$$\alpha \approx 1/267. \qquad (3)$$

This is a great achievement of the theory, since for the first time electromagnetic forces have been represented as a consequence of other, more primary laws. A distinguishing feature of the work is that the calculated fine-structure constant has a value close to that found experimentally.

We shall take as the basis of the theory a Lagrangian of general form

$$L = \bar{\psi}\gamma_\mu \frac{\partial\psi}{\partial x_\mu} + \frac{1}{2} l^2 \sum_n C_n : \bar{\psi} O_n \psi \cdot \bar{\psi} O_n \psi : . \qquad (4)$$

Here the colons indicate the normal product of the operators, and O_n are the 16 Dirac matrices

$$O_n = 1, \quad \gamma_\mu, \quad \gamma_{\mu\nu} = (i/2)[\gamma_\mu, \gamma_\nu], \quad i\gamma_5\gamma_\mu, \quad \gamma_5, \qquad (5)$$

which satisfy the relations

$$O_n^+ = O_n, \quad \mathrm{Sp}\, O_m O_n = 4\delta_{mn}. \qquad (6)$$

Thus the objections connected with the arbitrary choice of the Lagrangian in the papers of Heisenberg and others[1-3] are removed, and the introduction of the normal product removes from the theory the so-called vacuum divergences[4] and the indefinite quantity $S_F(0)$.

The Lagrangian (4) retains its form when the two operators ψ in the normal product are interchanged, if the coefficients C are subjected to the transformation

$$C_n \to C_n' = -\tfrac{1}{4} \sum_m C_m A_{mn}, \qquad (7)$$

where the A_{mn} are defined by the identity

$$O_m \Gamma_n O_m = A_{mn} \Gamma_n \qquad (8)$$

[Γ_n is any one of the matrices (5)]. The coefficients A_{mn} are shown in Table I. The requirement of invariance with respect to the transformation (7) is satisfied if the C_n appear only in the combinations

$$B_m = \sum_n C_n (A_{nm} - 4\delta_{nm}). \qquad (9)$$

TABLE I

	A_{mn}	Γ_n				
		1	γ_5	$\gamma_{\mu\nu}$	$i\gamma_5\gamma_\mu$	γ_5
O_m	1	1	1	1	1	1
	γ_5	4	−2	0	2	−4
	$\gamma_{\mu\nu}$	6	0	−2	0	6
	$i\gamma_5\gamma_\mu$	4	2	0	−2	−4
	γ_5	1	−1	1	−1	1

1. PHOTONS AND THEIR PROPERTIES

The wave function of a boson

$$\varphi_{\alpha\beta}(x, y) = \langle 0 / T\psi_\alpha(x)\bar{\psi}_\beta(y) / \Phi \rangle. \qquad (1.1)$$

obeys the equation

$$\varphi_{\alpha\beta}(x, x) = \int H_{\alpha\varepsilon\eta\beta}(x, u)\, \varphi_{\varepsilon\eta}(u, u)\, d^4u, \qquad (1.2)$$

which can be derived from the field equation

$$\gamma_\mu \partial\psi / \partial x_\mu + l^2 \sum_n C_n : O_n\psi \cdot \bar{\psi} O_n \psi : = 0 \qquad (1.3)$$

by means of the Tamm-Dancoff method. One thus finds that[5]

$$H_{\alpha\varepsilon\eta\beta}(x,u) = -\tfrac{1}{2} il^2 \sum_N \tfrac{1}{4} B_N \{G(x,u)\Gamma^N S(u,x) + S(x,u)\Gamma^N G(u,x)\}_{\alpha\beta} (\Gamma^N)_{\eta\varepsilon}$$
$$= \tfrac{1}{4} \sum_{M,N} H_{MN}(x,u) (\Gamma^M)_{\alpha\beta} (\Gamma^N)_{\eta\varepsilon}. \qquad (1.4)$$

Here

$$H_{MN}(x,u) = -\tfrac{1}{2} il^2 \tfrac{1}{4} B_N \operatorname{Sp} \{\Gamma^M G(x,u)\Gamma^N S(u,x) + \Gamma^M S(x,u)\Gamma^N G(u,x)\}$$
$$= (2\pi)^{-4} \int e^{ip(x-u)} H_{MN}(p)\, d^4p; \qquad (1.5a)$$

$$H_{MN}(p) = -\tfrac{1}{2} il^2 \tfrac{1}{4} B_N (2\pi)^{-4} \operatorname{Sp} \int d^4q \{\Gamma^M G(p+q)\Gamma^N S(q) + \Gamma^M S(q)\Gamma^N G(-p+q)\}. \qquad (1.5b)$$

In the momentum representation for the function

$$\varphi_M(p) = \operatorname{Sp}\Gamma^M \varphi(p)$$
$$= \operatorname{Sp}\Gamma^M \int e^{-ipx} \langle 0 | T\psi(x)\bar{\psi}(x) | \Phi\rangle\, d^4x \qquad (1.6)$$

(1.2) has the form of a linear homogeneous equation

$$\varphi_M(p) = \sum_N H_{MN}(p)\varphi_N(p). \qquad (1.7)$$

The spinor structure of G and S is such that

$$\frac{il^2}{(2\pi)^4} \int \Gamma^M G(p+q)\Gamma^N S(q)\, d^4q = \Gamma^M(\gamma p)\Gamma^N B(p^2) + \Gamma^M \gamma_\nu \Gamma^N \gamma_\nu C(p^2) + \Gamma^M(\gamma p)\Gamma^N(\gamma p) D(p^2). \qquad (1.8)$$

Therefore

$$H_{MN}(p) = -\tfrac{1}{4} B_N \operatorname{Sp}\{\Gamma^M(\gamma p)\Gamma^N(\gamma p) D(p^2) + \Gamma^M \gamma_\nu \Gamma^N \gamma_\nu C(p^2) + \tfrac{1}{2}[\Gamma^M(\gamma p)\Gamma^N - \Gamma^N(\gamma p)\Gamma^M] B(p^2)\}. \qquad (1.9)$$

Equation (1.7) with the coefficients H_{MN} given by Eq. (1.9) can be used to determine the mass spectrum of the bosons with nonvanishing rest mass.[5] The condition for the existence of such particles is that the determinant of the system (1.7) be equal to zero.

Equation (1.7) is also valid for photons, for which $p^2 = 0$. Here, however, the functions B and C are singular:

$$B \approx -\frac{i}{2}\left(\frac{\varkappa l}{4\pi}\right)^2 \ln|p^2|, \qquad C \approx \frac{1}{4}\left(\frac{\varkappa l}{4\pi}\right)^2 \ln|p^2| \qquad (1.10)$$

(the singularity of D is of no significance). Because of this a regular solution of Eq. (1.7) exists only in cases in which the coefficients of the singular functions go to zero:

$$\sum_N B_N \operatorname{Sp}\Gamma^M \gamma_\nu \Gamma^N \gamma_\nu \varphi_N = 0, \qquad (1.11a)$$

$$\sum_N B_N \operatorname{Sp}\Gamma^M (\gamma p)\Gamma^N \varphi_N = 0, \qquad (1.11b)$$

$$\sum_N B_N \operatorname{Sp}\Gamma^N (\gamma p)\Gamma^M \varphi_N = 0. \qquad (1.11c)$$

These three cases extend and improve Eq. (19) of Heisenberg's paper.[1] According to Eqs. (8) and (6) the first of these equations is equivalent to the equation

$$B_M A_{VM} \varphi_M = 0, \qquad (1.12)$$

from which it follows that there are two types of solutions:

1) $A_{VM} = 0$, $B_M \neq 0$ is the general solution, which exists for all the types of nonlinear term. This solution has the form

$$\varphi_M = a(p_\mu e_\nu - p_\nu e_\mu), \qquad (1.13)$$

and it follows from Eq. (1.11b) that

$$(p \cdot e) = 0. \qquad (1.14)$$

Thus we get an antisymmetric tensor of the second rank with two independent transverse polarizations. The conclusion about transversality loses its validity if

$$B_T = C_S - 6C_T + C_P = 0, \qquad (1.15)$$

which occurs, for example, for the nonlinear terms $(\bar{\psi}\gamma_5\gamma_\mu\psi)^2$ and $(\bar{\psi}\psi)^2 - (\bar{\psi}\gamma_5\psi)^2$ studied in reference 6.

2) $B_M = 0$, $A_{VM} \neq 0$; these are particular solutions, whose existence depends on the choice of the type of nonlinear term. By choice of the coefficients C_n one can construct any additional solution. In the cases of the pure types ($C_n = \pm\delta_{nn_0}$) they can all be enumerated:

S, *P*:	none
V, *A*:	$\gamma_{\mu\nu}$;
T:	γ_μ, $\gamma_5\gamma_\mu$.

(1.16)

The polarization of the tensor solution in a mixture of the types V, A can also be longitudinal, since the equations (1.11b), (1.11c) are satisfied identically.

It is important to emphasize that all the additional solutions with their nonphysical properties are automatically removed from the theory. In fact, if we average the nonlinear term of the La-

grangian (4) over a single-nucleon state, we get an effective interaction Lagrangian of the form

$$l^2\sum_n C_n\left(\frac{1}{4}A_{nN}-\delta_{nN}\right):\bar{\psi}\Gamma_N\psi:\varphi_N$$
$$=\frac{1}{4}\,l^2\sum_N B_N:\bar{\psi}\Gamma_N\psi:\varphi_N, \tag{1.17}$$

which describes the coupling of the boson with a spinor particle having the charge $\frac{1}{4}l^2B_N$. If the Lagrangian admits an additional solution of the N-th kind, then $B_N \equiv 0$, and the corresponding term in Eq. (1.17) drops out. Thus nonphysical photons cannot convey an interaction. Furthermore, in a mixture of the types V, A even the physical photons give no coupling, since in this case the main and additional solutions coincide.

It will be shown below that the vertex operator contains the factor

$$B_V = C_S - 6C_V + 2C_A - C_P, \tag{1.18}$$

which vanishes in the tensor type of theory, because of the presence of an additional solution. Therefore we can draw the general conclusion: the presence of additional solutions in any type of Lagrangian leads to the absence of electromagnetic interaction.

As is well known, Lagrangians that are mixtures of the vector and axial-vector types form a class invariant with respect to the transformation[7]

$$\psi' = e^{i\alpha\gamma_5}\psi. \tag{1.19}$$

The absence of electromagnetic forces in this class of Lagrangians speaks against the inclusion of the Touschek transformation in the invariance group of the Lagrangian.

2. THE INTERACTION IN A LOWER APPROXIMATION

It has been shown above that for particles with zero rest mass the theory gives just the kinematic properties that are observed for actual photons. The proof of their full identity is completed by the calculation of the propagation function

$$D_{MN}(x,\ y) = \langle 0\,|\,T\varphi_M(x)\,\varphi_N(y)\,|\,0\rangle$$
$$= \langle 0\,|\,T\psi_\alpha(x)\,\Gamma^M_{\beta\alpha}\bar{\psi}_\beta(x)\,\psi_\gamma(y)\,\Gamma^N_{\delta\gamma}\bar{\psi}_\delta(y)\,0\rangle$$
$$= -\,\Gamma^M_{\beta\alpha}S^F_{\alpha\delta}(x,\ y)\,\Gamma^N_{\delta\gamma}S^F_{\gamma\beta}(y,\ x)$$
$$= -\,\mathrm{Sp}\,\Gamma^M S_F(x,\ y)\,\Gamma^N S_F(y,\ x)$$
$$= (2\pi)^{-4}\int D_{MN}(p)\exp\left[ip(x-y)\right]d^4p, \tag{2.1}$$

$$D_{MN}(p) = -(2\pi)^{-4}\,\mathrm{Sp}\int d^4q\,\Gamma^M S(p+q)\,\Gamma^N S(q) \tag{2.2}$$

(the index F on the Fourier transforms S_F is omitted throughout in what follows).

The spinor structure of $S(q)$ is such that

$$\int d^4q\,\Gamma^M S(p+q)\,\Gamma^N S(q)$$
$$= \Gamma^M(\gamma p)\,\Gamma^N(\gamma p)\,K(p^2) + \Gamma^M\gamma_\nu\Gamma^N\gamma_\nu\,L(p^2)$$
$$+\,\Gamma^M\Gamma^N M(p^2) + \left[\Gamma^M(\gamma p)\,\Gamma^N - \Gamma^M\Gamma^N(\gamma p)\right]N(p^2). \tag{2.3}$$

Therefore

$$D_{MN}(p) = -\,4(2\pi)^{-4}\,\delta_{MN}\left[\varepsilon_N p^2 K(p^2) + A_{VN}L(p^2) + M(p^2)\right]$$
$$-\,4(2\pi)^{-4}\,\delta_{MN'}(1-\varepsilon_N)\,p_4\,N(p^2), \tag{2.4}$$

where ϵ_N and $\Gamma_{N'}$ are defined by the equations

$$(\gamma p)\,\Gamma_N(\gamma p) = \varepsilon_N p^2\,\Gamma_N, \tag{2.5}$$
$$\Gamma_{N'} = \gamma_4\Gamma_N. \tag{2.6}$$

The invariant functions K, L, M, N, calculated by means of Eq. (2) in the limit of small p^2/κ^2 (i.e., at distances much larger than the Compton wavelength of the nucleon), take the values

$$\frac{p^2K}{f(p^2)}\to 1,\quad \frac{L(p^2)}{f(p^2)}\to -\frac{1}{2},$$
$$\frac{M(p^2)}{f(p^2)}\to 0,\quad \frac{P_4N(p^2)}{f(p^2)}\to 0; \tag{2.7}$$

$$f(p^2) = -\frac{i\pi^2\varkappa^4}{p^2}. \tag{2.8}$$

Thus in the infrared region of momenta

$$D_{MN}(p) = \delta_{MN}\frac{4i\pi^2\varkappa^4}{(2\pi)^4p^2}\left(\varepsilon_N - \frac{1}{2}A_{VN}\right), \tag{2.9}$$

and we return to the Feynman propagation function. Since along with this the Lorentz condition holds as a consequence of Eq. (1.14), all the laws of linear electrodynamics are satisfied at large distances. Sizable deviations from linearity occur for $p^2 \sim \kappa^2$, at distances related to the structure of the core of the nucleon. Even before this, however, at $p^2 \sim M_\pi^2$, the structure of the meson cloud around the nucleon begins to show up (cf. Sec. 4).

By means of the propagation function that has been found one can calculate the matrix element for scattering of two nucleons

$$\mathfrak{M} = -\,\bar{u}(p',\ q')\,W(p',\ q';\ p,\ q)\,u(p,\ q). \tag{2.10}$$

Since in this case we can use (in lowest approximation) the effective interaction (1.17), we have

$$W(p'q',\ pq) = \sum_{M,\ N}\frac{1}{4}\,l^2B_M\,\frac{1}{4}\,l^2\,B_N\,D_{MN}(p'-p)$$
$$\times\,\Gamma^M\Gamma^N\delta(p'-p+q'-q), \tag{2.11}$$

$$\mathfrak{M} = -\,i\pi^2\,\frac{(\varkappa l)^4}{4\,(2\pi)^4}\,\frac{1}{(p'-p)^2}\sum_N B_N^2\,\varepsilon_N\,\bar{u}(p')\,\Gamma^N u(p)$$
$$\times\,\bar{u}(q')\,\Gamma^N u(q)\,\delta(p'-p+q'-q). \tag{2.12}$$

This formula is the same as the result of Heisenberg, Kortel, and Mitter,[2] which they obtained in a more complicated way. Comparing Eq. (2.12) with the matrix element of quantum electrodynamics,

$$\mathfrak{M}_{ed} = ie^2 \frac{\bar{u}\gamma_\mu u \cdot \bar{u}\gamma_\mu u}{(p'-p)^2} \delta(p'-p+q'-q), \qquad (2.13)$$

we conclude that there are tensor forces with the Coulomb dependence on the distance and with the fine-structure constant

$$\alpha = e^2/4\pi = \pi(\varkappa l/4\pi)^4 B_T^2.$$

In the scalar theory this quantity is equal to 1/2.7, i.e., 50 times the observed value. In the vector and axial vector theories there is no interaction.

Both the numerical discrepancy and the incorrect spin dependence are due to the absence of the vertex operator. The difference between this operator and unity must also be taken into account in the lowest approximation.

3. THE VERTEX OPERATOR

The vertex operator describing the emission (absorption) of a photon of type M can be written in the form

$$V_M = \langle\Phi'|\varphi_M(x)|\Phi\rangle = \langle\Phi'|\psi_\alpha(x)\Gamma^M_{\beta\alpha}\bar{\psi}_\beta(x)|\Phi\rangle, \qquad (3.1)$$

where Φ, Φ' are the states of the nucleon before and after the scattering.

Owing to the completeness of the set of eigenfunctions,

$$\langle 0|\psi_\mu(y)\psi_\alpha(x)\bar{\psi}_\beta(x)|\Phi\rangle = \sum_{\Phi'}\langle 0|\psi_\mu(y)|\Phi'\rangle\langle\Phi'|\psi_\alpha(x)\bar{\psi}_\beta(x)|\Phi\rangle, \qquad (3.2)$$

we have the equation

$$u_\mu e^{-iE't}\langle\Phi'|\psi_\alpha(x)\bar{\psi}_\beta(x)|\Phi\rangle = \int dy e^{-ip'y}\langle 0|\psi_\mu(y)\psi_\alpha(x)\bar{\psi}_\beta(x)|\Phi\rangle \qquad (3.3)$$

(u_μ is the spinor for the physical nucleon). The right member of Eq. (3.3) is easily calculated in the first approximation of the Tamm-Dancoff method:

$$\langle 0|\psi_\mu(y)\psi_\alpha(x)\bar{\psi}_\beta(x)|\Phi\rangle = \frac{il^2}{3}\sum_N \frac{B_N}{4}\int G_{\mu\rho}(y,z)\Gamma^N_{\rho\sigma}S_{\alpha\beta}(z,x) \times S_{\alpha\lambda}(x,z)\Gamma^N_{\lambda\nu}\langle 0|\psi_\nu(z)|\Phi\rangle d^4z + \ldots$$
$$= \frac{il^2}{3}(2\pi)^{-8}\sum_N \frac{B_N}{4}\int G_{\mu\rho}(q)\Gamma^N_{\rho\sigma}S_{\alpha\beta}(r)S_{\alpha\lambda}(p-q+r) \times \Gamma^N_{\lambda\nu}u_\nu e^{iqy+i(p-q)x}d^4q d^4r + \ldots, \qquad (3.4)$$

The terms indicated by the row of dots are omitted because they make no contribution to the infrared asymptotic behavior of the vertex operator. By using Eqs. (3.3) and (3.4) we get (for $t_x = t_y$)

$$V_M = \frac{il^2}{3}(2\pi)^{-5}\sum_N \frac{B_N}{4} e^{i(p-p')x}\int dq_0 G(p+q)\Gamma_N \times \int d^4r S(q+r)\Gamma^M S(r)\Gamma^N. \qquad (3.5)$$

Using Eq. (2.3) and averaging over the spins of the nucleons, we get ($q^2/\kappa^2 \to 0$)

$$\int S(q+r)\Gamma^M S(r)d^4r = -\frac{i\pi^2\varkappa^3}{q^2}(\hat{q}\Gamma^M - \Gamma^M\hat{r}). \qquad (3.6)$$

For the tensor photon, with $\Gamma_M = \gamma_{\mu\nu}$, we have

$$\hat{q}\gamma_{\mu\nu} - \gamma_{\mu\nu}\hat{q} = -2i(\gamma_\mu q_\nu - \gamma_\nu q_\mu),$$
$$\Gamma^N(\hat{q}\gamma_{\mu\nu} - \gamma_{\mu\nu}\hat{q})\Gamma^N = A_{NV}(\hat{q}\gamma_{\mu\nu} - \gamma_{\mu\nu}\hat{q}), \qquad (3.7)$$
$$\sum_N B_N A_{NV} = -4B_V.$$

The result is then

$$V_T = -\frac{(\varkappa l)^2}{3}(2\pi)^{-5}B_V e^{i(p-p')x}\pi^2\varkappa \times \int dq_0 \frac{\hat{p}+\hat{q}}{(p+q)^2}\cdot\frac{\hat{q}\gamma_{\mu\nu} - \gamma_{\mu\nu}\hat{q}}{q^2}. \qquad (3.8)$$

Calculating the momentum integral for $p^2 \to 0$,[3] we find

$$V_T = C\frac{(p'-p)_\mu}{|p'-p|}\gamma_\nu \exp[i(p-p')x], \qquad (3.9)$$

$$C = \frac{1}{12}\left(\frac{\varkappa l}{4\pi}\right)^2 B_V. \qquad (3.10)$$

The introduction of the vertex operator in the matrix element brings the latter to the form

$$\mathfrak{M} = -\sum_{M,N}\frac{l^2}{4}B_M\frac{l^2}{4}B_N D_{MN}(p'-p) \times \mathrm{Sp}\,\Gamma^M\gamma_{\mu\nu}\,\mathrm{Sp}\,\Gamma^N\gamma_{\rho\sigma}C^2\bar{u}'\frac{(\Delta p)_\mu}{|\Delta p|}\gamma_\nu u \times \bar{u}'\frac{(\Delta q)_\rho}{|\Delta q|}\gamma_\sigma u\,\delta(p'-p+q'-q') = \delta(p'-p+q'-q) \times l^4 B_N^2 D_N(p'-p)C^2\bar{u}'\gamma_\nu u\cdot\bar{u}'\gamma_\nu u \qquad (3.11)$$

($\Gamma^N = \gamma_{4\nu}$), i.e., we get vector forces with the fine-structure constant

$$\alpha = \pi(\varkappa l/4\pi)^4 B_T^2\cdot 16C^2 = (\pi/9)(\varkappa l/4\pi)^8 B_T^2 B_V^2, \qquad (3.12)$$

which in the scalar theory is equal to 1/202. The remaining numerical disagreement with experiment is due to the omission of higher-order corrections to D_{MN} (cf. Sec. 4).

It must be particularly emphasized that as the

result of the emission of tensor photons vector forces are produced. This is explained by the invariance of the vertex operator under charge conjugation and reflections of the space coordinates (cf. reference 3).

4. CORRECTIONS TO THE PHOTON PROPAGATION FUNCTION IN THE CHAIN APPROXIMATION

The expression for the photon propagation function

$$D_{\alpha\beta\mu\nu}(x, y) = \int [\delta_{\alpha\varepsilon}\delta_{\eta\beta}\delta(x, u) + L_{\alpha\varepsilon\eta\beta}(x, u)] \times D^0_{\varepsilon\eta\tau\varkappa}(u, v)[\delta_{\mu\tau}\delta_{\varkappa\nu}\delta(v, y) + L_{\mu\tau\varkappa\nu}(v, y)]\, d^4u\, d^4v \quad (4.1)$$

(D^0 is the propagation function calculated in Sec. 2) contains the operator L, which describes the effect of the higher approximations at one of the junctions of the diagram (Fig. 1, a) that represents the propagation function D^0 in lowest approximation.

a b

If we confine ourselves to the "chain" approximation, the function D_{MN} can be represented by the diagram of Fig. 1, b; to this diagram there corresponds the following integral equation for L:

$$L_{\alpha\varepsilon\eta\beta}(x, u) = H_{\alpha\varepsilon\eta\beta}(x, u) + \int H_{\alpha\rho\sigma\beta}(x, v)\, L_{\rho\varepsilon\eta\sigma}(v, u)\, d^4v. \quad (4.2)$$

The operator H(x, u) that appears here corresponds to one link of the chain; it has already been encountered in Eq. (1.2).

The two equations (4.1) and (4.2) are decidedly simplified by the substitution

$$L_{\alpha\varepsilon\eta\beta}(x, u) = -\delta_{\alpha\varepsilon}\delta_{\eta\beta}\delta(x, u) + Q_{\alpha\varepsilon\eta\beta}(x, u) \quad (4.3)$$

and passage to the momentum representation,

$$Q_{\alpha\varepsilon\eta\beta}(x, u) = (2\pi)^{-4}\int Q_{\alpha\varepsilon\eta\beta}(p)\, e^{ip(x-u)}\, d^4p. \quad (4.4)$$

They are thus reduced to linear algebraic equations:

$$D_{\alpha\beta\mu\nu}(p) = Q_{\alpha\varepsilon\eta\beta}(p)\, D^0_{\varepsilon\eta\tau\varkappa}(p)\, Q_{\mu\tau\varkappa\nu}(p), \quad (4.5)$$

$$Q_{\alpha\varepsilon\eta\beta}(p) = \delta_{\alpha\varepsilon}\delta_{\eta\beta} + H_{\alpha\rho\sigma\beta}(p)\, Q_{\rho\varepsilon\eta\sigma}(p). \quad (4.6)$$

Expressing Q(p) in terms of the Dirac matrices

$$Q_{\alpha\varepsilon\eta\beta}(p) = \tfrac{1}{4}\sum_{M, N} Q_{MN}(p)\,(\Gamma^M)_{\alpha\beta}(\Gamma^N)_{\eta\varepsilon} \quad (4.7)$$

and using Eqs. (1.4) and (6), we bring Eq. (4.6) to the form

$$Q_{MN}(p) = \delta_{MN} + \sum_K H_{MK}(p)\, Q_{KN}(p), \quad (4.8)$$

which is entirely analogous to Eq. (1.7). The only difference is the presence of the inhomogeneous term δ_{MN}. In view of this relation between the equations (1.7) and (4.8) it can be asserted that the eigenvalues of the equation for $\varphi_N(p)$ are the poles of Q(p); that is, that the boson masses are the poles of Q(p).

Equation (4.8) can be solved easily, since $H_{MK} \neq 0$ for M = K or M = K′ [cf. Eqs. (1.9) and (2.6)]. In our case of $p^2/\kappa^2 \to 0$ the solution is particularly simple, since

$$p^2 D(p^2) \to \tfrac{1}{2}(\varkappa l/4\pi)^2, \quad p_4 B(p^2) \to 0, \quad C(p^2) \to 0, \quad (4.9)$$

$$H_{MK}(p) \to -\tfrac{1}{2}(\varkappa l/4\pi)^2\, \delta_{MK}\, B_M\, \varepsilon_M. \quad (4.10)$$

The result is

$$Q_{MN} = \frac{\delta_{MN}}{1 + \frac{1}{2}(\varkappa l/4\pi)^2 B_M\, \varepsilon_M} = Q_M\, \delta_{MN}. \quad (4.11)$$

Using the expansions

$$D_{\alpha\varepsilon\mu\nu} = \sum_{A, B} D_{AB}(\Gamma^A)_{\alpha\beta}(\Gamma^B)_{\mu\nu}, \quad (4.12)$$

$$D^0_{\varepsilon\eta\tau\varkappa} = \sum_{A, B} D^0_{AB}(\Gamma^A)_{\varepsilon\eta}(\Gamma^B)_{\tau\varkappa} \quad (4.13)$$

and Eq. (4.7), we get

$$D_{AB}(p) = \sum_{M, N} Q_{AM}(p)\, D^0_{MN}(p)\, Q_{BN}(p). \quad (4.14)$$

Owing to Eq. (4.11) we have in the infrared region

$$D_{AB}(p) = Q_A Q_B D^0_{AB}(p) = Q_A^2 D^0_A(p)\, \delta_{AB}. \quad (4.15)$$

Thus inclusion of the higher-order corrections by the summation of "chain" diagrams leads to the appearance of a correction factor

$$Q_A^2 = [1 + \tfrac{1}{2}(\varkappa l/4\pi)^2 B_A\, \varepsilon_A]^{-2} \quad (4.16)$$

in the expression for the propagation function. This factor depends on the sign of the nonlinear term; it contains B_A to the first power, whereas B_A occurs squared in all the other expressions. Because of this there is a possibility of determining the sign of the nonlinear term. The value of the correction in the scalar theory is 0.17; that is, it is far from the nearest zero of the denominator. It increases very rapidly, however, with approach to the threshold for production of a vector meson. Below the threshold the main part is played by the virtual production of mesons, which smears out the structure of the nucleon and leads to other nonlocal effects.

In view of the fact that the threshold for the production of mesons by electrons is considerably higher than that for nucleons, deviations from the Coulomb law are easier to detect in the scattering of nucleons. Thus nonlinear (and nonlocal) effects appear at lower energies in mesodynamics than in electrodynamics. This in turn is closely connected with the large difference between the coupling constants, which receives a natural explanation in a unified nonlinear theory.[1] An intermediate position between these two cases is occupied by the scattering of electrons by nucleons.

The appearance of a correction factor in the propagation function can be understood in the sense of a charge renormalization, although here all quantities are finite. The presence of additional poles in the renormalized propagation function is due to an actual physical effect: the influence of the meson field on the electromagnetic field. This dispenses with the difficulty that several writers[8] have pointed out in the interpretation of the additional poles. The difficulty with the vanishing of the renormalized charge is also removed. It could occur only at energies sufficient for penetration into the nucleon core, where there is of course no point in talking about the Coulomb law. In this region mesic forces play the decisive role. The continuous transition between electromagnetic and mesic forces underlines the necessity of a unified theory of both types of interaction.

5. THE FINE-STRUCTURE CONSTANT

Inserting the renormalizing factor (4.16) in Eq. (3.12), we get the following expression for the fine-structure constant of the electromagnetic interaction:

$$\alpha = \frac{\pi}{9}\left(\frac{\varkappa l}{4\pi}\right)^8 B_T^2 B_1^2 \left[1 - \frac{1}{2}\left(\frac{\varkappa l}{4\pi}\right)^2 B_T\right]^{-2} \qquad (5.1)$$

($\epsilon_T = -1$, since $\Gamma^N = \gamma_4\nu$; cf. Sec. 3).

Using the values of the constants calculated in reference 5, we get for the pure types of nonlinear term the results shown in Table II (the small numerical disagreement with the result of Ascoli and Heisenberg[3] is due to an improvement in the value of the constant κl). Comparison with the experimental value 1/137.03 is strong evidence for the Lagrangian

$$L = \bar{\psi}\gamma_\mu \partial\psi/\partial x_\mu + \frac{1}{2} l^2 (\bar{\psi}\psi)(\bar{\psi}\psi). \qquad (5.2)$$

Precisely this Lagrangian was proposed in reference 2, but a mistake that got into the calculations led to a change of the sign of the nonlinear term.[3]

TABLE II

Type of theory	Sign of nonlinear term	
	+	−
S	1/138.1	1/277.4
P	1/10.8	1/37.2
V, A, T	0	0

In the pseudoscalar theory the forces are larger by an order of magnitude. The absence of forces in the vector, axial-vector, and tensor theories has been analyzed above (Sec. 1); it is due to the presence of longitudinal photons in these theories.

The accuracy of the expression (5.1) can be improved by the calculation of higher approximations to the vertex operator and by an estimate of the degree of correctness of the chain approximation for the photon propagation function.

6. CONCLUSION

As the result of the present treatment we conclude that it is possible to reduce the laws of electromagnetic forces to other, more primitive, laws. In the limiting case of small momenta the electrodynamics constructed on the basis of Heisenberg's theory goes over into the ordinary quantum electrodynamics with the fine-structure constant 1/138, and with the correct polarization properties of the photon. The last two facts are closely interconnected; the admission of a longitudinal polarization makes the charge vanish.

Moreover, with increase of the energies of the interacting particles departures from the Coulomb law appear because of the virtual production of mesons and nucleon-antinucleon pairs. Beginning at a certain value of the energy a separate treatment of the electromagnetic and mesic forces becomes impossible, and the concept of electric charge loses its meaning; the internal structure of the particles begins to manifest itself. Such difficulties of the linear theory as the vanishing of the renormalized charge, and so on, occur only beyond this threshold value of the energy and are of no physical interest. With further increase of the energy electrodynamics goes over continuously into the mesodynamics of vector mesons.

The existence of an upper limit to the applicability of the separate theory also shows the necessity of a unified theory of the elementary particles.

[1] W. Heisenberg, Revs. Modern Phys. **29**, 269 (1957).

[2] Heisenberg, Kortel, and Mitter, Z. Naturforsch. **10a**, 425 (1955).

[3] R. Ascoli and W. Heisenberg, Z. Naturforsch. **12a**, 177 (1957).

[4] N. N. Bogolyubov and D. V. Shirkov, Введение в теорию квантованных полей (Introduction to the Theory of Quantized Fields), GITTL, 1957 [Engl. transl: Interscience, 1959].

[5] Ya. I. Granovskiĭ, J. Exptl. Theoret. Phys. (U.S.S.R.) **36**, 1154 (1959), Soviet Phys. JETP **9**, 819 (1959).

[6] W. Heisenberg and W. Pauli, Preprint, 1958.

[7] B. F. Touschek, Nuovo cimento **5**, 754 (1957).

[8] Landau, Abrikosov, and Khalatnikov, Dokl. Akad. Nauk SSSR **95**, 497, 773, 1177; **96**, 261 (1954). Silin, Tamm, and Faĭnberg, J. Exptl. Theoret. Phys. (U.S.S.R.) **29**, 6 (1955), Soviet Phys. JETP **2**, 3 (1956).

Translated by W. H. Furry.
81

COUPLED MAGNETOELASTIC OSCILLATIONS IN ANTIFERROMAGNETICS

S. V. PELETMINSKIĬ

Physico-Technical Institute, Academy of Sciences, Ukrainian S.S.R.

Submitted to JETP editor February 9, 1959

J. Exptl. Theoret. Phys. (U.S.S.R.) **37**, 452-457 (August, 1959)

A phenomenological theory of coupled magnetoelastic oscillations in antiferromagnetics is given (the coupling between elastic and magnetic waves is due to magnetostriction and spontaneous magnetization). The velocities of sound in the antiferromagnetic are determined; they are found to depend on the magnetization and the applied magnetic field. The absorption coefficient of sound is found.

1. In an elastically strained antiferromagnetic, because of magnetostriction and because of ponderomotive action due to the presence of spontaneous magnetization, there should occur a coupling between elastic and magnetic (spin) waves. When the conductivity of the medium is high, the coupled magnetoelastic waves that thus originate are similar to the waves that can propagate in metals in the presence of an external magnetic field. The interaction between magnetic and elastic waves leads to a change in the velocity of sound and to an additional sound absorption. These changes are especially large at resonance, when the frequency and wave vector of the sound wave coincide with the frequency and wave vector of the magnetic wave. The present work is devoted to a treatment of these problems for the case of an antiferromagnet; the treatment is analogous to that given earlier by Akhiezer, Bar'yakhtar, and the author for ferromagnets.[1]

2. The free energy of an antiferromagnet, with account taken of the coupling between acoustic and magnetic oscillations, is[2]

$$\mathcal{H} = \int dV \left\{ \frac{1}{2}\alpha\left[\left(\frac{\partial \mathbf{M}_1}{\partial x_k}\right)^2 + \left(\frac{\partial \mathbf{M}_2}{\partial x_k}\right)^2\right] + \alpha' \frac{\partial \mathbf{M}_1}{\partial x_k}\frac{\partial \mathbf{M}_2}{\partial x_k} + \beta(\mathbf{M}_1, \mathbf{M}_2) - (\mathbf{M}_1 + \mathbf{M}_2)\mathbf{H}_0 + \frac{\mathbf{h}^2 + \mathbf{ed}}{8\pi} + \frac{1}{2}\rho\dot{\mathbf{u}}^2 + \frac{1}{2}\lambda_{iklm}u_{ik}u_{lm} + F_{lm}(\mathbf{M}_1, \mathbf{M}_2)u_{lm} \right\}, \quad (1)$$

where the last term in curly brackets is the magnetostrictive energy; $\beta(\mathbf{M}_1, \mathbf{M}_2)$ includes the anisotropy energy and the part of the exchange energy not related to nonuniformities of the magnetic moments $\mathbf{M}_1$ and $\mathbf{M}_2$ of the sublattices; α and α' are exchange integrals. The remaining symbols are the same as in reference 1. Just as in the theory of ferromagnetism, the constants α and α' can be determined from the specific heat or the temperature dependence of the magnetic susceptibility of the antiferromagnet. In order of magnitude, they are determined by the Curie temperature Θ_C in the following manner: $\alpha' \sim \alpha \sim \Theta_C a^2/g\mathbf{M}_0\hbar$.

The equations of motion of the magnetic moments $\mathbf{M}_1$ and $\mathbf{M}_2$ have the form

$$\frac{\partial \mathbf{M}_1}{\partial t} + \frac{\partial}{\partial x_k}(\mathbf{M}_1\dot{u}_k) = g[\mathbf{M}_1 \times \mathbf{H}_1^{(e)}] - \frac{\lambda}{M^2}\left[\mathbf{M}_1 \times [\mathbf{M}_1 \times \mathbf{H}_1^{(e)}]\right],$$

$$\frac{\partial \mathbf{M}_2}{\partial t} + \frac{\partial}{\partial x_k}(\mathbf{M}_2\dot{u}_k) = g[\mathbf{M}_2 \times \mathbf{H}_2^{(e)}] - \frac{\lambda}{M^2}[\mathbf{M}_2 \times [\mathbf{M}_2 \times \mathbf{H}_2^{(e)}]], \quad (2)$$

where $\mathbf{H}_1^{(e)}$ and $\mathbf{H}_2^{(e)}$ are the effective magnetic fields acting on the magnetic moments of the first and second sublattices, respectively. To Eqs. (2) must be added Maxwell's equations and the equations of elasticity,

$$\operatorname{curl}\mathbf{h} = \frac{1}{c}\frac{\partial \mathbf{d}}{\partial t} + \frac{4\pi}{c}\mathbf{j}, \qquad \operatorname{curl}\mathbf{e} = -\frac{1}{c}\frac{\partial}{\partial t}(\mathbf{h} + 4\pi\mathbf{M}),$$

$$\mathbf{j} = \sigma(\mathbf{e} + \frac{1}{c}[\dot{\mathbf{u}} \times \mathbf{B}]), \qquad \rho\ddot{\mathbf{u}} = \mathbf{f}, \quad (3)$$

where $\mathbf{f}$ is the force per unit volume of the medium, $\mathbf{M} = \mathbf{M}_1 + \mathbf{M}_2$, and $\mathbf{B} = \mathbf{H} + 4\pi\mathbf{M}$. We shall find the values of $\mathbf{H}_1^{(e)}$, $\mathbf{H}_2^{(e)}$, and $\mathbf{f}$ from the requirement that the free energy (1) be conserved by virtue of Eqs. (2) and (3).

On carrying out calculations analogous to those carried out in reference 1, we get

$$\mathbf{H}_1^{(e)} = \mathbf{H}_0 - \partial\beta/\partial\mathbf{M}_1 + \mathbf{h} - \mathbf{G}_1 + \alpha\Delta\mathbf{M}_1 + \alpha'\Delta\mathbf{M}_2,$$
$$\mathbf{H}_2^{(e)} = \mathbf{H}_0 - \partial\beta/\partial\mathbf{M}_2 + \mathbf{h} - \mathbf{G}_2 + \alpha\Delta\mathbf{M}_2 + \alpha'\Delta\mathbf{M}_1,$$
$$f_i = \frac{\partial \sigma_{ik}}{\partial x_k} + \frac{1}{c}[\mathbf{j} \times \mathbf{B}]_i + \mathbf{M}_1\frac{\partial}{\partial x_i}\mathbf{H}_1^{(e)} + \mathbf{M}_2\frac{\partial}{\partial x_i}\mathbf{H}_2^{(e)}, \quad (4)$$

where

$$\mathbf{G}_1 = u_{lm}\partial F_{lm}/\partial\mathbf{M}_1, \qquad \mathbf{G}_2 = u_{lm}\partial F_{lm}/\partial\mathbf{M}_2,$$
$$\sigma_{ik} = \lambda_{iklm}u_{lm} + F_{ik}(\mathbf{M}_1, \mathbf{M}_2).$$

An expression for $d\mathcal{H}/dt$ is given by the formula

$$\frac{d\mathcal{H}}{dt} = -\int \left\{ \frac{j^2}{\sigma} + \frac{\lambda}{M^2}[\mathbf{M}_1 \times \mathbf{H}_1^{(e)}]^2 + \frac{\lambda}{M^2}[\mathbf{M}_2 \times \mathbf{H}_2^{(e)}]^2 \right\} dV$$
$$+ \oint dS_k \left\{ \frac{c}{4\pi}[\mathbf{h} \times \mathbf{e}]_k + \alpha\left(\dot{\mathbf{M}}_1 \frac{\partial \mathbf{M}_1}{\partial x_k} + \dot{\mathbf{M}}_2 \frac{\partial \mathbf{M}_2}{\partial x_k}\right) \right.$$
$$+ \alpha'\left(\dot{\mathbf{M}}_1 \frac{\partial \mathbf{M}_2}{\partial x_k} + \dot{\mathbf{M}}_2 \frac{\partial \mathbf{M}_1}{\partial x_k}\right)$$
$$\left. + \dot{u}_i [\sigma_{ik} + \delta_{ik}(\mathbf{M}_1 \mathbf{H}_1^{(e)} + \mathbf{M}_2 \mathbf{H}_2^{(e)})] \right\}. \quad (5)$$

From formula (5) can be found the coefficient of absorption of the magnetoelastic oscillations,

$$\Gamma = -\frac{1}{\mathcal{H}} \frac{\overline{d\mathcal{H}}}{dt},$$

where $\overline{d\mathcal{H}/dt}$ is the time-average value of the volume integral in (5).

According to Eq. (2), in the linear approximation in the quantities $\mathbf{u}$, $\boldsymbol{\mu}_1 = \mathbf{M}_1 - \mathbf{M}_{10}$, and $\boldsymbol{\mu}_2 = \mathbf{M}_2 - \mathbf{M}_{20}$, and for small λ,

$$g[\mathbf{M}_1 \times \mathbf{H}_1^{(e)}] = \partial \boldsymbol{\mu}_{1\perp}/dt, \qquad g[\mathbf{M}_2 \times \mathbf{H}_2^{(e)}] = \partial \boldsymbol{\mu}_{2\perp}/dt,$$

therefore,

$$\frac{\overline{d\mathcal{H}}}{dt} = -\int \left\{ \frac{\overline{j^2}}{\sigma} + \frac{\lambda}{(gM)^2}\overline{\dot{\boldsymbol{\mu}}_{1\perp}^2} + \frac{\lambda}{(gM)^2}\overline{\dot{\boldsymbol{\mu}}_{2\perp}^2} \right\} dV. \quad (6)$$

3. We now consider the system of equations (2) – (3). First of all, this system must be linearized. For simplicity we shall suppose that the medium is isotropic in its magnetostrictive properties. This condition means that $F_{ik}(\mathbf{M}_1, \mathbf{M}_2)$ has the form

$$F_{ik}(\mathbf{M}_1, \mathbf{M}_2) = \delta_1 (M_{1i} M_{1k} + M_{2i} M_{2k})$$
$$+ \delta_2 (M_{1i} M_{2k} + M_{1k} M_{2i})$$
$$+ \delta_{ik}(\delta_3 \mathbf{M}_1 \mathbf{M}_2 + \delta_4 (\mathbf{M}_1^2 + \mathbf{M}_2^2)). \quad (7)$$

We further suppose that the quantities, δ_1, δ_2, δ_3, and δ_4 are independent of $\mathbf{M}_1^2$, $\mathbf{M}_2^2$, and $\mathbf{M}_1\mathbf{M}_2$. From (2), the equations of motion of the magnetic moments, in terms of the variables $\boldsymbol{\eta} = \boldsymbol{\mu}_1 - \boldsymbol{\mu}_2$ and $\boldsymbol{\mu} = \boldsymbol{\mu}_1 + \boldsymbol{\mu}_2$, have the form

$$\partial \boldsymbol{\eta}/\partial t + 2M_0 \mathbf{n} \operatorname{div} \dot{\mathbf{u}}$$
$$= gM_0 \mathbf{n} \times [\mathbf{H}_1^{(e)} + \mathbf{H}_2^{(e)}] - \lambda \mathbf{n} \times \left[\mathbf{n} \times [\mathbf{H}_1^{(e)} - \mathbf{H}_2^{(e)}]\right],$$
$$\partial \boldsymbol{\mu}/\partial t = gM_0 \mathbf{n} \times [\mathbf{H}_1^{(e)} - \mathbf{H}_2^{(e)}]$$
$$- \lambda \mathbf{n} \times \left[\mathbf{n} \times [\mathbf{H}_1^{(e)} + \mathbf{H}_2^{(e)}]\right]. \quad (8)$$

From Eq. (8) it follows that

$$\boldsymbol{\mu}\mathbf{n} = 0, \qquad \boldsymbol{\eta}\mathbf{n} = -2M_0 \operatorname{div} \mathbf{u}.$$

If we treat the body as isotropic in its elastic properties, and if we introduce the notation

$$\tilde{c}_t^2 = c_t^2 + (M_0^2/\rho)\{2\beta + a + 4(\delta_3 - 2\delta_4) + 2(\alpha' - \alpha)\Delta\}$$

(where a and β are constants related to exchange and to anisotropy), we get the following equation for the displacement vector $\mathbf{u}$:

$$\ddot{\mathbf{u}} = c_t^2 \Delta \mathbf{u} + (\tilde{c}_t^2 - c_t^2) \nabla \operatorname{div} \mathbf{u} + \frac{1}{\rho c}[\mathbf{j} \times \mathbf{B}]$$
$$- \frac{4M_0^2}{\rho}(\delta_1 - \delta_2) \nabla n_i u_{ik} n_k$$
$$\left. + \frac{M_0}{\rho}(\delta_1 - \delta_2)(\mathbf{n} \operatorname{div} \boldsymbol{\eta} + n_k \frac{\partial \boldsymbol{\eta}}{\partial x_k}) \right. . \quad (9)$$

The equations of motion of the magnetic moments, in expanded form, are

$$\frac{\partial \boldsymbol{\eta}}{\partial t} + 2M_0 \mathbf{n} \operatorname{div} \dot{\mathbf{u}}$$
$$= gM_0 \mathbf{n} \times [2\mathbf{h} - (2\gamma + \beta)\boldsymbol{\mu} - \frac{H_0}{M_0}\boldsymbol{\eta} + (\alpha + \alpha')\Delta\boldsymbol{\mu}]$$
$$- \lambda \mathbf{n} \times \left\{ \mathbf{n} \times [-\beta\boldsymbol{\eta} - \frac{H_0}{M_0}\boldsymbol{\mu} + (\alpha - \alpha')\Delta\boldsymbol{\eta} \right.$$
$$\left. - 4M_0(\delta_1 - \delta_2)\hat{u}\mathbf{n}] \right\},$$
$$\frac{\partial \boldsymbol{\mu}}{\partial t} = gM_0 \mathbf{n} \times [-\beta\boldsymbol{\eta} - \frac{H_0}{M_0}\boldsymbol{\mu} + (\alpha - \alpha')\Delta\boldsymbol{\eta} - 4M_0(\delta_1 - \delta_2)\hat{u}\mathbf{n}]$$
$$- \lambda \mathbf{n} \times \left\{ \mathbf{n} \times [2\mathbf{h} - (2\gamma + \beta)\boldsymbol{\mu} - \frac{H_0}{M_0}\boldsymbol{\eta} + (\alpha + \alpha')\Delta\boldsymbol{\mu}] \right\}, \quad (10)$$

where $\hat{u}\mathbf{n}$ is a vector with the components $u_{ik}n_k$, and where γ is an exchange constant. The magnetic field $\mathbf{H}_0$ is assumed to be directed along an axis of easiest magnetization $\mathbf{n}$.

Henceforth we shall treat in detail only the case in which the wave is propagated along the axis of easiest magnetization ($\mathbf{k} \parallel \mathbf{n}$). As usual, we seek a solution of the form $\exp\{-i(\omega t - \mathbf{k} \cdot \mathbf{x})\}$. Taking the component of Eqs. (9) and (10) parallel to the vector $\mathbf{n}$, we get

$$\mu_\parallel = 0, \qquad \eta_\parallel + 2iM_0 k u_\parallel = 0,$$
$$(\omega^2 - k^2\tilde{c}_t^2) u_\parallel + (2iM_0/\rho)(\delta_1 - \delta_2) k \eta_\parallel$$
$$+ (4M_0^2/\rho)(\delta_1 - \delta_2) k^2 u_\parallel = 0.$$

Hence we find the frequency and the phase velocity of longitudinal sound:

$$\omega^2 = v^2 k^2 = k^2 \{\tilde{c}_t^2 - (8M^2{}_0/\rho)(\delta_1 - \delta_2)\}, \quad (11)$$

where

$$\tilde{c}_t^2 = c_t^2 + (M_0^2/\rho)\{2\beta + a + 4(\delta_3 - 2\delta_4) - 2(\alpha' - \alpha)k^2\}. \quad (11')$$

The dependence of the phase velocity on the wave vector k through the term $2(M_0^2/\rho)(\alpha' - \alpha)k^2$ in formula (11′) can be neglected in the acoustic frequency range:

$$\omega \ll c_l/\sqrt{\alpha} \sim (\Theta_l/\hbar)(g\hbar M_0/\Theta_c)^{1/2} \sim 4\cdot 10^{11}\ \text{sec}^{-1}$$

for $\Theta_l = c_l\hbar/a \approx 3\times 10^{-14}$ ($\Theta_l \sim 300°$K), $M_0 \sim 10^3$ G, and $\Theta_c \sim 500°$K.

Equations (9) and (10), with Maxwell's equations taken into account, lead to the following dispersion equation for magnetoelastic oscillations that correspond to transverse sound:

$$\begin{aligned}&(\omega^2 - k^2\tilde{c}_t^2)\{(\omega - gH_0)^2 - \Omega\Omega_1 + i\frac{\lambda}{gM_0}\omega(\Omega+\Omega_1)\\ &-\left(\frac{\lambda}{gM_0}\right)^2(\Omega\Omega_1 - g^2H_0^2)\} + \frac{2M_0^2}{\rho}(\delta_1-\delta_2)k^2gM_0\\ &\times\left\{\left[(\delta_2-\delta_1)\Omega + gH_0\frac{H_0}{M_0}\zeta\right]\left[1+\left(\frac{\lambda}{gM_0}\right)^2\right]\right.\\ &\left.+\omega\left[\frac{i\lambda}{gM_0}(\delta_1-\delta_2) - \frac{H_0}{M_0}\zeta\right]\right\}\\ &+\frac{2M_0^2}{\rho}\zeta k^2gH_0\left\{\left[gH_0(\delta_1-\delta_2) - \Omega_1\frac{H_0}{M_0}\zeta\right]\left[1+\left(\frac{\lambda}{gM_0}\right)^2\right]\right.\\ &\left.+\omega\left[\frac{i\lambda}{gM_0}\frac{H_0}{M_0}\zeta+\delta_2-\delta_1\right]\right\} = 0, \qquad (12)\end{aligned}$$

$$\Omega = gM_0\{\beta + 2\gamma - 8\pi\zeta + (\alpha+\alpha')k^2\},$$

$$\Omega_1 = gM_0\{\beta + (\alpha-\alpha')k^2\},$$

$$\tilde{c}_t^2 = c_t^2 - H_0^2\zeta/4\pi\rho, \qquad \zeta = \{c^2k^2/4\pi i\omega\sigma - 1\}^{-1}. \qquad (13)$$

In the absence of coupling between acoustic and magnetic oscillations ($M_0^2/\rho c_t^2 \to 0$), we arrive at a dispersion equation for a magnetic wave with account taken of absorption through relaxation processes described by the constant λ and the conductivity σ:

$$\begin{aligned}&(\omega - gH_0)^2 - \Omega\Omega_1 + i(\lambda/gM_0)\omega(\Omega+\Omega_1)\\ &-(\lambda/gM_0)^2(\Omega\Omega_1 - g^2H_0^2) = 0. \qquad (14)\end{aligned}$$

Hence we find for $\lambda \ll gM_0$

$$\begin{aligned}&\omega = gH_0 \pm \sqrt{\Omega\Omega_1}\\ &- i(\lambda/2gM_0)(\Omega+\Omega_1)\{1 \pm gH_0/\sqrt{\Omega\Omega_1}\}. \qquad (14')\end{aligned}$$

Formula (14′) shows that the coefficient of absorption of a magnetic wave by virtue of relaxation processes when $\sigma = 0$ is

$$\Gamma = -2\,\text{Im}\,\omega|_{\sigma=0} = (\lambda/gM_0)(\Omega+\Omega_1)(1 \pm gH_0/\sqrt{\Omega\Omega_1}).$$

Absorption of the energy of the magnetic wave will take place if $\Gamma > 0$, i.e. if

$$gH_0 < \sqrt{\Omega\Omega_1}. \qquad (15)$$

This relation is the condition for existence of a ground state of an antiferromagnetic with $\mathbf{M}_{10} = -\mathbf{M}_{20}$ along $\mathbf{H}_0$. At fields $gH_0 > \sqrt{\Omega\Omega_1}$, the ground state corresponds to a structure with $\mathbf{M}_{10} = -\mathbf{M}_{20}$ perpendicular to $\mathbf{H}_0$.[3]

When $\sigma = \lambda = 0$ and $M_0^2/\rho c_t^2 \ll 1$, formula (12) leads to the following expression for the phase velocity of transverse sound:

$$v^2 = \frac{\omega^2}{k^2} = c_t^2\left\{1 + \frac{2M_0^2}{\rho c_t^2}(\delta_1-\delta_2)^2\frac{\Omega gM_0}{(\omega-gH_0)^2-\Omega\Omega_1}\right\}. \qquad (16)$$

When $\sigma = \infty$, $\lambda = 0$, and $M_0^2/\rho c_t^2 \ll 1$, the same formula (12) leads to the following expression for the phase velocity of transverse sound:

$$v^2 = \frac{\omega^2}{k^2} = \tilde{c}_t^2\left\{1 - \frac{2M_0^2}{\rho c_t^2}\frac{gH_0[2(\delta_1-\delta_2)(\omega-gH_0) - \Omega_1H_0/M_0 - (\Omega M_0/H_0)(\delta_1-\delta_2)^2]}{(\omega-gH_0)^2-\Omega\Omega_1}\right\}. \qquad (16')$$

When $M_0 = \delta_1 = \delta_2 = 0$, formulas (11) and (16′) reduce to the formulas for the velocity of sound in a metal in the presence of an external magnetic field.

Formulas (16) and (16′) are valid when the sound frequency ω is not close to $gH_0 \pm \sqrt{\Omega\Omega_1}$; in the contrary case, "entanglement" of the acoustic and magnetic oscillations occurs, just as in the case of a ferromagnet.

Inclusion of the terms containing λ and σ leads, first, to an additional change of the phase velocity of the waves; and second, to damping of the oscillations. We consider first the change of the phase velocity of transverse sound.

The dispersion equation (12) leads in the case $\sigma = 0$ to the following formula instead of formula (16):

$$\begin{aligned}&v^2 = c_t^2\left\{1 + \frac{2M_0^2}{\rho c_t^2}(\delta_1-\delta_2)^2\Omega gM_0\right.\\ &\left.\times\frac{(\omega-gH_0)^2-\Omega\Omega_1}{[(\omega-gH_0)^2-\Omega\Omega_1]^2 + (\lambda/gM_0)^2\omega^2(\Omega+\Omega_1)^2}\right\}. \qquad (17)\end{aligned}$$

The relative change of sound velocity at resonance, $\Delta v/v$, for $\lambda/gM_0 \sim 10^{-1}$, $gM_0/\omega \sim 10^2$, and $\delta_1 \sim \delta_2 \sim 1$, is about 1%, as can be seen from formula (17).

We note that in the case of antiferromagnets, the phenomenon of resonance (reinforcement of the coupling between acoustic and magnetic oscillations) takes place both for $\sigma = 0$ and for $\sigma = \infty$, as can be seen from formula (13) in view of the large value of the exchange constant γ. But in contrast to ferromagnets, the resonance frequencies can be made small in comparison with gM_0 ($\sim 10^{10}$ sec^{-1}) only

in strong magnetic fields H_0:

$$gH_0/\sqrt{\Omega\Omega_1}-1\approx H_0/M_0\sqrt{2\beta\gamma}-1\ll 1. \qquad (18)$$

From this it is clear that these fields must be on the scale of $M_0\sqrt{2\beta\gamma}\sim 10M_0\sim 10^4$ G. Smaller values of the field H_0 may be obtained if antiferromagnets are chosen with small anisotropy and a small exchange constant γ.

4. The absorption coefficient Γ of magnetoelastic oscillations in an antiferromagnet can be determined from formula (6) in exactly the same way as for a ferromagnet or ferrodielectric.

However, it is now easier to determine the absorption coefficient from the exact dispersion equation (12). The absorption coefficient Γ is found from the solution ω of the dispersion equation by the formula

$$\Gamma=-2\,\mathrm{Im}\,\omega. \qquad (19)$$

Formulas (12) and (19) lead to the following expression for the coefficient of absorption of magnetoelastic oscillations by virtue of relaxation processes described by the constant λ:

$$\Gamma_\lambda=2\omega^2\frac{M_0^2}{\rho c_t^2}(\delta_1-\delta_2)^2\lambda \times\frac{\Omega^2+(\omega-gH_0)^2}{[(\omega-gH_0)^2-\Omega\Omega_1]^2+(\lambda/gM_0)^2\omega^2(\Omega+\Omega_1)^2}. \qquad (20)$$

The absorption is especially large at resonance, when $\omega=gH_0-\sqrt{\Omega\Omega_1}$ (magnetic fields of order $M_0\sqrt{2\beta\gamma}$). The value of the absorption at resonance is

$$\Gamma_\lambda=gM_0\frac{M_0^2}{\rho c_t^2}(\delta_1-\delta_2)^2\frac{gM_0}{\lambda}\frac{\Omega}{\Omega+\Omega_1} \approx gM_0\frac{M_0^2}{\rho c_t^2}(\delta_1-\delta_2)^2\frac{gM_0}{\lambda}, \qquad (20')$$

since $\Omega_1\ll\Omega$ in view of the large value of the exchange constant γ by comparison with the anisotropy constant β.

We shall compare the absorption coefficient at resonance with the absorption coefficient resulting from heat conductivity. The latter is determined by the formula[4]

$$\gamma\approx\omega^2C^{-2}\varkappa T\alpha_T^2\rho=(gH_0-\sqrt{\Omega\Omega_1})^2C^{-2}\varkappa T\alpha_T^2\rho,$$

where κ is the coefficient of heat conductivity, T is the temperature in degrees, C is the volume specific heat, and α_T is the coefficient of thermal expansion.

The ratio Γ_λ/γ is equal to

$$\Gamma_\lambda/\gamma\sim(M_0^2/\rho c_l^2)(\delta_1-\delta_2)^2C^2/\lambda\varkappa T\alpha_T^2\rho.$$

For $\alpha_T=10^{-5}$, $C=10^6$, $\kappa=10^6$, $T\sim 10^2\,^\circ$K, $\lambda/gM_0\sim 10^{-1}$, $\delta_1\sim\delta_2\sim 1$, $c_l\sim 5\times 10^5$, and $M_0\sim 500$, this ratio amounts to $\Gamma/\gamma\sim 10^2$.

The amount of absorption of magnetoelastic oscillations by virtue of the conductivity σ, for small values of σ, is given by the formula

$$\Gamma_\sigma=\frac{\sigma}{\rho c^2}\frac{\{H_0[(\omega-gH_0)^2-\Omega\Omega_1]-8\pi gM_0^2(\omega-gH_0)(\delta_1-\delta_2)\}^2}{[(\omega-gH_0)^2-\Omega\Omega_1]^2}. \qquad (21)$$

The absorption of sound by virtue of conductivity σ in the vicinity of resonance is obtained from formula (21) by the substitution

$$[(\omega-gH_0)^2-\Omega\Omega_1]^2\to[(\omega-gH_0)^2-\Omega\Omega_1]^2+\left|\frac{\lambda}{gM_0}\omega(\Omega+\Omega_1)+gM_0\Omega_1\frac{32\pi^2\omega\sigma}{c^2k^2}\right|^2.$$

The author expresses his gratitude to A. I. Akhiezer, V. G. Bar'yakhtar, and M. I. Kaganov for discussion of the results of his work.

[1] Akhiezer, Bar'yakhtar, and Peletminskiĭ, J. Exptl. Theoret. Phys. (U.S.S.R.) **35**, 228 (1958), Soviet Phys. JETP **8**, 157 (1959).

[2] M. I. Kaganov and V. M. Tsukernik, J. Exptl. Theoret. Phys. (U.S.S.R.) **34**, 106 (1958), Soviet Phys. JETP **7**, 73 (1958).

[3] A. Amatuni, Физика металлов и металловедение (Phys. of Metals and Metal Research) **3**, 411 (1956); **4**, 17 (1957); E. A. Turov, J. Exptl. Theoret. Phys. (U.S.S.R.) **34**, 1009 (1958), Soviet Phys. JETP **7**, 696 (1958).

[4] Akhiezer, Kaganov, and Lyubarskiĭ, J. Exptl. Theoret. Phys. (U.S.S.R.) **32**, 837 (1957), Soviet Phys. JETP **5**, 685 (1957).

Translated by W. F. Brown, Jr.
82

APPLICATION OF THE VARIATIONAL PRINCIPLE FOR THE DETERMINATION OF THE BINDING ENERGY OF A PROTON-ELECTRON-POSITRON SYSTEM

V. P. SHMELEV

Moscow State University

Submitted to JETP editor February 13, 1959

J. Exptl. Theoret. Phys. (U.S.S.R.) **37**, 458-466 (August, 1959)

The energy of a system of three particles, proton, electron, and positron, has been determined by the variational method. It is found to be $E \leq 0.563$ Ry. The system can only dissociate into a proton and a positronium atom, with the dissociation energy $|\epsilon| \geq 0.063$ Ry.

1. FORMULATION OF THE PROBLEM

We consider the problem of the determination of the ground state of a system consisting of a fixed (at the origin) proton and two particles, an electron and a positron, moving in the field of the proton.

Let r_1 be the distance between the proton and the electron, r_2, that between the proton and the positron, and r_{12}, the distance between the electron and the positron. The potential energy of the system is

$$U_1 = e^2/r_2 - e^2/r_1 - e^2/r_{12}. \quad (1)$$

It was shown by Hylleraas[1] and Breit[2] that it is possible to separate the variables in the wave function of two particles moving in a Coulomb field. The equation in six variables is thus reduced to an equation in three variables, r_1, r_2, and the angle θ between r_1 and r_2, which determine the relative position of the particles. The three remaining variables determine the total angular momentum L of the whole system. This method leads to the following Schrödinger equation for the ground state (L = 0):

$$\frac{1}{r_1^2}\frac{\partial}{\partial r_1}\left(r_1^2\frac{\partial\psi}{\partial r_1}\right) + \frac{1}{r_2^2}\frac{\partial}{\partial r_2}\left(r_2^2\frac{\partial\psi}{\partial r_2}\right) + \left(\frac{1}{r_1}+\frac{1}{r_2}\right)\left[\frac{1}{\sin\theta}\frac{\partial}{\partial\theta}\left(\sin\theta\,\frac{\partial\psi}{\partial\theta}\right)\right] + \frac{2m}{\hbar^2}(E-U_1)\psi = 0. \quad (2)$$

In solving the analogous problem of the helium atom one chooses as a first approximation that solution in which the interaction between the electrons is neglected. In our case this is not possible, since our system would not even exist without the attraction between the electron and the positron. A separation of variables in Eq. (2) is therefore impossible.

We find the solution to Eq. (2) by the variational method. In choosing a trial function we must use those methods of solution of the problem of the helium atom in which the variables are not separated. The solutions of Hylleraas[3] and Slater[4] are of this kind. We must also consider the physical characteristics of the system; we note that it is analogous to the ionized hydrogen molecule consisting of two protons and one electron. In deciding what should be the form of the solution of Eq. (2) we must therefore pay attention to the following facts. It is known that the problem of the hydrogen ion reduces mathematically to the problem of two centers: find the stationary states of the electron in the field of two fixed positive charges with the relative distance R. The solution can be found using the methods of Born and Oppenheimer,[5] who made a general study of the system consisting of several protons and electrons. These authors show that the wave functions of the protons can generally be regarded as solutions of the equation of motion of particles in a potential well given by the electrons moving in the field of the protons. Let ξ be the set of electron coordinates relative to the protons, and x the set of relative proton coordinates. The wave function can then be written in the form

$$\psi(x, \xi) = \Phi_0(x)F_0(x, \xi) + \Phi_1(x)F_1(x, \xi) + \cdots$$

Here $F_0(x, \xi)$, as a function of the coordinates ξ, is the wave function of the ground state of the electrons in the field of the fixed protons. It depends on the proton coordinates x parametrically. The energy of the system of electrons, $V(x)$, is then also a function of the parameters x. The function $\Phi_0(x)$ is the wave function of the system of protons in the first approximation. The quantity

V(x) appears as the potential energy of the coupling of the system of protons:

$$\nabla_x^2\Phi_0(x) + (2M/\hbar^2)(E_p - V(x))\Phi_0(x) = 0,$$

where M is the mass of the proton. The potential V(x) is no other than the potential of the exchange forces which couple the heavy nuclei of the molecules.

These results not only suggest the choice of the trial function, but also play a decisive role in the analysis of the solution and of the character of the forces binding our system. It should be recalled at this point that the potential V(x) for the ionized hydrogen molecule has the form of a well similar to the one shown in the figure (see below), where x stands for the distance between the protons, r. The minimum of 0.1025 atomic units is located at the distance $r_m = 2a_0$ (a_0 is the Bohr radius) between the protons; as the protons come closer to each other the potential increases according to the Coulomb law e^2/r, while it goes to zero as $-\frac{4}{3}re^{-r}$ at large relative proton distances.

The Born-Oppenheimer method is based on the fact that the ratio of the electron mass m to the proton mass M is small, so that the wave function can be expanded in powers of m/M. In our case the proton is replaced by the positron, which has a mass equal to that of the electron. However, a method of solution analogous to that of Born can be found even for this system. This was done by Slater[4] in the solution of the problem of the helium atom. He regarded one electron as fixed at the distance r_1, and determined the motion of the other electron in the field of the two centers (+e) and (−e). Slater first found the energy of the second electron, $V(r_1)$, as a function of the distance r_1 between the nucleus and the first electron (which enters as a parameter), and then regarded this energy as a field of conservative forces imposed on the first electron by the remaining part of the system. This is equivalent to the Born method. Slater pointed out the great accuracy of this method, which allowed him to restrict himself to the first approximation. Hylleraas[3] also remarks on the accuracy of the Slater method.

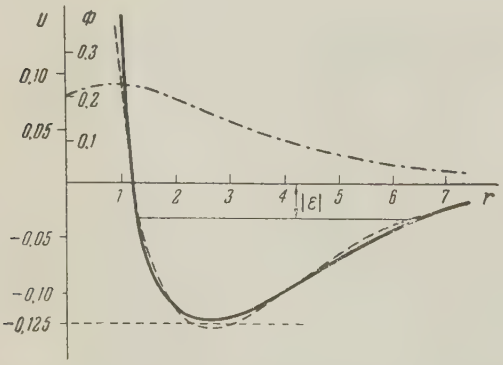

Solid curve: potential U of formula (23) in atomic units, counted from (−1/4) as the zero point; dotted curve: the function (24); dash-dotted curve: the wave function Φ(r).

In our problem we denote the position of the proton by the point a, and put the positron at the fixed point b. The coordinate of the positron, $r_2 = R$, will then be a constant parameter in Eq. (2). This leads us to the problem of two centers. Its solution is given by a system of wave functions of the hydrogen ion which depend on the distance $r_2 = R$ as on a parameter. This system of functions is found in a known fashion by separating the variables in elliptic coordinates:

$$\xi_0 = (r_1 + r_{12})/R, \qquad \eta_0 = (r_1 - r_{12})/R \tag{3}$$

The functions can be written in the form

$$F_{nlm}(R;\ \xi_0,\ \eta_0) = X_n(R,\ \xi_0)\,Y_{lm}(R,\ \eta_0). \tag{4}$$

We shall seek the solution of the equation in the form of an expansion in terms of the normalized eigenfunctions of the problem of two centers, $F_{nlm}(r_2;\ r_1,\ r_2)$:

$$\psi = \Phi_0(r_2)\,F_{00\sigma}(r_2;\ r_1,\ r_{12}) + \Phi_1(r_2)\,F_{10\sigma}(r_2;\ r_1,\ r_2) + \cdots.$$

We note that the expansion includes only functions $F_{nl\sigma}$ with the index σ, which corresponds to the vanishing of the projection of the angular momentum on the proton-positron axis. In the present paper we restrict ourselves to the first term in the expansion only. As we are using the variational principle, the corrections to the wave function can only lower the energy level. According to Slater and Born, Φ_0 must be the first approximation to the positron wave function. However, this function is somewhat more complicated than in the aforementioned papers.

2. THE LAGRANGE FUNCTION AND THE WAVE FUNCTION

We introduce the variables

$$r = r_2, \qquad \xi = r_1 + r_{12}; \qquad \eta = r_1 - r_{12}. \tag{5}$$

Fixing the positron coordinate r, we obtain the elliptic coordinates (3) of the electron: $\xi_0 = \xi/r$, $\eta_0 = \eta/r$. Let $F(r;\ \xi,\ \eta)$ be the wave function (4) of the ground state of the electron in the field of the positive charges fixed at the distance r. For the trial function we take

$$\psi(r,\ \xi,\ \eta) = \Phi(r)\,F(r;\ \xi,\ \eta), \tag{6}$$

in analogy to Slater's solution of the problem of the

helium atom.[4] Following Slater, we must regard $F(r;\ \xi,\ \eta)$ as a wave function in the variables ξ_0 and η_0, normalized to unity. The normalization factor $A(r)$ is a function of the parameter r:

$$F(r;\ \xi,\ \eta) = A(r) f(r;\ \xi,\ \eta). \tag{7}$$

Knowing the volume element and the normalization condition in elliptic coordinates, we can write this condition also in the coordinates (5):

$$\frac{1}{r}\frac{\pi}{4}\int_r^\infty d\xi \int_{-r}^{+r} d\eta\,(\xi^2-\eta^2)\,F^2(r;\ \xi,\ \eta) = 1. \tag{8}$$

Substituting in this formula the expression (7) for F, we obtain the following relation:

$$\frac{\pi}{4} A^2(r)\, J(r) = 1,$$

$$J(r) = \frac{1}{r}\int\int f^2(r;\ \xi,\ \eta)\,(\xi^2-\eta^2)\,d\xi d\eta. \tag{9}$$

The quantity $J(r)$ can be used to simplify the later calculations. According to Slater, the function $\Phi(r)$ is the wave function for the motion of a particle in some spherically symmetric potential well, normalized to unity. However, the simple method for finding this function which Slater employed in the helium problem cannot be applied in the present case.

We solve the problem in the following fashion. The wave function (6) and the lowest energy level E are determined by the minimum condition for the functional

$$E = \int\int\int L(r,\ \xi,\ \eta,\ \partial\psi/\partial r,\ \partial\psi/\partial\xi,\ \partial\psi/\partial\eta,\ \psi)\,d\tau. \tag{10}$$

Here L is the Lagrange function for the proton-electron-positron system in the coordinates (5). It is known that the integral (10) is equal to the energy of the system if ψ is the solution of Eq. (2), normalized to unity. We find the volume element $d\tau$ and the normalization condition in terms of the coordinates (5) from the analogous formulas in terms of the coordinates r_1, r_2, and r_{12}:[3]

$$\iiint \psi^2 d\tau = \pi^2 \int_0^\infty r\,dr \int_r^\infty d\xi \int_{-r}^{+r} d\eta\,(\xi^2-\eta^2)\,\psi^2 = 1. \tag{11}$$

With condition (8), this leads to the following normalization for the function $\Phi(r)$:

$$4\pi\int_0^\infty \Phi^2 r^2 dr = 1.$$

For the determination of the Lagrange function it is convenient to use the analogous function for the helium atom, derived by Hylleraas[3] in terms of the coordinates r_1, r_2, and r_{12}, but to define the potential according to formula (1). We note that the transformation (5) is reminiscent of the transformation used by Hylleraas in the paper just mentioned. Making use of this analogy, we find the Lagrange function for the proton-electron-positron system in terms of the coordinates (5):

$$\begin{aligned} L d\tau = \pi^2 e^2 r \Big\{ a_0 \Big[& \frac{5\xi^2-\eta^2-4r^2}{2}\left(\frac{\partial\psi}{\partial\xi}\right)^2 \\ & + \frac{\xi^2-5\eta^2+4r^2}{2}\left(\frac{\partial\psi}{\partial\eta}\right)^2 + \frac{\xi^2-\eta^2}{2}\left(\frac{\partial\psi}{\partial r}\right)^2 \\ & - (\xi^2-\eta^2)\frac{\partial\psi}{\partial\eta}\frac{\partial\psi}{\partial\xi} + \frac{r^2-\xi\eta}{r}(\xi+\eta)\frac{\partial\psi}{\partial r}\left(\frac{\partial\psi}{\partial\xi}-\frac{\partial\psi}{\partial\eta}\right)\Big] \\ & + \left(\frac{\xi^2-\eta^2}{r} - 4\xi\right)\psi^2 \Big\} dr d\xi d\eta. \end{aligned} \tag{12}$$

In the following we shall use atomic units (the energy unit in this system is twice the energy of the hydrogen atom, i.e., 2 Ry). In going over to this system we must set $a_0 = 1$ and $e = 1$ in the Lagrangian (12).

We must now write down the explicit expression for the wave function of the ground state of the hydrogen ion (4): $n = 0$, $l = 0$, and $m = \sigma$. At this point we note the following peculiarity. The system of functions (4) was obtained by separating the variables in elliptic coordinates (3). For each value of the distance R between the positive charges we separately determine a set of eigenvalues and eigenfunctions. The function F, therefore, depends on R as on a parameter, but there is no analytic expression for this dependence. As for the analytic dependence on ξ_0 and η_0, it is natural to refer to that form of the wave function (4) which was found by the variational method. Teller[6] has used the variational principle to calculate those functions $X_n(R, \xi_0)$ of the system (4) which have no nodes. He found the following approximate expression for the ground state:

$$X_0(R,\ \xi_0) = C\exp(-\sqrt{\gamma_0}\xi_0), \tag{13}$$

where γ_n is the eigenvalue in the equation for the function $X_n(R, \xi_0)$. The magnitude of this eigenvalue depends, first, on its number, but it is also a function of the distance R. Teller has given a table of the first few eigenvalues as a function of R. Guillemin and Zener[7] also determined the ground state wave function from the system (4) with great accuracy. Their choice was based on the following considerations.

It is known that, if the distance between the centers a and b is increased to infinity, then the elliptic coordinates (3) go over into parabolic coordinates with respect to that center which is at a finite distance from the electron. If, on the other hand, the charges a and b are brought together in the point O, the equations for X_n

and Y_{lm} go over into the equations of the Laguerre polynomials for the radial function of the helium atom and into the equations of the spherical functions, respectively. For large distances R between the centers a and b the wave functions (4) themselves go over into a symmetric combination of the wave functions of the hydrogen atom at the points a and b. If the charges are brought together at one point, these functions go over into the wave function of the helium atom:

$$\Psi_{R\to 0} = 2\sqrt{2/\pi}e^{-2r_0}, \qquad \Psi_{R\to\infty} = (e^{-r_a} + e^{-r_b})/\sqrt{2\pi}. \quad (14)$$

Guillemin and Zener therefore require that the wave function, firstly, satisfy the boundary conditions (14), and, secondly, that it can be expressed in the form of the product $X(\xi_0)\,Y(\eta_0)$. This function then has the form

$$\Psi(R;\ \xi_0,\ \eta_0) = Ce^{-\alpha R\xi/2}\,(e^{-\beta R\eta_0/2} + e^{+\beta R\eta_0/2}). \quad (15)$$

The normalization factor $C(R)$ and the quantities $\alpha(R)$ and $\beta(R)$ are continuous functions of the parameter R. In virtue of the foregoing properties of the elliptic coordinates (3), the function (15) satisfies the boundary conditions (14) if $\alpha(R)$, $\beta(R)$, and $C(R)$ satisfy the boundary conditions

$$\alpha(0) = 2, \qquad \beta(0) \text{ finite}, \qquad C(0) = 2/\sqrt{2\pi};$$
$$\alpha(\infty) = 1, \qquad \beta(\infty) = 1, \qquad C(\infty) = 1/\sqrt{2\pi}. \quad (16)$$

Guillemin and Zener find $\alpha(R)$ and $\beta(R)$ from the minimum conditions for the functional. They also give a table of these quantities for several values of R together with a derivation of the general formula. Teller's[6] tables for the function $\gamma(R)$ in formula (13) correspond to the quantity $2\sqrt{\gamma} = R\alpha$.

We therefore seek the wave function in the form (6). Here F is the ground state function for the problem of two centers, the parameter R becoming the independent variable r. In the coordinates (5) this function is written, according to (7) and (15),

$$F = Af, \qquad f = e^{-\alpha\xi/2}\cosh(\beta\eta/2). \quad (17)$$

$\alpha(R)$ and $\beta(R)$ are continuous functions determined from the tables of references 6 and 7 and the boundary conditions (16). The normalization factor $A(r)$ has, according to (16), the following values at the ends of the half axis $0 \le r < \infty$:

$$A(0) = 4/\sqrt{2\pi}, \qquad A(\infty) = 2/\sqrt{2\pi}. \quad (16a)$$

Integrating over ξ and η in (9), we can write the function $J(r)$ in the explicit form

$$J(r) = \frac{2e^{-\alpha r}}{\alpha}\left\{\frac{r^2}{3} + \frac{1}{\alpha}\left(r + \frac{1}{\alpha}\right)\left(1 + \frac{\sinh\beta r}{\beta r}\right) + \frac{1}{\beta^2}\left(\cosh\beta r - \frac{\sinh\beta r}{\beta r}\right)\right\}. \quad (18)$$

Using the boundary conditions (16) for α and β, we can show that

$$J(0) = 1/2, \qquad J(\infty) = 2. \quad (18a)$$

Substitution of the numerical values of references 7 and 6 shows that J is a monotonically increasing function of r. The normalization conditions (8) and (9) at the points $r = 0$ and $r \to \infty$ are automatically fulfilled by virtue of Eqs. (16a) and (18a). At intermediate points the factor $A(r)$ is determined by the first of the formulas (9) and formula (18).

3. SOLUTION OF THE PROBLEM

In solving the problem by the variational method we substitute the Lagrangian (12) in the integral (10) and integrate over the volume in the manner indicated in formula (11). The trial function (6) is conveniently written in the form

$$\psi = \Phi F = \varphi(r)\,f(r;\xi,\eta), \qquad \varphi(r) = \Phi(r)\,A(r). \quad (19)$$

The function $\varphi(r)$ is unknown. The integration over the variables ξ and η does not cause any basic difficulties but is very cumbersome. With the help of the function $J(r)$ the calculations can be somewhat simplified. Using Eq. (18), we can write the result in the form

$$E = \pi^2\int_0^\infty \left\{\frac{r^2}{2}\frac{d\varphi}{dr}\frac{d}{dr}(J\varphi) + r\chi(r)\varphi^2\right\}dr,$$
$$\pi^2\int_0^\infty \varphi^2 J r^2 dr = 1. \quad (20)$$

Here $\chi(r)$ is a function of r, both explicitly and implicitly through $\alpha(r)$ and $\beta(r)$. After some simple calculations, using (9) and (19), we can replace the function $\varphi(r)$ in the integral (20) by the normalized function $\Phi(r)$. Then formulas (20) take the form

$$E = 4\pi\int_0^\infty \left\{\frac{1}{2}\left(\frac{d\Phi}{dr}\right)^2 + \left[\frac{\chi(r)}{rJ} - \frac{J_r^2}{8J^2}\right]\Phi^2\right\} r^2\,dr,$$
$$4\pi\int_0^\infty \Phi^2 r^2 dr = 1. \quad (21)$$

Here J_r is a total derivative:

$$J_r \equiv dJ/dr = \partial J/\partial r + \alpha_r \partial J/\partial\alpha + \beta_r \partial J/\partial\beta.$$

Equations (21) define the isoperimetric problem of variational calculus, which can be reduced

to the problem of the absolute minimum of the functional

$$S^* = 4\pi \int_0^\infty L^* r^2 \, dr, \tag{21a}$$

where we take $L^* = L + \lambda\Phi^2$ for the new Lagrangian. It is known from quantum mechanics that the factor λ in the Lagrangian in this case determines the energy of the system: $\lambda = -E$. The Euler equation for the functional S^* gives

$$\frac{1}{r^2}\frac{d}{dr}\left(r^2\frac{d\Phi}{dr}\right) - 2\left[\left(\frac{\chi(r)}{rJ} - \frac{J_r^2}{8J^2}\right) + \lambda\right]\Phi^2 = 0.$$

This is the equation of motion of a particle in a spherically symmetric potential field,

$$\frac{1}{2}\frac{1}{r^2}\frac{d}{dr}\left(r^2\frac{d\Phi}{dr}\right) - (U(r) - E)\,\Phi = 0 \tag{22}$$

with the potential energy (in atomic units)

$$U(r) = \chi / rJ - J_r^2 / 8J^2, \tag{23}$$

given by the explicit formula

$$\begin{aligned} U(r) = {} & \frac{1}{r} + \frac{5\beta^2}{8} + \frac{1}{8rJ}\left(\frac{\partial}{\partial r} + \alpha_r\frac{\partial}{\partial\alpha} + \beta_r\frac{\partial}{\partial\beta}\right)^2 (rJ) \\ & - \frac{J_r^2}{8J} + \frac{e^{-\alpha r}}{J\alpha}\left\{\left(r + \frac{1}{\alpha}\right)\left(\frac{5\alpha}{4} - \frac{5\beta^2}{4\alpha} - 4\right)\left(\frac{\sinh r\beta}{r\beta} + 1\right)\right. \\ & \left. - \beta^2\left(\frac{5r^2}{6} + \frac{r}{4\alpha} + \frac{1}{4\alpha^2}\right) + \left(\frac{1}{4}\cosh r\beta + \frac{\alpha}{\beta}\sinh r\beta + \alpha r + 1\right)\right\} \\ & + \frac{\alpha_r}{2}\left(1 + \frac{1}{\alpha r}\right) - \frac{\alpha_r}{2}\frac{e^{-\alpha r}}{J\alpha}\left(\frac{r}{\alpha} + \frac{1}{\alpha^2} + \frac{1}{r\alpha^3}\right)\left(\frac{\sinh r\beta}{r\beta} + 1\right) \\ & - \beta_r^2\frac{e^{-\alpha r}}{J\alpha}\frac{r^2}{12}\left(\frac{r^2}{5} + \frac{r}{\alpha} + \frac{1}{\alpha^2}\right) \\ & + \frac{\beta_r}{2\beta}\frac{e^{-\alpha r}}{J\alpha}\left\{\left(r + \frac{1}{\alpha}\right)\left[\frac{2}{\alpha r}\left(\cosh r\beta - \frac{\sinh r\beta}{r\beta}\right) - \frac{r\beta^2}{3\alpha}\right]\right. \\ & \left. + \frac{3}{r\beta^3}\left(\cosh r\beta - \frac{\sinh r\beta}{r\beta}\right) - \frac{\sinh r\beta}{\beta}\right\}. \end{aligned} \tag{23a}$$

For $r \to 0$ the potential increases according to the Coulomb law:

$$U_{r\to 0} \approx 0.63 / r.$$

As the proton and the positron come close to each other there should be a repulsion given by the potential (1/r). Hence we have here a screening effect. The behavior of the potential at infinity is determined by the boundary conditions (16) and (18a):

$$\lim U_{r\to\infty} = -\tfrac{1}{4} \text{ at. units.}$$

The first (Coulomb) term in formula (23a) cancels out, and the potential decreases exponentially as $r \cdot \exp(-0.49\,r)$. The intermediate points were calculated with the help of the tables of references 7 and 6. The resulting curve is shown in the figure (solid curve). It has the same behavior for $r \to 0$ and $r \to \infty$ as the potential for the ionized hydrogen molecule. Its minimum (0.375 at. un.) lies at $r_m = 2.5$. The limit at infinity of this quantity is the energy of the positronium atom ($-\frac{1}{4}$). Thus the "free energy" amounts to only 0.125 at. un. of the total depth of the potential well (0.375 at. un.), while the remaining 0.25 at. un. represent the "bound" (internal) energy of positronium. The quantity $U(r)$ and the potential of the hydrogen ion are therefore comparable with each other: the minimum of $U(r)$ is somewhat lower and is located further away from the proton than is the case for the hydrogen atom.

The potential (23), therefore, has the same properties as the potential of the molecular forces binding the atomic nuclei in a homeopolar molecule. Hence the forces binding the positron have a quantum nature. They arise from the fact that the electron may be observed near the proton as well as near the positron, i.e., it belongs to both these particles simultaneously. This circumstance is incorporated in the choice of the form of the trial function (5). It was proposed by Ferrell[8] that the forces coupling the positron to the molecules of the medium have a potential of the same form as the $U(r)$ shown in the figure. In the calculation of the potential of the hydrogen molecule Hylleraas[9] assumed 50% screening of the nuclei, since a screening of this magnitude leads to good agreement with experiment. In our case the screening is also close to 50%.

We now compute the ground energy level in Eq. (22). We use the following approximate formula for the potential (23):

$$\begin{aligned} U = U_0 + U_q = {} & 0.13\,[\exp(-0.96x) - 2\exp(-0.48x)] \\ & + (2r)^{-1}\exp(-2r) \end{aligned} \tag{24}$$

(in atomic units), where $x = r - 2.5$. This potential has the level $-\frac{1}{4}$ as zero point. Accordingly we introduce $\epsilon = E + \frac{1}{4}$ instead of the energy E. The dotted curve representing the potential (24) in the figure runs very close to the curve representing the potential (23). The main term in formula (24), U_0, is the well-known Morse potential.[10] The other term in (24) vanishes everywhere except near the origin of the coordinate system. We can obtain an exact solution of Eq. (22) by taking U_0 instead of U. For this purpose we make use of the method given in the book of Schiff.[11] After the substitution $\Phi(r) = v(r)/r$ Eq. (22) goes over into

$$v''(r) = (U_0 - \varepsilon_0)\,v(r) = 0$$

According to Schiff we must find a solution $v(r)$ which is zero at $r = 0$ and $r = \infty$. We solve the abovementioned equation by the method outlined in the book of Landau and Lifshitz.[10] After the substitution

$$z = (2\sqrt{0.13}/0.48)\, e^{-0.43x}, \qquad s = \sqrt{-\varepsilon_0}/0.48,$$
$$n = \sqrt{0.13}/0.48 - (s + 1/2), \qquad v(z) = e^{-z/2} z^s w(z),$$

we obtain the hypergeometric equation

$$zw'' + (2s + 1 - z)\, w' + nw = 0.$$

The characteristic equations for its roots are $\rho_1 = 0$ and $\rho_2 = -2s$. Since $z \to 0$ for $x \to \infty$, the only solution is the first hypergeometric function $w(z) = {}_1F_1(-n, 2s+1, z)$. The energy ϵ_0 is determined by the second boundary condition

$$\varepsilon_0 = -0.035. \tag{25}$$

We now turn to the potential (23), which is counted from the level -0.5. Equation (22) has the following form near the origin:

$$\nabla_r^2 \Phi - (1.25/r - \varepsilon)\, \Phi = 0.$$

Its characteristic roots are $\rho_1 = 0$ and $\rho_2 = -1$. The first solution therefore does not vanish at the origin. The second solution has there either a pole or a logarithmic divergence and must be discarded. Since the wave function of the ground state has no nodes, we may conclude, after integrating this equation once, that the derivative $\Phi'(r)$ is positive for small r. Assuming that the potential (23) has for large r the form $-k \exp(-\alpha r)$, we transform Eq. (22) to Bessel's equation by the substitution $y = \exp(-\alpha r/2)$. This problem was proposed in the book of Schiff.[11] Its solution is

$$\Phi(r) = J_\nu(by)/r = \frac{1}{r} e^{-\nu\alpha r/2}(B_0 + B_1 e^{-\alpha r/2} + \ldots). \tag{26}$$

The wave function has the form shown in the figure.

We shall solve Eq. (22) by the variational method:

$$\varepsilon = \tfrac{1}{2}\int_0^\infty (d\Phi/dr)^2 r^2\, dr + \int_0^\infty U(r) r^2\, dr, \qquad \int_0^\infty \Phi^2 r^2 dr = 1, \tag{27}$$

where $U = U_0 + U_q$ is the potential (24). Substituting the function

$$\Phi_i(r) = e^{-0.28r}(1 + 0.12\, re^{-0.1r})/4.82 \tag{28}$$

in the integral (27), we find the energy value

$$\varepsilon_i = \varepsilon_{0i} + \varepsilon_{qi} = -0.028 + 0.004 = -0.024.$$

Here ϵ_{qi} is the "Coulomb" part of the energy arising from the integral over U_q. The solution of Eq. (22) must have the asymptotic behavior (26). The value of ϵ_i is therefore higher than the actual level. From the minimizing sequence of functions Φ_i we can find the sequence of energies ϵ_i. The calculations show that the absolute value of ϵ_{qi} decreases as the absolute value of the energy ϵ_i increases with the number i. We can therefore assume that the energy $\epsilon_i = \epsilon_{0i} + \epsilon_{qi}$ approaches the limit ϵ_0, corresponding to the solution of Eq. (27) with the potential U_0, plus a correction ϵ_q which does not exceed 0.004. The sequence of ϵ_{0i}, however, has an exact lower limit, namely the solution (25). We can therefore regard

$$\varepsilon = -0.032 \text{ at. units}$$

as the solution of Eq. (22).

4. DISCUSSION

By this method the solution of the variational problem (10) with the boundary conditions (14) to (16) gives in first approximation the value $E = -0.282$ at. un. for the energy of the system. The ionization energy is equal to 0.032, i.e., about one third of that of the hydrogen ion. The system can only disintegrate into a proton and a positronium atom. Since we have used the variational method, the ionization energy found is lower than the actual one. With an appropriate choice of the functions $\alpha(r)$ and $\beta(r)$ (with the same boundary conditions) the potential well (23) can be made deeper. From a theoretical point of view this corresponds to solving the following variational problem: find those functions α and β, satisfying the boundary conditions (14) to (16), which lead to a minimum of the functional (21a). This variation leaves the limit $(-1/4)$ unchanged, since the latter depends only on the boundary conditions (14) to (16).

In comparing these results with those of other authors, we should recall that Simons[12] has made calculations for the "positronium chloride" molecule. He used the electrostatic field due to the negative chlorine ion. This field has been calculated by Hartree by the method of the self-consistent field in order to determine the energy of, for example, a sodium ion located in it. Simons developed a method to solve the problem of the motion of a positron in the field of the chlorine ion and found that the potential well of this ion is sufficiently deep to bind the positron. He obtained a heteropolar molecule analogous to sodium chloride.

By the method given in the present paper we can compute the forces of attraction between a positron (or positronium) and neutral atoms.

The method can also be applied to the helium atom. The calculations would probably confirm the assertion of Ferrell[8,13] that two counter-acting forces act between the positronium and the helium atom: the attractive Van-der-Waals forces and the repulsive forces arising from the fact that the two electrons of the helium atom form a closed shell. These repulsive forces should be the main reason for the formation of the long-lived component in liquid helium, but the Van-der-Waals forces work against this effect. The solution of an equation analogous to equation (2) for the helium-positronium system would lead to results which could be compared with presently available experimental data on positronium in liquid helium.[14] In another article,[15] published recently, Ferrell casts some doubt on the existing belief that the quenching of positronium atoms in gases by adding NO is caused by the exchange of electrons with opposite spins. He assumes that the annihilation is caused by the exchange interaction between the electron of the positronium and the valence electrons of the molecule. After an analysis of the experimental work on the quenching of positronium by DPH (diphenyl picryl hydrazyl) in benzene, Ferrell asserts the following: the annihilation of positronium is due to the capture of the whole positronium atom by the DPH molecule under the action of the covalent coupling between the electron of the positronium and the valence electrons of DPH. Further calculations based on the methods presented in the present paper could, perhaps, help in the resolution of the abovementioned questions.

In conclusion the author expresses his deep gratitude to his adviser, Prof. A. A. Sokolov.

[1] E. A. Hylleraas, Z. Physik **48**, 469 (1928).
[2] G. Breit, Phys. Rev. **35**, 569 (1930).
[3] E. A. Hylleraas, Z. Physik **54**, 347 (1929).
[4] J. C. Slater, Proc. Nat. Acad. Sci. Amer. **13**, 423 (1927).
[5] M. Born and J. R. Oppenheimer, Ann. Physik **84**, 457 (1927).
[6] E. Teller, Z. Physik **61**, 458 (1930).
[7] V. Guillemin and C. Zener, Proc. Nat. Acad. Sci. Amer. **15**, 314 (1929).
[8] R. A. Ferrell, Revs. Modern Phys. **28**, 308 (1956).
[9] E. A. Hylleraas, Z. Physik **71**, 739 (1931).
[10] L. D. Landau and E. M. Lifshitz, Квантовая механика (Quantum Mechanics), Gostekhizdat (1948); Engl. Transl. Addison–Wesley, Reading, Mass. (1958).
[11] L. Schiff, Quantum Mechanics, McGraw-Hill Book Co., N. Y. (1955).
[12] L. Simons, Finska Vetenskaps Societeten, Suomen Tiedeseura (Societas Scientiarium Fennica, Comm. Phys.-Math., Helsingfors) **14**, 2 (1950).
[13] R. A. Ferrell, Phys. Rev. **108**, 167 (1957).
[14] D. A. L. Paul and R. L. Graham, Phys. Rev. **106**, 16 (1957). J. Wackerle and R. Stump, Phys. Rev. **106**, 18 (1957);
[15] R. A. Ferrell, Phys. Rev. **110**, 1355 (1958).

Translated by R. Lipperheide
83

ON THEORIES WITH AN INDEFINITE METRIC

V. G. VAKS

Submitted to JETP editor February 13, 1959

J. Exptl. Theoret. Phys. (U.S.S.R.) 37, 467-469 (August, 1959)

The conditions of unitarity and macro-causality for the Lee model with an indefinite metric are investigated.

We consider the Lee model with an indefinite metric,[1,2] regarding the coordinates of the "heavy" N and V particles as fixed. The unrenormalized Hamiltonian has the form

$$H = -m_V \sum_i \psi^+_{V_i}\psi_{V_i} + \sum_k \omega_k a_k^+ a_k$$
$$-g_0 \sum_k \frac{f_k}{\sqrt{2\omega_k}} (\psi^+_{V_i}\psi_{N_i} a_k e^{ikR_i} + \psi_{V_i}\psi^+_{N_i} a_k^+ e^{-ikR_i}).$$

Here $\psi^+_{V_i}$, ψ_{V_i}, $\psi^+_{N_i}$, and ψ_{N_i} are the creation and absorption operators for the V and N particles at the point $\mathbf{R}_i$; the mass of the N particle is $m_N = 0$;[2] g_0 is pure imaginary; for point interactions the cut-off factor f_k goes to unity: $f_k \to 1$.

The constants m_V and g_0 are chosen such that the denominator of the Green's function of the V particles,

$$g_0^2 h(\varepsilon) = \varepsilon + m_V + g_0^2 \sum_k \frac{f_k^2}{2\omega_k} \frac{1}{\omega_k - \varepsilon}$$

has a multiple root at $E_0 < \mu$ (dotted curve in the figure). Let us consider the problem of the bound states of the θ particles in the field of the two particles N_a and N_b. The distance $|\mathbf{R}_a - \mathbf{R}_b|$ is arbitrary. The state vector has the form

$$\Phi = c_a |V_a N_b\rangle + c_b |V_b N_a\rangle + \sum_k \varphi_k |N_a N_b \theta_k\rangle.$$

Solving the Schrödinger equation $H\Phi = E\Phi$, we obtain a homogeneous system of equations for c_a and c_b for the bound states with $E < \mu$. The secular equation for this system yields

$$(h(\varepsilon) - J(\varepsilon))(h(\varepsilon) + J(\varepsilon)) \equiv g_{as}(\varepsilon) g_s(\varepsilon) = 0,$$
$$J(\varepsilon) = \sum_q \frac{f_q^2}{2\omega_q} \frac{\exp\{iq(\mathbf{R}_a - \mathbf{R}_b)\}}{\omega_q - \varepsilon}.$$

The dispersion curves $g_s(\epsilon)$ and $g_{as}(\epsilon)$ are given in the figure. The presence of a second center leads, of course, to the splitting of the "degenerate term" E_0. The function $g_s(\epsilon)$ has no real roots, where the function $g_{as}(\epsilon)$ has two real roots, E_1 and E_2; the state with energy E_2 has a negative norm. This consequence of the Lee model suggests that the presence of a multiple pole in the single nucleon Green's function gives rise to states with negative norm in the deuteron problem.

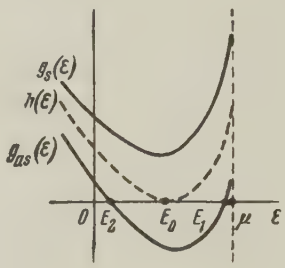

Bogolyubov, Medvedev, and Polivanov[3] proposed a method for the description of the more general case which allows for states with negative norm ("ghost states"). According to these authors, the state vector is given by a superposition of states with positive and negative norms. The contribution of the latter states is determined from the preceding ("preparatory") experiment as well as from the one that follows, and in such a way that the "ghost state" does not change in this later experiment. Then the presence of the state with negative norm cannot be detected in any experiment which measures the difference of physical quantities (for example, the particle flow) before and after the experiment, and the conservation of the total norm guarantees the unitarity of the observed S matrix. We shall show that this violates the condition of macro-causality. This condition is, for two remote centers, given by the relation $S(A+B) = S(B)S(A)$, where $S(A)$, $S(B)$, and $S(A+B)$ are the S matrices for the scatterers A, B, and A+B.

We assume that $h(\epsilon)$ has the distinct real roots E_p and $E_g < E_p$, and solve the problem of the scattering of two θ particles by the separated particles V_{ap} and N_b. According to the proposed scheme we have

$$\tilde{S}^{k_1k_2V_{ap}N_b}_{\cdots} = S^{k_1k_2V_{ap}N_b}_{\cdots} + \sum_{q_1q_2} g^a_{q_1q_2}\delta(\omega_{q_1}+\omega_{q_2}+E_g-E)$$
$$\times S^{q_1q_2V_{ag}N_b}_{\cdots} + \sum_q g^b_q\delta(\omega_q+E_p+E_g-E)S^{qV_{ap}V_{bg}}.$$

The upper indices of S denote the incoming particles and the lower indices correspond to the possible outgoing channels; V_{ap}, V_{bp} and V_{ag}, V_{bg} are the physical and ghost states of the V particle at the points A and B; $S^{\cdots}_{\cdots}$ are standard S matrices obtained from the solution of the Schrödinger or Dyson equation; $\tilde{S}^{\cdots}_{\cdots}$ is the observed S matrix. The functions $g^a_{q_1q_2}$, g^b_q describe the initial distribution of the θ particles in the "ghost" state. They are determined from the condition that there be no scattering of "ghost" states:

$$S^{k_1k_2V_{ap}N_b}_{k'k''V_{ag}N_b} + \sum_{q_1q_2} g_{q_1q_2}\delta(\omega_{q_1}+\omega_{q_2}+E_g-E)(S-1)^{q_1q_2V_{ag}N_b}_{k'k''V_{ag}N_b}$$
$$+\sum_q g^b_q\delta(\omega_q+E_p+E_g-E)S^{qV_{ap}V_{bg}}_{k'k''V_{ag}N_b}=0$$

and analogously for V_{bg}.

We restrict ourselves to the zeroth approximation with respect to $1/|\mathbf{R_a}-\mathbf{R_b}|$. The problem is readily solved by graphic methods. The answer is of the form

$$\tilde{S}(A+B)=\tilde{S}(B)\tilde{S}(A)+R.$$

The meaning of R is the following. Suppose we have determined, in the absence of the center B, that admixture of ghost states which leads to no scattering of ghost states by the center A, i.e., we have found $\tilde{S}(A)$. If now the particles N_b are added at the point B, the real scattering will be accompanied by the scattering of "ghost" states of the θ particles, so that the previous superposition has to be changed. The absence of "ghost" scattering in the complete problem can be achieved by changing the state vector, but this gives rise to additional transitions from ghost states to physical states at the point A, which are described by the matrix R. In the problem of the scattering of two θ particles, R does not decrease with the distance. This is precisely the reason why this problem was selected to illustrate the contradiction.

A unitary matrix $\tilde{S}$ can also be constructed by calling the states which involve ghost states, "auxiliary" or "unobservable" states, which may therefore undergo arbitrary elastic processes as long as these conserve the norm in the ghost subspace. However, with this approach the theory has to forego uniqueness and a clear interpretation.

Let us now assume that the roots of $h(\epsilon)$ are complex (and conjugate to each other). Following Källén and Pauli,[1] we show by direct calculation that the S matrix is in this case automatically unitary. Let us consider, for example, the scattering of 2θ from N. From the equation $H\Phi = E\Phi$ with the usual boundary conditions we obtain

$$\Phi=\sum_k \varphi_{k,k_0q_0}\big|V\theta_k\rangle+\sum_{kq}\psi_{kq,k_0q_0}\big|\theta_k\theta_qN\rangle,$$

$$\psi_{kq,k_0q_0}=\tfrac{1}{2}(\delta_{kk_0}\delta_{qq_0}+\delta_{kq_0}\delta_{qk_0})$$
$$+\frac{g_0}{2}\frac{1}{\omega_k+\omega_q-E-i\gamma}\left(\frac{f_k}{\sqrt{2\omega_k}}\varphi_{q,k_0q_0}+\frac{f_q}{\sqrt{2\omega_q}}\varphi_{k,k_0q_0}\right),$$

$$h(E-\omega_k+i\gamma)\varphi_{k,k_0q_0}=-\varphi_{0k,k_0q_0}$$
$$-\sum_q\frac{f_kf_q}{\sqrt{4\omega_k\omega_q}}\frac{\varphi_{q,k_0q_0}}{\omega_k+\omega_q-E-i\gamma}\equiv iU_{k,k_0q_0},$$

where

$$E=\omega_{k_0}+\omega_{q_0},\quad \gamma\to+0,$$

$$\varphi_{0k,k_0q_0}=\frac{1}{g_0}\left(\frac{f_{q_0}}{\sqrt{2\omega_{q_0}}}\delta_{kk_0}+\frac{f_{k_0}}{\sqrt{2\omega_{k_0}}}\delta_{kq_0}\right).$$

Calculations similar to those of reference 1 lead to the equation

$$2\pi\delta(E-E')|g_0|^2\Big\{i\Big(\sum_{E-\omega_k<\mu}+\sum_{E-\omega_k>\mu}\Big)U^+_{k_0q_0,k}U_{k,k_0q_0}$$
$$\times\left(\frac{1}{h(E-\omega_k+i\gamma)}-\frac{1}{h(E-\omega_k-i\gamma)}\right)$$
$$-i\sum_k(\varphi^+_{k_0q_0,k}\varphi_{0k,k_0q_0}-\varphi^+_{k_0q_0,0k}\varphi_{k,k_0q_0})$$
$$+2\pi\sum_{kq}\frac{f_kf_q}{\sqrt{4\omega_k\omega_q}}\varphi^+_{k_0q_0,k}\varphi_{k,k_0q_0}\delta(\omega_k+\omega_q-E)\Big\}=0.$$

The sum over $\mathbf{k}$ with $E-\omega_k<\mu$ in the first term, which describes transitions to bound states in the paper of Källén and Pauli, is here equal to zero, since $h(\epsilon)$ has no zeros on the real axis. With the notation

$$\langle kq|R|k_0q_0\rangle=\pi ig_0\delta(\omega_k+\omega_q-E)$$
$$\times\left(\frac{f_k}{\sqrt{2\omega_k}}\varphi_{q,k_0q_0}+\frac{f_q}{\sqrt{2\omega_q}}\varphi_{k,k_0q_0}\right),$$

we obtain from the preceding equation

$$\langle k_0'q_0'|R+R^+R+R^+R|k_0q_0\rangle=0.$$

The proof is easily generalized for the other sectors, as for example, for the problem of the scattering of two θ particles by two N particles, if, as before, the functions $g_S(\epsilon)$ and $g_{AS}(\epsilon)$ do not intersect the real axis.

In the case of complex roots of $h(\epsilon)$ the stationary S matrix of the Lee model is therefore unitary[4] without any trivial violations of the causality principle. The scattering amplitude has a pole in the upper half of the energy plane, so that the dispersion relations have to be modified. In the sector $N+\theta$ we have two nonorthogonal state vectors with vanishing norm, $\Phi_{1,2}$, corresponding to the eigenvalues $\lambda_0 \pm i\lambda_1$ of the Hamiltonian. As solutions of the equation $i\partial\Phi/\partial t = H\Phi$ both of these vectors depend exponentially on the time: $\Phi_{1,2} \sim \exp[-i(\lambda_0 \pm i\lambda_1)t]$, but the norm of an arbitrary superposition is, of course, preserved.

The author thanks K. A. Ter-Martirosyan and L. A. Maksimov for their interest in this work and comments.

[1] G. Källén and W. Pauli, Kgl. Danske Videnskab. Selskab, Mat.-fys. Medd. **30**, No. 7 (1955).

[2] W. Heisenberg, Nucl. Phys. **4**, 532 (1957).

[3] Bogolyubov, Medvedev, and Polivanov, Preprint, Joint Institute of Nuclear Research, (1958).

[4] R. Ascoli and E. Minardi, Nuovo cimento **8**, 951 (1958); Nucl. Phys. **9**, 242 (1958).

Translated by R. Lipperheide
84

WAVE EQUATIONS WITH ZERO AND NONZERO REST MASSES

V. I. OGIEVETSKIĬ and I. V. POLUBARINOV

Joint Institute for Nuclear Research

Submitted to JETP editor February 27, 1959

J. Exptl. Theoret. Phys. (U.S.S.R.) **37**, 470-476 (August, 1959)

It is shown that wave equations with nonzero rest mass are invariant with respect to a 15-parameter group of transformations which is a representation of the conformal group.

1. INTRODUCTION

THE Klein-Gordon and Dirac equations are invariant with respect to a 10-parameter group of transformations which is a representation of the inhomogeneous Lorentz group L_{10}.

It has been shown by Cunnigham,[1] Bateman,[2] Dirac,[3] Bhabha,[4] Pauli,[5] McLennan,[6] and others that in the case of zero rest mass the wave equations are invariant under a wider, 15-parameter group of transformations which forms a representation of the conformal group C_4 including L_{10}. The Dirac equation for the neutrino is in addition invariant under the 4-parameter Pauli group.

It is generally believed that these invariance properties are peculiar to wave equations with zero rest mass.

However, we show below that both the Klein-Gordon and the Dirac equations with nonzero rest mass are also invariant under a 15-parameter group of transformations G_{15} which is a representation of the conformal group C_4. The analogue of Pauli's group also exists for the Dirac equation. The operators for all these transformations contain as a parameter the mass m, and in the limit $m = 0$ go over into the well known operators.

Some of the operators of the representation of the Lorentz group L_{10} assume an unusual form in the group G_{15}. This causes certain difficulties: under Lorentz rotations the momentum of a particle does not transform as a four-vector.

In the derivation of the transformations for nonzero rest mass we shall made use of the known form of the transformation for $m = 0$.

In this connection we discuss in Sec. 2 the representation of the conformal group C_4 for rest mass zero. In Sec. 3 we establish the method for deriving the corresponding transformations for $m \neq 0$. In Sec. 4 we give the infinitesimal operators of the G_{15} for wave equations with $m \neq 0$ and the analogue of the Pauli group.

2. CONFORMAL GROUP AND WAVE EQUATIONS WITH ZERO REST MASS

As indicated in the introduction, many papers exist[1-6] dealing with the proof of conformal invariance of wave equations with zero rest mass. In this section we give a summary of the principal results, some of which appear in references 3 — 8, relevant to the problem of the conformal group and the invariance of the Klein-Gordon and Dirac equations with zero rest mass. The 15-parameter conformal group C_4 consists of the Lorentz group L_{10} (translations and rotations), of the scale transformation, and of the four properly conformal transformations (see first line, Table I). Properly conformal transformations correspond to the product of an inversion in the unit hyper-sphere $x^1 = x_\mu/x^2$, then a translation, and then again an inversion. Three of them (spatial) are related to transitions to a uniformly accelerating frame of reference.[9-13]

The transformation laws for solutions of the Klein-Gordon and Dirac equations with rest mass zero

$$\Box^2 \varphi_0(x) = 0, \tag{1}$$

$$\gamma_\mu \frac{\partial}{\partial x_\mu} \psi_0(x) = 0. \tag{2}$$

are given in lines 3 and 4 of Table I.

As can be seen from Table I the solution of even the Klein-Gordon equation does not behave like a scalar under scale transformations and properly conformal transformations.

Functions transforming according to any of the representations of the conformal group change according to the following law under infinitesimal transformations:*

$$\psi'(x) = (1 + ia_\mu P_\mu)\psi(x), \tag{3}$$

*We take the physical momentum and angular momentum operators for P_μ and $M_{\mu\nu}$ — hence the appearance of the imaginary unit i.

TABLE I. Finite transformations

	Scale transformation (1 parameter)*	Properly conformal transformations (4 parameters)**
Transformation of coordinates	$x'_\mu = \frac{x_\mu}{a}$	$x'_\mu = \frac{x_\mu - \alpha_\mu x^2}{1-2(\alpha x)+\alpha^2 x^2}$
Transformation of a scalar function	$f'(x_\mu) = f(ax_\mu)$	$f'(x_\mu) = f\left(\frac{x_\mu + \alpha_\mu x^2}{1+2(\alpha x)+\alpha^2 x^2}\right)$
Transformation of solutions of the Klein-Gordon equation with m = 0	$\varphi'_0(x_\mu) = a\varphi_0(ax_\mu)$	$\varphi'_0(x_\mu) = [1+2(\alpha x)+\alpha^2 x^2]^{-1}\varphi_0\left(\frac{x_\mu+\alpha_\mu x^2}{1+2(\alpha x)+\alpha^2 x^2}\right)$
Transformation of solutions of the Dirac equation with m = 0.	$\psi'_0(x_\mu) = a^{3/2}\psi_0(ax_\mu)$	$\psi'_0(x_\mu) = \frac{1+2(\alpha x)-(\alpha\gamma)(\gamma x)}{[1+2(\alpha x)+\alpha^2 x^2]^2}\psi_0\left(\frac{x_\mu+\alpha_\mu x^2}{1+2(\alpha x)+\alpha^2 x^2}\right)$

*The numerical value of the power to which a must be raised in the case of $\phi_0(ax)$ and $\psi_0(ax)$ is determined by the requirement that ϕ_0 and ψ_0 transform according to a representation of the group C_4 in its entirety, and may be found from the structural relation (15).

**$x^2 = x_\mu x_\mu$, $\alpha^2 = \alpha_\mu\alpha_\mu$, $(\alpha x) = \alpha_\mu x_\mu$, $\mu = 1,2,3,4$.

$$\psi'(x) = (1 + i\omega_{\mu\nu}M_{\mu\nu})\psi(x), \tag{4}$$

$$\psi'(x) = (1 + \varepsilon I)\psi(x), \tag{5}$$

$$\psi'(x) = (1 + \alpha_\mu I_\mu)\psi(x), \tag{6}$$

where P_μ, $M_{\mu\nu}$, I, and I_μ are the infinitesimal operators for the translation, rotation, scale and properly conformal transformations, and a_μ, $\omega_{\mu\nu}$, ϵ and α_μ are the corresponding infinitesimal transformation parameters.

The infinitesimal operators of the conformal group and its representations satisfy the following structural relations:

$$[P_\mu,\ P_\nu] = 0, \tag{7}$$

$$[P_\mu,\ M_{\nu\lambda}] = -i(\delta_{\mu\nu}P_\lambda - \delta_{\mu\lambda}P_\nu), \tag{8}$$

$$[M_{\mu\nu},\ M_{\lambda\rho}] = i(\delta_{\mu\lambda}M_{\nu\rho} + \delta_{\nu\rho}M_{\mu\lambda} - \delta_{\mu\rho}M_{\nu\lambda} - \delta_{\nu\lambda}M_{\mu\rho}), \tag{9}$$

$$[I_\mu,\ M_{\nu\lambda}] = -i(\delta_{\mu\nu}I_\lambda - \delta_{\mu\lambda}I_\nu), \tag{10}$$

$$[I_\mu,\ I_\nu] = 0, \tag{11}$$

$$[P_\mu,\ I] = P_\mu, \tag{12}$$

$$[M_{\mu\nu},\ I] = 0, \tag{13}$$

$$[I_\mu,\ I] = -I_\mu, \tag{14}$$

$$[P_\mu,\ I_\nu] = 2(M_{\mu\nu} + i\delta_{\mu\nu}I). \tag{15}$$

For solutions of the Klein-Gordon equation with zero mass the infinitesimal operators in x- and p-representations respectively [$\psi(p) = (2\pi)^{-2} \times \int \exp(-ipx)\psi(x)\,dx$] are given as follows

$$P_\mu = -i\partial/\partial x_\mu, \qquad P_\mu = p_\mu,$$

$$M_{\mu\nu} = -i(x_\mu\partial/\partial x_\nu - x_\nu\partial/\partial x_\mu),$$

$$M_{\mu\nu} = -i(p_\mu\partial/\partial p_\nu - p_\nu\partial/\partial p_\mu),$$

$$I = x_\mu\partial/\partial x_\mu + 1, \qquad I = -p_\mu\partial/\partial p_\mu - 3,$$

$$I_\mu = x^2\partial/\partial x_\mu - 2x_\mu x_\nu\partial/\partial x_\nu - 2x_\mu,$$

$$I_\mu = -i\{p_\mu\partial^2/\partial p_\nu^2 - 2[3 + p_\nu\partial/\partial p_\nu]\partial/\partial p_\mu\}. \tag{16}$$

For solutions of the Dirac equation with m = 0 the corresponding quantities are

$$P_\mu = -i\partial/\partial x_\mu, \qquad P_\mu = p_\mu,$$

$$M_{\mu\nu} = -i(x_\mu\partial/\partial x_\nu - x_\nu\partial/\partial x_\mu) + \tfrac{1}{2}\sigma_{\mu\nu},$$

$$M_{\mu\nu} = -i(p_\mu\partial/\partial p_\nu - p_\nu\partial/\partial p_\mu) + \tfrac{1}{2}\sigma_{\mu\nu},$$

$$I = x_\mu\partial/\partial x_\mu + 3/2, \qquad I = -p_\mu\partial/\partial p_\mu - 5/2,$$

$$I_\mu = x^2\partial/\partial x_\mu - 2x_\mu x_\nu\partial/\partial x_\nu - 2x_\mu - \gamma_\mu(\gamma x),$$

$$I_\mu = -i(p_\mu\partial^2/\partial p_\nu^2 - 2(3 + p_\nu\partial/\partial p_\nu)\partial/\partial p_\mu + \gamma_\mu\gamma_\nu\partial/\partial p_\nu), \tag{17}$$

where $\sigma_{\mu\nu} = -i(\gamma_\mu\gamma_\nu - \delta_{\mu\nu})$.

Whereas the operators P_μ, $M_{\mu\nu}$ commute with the wave equation operators, the corresponding commutators for the operators I and I_μ are (in the p-representation):
for the Klein-Gordon equation

$$[I,\ p^2] = -2p^2, \quad [I_\mu,\ p^2] = 4i\partial p^2/\partial p_\mu, \tag{18}$$

and for the Dirac equation

$$[I,\ i\gamma p] = -i\gamma p, \quad [I_\mu,\ i\gamma p] = 2i\partial(i\gamma p)/\partial p_\mu. \tag{19}$$

Consequently these commutators vanish when ap-

plied to solutions of the wave equations and therefore the transformed functions will also be solutions of the wave equations.

If instead of I_μ, P_μ, and I one introduces the operators

$$M_{\mu 5} = \tfrac{1}{2}(I_\mu + iP_\mu), \quad M_{\mu 6} = \tfrac{1}{2}(P_\mu + iI_\mu),$$
$$M_{56} = -I \quad (\mu \neq 5,6), \tag{20}$$

then the relations (7) — (15) may be written in the form of structural relations for the rotation group in six dimensions, i.e., in the form (9) with μ, ν, λ, $\rho = 1, 2, 3, 4, 5, 6$. A number of authors[3,4,14] have studied the conformal group and invariance with respect to it of wave equations with zero rest mass by going over to a 6-dimensional space.

3. RELATION BETWEEN WAVE EQUATIONS WITH $m \neq 0$ AND $m = 0$

The proof of invariance of the Klein-Gordon and Dirac equations with mass under the 15-parameter group will be accomplished by establishing a relation between the equations with and without mass. All considerations will be carried out in momentum space.

If in the Klein-Gordon equation

$$[\mathbf{p}^2 - p_0^2 + m^2]\,\varphi(\mathbf{p}, p_0) = 0 \tag{21}$$

one makes the substitution

$$\mathbf{q} = \mathbf{p}, \quad q_0 = \varepsilon(p_0)\sqrt{p_0^2 - m^2}, \tag{22}$$
$$\varphi_0(\mathbf{q}, q_0) = \varphi(\mathbf{p}, p_0), \tag{23}$$

then Eq. (21) takes on the form of a Klein-Gordon equation with zero mass

$$(\mathbf{q}^2 - q_0^2)\,\varphi_0(\mathbf{q}, q_0) = 0. \tag{24}$$

Similarly, the Dirac equation

$$(i\gamma p + m)\,\psi(\mathbf{p}, p_0) = 0 \tag{25}$$

goes over, under the substitution (22) and

$$\psi_0(\mathbf{q}, q_0) = S\psi(\mathbf{p}, p_0), \tag{26}$$

where

$$S = \cosh\frac{\chi}{2} - \gamma_4 \sinh\frac{\chi}{2}, \quad \chi = \tanh^{-1}\frac{m}{p_0}, \tag{27}$$

into the Dirac equation for zero mass

$$i\gamma q\,\psi_0(\mathbf{q}, q_0) = 0, \tag{28}$$

since

$$S^{-1}(i\gamma p + m)\,S^{-1} = i\gamma q. \tag{29}$$

There exists a whole class of transformations of this kind which reduce the Klein-Gordon and Dirac equations to mass $m = 0$. They are all noncovariant. One of them, with a unitary S matrix, was utilized by Cini and Touschek.[15]

Equations (25) and (28) are invariant with respect to the 15-parameter conformal group. The laws of transformation for the solutions of these equations are given in Sec. 2. The 15-parameter transformation group G_{15} which leaves the equation with nonzero mass invariant may be obtained as follows:

1) Using (22) and (23) for the Klein-Gordon equation, or (22) and (26) for the Dirac equation, we perform the reduction to the massless equations.

2) We perform any of the transformations of the 15-parameter group for $m = 0$.

3) Finally we perform the operations inverse to (22) and (23) or (22) and (26) and thus obtain the operators of the 15-parameter group for nonzero mass.

4. INFINITESIMAL OPERATORS OF THE 15-PARAMETER GROUP FOR KLEIN-GORDON AND DIRAC EQUATIONS WITH $m \neq 0$.

Finite transformation of the 15-parameter group G_{15} for $m \neq 0$ are very complicated. However, since they are fully determined by their corresponding infinitesimal operators we give below only the latter, derived in the manner described in the previous section.

The infinitesimal operators are as follows:*

a) For the Klein-Gordon equation

$$P_r^K = p_r \ (r = 1, 2, 3), \quad P_0^K = \sqrt{p_0^2 - m^2}; \tag{30}$$

$$M_{rn}^K = \frac{1}{i}\left(p_r\frac{\partial}{\partial p_n} - p_n\frac{\partial}{\partial p_r}\right),$$

$$M_{r4}^K = \frac{1}{i}\frac{\sqrt{p_0^2 - m^2}}{p_0}\left(p_r\frac{\partial}{\partial p_4} - p_4\frac{\partial}{\partial p_r}\right) \quad (p_4 = ip_0); \tag{31}$$

$$I^K = -\left[3 + p_\mu\frac{\partial}{\partial p_\mu} - \frac{m^2}{p_0}\frac{\partial}{\partial p_0}\right]; \tag{32}$$

$$I_r^K = -ip_r\left[\frac{\partial^2}{\partial p_\mu^2} + \frac{m^2}{p_0^2}\frac{\partial^2}{\partial p_0^2} - \frac{m^2}{p_0^3}\frac{\partial}{\partial p_0}\right] - 2iI^K\frac{\partial}{\partial p_r},$$

$$I_0^K = -i\frac{\sqrt{p_0^2 - m^2}}{p_0}\left\{p_0\left[\frac{\partial^2}{\partial p_\mu^2} + \frac{m^2}{p_0^2}\frac{\partial^2}{\partial p_0^2} + \frac{m^2}{p_0^3}\frac{\partial}{\partial p_0}\right] - 2I^K\frac{\partial}{\partial p_0}\right\}. \tag{33}$$

*For the sake of simplicity we consider only the case of positive frequencies, $p_0 \geqslant m$.

b) For the Dirac equation

$$P_r^D = p_r, \qquad P_0^D = \sqrt{p_0^2 - m^2}; \tag{34}$$

$$M_{rn}^D = M_{rn}^K + {}^1/_2\sigma_{rn},$$

$$M_{r4}^D = M_{r4}^K + \frac{\sqrt{p_0^2 - m^2}}{2p_0}\sigma_{r4} + \frac{m}{2p_0\sqrt{p_0^2 - m^2}}(\gamma_r p_4 - \gamma_4 p_r + m\sigma_{r4}); \tag{35}$$

$$I^D = -\left[\frac{5}{2} + p_\mu\frac{\partial}{\partial p_\mu} - \frac{m^2}{p_0}\frac{\partial}{\partial p_0} + \gamma_4\frac{m}{2p_0}\right]; \tag{36}$$

$$I_r^D = I_r^K + \frac{im}{4p_0^3(p_0^2 - m^2)}[mp_0p_r - 2p_r\gamma_4(2p_0^2 - m^2) + 2i\gamma_r p_0^2(p_0 - \gamma_4 m)] - i\gamma_r\left(\gamma_\mu\frac{\partial}{\partial p_\mu} + \frac{im}{p_0}\frac{\partial}{\partial p_0}\right) + \frac{im\gamma_4}{p_0^2}\left(p_r\frac{\partial}{\partial p_0} + p_0\frac{\partial}{\partial p_r}\right),$$

$$I_0^D = I_0^K + \frac{im}{4p_0^3\sqrt{p_0^2 - m^2}}[2\gamma_4(2p_0^2 - m^2) + mp_0] + \frac{im\gamma_4}{p_0\sqrt{p_0^2 - m^2}}I^D - \frac{m + \gamma_4 p_0}{\sqrt{p_0^2 - m^2}}\left(\gamma_\mu\frac{\partial}{\partial p_\mu} + \frac{im}{p_0}\frac{\partial}{\partial p_0}\right). \tag{37}$$

The infinitesimal operators (30) — (33) and (34) — (37) satisfy the structural relations (7) — (15). Consequently the transformations determined by them form a representation of the conformal group C_4. In the limit $m = 0$ they go over into the corresponding operators for the massless equations [see Eqs. (16) and (17)].

All these infinitesimal operators either commute with the appropriate wave equation operator, or commute in application to the solutions of these equations, in a manner similar to the $m = 0$ case [see Eqs. (18) and (19)], e.g.,

$$[I^D,\ i\gamma p + m] = -(1 + \gamma_4 m/p_0)(i\gamma p + m). \tag{38}$$

Let us note that all commutators that vanish for the $m = 0$ case also vanish for $m \neq 0$ with the exception of

$$[M_{r4}^D,\ i\gamma p + m] = \frac{m}{p_0\sqrt{p_0^2 - m^2}}(p_r\gamma_4 - p_4\gamma_r)(i\gamma p + m). \tag{39}$$

Thus, the Klein-Gordon and Dirac equations with mass are invariant with respect to the 15-parameter group G_{15}.

However in order to obtain a representation of the conformal group C_4 in its entirety it was necessary to modify the representation of the inhomogeneous Lorentz group L_{10} (the operators P_0 and M_{r4} were changed). As a consequence the law of transformation for the four-momentum of a particle p_μ (which is not the same, in general, as the operator of infinitesimal translation P_μ) will differ from the transformation law obeyed by four-vectors.* Analogous difficulties may also arise for other physical quantities.

In conclusion we note that the method described in Sec. 2 may be used to derive the analogue of the Pauli group for the Dirac equation with mass. For example, the one-parameter group is given by

$$\psi'(p) = \exp(i\alpha\Gamma_5)\psi(p), \tag{40}$$

where

$$\Gamma_5 = \varepsilon(p_0)\frac{p_0 + \gamma_4 m}{\sqrt{p_0^2 - m^2}}\gamma_5, \qquad \Gamma_5^2 = 1. \tag{41}$$

In the representation discussed above of the conformal group C_4 the quantity Γ_5 behaves like a Lorentz pseudoscalar.

The authors are grateful to Prof. M. A. Markov for his interest in this research and to L. G. Zastavenko for useful discussions.

[1] E. Cunnigham, Proc. Lond. Math. Soc. **8**, 77 (1910).
[2] H. Bateman, Proc. Lond. Math. Soc. **8**, 223 (1910).
[3] P. A. M. Dirac, Ann. of Math. **37**, 429 (1936).
[4] H. Bhabha, Proc. Cambr. Phil. Soc. **32**, 622 (1936).
[5] W. Pauli, Helv. Phys. Acta **13**, 204 (1940).
[6] J. A. McLennan Jr., Nuovo cimento **3**, 1360 (1956).
[7] R. L. Ingraham, Nuovo cimento **9**, 886 (1952); **12**, 825 (1954).
[8] S. A. Bludman, Phys. Rev. **107**, 1163 (1957).
[9] L. Page, Phys. Rev. **49**, 254 (1936).
[10] H. P. Robertson, Phys. Rev. **49**, 755 (1936).
[11] H. T. Engstrom and M. Zorn, Phys. Rev. **49**, 701 (1936).
[12] J. Haantjes, Proc. Med. Akad. Wet. **43**, 1288 (1940).
[13] E. L. Hill, Phys. Rev. **67**, 358 (1945); **72**, 143 (1947); **84**, 1165 (1951).
[14] Y. Murai, Prog. Theoret. Phys. **9**, 147 (1953); **11**, 441 (1954).
[15] M. Cini and B. Touschek, Nuovo cimento **7**, 422 (1958).

Translated by A. M. Bincer
85

*p_μ transforms as a four-vector.

ON THE RELATIVISTIC OPERATORS FOR MOMENTUM AND ANGULAR MOMENTUM

A. P. GEL' MAN

Submitted to JETP editor March 4, 1959

J. Exptl. Theoret. Phys. (U.S.S.R.) **37**, 477-481 (August, 1959)

Correct expressions for the relativistic operators for momentum and angular-momentum components in orthogonal curvilinear coordinates are derived by a systematic application of the theory of spinors.

INTRODUCTION

IT is well known that the operators for momentum and for covariant differentiation differ only by a constant factor. Since the Dirac equation contains a linear combination of products of momentum components by a spinor, one must then use covariant derivatives of a spinor to write this equation in curvilinear coordinates. Operators for covariant differentiation of a spinor have been calculated by Fock and by Ivanenko and are given in the books of these authors.[1,2] The virtue of these operators is that they agree with the rule for differentiation of a vector and give the correct result when a certain linear combination of them is substituted in the Dirac equation. Individually, however, these operators are incorrect, as is shown below by a particular example. The purpose of the present paper is to use an elementary but systematic application of the theory of spinors to get the correct expression for the operator of covariant differentiation of a spinor, and along with it the expressions for the momentum and angular-momentum operators.

1. THE COVARIANT DERIVATIVE OF A SPINOR

The spinor ξ is to be regarded as a one-column matrix with four complex components.

It is convenient to represent vectors and bivectors by square matrices, as Cartan[3] does. Thus one puts in correspondence with the vector V^i the matrix $V \equiv V^i H_i$ (summation from 1 to 4), where

$$H_1 = \begin{pmatrix} 0 & 0 & 1 & 0 \\ 0 & 0 & 0 & -1 \\ 1 & 0 & 0 & 0 \\ 0 & -1 & 0 & 0 \end{pmatrix}, \quad H_2 = \begin{pmatrix} 0 & 0 & i & 0 \\ 0 & 0 & 0 & i \\ -i & 0 & 0 & 0 \\ 0 & -i & 0 & 0 \end{pmatrix},$$

$$H_3 = \begin{pmatrix} 0 & 0 & 0 & 1 \\ 0 & 0 & 1 & 0 \\ 0 & 1 & 0 & 0 \\ 1 & 0 & 0 & 0 \end{pmatrix}, \quad H_4 = \begin{pmatrix} 0 & 0 & 0 & -1 \\ 0 & 0 & 1 & 0 \\ 0 & -1 & 0 & 0 \\ 1 & 0 & 0 & 0 \end{pmatrix}. \tag{1}$$

Any two of the matrices H_i anticommute, and $H_i^2 = e_i$, $e_1 = e_2 = e_3 = 1$, $e_4 = -1$. We shall confine our treatment to orthogonal bases consisting of unit vectors (a Galilean frame) relative to which the components of vectors and bivectors are real, the space axes having the numbers 1, 2, 3, and the time axis being taken as the fourth.

In finding the covariant derivative of a spinor, $D_k\xi$, we follow Cartan in using the following definition of the covariant derivative $D_i f$ of any quantity f:

$$Df = D_i f \omega^i, \tag{2}$$

where Df is the actual increase (the absolute differential) of the quantity f, and ω^i is the i-th Galilean component of the vector connecting two neighboring points:

$$ds^2 = (\omega^1)^2 + (\omega^2)^2 + (\omega^3)^2 - (\omega^4)^2. \tag{3}$$

The form of the operator D_i depends on the object f to which it is applied. If we denote by ω^{ik} the components of the bivector of an infinitesimal rotation ($\omega^{ii} = 0$) and by Ω the Cartan matrix of this bivector

$$\Omega \equiv \tfrac{1}{2}\omega^{ik} H_i H_k, \tag{4}$$

we have for the absolute differential of a spinor[3]

$$D\xi = d\xi - \tfrac{1}{2}\Omega\xi. \tag{5}$$

The components of the bivector Ω are found by an elementary calculation (cf., e.g., reference 4, p. 217). Let the standard form of the line element in our orthogonal coordinates x^k be

$$ds^2 = \sum_{k=1}^{4} g_{kk} (dx^k)^2, \tag{6}$$

where $x^4 = ct$ (c is the speed of light, t the time). Let us introduce the briefer notations $e_k g_{kk} = g_k$; then

$$\omega^{ik} = \frac{1}{2\sqrt{g_i g_k}} \left(e_i \frac{\partial g_k}{\partial x^i} dx^k - e_k \frac{\partial g_i}{\partial x^k} dx^i \right). \tag{7}$$

From Eqs. (2), (5), and (4) it follows that

$$\sum_{i=1}^{4} D_i\xi\omega^i = d\xi - \frac{1}{4}\sum_{i,k=1}^{4}\omega^{ik}H_iH_k\xi.$$

Inserting the quantities (7), we find

$$\sum_{i=1}^{4} D_i\xi\omega^i = d\xi - \frac{1}{8}\sum_{i,k=1}^{4}\frac{e_i}{\sqrt{g_ig_k}}\frac{\partial g_k}{\partial x^i}H_iH_k\xi dx^k$$

$$+\frac{1}{8}\sum_{i,k=1}^{4}\frac{e_k}{\sqrt{g_ig_k}}\frac{\partial g_i}{\partial x^k}H_iH_k\xi dx^i.$$

In the first double sum we interchange the summation indices i and k; the right member of the last equation is then written in the form

$$d\xi + \frac{1}{8}\sum_{i,k=1}^{4}\frac{e_k}{\sqrt{g_ig_k}}\frac{\partial g_i}{\partial x^k}(H_iH_k - H_kH_i)\xi dx^i.$$

The terms with i = k cancel. Using the fact that the matrices H_k anticommute, we get finally

$$\sum_{i=1}^{4} D_i\xi\omega^i = d\xi + \frac{1}{4}\sum_{i=1}^{4}\sum_{k\neq i}\frac{e_k}{\sqrt{g_ig_k}}\frac{\partial g_i}{\partial x^k}H_iH_k\xi dx^i, \qquad (8)$$

and from a comparison of Eqs. (3) and (6) it follows that

$$\omega^i = \sqrt{g_i}\,dx^i. \qquad (9)$$

In virtue of the arbitrariness of the differentials dx^i we get from Eqs. (8) and (9)

$$D_i\xi = \frac{1}{\sqrt{g_i}}\frac{\partial\xi}{\partial x^i} + \frac{1}{4g_i}\sum_{k\neq i}\frac{e_k}{\sqrt{g_k}}\frac{\partial g_i}{\partial x^k}H_iH_k\xi. \qquad (10)$$

This is the expression for the covariant derivative of a spinor prescribed in terms of its components relative to the Galilean coordinate frame x^k. Because of the presence of the matrices the operator D_i is nondiagonal, and this nondiagonality cannot be removed by any kind of unitary transformation.*

2. RELATION OF THE COVARIANT DERIVATIVE TO THE DIRAC EQUATION

Since the basis for the derivation of Eq. (10) is Eq. (2), in which the symbol D has scalar character, it is clear that the index i in the expression $D_i\xi$ is a full-fledged covariant index, and the quantities $D_i\xi$ form a tensor of rank three halves (a spinor being regarded as a tensor of rank one half). Thus we have a right to put in correspondence with the canonical momentum P_k the expression $P_k \to -i\hbar D_k$. The treatments by Fock[1] and by Ivanenko and Sokolov[2] give expressions for the momentum operator in which the index k is not a covariant index. The correctness of the results so obtained is due to a peculiarity of the Dirac equation, which we shall now analyze very briefly.

It is well known that the momentum components P^k, k = 1, 2, 3 and $P^4 = E/c$ (where E is the total energy of the particle) form a contravariant four-vector. The Cartan matrix of this vector is $P = P^kH_k$.

The eigenvalue equation of the energy-momentum operator, written in the form

$$P\xi = \lambda H_0\xi, \qquad (11)$$

gives the value of the spinor for a free electron, at the origin of the coordinates. The matrix

$$H_0 = \begin{pmatrix} -1 & 0 & 0 & 0 \\ 0 & -1 & 0 & 0 \\ 0 & 0 & 1 & 0 \\ 0 & 0 & 0 & 1 \end{pmatrix}$$

is introduced so that the left and right members of Eq. (11) will transform in the same way.[3] For agreement with the theory of relativity we must have $\lambda = \pm m_0c$, where m_0 is the rest mass of the electron. To get the value of the spinor at the other points of the space, we must make the replacement $P_k \to -i\hbar D_k$, or $P^k \to -i\hbar e_k D_k$, and add the matrix V of the electromagnetic potential, multiplied by e/c (−e is the charge of the electron), if there is an external field. Furthermore one sets $\lambda = +m_0c$, and the Dirac equation takes the form

$$(-i\hbar\nabla + eV/c - m_0cH_0)\xi = 0,$$

where

$$\nabla\xi = \sum_{i=1}^{4} e_iH_iD_i\xi$$

Using Eq. (10) and recalling that $H_i^2 = e_i$, we get

$$\nabla\xi = \sum_{i=1}^{4}\frac{e_i}{\sqrt{g_i}}\frac{\partial}{\partial x^i}H_i\xi + \frac{1}{4}\sum_{i=1}^{4}\sum_{k\neq i}\frac{e_k}{g_i\sqrt{g_k}}\frac{\partial g_i}{\partial x^k}H_k\xi.$$

In the double sum we may sum over k from 1 to 4, and over the same values of i, except the value i = k:

$$\nabla\xi = \sum_{k=1}^{4}\frac{e_k}{\sqrt{g_k}}\frac{\partial}{\partial x^k}H_k\xi + \frac{1}{4}\sum_{k=1}^{4}\sum_{i\neq k}\frac{e_k}{g_i\sqrt{g_k}}\frac{\partial g_i}{\partial x^k}H_k\xi. \qquad (12)$$

Thus we can set

$$\nabla = \sum_{k=1}^{4} e_kH_k\tilde{D}_k,$$

*It is also easy to get from Eq. (2) the rule for differentiation of the product of a matrix A and a spinor ξ: $D_iA\xi = (D_iA)\xi + AD_i\xi$. When we use Eq. (10) to differentiate a vector expressed as a bilinear combination of the components of a spinor, we get the correct result on the basis of the remark just made. If, on the other hand, we take the requirement that the rule for differentiation of a vector shall hold as the basis for finding $D_i\xi$, the result obtained is not only incorrect, but also ambiguous. But if we follow the Cartan procedure there are, as we see, no ambiguities.

where, according to Eq. (12),

$$\tilde{D}_k = \frac{1}{\sqrt{g_k}}\left(\frac{\partial}{\partial x^k} + \frac{1}{4}\sum_{i\neq k}\frac{1}{g_i}\frac{\partial g_i}{\partial x^k}\right). \qquad (13)$$

The operator $-i\hbar\tilde{D}_k$ is also taken for the momentum P_k.[1] It has, however, nothing in common with the covariant differentiation operator D_k, as can be verified easily by particular examples. The correctness of the results obtained by the use of Eq. (13) is explained by the fact that

$$\sum_{k=1}^{4} e_k H_k D_k \xi = \sum_{k=1}^{4} e_k H_k \tilde{D}_k \xi.$$

If, however, one uses the operators $\tilde{D}_k$ not in the linear combination with the matrices H_k, but separately, then they naturally lead to incorrect results.

Let us consider, for example, the cylindrical coordinates ρ, φ, z, x^4, for which

$$ds^2 = d\rho^2 + \rho^2 d\varphi^2 + dz^2 - (dx^4)^2,$$

i.e.,

$$g_1 = g_3 = g_4 = 1, \quad g_2 = \rho^2.$$

From Eqs. (10) and (13) we find

$$D_1 = \partial/\partial\rho, \quad D_2 = (\partial/\partial\varphi + H_2H_1/2)/\rho \text{ etc.}$$
$$\tilde{D}_1 = \partial/\partial\rho + 1/2\rho, \quad \tilde{D}_2 = \partial/\partial\varphi \text{ etc.}$$

Let ξ be a constant spinor, prescribed in terms of its Cartesian components. In cylindrical coordinates the column representing the same spinor field is[1]

$$\xi' = \left(\cos\frac{\varphi}{2} + \sin\frac{\varphi}{2} H_1H_2\right)\xi.$$

Since the field is constant, we must have $D_1\xi' = 0$, $D_2\xi' = 0$, and these equations are indeed verified. But $\tilde{D}_1\xi' \neq 0$, $\tilde{D}_2\xi' \neq 0$, so that the operators D_1, D_2 cannot possibly be called covariant derivatives.

We note that the expression (10) can also be obtained by starting from the requirement that the covariant derivative of a constant spinor field must be zero.

3. THE ANGULAR-MOMENTUM OPERATOR

The components of the operator for the orbital angular momentum are defined by the equations

$$K_1 = -i\hbar(R_2D_3 - R_3D_2) \text{ etc.}$$

where R_k is a Galilean covariant component of the radius vector. The complete (three-dimensional) operator for the angular momentum is

$$K = K_1H_1 + K_2H_2 + K_3H_3.$$

In spherical coordinates θ, φ, r we get

$$K = \frac{\hbar}{i}\left\{\left(\frac{\partial}{\partial\theta} + \frac{1}{2}\cot\theta\right)H_2 - \frac{1}{\sin\theta}\frac{\partial}{\partial\varphi}H_1 - H_1H_2H_3\right\}, \qquad (14)$$

whereas the use of the operators $\tilde{D}_k$ instead of D_k would give

$$\tilde{K} = \frac{\hbar}{i}\left\{\left(\frac{\partial}{\partial\theta} + \frac{1}{2}\cot\theta\right)H_2 - \frac{1}{\sin\theta}\frac{\partial}{\partial\varphi}H_1\right\}. \qquad (15)$$

The eigenvalues of the operator (15) are all positive integers, excluding zero,[1] whereas in the nonrelativistic theory the angular momentum can also have the value zero. The operator (14), on the other hand, admits also the zero eigenvalue, because the eigenvalues of the matrix $iH_1H_2H_3$ are ± 1 and this matrix commutes with $\tilde{K}$.

There is, however, also a third possibility. Let us define the angular momentum as the (three-dimensional) bivector with the components

$$K_{mn} = R_mP_n - R_nP_m.$$

According to Eq. (4) the Cartan matrix of this bivector is

$$\hat{K} = H_2H_3K_{23} + H_3H_1K_{31} + H_1H_2K_{12}. \qquad (16)$$

The operator (16) is antihermitian, and therefore we must multiply it by i. In spherical coordinates we get

$$\hat{\tilde{K}} = -\hbar\left\{\left(\frac{\partial}{\partial\theta} + \frac{1}{2}\cot\theta\right)H_1H_3 + \frac{1}{\sin\theta}\frac{\partial}{\partial\varphi}H_2H_3\right\}. \qquad (17)$$

The eigenvalues and eigenfunctions of the operators (17) and (15) are the same (apart from interchanges of components), but from the point of view of the representation of operators by Cartan matrices the expression (17) must be given preference.

The results obtained in this paper are also correct in the presence of gravitational fields, provided the coordinate bases remain orthogonal, as, for example, in the case of the Schwartzschild line element.[3]

---

[1] V. A. Fock, Начала квантовой механики (Principles of Quantum Mechanics), KUBUCh, 1932.

[2] A. A. Sokolov and D. D. Ivanenko, Квантовая теория поля (Quantum Field Theory), Gostekhizdat, 1952.

[3] É. Cartan, Théorie des Spineurs, Hermann, Paris, 1938; Russian Transl., IIL, 1947.

[4] N. E. Kochin, Векторное исчисление и начала тензорного исчисления (Vector Calculus and Principles of Tensor Calculus), GONTI, 1938.

Translated by W. H. Furry
86

THEORY OF PARAMAGNETIC RESONANCE IN SYSTEMS CONTAINING TWO KINDS OF MAGNETIC MOMENTS

A. A. KOKIN and G. V. SKROTSKIĬ

Ural' Polytechnic Institute

Submitted to JETP editor March 5, 1959

J. Exptl. Theoret. Phys. (U.S.S.R.) 37, 482-489 (August, 1959)

Equations of motion for the partial magnetizations of a system containing two kinds of interacting magnetic moments situated in a weak variable magnetic field are obtained by methods of thermodynamics of irreversible processes. The same equations can be derived from the microscopic theory in the case of sufficiently rapid thermal fluctuations of the local fields. The relaxation times and the shift of the resonance frequency are computed. It is shown that a universal relation, similar to the Kramers-Kronig relation, exists between the quantities determining the transverse relaxation time and the resonance frequency shift.

1. In many problems of the theory of magnetic resonance one has to deal with systems containing two kinds of magnetic moments. Such systems are substances whose molecules contain two kinds of nuclei with different gyromagnetic ratios, viz: isotope mixtures, paramagnetic solutions, metals. In some cases these systems are described by two uncoupled equations for the partial magnetizations. In spite of this, the behavior of the magnetic moments of one kind may depend in an essential manner on the nature of the interaction between the magnetic moments of the other kind, through the relaxation times and the shift of the resonance frequency. An example of such a system is a solution of Mn^{++} in water.[1]

The microscopic theory of relaxation processes in systems which contain the same number of magnetic moments of each kind with spin $\frac{1}{2}$, and which differ only in their gyromagnetic ratios, was developed in Solomon's paper[2] and was applied to the description of nuclear resonance in hydrogen fluoride.[3]

On the other hand, by the method of the thermodynamics of irreversible processes, one of us[4] has obtained equations for the partial magnetizations $\mathbf{M}_1$ and $\mathbf{M}_2$ in weak variable fields of arbitrary orientation with respect to the constant field.

In the present paper we develop a thermodynamic theory more complete than the one given in reference 4, and also a microscopic theory of systems containing two kinds of magnetic moments for weak magnetic fields; we also obtain equations for the partial magnetizations $\mathbf{M}_1$ and $\mathbf{M}_2$.

2. The thermodynamic theory of the systems under consideration may be developed on the basis of the methods of thermodynamics of irreversible processes.[5]

We suppose that the paramagnetic sample is situated in a constant magnetic field $H = H_z$ and in a variable magnetic field $\mathbf{h}(t)$ which violates thermodynamic equilibrium only to a small extent. In this case the partial magnetizations of the subsystems $M_j = M_j(t)$ $(j = 1, 2)$ satisfy the following equations linear in the variable field:[6]

$$\dot{M}_{lj} = \sum_{m,k} L_{lm,jk}(h_m(t) - h_m^k), \qquad l, m = x, y, z; \quad j, k = 1, 2, \tag{1}$$

where

$$\mathbf{h}^k = \chi_k^{-1}(\mathbf{M}_k(t) - \mathbf{M}_k^0), \tag{2}$$

while

$$\mathbf{M}_k^0 = \chi_k \mathbf{H} \tag{3}$$

are the equilibrium partial magnetizations of the magnetic subsystems.

On going over to circularly polarized components

$$M_{\pm 1} = \mp (M_x \pm iM_y)/\sqrt{2}, \qquad M_0 = M_z, \tag{4}$$

$$h_{\pm 1} = \mp (h_x \pm ih_y)/\sqrt{2}, \qquad h_0 = h_z, \tag{5}$$

we shall obtain in accordance with (1)

$$\dot{M}_{\alpha j} = \sum_{\beta k} L_{\alpha\beta,jk}(h_\beta(t) - h_\beta^k), \qquad \alpha, \beta = \pm 1, 0. \tag{6}$$

The kinetic coefficients $L_{\alpha\beta,jk}$ satisfy the Onsager relations, which in the case of paramagnetic media $(\chi_j \ll 1)$ have the form

$$\alpha \neq \beta, \quad L_{\alpha\beta,\,jk}(H_0) = -L^{*}_{\beta\alpha,\,jk}(-H_0) = -L_{-\beta-\alpha,\,jk}(-H_0),$$
$$\alpha = \beta, \quad L_{\alpha\alpha,\,jk}(H_0) = L^{*}_{\alpha\alpha,\,jk}(-H_0) = L_{-\alpha-\alpha,\,jk}(-H_0). \quad (7)$$

Requirements of axial symmetry with respect to the direction of the constant field H lead to the additional relations

$$L_{\alpha\beta,\,jk}(H_0) = \delta_{\alpha\beta} L_{\alpha\beta,\,jk}(H_0),$$
$$L_{11,\,jk} = L^{*}_{-1\,-1,\,jk} \neq L_{00,\,jk}, \quad (8)$$

Equations (7) and (8) can be satisfied if we set

$$L_{\alpha\alpha,\,jk}(H_0) = \sqrt{\chi_j \chi_k}\,(1/T^{jk}_{\alpha} + i\alpha\omega^{jk}), \quad \omega^{jk} = \gamma^{jk} H_0, \quad (9)$$

where γ^{jk} and T^{jk}_{α} are even functions of H_0 symmetric with respect to an interchange of the indices jk:

$$T^{jk}_{\perp} = T^{jk}_{\pm 1}(H_0), \quad T^{jk}_{\parallel} = T^{jk}_{0}(H_0), \quad \gamma^{jk} = \gamma^{jk}(H_0). \quad (10)$$

In weak fields ($H_0 \to 0$) the system possesses spherical symmetry, and therefore

$$T^{jk}_{\perp} = T^{jk}_{\parallel} = T^{jk}. \quad (11)$$

On substituting (9) into (6), and on taking (2) and (3) into account, we obtain a system of linear equations of motion for the partial magnetizations

$$\dot{M}_{\alpha j} + \sum_k \sqrt{\chi_j/\chi_k}\,(1/T^{jk}_{\alpha} + i\alpha\omega^{jk})(M_{\alpha k} - M^0_{\alpha k})$$
$$= \sum_k \sqrt{\chi_j \chi_k}\,(1/T^{jk}_{\alpha} + i\alpha\omega^{jk}) h_{\alpha}(t), \quad (12)$$

which contain undetermined (within the framework of thermodynamics) coefficients T^{jk}_{α} and γ^{jk}.

For a system containing one kind of magnetic moments (j = k = 1) we obtain the equations

$$\dot{M}_{\alpha} + (1/T_{\alpha} + i\alpha\omega_0)(M_{\alpha} - M^0_{\alpha})$$
$$= \chi_0 (1/T_{\alpha} + i\alpha\omega_0) h_{\alpha}(t), \quad (13)$$

which agree with those which we have obtained earlier in microscopic theory.[7]

In the absence of a radio-frequency field $\mathbf{h}(t) = 0$ and when $\chi_j/\chi_k = (\gamma_j/\gamma_k)^2$ Eqs. (12) reduce to the equations obtained by Solomon.[2] They differ from the equations obtained in reference 4 by the presence of terms containing ω^{12}.

The static susceptibilities appearing in (12) depend on the thermodynamic temperatures of the subsystems which, generally speaking, may differ from the temperature of the remaining degrees of freedom of the magnetic material — the equilibrium lattice temperature. By restricting ourselves in this paper to the case of weak fields $\mathbf{h}(t)$, we neglect variations in the temperatures of the subsystems by setting them equal to the temperature of the sample. The transfer of heat from the spin system to the "lattice" may be taken into account in a manner analogous to that used in reference 6.

3. In order to interpret the coefficients T^{jk}_{α} and ω^{jk} appearing in Eqs. (12) we consider the case of the free precession of the magnetization $\mathbf{h}(t) = 0$ in the constant field H_0.

On setting

$$M_{\alpha j}(t) = M^0_{\alpha j} + A_{\alpha j} \exp(-\lambda_{\alpha} t), \quad (14)$$

we obtain for the determination of $A_{\alpha j}$ a system of homogeneous equations, the condition for the solution of which has the form

$$(-\lambda_{\alpha} + 1/T^{11}_{\alpha} + i\alpha\omega^{11})(-\lambda_{\alpha} + 1/T^{22}_{\alpha} + i\alpha\omega^{22})$$
$$= (1/T^{12}_{\alpha} + i\alpha\omega^{12})^2. \quad (15)$$

Solving the quadratic equation (15) with respect to λ_{α}, we obtain the complex eigenvalues $\lambda^{\pm}_{\alpha}$. Now the solutions of (12) can be written

$$M_{\alpha 1}(t) = M^0_{\alpha 1} + A^{+}_{\alpha}(-\lambda^{+}_{\alpha} + 1/T^{22}_{\alpha} + i\alpha\omega^{22}) \exp(-\lambda^{+}_{\alpha} t)$$
$$- A^{-}_{\alpha} \sqrt{\chi_1/\chi_2}\,(1/T^{12}_{\alpha} + i\alpha\omega^{12}) \exp(-\lambda^{-}_{\alpha} t),$$
$$M_{\alpha 2}(t) = M^0_{\alpha 2} - A^{+}_{\alpha} \sqrt{\chi_2/\chi_1}\,(1/T^{12}_{\alpha} + i\alpha\omega^{12}) \exp(-\lambda^{+}_{\alpha}(t))$$
$$+ A^{-}_{\alpha}(-\lambda^{-}_{\alpha} + 1/T^{11}_{\alpha} + i\alpha\omega^{11}) \exp(-\lambda^{-}_{\alpha} t). \quad (16)$$

In two limiting cases they assume a particularly simple form. If

$$(1/T^{12}_{\alpha} + i\alpha\omega^{12})^2$$
$$\ll (1/T^{11}_{\alpha} - 1/T^{22}_{\alpha} + i\alpha\omega^{11} - i\alpha\omega^{22})^2, \quad (17)$$

then, in accordance with (15),

$$\lambda^{+}_{\alpha} = \lambda^{2}_{\alpha} = 1/T^{22}_{\alpha} + i\alpha\omega^{22},$$
$$\lambda^{-} = \lambda^{1}_{\alpha} = 1/T^{11}_{\alpha} + i\alpha\omega^{11}. \quad (18)$$

In this case

$$M_{\alpha j}(t) = M^0_{\alpha j} + A_{\alpha j} \exp(-\lambda^{j}_{\alpha} t), \quad (19)$$

where T^{jj}_{α} have the meaning of relaxation times, while ω^{jj}_{α} have the meaning of characteristic frequencies.

If the inequality of (17) is reversed, the eigenvalues are determined in the following manner:

$$\lambda^{\pm}_{\alpha} = {}^1/_2 (1/T^{11}_{\alpha} + 1/T^{22}_{\alpha} \pm 2/T^{12}_{\alpha})$$
$$+ {}^1/_2 i\alpha (\omega^{11} + \omega^{22} \pm 2\omega^{12}), \quad (20)$$

and the solutions for $M_{\pm 1 j}(t)$ have the form of damped beats, which are due to the existence of coupling (T^{12}_{α}, ω^{12}) between the equations for the partial magnetizations.

4. The microscopic theory of relaxation and resonance phenomena in systems containing two kinds of magnetic moments can be developed on the basis of the method of Kubo and Tomita[8] in a manner analogous to the one which we used in the case of one kind of spins.[7]

We shall assume that the g-factors of the par-

ticles are isotropic, while the spin-Hamiltonian of the system does not contain products of more than two spin operators $\hat{I}_s^{(j)}$, and therefore contains them in combinations which transform according to the irreducible representations of the rotation group D_0, D_1, and D_2. Then, on taking into account the fact that $\hat{I}_s^{(j)}\hat{I}_s^{(j)} = \text{const}$, we can write

$$\hat{\mathcal{H}} = \hat{\mathcal{H}}_1 + \hat{\mathcal{H}}_2 + \hat{\mathcal{H}}', \tag{21}$$

where

$$\hat{\mathcal{H}}_1 = -\sum_j \hbar\omega_j \sum_s^{N_j} \hat{I}_{s0}^j \tag{22}$$

is the operator for the interaction of the magnetic moments with the constant external field H_0, $\omega_j = \gamma_j H_0$; $\hat{\mathcal{H}}_2$ represents the part of the total Hamiltonian $\hat{\mathcal{H}}$ which is independent of the spins; $\hat{\mathcal{H}}'$ is the perturbation:

$$\hat{\mathcal{H}}' = \hat{\mathcal{H}}^{11} + \hat{\mathcal{H}}^{12} + \hat{\mathcal{H}}^{22} = \sum_{j\leqslant k}\sum_{\lambda\nu}\hat{\mathcal{H}}_{\lambda\nu}^{jk} = \sum_{j\leqslant k}\sum_{\lambda\nu}\sum_{s<m}^{N_j N_k} (F_{sm}^{-(\lambda+\nu),jk} \times \{\hat{I}_s^{(j)}\hat{I}_m^{(k)}\}_{\lambda\nu} + \delta_{\nu,-\lambda}A_{sm}^{-\lambda,jk}\hat{I}_{s\lambda}^{(j)}\hat{I}_{m-\lambda}^{(k)}) + \sum_{j\leqslant k}\sum_{\lambda\nu}\sum_s^{N_j}\delta_{jk}F_s^{-(\lambda+\nu),j}\{\hat{I}_s^{(j)}\hat{I}_s^{(j)}\}_{\lambda\nu}, \tag{23}$$

where

$$\{\hat{I}_s^{(j)}\hat{I}_m^{(k)}\}_{\pm1\,\pm1} = \sqrt{15/2\pi}\,\hat{I}_{s\pm1}^{(j)}\hat{I}_{m\pm1}^{(k)},$$
$$\{\hat{I}_s^{(j)}\hat{I}_m^{(k)}\}_{\pm10} = \sqrt{15/4\pi}\,\hat{I}_{s\pm1}^{(j)}\hat{I}_{m0}^{(k)},$$
$$\{\hat{I}_s^{(j)}\hat{I}_m^{(k)}\}_{0\pm1} = \sqrt{15/4\pi}\,\hat{I}_{s0}^{(j)}\hat{I}_{m\pm1}^{(k)},$$
$$\{\hat{I}_s^{(j)}\hat{I}_m^{(k)}\}_{00} = \sqrt{5/\pi}\,\hat{I}_{s0}^{(j)}\hat{I}_{m0}^{(k)},$$
$$\{\hat{I}_s^{(j)}\hat{I}_m^{(k)}\}_{\pm1\mp1} = \sqrt{5/4\pi}\,\hat{I}_{s\pm1}^{(j)}\hat{I}_{m\mp1}^{(k)}.$$

Under a rotation of coordinates the coefficients $F_{sm}^{-(\lambda+\nu),jk}$, $F_s^{-(\lambda+\nu)j}$ transform according to the representation D_2, while $A_{sm}^{-\lambda,jk}$ transform according to D_0; this determines their angular dependence.

Expression (23) may, in principle, contain combinations of spins which transform according to the representation D_1. However, in this case the coefficients must be functions not only of the coordinates but also of a certain axial vector. The only such vector in the case under consideration is **H**. We shall obtain such an expression, for example, if we take into account the anistropy of the g-factor.[9]

The choice of the Hamiltonian in the form (21) — (23) enables us to take into account the quadrupole moments of nuclei, atoms and ions and their interaction with the local inhomogeneous and, generally speaking, fluctuating field (for nuclei and atoms inside the molecule or for ions inside the complex), and also weak direct and indirect exchange interactions leading to hyperfine splitting. The singling out of coefficients which depend on spherical harmonics leads to simpler calculations in the case of a homogeneous and isotropic medium.

According to reference 7, to compute

$$M_{\alpha j}(t) - M_{\alpha j}^0 = -\sum_\beta \int_0^\infty \frac{dG_{\alpha\beta}(\tau)}{d\tau} h_\beta^*(t-\tau)\,d\tau \tag{24}$$

it is sufficient to determine the form of the relaxation function

$$G_{\alpha\beta}(\tau) = G_{\alpha\beta}^*(-\tau) = \sum_j G_{\alpha\beta j}(\tau), \qquad G_{\alpha\beta}(\infty) = 0, \tag{25}$$

where for the fields ordinarily used ($\hbar\omega_j \ll kT$)

$$G_{\alpha\beta j}(\tau) = \frac{1}{kT}\sum_k \mathrm{Sp}\hat{\rho}_0\{\hat{M}_{\alpha j}(\tau)\hat{M}_{\beta k}\}, \tag{26}$$

and $M_{\alpha j}(\tau)$ is a time-dependent operator in the Heisenberg representation determined by the Hamiltonian $\mathcal{H}$:

$$M_{\alpha j}(\tau) = \exp(i\hat{\mathcal{H}}\tau/\hbar)\hat{M}_{\alpha j}\exp(-i\hat{\mathcal{H}}\tau/\hbar). \tag{27}$$

We seek expressions for $C_{\alpha\beta j}(\tau)$ in the form of expansions in terms of the parameter characterizing the perturbation:

$$G_{\alpha\beta j}(\tau) = G_{\alpha\beta j}^{(0)}(\tau) + G_{\alpha\beta j}^{(1)}(\tau) + G_{\alpha\beta j}^{(2)}(\tau) + \ldots, \tag{28}$$

where

$$G_{\alpha\beta j}^{(0)}(\tau) = \frac{1}{kT}\sum_k \mathrm{Sp}\,\hat{\rho}_0\{\hat{M}_{\alpha j}^0(\tau),\ \hat{M}_{\beta k}\},$$

$$G_{\alpha\beta j}^{(1)}(\tau) = -\frac{i}{kT\hbar}\sum_k \int_0^\tau d\vartheta\,\mathrm{Sp}\,\hat{\rho}_0\{[\hat{M}_{\alpha j}^0(\tau),\ \hat{\mathcal{H}}'(\vartheta)]\hat{M}_{\beta k}\}\ \text{etc.},$$

while the dependence of the operators $M_{\alpha j}^0(\tau)$ and $\hat{\mathcal{H}}'(\tau)$ on the time is determined by the Hamiltonian $\hat{\mathcal{H}}_0$ according to the usual formulas analogous to (27).

The character of the subsequent calculations depends on the magnitude of the interactions determined by the operators $\hat{\mathcal{H}}^{11}$, $\hat{\mathcal{H}}^{12}$ and $\hat{\mathcal{H}}^{22}$. If $\hat{\mathcal{H}}^{11} \sim \hat{\mathcal{H}}^{12} \sim \hat{\mathcal{H}}^{22}$ then one should consider to the same extent all terms of the perturbing operator (23). On the other hand, if $\hat{\mathcal{H}}^{11} \gg \hat{\mathcal{H}}^{12} \gg \hat{\mathcal{H}}^{22}$, then in considering the first subsystem we may neglect $\hat{\mathcal{H}}^{12}$ and $\hat{\mathcal{H}}^{22}$, while in considering the second subsystem we may neglect $\hat{\mathcal{H}}^{22}$.

5. In the first case we have for a homogeneous and isotropic medium, if the density matrix may be assumed constant,

$$G_{\alpha\beta j}^{(0)}(\tau) = (-1)^\alpha \chi_j \delta_{\alpha,-\beta}\exp(-i\alpha\omega_j\tau), \tag{29}$$

$$G_{\alpha\beta j}^{(1)}(\tau) = i\alpha\tau G_{\alpha\beta j}^{(0)}(\tau)\frac{1}{\hbar}\sum_m^{N_k}\langle A_{sm}^{jk}\hat{I}_{m0}^{(k)}\rangle = i\alpha\tau G_{\alpha\beta j}^{(0)}(\tau)\,\Delta\omega^{(1)}\ //. \tag{30}$$

Using the property of the independence of the trace of the time origin, and neglecting the terms with $\lambda,\ \nu \neq -\lambda',\ -\nu'$, we obtain in a manner analogous to the one used in references 7 and 8,

$$G^{(2)}_{\alpha\beta j}(\tau) = -G^{(0)}_{\alpha\beta j}(\tau)\sum_k\sum_{\lambda\nu}\left\{\int_0^\tau d\vartheta_1\int_0^{\vartheta_1} d\vartheta_2 \times \exp[(i\lambda\omega_j + i\nu\omega_k)(\vartheta_1-\vartheta_2)]\ P^{jk}_{\alpha\lambda\nu}(\vartheta_1-\vartheta_2) + \int_0^\tau d\vartheta_1\int_0^{\vartheta_1} d\vartheta_2 \exp[(i\lambda\omega_j + i\nu\omega_k)\vartheta_1 + (i(\alpha-\lambda)\omega_j - i(\alpha+\nu)\omega_k)\vartheta_2]\sqrt{\frac{\chi_k}{\chi_j}}\,Q^{jk}_{\alpha\lambda\nu}(\vartheta_1-\vartheta_2)\right\} - G^{(0)}_{\alpha\beta j}(\tau)(\alpha\Delta\omega^{(1)\,jj})^2\frac{\tau^2}{2}, \tag{31}$$

where the functions

$$P^{jk}_{\alpha\lambda\nu}(\vartheta_1-\vartheta_2) = \frac{\langle\{[\hat M_{\alpha j}\hat{\mathcal{H}}^{jk}_{-\lambda-\nu}(\vartheta_1-\vartheta_2)][\hat{\mathcal{H}}^{jk*}_{-\lambda-\nu}(0)\,\hat M^*_{\alpha j}]\}\rangle}{\hbar^2\langle|M_{\alpha j}|^2\rangle} - \delta_{\lambda 0}\delta_{\nu 0}\langle\alpha\Delta\omega^{(1)\,jj}\rangle^2, \tag{32}$$

$$\sqrt{\frac{\chi_k}{\chi_j}}\,Q^{jk}_{\alpha\lambda\nu}(\vartheta_1-\vartheta_2) = \frac{\langle\{[\hat M_{\alpha j}\hat{\mathcal{H}}^{jk}_{-\lambda-\nu}(\vartheta_1-\vartheta_2)][\hat{\mathcal{H}}^{jk*}_{\alpha-\lambda,\,-(\alpha+\nu)}(0)\,\hat M^*_{\alpha k}]\}\rangle}{\hbar^2\langle|M_{\alpha j}|^2\rangle} \tag{33}$$

satisfy the conditions $P^{jk}_{\alpha\lambda\nu}(\infty) = Q^{jk}_{\alpha\lambda\nu}(\infty) = 0$.

The angle brackets denote everywhere averaging over the coordinates and the spins, using a constant density matrix, while figure brackets indicate the symmetrized product of the operators.

The Heisenberg operators $\hat{\mathcal{H}}^{jk}_{\lambda\nu}(t)$ appearing in (32) and (33) contain a dependence on the time determined by the Hamiltonian $\hat{\mathcal{H}}_2$.

To ascertain the type of equations of motion for the partial magnetizations $M_{\alpha j}(t)$, we differentiate (24) with respect to the time. Then, after integration by parts we obtain

$$\frac{dM_{\alpha j}(t)}{dt} = -\sum_\beta \frac{dG_{\alpha\beta j}(0)}{d\tau}h^*_\beta(t) - \sum_\beta\int_0^\infty \frac{d^2G_{\alpha\beta j}(\tau)}{d\tau^2}h^*_\beta(t-\tau)\,d\tau. \tag{34}$$

Differentiating (29), (30), and (31) with respect to τ, and adding them together we obtain

$$dG_{\alpha\beta j}(\tau)/d\tau = -i\alpha\omega_j G_{\alpha\beta j}(\tau) - i\alpha G^{(0)}_{\alpha\beta j}(\tau)\,\Delta\omega^{(1)\,jj}_\alpha\,(1 - i\alpha\Delta\omega^{(1)\,jj}_\alpha\tau) - G^{(0)}_{\alpha\beta j}(\tau)\sum_k\sum_{\lambda\nu}\int_0^\tau d\vartheta\exp[(i\lambda\omega_j + i\nu\omega_k)\vartheta]\,P^{jk}_{\alpha\lambda\nu}(\vartheta) - G^{(0)}_{\alpha\beta k}(\tau)\sqrt{\chi_j/\chi_k}\sum_{\lambda\nu}\int_0^\tau d\vartheta\exp[i\alpha(\omega_k-\omega_j)\vartheta]\,Q^{jk}_{\alpha\lambda\nu}(\vartheta), \tag{35}$$

where $P^{jk}_{\alpha\lambda\nu}(t)$ and $Q^{jk}_{\alpha\lambda\nu}(t)$, in the case of an isotropic sample, are made up of parts corresponding to different terms in the interaction Hamiltonian (23). If the characteristic times for these functions satisfy the condition of strong narrowing*

$$\tau_p \ll (P^{jk}_{\alpha\lambda\nu}(0))^{-1/2} \qquad \tau_q \ll (Q^{jk}_{\alpha\lambda\nu})^{-1/2}, \tag{36}$$

then the integrals in (35) may be replaced by their asymptotic expressions:[7]

$$P^{jk}_{\alpha\lambda\nu}\tau_{\lambda\nu} = P^{jk}_{\alpha\lambda\nu}(0)(\tau'_{\lambda\nu} + i\tau''_{\lambda\nu}) = \int_0^\infty d\vartheta\exp[(i\lambda\omega_j + i\nu\omega_k)\vartheta]\,P^{jk}_{\alpha\lambda\nu}(\vartheta),$$

$$Q^{jk}_{\alpha\lambda\nu}\varkappa_{\lambda\nu} = Q^{jk}_{\alpha\lambda\nu}(0)(\varkappa'_{\lambda\nu} + i\varkappa''_{\lambda\nu}) = \int_0^\infty d\vartheta\exp[i\alpha(\omega_k-\omega_j)\vartheta]\,Q^{jk}_{\alpha\lambda\nu}(\vartheta). \tag{37}$$

Further, on introducing the notation

$$1/T^{jj}_\alpha + i\alpha\Delta\omega^{(2)\,jj} = \sum_k\sum_{\lambda\nu}P^{jk}_{\alpha\lambda\nu}(0)\,\tau_{\lambda\nu},$$

$$1/T^{jk}_\alpha + i\alpha\Delta\omega^{jk} = \sum_{\lambda\nu}Q^{jk}_{\alpha\lambda\nu}(0)\,\varkappa_{\lambda\nu}, \tag{38}$$

$$\Delta\omega^{jj} = \Delta\omega^{(1)jj} + \Delta\omega^{(2)jj}, \qquad \omega^{jk} = \omega_j\delta_{jk} + \Delta\omega^{jk}, \tag{39}$$

we obtain, up to terms of second-order perturbation theory, the equation satisfied by the relaxation function $G_{\alpha\beta j}$:

$$dG_{\alpha\beta j}(\tau)/d\tau = -\sum_k\sqrt{\chi_j/\chi_k}\,(1/T^{jk}_\alpha + i\alpha\omega^{jk})\,G_{\alpha\beta k}(\tau), \tag{40}$$

where we have approximately replaced

$$G^{(0)}_{\alpha\beta j}(\tau)\,(1 - i\alpha\Delta\omega^{(1)jj}\tau) \to G_{\alpha\beta j}(\tau).$$

On substituting (40) into (34) we return to Eqs. (12) for the partial magnetizations. If the specific nature of the interaction is given, then the coefficients T^{jk}_α and ω^{jk} appearing in (12) are determined by (38) and (39).

6. In the case when $\hat{\mathcal{H}}^{22} \ll \hat{\mathcal{H}}^{12} \ll \hat{\mathcal{H}}^{11}$ we can write

$$G_{\alpha\beta 1}(\tau) = \frac{1}{kT}\langle\{\hat M_{\alpha 1}(\tau)\,\hat M_{\beta 1}\}\rangle = \frac{\gamma_1^2\hbar^2N_1}{kT}\langle\hat I^{(1)}_{s\alpha}(\tau)\,\hat I^{(1)}_{s\beta}\rangle, \tag{41}$$

$$G_{\alpha\beta,\,2}(\tau) = \frac{1}{kT}\sum_k\langle\{\hat M_{\alpha 2}(\tau),\,\hat M_{\beta k}\}\rangle, \tag{42}$$

where $\hat I^{(1)}_{S\alpha}(\tau)$ and $\hat M_{\alpha 2}(\tau)$ are operators in the Heisenberg representations defined respectively by the Hamiltonians $\hat{\mathcal{H}}_0 + \hat{\mathcal{H}}^{11}$ and $\hat{\mathcal{H}}_0 + \hat{\mathcal{H}}^{11} + \hat{\mathcal{H}}^{12}$.

As may be seen from (41), an independent equation is obtained for the first subsystem in this case. If $P^{11}_{\alpha\lambda\nu}(t)$ is a rapidly varying function of time, we obtain, as in the preceding case,

$$dG_{\alpha\beta 1}(\tau)/d\tau = -(1/T^{11}_\alpha + i\alpha\omega^{11})\,G_{\alpha\beta 1}(\tau), \tag{43}$$

*In this case the local fields fluctuate rapidly because of the thermal motion of the magnetic moments.

where T_α^{11} and ω^{11} are calculated for the case of the interaction $\hat{\mathcal{H}}^{11}$ by means of the formulas given earlier. On solving this equation under the condition $G_{\alpha\beta_1}(0) = (-1)^\alpha \chi_1 \delta_{\alpha,-\beta}$ we obtain for the second subsystem

$$dG_{\alpha\beta_2}(\tau)/d\tau = -(1/T_\alpha^{22} + i\alpha\omega^{22})\, G_{\alpha\beta_2}(\tau) - \sqrt{\chi_2/\chi_1}\,(1/T_\alpha^{21} + i\alpha\omega^{21})\, G_{\alpha\beta_1}(\tau), \quad (44)$$

where

$$\frac{1}{T_\alpha^{22}} + i\alpha\Delta\omega^{(2)\,22} = \sum_{\lambda\nu}\int_0^\infty d\vartheta P_{\alpha\lambda\nu}^{21}(\vartheta) \exp\left[\left(i\lambda\omega_2 + i\nu\omega^{11} - \frac{1}{T_\nu^{11}}\right)\vartheta\right],$$

$$\frac{1}{T_\alpha^{21}} + i\alpha\omega^{21} = \sum_{\lambda\nu}\int_0^\infty d\vartheta Q_{\alpha\lambda\nu}^{21}(\vartheta) \exp\left[\left(i\alpha(\omega^{11} - \omega_2) - \frac{1}{T_\alpha^{11}}\right)\vartheta\right]. \quad (45)$$

If $\gamma_1 \gg \gamma_2$, we can neglect the last term in (44), and the equations for the separate subsystems are completely separated, but the coefficients in these equations turn out to be coupled. If T_α^{11} is considerably less than the characteristic time for the function $P_{\alpha\lambda\nu}^{21}(t)$, then we may set in (45) $P_{\alpha\lambda\nu}^{21}(t) = P_{\alpha\lambda\nu}^{21}(0)$. Then, if the condition $T_\nu^{11} \ll (P_{\alpha\lambda\nu}^{21}(0))^{-1/2}$ is satisfied, we shall have

$$\frac{1}{T_\alpha^{22}} + i\alpha\Delta\omega^{(2)\,22} = \sum_{\lambda\nu} P_{\alpha\lambda\nu}^{21}(0)\, \frac{i\lambda\omega_2 + i\nu\omega^{11} + 1/T_\nu^{11}}{(\lambda\omega_2 + \nu\omega^{11})^2 + (T_\nu^{11})^{-2}}. \quad (46)$$

The relaxation time and the shift of the resonance frequency for one substystem turn out to be related to the relaxation time and the resonance frequency of the other subsystem.

7. The real and the imaginary parts of the coefficients $\tau_{\lambda\nu}(\omega_j, \omega_k)$ and $\kappa_{\lambda\nu}(\omega_j, \omega_k)$ which were determined earlier in (37) satisfy the dispersion relations.

We consider the integral ($\omega_j \neq \omega_k$)

$$\tau_{\lambda\nu}(\omega_j, \omega_k) = \tau'_{\lambda\nu}(\omega_j, \omega_k) + i\tau''_{\lambda\nu}(\omega_j, \omega_k) = [1/P_{\alpha\lambda\nu}^{jk}(0)] \int_0^\infty d\vartheta \exp[(i\lambda\omega_j + i\nu\omega_k)\vartheta]\, P_{\alpha\lambda\nu}^{jk}(\vartheta). \quad (47)$$

We let ω_j take on not only real, but also complex values. Then, for $\lambda > 0$ in the upper half-plane, and for $\lambda < 0$ in the lower half-plane, $\tau_{\lambda\nu}$ vanishes when $|\omega_j| \to \infty$. If we represent $\tau_{\lambda\nu}(\omega_j, \omega_k)$ by means of Cauchy's theorem in the form of an integral along a contour consisting of the entire real axis and of a semi-circle of infinite radius (taken, respectively, in the upper half-plane in the case $\lambda > 0$, and in the lower half-plane in the case $\lambda < 0$) then we obtain in the usual way the following dispersion relations

$$\tau'_{\lambda\nu} = \pm \int_{-\infty}^{+\infty} \frac{\tau''_{\lambda\nu}(x, \omega_k)\, dx}{x - \omega_j}, \quad \tau_{\lambda\nu} = \mp \frac{1}{\pi} \int_{-\infty}^{+\infty} \frac{\tau'_{\lambda\nu}(x, \omega_k)\, dx}{x - \omega_j}, \quad (48)$$

where $\lambda = \pm 1$. We can, evidently, write down completely analogous relations with respect to the variable ω_k.

Thus, a universal relation, analogous to the Kramers-Kronig relations, exists between $\tau'_{\lambda\nu}$ and $\tau''_{\lambda\nu}$. Expressions (48) are of a very general nature, and do not depend on the specific form of the functions $P_{\alpha\lambda\nu}^{jk}(t)$. Expressions (38) provide a simple connection between the relaxation time and the resonance frequency shift on the one hand, and the quantities $\tau'_{\lambda\nu}$ and $\tau''_{\lambda\nu}$ on the other.

8. When the characteristic time for $P_{\alpha\lambda\nu}^{jk}$ and $Q_{\alpha\lambda\nu}^{jk}$ is great, then we can no longer make use of the asymptotic expressions for the integrals in (35). The concept of relaxation times in this case has no meaning, and we cannot write down simple macroscopic equations for the partial magnetizations. In this case we can calculate directly the partial susceptibilities. By expanding $M_{\alpha j}(t) - M_{\alpha j}^0$ and $h_\beta(t)$ into Fourier integrals with respect to time we shall obtain for the corresponding Fourier components $m_{\alpha j}(\omega)$ and $h_\beta(\omega)$ the following equations

$$m_{\alpha j}(\omega) = \sum_\beta (\chi'_{\alpha\beta j}(\omega) + i\chi''_{\alpha\beta j}(\omega)) h_{-\beta}(\omega), \quad (49)$$

where

$$\chi'_{\alpha\beta j}(\omega) = \chi_0 \delta_{\alpha-\beta} - (-1)^\beta \omega\, \mathrm{Im} \int_0^\infty G_{\alpha\beta j}(\tau) \exp(i\omega\tau)\, d\tau,$$

$$\chi''_{\alpha\beta j}(\omega) = (-1)^\beta \frac{\omega}{2} \int_{-\infty}^{\infty} G_{\alpha\beta j}(\tau) \exp(i\omega\tau)\, d\tau. \quad (50)$$

The real and imaginary parts of the susceptibility are related to one another by the Kramers-Kronig relations.

[1] N. Bloembergen, J. Chem. Phys. **27**, 572 (1957).

[2] I. Solomon, Phys. Rev. **99**, 559 (1955).

[3] I. Solomon and N. Bloembergen, J. Chem. Phys. **25**, 261 (1956).

[4] G. V. Skrotskiĭ, J. Exptl. Theoret. Phys. (U.S.S.R.) **35**, 793 (1958), Soviet Phys. JETP **8**, 550 (1959).

[5] S. R. de Groot, Thermodynamics of Irreversible Processes, Interscience, New York, 1951; Russ. transl. GITTL, Moscow, 1956.

[6] G. V. Skrotskiĭ and V. T. Shmatov, J. Exptl. Theoret. Phys. (U.S.S.R.) **34**, 740 (1958), Soviet Phys. JETP **7**, 508 (1958).

[7] G. V. Skrotskiĭ and A. A. Kokin, J. Exptl. Theoret. Phys. (U.S.S.R.) **36**, 169 (1959), Soviet Phys. JETP **9**, 116 (1959).

[8] R. Kubo and K. Tomita, J. Phys. Soc. Japan **9**, 888 (1954).

[9] A. A. Kokin, J. Exptl. Theoret. Phys. (U.S.S.R.) **36**, 508 (1959), Soviet Phys. JETP **9**, 353 (1959).

Translated by G. Volkoff
87

EFFECT OF INELASTIC COLLISIONS ON THE VELOCITY DISTRIBUTION OF ELECTRONS

L. M. KOVRIZHNYKH

P. N. Lebedev Physics Institute, Academy of Sciences, U.S.S.R.

Submitted to JETP editor March 7, 1959

J. Exptl. Theoret. Phys. (U.S.S.R.) **37**, 490-500 (August, 1959)

The velocity distribution function for electrons in a weakly ionized plasma has been found with account of inelastic collisions. It is shown that the inelastic collisions lead to a sharp drop in the distribution function for electron energies exceeding the excitation (or ionization) energy.

INTRODUCTION

IN finding the velocity distribution function for electrons in inelastic collisions, one usually neglects completely the fact that the function is valid only under the condition that the mean energy of the electrons is much smaller than the excitation (or ionization) energy. In many cases, and in particular, in the study of phenomena taking place in gas discharges, this proves to be a serious limitation. In a number of researches,[1-3] approximate methods of solution have been found which permit the energy losses in inelastic collisions to be taken into account. However, these methods have limited applicability, and apply essentially to cases in which the mean energy of the electrons is not very great, so that the inelastic collisions affect chiefly the tail of the distribution function. Moreover, they assume some particular form for the dependence of the cross section on the velocity; the model of inelastic collisions used by Davydov[3] is very rough, and leads to the divergence of the distribution at small velocities. It should also be noted that there is an error in the work of Smit[2] (see below); however, in the case considered there of small E/p (E is the electric field intensity, p the gas pressure), the error is shown to be unimportant.

Under these conditions, it is desirable to develop a method free from these limitations; the present paper is devoted to such a development.

We consider the case of a spatially homogeneous plasma, in which the ionization is so small that we can neglect the Coulomb interaction. The generalization of this method to the case of a sufficiently strong ionization, in which the electron-electron interaction becomes important, will be considered below.

1. FUNDAMENTAL EQUATIONS

Let us first consider the case in which the electric and magnetic fields do not depend on the time. Then the kinetic equation for the determination of the stationary electron distribution function has the form

$$\{\gamma + [\mathbf{v}\Omega]\}\,\partial f/\partial \mathbf{v} = St_a + \sum_m^M St_e^{(m)} + \sum_n^N St_i^{(n)} + St_r, \quad (1.1)$$

where $\gamma = e\mathbf{E}/m_e$, $\Omega = e\mathbf{H}/m_e c$ while St_a, $St_e^{(m)}$, $St_i^{(n)}$ and St_r are terms taking into account, respectively, the elastic collisions of electrons with molecules, excitation of the m-th level, ionization (n-fold), and recombination (volume for high pressures and surface for low). Here we have neglected collisions of second order, inasmuch as these do not play an important role for weak ionization. Moreover, we confine ourselves to monatomic molecules. In the case of polyatomic molecules, it is necessary to take into consideration the excitation of vibrational and rotational levels, and also dissociation. This can easily be done by an analogous method.

The expression for St_a has the usual form (see, for example, reference 4), while for the inelastic collisions we assume an approximate model and set

$$St_e^{(m)} = -\nu_e^{(m)}(v) f(v,\theta,\varphi) + \nu_e^{(m)}(v_e^{(m)}) \frac{v_e^{(m)}}{v} f(v_e^{(m)},\theta,\varphi) \quad (1.2)$$

$$St_i^{(n)} = -\nu_i^{(n)}(v) f(v,\theta,\varphi) + \eta\nu_i^{(n)}(v_i^{(n)}) \frac{\tilde{v}_i^{(n)}}{v} f(v_i^{(n)},\theta,\varphi) + \tilde{\eta}\nu_i^{(n)}(\tilde{v}_i^{(n)}) \frac{\tilde{v}_i^{(n)}}{v} f(\tilde{v}_i^{(n)},\theta,\varphi), \quad (1.3)$$

where $\nu_e^{(m)} = N_0 v \sigma_e^{(m)}$, $\nu_i^{(n)} = N_0 v \sigma_i^{(n)}$; N_0 is the number of atoms per unit volume; $\sigma_e^{(m)}$ and $\sigma_i^{(n)}$ are the excitation cross sections of the m-th level and the n-fold ionization, averaged over the angles;

$$v_e^{(m)} = (v^2 + 2\varepsilon_e^{(m)}/m_e)^{1/2},\quad v_i^{(n)} = (\eta v^2 + 2\varepsilon_i^{(n)}/m_e)^{1/2},$$
$$\tilde{v}_i^{(n)} = (\tilde{\eta} v^2 + 2\varepsilon_i^{(n)}/m_e)^{1/2},$$

$\epsilon_e^{(m)}$ and $\epsilon_i^{(n)}$ are the corresponding energies of excitation and ionization, while the quantities $1 < \eta < \infty$ and $\tilde{\eta} = \eta/(\eta - 1)$ take into account the energy distribution between the primary scattered and the secondary electrons in the ionization. Inasmuch as the distribution of secondary electrons has a maximum for low velocities, while the scattered distribution has one at high velocities,[5] we can usually assume $\eta \sim 1$.

As regards the term St_r, it is introduced to satisfy the law of conservation of the number of particles. Account of it in the stationary case has importance in principle, although the specific form is shown to be unimportant. We set

$$St_r = -\nu_r(v) f(v, \theta, \varphi), \tag{1.4}$$

where, as follows from (1.1), the relation

$$\int \left(St_r + \sum_{n=1}^{N} St^{(n)}\right) d\mathbf{v} = 0 \tag{1.5}$$

must hold. (N is the maximum multiplicity of ionization.) It is easy to prove that if $St_e^{(m)}$ and $St_i^{(n)}$ are written in this manner, the laws of conservation of energy and of the number of particles are satisfied. The law of conservation of momentum is not satisfied. However, inasmuch as the form of the non-isotropic part of the distribution function is fundamentally determined by elastic collisions, this does not have a significant effect on the isotropic part of the distribution function.

Following Davydov,[3] let us expand f in a series of spherical harmonics in velocity space:

$$f(v, \theta, \varphi) = f_0(v) + \mathbf{v}\mathbf{f}_1(v) + \chi(v, \theta, \varphi), \tag{1.6}$$

where $\chi(v, \theta, \varphi)$ represents the remaining terms in the expansion.

If neutral atoms have a Maxwellian distribution with temperature T_0, then it can be shown (see, for example, reference 4) that, accurate to quantities of first order of smallness in $\delta = m_e/m_i$, we obtain

$$St_a(f_0) = \frac{\delta}{v^2}\frac{\partial}{\partial v} v^3 \nu_a(v)\left[f_0 + \frac{kT_0}{m_e v}\frac{\partial f_0}{\partial v}\right], \tag{1.7}$$

$$St_a(\mathbf{v}\mathbf{f}_1) = -\nu_a(v)\mathbf{v}\mathbf{f}_1, \tag{1.8}$$

where ν_a is the frequency of the elastic collisions.

We substitute Eq. (1.6) in Eq. (1.1), and integrate over the angles θ and φ. Taking Eq. (1.7) into account, and also the condition of the orthogonality of the spherical harmonics, we obtain, after a single integration over v:

$$\delta\nu_a(v)\left[f_0 + \frac{kT_0}{m_e v}\frac{\partial f_0}{\partial v}\right] - \frac{1}{3}\gamma\mathbf{f}_1 - \frac{S(f_0)}{v} = 0, \tag{1.9}$$

where

$$S(f) = -\frac{1}{v^2}\left\{\sum_m^M \int_v^{v_e^{(m)}} \nu_e^{(m)}(v) f(v) v^2 dv - \int_0^v \nu_r(v) f(v) v^2 dv\right.$$
$$\left. + \sum_n^N \left[\int_v^{v_i^{(n)}} \nu_i^{(n)}(v) f(v) v^2 dv + \int_0^{\tilde{v}_i^{(n)}} \nu_i^{(n)}(v) f(v) v^2 dv\right]\right\}. \tag{1.10}$$

Multiplying (1.1) by $\mathbf{v}$, and again integrating over the angles, we find (neglecting* the correction χ in comparison with f_0):

$$\nu_a(v)\mathbf{f}_1 + [\Omega \times \mathbf{f}_1] + \frac{1}{v^3}\frac{\partial}{\partial v} v^2 S(v\mathbf{f}_1) = -\frac{\gamma}{v}\frac{\partial f_0}{\partial v}. \tag{1.11}$$

Since, in writing down the initial equation, we have neglected the law of conservation of momentum for inelastic collisions, we can also neglect the third term on the left in Eq. (1.11) in comparison with the first. Then, solving (1.11) relative to $\mathbf{f}_1$, and substituting the resultant expression in (1.9), we obtain an equation for the isotropic part of the distribution function $f_0(v)$:

$$\delta\nu_a(v)\left[f_0 + \frac{kT_0}{m_e v}\frac{\partial f_0}{\partial v}\right] + \frac{\alpha\gamma}{3\nu_a}\frac{1}{v}\frac{\partial f_0}{\partial v} - \frac{S(f_0)}{v} = 0, \tag{1.12}$$

where

$$\alpha(v) = \frac{\gamma + [\gamma \times \Omega]/\nu_a + \Omega(\gamma\Omega)/\nu_a^2}{1 + \Omega^2/\nu_a^2}. \tag{1.13}$$

Inasmuch as the magnetic field enters into Eq. (1.12) only in the form of the product $\alpha \cdot \gamma$, we shall everywhere below assume for simplicity that $\Omega = 0$, having in view that the generalization of results to the case $\Omega \neq 0$ reduces simply to replacing the quantity $\mu(u)$ in the obtained formulas (see 1.18) by

$$\mu_H(u) = \frac{3kT_0\,\delta\tilde{\nu}_a^2}{m_e\gamma^2}\varphi_a^2(u) + \frac{\tilde{\nu}_a^2\varphi_a^2(u) + \Omega^2\cos^2(\widehat{\gamma\Omega})}{\tilde{\nu}_a^2\varphi_a^2(u) + \Omega^2}. \tag{1.13a}$$

We change in (1.12) to a new independent variable u and to a new function A(u) by the formulas

$$u = m_e v^2/2\varepsilon_e^{(1)},\quad f_0(v)|_{v=v(u)} = f_{00}(u)A(u), \tag{1.14}$$

where $f_{00}(u)$ is the solution of the equation in the absence of the inelastic collisions. Now, setting

$$\nu_a = \tilde{\nu}_a\varphi_a(u),\quad \nu_r = \tilde{\nu}_r\varphi_r(u)u^{-1/2},$$
$$\nu_e^{(m)} = \tilde{\nu}_e^{(m)}\varphi_e^{(m)}(u)u^{-1/2},\quad \nu_i^{(n)} = \tilde{\nu}_i^{(n)}\varphi_i^{(n)}(u)u^{-1/2}, \tag{1.15}$$

where $\tilde{\nu}_a$, $\tilde{\nu}_r$, $\tilde{\nu}_e^{(m)}$ and $\tilde{\nu}_i^{(n)}$ are certain constants, chosen to make $\varphi_a(1) = \varphi_r(1) = 1$ and to make the functions $\varphi_e^{(m)}$ and $\varphi_i^{(n)}$ of the order of unity for $u \gg 1$, we get

$$\frac{dA}{du} + Q(u)\left[F\{A\} - \lambda_r^2\int_0^u \varphi_r f_{00} A\, du\right] = 0. \tag{1.16}$$

*It can be shown that for $\lambda_e^2 \gg 1$, the function $\chi \sim (f_0\tilde{\nu}_e/\tilde{\nu}_a)\lambda_e^{-(2q+1)/(q+1)} \ll f_0$.

Here

$$F\{A\} = \sum_{m}^{M} \lambda_{e,m}^2 \int_{u}^{u+u_e^{(m)}} f_{00}(u)\,\varphi_e^{(m)}(u)\,A(u)\,du + \sum_{n}^{N} \lambda_{in}^2 \Big[\int_{u}^{\eta u + u_i^{(n)}} f_{00}(u)\,\varphi_i^{(n)}(u)\,A(u)\,du + \int_{0}^{\tilde{\eta} u + u_i^{(n)}} f_{00}(u)\,\varphi_i^{(n)}(u)\,A(u)\,du \Big], \quad (1.17)$$

$$Q(u) = \varphi_a(u)/u^{3/2} f_{00}\mu, \qquad \mu = (3kT_0\,\delta\tilde{\nu}_a^2/m_e\gamma^2)\,\varphi_a^2(u) + 1,$$

$$f_{00} = \exp\Big\{-\int_0^u du/u_T\Big\}, \qquad u_T = \gamma^2 m_e \mu(u)/3\delta\tilde{\nu}_a^2\varepsilon_e^{(1)}\varphi_a^2(u), \quad (1.18)$$

$$\lambda_{em}^2 = 3\varepsilon_e^{(1)}\tilde{\nu}_a\tilde{\nu}_e^{(m)}/2m_e\gamma^2, \quad \lambda_{in}^2 = 3\varepsilon_e^{(1)}\tilde{\nu}_a\tilde{\nu}_i^{(n)}/2m_e\gamma^2 = \lambda_{em}^2\beta_{nm}^2,$$

$$\lambda_r^2 = 3\varepsilon_e^{(1)}\tilde{\nu}_a\tilde{\nu}_r/2m_e\gamma^2,$$

$$u_e^{(m)} = \varepsilon_e^{(m)}/\varepsilon_e^{(1)} \geqslant 1, \qquad u_i^{(n)} = \varepsilon_i^{(n)}/\varepsilon_e^{(1)} > 1.$$

We note that, in accord with (1.5),

$$\lambda_r^2 \int_0^\infty \varphi_r f_{00} A\,du = \sum_n^N \lambda_{in}^2 \int_0^\infty \varphi_i^{(n)} f_{00} A\,du. \quad (1.19)$$

This condition is very important. Actually, if it is not satisfied, then, as follows from (1.16), A(u) vanishes for a finite value of u, whereas its derivative at this point undergoes a jump, which is physically without meaning. In essence, (1.19) is equivalent to the requirement

$$\partial A/\partial u \to 0 \quad \text{for } u \to \infty, \qquad A(u) \to 0. \quad (1.20)$$

In the work of Smit,[2] the loss of particles as the result of recombination was not taken into account; hence condition (1.19) was not fulfilled. However, in the solution of the equation, the author used the condition (1.20) (which is not compatible with the initial equation in this case), and thus obtained correct results for u > 1.

2. SOLUTION OF THE EQUATION FOR A(u)

To avoid needless complications, we first consider the case in which only a single ionization (N = 1) is possible, and there is either only one level of excitation (M = 1), or the distance between the levels is so small ($u_e^{(M)} - 1 \ll 1$) that $\epsilon_e^{(1)}$ can be replaced by some average excitation energy $\bar{\epsilon}_e$, while $\varphi_e^{(m)}$ can be replaced by the mean frequency of excitation.

An exact solution of Eq. (1.16) is evidently impossible without going to numerical integration. However, one can attempt to apply an approximate method of solution, which is essentially the expansion of A(u) in inverse powers of the parameter λ_{e1}^2. Actually, as follows from its definition, this parameter is of the same order of magnitude as the ratio of the energy lost per unit time by the electron (with velocity corresponding to the maximum of the frequency of ionization) on excitation to the energy obtained by it from the external field, i.e., it is usually much greater than unity.* Thus, we shall solve the equation for A(u) under the assumption that $\lambda_{e1}^2 \gg 1$.

We note that, as follows from the discussion below, the function A(u) falls off with distance as $\sim 1/\lambda_{e1}$, whereas $f_{00}(u)$ depends on distance as $\sim 1/\delta\lambda_{e1}^2$. Consequently, since $\delta \ll 1$, we can, for not very large λ_{e1} (less than δ^{-1}), remove the function f_{00} in Eqs. (1.16), (1.17) from under the integral sign.† Then, denoting by $A_I(u)$ the solution for $u \leq 1$, and by $A_{II}(u)$ the solution for $u \geq 1$, and dropping the index (1) in λ_{e1}, ϵ_{11}, $\varphi_e^{(1)}$ and $\varphi_i^{(1)}$, we obtain

$$A_{II}'(u) + Q_1(u)\Big[\lambda_e^2 F_1\{A_{II}\} - \lambda_r^2 \int_0^u \varphi_r A_{II}\,du\Big] = 0 \quad (2.1)$$

for $u \geq 1$ and

$$A_I'(u) - \lambda_r^2 Q_1(u) \int_0^u \varphi_r A_I\,du = -\lambda_e^2 Q_1(u) F_1\{A_{II}\} \quad (2.2)$$

for $u \leq 1$, where

$$F_1\{A_{II}\} = \int_u^{u+1} \varphi_e(u)\,A_{II}(u)\,du + \beta^2\Big[\int_u^{\eta u + u_i} \varphi_i(u)\,A_{II}(u)\,du + \int_0^{\tilde{\eta} u + u_i} \varphi_i(u)\,A_{II}(u)\,du\Big], \quad (2.3)$$

$$Q_1(u) = \varphi_a(u)/u^{3/2}\mu(u). \quad (2.4)$$

The prime here and below denotes differentiation with respect to the argument.

To begin, let us consider Eq. (2.1). We assume that the condition

$$[\ln A_{II}(u)]' \gg 1, \quad (2.5)$$

is satisfied, i.e., the function $A_{II}(u)$ falls off rapidly in the interval [u, u+1], and differentiate (2.1) with respect to u. Then, considering that, by (1.19), $\lambda_r^2 \lesssim 1$ and $\lambda_e^2 \gg 1$, and neglecting $A_{II}(u+1)$ in comparison with $A_{II}(u)$, we find, with accuracy $\gtrsim \lambda_e^{-2}$, the equation of first approximation

*The case of very large E/p, when the quantity λ_{e1}^2 becomes smaller than unity, will not now be considered, inasmuch as for such values of E/p, the percent ionization is sufficiently high and it is necessary to take into account the electron-electron interaction.

†The case $\lambda_{e1} > \delta^{-1}$ always corresponds to low (of the order of several hundred degrees) mean energies of electrons, when the inelastic collisions no longer play a role.

$$(A_{II}^{(1)})'' - (\ln Q_1(u))'(A_{II}^{(1)})' - \lambda_e^2 p^2(u) A_{II}^{(1)} = 0, \quad (2.6)$$

where

$$p^2(u) = Q_1(u)[\varphi_e(u) + \beta^2\varphi_i(u)]. \quad (2.7)$$

Up to now we have made no assumptions concerning the form of the dependence of the cross section on the velocity. We now assume that φ_e, φ_i, and φ_a are such that p^2 vanishes nowhere, except at the point $u = 1$, while as $u \to 1$,

$$p^2(u) = p_0^2(u-1)^{2q}, \quad (2.8)$$

where $q > 0$ and $p_0^2 > 0$ are certain constants which depend on the behavior of the functions φ_e and φ_i close to the thresholds of excitation and ionization.

Let us change variables in Eq. (2.6), introducing the independent variable

$$x(u) = \left[(q+1)\lambda_e \int_1^u p(u)\,du\right]^{1/(1+q)} \quad (2.9)$$

and the new function

$$Y(x) = (x'(u)/Q_1(u))^{1/2} A_{II}^{(1)}(u)|_{u(x)}. \quad (2.10)$$

We then get for $Y(x)$ the equation

$$Y''(x) - [\zeta(x) + x^{2q}]Y(x) = 0, \quad (2.11)$$

where

$$\zeta(x) = \tfrac{1}{2}\{(x')^{-3/2}[(x')^{-3/2}x'']' + (x'Q_1)^{-2}[\tfrac{3}{2}(Q_1')^2 - Q_1Q_1'']\}|_{u(x)}.$$

An estimate shows that the function $\zeta(x)$ will, generally speaking, be of the order of $2^{-1/q}(\lambda_e p_0)^{-1/q(q+1)}$, i.e., very small both for x close to zero and for large values of x. It can become large only if u approaches the next root of the function $p^2(u)$. Inasmuch as we have assumed that the function $p^2(u)$ never vanishes for $u > 1$, we can neglect $\zeta(x)$ in Eq. (2.11) in comparison with x^{2q} and obtain

$$Y'' - x^{2q}Y = 0, \quad (2.12)$$

whence, by taking account of the condition (1.20),

$$Y = \text{const}\cdot C_0 K_{1/2(q+1)}\left(\frac{x^{q+1}}{q+1}\right)x^{1/2} = \text{const}\cdot V_q(x), \quad (2.13)$$

where K_n is the MacDonald function of order n and C_0 is a constant, so chosen that $V_q(0) = 1$. Thus

$$A_{II}^{(1)}(u) = \text{const}\cdot[Q_1/x']^{1/2}V_q(x)|_{x(u)}, \quad (2.14)$$

and the condition (2.5) takes the form

$$\lambda_e^2 p^2(u) \gg 1. \quad (2.15)$$

It then follows that, for sufficiently large u, when $\lambda_e^2 p^2(u) \sim 1$, the solution (2.14) turns out to be invalid. However, for these values of u, the function $A_{II}^{(1)}$ is already very small ($\sim \exp[-\lambda_e^2 p_0]$) and consequently is not of interest.

For $\lambda_e^2 p_0^2 \gg 1$, we can limit ourselves entirely to the first approximation $A_{II}^{(1)}$. If $\lambda_e p_0$ becomes of the order of unity, then it is necessary to use the solution $A_{II}^{(2)}$, obtained in second approximation. Assuming, as before, that for $u > 1$,

$$\lambda_i^2 \int_0^{\eta u + u_i} \varphi_i A\,du \approx \lambda_r^2 \int_0^u \varphi_r A\,du,$$

we find from (2.1) that

$$A_{II}^{(2)}(u) = \lambda_e^2 \int_u^\infty Q_1(u) J\{A_{II}^{(1)}\}\,du, \quad (2.16)$$

where

$$J\{A_{II}^{(1)}\} = \int_u^{u+1} \varphi_e A_{II}^{(1)}\,du + \beta^2 \int_u^{\tilde{\eta}u + u_i} \varphi_i A_{II}^{(1)}\,du. \quad (2.17)$$

We now proceed to the finding of the function $A_I(u)$. Generally speaking, for an exact solution of Eq. (2.2) it is necessary to give an explicit form for $\varphi_r(u)$, which, unfortunately, is very little known. We can prove, however, that in the case under discussion here, the term proportional to λ_r^2 plays an important role only in the region of small values of u, where it leads to a certain increase in $A_I(u)$. Moreover, inasmuch as the distribution function for $u < 1$ is needed essentially only for the calculation of the normalizing factor, then, taking it into account that $\tilde{\eta} \gg \eta$, we can set, without excessive error,

$$\lambda_e^2 F_1\{A_{II}^{(1)}\} - \lambda_r^2 \int_0^u \varphi_r A_I\,du = \lambda_e^2 J\{A_{II}^{(1)}\},$$

whence

$$A_I(u) = A_{II}^{(2)}(1) + \lambda_e^2 \int_u^1 Q_1(u) J\{A_{II}^{(1)}\}\,du$$
$$= \lambda_e^2 \int_u^\infty Q_1(u) J\{A_{II}^{(1)}\}\,du. \quad (2.18)$$

The results obtained for $A_I(u)$ and $A_{II}(u)$ can be materially simplified by making use of the fact that $V_q(x)$ is a rapidly decreasing function. We first note that: a) if u_i is close to unity, so that $\alpha(u_i - 1) < 1$, where $\alpha = (\lambda_e p_0)^{1/(q+1)}$, then we can write

$$J = [1+\beta^2]^{-1}\left\{\int_u^{u+1} Q_1^{-1}p^2 A_{II}^{(1)}\,du + \beta^2 \int_u^{\tilde{\eta}u+1} Q_1^{-1}p^2 A_{II}^{(1)}\,du\right\}; \quad (2.19)$$

b) in the opposite case, when $\alpha(u_i - 1) > 1$, we can neglect the second component in (2.17) and get

$$J = \int_u^{u+1} Q_1^{-1}p^2 A_{II}^{(1)}\,du, \quad (2.19')$$

i.e., case b) is obtained from a) if we set $\beta^2 = 0$ in the latter. Therefore, we limit our considerations to the case a).* Substituting (2.14) in Eqs. (2.16) and (2.18), and integrating, we obtain [bearing in mind that, for $u > 1$, the function $A_{II}^{(1)}(u)$ decreases rapidly]:

$$A_{II}(u) = \text{const} \cdot \left[\frac{\alpha Q_1(u)}{x' Q_1(1)}\right]^{1/2} \left\{V_q(x(u)) - (1+\beta^2)^{-1}\left[\frac{x'(u)}{x'(u+1)} V_q(x(u+1)) + \frac{\beta^2}{\tilde{\eta}} \frac{x'(u)}{x'(\tilde{\eta}u+1)} V_q(x(\tilde{\eta}u+1))\right]\right\}, \quad (2.20)$$

where the index (2) in $A_{II}^{(2)}(u)$ is omitted, and

$$A_I(u) = A_{II}(1) - (1+\beta^2)^{-1}\alpha\left\{\tau(u)\left[(1+\beta^2)V_q'(0) - V_q'(x(u+1)) - \beta^2 V_q'(x(\tilde{\eta}u+1))\right] - x'(u+1)\int_{u+1}^{2}\tau(u-1)x^{2q}V_q(x(u))\,du - \beta^2 x'(\tilde{\eta}u+1)\int_{\tilde{\eta}u+1}^{\tilde{\eta}+1}\tau\left(\frac{u-1}{\tilde{\eta}}\right)x^{2q}V_q(x(u))\,du\right\}, \quad (2.21)$$

where

$$\tau(u) = \int_u^1 \frac{Q_1(u)}{Q_1(1)}\,du. \quad (2.22)$$

The resulting values apply to the case in which only single ionization is possible ($N = 1$) and there is only one excitation level ($M = 1$). However, it is easy to generalize it to the case of arbitrary N and M. Actually, Eqs. (2.9) and (2.14) for $A_{II}^{(1)}$ and Eqs. (2.16) and (2.18) for $A_I(u)$ and $A_{II}^{(2)}(u)$ evidently remain valid even in the case in which we replace the quantity $\lambda_e^2 p^2(u)$ appearing in it by

$$P^2(u) = Q_1(u)\left\{\sum_m^M \lambda_{em}^2 \varphi_e^{(m)} + \sum_n^N \lambda_{in}^2 \varphi_i^{(n)}\right\}, \quad (2.7')$$

and the expression $\lambda_e^2 J\{A_{II}^{(1)}\}$ by

$$I\{A_{II}^{(1)}\} = \sum_m^M \lambda_{em}^2 \int_u^{u+u_e^{(m)}} \varphi_e^{(m)} A_{II}^{(1)}\,du + \sum_n^N \lambda_{in}^2 \int_u^{\tilde{\eta}u+u_i^{(n)}} \varphi_i^{(n)} A_{II}^{(1)}\,du. \quad (2.17')$$

It follows from the expression for $A_{II}(u)$ that the presence of inelastic collisions leads to a sharp decrease in the distribution function when $u > 1$. Thus, with increase in the intensity of the electric field, the mean energy of the electrons at first increases rapidly and then, beginning with some value $E = E(N_0)$ (corresponding to $\lambda_e^2 \delta \sim 1$), it remains practically constant until values are reached, for which the energy drawn from the field per unit time is comparable with the losses due to excitation and ionization ($\lambda_e^2 \sim 1$), after which it again begins to increase.

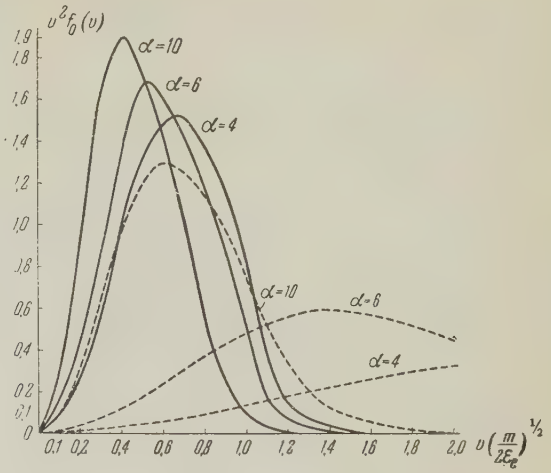

The formulas given above are valid, in general, for all $q > 0$. However, the greatest interest attaches to the case $q = 1/2$, inasmuch as the function V_q coincides in this case (with accuracy up to some constant) with the excellently tabulated Airy functions,[6] which simplifies appreciably the use of the formulas. In the same way, the case $q = 1/2$ agrees well with the actual course of the cross section close to the threshold for excitation and ionization.[7]

By way of illustration we have plotted the function $v^2 f_0(v)$ for the case in which the frequency of elastic collisions does not depend on the velocity:

$$\varphi_a = 1, \quad \varphi_e = u(u-1)/(u^2+u_0^2), \quad \tilde{\nu}_e = 2u_0\tilde{\nu}_a, \quad \delta = 5\cdot 10^{-4}, \quad u_0 = 5, \quad \beta^2 = 0, \quad T = 300^\circ\,\text{K}.$$

The dashed curves correspond to distribution functions computed without consideration of inelastic collisions, the solid curves, with consideration of losses by excitation.

In conclusion, it should be noted that although the method of solution used here is valid, strictly speaking, only for the condition (2.15), an analysis shows that the expressions obtained for $A(u)$ remain valid up to values $\alpha \sim 1$, which corresponds to quite large values of E/p.

3. DISTRIBUTION FUNCTION IN AN ALTERNATING ELECTRIC FIELD

In previous section we found an expression for the electron distribution function in electric and magnetic fields that were constant in time. The results are easily generalized to the case of an alternating electric field. We assume, for sim-

*Similar simplifications can be carried out also in the case of an intermediate value of u_i. However, inasmuch as the resulting formulas are very cumbersome, we shall not write them out.

plicity, that $\mathbf{E}(t) = \mathbf{E}_0 \cos \omega t$. We then have in place of (1.9) and (1.11):

$$\frac{\partial f_0}{\partial t} = \frac{1}{v^2}\frac{\partial}{\partial v} v^3 \left\{ \delta\nu_a \left[f_0 + \frac{kT_0}{m_e v}\frac{\partial f_0}{\partial v} \right] - \frac{\gamma(t)\,\mathbf{f}_1}{3} - \frac{S(f_0)}{v} \right\}, \quad (3.1)$$

$$\frac{\partial \mathbf{f}_1}{\partial t} + \nu_a \mathbf{f}_1 + [\Omega \times \mathbf{f}_1] = -\frac{\gamma(t)}{v}\frac{\partial f_0}{\partial v}, \quad (3.2)$$

where $\boldsymbol{\gamma}(t) = \boldsymbol{\gamma}_0 \cos \omega t$, and $S(f)$ is determined by (1.10) as before.

Before undertaking the solution of these equations, we note that in a variable field the mean energy of the electrons changes only as a result of a change in the external electric field. Therefore, depending on the ratio between the characteristic time $\tau_E \sim 1/\omega$ of change in the field and the time τ of the relaxation of the energy of the electrons, we can segregate the cases of slowly ($\omega\tau \ll 1$) and rapidly ($\omega\tau \gg 1$) changing fields. In the first case (quasi-stationary), the energy distribution is established in a time much shorter than $1/\omega$ and thus the stationary solution is valid provided we replace γ^2 in it by $\gamma^2(t)$. In the second case the mean energy of the electrons does not succeed in changing within the time $\sim 1/\omega$ and, consequently, the isotropic part of the distribution function $f_0(v)$ should not, in first approximation, depend on the time. Consequently, we can solve the set of equations (3.1) and (3.2) by successive approximation, expanding f_0 and $\mathbf{f}_1$ in positive (for $\omega\tau \ll 1$) or negative (for $\omega\tau \gg 1$) powers of the parameter $\omega\tau$. A logical exposition of this method, for the case in which we can neglect the inelastic collisions [$S(f) = 0$], has been given by A. V. Gurevich.[8] In the presence of inelastic collisions, the problem is somewhat complicated, inasmuch as for $S(f) \neq 0$ it is no longer possible to introduce a single parameter independent of the value of the applied electric field capable of characterizing the rate of establishment of the symmetric part of the distribution function. Actually, in weak fields, when the inelastic collisions do not play an important role, the relaxation time is determined essentially by the elastic interaction and $\tau \sim 1/\delta\nu_a$. With increasing electric field, the frequency of the inelastic collisions increases, and the inelastic interaction begins to play a decisive role, i.e., the relaxation time decreases. However, in spite of this indeterminacy in the choice of τ, we can nevertheless evaluate the lower (τ_1) and upper (τ_2) bounds of τ; thus, for frequencies $\omega \ll \tau_2^{-1}$ and $\omega \gg 1/\tau_1$, we apply the method of successive approximations as before, expanding f_0 and $\mathbf{f}_1$ in powers of the parameter $\omega\tau_2$ (for $\omega\tau_2 \ll 1$) or $(\omega\tau_1)^{-1}$ (for $\omega\tau_1 \gg 1$). Solution of these equations in the case of intermediate frequencies $1/\tau_1 > \omega > 1/\tau_2$ entails great mathematical difficulty and will not be considered here.

1. Let $\omega\tau_2 \ll 1$. Then the equations for the functions of first approximation, $f_0^{(1)}$ and $\mathbf{f}_1^{(1)}$, are obtained from (3.1) and (3.2) by discarding the time derivatives, after which we get for $f_0^{(1)}$:

$$\delta\nu_a \left[f_0^{(1)} + \frac{kT_0}{mv}\frac{\partial f_0^{(1)}}{\partial v} \right] + \frac{\alpha(t)\,\gamma(t)}{3\nu_a v}\frac{\partial f_0^{(1)}}{\partial v} - \frac{S(f_0^{(1)})}{v} = 0,$$

where

$$\alpha(t) = \frac{\gamma(t) + [\gamma(t) \times \Omega]/\nu_a + \Omega(\Omega\gamma(t))/\nu_a^2}{1 + \Omega^2/\nu_a^2}.$$

It is easy to see that this equation is identical with Eq. (1.12), the solution of which was obtained above. An estimate of next higher approximations shows that the parameter τ_2 is equal, in order of magnitude, to $1/\delta\bar{\nu}_a$, where $\bar{\nu}_a$ is the average frequency of elastic collisions of the electron with the atoms of the gas.

Thus, for $\omega/\delta\bar{\nu}_a \ll 1$,

$$f_0^{(1)}(v, t) = C(t)\, f_{00}(u, t)\, A(u, t) \quad (3.3)$$

[with $u = u(v)$], where the function $C(t)$ is determined from the normalization condition, and the expressions for $f_{00}(u, t)$ and $A(u, t)$ are given by Eqs. (1.18), (2.16), and (2.18), in which the quantity γ^2 has been replaced by $\gamma^2(t) = \gamma_0^2 \cos^2 \omega t$.

2. For $\omega\tau_1 \gg 1$, the equations of first approximation give

$$\frac{\partial f_0^{(1)}}{\partial t} = 0, \quad \mathbf{f}_1^{(1)} = -\frac{1}{v}\frac{\partial f_0^{(1)}}{\partial v} \operatorname{Re}\left\{ \frac{\gamma_0(\nu_a + i\omega)^2 + (\nu_a + i\omega)[\gamma_0 \times \Omega] + \Omega(\Omega\gamma_0)}{(\nu_a + i\omega)[(\nu_a + i\omega)^2 + \Omega^2]} e^{i\omega t} \right\}. \quad (3.4)$$

Proceeding to the second approximation, $f_0^{(2)}$, and bearing in mind that $f_0^{(2)}$ is bounded as $t \to \infty$, we find an equation for $f_0^{(1)}$ as a function of v:

$$\delta\nu_a \left[f_0^{(1)} + \frac{kT_0}{mv}\frac{\partial f_0^{(1)}}{\partial v} \right] + \frac{\gamma_0^2 \bar{\psi}}{6\nu_a v}\frac{\partial f_0^{(1)}}{\partial v} - \frac{S(f_0^{(1)})}{v} = 0, \quad (3.5)$$

where

$$\bar{\psi} = (1 + \omega^2/\nu_a^2)^{-1} \left\{ 1 - \Omega^2 \frac{(\nu_a^2 + \Omega^2 - 3\omega^2)\sin^2(\widehat{\gamma_0, \Omega})}{(\nu_a^2 + \omega^2 + \Omega^2) - 4\omega^2\Omega^2} \right\}. \quad (3.6)$$

Comparing (3.5) with (1.12), we find that they coincide if $\gamma \cdot \alpha$ in (1.12) is replaced by $\gamma_0^2\bar{\psi}/2$. Thus, as has already been pointed out, the isotropic part of the distribution function does not depend in first approximation on the time, and is equal to

$$f_0^{(1)}(v) = \text{const} \cdot f_{00}(u)\, A(u), \quad (3.7)$$

where $f_{00}(u)$ and $A(u)$ are determined, as above, by Eqs. (1.18), (2.16), and (2.18), in which γ^2 is

replaced by $\gamma_0^2\overline{\psi}/2$ and the function $\mu(u)$ [see Eq. (1.18)] is replaced by

$$\widetilde{\mu}(u) = (6kT_0\delta\widetilde{\nu}_a^2/\gamma_0^2 m)\varphi_a^2 + \overline{\Psi}(v), \qquad v = v(u). \quad (3.8)$$

By computing the higher approximations, we find that the solution (3.7) is valid only for frequencies ω satisfying the inequality

$$\omega \gg \widetilde{\nu}_e \lambda_e^{-(2q+1)/(q+1)}. \quad (3.9)$$

The author thanks M. S. Rabinovich for his interest in the research.

[1] M. Druyvestyn, Physica **3**, 65 (1936).

[2] J. A. Smit, Physica **3**, 543 (1937).

[3] B. I. Davydov, J. Exptl. Theoret. Phys. (U.S.S.R.) **6**, 463 (1936).

[4] S. Chapman and T. G. Cowling, The Mathematical Theory of Nonuniform Gases. (Cambridge, 1952).

[5] H. S. W. Massey and E. Burhop, Electronic and Ionic Impact Phenomena, Clarendon Press, Oxford, 1952; Russ. transl. IIL, 1958.

[6] V. A. Fok, Таблицы функций Эйри (Tables of Airy Functions), Moscow, 1946.

[7] V. L. Granovskiĭ, Электрический ток в газе (Electric Currents in Gases) Gostekhizdat, vol. 1, Moscow-Leningrad, 1952.

[8] A. V. Gurevich, Dokl. Acad. Nauk SSSR **104**, 201 (1955).

Translated by R. T. Beyer
88

ON THE POSSIBILITY OF DETERMINING THE AMPLITUDE FOR CHARGE EXCHANGE PION-PION SCATTERING FROM AN ANALYSIS OF THE $\pi^- + p = N + \pi^+ + \pi^-$ REACTIONS NEAR THRESHOLD

A. A. ANSEL'M and V. N. GRIBOV

Submitted to JETP editor March 9, 1959

J. Exptl. Theoret. Phys. (U.S.S.R.) **37**, 501-503 (August, 1959)

It is shown that an analysis of experimental data on the energy distribution and angular correlations in the $\pi^- + p \to n + \pi^+ + \pi^-$, $n + \pi^0 + \pi^0$, and $p + \pi^- + \pi^0$ reactions makes it possible to determine the amplitude for charge-exchange scattering of charged mesons into neutral ones: $\pi^+ + \pi^- \to 2\pi^0$.

IN a previous paper by the authors[1] it was shown that the experimental study of the photoproduction of two π mesons near threshold may give information on the charge exchange amplitude $(\pi^+, \pi^-) \to 2\pi^0$ at zero energy. In this note analogous results are presented for the case of production of a π-meson pair in a pion-proton collision. In this case knowledge of pion-nucleon scattering phase shifts (δ_{31} and δ_{11}) makes it possible to indicate a somewhat different method for analyzing the experimental data.

Three reactions accompanied by production of two π mesons are possible in the collision of a π^- meson with a proton:

$$\pi^- + p \to n + \pi^+ + \pi^-, \quad (1a)$$
$$\pi^- + p \to n + \pi^0 + \pi^0, \quad (1b)$$
$$\pi^- + p \to p + \pi^- + \pi^0. \quad (1c)$$

The squares of the matrix elements for reactions (1), with final-state interactions taken into account, can be written, analogously to the case of photoproduction of two π mesons, as follows (accurate up to terms linear in kr_0):[1]

$$|\langle \pi^+\pi^- n | S | \pi^- p\rangle|^2 = \rho_1^2 [1 + \rho_{12}\sin\varphi_{12}\cdot \tfrac{2}{3}(a_2 - a_0)k_{12} + \rho_{13}\sin\varphi_{13}\cdot \tfrac{2}{3}\sqrt{2}(b_{3/2} - b_{1/2})k_{13}],$$
$$|\langle \pi^0\pi^0 n | S | \pi^- p\rangle|^2 = \rho_2^2 [1 + \rho_{21}\sin\varphi_{21}\cdot \tfrac{4}{3}(a_2 - a_0)k_{12} + \rho_{23}\sin\varphi_{23}\cdot \tfrac{2}{3}\sqrt{2}(b_{3/2} - b_{1/2})(k_{13} + k_{23})],$$
$$|\langle \pi^-\pi^0 p | S | \pi^- p\rangle|^2 = \rho_3^2 [1 + \rho_{31}\sin\varphi_{31}\cdot \tfrac{2}{3}\sqrt{2}(b_{3/2} - b_{1/2})k_{13} + \rho_{32}\sin\varphi_{32}\cdot \tfrac{2}{3}\sqrt{2}(b_{3/2} - b_{1/2})k_{23}],$$
$$\rho_{ik} = \rho_k/\rho_i, \qquad \varphi_{ik} = \varphi_i - \varphi_k. \quad (2)$$

Here ρ_i and φ_i are determined by the relations $\lambda_i = \rho_i \exp(i\varphi_i)$ where λ_i are the matrix elements of reactions (1a) – (1c) at threshold; $(a_2 - a_0)/3$ and $\sqrt{2}\,(b_{3/2} - b_{1/2})/3$ are, as before, charge exchange amplitudes for π-π and π-N scattering at zero energy; k_{lm} is the absolute value of the relative momentum of the l-th and m-th particles, which are numbered in the order in which they are written out in the left hand sides of Eq. (2).

To determine $a_2 - a_0$ it is sufficient, as in reference 1, to study the angular or energy distribution of the reaction 1a because the coefficients $\rho_{12}\sin\varphi_{12}$ and $\rho_{13}\sin\varphi_{13}$ are related due to charge independence by

$$\rho_{12}\sin\varphi_{12} = -\sqrt{2/3}\,\rho_{13}\sin\varphi_{13}. \quad (3)$$

Below we discuss in some detail the quantity $\rho_{12}\sin\varphi_{12}$ which enables us to give a rough estimate of the magnitude of the effect and indicate a method for a determination of $(a_2 - a_0)$ without a measurement of the ratio of the coefficients of k_{12} and k_{13}.

Near threshold the contribution to the matrix elements of reactions (1a) – (1c) comes from the $P_{1/2}$ state of the (π^-, p) system. The (π^-, p) system is a superposition of isospin $T = \frac{1}{2}$ and $\frac{3}{2}$ states. Consequently, if we characterize the system (N, π, π) by its total isospin T and the isospin of the two mesons T_{12}, then in the final state there are only the following possibilities: $T = \frac{1}{2}$, $T_{12} = 0$ or $T = \frac{3}{2}$, $T_{12} = 2$ ($T_{12} = 1$ is forbidden for zero-energy π mesons). Therefore the three amplitudes λ_i may be expressed in terms of two isospin invariant matrix elements $\langle \frac{1}{2}\, 0 | S | \frac{1}{2}\rangle$ and $\langle \frac{3}{2}\, 2 | S | \frac{3}{2}\rangle$.

It is easy to show (see reference 2) that the phases of these matrix elements arise from initial-state interactions and coincide with the scattering phase shifts of π mesons on nucleons, δ_{11} and δ_{31}, in the $P_{1/2}$ state with isospin $T = \frac{1}{2}$ and $\frac{3}{2}$ at the energy corresponding to the

threshold of the reactions under study. We can write

$$\langle \tfrac{1}{2}0|S|\tfrac{1}{2}\rangle = F_{11}e^{i\delta_{11}}, \qquad \langle \tfrac{3}{2}0|S|\tfrac{3}{2}\rangle = F_{31}e^{i\delta_{31}}, \quad (4)$$

where F_{11}, F_{31} are real (but may be positive as well as negative).

It is then easy to find for λ_1, λ_2, and λ_3:

$$\lambda_1 = \rho_1 e^{i\varphi_1} = -(\sqrt{2}/3)F_{11}e^{i\delta_{11}} + (1/3\sqrt{5})F_{31}e^{i\delta_{31}},$$
$$\lambda_2 = \rho_2 e^{i\varphi_2} = (\sqrt{2}/3)F_{11}e^{i\delta_{11}} + (2/3\sqrt{5})F_{31}e^{i\delta_{31}},$$
$$\lambda_3 = \rho_3 e^{i\varphi_3} = -\sqrt{3/10}F_{31}e^{i\delta_{31}}. \quad (5)$$

Equation (5) leads in particular, to Eq. (3).

Let us express $\rho_{12}\sin\varphi_{12}$ in terms of F and δ:

$$\rho_{12}\sin\varphi_{12} = \frac{3\sin(\delta_{31}-\delta_{11})}{x\sqrt{10}+1/x\sqrt{10}-2\cos(\delta_{31}-\delta_{11})}, \quad x = \frac{F_{11}}{F_{31}}. \quad (6)$$

Thus the quantity $\rho_{12}\sin\varphi_{12}$, which determines the order of magnitude of the effect, depends on $\delta_{31}-\delta_{11}$ and x. The scattering phase shifts δ_{31} and δ_{11}, at energies 140-220 Mev in the center of mass system, are but poorly known.[3] It is expected, however, that $|\delta_{11}-\delta_{31}| \lesssim 10$ deg (B. M. Pontecorvo, private communication).

The quantity $\rho_{12}\sin\varphi_{12}$ behaves as a function of x (with $\delta_{31}-\delta_{11} = 10$ deg) as shown in the figure. For $x < 0$ the effect is small. In that case it would be more favorable to study the reaction (1b).

In order to determine $\rho_{12}\sin\varphi_{12}$, assuming the phase shifts δ_{11} and δ_{31} to be known, it is necessary to know x. A measurement of the ratio (ρ_k^2/ρ_i^2) of the rates of any two of the reactions (1a — 1c) at threshold would determine x, using Eq. (5). However, the x so determined will be two-valued. One may also determine x by measuring the ratio of the rate of reaction (1a) to the rate of either of the reactions $\pi^+ + p \to \pi^+ + \pi^0 + p$, $\pi^+ + \pi^+ + n$ (the cross sections for these reactions are $\sim F_{31}^2$). Here again x will be two-valued. To obtain a unique value for x it must be measured by any two of the indicated methods. Otherwise two alternatives for the sign of $a_2 - a_0$ will be obtained.

Once the quantity $\rho_{12}\sin\varphi_{12}$ has been determined, it is sufficient to study, for example, the dependence of the total cross section for reaction (1a) on the energy of the incident π^- meson. This cross section is given by (see reference 3):

$$\sigma = \rho_1^2 T^2\left\{1 + \frac{64}{45\pi}\rho_{12}\sin\varphi_{12}\left[(a_2-a_0)\sqrt{2\mu_{12}T}\right.\right.$$
$$\left.\left. - (b_{3/2}-b_{1/2})\sqrt{6\mu_{13}T}\right]\right\},$$
$$\mu_{12} = \mu/2, \quad \mu_{13} = m\mu/(m+\mu), \quad (7)$$

where m and μ are the nucleon and meson masses, and T is the kinetic energy of the three particles in the center of mass system.

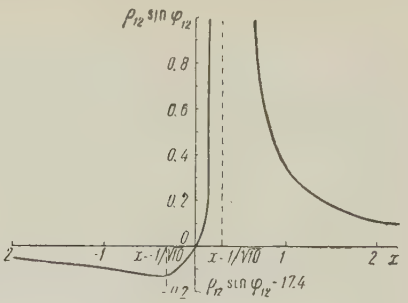

The method described for determining $a_2 - a_0$ can also be used in principle in the photoproduction of two π mesons on a proton.[1] Instead of Eq. (6) we have in that case

$$\rho_{12}\sin\varphi_{12} = \frac{3\sin(\alpha_{31}-\alpha_{11})}{y\sqrt{5}+1/y\sqrt{5}-2\cos(\alpha_{31}-\alpha_{11})}, \quad y = \frac{G_{11}}{G_{31}}, \quad (8)$$

where $G_{31}e^{i\alpha_{31}}$ and $G_{11}e^{i\alpha_{11}}$ are the matrix elements for photoproduction in the isospin states $\frac{3}{2}$ and $\frac{1}{2}$ (with a total angular momentum $\frac{1}{2}$). The phases α_{11} and α_{31} differ from zero because of the existence of a real intermediate state $\gamma + N \to N + \pi \to N + \pi + \pi$, and can be expressed, with the help of the unitarity condition,[2] in terms of photoproduction amplitudes and the matrix elements F_{11} and F_{31} (see reference 4) for the π into 2π transition:

$$G_{11}\sin\alpha_{11} = \pm|M_{11}||F_{11}|\Gamma^{1/2},$$
$$G_{31}\sin\alpha_{31} = \pm|M_{31}||F_{31}|\Gamma^{1/2}. \quad (9)$$

Here M_{11} and M_{31} are the amplitudes for the photoproduction of a single π meson by an M1 photon at a photon energy $E = m + 2\mu$ in a state of total angular momentum $\frac{1}{2}$ and isospin $\frac{1}{2}$ and $\frac{3}{2}$ respectively.[4] Γ is the phase space volume $(k^2\,dk/dE)$ of the nucleon + pion system at energy $E = \sqrt{k^2+m^2} + \sqrt{k^2+\mu^2} = m + 2\mu$. If the photoproduction amplitudes M are normalized so that the cross section is given by $\sigma = \int|M|^2 d\Omega$, then $\sqrt{\Gamma} = 1.5\mu$.

The authors express gratitude to B. M. Pontecorvo for his interest in this work and discussion of the results.

[1] A. A. Ansel'm and V. N. Gribov, J. Exptl. Theoret. Phys. (U.S.S.R.) **36**, 1890 (1959), Soviet Phys. JETP **9**, 1345 (1959).

[2] E. Fermi, Suppl. Nuovo cimento **2**, 17 (1955). V. N. Gribov, J. Exptl. Theoret. Phys. (U.S.S.R.) **33**, 1431 (1957), Soviet Phys. JETP **6**, 1102 (1958).

[3] G. Puppi, Report at the VIII Rochester Conference in Geneva, 1958.

[4] Watson, Keck, Tollestrup, and Walker, Phys. Rev. **101**, 1159 (1956).

Translated by A. M. Bincer
89

ON THE INTRODUCTION OF AN "ELEMENTARY LENGTH" IN THE RELATIVISTIC THEORY OF ELEMENTARY PARTICLES

Yu. A. GOL'FAND

P. N. Lebedev Physics Institute, Academy of Sciences U.S.S.R.

Submitted to JETP editor March 11, 1959

J. Exptl. Theoret. Phys. (U.S.S.R.) 37, 504-509 (August, 1959)

A momentum space of constant curvature is introduced into the theory in place of the pseudo-Euclidean momentum space. The Feynman diagram technique is suitably generalized. Finite results are obtained in the lowest order perturbation theory approximation for the fermion and boson self-energy.

INTRODUCTION

THE formulation of a theory of elementary particles free of the "ultraviolet catastrophe" is, apparently, impossible without the introduction of an "elementary length" l_0 which defines the limit down to which the ordinary concepts of space are still valid. Another equivalent possibility is the introduction into the theory of a "limiting mass" $\mu \sim 1/l_0$, which establishes corresponding limitations in momentum space. The present paper is devoted to an attempt of formulation of such a theory. A brief formulation of the principal idea consists of the following. The four-dimensional momentum space is a space of constant curvature. The radius of curvature of this space is the limiting mass μ_0. The theory must be formulated in accordance with the geometry of a p-space of constant curvature.

The existence of a geometric principle introduces a considerable degree of uniqueness into the formulation of the theory. At the same time a consistent development of this principle leads to far-reaching consequences, the most important of which is the conclusion that in this theory the law of conservation of energy and momentum appears in an altered form. Apparently other physical concepts, for example, coordinate space and the condition of microcausality, will also have to undergo a similarly serious alteration.

In the present paper Feynman's diagram technique is generalized in the spirit of the geometry of a p-space of constant curvature (Sec. 3). Preliminary investigations (Sec. 4) show that "ultraviolet" divergences are not very likely to arise within such a scheme.

Diagram technique is one of the fundamental tools of the modern theory of elementary particles. Therefore the possibility of generalizing this technique to the case of a p-space of constant curvature may be regarded as a hopeful result. However, to formulate a consistent theory of elementary particles it is necessary to subject to a similar generalization many other aspects which play an important role in modern theory.

1. MOMENTUM SPACE OF CONSTANT CURVATURE

The principal role in the theory under discussion is played by the p-space of constant curvature. The radius of curvature of this space μ_0 has the dimensions of a mass. The usual theory corresponds to the case $\mu_0 = \infty$. We shall consider the magnitude of μ_0 to be finite, and shall assume only that the masses of the elementary particles satisfy the condition $m \ll \mu_0$. The numerical value of the constant μ_0 must be determined from experiment. In the following we adopt a system of units in which $\mu_0 = c = \hbar = 1$, so that all the relationships take on dimensionless form.

The general method of constructing spaces of constant curvature, based on the introduction of a projective metric into the space, was developed by F. Klein.[1] In following this method we isolate in the four dimensional p-space the hypersurface

$$p^2 = 1 \tag{1.1}$$

and we define the non-Euclidean distance between the points p and q in the form

$$D(p, q) = \ln(J + \sqrt{J^2 - 1}),$$
$$J = (1 - pq) / \sqrt{(1 - p^2)(1 - q^2)}. \tag{1.2}$$

We henceforth adopt the following notation: p, q, . . . denote four-vectors in p-space, for example $p = (p_1, p_2, p_3, p_4)$. The scalar product

of the vectors p and q is given by $pq = p_4q_4 - p_1q_1 - p_2q_2 - p_3q_3$; $p^2 \equiv pp$.

If all the components of the vectors p and q are much less than unity, then up to terms of higher order

$$D(p, q) \approx \sqrt{(p-q)^2},$$

i.e., the metric is pseudo-Euclidean near the origin. The hypersurface (1.1) divides the whole p-space into two parts, interior ($p^2 < 1$) and exterior ($p^2 > 1$). According to (1.2) the "distance" D between points lying in the interior and exterior regions is complex. The momenta of real particles always lie in the interior region. However, there are no reasons for considering that the momenta of virtual particles cannot take on values lying in the exterior part.

From expression (1.2) we can easily obtain for our space the differential metric form which defines the square of the distance between two infinitely close points p and q = p + dp

$$ds^2 = (1-p^2)^{-1}\{dp^2 + (1-p^2)^{-1}(pdp)^2\},$$

from which we find in the usual manner the magnitude of the volume element

$$d\Omega = (1-p^2)^{-5/2}\,d^4p. \qquad (1.3)$$

To compute the volume of the whole space it is necessary to indicate the manner of going around the singularities situated on the hypersurface $p^2 = 1$. We define the volume of the space in the following manner

$$\Omega = \lim_{\delta\to 0}\int (1 - i\delta - p^2)^{-5/2}\,d^4p. \qquad (1.4)$$

The manner of evaluating the integral (1.4) is illustrated in Fig. 1. Cuts are introduced in the complex plane of p_4 from the branch points $p_4 = \pm\sqrt{1 + p^2 - i\delta}$. The path of integration 1 — 2 can be transformed without crossing the cuts into the path of integration 3 — 4 (the integrals along the arcs of the large circles tend to zero).

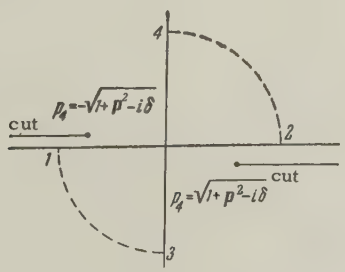

FIG. 1

As a result we obtain

$$\Omega = i\int (1 + p_1^2 + p_2^2 + p_3^2 + p_4^2)^{-5/2}\,d^4p = \tfrac{4}{3}\,i\pi^2.$$

The imaginary value of the volume Ω of the space does not lead to any difficulties. In view of the fact that the volume Ω is finite, the integrals over the momenta of the virtual particles of the self-energy type converge. In evaluating these integrals, the same procedure is utilized as for the evaluation of the volume Ω.

2. THE GROUP OF MOTIONS OF p-SPACE

The group of motions in p-space consists of all the point transformations that leave invariant the distance (1.2). According to the general theory due to Klein,[1] the motions in p-space are described by projective (i.e., linear or fractionally linear with respect to the components of the vector p) transformations which transform the hypersurface (1.1) into itself. Evidently the group of motions in p-space contains the group of Lorentz transformations which leave invariant the magnitude of p^2 and which transform the point p = 0 into itself.

In addition to the Lorentz transformations, the group of motions contains also the "displacement" transformations. Each displacement transforms the point p = 0 into some point k, with a one-to-one correspondence existing between the vectors k and the operations of displacement. This enables us to speak of "displacements by a vector k." Symbolically we shall represent the effect of displacements by equalities of the following type

$$q = p(+)k, \qquad (2.1)$$

by which we understand that the vector q was formed as the result of displacing the vector p by the vector k. The relation (2.1) establishes a certain law of addition of vectors in p-space. The most characteristic feature of this "addition" is that it does not commute

$$p(+)k \neq k(+)p.$$

The operation which is the inverse of the displacement by a vector k is a displacement by a vector −k. The result of such a displacement we shall denote by an equality of the type

$$q = p(-)k.$$

These definitions may be generalized in an obvious manner to a "sum" of several vectors. For example, the equality

$$q = p(+)k(-)l(+)n, \qquad (2.2)$$

denotes the consecutive application to the vector p

of displacements by k, by $-l$ and by n. Of course the order of the "addends" in (2.2) is important.

We note that the operations of displacement do not form a group; the product of two displacements will no longer be a displacement. One may show that displacements generate the whole group of motions in p-space.

Explicitly the "sum" of two vectors is defined by the expression

$$q = p(+)k = \frac{p\sqrt{1-k^2} + k(1+pk)/(1+\sqrt{1-k^2})}{1+pk}. \qquad (2.3)$$

If both vectors p and k are small ($p_\mu, k_\mu \ll 1$) then

$$p(+)k \approx p + k,$$

i.e., near the origin of coordinates the "addition" of vectors defined by formula (2.3) coincides, up to higher order terms, with ordinary addition. The following equality follows immediately from (2.3):

$$1/\sqrt{1-q^2} = (1+pk)/\sqrt{(1-p^2)(1-k^2)}, \qquad (2.4)$$

from which it can be seen that the transformation (2.3) describes the motion in p-space, since it follows from $p^2 = 1$ that $q^2 = 1$.

In going over to a p-space of constant curvature a new feature arises, associated with the transformation of spinors under displacements. While in the case of a pseudo-Euclidean space spinors do not transform under a displacement, in the case of a "curved" space it is neeessary to make a displacement by a vector k correspond to the following transformation of the bispinor ψ:

$$\psi \to d(k)\psi, \qquad d(k) = [(1-\hat{k})/(1+\hat{k})]^{1/4}, \qquad (2.5)$$

where

$$\hat{k} = k_\mu \gamma_\mu.$$

The relation (2.5) follows from the connection between the group of motions in p-space considered by us with the rotation group of a certain pseudo-Euclidean five-dimensional space.

3. PRINCIPLES OF THE DIAGRAM TECHNIQUE

To describe interactions between elementary particles, we make use of Feynman's diagram technique,[2] altered in the spirit of the geometry of p-space of constant curvature. We consider the interaction of a Fermi-field with a Bose-field. Let us trace the changes in the momentum of the fermion along a line (we shall consider both fermion and boson lines to be directed). In the usual theory, the law of conservation of energy-momentum holds at each vertex of the diagram. If the momentum of the fermion is p "before" the absorption of the boson, then "after" absorption it becomes equal to p + k, where k is the momentum of the absorbed boson. In going over to "curved" p-space, it is necessary to alter the rule for the addition of momenta at the vertices of the diagram: ordinary geometric addition of momenta is replaced by addition in the sense of Eq. (2.3). This rule is formulated more exactly in the following manner: if at the beginning of the line the fermion had a momentum p, then after the vertex of the diagram which corresponds to the absorption of a boson of momentum k, we must replace p by p(+)k, while after a vertex which corresponds to the emission of a boson with momentum k', we should replace it by p(−)k'. In moving along a fermion line in this manner we obtain a unique result for the final momentum p'. The sequence of operations required for this is determined by the sequence of vertices along the fermion line. Figure 2 shows several of the simplest diagrams which illustrate the rule of addition of momenta. As can be seen in the examples of the diagrams of Fig. 2, the relation between the values of the energy-momentum vectors of the particles before and after scattering is no longer universal, but depends on the nature of the scattering process.

Thus we conclude that the introduction into the theory of a p-space of constant curvature instead of the pseudo-Euclidean space requires the alteration of the usual form of the law of conservation of energy-momentum. In the new scheme the latter is only approximate, and is valid in the case when the energy and the momentum of the interacting particles are small. This follows directly from the fact that for small values of energy and momentum the new law of addition goes over into the ordinary

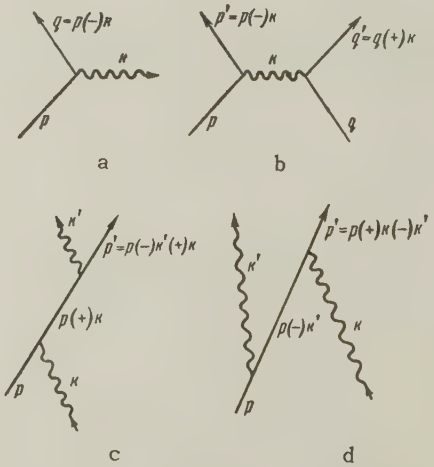

FIG. 2

law of geometric addition of vectors (Sec. 2).

After the nature of the change in the momenta along a fermion line has been established, all the Feynman rules for the calculation of matrix elements corresponding to a given diagram can be directly generalized. The propagation factor $D(k)$ corresponds to the boson line with momentum k, while the propagation factor $G(p)$ corresponds to the fermion line of momentum p. To the segment of an internal fermion line with momentum $p(+)k$ there corresponds the propagation factor

$$d^{-1}(k)\,G(p(+)k)d(k). \tag{3.1}$$

The appearance in the expression (3.1) of the matrix $d(k)$ is associated with the transformation of spinors (2.5) under displacements by vector k. For the sake of simplicity we set the vertex operator Γ equal to unity, i.e., we consider the case of scalar bosons with scalar coupling. Finally, it is necessary to integrate over the volume of the whole p-space over the momenta of all the virtual particles which are not defined uniquely by the law of addition. In carrying out this integration, it is necessary to take into account Feynman's rule for going around the poles and to rotate through quadrants the contour of integration over the momentum components as shown in Fig. 1.

4. SOME CONSEQUENCES OF NON-COMMUTATIVITY OF "ADDITION" OF MOMENTA

We shall illustrate by means of simplest examples results due to non-commutativity of "addition" of momenta. We first consider a first-order process (diagram a, Fig. 2). It can be easily shown that, just as in the usual theory, a free particle cannot emit a boson. This follows directly from relation (2.4), in which we must set $q^2 = p^2 = m^2$, $k^2 = \mu^2$. In going over to the fermion rest system, we obtain

$$1 + m\omega = \sqrt{1 - \mu^2}. \tag{4.1}$$

Obviously Eq. (4.1) cannot hold for positive values of the boson energy ω.

As a second example, we consider the scattering of a boson by a fermion. This process corresponds to two second-order diagrams (Fig. 2, b, c), which differ in the order of emission and absorption of the boson. Whereas in the usual theory both these diagrams contribute to the same scattering process, in our case, because of the non-commutativity of the "addition" of momenta, they lead to different final states starting from the same initial momenta p and k of the colliding particles. In other words, these diagrams describe two different scattering processes. For the sake of simplicity we write for the boson mass $\mu = 0$ and establish certain generalizations of the well-known Compton formula. By assuming that the fermion is at rest in the initial state, while the momenta of the quantum before and after scattering are respectively equal to $k = (\mathbf{k}, \omega)$ and $k' = (\mathbf{k}', \omega')$, we easily obtain, with the aid of relations (2.3) and (2.4), expressions for the energy of the scattered quantum ω' as a function of the energy of the incident quantum ω and of the scattering angle θ. For the case of the diagram of Fig. 2c we obtain:

$$\omega_1' = 2\omega_c/[1 + \sqrt{1 - 4\omega_c^2 \sin^2(\theta/2)}]. \tag{4.2}$$

For the case of the diagram of Fig. 2d we have:

$$\omega_2' = \omega_c/[1 + \omega\omega_c \sin^2(\theta/2)], \tag{4.3}$$

where ω_C is the energy of the scattered quantum which corresponds to the Compton formula

$$\omega_c = \omega/[1 + (\omega/m)(1 - \cos\theta)].$$

It is clear that for ω or $\omega_C \ll 1$

$$\omega_1' \approx \omega_2' \approx \omega_c.$$

However, when $\omega \gtrsim 1$ considerable deviations from the Compton formula do occur. We consider scattering through an angle $\theta = 90°$. When $\omega \gg m$ we have $\omega_C = m \ll 1$. At the same time

$$\omega_1' = m, \quad \omega_2' = m/(1 + m\omega/2).$$

The "line splitting" arising in this case

$$\Delta\omega/\omega_2' = (\omega_1' - \omega_2')/\omega_2' = m\omega/2$$

increases proportionally to the energy of the incident quantum.

5. SIMPLEST SELF-ENERGY DIAGRAMS

Let us consider the expressions for the self-energy of the fermion and the boson in second-order perturbation theory, corresponding to the diagrams of Fig. 3. According to the general rules of Sec. 4 we obtain for the self-energy of the fermion

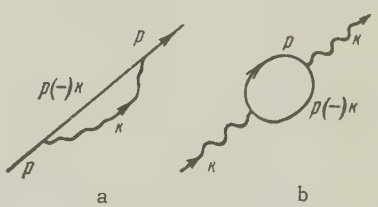

FIG. 3

$$\Sigma(p) = \frac{g^2}{(2\pi)^4 i}\int d(k)\, G(p(-)k)\, d^{-1}(k)\, D(k)\, d\Omega_k, \quad (5.1)$$

while for the self-energy of the boson we obtain

$$\Pi(k) = \frac{g^2}{(2\pi)^4 i}\int \mathrm{Sp}\{G(p)\, d(k)\, G(p(-)k)\, d^{-1}(k)\}\, d\Omega_p. \quad (5.2)$$

To estimate the integrals (5.1) and (5.2) it is necessary to know the explicit form of the propagation factors D(k) and G(p).

However, within the framework of the preliminary outline of the theory developed here, we cannot determine uniquely the forms of these factors. Therefore as an additional hypothesis we set

$$D(k) = (1-k^2)/(k^2-\mu^2),$$
$$G(p) = \sqrt{1-p^2}/(\hat{p}-m). \quad (5.3)$$

The choice of expressions (5.3) is based, on the one hand, on the correspondence principle for small values of the momenta and, on the other hand, on the special nature of the hypersurface (1.1) which plays a fundamental role in the whole theory. We particularly emphasize the utterly tentative nature of expressions (5.3), the form of which may undergo significant changes in a consistent theory.

Fairly simple calculations yield

$$d(k)\, G(p(-)k) d^{-1}(k)$$
$$= \frac{\sqrt{(1-k^2)(1-p^2)}\{(1-m)(1-kp)-(1-\hat{k})(1+\hat{p})\}}{(1+k^2)(1-p^2)-(1-m^2)(1-kp)^2}. \quad (5.4)$$

Substituting (5.3) and (5.4) into the expressions for the self-energy we obtain

$$\Sigma(p) = \frac{g^2\sqrt{1-p^2}}{(2\pi)^4 i}$$
$$\times\int \frac{(1-m)(1-kp)-(1-\hat{k})(1+\hat{p})}{[(1-k^2)(1-p^2)-(1-m^2)(1-kp)^2](k^2-\mu^2)(1-k^2)}\, d^4k, \quad (5.5)$$

$$\Pi(k) = \frac{g^2\sqrt{1-k^2}}{4\pi^4 i}$$
$$\times\int \frac{1-p^2-(1+m^2)(1-kp)}{[(1-k^2)(1-p^2)-(1-m^2)(1-kp)^2](p^2-m^2)(1-p^2)^{3/2}}\, dp^4. \quad (5.6)$$

To evaluate the integrals (5.5) and (5.6) we must utilize the procedure indicated at the end of Sec. 3. In this way, convergent results are obtained. There is no point in carrying out a more detailed analysis of the singularities of the foregoing expressions, since such an investigation depends on the forms of the functions D and G. The most important result is the absence of the ultraviolet catastrophe, and this result most probably will hold also in a consistent theory.

[1] F. Klein, Non-Euclidean Geometry (Russian transl.) Moscow-Leningrad, 1936.

[2] R. P. Feynman, Phys. Rev. **76**, 796 (1949).

Translated by G. Volkoff
90

LIGHT WAVES IN CRYSTALS IN THE EXCITON ABSORPTION REGION AND THE IMPURITY PHOTOEFFECT

I. M. DYKMAN and S. I. PEKAR

Institute of Physics, Academy of Sciences, Ukrainian S.S.R.

Submitted to JETP editor March 10, 1959

J. Exptl. Theoret. Phys. (U.S.S.R.) 37, 510-521 (August, 1959)

We have used a new theory of electromagnetic waves in a crystal[1,2] to evaluate, in the exciton light absorption region, the amplitudes of the waves occurring in a crystal for a given amplitude of the wave incident from the vacuum. We have considered the case of cubic crystals. We show that in the frequency region where the refractive index is much less than unity the amplitudes of the normal and the longitudinal waves in the crystal are appreciably larger (by factors of the order of several hundred) than the amplitude of the incident wave. The photoionization of impurities is therefore much more intensive in this frequency range than in the neighboring regions. This explains the frequently-observed sharp maximum of the external and internal photoeffects in the frequency range corresponding to exciton absorption. We show that there can occur in the crystal waves with an amplitude which increases linearly with the penetration depth into the crystal.

ONE of the authors has shown in previous papers[1-4] that if a monochromatic light wave, with a frequency which lies within the exciton absorption range, is incident upon a crystal from the vacuum, several light waves appear in the crystal, among which strictly longitudinal waves are also possible. In particular, four transverse waves and one longitudinal wave appear in cubic crystals.[2] The amplitudes of the two anomalous transverse waves tend rapidly to zero when the frequency of the light moves out of the exciton absorption range on the red or the violet side. The remaining two transverse waves then go over into the usual waves known in optics. As far as the longitudinal wave is concerned, its amplitude remains appreciable (of the order of the amplitude of the wave incident from the vacuum) in a much wider range of frequencies and important changes must be introduced into the usual electromagnetic optics for this range.

In the present paper, as in reference 2, we restrict our considerations only to cubic crystals and only to those cases where the coefficients of the expansion of the exciton energy in powers of the absolute magnitude of its wave vector do not depend on the direction of that vector (isotropy). In particular, the effective mass of the exciton will not depend on the direction of the wave vector. We emphasize that for excitons with a longitudinal and a transverse polarization (called henceforth longitudinal and transverse excitons) these expansion coefficients will be different. We shall restrict ourselves, as was done earlier,[2] to considering the case where the expansion of the exciton energy in powers of the absolute magnitude of the wave vector does not contain a linear term.

The aim of the present paper is to estimate the amplitudes of all five waves appearing in the crystal in relation to the amplitude of the incident wave. The equations obtained will be used to determine the intensity and the frequency dependence of the impurity photoeffect, which will be shown to possess a number of peculiarities in the exciton absorption region.

1. AMPLITUDES OF ELECTRICAL FIELD INTENSITY OF WAVES PRODUCED IN A CUBIC CRYSTAL ILLUMINATED BY MONOCHROMATIC LIGHT

The amplitudes of the transverse waves ($\mathbf{E}_+$, $\mathbf{E}_-$) and of the longitudinal wave ($\mathbf{E}_\parallel$) which appear in a crystal, and also the amplitude of the wave reflected into the vacuum $\mathbf{R}$ can be expressed in terms of the amplitude of the wave incident from the vacuum $\mathbf{A}$ through Eqs. (23) – (29) of reference 2. For the purpose of interest to us, we can simplify these equations in some limiting cases. Below we consider two such cases (we retain the notation of reference 2).

A. The case where the indices of refraction of the transverse waves, n_+ and n_-, have absolute magnitudes appreciably larger than unity. Let the

subscript s denote the component of the amplitude of the wave in the direction perpendicular to the plane of incidence, and subscript p the component in the plane of incidence. If $|n_\pm| \gg 1$, Eqs. (23), (24), and (25) of reference 2 can be rewritten in the following simplified manner:

s -components:

$$E_{\pm s} = u_\pm A_s, \qquad R_s = (u_+ + u_- - 1) A_s, \tag{1}$$

$$u_+ = 2\cos\varphi/(n_+ - qn_-), \qquad u_- = 2\cos\varphi/(n_- - n_+/q),$$

$$u_- = -qu_+, \tag{2}$$

$$q \equiv (n_-^2 - \mu)/(n_+^2 - \mu), \qquad \mu \equiv (2Mc^2/\hbar\omega_0^2)(\omega - \omega_0). \tag{3}$$

Here φ is the angle of incidence of the light on the crystal, M the effective mass of the transverse exciton, c the velocity of light in vacuo, $\omega_0 = \mathcal{E}_0/\hbar$ where $\mathcal{E}_0$ is the energy of a transverse exciton with a zero wave vector, and ω the light frequency.

We can write down similarly Eqs. (26) — (29) of reference 2 in simplified form.

p -components:

$$E_{\pm p} = v_\pm A_p, \qquad R_p = (v_+ n_+ + v_- n_- - 1) A_p, \tag{4}$$

$$v_+ = 2/(n_+ - qn_-), \qquad v_- = 2/(n_- - n_+/q),$$

$$v_- = -qv_+, \tag{5}$$

$$E_\parallel = -(2\sin\varphi/\vartheta) A_p. \tag{6}$$

We have assumed that the other absorption bands are sufficiently far away from the one considered (or have low intensities), and thus the refractive index of the normal transverse waves tends asymptotically to a constant value $\sqrt{\vartheta}$, when the light frequency moves away from the exciton absorption region under consideration. The refractive indices of the transverse waves are determined in that case by the formulae[1]

$$n_\pm^2 = (\mu + \vartheta)/2 \pm \sqrt{(\mu - \vartheta)^2/4 + b}, \tag{7}$$

$$b = 8\pi Mc^2 a/\hbar^2\omega_0^3, \tag{8}$$

where a is a constant proportional to the oscillator strength of the phototransition of the crystal in the exciton state; its exact meaning is explained in reference 1.

If the oscillator strength of the transition referred to an elementary cell of the crystal is of the order of 0.1, and if we assume that M is of the order of the free electron mass, b turns out to be of the order of several times ten thousand, as shown in reference 2. Correspondingly, $|n_\pm|$ turns out, from Eq. (7), to be of the order of 10 or larger. Such a large dispersion does, however, not yet mean an intensive absorption. The popular point of view, according to which a large dispersion is always combined with an intensive absorption, is in general incorrect, as shown in references 2 and 4.

The refractive index for the longitudinal waves is equal to[2]

$$n_\parallel^2 = (2M'c^2/\hbar\omega_0')(\omega - \omega_0'), \tag{9}$$

where M′ is the effective mass of a longitudinal exciton, $\omega_0' = \mathcal{E}_0'/\hbar$, and $\mathcal{E}_0'$ is the energy of a longitudinal exciton with zero wave vector. The connection between $\mathcal{E}_0'$ and $\mathcal{E}_0$ is given in Eq. (8) of reference 3 and Eq. (35) of reference 4. This connection can be written in the form

$$\mathcal{E}_0' - \mathcal{E}_0 = b\hbar^2\omega_0^2/2\vartheta Mc^2. \tag{10}$$

using the notation of the present paper. If μ is evaluated at the frequency $\omega = \omega_0'$ using Eq. (3), we get

$$\mu(\omega = \omega_0') = b/\vartheta. \tag{11}$$

From this it follows that ω_0' is just the frequency for which, according to Eq. (7), the refractive index of one of the transverse waves (the normal wave) is equal to zero. At the frequency ω_0' the macroscopic dielectric constant of the crystal is equal to zero.

We now proceed to estimate the relative magnitude of the amplitudes of the waves occurring in the crystal. In the case $M > 0$ the denominators in the expressions for $v_\pm$ and $u_\pm$ will, according to (7), not have a small absolute magnitude in the region $|n_\pm| \gg 1$. Hence, $|v_\pm| \ll 1$ and $|u_\pm| \ll 1$, i.e., the amplitudes of both transverse waves are appreciably less than the amplitude of the incident wave. As far as the longitudinal wave is concerned its amplitude is, according to (6), of the order of magnitude of the amplitude of the incident wave for not too small φ. The longitudinal wave is thus intense and dominates over the transverse waves. When $M < 0$, the longitudinal wave is determined in the region $|n_\pm| \gg 1$ by the same Eq. (6), and has the same amplitude as in the previous case. $u_\pm$ and $v_\pm$ are also small, except in the frequency region where $n_+ \approx n_-$, i.e., where the denominator of $u_\pm$ or $v_\pm$ tends to zero. $u_\pm$ and $v_\pm$ become then infinite. This anomaly deserves a special detailed consideration which shall be given in the following section.

In Figs. 1 — 4 are shown the frequency dependences of $|u_\pm|$, $|v_\pm|$, and $|E_\parallel/A_p|$ in the region $\omega \approx \omega_0$ evaluated by the exact formulae of reference 2. The following values of the parameters were used: $\hbar\omega_0 = 2$ ev, $\vartheta = 2$, $M' = M$, lattice constant equal to 10 Bohr radii of the hydrogen atom, and an oscillator strength of the transition equal to 0.1 (referred to the elementary cell of the crystal).

B. The case $\omega \approx \omega_0'$, when the refractive in-

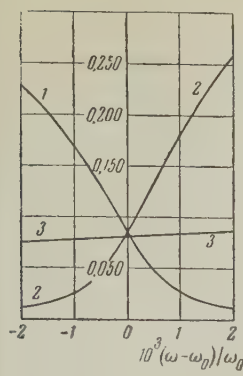

FIG. 1. Frequency dependence curves: 1) $|u_+| \approx |v_+|$; 2) $|u_-| \approx |v_-|$; 3) $|E_\parallel/A_p|$. M = m (m is the mass of a free electron), b = 58400, $\varphi = 5°$.

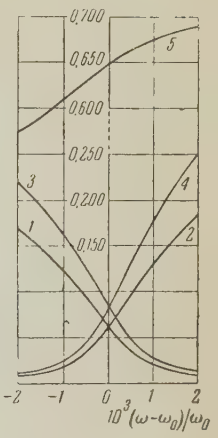

FIG. 2. Frequency dependence curves: 1) $|u_+|$; 2) $|u_-|$; 3) $|v_+|$; 4) $|v_-|$; 5) $|E_\parallel/A_p|$. M = m, b = 58400, $\varphi = 45°$.

dex of the normal transverse wave is much less than unity. In this frequency range we get $|q| \ll 1$, for $M > 0$ and $|q| \gg 1$ for $M < 0$. On the basis of these inequalities we can show that, according to Eqs. (23) – (29) of reference 2, the amplitude of one of the transverse waves (the anomalous wave) becomes negligibly small and all the properties of the second transverse wave (the normal one) approach the properties that follow from the usual electromagnetic crystal optics. The refractive index and the amplitude of the normal wave will henceforth be denoted by n and E, without the subscript ±. On the basis of the above-mentioned inequalities, Eqs. (23) – (29) of reference 2 can be simplified and written in the following form:

s -components:

$$E_s = uA_s, \qquad u = 2/[1 + \sqrt{n^2 - \sin^2\varphi}/\cos\varphi], \tag{12}$$

$$\sin\psi = n^{-1}\sin\varphi, \qquad \cos\psi = \sqrt{1 - n^{-2}\sin^2\varphi}. \tag{13}$$

Here ψ is the angle of refraction of the normal wave.

p -components:

$$E_p = vA_p, \quad v = 2\cos\varphi/[\sqrt{1 - n^{-2}\sin^2\varphi} + n\cos\varphi + \sin^2\varphi/n\sqrt{\alpha^2 n^2 - \sin^2\varphi}], \tag{14}$$

$$E_\parallel = E_p \sin\varphi/n\sqrt{1 - \sin^2\varphi/\alpha^2 n^2}. \tag{15}$$

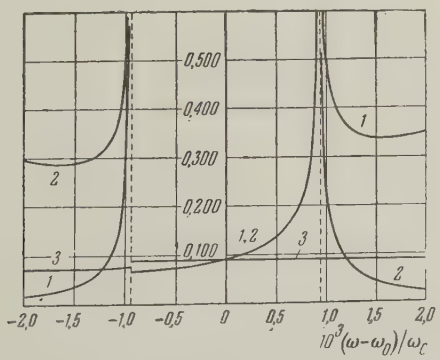

FIG. 3. Frequency dependence curves: 1) $|u_+| \approx |v_+|$; 2) $|u_-| \approx |v_-|$; 3) $|E_\parallel/A_p|$. M = –m, b = –58400, $\varphi = 5°$. The region of complex values of n^2 lies between the dotted straight lines.

Here

$$\alpha^2 \equiv n_\parallel^2/n^2 = (M'\omega_0^2/M\omega_0'^2)\, b/\varepsilon^2. \tag{16}$$

To obtain the right hand side of Eqs. (16), we expanded $n_\parallel^2$ and n^2 in a power series in $\omega - \omega_0'$ and limited ourselves to the first terms of the expansion, since we were considering the region $\omega \approx \omega_0'$.

In Eq. (14) we can always neglect $\sin^2\varphi$ compared to $\alpha^2 n^2$ in $\sqrt{\alpha^2 n^2 - \sin^2\varphi}$ since α is a very large quantity; we have, for instance $\alpha^2 \sim b/\varepsilon^2$ in the case when $M'\omega_0^2/M\omega_0'^2 \sim 1$. In the numerical example considered above, α^2 was of the order of several thousands. Thus, even when the real part of n^2 goes through zero, $|\alpha^2 n^2|$ will in practice always be larger than $\sin^2\varphi$, since the imaginary part of n^2 is then different from zero. The second of Eqs. (14) can therefore simplified to

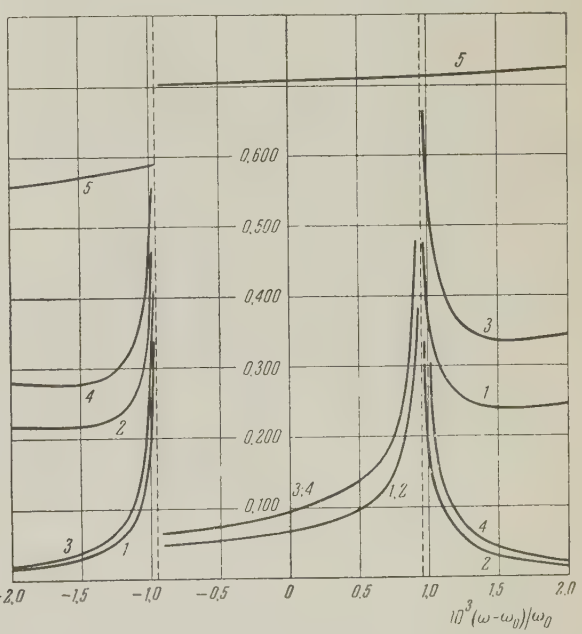

FIG. 4. Frequency dependence curves: 1) $|u_+|$; 2) $|u_-|$; 3) $|v_+|$; 4) $|v_-|$; 5) $|E_\parallel/A_p|$. M = –m, b = –58400, $\varphi = 45°$.

$$v = 2\cos\varphi / [\sqrt{1 - n^{-2}\sin^2\varphi} + n\cos\varphi + \sin^2\varphi / n^2\alpha]. \quad (17)$$

We now go over to an estimate of the relative magnitude of the amplitudes of the waves occurring in the crystal. According to Eq. (12), u attains its largest absolute magnitude, u = 2, at the frequency for which $n = \sin\varphi$. In that point E_S is twice the amplitude of the incident wave A_S (assuming that $\varphi \neq \frac{1}{2}\pi$). From (17) it follows, for the p-components, that if $n > \sin\varphi$ we can neglect the last term in the denominator of expression (17), after which it is clear that v is a monotonically decreasing function of n and thus also of ω. v attains its largest value at the frequency for which $n = \sin\varphi$. This value is

$$[v]_{n=\sin\varphi} = 2\cos\varphi / (\sin\varphi\cos\varphi + 1/\alpha). \quad (18)$$

We have retained here also the third term in the denominator of Eq. (17), since $\sin\varphi$ can be very small. The quantity (18) has a very sharp maximum as a function of φ at the point $\varphi = 0$: when $\varphi = 0$, $[v]_{n=\sin\varphi} = 2\alpha$, i.e., it can take on a value of the order of 10^2. This means that the amplitude of the normal transverse wave in a crystal can be larger than the amplitude of the incident wave by a factor of the order of a hundred. When φ is of the order of 5 or 6 degrees, the magnitude of $[v]_{n=\sin\varphi}$ falls to 20 and varies further as $2/\sin\varphi$ with increasing φ (one must bear in mind that following a change in φ one must change here the frequency, to keep the condition $n = \sin\varphi$ satisfied).

In the region $\omega < \omega_0'$, when $n^2 < 0$, $|v|$ goes through a maximum at a frequency determined by the condition $\tan\varphi = -n^2$. The maximum value of $|v|$ is then equal to $2\cos\varphi/\sqrt{1+2\sin\varphi\cos\varphi}$, i.e., it does not exceed two. The amplitude of the transverse wave in the crystal can thus not exceed appreciably the amplitude of the incident wave in this frequency range.

Figure 5 shows the frequency dependences of the absolute magnitudes of the coefficients u (curve 1) and v (curve 2) for angles of incidence $\varphi = 5°$ and $\varphi = 45°$, evaluated by the exact formulae of reference 2 [the values of the parameters are the same as for Figs. 1 — 4 (see case A)].

The amplitude of the longitudinal wave in the frequency range $\omega \approx \omega_0'$ can be estimated using Eq. (15), which can be written in simplified form:

$$E_\parallel = n^{-1}E_p\sin\varphi. \quad (19)$$

From this it is clear that if $|n| \sim \sin\varphi$ the amplitude of the longitudinal wave is of the same order of magnitude as the amplitude of the transverse wave considered above, i.e., it can exceed by a factor of the order of a hundred the amplitude of the incident wave. But if $|n| < \sin\varphi$, the amplitude of the longitudinal wave is larger than the normal transverse wave. Figure 5 (curve 3) shows the frequency dependence of $|E_\parallel/A_p|$. As is clear from the figure the peaks of the curves for $|E_\parallel/A_p|$ and $|v|$ coincide approximately both in height and in their position along the frequency scale.

We must emphasize that the estimates given are made assuming that the absorption is so small that we can neglect the imaginary part of n^2. In selected frequency intervals, however, it turns out that even a small imaginary part of n^2 plays an essential role. The condition $n = \sin\varphi$, for instance, used above, cannot even approximately be satisfied in the case $\varphi \to 0$ if n possesses an imaginary part. (The fact is that the imaginary part of n^2 does, generally speaking, not vanish at the fre-

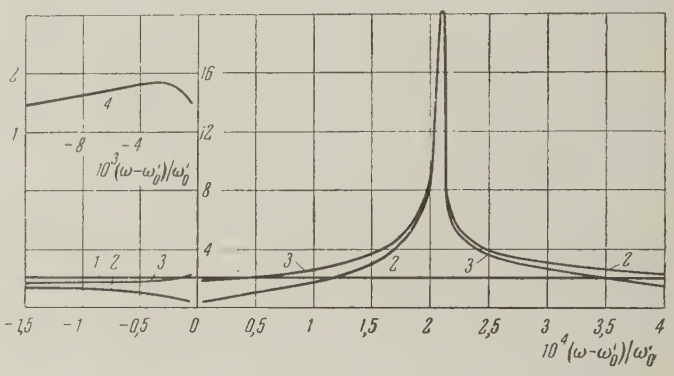

a

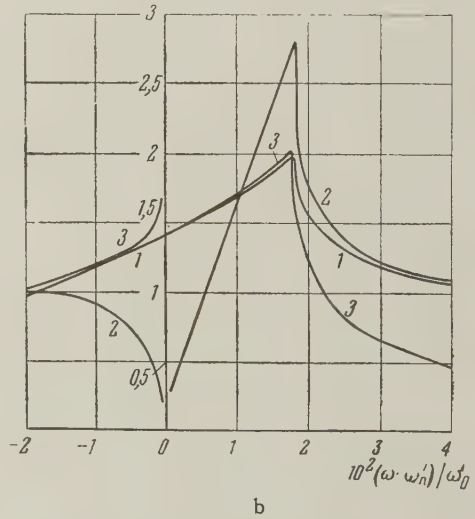

b

FIG. 5. Frequency dependence of |u| (curve 1), |v| (curve 2), and $|E_\parallel/A_p|$ (curve 3) in the region $\omega \approx \omega_0'$: a for $\varphi = 5°$, and b for $\varphi = 45°$. In the point $\omega = \omega_0'$ the quantities |v| and $|E_\parallel/A_p|$ tend to infinity; it is difficult to depict the corresponding delta-function curves in the figures and they are therefore not given. Curve 4 in Fig. 5a is the function |v| in the neighborhood of the additional maximum at $n^2 = -\tan\varphi$ (different scale).

quency at which the real part of n^2 vanishes.) This causes in fact a deformation of the curves of Fig. 5: the peaks are lowered and their position along the frequency scale is determined approximately by the condition that $|1-n^{-2}\sin^2\varphi|$ be a minimum. Moreover, in the region $\omega = \omega_0'$ the condition $n = 0$ will be violated if account is taken of the fact that the imaginary part of n is different from zero. In that point $|v|$ does therefore not attain, strictly speaking, an infinite value. One can take these changes explicitly into account only if the frequency dependence of the absorption coefficients of the normal and the longitudinal waves are known.

In case A, when the amplitudes of the four transverse waves have the same order of magnitude, the results obtained above differ appreciably from the results of the usual crystal optics. In case B, however, it turns out that the normal transverse wave possesses almost the same properties as follow from the usual crystal optics, since the amplitude of the anomalous transverse wave is very small. Equation (12) is thus, for instance, exactly the same as the corresponding usual Fresnel equation, and Eq. (17) goes over into the usual Fresnel equation if we neglect the last term in the denominator. The amplitude of the transverse wave in the crystal has thus, as in the usual crystal optics, a sharp maximum as function of the frequency at the frequency for which the condition $n = \sin\varphi$ is satisfied. One can easily understand this by considering that under the condition mentioned the angle of refraction is equal to 90°, i.e., the refracted light goes along the crystal surface. The ratio of the cross section of the light beam in the crystal to the cross section of the corresponding light beam in vacuo is then equal to zero. Hence, even though E_p is large, the energy flux in the crystal, integrated over the cross section, may anyhow be small. All the same, however, such a wave propagating under the crystal surface itself, and possessing a large amplitude, can cause an intensive external photoeffect and also a surface internal photoeffect.

As to longitudinal waves in crystals, they do not arise, generally speaking, in the usual crystal optics, and are the consequence of the new boundary conditions formulated in references 1 and 2. We must emphasize that these boundary conditions do not go over into the boundary conditions of the usual crystal optics, not even in the limiting case of very long waves, when one may neglect the effects of the spatial dispersion in the volume equations. Under the condition $n = \sin\varphi$ the amplitude of the longitudinal wave has also a steep maximum as a function of the frequency and can exceed the amplitude of the incident wave by a factor of the order of a hundred. But the angle of refraction $\psi_\parallel$ is smaller by the same factor:

$$\sin\psi_\parallel = \sin\varphi / n_\parallel = \sin\varphi / \alpha n = 1/\alpha.$$

The cross section of the light beam in the crystal is therefore not small; there is no energy flux into the crystal because there is no magnetic field in the longitudinal wave.[1,4] This wave is, however, able to cause an intensive internal or external photoeffect.

A non-zero energy flux into the crystal, due to the expenditure of energy on photoionization can be obtained in the next approximation, by introducing a weak absorption of the waves in the crystal.

2. THE CASE OF TWO WAVES OF THE SAME POLARIZATION WITH THE SAME REFRACTIVE INDEX

In the following we consider the case where the dispersion follows the curve of Fig. 6, i.e., where ω has an extremum as a function of n^2. Equations (20) — (22) which follow refer not only to crystals, but also to any dielectric medium with a dispersion of the kind shown in Fig. 6 (for instance, to a plasma in a magnetic field). Such a dispersion occurs, for instance, when the refractive index is expressed by Eq. (7) with negative b. In particular, if we are dealing with excitons, this case corresponds to $M < 0$. At the point B (Fig. 6) we have $n_+^2 = n_-^2$. The two solutions, which have the form of plane waves with refractive indices n_+ and n_- and which are usually linearly independent, are thus identical at the point B and are, therefore, only one solution. The second linearly independent solution is obtained in that case, as is well known, by differentiating the first solution with respect to the parameter n. If we write the first solution in the form $\exp\{i(\omega/c)n(\mathbf{s},\mathbf{r})\}$ and take it into account that at the boundary between the medium under consideration and the

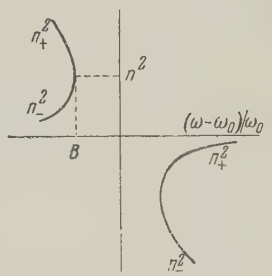

FIG. 6

vacuum (the plane $z = 0$) the relations

$$ns_x = s_{0x}, \qquad ns_y = s_{0y} \tag{20}$$

must be satisfied by virtue of the usual boundary conditions ($\mathbf{s}_0$ is a unit vector in the direction of the propagation of the incident wave in the vacuum, which is independent of n), the second linearly-independent solution is of the form

$$z \exp\left\{i \frac{\omega}{c} n(\mathbf{s}, \mathbf{r})\right\}. \tag{21}$$

The solution (21) is thus a wave whose amplitude increases linearly with the distance z from the surface of the medium.

Both solutions are waves with a zero group velocity. This follows from the fact that $k = \omega n/c$ and the reciprocal of the group velocity is

$$\frac{1}{g} = \frac{dk}{d\omega} = \frac{n}{c} + \frac{\omega}{c}\frac{dn}{d\omega} = \infty, \tag{22}$$

since the derivative $dn/d\omega = \infty$ in the point B, because ω, as a function of n^2, possesses an extremum at that point. The energy flux into the medium is therefore equal to zero.

The amplitudes of both waves mentioned above can be related to the amplitude of the wave incident from the vacuum if the appropriate boundary conditions are known. Turning from the general case to the case of light waves in a crystal near the exciton absorption band, we can again use Eqs. (23) to (29) of reference 2. From these equations we get $u_+ \to -u_- \to \infty$ and $v_+ \to -v_- \to \infty$ if $n_+ \to n_-$. If, however, we write down the total field of the +wave and the −wave, we get an indeterminate expression of the kind $\infty - \infty$. Writing it out explicitly under the assumption that $n_+ \to n_-$, and taking it into account that the quantities

$$n_+ s_{+x} = n_- s_{-x} = s_{0x}, \qquad n_+ s_{+y} = n_- s_{-y} = s_{0y} \tag{23}$$

are independent of $n_\pm$, we get the following results:

For the s-components:

$$E_s(\mathbf{r}, t) = 2\cos\varphi \frac{2n\cos\psi + (i\omega/c)(n^2 - \mu)z}{2n\cos\psi(\cos\varphi + n\cos\psi) + n^2 - \mu} \times A_s \exp\left\{i\omega\left[\frac{n}{c}(\mathbf{s}, \mathbf{r}) - t\right]\right\},$$
$$\sin\psi = \sin\varphi / n; \tag{24}$$

where n is the value of the refractive index for the frequency for which n_+ and n_- are the same.

For the p-components:

$$E_{px}(\mathbf{r}, t) = 2A_p \frac{Q_x}{R} \exp\left\{i\frac{\omega}{c} n(\mathbf{s}, \mathbf{r})\right\},$$
$$E_{pz}(\mathbf{r}, t) = 2A_p \frac{Q_z}{R} \exp\left\{i\frac{\omega}{c} n(\mathbf{s}, \mathbf{r})\right\}, \tag{25}$$

where

$$Q_x = \cos\psi\left[2n + \frac{n^2 - \mu}{n}\tan^2\psi - \frac{n^2 - \mu}{n}\tan\psi\tan(\psi - \psi_\parallel) + \frac{i\omega z}{c\cos\psi}(n^2 - \mu)\right],$$
$$Q_z = -\sin\psi\left[2n - \frac{n^2 - \mu}{n} - \frac{n^2 - \mu}{n}\tan\psi\tan(\psi - \psi_\parallel) + \frac{i\omega z}{c\cos\psi}(n^2 - \mu)\right],$$
$$R = 2n\frac{\cos\psi}{\cos\varphi} + 3n^2 - \mu + \frac{b\sin\psi_\parallel\tan\psi}{3n\cos\varphi\cos(\psi - \psi_\parallel)} + \frac{n^2 - \mu}{n}\frac{\sin\psi\tan\psi}{\cos\varphi} - \frac{n^2 - \mu}{n}\left(\frac{\cos\psi}{\cos\varphi} + n\right)\tan\psi\tan(\psi - \psi_\parallel),$$
$$\sin\psi_\parallel \equiv \frac{\sin\varphi}{n_\parallel}. \tag{26}$$

The solution (25), (26) is the linear combination of the usual wave, of the type $\exp\{i(\omega/c)n(\mathbf{s}, \mathbf{r})\}$, with a wave (21) satisfying the boundary conditions formulated in references 1 and 2.

We must emphasize that the solution (25), (26) is a wave which is not transverse. All the same, we can verify that for this solution, too, div $\mathbf{E} = 0$, as should be the case in cubic crystals. Equations (24) – (26) can be simplified if $n^2 \gg 1$. We then get $\cos\psi \approx 1$, $\mu \approx 2n^2$ and Eq. (24) takes on the following form:

s-components:

$$E_s(\mathbf{r}, t) = 2\cos\varphi \frac{2 - (i\omega/c)nz}{2\cos\varphi + n} \times A_s \exp\left\{i\omega\left[\frac{n}{c}(\mathbf{s}, \mathbf{r}) - t\right]\right\}. \tag{27}$$

Equations (25) reduce approximately to the following ones:

p-components:

$$E_{px}(\mathbf{r}, t) = 2\cos\varphi \frac{2 - (i\omega n/c)z}{2 + n\cos\varphi} A_p \exp\left\{i\omega\left[\frac{n}{c}(\mathbf{s}, \mathbf{r}) - t\right]\right\},$$
$$E_{pz}(\mathbf{r}, t) \approx 0. \tag{28}$$

These formulae show that (if $\cos\varphi$ is approximately of order unity) the amplitude of the wave in the crystal exceeds the amplitude of the incident wave by a factor $(4\pi/\lambda)z$, where λ is the wavelength of the light in the vacuum.

3. FREQUENCY DEPENDENCE OF THE IMPURITY PHOTOEFFECT IN THE EXCITON ABSORPTION REGION

It has been established in several experimental papers that both for the internal and for the external impurity photoeffect the frequency dependence of the photocurrent has a maximum in the frequency range corresponding to the exciton absorption of light in the crystal. In this way, for instance, Zhuze and Ryvkin[5] were the first to discover in

cuprous oxide a maximum in the frequency dependence of the photoconductivity at the same frequencies at which Gross and collaborators[6] detected exciton absorption in cuprous oxide. The frequency dependence of the external impurity photoeffect also often shows a maximum at the frequencies corresponding to the exciton absorption of light. This was shown experimentally by Apker and Taft[7] for KI and RbI films in which F-centers played the role of impurities, and by Borzyak[8] for a cesium-antimony photocathode. Later similar maxima were detected by Taft and Philipp[9] in the spectral distribution of the external photoeffect in a number of other alkali halide films and in single crystals of KI, and also by Philipp[10] in BaO. In all these cases the intensity of the photoeffect was proportional to the impurity concentration, indicating the impurity character of the photoeffect. In the experiments of Apker and Taft the proportionality of the photocurrent to the intensity of the incident light was also noted.

One usually explains the connection between the photoeffect and the exciton absorption of the light (position of the photoeffect maximum in the exciton absorption region) as follows. It is assumed that the direct influence of the light on the electrons of the impurity centers is not very great, because of the small impurity concentration. In the exciton absorption region, however, the light creates in the crystal, a large number of excitons, which diffuse and collide with and ionize the impurity centers. The energy of light spent on the ionization of the impurity centers is thus not determined by the impurity absorption, which is small, but by the intrinsic absorption.

The exciton photoeffect mechanism described here is perfectly feasible and is, perhaps, in some cases the dominant one. There is, however, another possible explanation of the photoeffect, to which we wish to call attention. This explanation assumes normal photoionization of the impurity centers directly by the electrical field of the light wave. It is well known that the probability of such an ionization, per unit intensity of the light incident from the vacuum, is equal to

$$w = C(\omega)|\mathbf{E}|^2/|\mathbf{A}|^2, \qquad (29)$$

where $\mathbf{E}$ is the amplitude of the electrical field of the light wave in the crystal, and $C(\omega)$ a coefficient of proportionality independent of the field of the light wave and determined by the properties of the impurity center and the crystal. $C(\omega)$ is a smooth function of the light frequency ω. As far as $|\mathbf{E}|/|\mathbf{A}|$ is concerned, however, this ratio has a sharp maximum as a function of ω in the exciton absorption region, as was shown in the preceding sections. In the frequency region $\omega \approx \omega_0'$, for instance, we thus have from Eqs. (17) — (19) that $|v|$ and $|E_{||}/A|$ can attain values of the order of one hundred (for small angles of incidence φ). The dependence of $|v|$ and $|E_{||}/A|$ on the frequency is shown in Fig. 5. For $\omega \approx \omega_0'$, the probability for photoionization can thus, according to (29), be larger by a factor 10^4 than in the neighboring frequency regions. A similar peak in the frequency dependence can also occur for the photoconductivity and the external photocurrent, since they are proportional to w while the coefficient of proportionality is like $C(\omega)$, a smooth function of ω.

We must emphasize that such a high photoeffect peak is obtained in the exciton absorption region precisely because $n^2 \approx 0$ in the region $\omega \approx \omega_0'$. This however, is not always realized, but only when the following conditions are fulfilled: a) The oscillator strength for the phototransition in the exciton state must not be very small, so as to make the constant b in Eq. (7) large. This insures the vanishing of n_+^2 or n_-^2 in the frequency range $\omega = \omega_0'$, which lies outside the region of strong absorption of light. b) The violet side of the band under consideration must have no intensive absorption bands, the presence of which can lead to such deviations from Eq. (7), that neither n_+^2 nor n_-^2 vanish. c) In the region $\omega \approx \omega_0'$ the light in the crystal must be absorbed only very weakly (at the same time, the absorption background must also be weak), so that n^2 is almost real. Otherwise the condition $n = \sin\varphi$, which is necessary in order that the quantity (17) take on the particularly large value (18), will not be satisfied even approximately. If these three conditions are not realized, the photoeffect peak will be appreciably lower.

We note that our explanation of the photoeffect peak in the region of the exciton absorption is essentially different from the explanation based upon the mechanism of a photocreation of excitons, their diffusion and the subsequent transfer of their energy to the electrons of the impurity centers. The present explanation requires neither the absorption of light in general nor the formation of real excitons. If the latter do appear, it is only as an accompanying phenomenon, which is not used for the explanation. The whole effect is caused only by a large dispersion (connected with the formation of virtual excitons) which causes n^2 to take on the value zero. It turns out in this case that even the boundary conditions at the surface of the crystal lead to such relations between the ampli-

tudes of the incident wave and the waves occurring in the crystal, as to cause $|E_p/A|$ and $|E_{||}/A|$ to have a steep maximum as functions of the frequency ω.

The value $n^2 = 0$ as a result of a large dispersion can be realized not only near the exciton absorption band, but also near other bands, for instance, the impurity absorption band. In that case $|E_p/A|$ will also have a sharp maximum as a function of the frequency which leads to a corresponding peak in the photoeffect. The longitudinal wave, however, will not occur then, since its appearance is caused by the special boundary conditions[1,2] ($P = 0$ at the crystal surface) which occur near the exciton absorption band, but not near the impurity absorption band.

The probability for the photoionization of an impurity center is determined by the total electrical field at the point where the center is situated. We must thus take $\mathbf{E}$ in Eq. (29) to mean the amplitude of the vector sum of the electrical fields of all waves occurring in the crystal.

When $n = \sin\varphi$ the angle of refraction of the transverse wave $\psi = 90°$. This wave does therefore not penetrate into the crystal but is propagated along its surface, causing an external photoeffect and an internal surface photoeffect. Photoionization inside the crystal, however, can be caused only by the longitudinal wave, the amplitude of which has a peak of the same height as the transverse wave and the angle of refraction of which, $\psi_{||}$, is determined by the condition $\sin\psi_{||} = \sin\varphi/\alpha n$. In the case $n_+^2 = n_-^2$ (this is possible only for a negative effective exciton mass and only for a well defined value of the frequency ω) a wave occurs with an amplitude which increases from the surface into the crystal according to Eqs. (24) — (26). If we assume that absorption is weak and that the complex refractive index is of the form $n = n' + i\kappa$, $\kappa \ll n'$, where n' and κ are real, the wave of Eq. (21) will have an amplitude that depends on z, its depth of penetration into the crystal, according to the law

$$z\exp\left\{-\frac{\omega\kappa}{c}\frac{z}{\cos\psi}\right\}. \qquad (30)$$

This amplitude has a maximum at $z = c\cos\psi/\omega\kappa$. The probability for ionization of an impurity will thus change with z as the square of the amplitude (30). Therefore, when a thin plane-parallel crystal plate is illuminated, the intensity of the external photoeffect will turn out to be less at the illuminated side of the plate than at the back side.

An experimental verification of the theory given here would be a quantitative agreement between the formulae obtained and experiment. In particular, the theory predicts the appearance of a peak in the photoeffect only then when the refractive index becomes much less than unity. Moreover, Eqs. (17) and (18) predict a definite dependence of the peak height on φ. The peak height must also depend essentially on the polarization of the incident light, since for p-components the ratio $|E_p/A_p|$ can be very large (of the order of a hundred), and a longitudinal wave with the same peak in amplitude occurs as well, while for the s-component $|E_s/A_s|$ does not exceed two and no longitudinal wave appears. For the s-component the peak in the photocurrent can thus not be large in the exciton absorption region.

In conclusion we note that the present idea of the explanation of the photoeffect peak in the region of exciton absorption of light was first proposed by one of the authors at the First All-Union Conference on Photoelectrical and Optical Phenomena in Semiconductors (Kiev, 1957).[11]

The authors express their gratitude to I. G. Zaslavskaya for performing the numerical calculations.

[1] S. I. Pekar, J. Exptl. Theoret. Phys. (U.S.S.R.) **33**, 1022 (1957), Soviet Phys. JETP **6**, 785 (1958).

[2] S. I. Pekar, J. Exptl. Theoret. Phys. (U.S.S.R.) **34**, 1176 (1958), Soviet Phys. JETP **7**, 813 (1958).

[3] S. I. Pekar, J. Exptl. Theoret. Phys. (U.S.S.R.) **35**, 522 (1958), Soviet Phys. JETP **8**, 360 (1959).

[4] S. I. Pekar, J. Exptl. Theoret. Phys. (U.S.S.R.) **36**, 451 (1959), Soviet Phys. JETP **9**, 314 (1959).

[5] V. P. Zhuze and S. M. Ryvkin, Izv. Akad. Nauk SSSR, Ser. Fiz. **11**, 93 (1952).

[6] E. F. Gross and N. A. Karryev, Dokl. Akad. Nauk SSSR **84**, 261 471 (1952); E. F. Gross and B. P. Zakharchenya, Dokl. Akad. Nauk SSSR **90**, 745 (1953).

[7] L. Apker and E. Taft, Phys. Rev. **79**, 964 (1950); **81**, 698 (1951); **82**, 814 (1951); E. Taft and L. Apker, J. Chem. Phys. **20**, 1648 (1952).

[8] P. G. Borzyak, Тр. Ин-та физики АН УССР (Proc. Inst. Phys. Acad. Sci. Ukr. S.S.R.) **4**, 28 (1952).

[9] H. R. Philipp and E. A. Taft, J. Phys. Chem. Solids **1**, 159 (1956); Phys. Rev. **106**, 671 (1957); E. A. Taft and H. R. Philipp, J. Phys. Chem. Solids **3**, 1 (1957).

[10] H. R. Philipp, Phys. Rev. **107**, 687 (1957).

[11] S. I. Pekar, Тр. 1-го Всесоюзн. совещания по фотоэлектрич. оптич. явлениям в полупроводн. (Proc. First All-Union Conference on Photoelectrical and Optical Phenomena in Semiconductors) Acad. Sci. Ukr. S.S.R, 1959; see also the survey by Rashba, Snitko, and Tolpygo, J. Tech. Phys. (U.S.S.R.) **28**, 2696 (1958) (p. 2699, Sec. II), Soviet Phys.—Tech. Phys. **3**, 2464 (1959).

Translated by D. ter Haar
91

POLARIZATION EFFECTS IN THE ELASTIC SCATTERING OF ELECTRONS FROM DEUTERONS

G. V. FROLOV

Radium Institute, Academy of Sciences, U.S.S.R.

Submitted to JETP editor March 11, 1959

J. Exptl. Theoret. Phys. (U.S.S.R.) 37, 522-526 (August, 1959)

The differential scattering cross section and the change of electron polarization are calculated for the elastic scattering of polarized electrons on polarized deuterons.

INTRODUCTION

IF we look at the electron-nucleon interaction, to first order in the electromagnetic field but taking into account all mesonic-radiation corrections, the nucleon structure is given by two material form factors $a(q^2)$ and $b(q^2)$ (see for example the work of Akhiezer, Rozentsveĭg, and Shmushkevich[1]). Here $q^2 = (p_1 - p_2)^2$, where p_1 and p_2 are the four-momenta of the electron before and after scattering, $a(q^2)$ characterizes the charge distribution, and $b(q^2)$ the distribution of the anomalous nuclear magnetic moment.

In the static limit $(q^2 \to 0)$ we have $a_p = 1$ and $b_p = \mu_p$ for the proton, and $a_n = 0$ and $b_n = \mu_n$ for the neutron, where μ_p and μ_n are the anomalous magnetic moments of the proton and the neutron.

Experiments on the elastic scattering of electrons on deuterons[2,3] permit the possible determination of the neutron form factor. Both the nucleon form factors and the form factor of the deuteron as a whole enter into the formula for the electron-deuteron differential cross section.[4] Therefore, experiments with polarized particles, some of which are considered in the present work, are useful in determining these quantities.

DIFFERENTIAL ELASTIC SCATTERING CROSS SECTION

The matrix element for the electron-nucleon interaction has the following form:[1]

$$V_{if} = (\bar{U}_2 \Gamma_\mu U_1) g_\mu,$$
$$\Gamma_\mu = a(q^2)\gamma_\mu + \frac{ib(q^2)}{2M}\gamma_\mu \hat{q}, \qquad g_\mu = \frac{e^2}{q^2}(\bar{u}_2 \gamma_\mu u_1). \quad (1)$$

Capital letters indicate quantities related to the nucleon, while lower-case letters refer to the electron; M is the nucleon mass. In the nonrelativistic approximation, which will be applied later to the deuteron, we have

$$V_{if} = v_2^* [R_1 g_4 + \mathbf{R}\mathbf{g}] v_1, \qquad R_4 = a,$$
$$\mathbf{R} = -(i/2M)\{a(\mathbf{P}_1 + \mathbf{P}_2) - i(a+b)[\mathbf{q}\times\boldsymbol{\sigma}]\}; \quad (2)$$

v is a two-component spinor, and $\mathbf{P}_1$ and $\mathbf{P}_2$ are the initial and final nucleon momenta.

As applied to the bound nucleon, we can write instead of (2)

$$V_{if} = \int \psi_f^* V \psi_i d\tau, \quad (3)$$

$$V = g_4 a e^{i\mathbf{q}\mathbf{r}} - (\mathbf{g}/2M)\{a[\nabla e^{i\mathbf{q}\mathbf{r}} + e^{i\mathbf{q}\mathbf{r}}\nabla]$$
$$- i(a+b)([\nabla\times\boldsymbol{\sigma}]e^{i\mathbf{q}\mathbf{r}} - e^{i\mathbf{q}\mathbf{r}}[\nabla\times\boldsymbol{\sigma}])\}. \quad (4)$$

Corresponding to this, the matrix element for electron-deuteron scattering is written

$$V_{if} = \int \Psi_f^* [V_p + V_n] \Psi_i d\tau_p d\tau_n. \quad (5)$$

Here Ψ_i and Ψ_f are the deuteron wave functions before and after the collision, and V_p and V_n are determined by Eq. (4), where the form factors a and b correspond respectively to the proton and neutron. Writing the matrix element in the form (5) actually corresponds to using the impulse approximation for the deuteron. For elastic electron-deuteron scattering we get with the help of (5)

$$V_{if} = \langle \chi_f | S | \chi_i \rangle. \quad (6)$$

Here χ_i and χ_f are deuteron spin functions,

$$S = A + \mathbf{B}(\boldsymbol{\sigma}_1 + \boldsymbol{\sigma}_2)/2,$$
$$A = I_1\left(g_4 - \frac{i}{2M}\mathbf{g}\mathbf{q}\right) - \frac{1}{2M}\mathbf{I}_2\mathbf{g}, \qquad \mathbf{B} = I_3[\mathbf{q}\times\mathbf{g}];$$
$$I_1 = \int (a_p e^{i\mathbf{q}\mathbf{r}/2} + a_n e^{-i\mathbf{q}\mathbf{r}/2}) |\varphi_d|^2 d\mathbf{r},$$
$$\mathbf{I}_2 = 2\int \varphi_d^* (a_p e^{i\mathbf{q}\mathbf{r}/2} - a_n e^{-i\mathbf{q}\mathbf{r}/2}) \nabla\varphi_d d\mathbf{r},$$
$$I_3 = \frac{1}{2M}\int [(a_p + b_p) e^{i\mathbf{q}\mathbf{r}/2} + (a_n + b_n) e^{-i\mathbf{q}\mathbf{r}/2}] |\varphi_d|^2 d\mathbf{r} \quad (7)$$

$\mathbf{r}$ is the relative coordinate of the nucleons, σ_1 and σ_2 are proton and neutron spin operators, and φ_d is the deuteron coordinate wave function. The D-wave admixture in the deuteron ground state is neglected.

We look at the general case for the scattering of polarized electrons on polarized deuterons. The initial state is described by the density matrix ρ_0, represented as the direct product of the electron and neutron density matrices

$$\rho_0 = \rho_e \times \rho_d,$$

$$\rho_e = {}^1/_2 (1 + i\gamma_5 \hat{\zeta}_1)\, \eta^{(+)}(p_1),$$

$$\rho_d = \tfrac{1}{4}\left[1 + \tfrac{1}{3}\sigma_1\sigma_2 + \alpha(\sigma_1 + \sigma_2) + \beta_{im}(\sigma_{1i}\sigma_{2m} + \sigma_{2i}\sigma_{1m})\right].$$

Here

$$\eta^{(+)}(p) = \frac{i\hat{p} - m}{2\varepsilon}\gamma_4$$

is the positive energy state projection operator. The four-component vector $\zeta_\mu = (\boldsymbol{\zeta}, \zeta_4)$ describes the electron polarization. In the rest system $\zeta_\mu = (\boldsymbol{\zeta}^0, 0)$, and in an arbitrary system

$$\zeta = \zeta_t^0 + (\varepsilon/m)\zeta_l^0, \qquad \zeta_4 = i(\mathbf{p}\boldsymbol{\zeta}^0)/m,$$

where ζ_t^0 and ζ_l^0 are the transverse and longitudinal components of the vector $\boldsymbol{\zeta}^0$, $\mathbf{p}$ is the momentum; ϵ the energy, m the electron mass; α and β_{im} describe the deuteron polarization, where $\mathrm{Sp}\,\beta_{im} = \beta_{ii} = 0$. The term "polarization" in the present case includes that process usually called "alignment."

The following expression is obtained for the differential cross section*

$$\frac{d\sigma}{d\Omega} = \frac{1}{4}\left(\frac{e^2}{4\pi}\right)^2 \frac{\mathrm{Sp}\{\eta^{(+)}(p_2)\, S\rho_0 S^+\}}{\varepsilon_1^2 \sin^4(\vartheta/2)\,(1 + \xi\sin^2(\vartheta/2))}. \qquad (8)$$

Here ϑ is the scattering angle, $\xi = \epsilon_1/M$. Carrying out the summation on the electron and nucleon spin indices, we get

$$\begin{aligned}\mathrm{Sp}\{\eta^{(+)}(p_2)\, S\rho_0 S^+\} &= |I_1|^2 \cos^2\frac{\vartheta}{2} + |I_3|^2\left\{\frac{2}{3}\mathbf{q}^2\left(1 + \sin^2\frac{\vartheta}{2}\right)\right.\\ &+ \beta_{im}\left[(p_{1i}p_{2m} + p_{2i}p_{1m})\cos^2\frac{\vartheta}{2}\right.\\ &- p_{1m}p_{1i}\left(1 + \sin^2\frac{\vartheta}{2} - \xi\sin^2\frac{\vartheta}{2}\right)\\ &\left.\left. - p_{2i}p_{2m}\left(1 + \sin^2\frac{\vartheta}{2} + \xi\sin^2\frac{\vartheta}{2}\right)\right]\right\}\\ &+ \frac{m}{2\varepsilon_1\varepsilon_2}\{i|I_3|^2(\alpha\mathbf{q})[\boldsymbol{\zeta}_1\mathbf{q}^2 - i(\varepsilon_1 - \varepsilon_2)(\boldsymbol{\zeta}\mathbf{q})]\\ &- 2I_1I_3[(\alpha\boldsymbol{\zeta})\,\mathbf{q}^2 - (\alpha\mathbf{q})(\boldsymbol{\zeta}\mathbf{q})]\}. \qquad (9)\end{aligned}$$

In the computations it is everywhere assumed that $\epsilon_1 \gg m$ and $\vartheta \gg m/\epsilon_1$. The final expression for the differential cross section is conveniently written with the following choice of axes:

$$\mathbf{k} = \mathbf{p}_1/|\mathbf{p}_1|, \qquad \mathbf{n} = [\mathbf{p}_1\times\mathbf{p}_2]/|[\mathbf{p}_1\times\mathbf{p}_2]|, \qquad \mathbf{l} = [\mathbf{k}\times\mathbf{n}].$$

We get

$$d\sigma/d\Omega = (d\sigma/d\Omega)_0\,(1 - N/N_0), \qquad (10)$$

where

$$\begin{aligned}N_0 &= (a_p + a_n)^2 - \frac{2}{3}\mathbf{q}^2\,\frac{(a_p + a_n + b_p + b_n)^2}{4M^2}\left(1 - \frac{2}{\cos^2(\vartheta/2)}\right),\\ N &= \frac{(a_p + a_n + b_p + b_n)^2}{4M^2}\left\{(\boldsymbol{\zeta}^0\mathbf{k})\tan\frac{\vartheta}{2}\left[\frac{1}{2}\mathbf{q}^2\left(2 - \xi\sin^2\frac{\vartheta}{2}\right)\right.\right.\\ &\times\left[2(\alpha\mathbf{l}) + (\alpha\mathbf{k})(2 + \xi)\tan\frac{\vartheta}{2}\right]\\ &+ \frac{2M\varepsilon_2\sin\vartheta\,(a_p + a_n)}{a_p + a_n + b_p + b_n}\left[2(\alpha\mathbf{k}) - (\alpha\mathbf{l})\tan\frac{\vartheta}{2}(2 + \xi)\right]\Big]\\ &+ \mathbf{q}^2\beta_{im}\left[k_ik_m\left(\cos^2\frac{\vartheta}{2} + \tan^2\frac{\vartheta}{2} + \xi\sin^4\frac{\vartheta}{2}\right)\right.\\ &+ l_il_m\left(1 + \sin^2\frac{\vartheta}{2} - \xi\sin^4\frac{\vartheta}{2}\right)\\ &\left.\left. + l_ik_m\sin^2\frac{\vartheta}{2}\tan\frac{\vartheta}{2}(2 + \xi\cos\vartheta)\right]\right\}. \qquad (11)\end{aligned}$$

The scattering cross section for unpolarized particles is

$$\left(\frac{d\sigma}{d\Omega}\right)_0 = \frac{1}{4}\left(\frac{e^2}{4\pi}\right)^2 \frac{f_d^2 N_0\cos^2(\vartheta/2)}{\varepsilon_1^2\sin^4(\vartheta/2)\,(1 + \xi\sin^2(\vartheta/2))}. \qquad (12)$$

The deuteron form factor is

$$f_d = \int |\varphi_d|^2 e^{i\mathbf{q}\mathbf{r}/2}\, d\mathbf{r} = \int_0^\infty u^2 j_0(qr/2)\, dr,$$

where j_0 is the spherical Bessel function. In particular, if

$$\varphi_d = \sqrt{\gamma/2\pi}\, e^{-\gamma r}/r, \quad \text{then } f_d = (4\gamma/q)\tan^{-1}(q/4\gamma).$$

Formula (12) coincides with the expression given by Jankus.[4]

The following circumstance is essential: the ratio of the scattering cross sections for polarized and unpolarized particles does not depend on the deuteron form factor. It is evident from formula (11) that, in the approximation used, the differential cross section does not depend on the transverse component of the polarization of the electrons. It is interesting to note the following: if the cross section does not depend on the proton polarization in the scattering of unpolarized electrons by protons, then in the present case the influence of the deuteron polarization shows up even for the scattering of unpolarized electrons, and the problem has azimuthal symmetry.

THE CHANGE IN ELECTRON POLARIZATION

The basic expression for the final polarization of the electrons $\boldsymbol{\zeta}_2$ in the scattering of electrons

*The factor e^2/q^2 has been removed from S.

with polarization ζ_1 from polarized deuterons has the following form:

$$\zeta_{2}=\frac{i\,(\varepsilon_2/m)\,\mathrm{Sp}\,\{\gamma\gamma_4\gamma_5\gamma_l^{(+)}(p_2)\,S\rho_0 S^{+}\eta^{(+)}(p_2)\}}{\mathrm{Sp}\,\{\eta^{(+)}(p_2)\,S\rho_0 S^{+}\}}. \qquad (13)$$

The method of computation is exactly the same as for deriving the differential cross section. We set down the result:

$$\begin{aligned}\zeta_{2}^{0}=\mathbf{k}\,[&C_{11}(\zeta_{1}^{0}\mathbf{k})+C_{12}(\zeta_{1}^{0}\mathbf{n})+C_{13}(\zeta_{1}^{0}\mathbf{l})+D_{11}(\alpha\mathbf{k})+D_{13}(\alpha\mathbf{l})]\\ &+\mathbf{n}\,[C_{22}(\zeta_{1}^{0}\mathbf{n})+C_{23}(\zeta_{1}^{0}\mathbf{l})]+\mathbf{l}\,[C_{31}(\zeta_{1}^{0}\mathbf{k})+C_{32}(\zeta_{1}^{0}\mathbf{n})\\ &+C_{33}(\zeta_{1}^{0}\mathbf{l})+D_{31}(\alpha\mathbf{k})+D_{33}(\alpha\mathbf{l})]. \qquad (14)\end{aligned}$$

The coefficients in formula (14) have the following meaning:

$$\begin{aligned}C_{11}=&\frac{\cos\vartheta}{N_0-N}\Big\{(a_p+a_n)^2+\frac{\mathbf{q}^2}{4M^2}(a_p+a_n+b_p+b_n)^2\\ &\times\Big[\frac{2}{3}\Big(1+2\tan^2\frac{\vartheta}{2}\Big)\\ &-\beta_{lm}\Big[k_lk_m\Big(\cos^2\frac{\vartheta}{2}+\tan^2\frac{\vartheta}{2}+\xi\sin^4\frac{\vartheta}{2}\Big)\\ &+l_il_m\Big(1+\sin^2\frac{\vartheta}{2}-\xi\sin^4\frac{\vartheta}{2}\Big)\\ &+l_ik_m\tan\frac{\vartheta}{2}\sin^2\frac{\vartheta}{2}(2+\xi\cos\vartheta)\Big]\Big]\Big\},\end{aligned}$$

$$\begin{aligned}C_{22}=&\frac{1}{N_0-N}\Big\{(a_p+a_n)^2+\frac{\mathbf{q}^2}{4M^2}(a_p+a_n+b_p+b_n)^2\Big[\frac{2}{3}\\ &-\beta_{lm}\Big[k_lk_m\Big(1+\tan^2\frac{\vartheta}{2}+\sin^2\frac{\vartheta}{2}-\xi\sin^4\frac{\vartheta}{2}\Big)\\ &-l_ik_m\tan\frac{\vartheta}{2}\sin^2\frac{\vartheta}{2}(2+\xi\cos\vartheta)\\ &+l_il_m\Big(\cos^2\frac{\vartheta}{2}+2\tan^2\frac{\vartheta}{2}+\xi\sin^4\frac{\vartheta}{2}\Big)\Big]\Big]\Big\},\end{aligned}$$

$$\begin{aligned}C_{23}=&\frac{\mathbf{q}^2(a_p+a_n+b_p+b_n)^2\tan(\vartheta/2)\beta_{lm}}{4M^2(N_0-N)}\\ &\times\Big\{n_il_m\tan\frac{\vartheta}{2}\Big(2+\xi\cos^2\frac{\vartheta}{2}\Big)-k_in_m\Big(2-\xi\sin^2\frac{\vartheta}{2}\Big)\Big\},\end{aligned}$$

$$\begin{aligned}D_{11}=&-\frac{\cos\vartheta\tan(\vartheta/2)(a_p+a_n+b_p+b_n)}{M(N_0-N)}\Big\{\varepsilon_2\sin\vartheta(a_p+a_n)\\ &+\frac{(a_p+a_n+b_p+b_n)\mathbf{q}^2}{8M}\tan\frac{\vartheta}{2}\Big(2+\xi\cos^2\frac{\vartheta}{2}\Big)\Big\},\end{aligned}$$

$$\begin{aligned}D_{13}=&\frac{\cos\vartheta\tan(\vartheta/2)(a_p+a_n+b_p+b_n)}{M(N_0-N)}\\ &\times\Big\{\varepsilon_2\sin^2\frac{\vartheta}{2}(2+\xi)(a_p+a_n)\\ &-\frac{(a_p+a_n+b_p+b_n)\mathbf{q}^2}{8M}(2-\xi\sin^2\frac{\vartheta}{2})\Big\},\end{aligned}$$

$$\begin{aligned}&C_{13}=C_{22}\sin\vartheta, \quad C_{12}=-C_{23}\sin\vartheta, \quad C_{31}=-C_{11}\tan\vartheta,\\ &C_{33}=C_{22}\cos\vartheta, \quad C_{32}=-C_{23}\cos\vartheta, \quad D_{31}=-D_{11}\tan\vartheta,\\ &\qquad\qquad D_{33}=-D_{13}\tan\vartheta.\end{aligned}$$

It is obvious from these expressions that the final electron polarization does not depend on the deuteron form factor. It is more convenient to represent the final polarization in the coordinate system connected with the scattered electron:

$$\zeta_{2l}=\zeta_{2}\mathbf{p}_2/p_2, \qquad \zeta_{2t}^{\perp}=\zeta_{2}\mathbf{n}; \qquad \zeta_{2t}^{\parallel}=(\zeta_2\,[\mathbf{p}_2\times\mathbf{n}])/p_2,$$

ξ_{2l} is the longitudinal component, $\xi_{2t}^{\perp}$ the transverse component perpendicular to the plane of the reaction, and $\xi_{2t}^{\parallel}$ the transverse component lying in the plane of the reaction. For the incident electron $\zeta_{1l}=\zeta_1\mathbf{k}$, $\zeta_{1t}^{\perp}=\zeta_1\mathbf{n}$, and $\zeta_{1t}^{\parallel}=\zeta_1\mathbf{l}$. In terms of these the result is written

$$\begin{aligned}\zeta_{2l}^{0}&=[C_{11}\zeta_{1l}^{0}+D_{11}(\alpha\mathbf{k})+D_{13}(\alpha\mathbf{l})]/\cos\vartheta,\\ \zeta_{2t}^{0\parallel}&=[C_{13}\zeta_{1t}^{0\parallel}+C_{12}\zeta_{1t}^{0\perp}]/\sin\vartheta,\\ \zeta_{2t}^{0\perp}&=[C_{13}\zeta_{1t}^{0\perp}-C_{12}\zeta_{1t}^{0\parallel}]/\sin\vartheta.\end{aligned}$$

It is evident that the longitudinal and transverse components of the polarization change independently of each other during the scattering.

If the deuteron is not polarized at first, we get

$$\begin{aligned}\zeta_{2l}^{0}&=\zeta_{1l}^{0},\\ \zeta_{2t}^{0\parallel}&=\zeta_{1t}^{0\parallel}\Big[1-\frac{\mathbf{q}^2(a_p+a_n+b_p+b_n)^2\tan^2(\vartheta/2)}{3M^2N_0}\Big],\\ \zeta_{2t}^{0\perp}&=\zeta_{1t}^{0\perp}\Big[1-\frac{\mathbf{q}^2(a_p+a_n+b_p+b_n)^2\tan^2(\vartheta/2)}{3M^2N_0}\Big].\end{aligned}$$

In this case the longitudinal component of the electron polarization does not change during the scattering, but both transverse components change in the same way. This statement is true also for the scattering of electrons on unpolarized protons, as follows from the formulas obtained before.[5]

If the electrons are initially unpolarized, we have

$$\zeta_{2l}^{0}=[D_{11}(\alpha\mathbf{k})+D_{13}(\alpha\mathbf{l})]/\cos\vartheta, \qquad \zeta_{2t}^{0\perp}=\zeta_{2t}^{0\parallel}=0.$$

The electrons appear longitudinally polarized. Other polarization effects may be interesting, for example, those arising in inelastic electron-deuteron scattering, which effects are now being calculated.

The author is grateful to I. M. Shmushkevich for his constant interest in the work.

[1] Akhiezer, Rozentsveĭg, and Shmushkevich, J. Exptl. Theoret. Phys. (U.S.S.R.) **33**, 765 (1957), Soviet Phys. JETP **6**, 588 (1958).

[2] J. A. McIntyre, Phys. Rev. **103**, 1464 (1956).

[3] J. A. McIntyre and S. Dhar, Phys. Rev. **106**, 1074 (1957).

[4] V. Z. Jankus, Phys. Rev. **102**, 1586 (1956).

[5] G. V. Frolov, J. Exptl. Theoret. Phys. (U.S.S.R.) **34**, 764 (1958), Soviet Phys. JETP **7**, 525 (1958).

Translated by W. Ramsay
92

TRANSITION RADIATION EFFECTS IN PARTICLE ENERGY LOSSES

G. M. GARIBYAN

Physics Institute, Academy of Sciences, Armenian S.S.R.

Submitted to JETP editor March 19, 1959; resubmitted April 29, 1959

J. Exptl. Theoret. Phys. (U.S.S.R.) 37, 527-533 (August, 1959)

The energy lost by a particle that passes through a layer of matter of finite thickness is computed. It is found that at high energies the particle losses due to passage through the interface between two media (transition radiation) can become important.

THE energy lost by a particle (per unit path length) is usually computed under the assumption that the particle moves in an unbounded uniform medium (cf., for example, reference 1). In the present paper we calculate the energy lost by a particle in traversing a layer of finite thickness. As has been shown by Ginzburg and Frank,[2] when a charged particle passes from one medium into another a readjustment must take place in the field associated with the particle; as a result part of the field is "shaken off." This effect is the so-called transition radiation. It is of interest to consider the total energy lost by a particle in passing through the boundary separating two media.

Before solving this problem for finite slabs we consider the case in which the particle moves from one semi-infinite medium into another. The particle losses are computed by the method developed by Landau (cf. reference 1). The fields produced by the charged particle in cases of this kind have been given earlier.[3,4]

1. CASE OF A SINGLE BOUNDARY DIVIDING TWO MEDIA

Suppose that the particle moves along the z axis with velocity v and goes from one medium into another [with dielectric permittivities $\epsilon_1(\omega)$ and $\epsilon_2(\omega)$ respectively]; the plane $z = 0$ is taken as the plane of separation between these media. The fields in both half-spaces will consist of two parts: one is the same as the field associated with a charge which moves in an infinite uniform medium while the other is the radiation field. We write the expressions for the Fourier components of the longitudinal (in the direction of motion of the particle) radiation fields in the first and second media:

$$E'_{1n}(\mathbf{k}) = \frac{ei}{2\pi^2}\frac{\varkappa^2}{\varepsilon_2\lambda_1+\varepsilon_1\lambda_2}\left\{\frac{\varepsilon_2/\varepsilon_1-v\lambda_2/\omega}{k^2-\omega^2\varepsilon_1/c^2}+\frac{-1+v\lambda_2/\omega}{k^2-\omega^2\varepsilon_2/c^2}\right\}, \quad (1)$$

$$E'_{2n}(\mathbf{k}) = \frac{ei}{2\pi^2}\frac{\varkappa^2}{\varepsilon_2\lambda_1+\varepsilon_1\lambda_2}\left\{\frac{1+v\lambda_1/\omega}{k^2-\omega^2\varepsilon_1/c^2}+\frac{-\varepsilon_1/\varepsilon_2-v\lambda_1/\omega}{k^2-\omega^2\varepsilon_2/c^2}\right\}. \quad (2)$$

Here, in contrast with the expressions given earlier[3] the real and imaginary parts of λ_1 and λ_2 are taken as positive ($\lambda_{1,2}^2 = \omega^2\epsilon_{1,2}/c^2 - \kappa^2$).

As in all problems of this type we assume that the energy lost by the particle is small compared with the kinetic energy so that the velocity remains constant.

To calculate effects due to interactions over distances much larger than interatomic distances (in which case a macroscopic analysis can be used) it is sufficient to compute the work done on the particle by its field. The work done by the first part of the field is similar to that computed in reference 1. We compute the work associated with the fields given by Eqs. (1) and (2). In this case it is more pertinent to consider the total work done in each medium rather than the work done per unit length of path.

First we calculate the work done by the Fourier field component in Eq. (2):

$$F_2 = ev\int_0^\infty dt\int E'_{2n}(\mathbf{k})\,e^{i(\lambda_2 v-\omega)t}\,d\mathbf{k} = \frac{e^2}{\pi v^2}(F_2^{(1)}-F_2^{(2)}), \quad (3)$$

where

$$F_2^{(1)} = \int\frac{\varkappa^3\,d\varkappa}{\varepsilon_2\lambda_1+\varepsilon_1\lambda_2}\frac{(1+v\lambda_1/\omega)(\lambda_2 v+\omega)}{(k^2-\omega^2\varepsilon_2/c^2)(k^2-\omega^2\varepsilon_1/c^2)}\,d\omega, \quad (4)$$

$$F_2^{(2)} = \int\frac{\varkappa^3\,d\varkappa}{\varepsilon_2\lambda_1+\varepsilon_1\lambda_2}\frac{(\varepsilon_1/\varepsilon_2+v\lambda_1/\omega)(\lambda_2 v+\omega)}{(k^2-\omega^2\varepsilon_2/c^2)^2}\,d\omega. \quad (5)$$

From these expressions it is apparent that by computing the integral

$$J = \int\frac{\varkappa^3\,d\varkappa}{\varepsilon_2\lambda_1+\varepsilon_1\lambda_2}\frac{([\varepsilon_1/\varepsilon_2]+v\lambda_1/\omega)(\lambda_2 v+\omega)}{(k^2-\omega^2\varepsilon_2/c^2)(k^2-\omega^2\varepsilon_3/c^2)}\,d\omega, \quad (6)$$

and then letting $\epsilon_1/\epsilon_2 \to 1$ (in the places denoted by the square brackets) and $\epsilon_3 \to \epsilon_1$, we can obtain $F_2^{(1)}$; then, by taking the limiting case $\epsilon_3 \to \epsilon_2$, we obtain $F_2^{(2)}$. In Eqs. (4) — (6) the integration over κ is carried out from zero to some value κ_0,

corresponding to the minimum distance from the particle trajectory at which the macroscopic analysis is still valid.

First we carry out the integration over ω from $-\infty$ to $+\infty$. For this purpose we close the path of integration by a half-circle in the upper half of the plane. Since the integral along this half-circle vanishes the expression being sought will be equal to the sum of the residues in the upper half of the plane. The residues are taken at the zeros of the functions $(k^2-\omega^2\epsilon_2/c^2)$ and $(k^2-\omega^2\epsilon_3/c^2)$. In the upper half of the plane these functions have one zero, at the imaginary axis (cf. reference 1).* Then, we integrate with respect to $\omega(\kappa)$ instead of κ (cf. reference 1). For an ultrarelativistic particle the limits of integration are

$$\sqrt{\sigma_{2,3}/(1-\beta^2)} \quad \text{and} \quad c\sqrt{(\varkappa_0^2+\sigma_{2,3}/c^2)/(1-\beta^2)},$$

$$\sigma_{2,3}=4\pi N_{2,3}e^2/m$$

(N is the number of electrons per unit volume and m is the mass of the electron). Thus, we have in the ultrarelativistic case

$$J=\frac{2\pi c}{\sqrt{1-\beta^2}}\left\{\frac{c\varkappa_0}{2}-\frac{2}{3}\frac{\sigma_2^{3/2}-\sigma_3^{3/2}}{\sigma_2-\sigma_3}+\frac{3}{8\varkappa_0 c}(\sigma_2+\sigma_3)\right\}. \quad (7)$$

Whence it is not difficult to obtain the values of $F_2^{(1)}$ and $F_2^{(2)}$; finally, from Eq. (3) we have

$$F_2=\frac{2e^2}{c\sqrt{1-\beta^2}}\left\{\sqrt{\sigma_2}-\frac{2}{3}\frac{\sigma_2^{3/2}-\sigma_1^{3/2}}{\sigma_2-\sigma_1}-\frac{3}{8\varkappa_0 c}(\sigma_2-\sigma_1)\right\}. \quad (8)$$

It is apparent from this formula that reasonable accuracy can be obtained if we take $\kappa_0=\infty$, i.e., the effect is macroscopic and vanishes at small distances. We may note that $F_2>0$ when $\sigma_2>\sigma_1$ and $F_2<0$ when $\sigma_2<\sigma_1$.

By a similar calculation we can show that in contrast with F_2, F_1, the work of the radiation field on the particle in the first medium, falls off with increasing particle energy; we shall not consider it further.

Our analysis is not complete until we take account of the fact that a particle with the same velocity will have different energies in different media; this might be called macroscopic "renormalization" of the particle mass. We compute the amount of electromagnetic energy which the particle carries through a plane perpendicular to its trajectory for motion in an unbounded uniform medium:

$$W=\frac{c}{4\pi}\int_{-\infty}^{\infty}[\mathbf{E}\times\mathbf{H}]_z\,dx\,dy\,dt$$

$$=\frac{e^2}{\pi v}\int\frac{\varkappa^3\,d\varkappa\,d\omega}{\varepsilon(\omega)\,(k^2-\omega^2\varepsilon(\omega)/c^2)\,(k^2-\omega^2\varepsilon(-\omega)/c^2)}. \quad (9)$$

The integration over κ is taken from 0 to κ_0 so that the numerical expression gives the flux through the entire plane except for a circle of radius $1/\kappa_0$ whose center coincides with the particle trajectory. Assuming for simplicity that $\epsilon(-\omega)=\epsilon(\omega)$, we compute the following integral (the zeros in the denominator are traversed from above):

$$W'=\frac{e^2}{\pi v}\int\frac{\varkappa^3\,d\varkappa\,d\omega}{\varepsilon(\omega)\,(k^2-\omega^2\varepsilon(\omega)/c^2)\,(k^2-\omega^2\varepsilon'(\omega)/c^2)}.$$

By taking $\epsilon'=\epsilon$ in the final result we obtain an expression for W. Thus,

$$W=\frac{e^2}{c\sqrt{1-\beta^2}}\left\{\frac{\varkappa_0 c}{2}-\sqrt{\sigma}\right\}, \quad (10)$$

where $\sigma=4\pi Ne^2/m$.

It can be shown that the field at distances up to $1/\kappa_0$ is the same in all media. Thus, if a particle has an energy $\mu c^2\sqrt{1-\beta^2}$ in the first medium, a particle of the same velocity will have in the second medium an energy

$$\mu' c^2/\sqrt{1-\beta^2},$$

where $\mu'=\mu+(W_2-W_1)/c^2=\mu+e^2(\sqrt{\sigma_1}-\sqrt{\sigma_2})/c^2$.

Returning to our problem, we now take account of the force F_2 which also acts on the particle; the energy of the particle is

$$\frac{1}{\sqrt{1-\beta^2}}\left\{\mu c^2-\left[\frac{4}{3}\frac{e^2}{c}\frac{\sigma_2^{3/2}-\sigma_1^{3/2}}{\sigma_2-\sigma_1}-\frac{e^2}{c}(\sqrt{\sigma_1}+\sqrt{\sigma_2})\right]\right\}.$$

It is easy to show that the quantity in the square brackets is always positive, i.e., in passing through the boundary between the two media the particle always loses an amount of energy given by

$$I=\frac{2e^2}{c\sqrt{1-\beta^2}}\left\{\frac{2}{3}\frac{\sigma_2^{3/2}-\sigma_1^{3/2}}{\sigma_2-\sigma_1}-\frac{1}{2}(\sqrt{\sigma_1}+\sqrt{\sigma_2})\right\} \quad (11)$$

For vacuum-medium and medium-vacuum cases this energy loss is $(e^2/3c)\sqrt{\sigma/(1-\beta^2)}$.

We now show that the indicated energy losses are completely due to the transition radiation.* We compute the electromagnetic radiation flux through some plane perpendicular to the z axis (in the second medium) for the entire particle time of flight:

$$S_{2z}=\frac{c}{4\pi}\int_{-\infty}^{+\infty}[\mathbf{E}_2\times\mathbf{H}_2]_z\,dt\,dx\,dy. \quad (12)$$

*In a similar manner it can be shown that λ_1 and λ_2 do not have zeros in the upper half of the plane. Furthermore, since ϵ_1 and ϵ_2 do not have zeros in the upper half of the plane and are positive along the real axis it is easy to show that the sum $\epsilon_2\lambda_1+\epsilon_1\lambda_2$ has no zeros in the upper half of the plane.

*Attention has been directed to this fact by K. A. Barsukov in a similar calculation for a waveguide.

We use the formulas for E_2 and H_2 which have been derived in reference 3, and make use of the δ-function in the integration over t, x, and y. Then, converting from integration over κ to ω, as in the preceding cases, we find that this flux consists of three parts: one is due to the field of the charged particle itself and is given by Eq. (10) (with $\sigma = \sigma_2$); the second is the radiation field (given by I); the third is due to interference between these fields and vanishes when $(\omega/v - \lambda_2)z \gg 1$.

We now find the angular distribution and frequency dependence of the transition radiation field in the second medium. To find the conditions under which the interference term vanishes (i.e., the transition radiation zone), after integrating over t, x, and y in Eq. (12) we make the substitution $\kappa = (\omega/c)\sqrt{\epsilon_2}\sin\theta$, where θ is the angle between the wave vector of the radiation field and the z axis. Assuming for simplicity that $\epsilon_2 = 1$ and $\epsilon_1 = \epsilon$, we find the energy flux in the second medium due to transition radiation

$$dS'_{2z} = \frac{2e^2\beta^2}{\pi c}\frac{\sin^3\theta\cos^2\theta\,d\theta}{(1-\beta^2\cos^2\theta)^2} \times \int_0^\infty \left(\frac{(\epsilon-1)(1-\beta^2-\beta\sqrt{\epsilon-\sin^2\theta}}{(\epsilon\cos\theta+\sqrt{\epsilon-\sin^2\theta})(1-\beta\sqrt{\epsilon-\sin^2\theta})}\right)^2 d\omega \qquad (13)$$

(we assume that the medium is transparent).* It is apparent from this formula that the radiation vanishes at small angles ($\theta \sim \sqrt{1-\beta^2}$) with respect to the direction of motion of the particle. Taking account of this fact, it is easy to show that the main contribution in the integral in Eq. (13) is at frequencies larger than the optical frequencies [because of the small factor $(1-\beta\sqrt{\epsilon-\sin^2\theta})$ which appears in the denominator of Eq. (13)]. Then, substituting the expression $\epsilon(\omega) = 1-\sigma/\omega^2$ in Eq. (13) and replacing $\sin\theta$ by θ, we integrate first over the frequencies, and then over the angles from 0 to ∞. We find $S'_{2z} = e^2\sqrt{\sigma}/3c\sqrt{1-\beta^2}$.

As to the frequency distribution of the transition radiation spectrum, we find from Eq. (13) that the radiation intensity is almost constant from optical frequencies to the limiting frequency $\omega_{lim} = \sqrt{\sigma}/2\sqrt{1-\beta^2}$. At this frequency the radiation intensity falls off by a factor of 2 as compared with the intensity at lower frequencies. The main contribution in the integral is due to frequencies which are not too small compared with the limiting frequency.

The transition radiation in the first medium can be obtained in essentially the same way. The well-known formula given by Ginzburg and Frank is used (cf. also references 3, 5, and 6); this formula differs from Eq. (13) in that β is replaced by $-\beta$. As a result, the small factor in the denominator vanishes and the backward transition radiation encompasses only the optical part of the spectrum, being given by an expression which diverges logarithmically with energy.

If we now assume that the first medium is a vacuum and that the second is a dielectric, Eq. (13) undergoes changes which are unimportant at high frequencies, so that the foregoing results still apply.

As has been noted, the transition radiation zone is determined by the inequality $z \gg |\omega/v - \lambda_2|^{-1}$. If the second medium is a vacuum the transition radiation zone is determined, for all frequencies, by the inequality $z \gg \lambda\!\!\!^{-}/(1-\beta^2)$ ($\lambda\!\!\!^{-}$ is the wavelength of the radiation divided by 2π). However, if the second medium is not vacuum, the transition radiation zone is of the order of the optical wavelength for optical frequencies so that $z \gg \lambda\!\!\!^{-}/(1-\beta^2+\sigma\lambda\!\!\!^{-2}/2c^2)$ for frequencies close to the limiting frequency. At the limiting frequency $z_{lim} \gg c/\sqrt{\sigma(1-\beta^2)}$, i.e., the transition radiation zone grows much larger.

Finally we consider the number of transition radiation photons. Again limiting ourselves to the medium–vacuum or the vacuum–medium case, the number of photons with frequencies $\omega' \gtrsim \omega_{opt}$, up to the hardest, is given by the expression

$$N'_2 = \frac{1}{137}\frac{2}{\pi}\left[\ln\left(\frac{1}{\omega'}\sqrt{\frac{\sigma}{2(1-\beta^2)}}\right) - \frac{1}{2}\right]. \qquad (14)$$

Whence it is apparent for example that if $E/\mu \sim 10^{10}$ and $\omega' \sim \sqrt{\sigma/2}$, $N'_2 \sim 0.1$, i.e., out of ten particles on the average only one emits a transition photon. If the frequency of the transition photon is close to the limiting frequency its energy is approximately $\sim\sqrt{\sigma/(1-\beta^2)}$, i.e., this energy is approximately 137 times greater than S'_{2z}. Thus, as follows from Eq. (14), a photon of this kind appears approximately once out of 137 particles).

In spite of the classical nature of the effect, the radiation of transition photons from singly charged particles is a rare phenomenon, sub-

*We may note that this formula coincides with Eq. (28) of reference 3, bearing in mind that the significance of the angle θ in both formulas is the same for transition radiation, but not for Cerenkov radiation. The infinity which appears in Eq. (13) when $1-\beta\sqrt{\epsilon-\sin^2\theta} = 0$ is due to the fact that this formula also gives the intensity of the Cerenkov radiation emitted with a semi-infinite trajectory in the first medium, which is assumed to be transparent. The intensity of the transition radiation itself, however, is always finite (cf. reference 3).

ject to large fluctuations. This effect can be made classical if the number of emitted photons is increased. This can be achieved, for example, if the particle is multiply charged or if it passes through a large number of boundaries. In the first case the number of emitted photons and the total energy increases quadratically with the charge of the particle; in the second case these quantities increase in proportion to the number of boundaries traversed. In both cases the limiting frequency of the photon remains the same. However in the second case the transition photon zone must be considered.

All the results cited above refer to the vacuum–medium or medium–vacuum case. However, as is apparent from Eq. (11), these results apply qualitatively for the medium–medium case, which differs from the preceding cases only in certain small numerical factors.

2. CASE OF A FINITE SLAB

Suppose now that a particle which moves in vacuum enters a slab whose boundaries are the planes[4] $z = 0$ and $z = a$ (cf. also reference 7).

Because the particle moves in the same medium (vacuum) on both sides of the slab it is not necessary to "renormalize" the particle mass.

As in the preceding case we consider the work done on the particle by the radiation field and obtain the following expressions for the region in front of the slab (W_0), in the slab (w_1) and behind the slab (W_1):

$$W_0 = -\frac{e^2}{\pi}\int \frac{\varkappa^3\xi\, d\varkappa\, d\omega}{\lambda_0 F(\lambda_0 v+\omega)}, \tag{15}$$

$$w_1 = -\frac{e^2}{\pi}\int \frac{\varkappa^3\eta'\, d\varkappa\, d\omega}{\lambda F(\lambda v-\omega)}\left(e^{i(\lambda v-\omega)a/v}-1\right) - \frac{e^2}{\pi}\int \frac{\varkappa^3\eta''\, d\varkappa\, d\omega}{\lambda F(\lambda v+\omega)}\left(e^{-i(\lambda v+\omega)a/v}-1\right), \tag{16}$$

$$W_1 = -\frac{e^2}{\pi}\int \frac{\varkappa^3\zeta\, d\varkappa\, d\omega}{\lambda_0 F(\lambda_0 v-\omega)}, \tag{17}$$

where

$$\left.\begin{matrix}\xi\\ \zeta\end{matrix}\right\} = \left(\frac{\varepsilon}{\lambda}\pm\frac{1}{\lambda_0}\right)\varkappa e^{\mp i\lambda a} + \left(\frac{\varepsilon}{\lambda}\mp\frac{1}{\lambda_0}\right)\beta e^{\pm i\lambda a} + \frac{2\varepsilon}{\lambda}\left\{\begin{matrix}\gamma\\ \delta\end{matrix}\right\} e^{\pm i\omega a/v},$$

$$\left.\begin{matrix}\eta'\\ \eta''\end{matrix}\right\} = -\left(\frac{\varepsilon}{\lambda}\pm\frac{1}{\lambda_0}\right)\delta e^{\mp i\lambda a} + \left(\frac{\varepsilon}{\lambda}\mp\frac{1}{\lambda_0}\right)\gamma e^{+i\omega a/v},$$

$$\left.\begin{matrix}\alpha\\ \beta\end{matrix}\right\} \quad \frac{\mp\varepsilon/\lambda - v/\omega}{k^2-\omega^2/c^2} \qquad \frac{\mp 1/\lambda + v/\omega}{k^2-\omega^2\varepsilon/c^2},$$

$$\left.\begin{matrix}\gamma\\ \delta\end{matrix}\right\} = \frac{\mp 1/\lambda_0 + v/\omega}{k^2-\omega^2/c^2} + \frac{\pm 1/\lambda_0\varepsilon - v/\omega}{k^2-\omega^2\varepsilon/c^2},$$

$$F = (\varepsilon/\lambda + 1/\lambda_0)^2 e^{-i\lambda a} - (\varepsilon/\lambda - 1/\lambda_0)^2 e^{i\lambda a}.$$

It is easy to show that F has no zeros in the upper half of the complex ω plane. Furthermore, in the expression for F only the first term need be used. As in the preceding case, we find that W_0 falls off with increasing particle energy; hence this term will not be considered here.

In integrating the expressions for w_1 and W_1 we limit ourselves to "thick" and "thin" slabs. We note that w_1 and W_1 contain exponential terms with the characteristic argument $i(\lambda - \omega/v)a$. A slab will be considered thick or thin depending on whether this argument is large or small compared with unity. In the first case we neglect terms containing this exponential; in the second case we expand the exponential and limit ourselves to the first nonvanishing term. We then analyze the manner in which ω and κ appear in the integrals to determine whether a slab is to be considered "thick" or "thin."

In the case of the thick slab, w_1 is given by an expression which coincides with F_2 for the motion of a particle from vacuum into a medium, while W_1 coincides with F_2 for the motion of a particle from a medium into vacuum. Thus, from Eq. (8) it follows that the total loss of energy is $-(2e^2/3c)\sqrt{\sigma/(1-\beta^2)}$. Obviously this loss approaches the transition radiation arising at each boundary of the slab. This same result can be obtained by direct calculation of the flux of electromagnetic energy which passes through a plane perpendicular to the z axis and located in the space beyond the slab.*

Assuming that the slab is thick, substituting the limiting value of the frequency, and assuming that $\kappa \sim \omega\sqrt{1-\beta^2}/c$, we obtain the following requirement for the slab thickness:

$$a \gg c/\sqrt{\sigma(1-\beta^2)}. \tag{18}$$

If the thickness of the slab is less than the limiting value (18), the transition radiation spectrum will not contain hard photons; these photons cannot be produced in the slab and it follows that they cannot be formed in the space beyond the slab.

We now consider the thin slab. The following expressions are obtained for w_1 and W_1:

$$w_1 = \frac{\sigma e^2}{c^2}a\left[\ln\frac{v\varkappa_0}{\sqrt{\sigma}} + \frac{1}{2}\right], \tag{19}$$

$$W_1 = -\frac{\sigma e^2}{c^2}a\left[\ln\frac{v\varkappa_0}{\sqrt{1-\beta^2}\,\Omega} + c_1\right],$$

$$c_1 = \frac{8}{\sigma}\int_0^\Omega \frac{\sqrt{\varepsilon}(\sqrt{\varepsilon}-1)}{(\sqrt{\varepsilon}+1)^2}\omega\, d\omega \tag{20}$$

*We may note that in references 4 and 8, in the calculation of the Poynting vector in the ultra-relativistic case, only the optical part of the transition radiation spectrum was investigated.

($\Omega \gtrsim I/\hbar$, where I is the ionization energy of the K-electron). Adding the last two expressions to the usual ionization losses in matter[1]* the energy loss of a particle in a thin slab is given by the expression

$$F = \frac{2\pi N e^4}{mc^2} a \left[\ln \frac{c^2 \varkappa_0^2}{(1-\beta^2)\Omega^2} + 2c_1 - 1 \right]. \qquad (21)$$

It is apparent from this formula that in thin slabs there is no density effect. To obtain the conditions under which a slab may be assumed thin we proceed as follows. In the expanded formulas (16) and (17) we compute the last term smaller than the first-order term in a. As a result the following condition is obtained for a thin slab:

$$a \ll 2 (c\Omega / \sigma) \ln (v\varkappa_0 / \sqrt{1-\beta^2}\Omega). \qquad (22)$$

It is apparent from these formulas that, after first levelling off, the ionization losses in the slab again start increasing logarithmically at some particle energy if the slab is in a vacuum. However if the slab is in a medium which has a smaller electronic density (than the slab), the ionization losses again reach a plateau corresponding to the electron density of the medium surrounding the slab.

As the slab thickness is reduced, the particle can radiate more or less hard photons in the region outside the intervals given by Eqs. (18) and (22), and the term without the density becomes important in the ionization losses.

Dnestrovskiĭ and Kostomarev have considered the radiation formed in the flight of a charge through a circular aperture in an infinite ideally-conducting plane.[9] The results obtained by them for the case of an ultrarelativistic electron are in agreement with the present results in that the total radiation energy is proportional to the particle energy. The coefficient of proportionality obtained by these authors is the ratio of the classical electron radius to the dimensions of the aperture and is several orders of magnitude smaller than the completely natural coefficient of proportionality obtained from Eq. (11).

The author wishes to express his gratitude for valuable discussions to Prof. V. L. Ginzburg, L. D. Landau, I. Ya. Pomeranchuk and also A. Ts. Amatuni, B. M. Bolotovskiĭ, I. I. Gol'dman and G. S. Saakyan.

*In view of the fact that Eq. (19) (with the exception of an additive constant) can be reduced to the usual expression for ionization losses, it would appear that braking forces do not operate on the particle in the slab. However account must be taken of the fact that the total field carried by the particle is different in vacuum and in the slab. When this factor is considered it can be shown that the braking force acts on the particle only in the slab.

[1] L. D. Landau and E. M. Lifshitz, Электродинамика сплошных сред (Electrodynamics of Continuous Media) Moscow, Gostekhizdat, 1957.

[2] V. L. Ginzburg and I. M. Frank, J. Exptl. Theoret. Phys. (U.S.S.R.) **16**, 15 (1946).

[3] G. M. Garibyan, J. Exptl. Theoret. Phys. (U.S.S.R.) **33**, 1403 (1957), Soviet Phys. JETP **6**, 1079 (1958).

[4] G. M. Garibyan and G. A. Chalikyan, J. Exptl. Theoret. Phys. (U.S.S.R.) **35**, 1282 (1958), Soviet Phys. JETP **8**, 894 (1959). Izv. Akad. Nauk. Arm SSR, Ser. Fiz-Mat, **12**, 3 (1959).

[5] N. P. Klepikov, Вестник МГУ, (Bull. Moscow State Univ.) **8**, 61 (1951).

[6] N. A. Korkhmazyan, Izv. Akad. Nauk. Arm SSR, Ser. Fiz-Mat, **10**, 4 (1957).

[7] V. E. Pafomov, J. Exptl. Theoret. Phys. (U.S.S.R.) **33**, 1074 (1957), Soviet Phys. JETP **6**, 829 (1958).

[8] G. M. Garibyan, J. Exptl. Theoret. Phys. (U.S.S.R.) **35**, 1435 (1958), Soviet Phys. JETP **8**, 1003 (1959).

[9] Yu. N. Dnestrovskiĭ and D. P. Kostomarev, Dokl. Akad. Nauk SSSR, **124**, 792, 1026 (1959), Soviet Phys.–Doklady **4**, 132, 158 (1959).

Translated by H. Lashinsky
93

THERMOELECTRIC PHENOMENA IN STRONG MAGNETIC FIELDS IN METALS POSSESSING VARIOUS FERMI SURFACES

Yu. A. BYCHKOV, L. É. GUREVICH, and G. M. NEDLIN

Institute for Physical Problems, Academy of Sciences, U.S.S.R.; Leningrad Physico-Technical Institute, Academy of Sciences, U.S.S.R.

Submitted to JETP editor March 19, 1959

J. Exptl. Theoret. Phys. (U.S.S.R.) 37, 534-539 (August, 1959)

The asymptotic behavior of the thermoelectric force, Peltier coefficients, and Thomson coefficients for metals with closed Fermi surfaces and open surfaces of the "corrugated cylinder" and "space net" types is investigated on the basis of the quasi-classical theory of kinetic phenomena in metals in strong magnetic fields, as developed by Lifshitz, Azbel', and Kaganov[1] and Lifshitz and Peschanskiĭ.[2]

LIFSHITZ, Azbel', Kaganov, and Peschanskiĭ[1,2] have given the theory of the asymptotic behavior of the kinetic coefficients in very strong magnetic fields, when the period of rotation of the electrons is much greater than the relaxation time. The asymptotic dependence of the coefficients on the magnetic field and on its direction relative to the crystal axes is then largely determined by the nature of the Fermi surface, and is very different for open and closed surfaces. The coefficients are weakly dependent on the actual form of the collision integral and on the dispersion law. The range of validity of this quasi-classical theory is indicated by Lifshitz et al. The asymptotic behavior of the electrical conductivity tensor was calculated in detail[1,2] and some aspects of the behavior of the heat conductivity tensor and of the Thomson coefficient were briefly considered[3] on the basis of the theory. In the present work we discuss in detail a number of thermoelectric phenomena.

As is well known, the electron distribution function, f, for a metal in an electric field and a temperature gradient differs from $f_0 = \{\exp[(\epsilon-\mu)/kT]+1\}^{-1}$ by an amount f_1 i.e., $f = f_0 + f_1$. f is derived from the solution of the corresponding kinetic equation. As a result of the additional term f_1 the current density vector, **j**, and the heat current vector, **q**, differ from zero, and are related to f_1 by the simple equations

$$\mathbf{j} = \frac{2e}{(2\pi\hbar)^3}\int \mathbf{v} f_1\, dp, \qquad \mathbf{q} = \frac{2}{(2\pi\hbar)^3}\int (\varepsilon-\zeta)\,\mathbf{v} f_1\, dp. \tag{1}$$

In general **j** and **q** can be written in the form[4]

$$j_i = \frac{a_{ik}}{T}E_k + b_{ik}\frac{\partial}{\partial x_k}\left(\frac{1}{T}\right),$$

$$q_i = \frac{c_{ik}}{T}E_k + d_{ik}\frac{\partial}{\partial x_k}\left(\frac{1}{T}\right). \tag{2}$$

In a magnetic field the kinetic coefficients are functions of the vector **H**. The coefficients in (2) are not independent, but are related by the well-known symmetry relations

$$a_{ik}(\mathbf{H}) = a_{ki}(-\mathbf{H}), \quad d_{ik}(\mathbf{H}) = d_{ki}(-\mathbf{H}),$$

$$b_{ik}(\mathbf{H}) = c_{ki}(-\mathbf{H}). \tag{3}$$

If **E** and **q** are expressed in terms of **j** and ∇T, we obtain

$$E_i = \sigma_{ik}^{-1} j_k + \alpha_{ik}\frac{\partial T}{\partial x_k}, \qquad q_i = \beta_{ik} j^k - \varkappa_{ik}\frac{\partial T}{\partial x^k} \tag{4}$$

where

$$\sigma_{ik} = T^{-1} a_{ik}, \qquad \alpha_{ik} = T^{-1} a_{il}^{-1} b_{lk},$$
$$\beta_{ik} = c_{il}\, a_{lk}^{-1}, \qquad \varkappa_{ik} = T^{-2}(d_{ik} - c_{il}\, a_{lm}^{-1} b_{mk}), \tag{5}$$

which satisfy the symmetry relation connected with (3):

$$\sigma_{ik}(\mathbf{H}) = \sigma_{ki}(-\mathbf{H}), \quad \varkappa_{ik}(\mathbf{H}) = \varkappa_{ki}(-\mathbf{H}),$$

$$T\alpha_{ik}(\mathbf{H}) = \beta_{ki}(-\mathbf{H}). \tag{6}$$

In these expressions σ_{ik} is the electrical conductivity tensor, $\varkappa_{ik}$ is the heat conductivity tensor, α_{ik} can be called the thermal emf tensor, and β_{ik} are the Peltier coefficients.[4] It can easily be shown that the Thomson effect and related phenomena are described by the quantity

$$\mu_{ik} = -\alpha_{ik} + \partial\beta_{ki}/\partial T.$$

In what follows we shall be interested in the asymptotic behavior of the thermal emf in a strong magnetic field. Evidently, knowing the dependence of α_{ik} on H, and using the symmetry relations, the asymptotic behavior of β_{ik} and μ_{ik} can easily be derived. In fact, we will first look for the asymptotic Peltier coefficients in each case, for the following reason. It can be seen from (5) that whereas α_{ik} is connected with a_{ik} and b_{ik} [i.e., it is found from the solution of the kinetic equation with an electric field (a_{ik}) and a temperature gradient (b_{ik}) present], the value of β_{ik} can be found if the solution of the kinetic equation in the presence of an electric field only is known so that α_{ik} can be determined by using relation (6).

1. CLOSED FERMI SURFACE

To find the dependence of the tensor β_{ik} on magnetic field one must know the behavior of a_{ik} and c_{ik}, and we shall base our calculation on the work of Lifshitz and Peschanskiĭ.[2] They examined in detail the asymptotic electrical conductivity tensor, $\sigma_{ik} = a_{ik}/T$, but it is clear that apart from some special cases (as can occur in the case of equal numbers of electrons and holes for closed surfaces), the form of the field dependence of a_{ik} and c_{ik} will be analogous. These cases will be examined separately.

a) Unequal numbers of electrons and holes. We use below the symbol $\gamma_0 = 1/\omega t_0$ where t_0 is some characteristic time of the order of the relaxation time, and ω is some frequency of revolution of an electron in its phase trajectory. We must look for the asymptote of quantities in a very high magnetic field, such that $\gamma_0 \ll 1$. According to Lifshitz and Peschanskiĭ, we have for this case

$$a_{ik} = \begin{pmatrix} \gamma_0^2 a_{xx}^{(0)} & \gamma_0 a_{xy}^{(0)} & \gamma_0 a_{xz}^{(0)} \\ -\gamma_0 a_{xy}^{(0)} & \gamma_0^2 a_{yy}^{(0)} & \gamma_0 a_{yz}^{(0)} \\ -\gamma_0 a_{xz}^{(0)} & -\gamma_0 a_{yz}^{(0)} & a_{zz}^{(0)} \end{pmatrix} \tag{7}$$

and the expansion of $a_{ik}^{(0)}$ in powers of γ_0 starts with the zero order term in general. The symmetry relations (3) are taken into account in (7). The most important fact turns out to be that the components a_{xy} and a_{yx} are independent of the collision integral and

$$a_{xy} = -a_{yx} = 2ecT\,(V_1 - V_2)/H(2\pi\hbar)^3 = ecT\,(n_1 - n_2)/H,$$

where V_1 and V_2 are the volumes in phase space occupied by electrons and holes, and n_1 and n_2 the corresponding numbers of electrons and holes. Using (1) we then obtain

$$c_{xy} = -c_{yx} = \frac{\pi^2 k^2 T^3}{3H}\frac{d}{d\varepsilon}(n_1 - n_2).$$

Evidently

$$c_{ik} = \begin{pmatrix} \gamma_0^2 c_{xx}^{(0)} & \gamma_0 c_{xy}^{(0)} & \gamma_0 c_{xz}^{(0)} \\ -\gamma_0 c_{xy}^{(0)} & \gamma_0^2 c_{yy}^{(0)} & \gamma_0 c_{yz}^{(0)} \\ -\gamma_0 c_{xz}^{(0)} & -\gamma_0 c_{yz}^{(0)} & c_{zz}^{(0)} \end{pmatrix},$$

$$a_{ik}^{-1} = \begin{pmatrix} d_{xx} & \gamma^{-1}{}_0 d_{xy} & d_{xz} \\ -\gamma^{-1}{}_0 d_{xy} & d_{yy} & d_{yz} \\ d_{xz} & d_{yz} & d_{zz} \end{pmatrix},$$

then

$$\beta_{ik} = \begin{pmatrix} \nu_{xx} & \gamma_0\nu_{xy} & \gamma_0\nu_{xz} \\ \gamma_0\nu_{yx} & \nu_{yy} & \gamma_0\nu_{yz} \\ \nu_{zx} & \nu_{zy} & \nu_{zz} \end{pmatrix}, \tag{8}$$

where

$$\nu_{xx} = \nu_{yy} = \frac{\pi^2 k^2 T^2}{3e}\frac{d}{d\varepsilon}\ln(n_1 - n_2). \tag{9}$$

Remembering that $\alpha_{ik} = [\beta_{ki}(-H)]/T$ and taking the symmetry relations into account, the coefficients of the thermal emf, α_{ik} are equal to

$$\alpha_{ik} = \frac{1}{T}\begin{pmatrix} \nu_{xx} & -\gamma_0\nu_{yx} & \nu_{zx} \\ -\gamma_0\nu_{xy} & \nu_{yy} & \nu_{zy} \\ -\gamma_0\nu_{xz} & -\gamma_0\nu_{yz} & \nu_{zz} \end{pmatrix}. \tag{10}$$

b) Equal numbers of electrons and holes. This corresponds to a whole range of metals. The expansion of the components a_{xy} in terms of γ_0 now starts with the quadratic term. i.e.,

$$a_{ik} = \begin{pmatrix} \gamma_0^2 a_{xx}^{(0)} & \gamma_0^2 a_{xy}^{(0)} & \gamma_0 a_{xz}^{(0)} \\ \gamma_0^2 a_{xy}^{(0)} & \gamma_0^2 a_{yy}^{(0)} & \gamma_0 a_{yz}^{(0)} \\ -\gamma_0 a_{xz}^{(0)} & -\gamma_0 a_{yz}^{(0)} & a_{zz}^{(0)} \end{pmatrix}. \tag{11}$$

If we make use of the fact that $d(n_1 - n_2)/d\epsilon \neq 0$, then $c_{xy} \sim \gamma_0$, as in the first case, i.e., the dependence of c_{ik} on H is unchanged. We then obtain

$$\beta_{ik} = \begin{pmatrix} \gamma_0^{-1}\nu_{xx} & \gamma_0^{-1}\nu_{xy} & \nu_{xz} \\ \gamma_0^{-1}\nu_{yx} & \gamma_0^{-1}\nu_{yy} & \nu_{yz} \\ \gamma_0^{-1}\nu_{zx} & \gamma_0^{-1}\nu_{zy} & \nu_{zz} \end{pmatrix}, \tag{12}$$

and

$$\alpha_{ik} = \frac{1}{T}\begin{pmatrix} -\gamma_0^{-1}\nu_{xx} & -\gamma_0^{-1}\nu_{yx} & -\gamma_0^{-1}\nu_{zx} \\ -\gamma_0^{-1}\nu_{xy} & -\gamma_0^{-1}\nu_{yy} & -\gamma_0^{-1}\nu_{zy} \\ \nu_{xz} & \nu_{yz} & \nu_{zz} \end{pmatrix}. \tag{13}$$

In the present case all the ν_{ik} depend on the angle between the vector H and the crystal axes, and their actual form is determined by the collision integral and the dispersion relation.

2. OPEN FERMI SURFACE

Lifshitz and Peschanskiĭ[2] have shown that in this case the kinetic coefficients are rapid functions of angle near certain particular directions of the magnetic field, when the character of the phase trajectory changes, i.e., goes from open to closed or vice versa. The field dependence of the coefficients varies rapidly near to these directions, and it is, in general, no longer possible to expand in powers of γ_0. These authors pointed out that there are three types of special field direction: a) directions for which a band of open trajectories exists, forming a one-dimensional set; b) directions giving open trajectories forming a two-dimensional region; c) an isolated direction of the vector **H** in the region of open trajectories, where the trajectories become closed.

We consider below the behavior of the thermoelectric coefficients near the special directions of all three types.

The "corrugated cylinder" is the simplest type of surface. For field directions which make a not too great angle with the cylinder axis, the trajectories are closed and the asymptotic expression for β_{ik} and, correspondingly, of α_{ik} will be just the same as for closed surfaces. The behavior of β_{ik}, however, changes rapidly when **H** approaches a direction perpendicular to the cylinder axis. The corresponding special field direction belongs to the first type. If we introduce $\eta = \gamma_0/\sin\theta$ (where θ is the angle between the cylinder axis and the plane perpendicular to the field vector), choose the direction of **H** as the z axis and take the x axis as lying in the plane passing through **H** and the cylinder axis, then[2]

$$a_{ik} = \begin{pmatrix} \gamma_0^2 b_{xx}(\eta) & \gamma_0 b_{xy}(\eta) & \gamma_0 b_{xz}(\eta) \\ -\gamma_0 b_{xy}(-\eta) & b_{yy}(\eta) & b_{yz}(\eta) \\ -\gamma_0 b_{xz}(-\eta) & b_{yz}(-\eta) & b_{zz}(\eta) \end{pmatrix}, \qquad (14)$$

where b_{ik} is a function of the type

$$b_{ik} = (b_{ik}^{(0)} + \eta b_{ik}^{(1)} + \eta^2 b_{ik}^{(2)})/(1 + \eta^2 \lambda_{ik}),$$

where $b_{ik}^{(n)}$ and λ_{ik} are relatively slow functions of the angle θ. Then

$$a_{ik}^{-1} = \begin{pmatrix} \gamma_0^{-2} d_{xx}(\eta) & \gamma_0^{-1} d_{xy}(\eta) & \gamma_0^{-1} d_{xz}(\eta) \\ -\gamma_0^{-1} d_{xy}(-\eta) & d_{yy}(\eta) & d_{yz}(\eta) \\ -\gamma_0^{-1} d_{xz}(-\eta) & d_{yz}(-\eta) & d_{zz}(\eta) \end{pmatrix}, \qquad (15)$$

$$c_{ik} = \begin{pmatrix} \gamma_0^2 f_{xx}(\eta) & \gamma_0 f_{xy}(\eta) & \gamma_0 f_{xz}(\eta) \\ -\gamma_0 f_{xy}(-\eta) & f_{yy}(\eta) & f_{yz}(\eta) \\ -\gamma_0 f_{xz}(-\eta) & f_{yz}(-\eta) & f_{zz}(\eta) \end{pmatrix}. \qquad (16)$$

From this it is easy to obtain

$$\beta_{ik} = \begin{pmatrix} \nu_{xx}(\eta) & \gamma_0 \nu_{xy}(\eta) & \gamma_0 \nu_{xz}(\eta) \\ \gamma_0^{-1} \nu_{yx}(\eta) & \nu_{yy}(\eta) & \nu_{yz}(\eta) \\ \gamma_0^{-1} \nu_{zx}(\eta) & \nu_{zy}(\eta) & \nu_{zz}(\eta) \end{pmatrix}, \qquad (17)$$

and the thermal emf is consequently

$$\alpha_{ik} = \frac{i}{T} \begin{pmatrix} \nu_{xx}(-\eta) & -\gamma_0^{-1} \nu_{yx}(-\eta) & -\gamma_0^{-1} \nu_{zx}(-\eta) \\ -\gamma_0 \nu_{xy}(-\eta) & \nu_{yy}(-\eta) & \nu_{zy}(-\eta) \\ -\gamma_0 \nu_{xz}(-\eta) & \nu_{yz}(-\eta) & \nu_{zz}(-\eta) \end{pmatrix}. \qquad (18)$$

For $\eta \to \infty$ ν_{ik} tends to a finite limit. By comparing their behavior for two limiting values of θ (0 and $\pi/2$) we see that all the ν_{ik}, except ν_{yx}, ν_{yz}, and ν_{zx}, are relatively slowly varying functions of θ, i.e., they retain the same dependence on H for all angles. At the same time, ν_{yx}, ν_{yz}, and ν_{zx} vary rapidly in the neighborhood of $\theta = 0$. By considering this behavior for $\theta = 0$ and $\theta = \pi/2$ one can obtain

$$\nu_{zx} = \frac{\eta^2 \gamma(\eta) + \eta\sigma(\eta)}{1 + \eta^2 \nu(\eta)},$$

$$\nu_{yx} = \frac{\eta^2 \beta(\eta)}{1 + \eta^2 \lambda(\eta)}, \qquad \nu_{yz} = \frac{\eta\delta(\eta) + \eta^2 \rho(\eta)}{1 + \eta^2 \varphi(\eta)}, \qquad (19)$$

where β, γ, δ etc. are slowly varying functions of angle, and their actual form depends on the dispersion law and on the collision integral.

For directions of **H** which make a not too large angle with the cylinder axis, we have

$$\beta_{xx} = \beta_{yy} = -\frac{\pi^2 k^2 T^2}{3e} \frac{d}{d\varepsilon} \ln R, \qquad (20)$$

where R is the Hall constant.

Another surface which lends itself easily to investigation is the "space net" type of surface. For this all three types of special field direction exist, and we will not consider the properties of the first type which is exactly equivalent to the case of $\theta = 0$ for a corrugated cylinder. We will discuss the other two cases, which refer to the magnetic field direction close to the direction of the crystallographic axes and of the boundary of the two-dimensional region of field directions which give open trajectories. In these cases the required choice of angle ϑ can be obtained from the fact that a_{ik} must be of the form

$$a_{ik} = \begin{pmatrix} \gamma_0^2 a_{xx}^{(0)} & \gamma_0 a_{xy}^{(0)} & \gamma_0 a_{xz}^{(0)} \\ -\gamma_0 a_{xy}^{(0)} & \gamma_0^2 a_{yy}^{(0)} + \vartheta c_1 & \gamma_0 a_{yz}^{(0)} + \vartheta c_2 \\ -\gamma_0 a_{xz}^{(0)} & -\gamma_0 a_{yz}^{(0)} + \vartheta c_2 & a_{zz}^{(0)} \end{pmatrix}, \qquad (21)$$

where a_{ik} is mainly determined by closed trajectories, apart from which there is a band of open trajectories with width proportional to the angle ϑ. Then

$$a_{ik}^{-1}=\begin{pmatrix} d_{xx}+\vartheta\gamma_0^{-2}d_{xx}^{(1)} & \gamma_0^{-1}d_{xy} & d_{xz}+\vartheta\gamma_0^{-1}d_{xz}^{(1)} \\ -\gamma_0^{-1}d_{xy} & d_{yy} & d_{yz} \\ d_{zx}+\vartheta\gamma_0^{-1}d_{zx}^{(1)} & d_{zy} & d_{zz} \end{pmatrix} \quad (22)$$

from which it is easy to deduce that

$$\beta_{ik}=\begin{pmatrix} \nu_{xx} & \gamma_0\nu_{xy} & \gamma_0\nu_{xz} \\ \gamma_0\nu_{yx}+\vartheta\gamma_0^{-1}\nu_{yx}^{(1)} & \nu_{yy} & \gamma_0\nu_{yz}+\vartheta\nu_{yz}^{(1)} \\ \nu_{zx}+\vartheta\gamma_0^{-1}\nu_{zx}^{(1)} & \nu_{zy} & \nu_{zz} \end{pmatrix}, \quad (23)$$

and the coefficients of the thermal emf are

$$\alpha_{ik}=\frac{1}{T}\begin{pmatrix} \nu_{xx} & -\gamma_0\nu_{yx}-\vartheta\gamma_0^{-1}\nu_{yx}^{(1)} & \nu_{zx}-\vartheta\gamma_0^{-1}\nu_{zx}^{(1)} \\ -\gamma_0\nu_{xy} & \nu_{yy} & \nu_{zy} \\ -\gamma_0\nu_{xz} & -\gamma_0\nu_{yz}+\vartheta\nu_{yz}^{(1)} & \nu_{zz} \end{pmatrix}. \quad (24)$$

In the same way we have found the form of the asymptotic behavior of the thermoelectric coefficients near the singularities of all three types.

We must make a comment on the asymptotic behavior of the heat conductivity coefficients. Azbel', Kaganov, and Lifshitz[3] have considered the heat conductivity of metals with closed surfaces. In metals with open surfaces the heat conductivity tensor κ_{ik} behaves completely analogously to the electrical conductivity σ_{ik} in its dependence on **H**. This is seen immediately by considering how κ_{ik} is composed of a_{ik}, b_{ik}, and c_{ik}.

The authors are grateful to Academician L. D. Landau for discussing the work. Yu. A. Bychkov is also grateful to I. M. Khalatnikov and I. M. Lifshitz for valuable discussion.

[1] Lifshitz, Azbel', and Kaganov, J. Exptl. Theoret. Phys. (U.S.S.R.) **31**, 63 (1956), Soviet Phys. JETP **4**, 41 (1957).

[2] I. M. Lifshitz and V. G. Peschanskiĭ, J. Exptl. Theoret. Phys. (U.S.S.R.) **35**, 1251 (1958), Soviet Phys. JETP **8**, 875 (1959).

[3] Azbel', Kaganov, and Lifshitz, J. Exptl. Theoret. Phys. (U.S.S.R.) **32**, 1188 (1957), Soviet Phys. JETP **5**, 967 (1957).

[4] L. D. Landau and E. M. Lifshitz, Электродинамика сплошных сред (Electrodynamics of Continuous Media), Gostekhizdat, 1957.

Translated by R. Berman
94

GROUND STATES OF NONSPHERICAL ODD NUCLEI ACCORDING TO THE INDEPENDENT PARTICLE MODEL

D. A. ZAIKIN

P. N. Lebedev Physics Institute, Academy of Sciences U.S.S.R.

Submitted to JETP editor April 2, 1959

J. Exptl. Theoret. Phys. (U.S.S.R.) **37**, 540-545 (1959)

The level scheme of nucleons in a spheroidal well with vertical walls is computed by using the asymptotic expansions of spheroidal wave functions. The results obtained are in good agreement with the experimental data on the spins and parities of the ground and isomeric states of nonspherical odd nuclei.

THE energy level scheme for nucleons in a nonspherical axially symmetric nucleus proposed by Nilsson[1] agrees satisfactorily with experiment. Nilsson's scheme was obtained on the assumption that the effective field in which the nucleons move is described by the potential of an anisotropic oscillator. As is well known the approximation of a harmonic oscillator for the self-consistent nuclear field is good only for light nuclei, whereas for heavy ones the self-consistent potential is closer to that of a rectangular well (cf., for example, reference[2]). Therefore Nilsson did not simply use the harmonic oscillator potential in constructing his scheme, but added to the Hamiltonian a term proportional to the operator of the square of the orbital angular momentum of the nucleon, and thereby made his potential closer to that of a rectangular well.

Nevertheless, it is of interest to construct an energy level scheme for nucleons in a rectangular spheroidal well. This problem entails considerable mathematical difficulties. It was first solved by Moszkowski[3] for the lowest states of the nucleons by the perturbation theory method. Later Gottfried[4] constructed an energy level scheme for nucleons in a rectangular deformed well. In his paper Gottfried expanded the potential in powers of a parameter that describes the deviation from the spherical shape, and starting with the spherically symmetrical case as the zero-order approximation, he solved the secular equation which refers to all the nucleon states under consideration. However, as was pointed out by Kumar and Preston,[5] in doing this he incorrectly took into account terms proportional to the square of the deformation, which is important in the case of nuclei whose shape deviates appreciably from spherical. Moreover, in his calculations Gottfried did not take into account the existence of the continuous spectrum which, certainly in the case of the higher lying levels, may affect the result appreciably. Finally, the choice of the zero-order approximation for the functions was no improvement, and this, of course, also adversely affected the convergence of the method, particularly for large values of the parameter describing the deviation from the spherical shape. Thus, it has become necessary to carry out the calculation of the energy levels of nucleons in a rectangular spheroidal well by a method which would be applicable to large deformations and to high nucleon energy levels.

Such a method was proposed in the preceding papers[6,7] by the present author. The problem of finding the energy levels of nucleons of mass M in a rectangular potential well having the spatial shape of an ellipsoid of revolution reduces, as is well known, to the solution of the Schrödinger equation

$$\left\{-\frac{\hbar^2}{2M}\Delta + V(\mathbf{r}) - \frac{\varkappa}{M^2c^2}\hat{\mathbf{s}}\left[\nabla V(\mathbf{r})\cdot\hat{\mathbf{p}}\right]\right\}\psi = E\psi, \qquad (1)$$

where c is the velocity of light, $\hat{\mathbf{s}}$ and $\hat{\mathbf{p}}$ are the nucleon spin and momentum operators, κ is a dimensionless constant. The potential V(r) has the form:

$$V(\mathbf{r}) = \begin{cases} 0 \text{ within the ellipsoid } (x^2+y^2)/a^2 + z^2/b^2 = 1 \\ V_0 \text{ outside the ellipsoid} \end{cases} \qquad (2)$$

The semi-axes of the ellipsoid a and b are related by the condition that its volume is independent of the degree of deviation from the spherical shape:

$$a^2 b = r_0^3, \qquad (3)$$

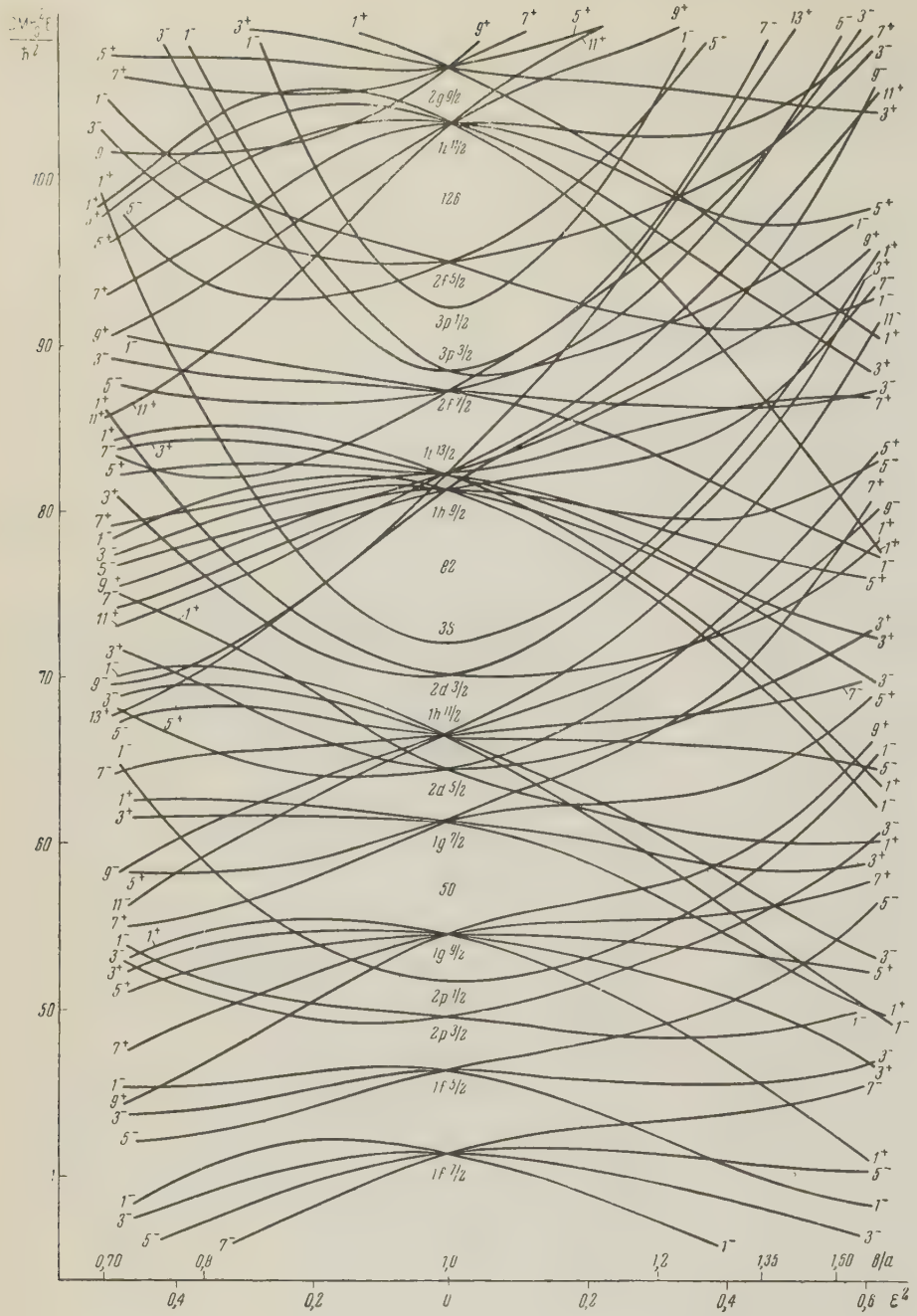

Nucleon energy level scheme in a rectangular spheroidal well. Along the horizontal axis are plotted the square of the eccentricity of the ellipsoid ε^2 and the corresponding ratio of the axes b/a, along the vertical axis is plotted the nucleon energy in units of $\hbar^2/2Mr_0^2$. The numbers opposite the curves denote twice the value of the component of the angular momentum along the symmetry axis, while the sign signifies the parity of the state.

where r_0 is the radius of a sphere of equal volume.

The solution of Eq. (1) can be expressed in terms of spheroidal functions for which asymptotic expansions have been obtained in inverse powers of the parameter $\gamma = f(2ME)^{1/2}/\hbar$, where f is half the distance between the foci of the ellipsoid (2). The details of the calculation and numerical estimates of the range of applicability of this method are described in references 6 and 7.

Numerical calculations of the nucleon energy levels were carried out on the "Ural" electronic computer of the P. N. Lebedev Physics Institute for values of the constant V_0 equal to 35, 42 and 50 Mev. The spin-orbit coupling constant κ was fixed by the condition that in the case of a spherically symmetric well the best approximation should be obtained to the scheme of Klinkenberg[8] arrived at by means of an analysis of experimental data on the basis of the shell model. This condition is best of all satisfied by the value $\kappa = 30$. The constant r_0 was everywhere taken equal to 8.4×10^{-13} cm (which corresponds to $A \approx 200$ in the formula $r_0 = 1.4 \times 10^{-13} A^{1/3}$ cm, where A is the atomic weight). The calculations were carried out for values of the ratio of the semi-axes b/a taken

TABLE I

Nucleus	β	I_0^{ω}		State of the odd nucleon $\Omega^{w}(n, l, j)$			Notes
		experiment	theory	Z scheme (present work)	N scheme[1]	G scheme[4]	
1	2	3	4	5	6	7	8
Eu^{153}	0.4	$5/2^+$	$5/2^+$	$5/2^+ (1g\,7/2)$	$5/2^+ (1g\,7/2)$	$5/2^+ (1g\,7/2)$	a
Gd^{155}	0.3	$3/2^-$	$3/2\pm$	$3/2^+ (1i\,13/2)$ or $3/2^- (1h\,9/2)$	$3/2^+ (1i\,13/2)$ or $3/2^- (1h\,9/2)$	$3/2^+ (1i\,13/2)$ or $3/2^- (1h\,9/2)$	
Gd^{157}	0.3	$3/2^-$	$3/2\pm$	$3/2^+ (1i\,13/2)$ or $3/2^- (1h\,9/2)$	$3/2^+ (1i\,13/2)$ or $3/2^- (1h\,9/2)$	$3/2^+ (1i\,13/2)$ or $3/2^- (1h\,9/2)$	
Tb^{159}	0.4	$3/2^+$	$3/2^+$	$3/2^+ (2d\,5/2)$	$3/2^+ (2d\,5/2)$	$3/2^+ (2d\,5/2)$	a
Dy^{161}	0.2	$5/2^+$	$5/2^+$	$5/2^+ (1i\,13/2)$	$5/2^+ (1i\,13/2)$	$5/2^+ (1i\,13/2)$	
Dy^{163}	0.2	$5/2^-$	$5/2^-$	$5/2^- (1h\,9/2)$	$5/2^- (1h\,9/2)$	$5/2^- (1h\,9/2)$	
Er^{167}	0.4	$7/2^+$	$7/2^+$	$7/2^+ (1i\,13/2)$	$7/2^+ (1i\,13/2)$	$7/2^+ (1i\,13/2)$	
Tm^{169}	0.3	$1/2^+$	$1/2^+$	$1/2^+ (2d\,3/2)$	$1/2^+ (2d\,3/2)$	$1/2^+ (2d\,3/2)$	b
Yb^{173}	0.3	$5/2^-$	$5/2^-$	$5/2^- (2f\,7/2)$	$5/2^- (1h\,9/2)$	$5/2^- (1h\,11/2)$	
Lu^{175}	0.4	$7/2^+$	$7/2^+$	$7/2^+ (1g\,7/2)$	$7/2^+ (1g\,7/2)$	$7/2^- (1h\,11/2)$	c
Hf^{177}	0.3	$7/2^-$	$7/2^-$	$7/2^- (1h\,9/2)$	$7/2^- (1h\,9/2)$	$7/2^- (2f\,7/2)$	
Hf^{179}	0.2	$9/2^+$	$9/2^+$	$9/2^+ (1i\,13/2)$	$9/2^+ (1i\,13/2)$	$9/2^+ (1i\,13/2)$	
Ta^{181}	0.3	$7/2^+$	$7/2^+$	$7/2^+ (1g\,7/2)$	$7/2^+ (1g\,7/2)$	$7/2^+ (1g\,7/2)$	a
W^{183}	0.2	$1/2^-$	$1/2^-$	$1/2^- (2f\,5/2)$	$1/2^- (2f\,5/2)$	?	d,e
$Re^{185,187}$	0.2	$5/2^+$	$5/2^+$	$5/2^+ (2d\,5/2)$	$5/2^+ (2d\,5/2)$	$5/2^+ (2d\,5/2)$	
Os^{189}	0.1	$3/2$	$3/2^-$	$3/2^- (3p\,3/2)$	$3/2^- (3p\,3/2)$	$1/2^- (3p\,3/2)$	f
$Ir^{191,193}$	0.2	$3/2^+$	$3/2^+$	$3/2^+ (2d\,3/2)$	$3/2^+ (2d\,3/2)$	$3/2^- (2f\,7/2)$	g
Ac^{227}	0.2	$3/2$	$3/2\pm$	$3/2^+ (1i\,13/2)$ or $3/2^- (1h\,9/2)$	$3/2^+ (1i\,13/2)$ or $3/2^- (1h\,9/2)$	$3/2^+ (1i\,13/2)$ or $3/2^- (1h\,9/2)$	h
U^{233}	±0.3	$5/2^+$	$5/2^+$	$5/2^- (2g\,9/2)$	$5/2^+ (1i\,11/2)$ or $5/2^+ (2g\,9/2)$	—	i
U^{235}	±0.3	$7/2$	$7/2^+$	$7/2^+ (2g\,9/2)$ or $7/2^+ (2g\,7/2)$	$7/2^+ (2g\,9/2)$ or $7/2^- (1j\,15/2)$	—	j
Np^{237}	±0.2	$5/2^+$	$5/2^+$	$5/2^+ (1i\,13/2)$	$5/2^+ (1i\,13/2)$	$5/2^+ (1i\,13/2)$	k
Pu^{239}	±0.2	$1/2^+$	$1/2^+$	$1/2^+ (2g\,7/2)$ or $1/2^+ (2g\,9/2)$	$1/2^+ (3d\,5/2)$ or $1/2^+ (2g\,9/2)$	—	l,m
$Am^{241,243}$	±0.3	$5/2^-$	$5/2^-$	$5/2^- (1h\,9/2)$	$5/2^- (2f\,7/2)$ or $5/2^- (1h\,9/2)$	$5/2^- (1h\,9/2)$	n

a. The odd nucleon state shown in the table which agrees with experiment is obtained in the N scheme if one supposes that the deformation is larger by a factor 1.5 or 2 than the experimentally observed one.

b. The coupling disruption factor in the Z scheme; $a_{theor} = -0.67$, $a_{exp} = -0.76$.

c. In the G scheme it is more natural to take $7/2^+(1g\,7/2)$, than $7/2^-(1h\,11/2)$ given in reference 4.

d. The coupling disruption factor in the Z scheme; $a_{theor} = -0.31$, $a_{exp} = -0.18$.

e. In the G scheme, no tolerable agreement with experiment can be obtained.

f. The result of the G scheme contradicts the experimental value of the spin of the ground state of Os^{189}.

g. In the G scheme it is more natural to take $3/2^+(2d\,3/2)$ than $3/2^-(2f\,7/2)$ given in reference 4.

h. As to the sign of the quadropole moment of Ac^{227}, see reference 17.

i. The identification of the state of the odd nucleon in the Z and N schemes does not depend on the sign of the deformation, however, in the N scheme the identification shown above is difficult to obtain for both states and for both signs of the deformation.

j. In the Z scheme the state $7/2^+(2g\,9/2)$ is obtained in the case $\beta > 0$, while $7/2^+(2g\,7/2)$ is obtained in the case $\beta < 0$. The states shown in the table for the N scheme refer to the case $\beta > 0$; in the case $\beta < 0$ the state of the odd nucleon is identified as $7/2^+(1i\,11/2)$.

k. In all three schemes the identification shown above for the state of the odd nucleon is more natural for $\beta > 0$, than for $\beta < 0$.

l. For the Z and N schemes the first of the states shown above refers to $\beta > 0$, the second refers to $\beta < 0$. In the Z scheme for $\beta > 0$ the coupling disruption factor is $a_{theor} = -0.61$, for $\beta < 0$ $a_{theor} = -0.64$, $a_{exp} = -0.58$.

m. In the case $\beta < 0$ the Z and N schemes admit the identification of the ground state as $1/2^-(3p\,1/2)$.

n. In all three schemes the result does not depend on the sign of the deformation.

TABLE II

Nucleus	β	I_0^W of the isomeric state (experiment)	State of the odd nucleon $\Omega^W(n, l, j)$			Notes
			Z scheme (present work)	N scheme[1]	G scheme[4]	
1	2	3	4	5	6	7
Er^{167}	0.4	$1/2^-$	$1/2^-(2f\,5/2)$	$1/2^-(2p\,3/2)$	$1/2^-(2f\,5/2)$	
Tm^{169}	0.3	$7/2^+$ and $7/2^-$	$7/2^+(1g\,7/2)$ and $7/2^-(1h\,11/2)$	$7/2^+(1g\,7/2)$ and $7/2^-(1h\,11/2)$	$7/2^+(1g\,7/2)$	b
Hf^{179}	0.2	$1/2^-$	$1/2^-(2f\,5/2)$	$1/2^-(2f\,5/2)$	$1/2^-(2f\,5/2)$	
W^{183}	0.2	unknown	$11/2^+(1i\,13/2)$	$11/2^+(1i\,13/2)$	?	a
Os^{189}	0.1	unknown	$13/2^+(1i\,13/2)$	$13/2^+(1\,i\,13/2)$	?	a
$Ir^{191,193}$	0.2	$11/2^-$	$11/2^-(1h\,11/2)$	$9/2^-(1h\,11/2)$	$11/2\,(1h\,11/2)$	
Ac^{227}	0.2	$1/2$	$1/2^+(3s\,1/2)$ or $1/2^-(2f\,7/2)$	$1/2^-(3p\,3/2)$	$1/2^-(2f\,5/2)$	
U^{235}	±0.3	$1/2^+$	$1/2^+(2g\,7/2)$ or $1/2^+(2g\,9/2)$	$1/2^+(3d\,5/2)$ or $1/2^+(2g\,9/2)$	—	c
Np^{237}	±0.2	$5/2^-$	$5/2^-(1h\,9/2)$	$5/2^-(1h\,9/2)$ or $5/2^-(2f\,7/2)$	$5/2^-(1h\,9/2)$	d

a. In the G scheme no isomeric state is obtained.

b. In the case of Tm^{169} two close long lived states are observed experimentally.

c. In the case of the Z and N schemes the first of the states shown refers to $\beta > 0$, while the second refers to $\beta < 0$. In the case $\beta < 0$ both schemes permit the isomeric state to be identified as $\frac{1}{2}(3p\,\frac{1}{2})$.

d. In all three schemes the identification shown is more natural in the case $\beta > 0$.

equal to 0.60; 0.70; 0.80 (oblate ellipsoid of revolution) and 1.20; 1.25; 1.35; 1.50; 1.70; 2.00 (prolate ellipsoid of revolution). For a spherically symmetric well the levels were calculated by the method described in reference 2. As shown by calculations, the behavior of the energy levels and their order do not depend strongly on the magnitude of the constant V_0, within the investigated limits of variation. A more significant effect on the order of levels was produced by variation of the spin-orbit coupling constant κ. In the diagram we show the nucleon energy level scheme in a rectangular spheroidal well calculated for the values $V_0 = 42$ Mev and $\kappa = 30$.

A comparison of the level scheme obtained here with Nilsson's[1] and Gottfried's[4] schemes shows that the behavior of the nucleon levels as a function of the deformation is qualitatively the same, but that there are certain differences of detail.

The results obtained were compared with experimental values of the spins and parities of the ground states of non-spherical odd nuclei. As usual it was assumed that the ground state of such nuclei is determined by the state of the odd nucleon, with the spin I_0 being equal to the component of Ω for this nucleon along the nuclear symmetry axis, with the exception of the case $\Omega = \frac{1}{2}$ when for the determination of I_0 the so-called "coupling disruption factor" was computed (cf. reference 9, and also reference 1). The experimental values of the spins and the parities of the ground states of the nuclei were taken from the tables of Seaborg et al.[10] The values of the parameter β describing the deviation from the spherical shape were calculated from the experimentally determined values of the quadrupole moments.[10,11] The results of comparison with experiment are shown in Table I, which also gives a comparison of the same quantities with Nilsson's[1] and Gottfried's results.

It has been established experimentally that many of the nuclei considered in this paper have low lying isomeric states. These states can be identified according to our scheme. The results of such identification are shown in Table II.

From the results given in the tables it may be seen that the nucleon level scheme obtained in this paper is in good agreement with the experimentally found values of the spins and parities of the ground states and of the low lying isomeric states of nonspherical odd nuclei. In our case the agreement is better than in Gottfried's case.[4]

The present level scheme, generally speaking, gives as good an agreement with experiment as does Nilsson's scheme;[1] at the same time, it is free of the defect of Nilsson's scheme associated with the fact that to make the latter agree with data on the ground states of a number of nuclei it is necessary to assume for these nuclei considerably larger values of the parameter that describes

the deviation from the spherical shape than are found experimentally.

A direct comparison of our nucleon level scheme with Nilsson's scheme shows that certain differences in level order existing in the spherical case, which are due to the different choice of potential, gradually disappear as the parameter β (describing the deviation from spherical shape) is increased. In the case of large deviations from the spherical shape, the order of levels in both schemes practically coincides. This fact indicates that the results of the shell model applied to strongly deformed nuclei are much less critical to the choice of the potential shape than in the case of spherical wells.

One should particularly note the odd isotopes of the actinides for which (with the exception of Ac^{227}) the sign of the quadrupole moment is either not known or is not known sufficiently reliably, and consequently the same uncertainty exists with respect to the sign of the parameter describing the deviation from the spherical shape. Neither our scheme nor Nilsson's scheme, contradicts the assumption of an oblate shape for some of these nuclei.

Let us investigate the conclusions to which we would be led by such an assumption in the case of U^{235}. First we note that it is in agreement with the measurements of B. Bleaney et al.,[12] who obtained for U^{235} a negative quadrupole moment. As seen from Table II, in this case (i.e. for $\beta < 0$) neither our scheme nor Nilsson's scheme contradicts the assumption that the isomeric state of U^{235} has negative parity (cf. note "c" of Table II). However, such an assumption would lead to changes in the properties of low lying levels of U^{235} and Pu^{239} from those adopted at present.[10,13]. Firstly, on the basis of data[13,14] on the multiplicity of the γ-transitions in U^{235}, we would have to change the parities of the low lying levels of this nucleus in the schemes of references 10 and 13. Secondly, on the basis of the data on the α-decay of Pu^{239}, one should expect that since the spins of the isomeric state of U^{235} and of the ground state of Pu^{239} coincide then, apparently, their parities also coincide. We should therefore ascribe $\frac{1}{2}^-$ to the ground state of Pu^{239}. According to both our scheme and Nilsson's scheme, such a possibility can be realized if the Pu^{239} nucleus is oblate (cf. note "m" to Table I). In this case, just as in the case of U^{235}, on taking into account the data[16] on the multiplicity of the γ-transitions in Pu^{239} one would also have to change the parities of the low lying levels of Pu^{239} in the schemes of references 10 and 13. However, the changes noted above would not contradict the available experimental data obtained from investigations of mutual transformations of the actinides (a detailed bibliography on this subject is contained in references 10 and 13). Thus, the problem of the shape of the actinides may be solved only by reliable measurement of the signs of their quadrupole moments.

[1] S. G. Nilsson, Dan. Mat.-fys. Medd. **29**, 16 (1955).

[2] W. Heisenberg, Theory of the Atomic Nucleus (Russian transl.) IIL, 1953 (Theorie des Atomkerns, Göttingen, 1951).

[3] S. A. Moszkowski, Phys. Rev. **99**, 803 (1955).

[4] K. Gottfried, Phys. Rev. **103**, 1017 (1956).

[5] K. Kumar and M. A. Preston, Phys. Rev. **107**, 1099 (1957).

[6] D. A. Zaikin, J. Exptl. Theoret. Phys. (U.S.S.R.) **33**, 1049 (1957), Soviet Phys. JETP **6**, 808 (1958).

[7] D. A. Zaikin, сб. Ядерные реакции при малых и средних энергиях (Collection: Nuclear Reactions at Low and Medium Energies) Acad. Sci. U.S.S.R., 1958, p. 579.

[8] P. F. A. Klinkenberg, Revs. Modern Phys. **24**, 63 (1952).

[9] A. Bohr and B. Mottelson, Dan. Mat.-fys. Medd. **27**, 16 (1953).

[10] Strominger, Hollander and Seaborg, Revs. Modern Phys. **30**, 585 (1958).

[11] C. H. Townes, Handb. d. Phys. **38**, 377 (1958).

[12] Bleaney, Hutchinson, Flewellyn, and Pope, Proc. Phys. Soc. B69, 1167 (1956).

[13] B. S. Dzhelepov and L. K. Peker, Схемы распада радиоактивных ядер (Decay Schemes of Radioactive Nuclei) Acad. of Sci. U.S.S.R., 1958.

[14] Gol'din, Grishuk, and Tret'yakov. Тезисы 8-го совещания по ядерной спектроскопии. (Abstracts of the 8th Conference on Nuclear Spectroscopy) Acad. Sci. U.S.S.R., 1958, p. 38.

[15] Novikova, Kondrat'ev, Sobolev, and Gol'din, J. Exptl. Theoret. Phys. (U.S.S.R.) **32**, 1018 (1957), Soviet Phys. JETP **5**, 832 (1957).

[16] Hollander, Smith, and Mihelich, Phys. Rev. **102**, 740 (1956).

[17] Ferd, Tomkins and Meggers, Phys. Rev. **111**, 747 (1958).

Translated by G. Volkoff
95

Letters to the Editor

ALPHA SPECTRUM OF THE NATURAL SAMARIUM ISOTOPE MIXTURE

A. A. VOROB'EV, A. P. KOMAR, V. A. KOROLEV and G. E. SOLYAKIN

Leningrad Physico-Technical Inst., Acad. Sci. U.S.S.R.

Submitted to JETP editor March 26, 1959

J. Exptl. Theoret. Phys. (U.S.S.R.) **37**, 546-548 (August, 1959)

1. Alpha Spectrum of Sm^{147}. The alpha spectrum of the natural mixture of Sm isotopes has been studied by means of a gridded pulse ionization chamber functioning by electron collection. The chamber was filled with chemically pure argon (99.9% A, 0.02% O_2, 0.08% N_2, and 0.005% CO_2).

The alpha-particle source, with an area of 400 cm^2, furnished a counting rate of 8 pulses per minute. However, to improve the quality of the spectrum, considerable electron collimation[1] was introduced, depressing the counting rate to 2 pulses per mintue. The measurements were made continuously during the course of 50 hours. The stability of the amplification coefficient requisite over the entire range under these conditions was assured by a forced stabilization scheme. The alpha spectrum obtained is presented in Fig. 1.

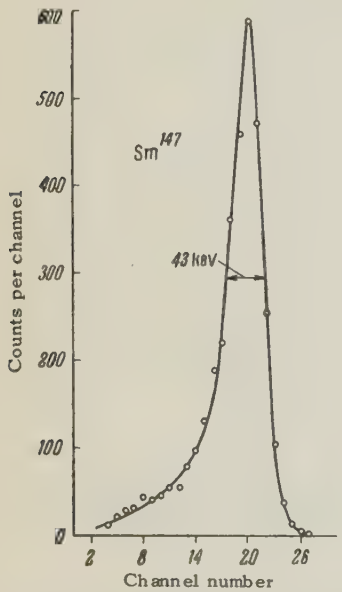

FIG. 1. Alpha-particle spectrum of Sm^{147}, obtained with electron collimation.

The half-width of the line amounts to 43 Kev. In work with intense alpha-emitters such as U^{234}, the half-width value is 30 Kev. The deterioration of the resolving power is connected with the large thickness of the samarium source. At the resolution attained, we observed no other groups of alpha particles radiated by other samarium isotopes or due to the fine structure of Sm^{147}.

2. Energy Measurement of Sm^{147} Alpha-Particles. Strictly speaking, the ionization chamber measures not the alpha-particle energy, but the ionization produced by the alpha particles in the chamber gas. From Fano's theoretical work[2] it follows that with argon these two quantities must be proportional. Experimentally,[3] such proportionality is observed in the high-energy range of alpha particles (> 4 Mev). Data[4,5] for this range are contradictory and inaccurate. It would therefore be interesting to measure, along with the ionization, the energy of the Sm^{147} alpha particles with a modern high-aperture spectrometer.

In our experiment the ionization measurement was executed in the following manner. U^{234} with an alpha-particle energy of 4.768 Mev served as a reference emitter. To eliminate the influence of the nonlinearity of the electronic apparatus, the amplitudes of the pulses from the test and reference emitters were compared by means of a generator which delivered input pulses to the preamplifier, and the amplitudes of these pulses were adjusted in such a way that the output value was exactly equal first to the pulses from the alpha particles of the test emitter and then to those from the reference emitter. The amplitude of the generated pulses was measured at the preamplifier input by means of a special instrument with an accuracy of 0.01 to 0.005%. After applying corrections for imperfect shielding of the chamber grid and for the rise time of the alpha pulse (a total correction of 10 Kev), the value obtained was $E_\alpha = 2.19 \pm 0.01$ Mev. Jesse and Sadauskis[6] give $E_\alpha = 2.18 \pm 0.02$ Mev.

3. Estimated Upper Limit of Sm^{146} Abundance in Natural Mixture. From previous work[7] the energy of Sm^{146} alpha particles is known to be ~ 2.55 Mev. The spectrum of natural samarium alpha particles in the 2.0 — 2.8 Mev energy range is shown in Fig. 2. To reduce the background effect, the operating volume of the ionization chamber was specially limited in such a way that the ionization produced outside this space did not register in the counting device.

Furthermore, by discriminating the pulses according to the time of their appearance at the collecting electrode and at the high-voltage electrode, it was possible to reduce considerably the cosmic radiation background and to exclude pulses due to alpha particles emitted by the chamber grid. The over-all background for the 1.5 — 2.5 Mev range amounted to ~ 1 pulse/hour.

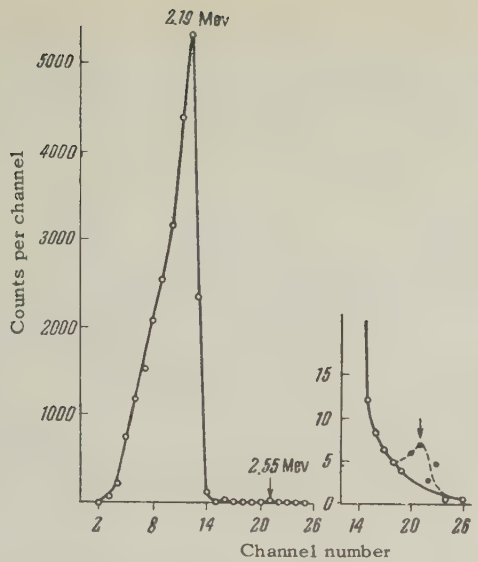

FIG. 2. Spectrum of alpha particles from the natural mixture of samarium isotopes (without collimation). At the right – part of the spectrum on a magnified scale. The observed counts in the energy range for the Sm^{146} alpha particles are indicated by black dots. The areal difference between the solid and dashed curves was employed to estimate the upper limit of the Sm^{146} content.

The number of fixed alpha particles at the decay energy of Sm^{146} does not exceed the background count. Comparing the count of pulses from Sm^{147} alpha particles possessing an energy of 2.19 Mev with the count of pulses which can be triggered by alpha particles having an energy of 2.55 Mev and taking into account the half-lives of these isotopes, viz., $T(Sm^{147}) = 10^{12}$ years and $T(Sm^{146}) = 5 \times 10^7$ years, (with allowance for the respective percentage contents in the natural isotopic mixture) we deduce that the natural mixture of samarium isotopes contains not less than $2.5 \times 10^{-6}\%$ of Sm^{146}.

According to the latest data of mass-spectrometric analysis[8] this value has been determined as equal to $8 \times 10^{-5}\%$.

[1] B. A. Bocharov, A. A. Vorob'ev, and A. P. Komar, Izv. Akad. Nauk SSSR, Ser. Fiz. **20**, 1455 (1956), Columbia Tech. Transl. p. 1331.

[2] U. Fano, Phys. Rev. **70**, 44 (1946).

[3] Harvey, Jackson, Eastwood, and Hanna, Can. J. Phys. **35**, 258 (1957).

[4] Facchini, Gatti, and Germagnoli, Phys. Rev. **81**, 475 (1951).

[5] Rhodes, Franzen, and Stephens, Phys. Rev. **87**, 141 (1952).

[6] W. P. Jesse and J. Sadauskis, Phys. Rev. **78**, 1 (1950).

[7] D. C. Dunlavey and G. T. Seaborg, Phys. Rev. **92**, 206 (1953).

[8] Collins, Rourke, and White, Phys. Rev. **105**, 196 (1957).

Translated by J. E. Viscardi
96

USE OF THE (d, p) REACTION TO EXCITE STATES WITH LARGE SPINS

B. G. NEUDACHIN, I. B. TEPLOV, and A. F. TULINOV

Inst. Nuc. Phys., Moscow State Univ.

Submitted to JETP editor May 8, 1959

J. Exptl. Theoret. Phys. (U.S.S.R.) **37**, 548-550 (August, 1959)

IT has been proposed to use the inelastic scattering of complex nuclei for the excitation of nuclear states with large spins.[1] We desire to call attention to the fact that (d, p) reactions can be effectively applied to light nuclei for the same purpose. In this case, not only can single-particle levels with large spins be excited, but, thanks to peculiarities of the angular distributions, it is possible to segregate such levels from the rest.

For the ordinary stripping process[2] the angular momentum summation rule has the following form

$$\mathbf{J}_i + \mathbf{j}_n = \mathbf{J}_f, \quad (\Delta J)_{max} = j, \tag{1}$$

where $\mathbf{J}_i$ and $\mathbf{J}_f$ are the initial and final states, and $\mathbf{j}_n$ is the total momentum of the capturing nucleon, determined by the shell structure of the nucleus. Ordinary stripping is forbidden if condition (1) is not fulfilled. In this event the following processes may occur, also characterized by differential cross-section peaks at small angles: stripping with change of spin orientation (spin-flip),[3] and the process of direct ejection of a proton from the nucleus with capture of the deuteron in the bound state ("knockout").[4,6] For the latter process we may write

$$\mathbf{J}_i + \mathbf{j}_{p_1} + \mathbf{j}_{n_1} = \mathbf{J}_f + \mathbf{j}_{p_2}, \quad (\Delta J)_{max} = 3j; \tag{2}$$

where $\mathbf{j}_{p_1}$ and $\mathbf{j}_{n_1}$ refer to the proton and neutron in the incident deuteron, and $\mathbf{j}_{p_2}$ to the expelled proton. From (1) and (2) it is evident that in a knockout process the difference between the spins of the initial and final states, ΔJ, can attain considerably larger values than in ordinary stripping.

As an example illustrating the general features of the knockout process, we calculated the angular distribution of the neutrons evolved as a result of

this process in the reaction $B^{10}(d, p)B^{11*}$ (E_{exc} = 2.14 Mev, $J^* = \frac{1}{2}^-$), for which ordinary stripping is forbidden. The calculation was carried out for deuteron energies of 4, 8, and 12 Mev ($R = 4.8 \times 10^{-13}$ cm), using the formula from reference 7. The computed results are exhibited in Fig. 1, wherein Butler's curves are reproduced for comparison. From these graphs it ensues that at all energies the maximum region is narrower for ordinary stripping than for the knockout process. Computed results for angular distributions in the same process were presented recently by Evans and French.[5] The curve obtained for E_d = 7.7 Mev, $R = 5 \times 10^{-13}$ cm, is shown in Fig. 1b. Unfortunately, formulas for the cross section are not given in reference 7, so that it is impossible to compare the calculation procedures.

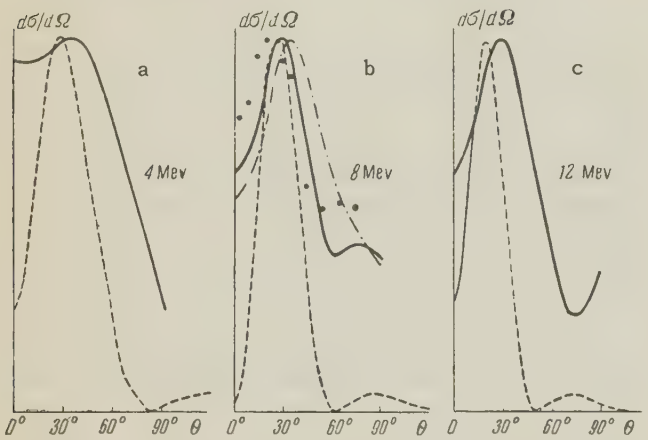

FIG. 1. Angular distribution of protons in the $B^{10}(d, p)B^{11*}$ reaction (the cross section is expressed in relative units). The solid curve was calculated in the present work, the dot-dash curve was calculated in reference 5, the dash curve is by Butler, and the experimental points are from reference 6. The Mev values on the charts correspond to the incident deuteron energy.

In Fig. 1b the dots represent the experimental data of Evans and Parkinson.[8] It is evident from the plot that the curve calculated for the knockout process agrees approximately with the experimental results, especially if we add some isotopic background, which can be due to a mechanism connected with the formation of a compound nucleus and with the "stripping of heavy particles."[4,9,10] At the same time it must be borne in mind that good accord between the calculated and experimental angular distributions should not be expected, since flip-spin is possible in this reaction. For the latter process the angular-momentum summation rule can be written in the form

$$\mathbf{J}_i + \mathbf{j}_n + \mathbf{s}_p + \mathbf{s}_p = \mathbf{J}_f, \quad (\Delta J)_{max} = j + 1, \qquad (3)$$

where s_p is the proton spin. According to estimates by Bowcock,[3] the angular distribution for this process also differs from that for ordinary stripping and agrees well with the experimental data.

Thus the task of detecting states with large spins (more precisely, states for which $\Delta J > j$) resolves itself into the most accurate possible determination of the differential cross-section peak and the segregation of the large-spin levels in relation to the location and width of the peak. At sufficiently high deuteron energies it is still possible to study such peaks experimentally in angular distributions which are several tenfolds smaller than for ordinary stripping and only a few times larger than the isotopic background level.

The knockout process, like stripping with change of spin orientation in the (d, p) reaction, is considerably more sensitive to the Coulomb field than the ordinary stripping process, since in the latter case the proton remains outside the limits of the nucleus. Furthermore, the orbital momenta of the deuteron, different from zero, play a substantial role in the excitation of states with large spins. For these reasons, in order to excite levels with large spins it is necessary to use deuterons with energies several times greater than the Coulomb-barrier height ($E_d \gtrsim 15$ Mev for $Z \sim 12$, $E_d \gtrsim 8$ Mev for $Z \sim 5$). At lower energies the forward peak will be suppressed. The reaction $Mg^{24}(d, p)Mg^{25*}$ (E_{exc} = 1.61 Mev, $J^* = \frac{7}{2}^+$),[11] for which Fig. 2 shows the experimental results at 8 Mev, can serve as an example of this.

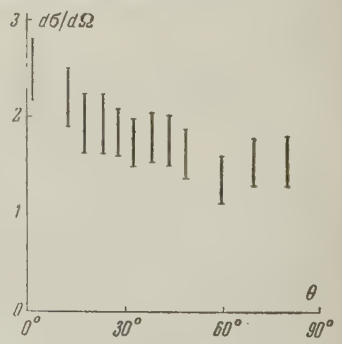

FIG. 2. Angular distribution of protons in the reaction $Mg^{24}(d, p)Mg^{25*}$.

The following reactions may be cited as examples of the possible utilization of the proposed method: a) $Li^6(d, p)Li^{7*}$, $J^* = \frac{7}{2}^-$, $E_{exc} \sim 4$ Mev;[12,13] b) $C^{12}(p, d)C^{11*}$, $J^* = \frac{5}{2}^-$, $\frac{7}{2}^-$, and $\frac{9}{2}^-$ in the excitation energy range 3 to 10 Mev;[13] c) $B^{11}(p, d)B^{10*}$, $J^* = 4^-$, $E_{exc} \sim 6$ Mev;[13] d) $C^{13}(p, d)C^{12*}$, $J^* = 4^+$, $E_{exc} \sim 8$ Mev.[13]

In conclusion we emphasize the fact that the

investigation of states with large spins by the proposed method possesses advantages over other means [reactions with complex nuclei, (α, p) reactions, and others], since the angular distribution features of the (d, p) reactions are revealed with significantly greater clarity.

[1] V. I. Gol'danskiĭ, J. Exptl. Theoret. Phys. (U.S.S.R.) **36**, 526 (1959), Soviet Phys. JETP **9**, 366 (1959).

[2] S. T. Butler, Proc. Roy. Soc. **A208**, 559 (1951).

[3] J. E. Bowcock, Phys. Rev. **112**, 923 (1958).

[4] Neudachin, Teplov, and Shevchenko, J. Exptl. Theoret. Phys. (U.S.S.R.) **36**, 850 (1959), Soviet Phys. JETP **9**, 599 (1959).

[5] N. T. S. Evans and A. P. French, Phys. Rev. **109**, 1272 (1958).

[6] Austern, Butler, and McManus, Phys. Rev. **92**, 350 (1953).

[7] V. G. Neudachin, J. Exptl. Theoret. Phys. (U.S.S.R.) **35**, 1165 (1958), Soviet Phys. JETP **8**, 815 (1959).

[8] N. T. S. Evans and W. C. Parkinson, Proc. Phys. Soc. **A67**, 684 (1954).

[9] G. Owen and L. Madansky, Phys. Rev. **105**, 1766 (1957).

[10] T. Fulton and G. Owen, Phys. Rev. **108**, 789 (1957).

[11] J. R. Holt and T. N. Marsham, Proc. Phys. Soc. **A66**, 258 (1953).

[12] V. V. Balashov, J. Exptl. Theoret. Phys. (U.S.S.R.) **36**, 1123 (1959), Soviet Phys. JETP **9**, 798 (1959).

[13] D. Kurath, Phys. Rev. **101**, 216 (1956).

Translated by J. E. Viscardi
97

THE PROTON SUBSHELL Z = 100

N. N. KOLESNIKOV and A. P. KRYLOVA

Moscow State University

Submitted to JETP editor April 1, 1959

J. Exptl. Theoret. Phys. (U.S.S.R.) **37**, 550-553 (August, 1959)

INVESTIGATIONS undertaken for the purpose of finding the new 102nd element were recently crowned with success. Groups headed by Flerov in the U.S.S.R. and by Seaborg and Ghiorso in the U.S.A. have synthesized the short-lived isotopes 102^{253} and 102^{254}, of which the first decays via emission of an 8.8-Mev alpha particle with a period from 2 to 30 seconds,[1,2] and second decays both via fission (30%) and via emission of alpha particles with energy close to 8.3 Mev with a period of approximately 3 seconds.[3] In addition, it was shown that the activity with a period of approximately 10 minutes, observed previously by the Swedish scientists,[3] was in all appearance not connected with the element 102.

We wish to call attention to the anomalous properties of the isotopes of the 102nd element, observed even on a simple graph showing the dependence of the alpha-decay energy on N (analogous to the graphs cited in reference 4). However, the observed slight excess of the alpha-decay energy of isotopes of the 102nd element over those of the neighboring even elements can be the consequence of the fact that these isotopes, which are quite far from the beta-stability curve[5] (as are, in general, all the lighter isotopes of the heavy elements), have excessive alpha-decay energies, other conditions being equal. To exclude the extraneous effect of the increase of the alpha-decay energy upon deviation from the beta-stability curve, we used the empirical dependence of the alpha-decay energy Q_α on Z, for nuclei with identical N but different Z (see reference 5):

$$Q_\alpha^*(N, Z) = Q_\alpha(N) - 0.8(Z - Z^*), \qquad (1)$$

where Z* is the value of Z corresponding to the most beta-stable nucleus for a given A, and $Q_\alpha^*(N, Z)$ is the alpha-decay energy of the nucleus (N, Z*) in Mev. One can put (see references 5 and 6)

$$Z^* = 0.356\,A + 9.1.$$

It follows from (1) that the $Q_\alpha^*(N)$ found from the experimental values of Q_α should coincide at each value of N, even in the presence of neutron shells and subshells; only in the case of proton subshells will the corresponding points deviate. Figure 1 shows the dependence of Q_α^* on N. For each of the values of N it was found here that the values of Q_α^*, calculated from different experimental values of Q_α (taken from reference 7), were almost the same. Nevertheless, to exclude the spread (which reaches ±0.15 Mev), we have drawn the curve $Q_\alpha^* = Q_\alpha^*(N)$ only through the averaged points. As can be seen from Fig. 1, in this region only two isotopes of the 102nd element lie without any doubt above the curve $Q_\alpha^* = Q_\alpha^*(N)$. Inasmuch as the isotopes of the 102nd element are converted into Fm by alpha decay, this is evidence of a reduced binding energy past Z = 100.

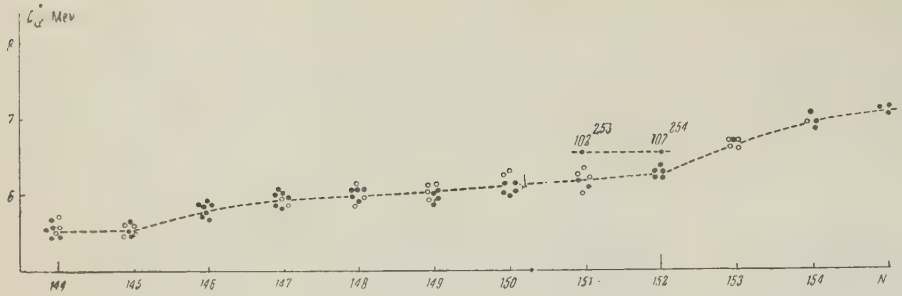

FIG. 1. Dependence of the reduced energies of alpha decay Q^*_α on the number of neutrons: ● – experimental and calculated values (Refs. 1, 2, 7), ○ – estimated values.[7]

We note that the rise of the curve $Q^*_\alpha = Q^*_\alpha(N)$ itself indicates the existence of subshells at $N = 152$ and $N = 144$, as has already been noted earlier.[6] The change in the properties of the nuclei past $Z = 100$ manifests itself also in a sharp decrease in the period of spontaneous fission at 102^{254}, which is observed when the spontaneous-fission period $\log \tau_f$ is plotted vs. Z^2/A (such a graph was plotted earlier[4]). At the same time one observes, in both isotopes of the 102nd element on the graph $\log \tau_\alpha = f(E_\alpha)$ (see Fig. 2), an increase in the forbiddenness in alpha decay.

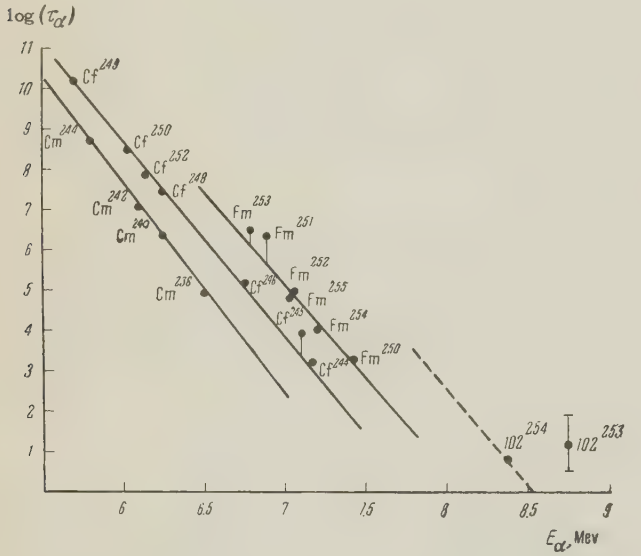

FIG. 2. Dependence of the period of alpha decay (τ_α, sec) on the energy of the alpha particles.[1,2,7]

Thus, the latest data in our possession are evidence that at $Z = 100$, apparently, there occurs either a filling of one of the subshells (which would be in accordance with the Mayer-Jensen or Nilsson scheme) or else a jump-like change in the deformations. In the former case, assuming the Nilsson scheme to be correct, one can assume, for example, a deformation parameter $\delta \approx 0.18$ to obtain jumps in the binding energies past $Z = 92$, 96, and 100 (see reference 8). The increase in the probability of spontaneous fission for 102^{254} is possibly connected in part with the appearance of spontaneous fission into three fragments,[9] as observed in the case of Cf^{252} (reference 10).

In connection with the reduced stability of the nuclei past $N = 152$ (references 4 and 6) and $Z = 100$, one must review all possible limits of the existence of nuclei[11,12] on the downward side, even compared with the pessimistic estimates of Ivanenko.[11] A preliminary estimate based on the spontaneous-fission curve shows now that the limit of nuclei with a lifetime of approximately $10^{-12} - 10^{-16}$ seconds should lie most likely between $Z = 108$ and 112, i.e., very far from the "optimistic" estimates of Wheeler.[11]

In conclusion, we express our gratitude to Prof. D. D. Ivanenko, Prof. A. Ghiorso, S. Thompson, and Prof. G. N. Flerov for valuable discussions and remarks, and also to S. I. Larin who graciously reported to us that the number $Z = 100$ stood out also on a curve he plotted for the dependence of the energy differences of the alpha decay of the neighboring isotopes on Z.

[1] G. N. Flerov, Report to the Eighth Mendeleev Congress, Moscow, March 1959.

[2] A. Ghiorso, Report to the Eighth Mendeleev Congress, Moscow, March 1959.

[3] Fields, Friedman, Milsted, Atterling, Forsling, Holm, and Astorom, Phys. Rev. **107**, 1460 (1957).

[4] J. R. Huizenga, Phys. Rev. **94**, 158 (1954); N. N. Kolesnikov and S. Larin, J. Exptl. Theoret. Phys. (U.S.S.R.) **28**, 244 (1955), Soviet Phys. JETP **1**, 179 (1955).

[5] N. N. Kolesnikov, J. Exptl. Theoret. Phys. (U.S.S.R.) **30**, 889 (1956), Soviet Phys. JETP **3**, 844 (1956).

[6] N. N. Kolesnikov and A. P. Krylova, J. Exptl. Theoret. Phys. (U.S.S.R.) **33**, 274 (1957), Soviet Phys. JETP **6**, 212 (1958).

[7] Strominger, Hollander, and Seaborg, Revs. Modern Phys. **30**, 585 (1958).

[8] S. G. Nilsson, Danske Vidensk. Selsk. Math.-Fys. Medd. **29**, 1-68 (1955).

[9] W. Swiatecki, Phys. Rev. **100**, 936 (1955).
[10] S. Thompson, Report to the Eighth Mendeleev Congress, Moscow, March 1959.
[11] D. D. Ivanenko, Сб. Менделеев, (Mendeleev Anthology), U.S.S.R. Acad. Sci. 1956.
[12] J. A. Wheeler, in Niels Bohr and the Development of Physics (Pergamon, London, 1955); F. G. Werner and J. A. Wheeler, Phys. Rev. **109**, 126 (1958).

Translated by J. G. Adashko
98

ON THE DISTRIBUTION FUNCTION FOR DISSIPATIVE PROCESSES IN A RAREFIED RELATIVISTIC GAS

S. S. MOĬSEEV

Poltava Construction Institute

Submitted to JETP editor April 4, 1959

J. Exptl. Theoret. Phys. (U.S.S.R.) **37**, 553-554 (August, 1959)

THE motion of a rarefied gas or of a gas with a large flow gradient, cannot, generally speaking, be treated as the motion of a continuous medium, and additional consequences of kinetic theory must be used.

As is known, Grad[1] considered such a flow by adding to the independent parameters (in addition to the mean velocity, density, and temperature) also the heat flow and the tensor of viscous stresses. Using a specific form of nonrelativistic Maxwellian distribution (which can be considered as a weighting function for three-dimensional Hermite polynomials in velocity space), Grad expanded the distribution function in Hermite polynomials. Retaining only the first three terms of the series, he obtained a distribution function over the coordinates and velocities, describing the processes of viscosity and heat conduction in the nonrelativistic approximation.

It is easy to obtain a distribution function for rarefied relativistic gas, with allowance for the phenomena of viscosity and heat conduction, by introducing orthogonal polynomials with a weight $\exp(-\sigma\sqrt{1+u^2})$. Here $\sigma = mc^2/kT$, where T is the temperature in the proper reference system of the given gas element; $u^2 = u_\alpha^2$, where u_α are the spatial components of the four-velocity of the gas particles.* By way of an example we cite the first two polynomials of this type

$$g^{(0)} = 1/2\sqrt{\pi}\,\sigma^{1/4}K_2^{1/2}(\sigma), \qquad g_\alpha^{(1)} = \xi_\alpha/2\sqrt{\pi}\,\sigma^{1/4}K_3^{1/2}(\sigma),$$
$$\xi_\alpha = \sigma^{1/2}u_\alpha. \tag{1}$$

Here $K_\nu(\sigma)$ is the MacDonald function.

As is known,[2] the scalar distribution can be written in the form

$$F = icf(x,p)\,\delta(H+mc). \tag{2}$$

Here H is the invariant Hamiltonian function, while x and p are the 4-coordinates and 4-momentum of the particle. The scalar f(x, p) coincides with the ordinary distribution function and its expression in the proper coordinate system of the gas in equilibrium differs from $\exp(-\sigma\sqrt{1+u^2})$ only by a multiplicative factor. If we now expand f $[\exp(-\sigma\sqrt{1+u^2})]^{-1/2}$ in terms of the functions $[\exp(-\sigma\sqrt{1+u^2})]^{1/2}g_\alpha^{(n)}$ (the expansion is valid in the sense of convergence in the mean) and confine ourselves to the first three terms of the expansion, we obtain after simple calculations an expression for f(x, p) in the proper system of reference of the given element of gas

$$f(x,p) = \exp(-\sigma\sqrt{1+u^2})\left\{\frac{n\sigma}{4\pi(mc)^3K_2(\sigma)} + \frac{\sigma^2\tau_{\alpha\beta}\xi_\alpha\xi_\beta}{8\pi m^4c^5K_3(\sigma)} + \frac{\sigma^{5/2}}{24\pi m^5c^6K_4(\sigma)}\left[T_{\alpha\beta\gamma}\xi_\alpha\xi_\beta\xi_\gamma - 3\frac{K_4(\sigma)}{K_3(\sigma)}T_{\alpha\beta\beta}\xi_\alpha\right]\right\}. \tag{3}$$

Here n is the density of the particles in a proper system of the given element of gas, $\tau_{\alpha\beta}$ is the additional term in the three-dimensional portion of the energy-momentum tensor due to the dissipative processes, and $T_{\alpha\beta\gamma}$ are the spatial components of the tensor $T_{ikl} = \int p_i p_k F_l d^4p$.

The expression for T_{ikl} in any system of reference can be obtained from its components in the proper system of reference. As a result we obtain

$$T_{ikl} = \frac{nm^2c^3}{\sigma}\frac{K_3(\sigma)}{K_2(\sigma)}(U_i\delta_{kl} + U_k\delta_{il} + U_l\delta_{ik}) + \frac{nm^2c^3K_4(\sigma)}{K_2(\sigma)}U_iU_kU_l + \frac{mcK_4(\sigma)}{K_3(\sigma)}(U_i\tau_{kl} + U_k\tau_{il} + U_l\tau_{ik}) + R_{ikl}, \tag{4}$$

where U_i is the 4-velocity corresponding to the average motion, and R_{ikl} is a tensor, whose components $R_{\alpha\beta4}$ and R_{444} vanish in the proper system and whose remaining components coincide with the components of T_{ikl} in the same system. The tensor T_{ikl} can be used in the study of transport phenomena, and also to investigate the structure of a shock wave. We note that for large values of σ, Eqs. (3) and (4) go into the corresponding nonrelativistic expressions.

Inasmuch as the function f is a scalar, its form for any system of reference should be

$$f(x,p) = \exp(p_l q_l)\left\{\frac{n\sigma}{4\pi (mc)^3 K_2(\sigma)} + \frac{\sigma^2 \tau_{ik}\,\xi_i\,\xi_k}{8\pi m^4 c^5 K_3(\sigma)}\right.$$
$$+ \frac{\sigma^{5/2}}{24\pi m^5 c^6 K_4(\sigma)}\left[R_{ikl} + \frac{(mc)^2\,[K_4^2(\sigma) - K_5(\sigma)\,K_3(\sigma)]}{[K_3^2(\sigma) - K_4(\sigma)\,K_2(\sigma)]}\right.$$
$$\times (\nu_i U_k U_l + \nu_k U_l U_l + \nu_l U_i U_k)\Big]$$
$$\left.\times\left[\xi_i\xi_k\xi_l - \frac{K_4(\sigma)}{K_3(\sigma)}(\xi_i\delta_{kl} + \xi_k\delta_{ll} + \xi_l\delta_{ik})\right]\right\},$$

where the q_i have the same meaning as in reference 2, and ν_i is an additional term in the vector of material flow density, due to the dissipative process.

Inasmuch as $T_{ii l} = -m^2c^2(cnU_l + \nu_l)$, the parameters that determine the state of the gas are n, T, U_i, τ_{ik}, and R_{ikl}. Using Eq. (3) and the requirement that the mean energy be expressed only in terms of the Maxwellian portion of the distribution function, it is easy to show that $\tau_{ii} = 0$.

In conclusion, I consider it my pleasant duty to thank Prof. V. L. German for interest in the work and for valuable advice, and to G. I. Budker and S. I. Braginskiĭ for very valuable discussions.

*The Greek indices run through three values, and the Latin ones through four; repeated indices imply summation.

[1] H. Grad, Commun. on Pure and Appl. Math. **2**, 331 (1949).

[2] S. T. Belyaev and G. I. Budker, Dokl. Akad. Nauk SSSR **107**, 807 (1956), Soviet Phys.-Doklady **1**, 218 (1956).

Translated by J. G. Adashko
99

ELECTRON RESONANCE IN CROSSED ELECTRIC AND MAGNETIC FIELDS

I. M. LIFSHITZ and M. I. KAGANOV

Technical Institute, Academy of Sciences, Ukrainian S.S.R.

Submitted to JETP editor May 21, 1959

J. Exptl. Theoret. Phys. (U.S.S.R.) **37**, 555-556 (August, 1959)

IT is known that a free electron placed in crossed electric and magnetic fields drifts in the direction perpendicular to the electric and magnetic fields. The drift velocity, i.e., the mean velocity of the electron's motion* (apart from a part dependent on its initial velocity), is equal to $\bar{\mathbf{v}} = cH^{-2}[\mathbf{E}\times\mathbf{H}]$, where $\mathbf{E}$ and $\mathbf{H}$ are the intensities of the electric and magnetic fields. In addition, the electron executes an oscillatory motion along the electric field, at a frequency eH/mc; that is, the frequency in crossed fields does not depend on the electric field.[1]

The situation is different for an electron in a metal or semiconductor. The complicated dispersion law has a pronounced effect on the character of the motion of a conduction electron. We shall start from the classical equation of motion, the Lorentz generalized equation,

$$d\mathbf{p}/dt = e\{\mathbf{E} + c^{-1}[\mathbf{v}\times\mathbf{H}]\}, \qquad \mathbf{v} = \partial\varepsilon/\partial\mathbf{p}. \tag{1}$$

It is easy to show that the integrals of the motion in this case are

$$\varepsilon^*(\mathbf{p}) \equiv \varepsilon(\mathbf{p}) - \mathbf{v}_0\mathbf{p} = \text{const},$$
$$\mathbf{v}_0 = cH^{-2}[\mathbf{E}\times\mathbf{H}],\ p_z = \text{const}. \tag{2}$$

The z axis is taken along the magnetic field; $\mathbf{v}_0$ coincides with the mean velocity of the electron's motion, i.e., with the drift velocity, only in case the trajectory of the electron in momentum space, as determined by Eq. (2), is closed. In fact, on introducing the velocity $\mathbf{v}_0$ in Eq. (1) we get

$$d\mathbf{p}/dt = (e/c)[\mathbf{v} - \mathbf{v}_0]\times\mathbf{H}. \tag{3}$$

From this it is clear that $\bar{\mathbf{v}} = \mathbf{v}_0$ if $\overline{d\mathbf{p}/dt} = 0$. This happens in the case of closed trajectories.[2]

Equation (3) shows that the motion in crossed fields of a particle with the dispersion law $\epsilon = \epsilon(\mathbf{p})$ can be treated as motion in a magnetic field alone of a particle with the dispersion law†

$$\varepsilon^*(\mathbf{p}) = \varepsilon(\mathbf{p}) - \mathbf{v}_0\mathbf{p}. \tag{4}$$

Therefore the results obtained before are easily transferred to this case. In particular, the period T^* of revolution of an electron around a closed orbit is[2,3]

$$T^* = -(c/eH)\,\partial S^*/\partial\varepsilon^*. \tag{5}$$

Here S^* is the area bounded by the curve determined by Eq. (2); it depends, naturally, on the electric field. It is interesting to note that this dependence disappears in the case of a quadratic dispersion law: the presence of the term $-\mathbf{v}_0\mathbf{p}$ in the Eq. (2) merely perturbs the trajectory without changing its area. Thus the dependence of the period of revolution on the electric field is an effect specific to an electron with a complicated (non-quadratic) dispersion law. It should be noticed that cases are possible in which a conduction

electron in a magnetic field executes a finite motion (its trajectory in momentum space being a closed curve), whereas in crossed fields it executes an infinite one, since the trajectory (2) is an open curve.

The explicit dependence of the period on the electric field can be obtained only for a definite law of dispersion. However, if $E/H \ll 1$, it is possible to obtain the result

$$T^* \approx T\left\{1 - (cv_0/eHT)\oint v_\perp^{-2}\, dl\,(\mathbf{n} + \mathbf{p}/R)\right\}. \qquad (6)$$

Here T is the period of revolution in a magnetic field, $\mathbf{n} = \mathbf{v}_\perp/|\mathbf{v}_\perp|$ is the normal to the trajectory of the electron in a magnetic field, and R is the radius of curvature of the trajectory. The integration extends over the trajectory in a magnetic field. Thus $\Delta T/T \sim (c/v)(E/H)$.

Once we know the frequency of revolution of the electron ($\omega^* = 2\pi/T^*$), it is easy to write down the distance between quantum energy levels in the classical approximation:[4,5]

$$\Delta\varepsilon^* = \hbar\omega^* = 2\pi|e|\hbar H/c\,(\partial S^*/\partial\varepsilon^*).$$

In connection with the dependence of the frequency of revolution of an electron in crossed fields on the size of the electric field, an interesting peculiarity should apparently occur in diamagnetic resonance in those semiconductors in which the dependence of the energy of the current carriers on the quasimomentum is appreciably nonquadratic: the resonance frequency should depend on the electric current passed through the specimen.

A nonquadratic dependence of the energy on the components of the quasi-momentum occurs not infrequently near the edge of the conduction band. Often it is a consequence of the crystal symmetry. Here the quadratic dependence on the magnitude of the momentum is retained near the edge of the band, but the angular dependence becomes complicated. Thus the energy spectrum of "holes" in Ge and Si crystals has the form[6]

$$\varepsilon = Ap^2 \pm [B^2p^4 + C^2\,(p_x^2p_y^2 + p_x^2p_z^2 + p_y^2p_z^2)]^{1/2},$$

where A, B, and C are constants.

To observe such effects in metals is in all probability impossible, since in a metal (in consequence of the large electrical conductivity) it is impossible to produce any appreciable electric field. To estimate the order of magnitude of the effect, we must start from formula (6), remembering however that the resonance frequencies are determined not by all the electrons but by those that have extremal effective masses.[7] It can be shown that for these electrons no effect linear in the electric field is present because of the symmetry of the trajectory. Therefore, apparently, $\Delta\omega/\omega \sim (c/v)^2(E/H)^2$.

*We have in mind the mean velocity in a plane perpendicular to the magnetic field.

†Except for an unimportant constant, ε^* coincides with the total energy of the particle.

[1] L. D. Landau and E. M. Lifshitz, Теория поля (Field Theory), Gostekhizdat, 1948 [Transl: Addison-Wesley, 1951].

[2] Lifshitz, Azbel', and Kaganov, J. Exptl. Theoret. Phys. (U.S.S.R.) **31**, 63 (1956), Soviet Phys. JETP **4**, 41 (1957).

[3] W. Shockley, Phys. Rev. **79**, 191 (1950).

[4] I. M. Lifshitz, Report at a session of the physics-mathematics section, Academy of Sciences, Ukr. S.S.R., 1951; I. M. Lifshitz and A. M. Kosevich, J. Exptl. Theoret. Phys. (U.S.S.R.) **29**, 730 (1955), Soviet Phys. JETP **2**, 636 (1956).

[5] L. Onsager, Phil. Mag. **43**, 1006 (1952).

[6] Dresselhaus, Kip, and Kittel, Phys. Rev. **98**, 368 (1955).

[7] M. Ya. Azbel' and É. A. Kaner, J. Exptl. Theoret. Phys. (U.S.S.R.) **32**, 896 (1957), Soviet Phys. JETP **5**, 730 (1957).

Translated by W. F. Brown, Jr.
100

IDENTIFICATION OF PARTICLES IN HIGH ENERGY STARS

G. I. KOPYLOV

Joint Institute for Nuclear Research

Submitted to JETP editor April 17, 1959

J. Exptl. Theoret. Phys. (U.S.S.R.) **37**, 557-558 (August, 1959)

THE identification of particles in high energy stars* is often made by comparing the measurements of the momentum p_1 of one of the particles with its possible limiting values under predetermined assumptions about the mass and the number of remaining particles 2, 3, ... , n. These last are united into one composite particle having some effective mass m_{eff}. The formula for the momentum of particle 1 at an angle of observation θ_1 under the assumption that the other particle has a mass m_{eff} gives the limiting pos-

sible values of the momentum of particle 1.[1,2,3] Ordinarily the value $\overline{m} = m_2 + m_3 + \ldots + m_n$ is taken for m_{eff}, a result which considers the velocities of particles 2, 3, ..., n to be equal in magnitude and direction.[2]

We shall show that the solution for the bounds $p_{1\,max}$, $p_{1\,min}$ of the momentum p_1 of particle 1 can be restricted if one takes into account the angles θ_{ij} between the other charged particles i and j (i, j = 2, 3, ..., n') and if the lower limit $\tilde{p}_i$ of their momenta p_i is estimated.

An attempt has been made earlier[4] to take into account information about the angles and momenta of the particles for purposes of identification. Unlike reference 4, the present work includes this information directly in m_{eff}. In this way only knowledge of the lower bounds of the momenta is required (in reference 4, knowledge of the values of p_i themselves is required, which is difficult for large p_i and leads to an indeterminacy in the limiting values for p_1).

To deduce a necessary formula, we note that the equation for the momentum p_1 (or energy E_1) of one of the secondary particles having the total energy E and momentum P coincides with the equation for p_1 in the decay of a particle with energy E and momentum P into two particles with masses m_1 and m_{eff}, if we take

$$m_{eff}^2 = (E_2 + \ldots + E_n)^2 - (\mathbf{p}_2 + \ldots + \mathbf{p}_n)^2. \qquad (1)$$

It is easy to show that the roots of the equation above for p_1 have the characteristic

$$dp_{1max}/dm_{eff} < 0, \quad dp_{1min}/dm_{eff} \geqslant 0.$$

This means that increasing the estimate for m_{eff} shrinks the region of solutions for the value p_1.

To increase this estimate, we write (1) as three positive terms

$$m_{eff}^2 \equiv \sum_{i=2}^{n} m_i^2 + 2\sum_{i<j}^{n} (E_iE_j - p_ip_j) + 2\sum_{i<j}^{n} p_ip_j(1 - \cos\vartheta_{ij}). \qquad (2)$$

Taking into account $E_iE_j - p_ip_j \geq m_im_j$ and $p_i > \tilde{p}_i$ (where $\tilde{p}_i$ is the lower bound of p_i),† we immediately get the following estimate:

$$m_{eff}^2 \geqslant \tilde{m}^2 \equiv \overline{m}^2 + \Delta^2 \equiv \overline{m}^2 + 2\sum_{2\leqslant i<j}^{n'} \tilde{p}_i\tilde{p}_j(1 - \cos\vartheta_{ij}). \qquad (3)$$

Here the sum is carried out over all pairs of charged particles, except particle 1. The masses of the neutral particles are included in $\overline{m}$.

Thus, if we take $\tilde{m}$ instead of $\overline{m}$ for the value of m_{eff}, p_{1min} and p_{1max} come closer and closer together as $\tilde{p}_i$ increases and θ_{ij} becomes larger. For narrow beams of secondary particles the use of formula (3) gives no effect.

If for some particles i and j not only $\tilde{p}$ but also p is known, $\tilde{p}$ can be changed to p in the equations and the term $E_iE_j - p_ip_j - m_im_j$ can be added. This makes $p_{1\,max}$ and $p_{1\,min}$ converge even more.

The most probable contribution from neutral particles to m_{eff} can be taken into account by adding to Δ^2 the term $\frac{1}{2}n'(\frac{1}{2}n'-1)\overline{p^2}(1-\cos\overline{\theta})$, where $\overline{p}$ and $\overline{\theta}$ are the average values of p_i and θ_{ij} in the given interaction.

The results of this work are given in more detail in reference 5.

The author takes this opportunity to thank I. M. Gramenitskiĭ and M. I. Podgoretskiĭ for their valuable comments.

*We consider high energy stars to be those in which there are tracks of relativistic particles.

†For gray tracks, for example, one can take $\tilde{p}_i = m_i$; for neutral particles, $\tilde{p}_i = 0$ is taken.

[1] I. L. Rozental', Usp. Fiz. Nauk **54**, 405 (1954).

[2] R. M. Sternheimer, Phys. Rev. **93**, 642 (1954).

[3] G. I. Kopylov, "On Estimating the Number of Secondary Particles Near Limiting Angles," preprint, Joint Inst. Nuc. Res. R-166 (1958).

[4] Birger, Grigorrov, Guseva, Zhdanov, Slavatinskiĭ, and Stashkov, J. Exptl. Theoret. Phys. (U.S.S.R.) **31**, 971 (1956), Soviet Phys. JETP **4**, 872 (1957).

[5] G. I. Kopylov, preprint, Joint Inst. Nuc. Res., R-341 (1959).

Translated by William Ramsay
101

NOTE ON A BARYON SCHEME

H. OIGLANE

Institute of Physics and Astronomy, Academy of Sciences, Estonian S.S.R.

Submitted to JETP editor April 16, 1959

J. Exptl. Theoret. Phys. (U.S.S.R.) **37**, 558-559 (August, 1959)

LET us assume that each of the eight known baryons is described by a four-component wave function. The general equation for all the baryons is in this case an equation for a 32-component spinor. A 32-dimensional spinor space can be treated as a rep-

resentation of a 10-dimensional vector space.[1] The basis vectors of this space are related to ten 32-row matrices Γ^a, where

$$\Gamma^a\Gamma^b + \Gamma^b\Gamma^a = 2\delta_{ab}, \quad a, b = 1, 2, \ldots, 10.$$

There corresponds to a reflection of the basis vectors e^b in the vector space the following transformation of the matrix Γ^a:

$$\Gamma^{a'} = -\Gamma^b\Gamma^a\Gamma^b, \quad a = 1, 2, \ldots, 10,$$

(no summation over b).

We divide the 10-dimensional vector space into a 4-dimensional Minkowski space (the matrices corresponding to the basis vectors are Γ^ν, $\nu = 1, 2, 3, 4$) and a 6-dimensional isotopic space (the matrices here are Γ^a, $a = 5, 6, \ldots, 10$). With the aid of the isotopic space transformations we can determine the following 3-component isotopic vectors, whose components satisfy the same relations as the components of ordinary spin:

$2\mathbf{J}^1 = (\Gamma^6, \Gamma^5, i\Gamma^5\Gamma^6)$, $2\mathbf{J}^2 = (\Gamma^8, \Gamma^7, i\Gamma^7\Gamma^8)$,
$2\mathbf{J}^3 = (\Gamma^{10}, \Gamma^9, i\Gamma^9\Gamma^{10})$, $2\mathbf{J}^4 = (i\Gamma^6\Gamma^7, i\Gamma^7\Gamma^5, i\Gamma^5\Gamma^6)$,
$2\mathbf{J}^5 = (i\Gamma^{10}\Gamma^8, i\Gamma^8\Gamma^9, i\Gamma^9\Gamma^{10})$.

We assume that the general equation for all baryons is of the type[2]

$$\left\{\Gamma^\nu \partial/\partial x_\nu - k_0 I \exp\left[\Gamma^0 \sum_{k=1}^{5} a_k \mathbf{J}^k\right]\right\}\psi = 0, \qquad (1)$$

where $\Gamma^0 = \Gamma^1\Gamma^2\Gamma^3\Gamma^4$, $I = i\Gamma^0\Gamma^6\Gamma^7\Gamma^{10}$, and $\mathbf{a}_k$ are some small isotopic vectors whose components depend on the potentials of the meson and lepton fields.

Equation (1) is solved by perturbation theory, where we express the Hamiltonian of the unperturbed problem as

$$H = \hbar c\left\{\Gamma^4\Gamma^k \partial/\partial x_k - k_0\Gamma^4 I \exp\left[\Gamma^0 \sum_{k=1}^{5} a_k^3 J_3^k\right]\right\}. \qquad (2)$$

The form of the baryon is characterized here by three quantum numbers τ_3, ω_3, and ζ_3, which appear as eigenvalues of the operators $(i/2)\Gamma^0\Gamma^7\Gamma^8$, $(i/2)\Gamma^0\Gamma^9\Gamma^{10}$, and $(i/2)\Gamma^0\Gamma^5\Gamma^6$ (see references 3 and 4). The baryon scheme can be described by a unit cube whose center lies at the origin of the coordinates τ_3, ω_3, and ζ_3 (see diagram).

From (1) and (2) we can determine the perturbation Hamiltonian which describes the weak interaction transitions between baryons. Every baryon can be displaced along the edges of the cube and along the diagonals marked in the diagram by dotted lines. All the indicated processes are possible in principle, although by the energy conservation law some of these, for example $\Xi^- \to \Sigma^- + \pi^0$, cannot be realized. Other processes, for example, $\Sigma^+ \to \Lambda^0 + \beta^+ + \nu$, are obviously realizable but are seldom found, since competing processes are more probable. The scheme described gives all known baryon transformations and does not give any forbidden transitions. All the weak interaction transitions noted can also proceed from positive energy states to negative energy states and vice versa. This means there can exist processes of the type $N + \overline{P} \to \beta^- + \nu$, whose probability is small compared with that of the strong interaction processes.

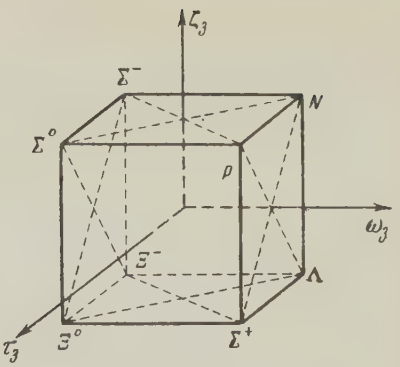

[1] P. K. Rashevskiĭ, Usp. Mat. Nauk **10**, 2 — 3 (1955).

[2] H. Oiglane, J. Exptl. Theoret. Phys. (U.S.S.R.) **33**, 1511 (1957), Soviet Phys. JETP **6**, 1167 (1958).

[3] J. Tiomno, Nuovo cimento **6**, 69 (1957).

[4] N. Dallaporta, Nuovo cimento **11**, 142 (1959).

Translated by Wm. Ramsay
102

ON THE DECAY SCHEME OF THE Bi^{210} *ISOMER*

S. V. GOLENETSKIĬ, L. I. RUSINOV, and Yu. I. FILIMONOV

Submitted to JETP editor April 27, 1959

J. Exptl. Theoret. Phys. (U.S.S.R.) **37**, 560-562 (August, 1959)

LEVY and Perlman[1] assumed that the α decay of the Bi^{210} isomer with $T_{1/2} = 2.6 \times 10^6$ yr and $E_\alpha = (4935 \pm 20)$ kev goes to the ground state of Tl^{206}. From the energy balance of the α and β transitions $Bi^{210} \to Pb^{206}$ the authors concluded that the long-lived state of Bi^{210} is the ground state and that RaE ($T_{1/2} = 5.01$ days) is metastable with an excitation energy of about 25 kev. We detected[2] the fine structure of the α spec-

trum of the long-lived bismuth with the most intensive group of α particles with E_α = (4930 ± 10) kev. These data did not contradict the assumption of Levy and Perlman about the subsequent levels in the Bi^{210} nucleus. In the present paper we give a further study of the radiation from the long-lived bismuth isotope which led to the necessity to change the decay scheme of Bi^{210}.

The measurements were performed by means of a burst ionization chamber with a grid and with a scintillation γ-spectrometer. The resolving power of the chamber was 28 kev for the α line of U^{233} with an energy of 4816 kev. In Tables I and II we give the results of measurements of the energy and of the relative intensities of α particles and γ transitions which accompany the α decay of the long-lived Bi^{210} isomer.

TABLE I. α-particle energies

	Energy, kev	Relative intensity, %
α_0	not detected	<0.03
α_1	5130±15	~0.1
α_2	4930±10	60
α_3	4890±10	34
α_4	4590±10	5±1
α_5	4480±15	~0.5
α_6 (Po^{210})	5300	$\leqslant 0.01$

TABLE II. γ-transition energies

	Energy, kev	Relative intensity, %
γ_1	260±10	60
γ_2	300±10	30
γ_3	340±10	
γ_4	620±20	

To explain the decay scheme of Bi^{210} we investigated α-γ coincidences. The γ-ray detector was a scintillation counter arranged in a coincidence set-up with the burst ionization chamber. The spectrum of γ lines which were in coincidence with α particles of well-defined energy was measured. The results of the measurement are given in Figs. 1 and 2. We observed coincidences of the most intensive group of α particles with an energy of 4930 kev with γ lines with an energy of 260 kev. These α particles correspond thus to the transition not to the ground state of Tl^{206}, as was assumed earlier, but to an excited one with an energy of 260 kev. Besides, we observed coincidences of γ lines with E_γ = 300 kev with α particles with an energy of 4890 kev and of γ lines with E_γ = 340 and 620 kev with α particles with an energy of 4590 kev. The maxima in Fig. 2 corresponding to E_γ = 260 and 300 kev are caused both by cascade transitions and by coincidences with scattered α particles with E_α = 4930 and 4890 kev. A comparison of the γ emission from the bismuth sample studied with a γ-ray reference source shows that the observed number of γ transitions is approximately equal to the total number of α decays.

On the basis of the data obtained we assumed a decay scheme for Bi^{210m} (Fig. 3). The energy of the α decay of RaE to the ground state of Tl^{206} can be evaluated from the energy balance and is

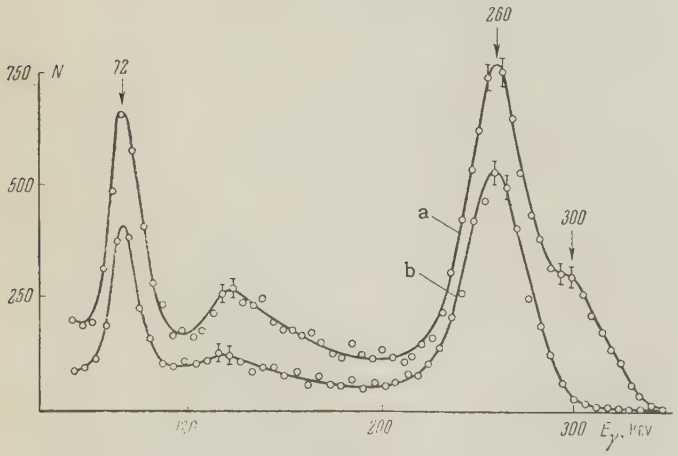

FIG. 1. Coincidences γ spectrum: a – with E_α = 4930 and 4890 kev, b – with E_α = 4930 kev.

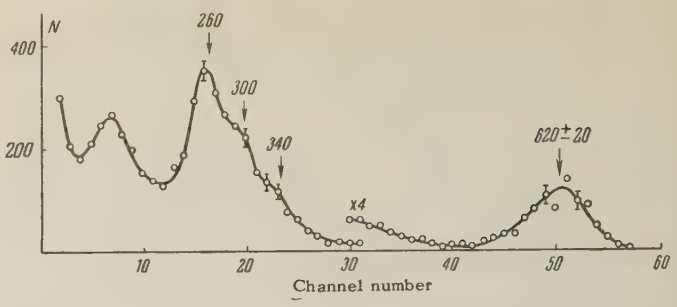

FIG. 2. Coincidences γ spectrum with E_α = 4590 kev.

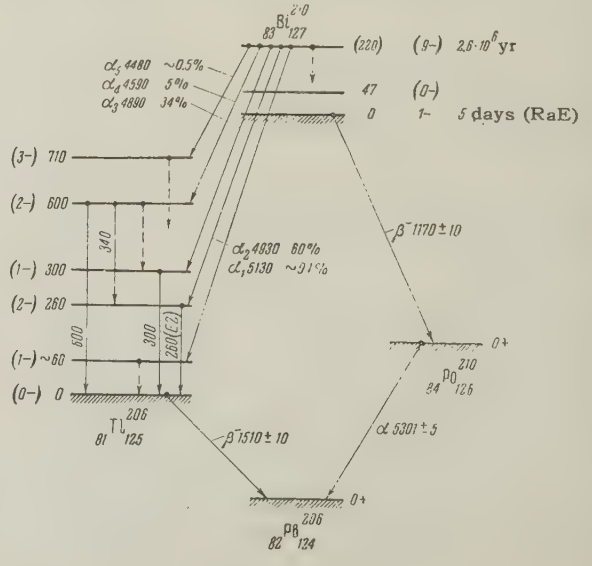

FIG. 3. Decay scheme of Bi^{210m}.

$Q_\alpha = (5064 \pm 15)$ kev, if we take the value $E_{\beta\,max} = (1510 \pm 10)$ kev[3] for Tl^{206}. The total α-decay energy of the long-lived Bi^{210} isomer is $Q_\alpha = (5286 \pm 15)$ kev if we take into account the recoil of the nucleus and the energy of the γ quanta. This value of Q_α is 220 kev larger than the above mentioned energy of the α decay of RaE. One must thus assume that RaE with $T_{1/2}$ = 5.01 days is the ground state of Bi^{210} and the state with $T_{1/2} = 2.6 \times 10^6$ yr a metastable one. The partial lifetime of Bi^{210m} relative to an electromagnetic transition T_γ can be estimated from the build up of Po^{210} from the subsequent decay through RaE. It is clear from Table I that the intensity of the α-line of Po^{210} with an energy of 5300 kev is $\leq 0.01\%$, which corresponds to $T_\gamma \geq 10^{10}$ yr.

The energy levels of Bi^{210} were calculated by Yu. I. Kharitonov on the nuclear shell model basis taking pair interaction and the interaction with the nuclear surface into account. It was shown that the lowest levels of Bi^{210} corresponded to the $(h_{9/2})^1_p(g_{9/2})^1_n$ configuration and that one should assign spins and parities 1^- and 0^- to the ground state and first excited state and 9^- to the isomeric state. Similar calculations for Tl^{206} point to a doublet structure of the levels and lead to spin values corresponding to the configurations $(s_{1/2})^{-1}_p(p_{1/2})^{-1}_n$, $(d_{3/2})^{-1}_p(p_{1/2})^{-1}_n$, $(d_{5/2})^{-1}_p(p_{1/2})^{-1}_n$ or $(s_{1/2})^{-1}_p(f_{5/2})^{-1}_n$ (Fig. 3). For the given values of the spins and parities the α decay to the ground state of Tl^{206} must be forbidden, because of parity, which agrees with the experimental data.

In conclusion the authors express their deep gratitude to L. A. Sliv for a discussion of the results obtained, and to E. G. Grachevaya, N. B. Obel'skaya, V. K. Makhnovskaya, and L. Ya. Rudaya for the chemical purification of the specimen from radioactive impurities and for the preparation of the samples.

[1] H. B. Levy and I. Perlman, Phys. Rev. **94**, 152 (1954).

[2] Golenetskiĭ, Rusinov, and Filimonov, J. Exptl. Theoret. Phys. (U.S.S.R.) **35**, 1313 (1958), Soviet Phys. JETP **8**, 917 (1959).

[3] D. E. Alburger and G. Friedlander, Phys. Rev. **82**, 977 (1951).

Translated by D. ter Haar
103

*EXPERIMENTAL INVESTIGATION OF THE HARMONIC OSCILLATIONS OF A DISK IN ROTATING HELIUM II**

É. L. ANDRONIKASHVILI and D. S. TSAKADZE

Tbilisi State University

Submitted to JETP editor April 28, 1959

J. Exptl. Theoret. Phys. (U.S.S.R.) **37**, 562-564 (August, 1959)

THE problem of the oscillations of a system of circular disks suspended from a torsion fiber in helium II, and participating together with the latter in uniform rotational motion, has been investigated by us[1,2] and by Hall.[3,4] It has been shown that the period of oscillation of such a stack of disks depends upon the ratio of the frequencies Ω (the frequency of the oscillations) and ω (the rotational frequency), as well as upon the spacing of the disks and the condition of their surfaces. These investigations, however, failed completely to take into account the possibility of changes in the damping processes in rotating helium II.

With the object of studying this aspect of the problem, we constructed an apparatus in which a transparent beaker of organic glass 44 mm in diameter filled with liquid helium performed uniform rotational motion at angular velocities of from $\omega = 13 \times 10^{-3}$ sec^{-1} to $\omega = 129 \times 10^{-3}$ sec^{-1}. A single circular disk 1 mm thick and 30 mm in diameter, suspended within the beaker of helium, took part simultaneously in two types of motion: rotation, with the same velocity as the beaker; and harmonic oscillation about an axis perpendicular to its own plane and parallel to that of the beaker. The surface of the disk was alternatively covered with granules with linear dimensions $l \approx 50\,\mu$, or polished. The frequency of the oscillations of the disk was 0.581 sec^{-1} in the case of the rough surface and 0.551 sec^{-1} for the smooth surface case.

The logarithmic damping decrement δ of the oscillations of the disk was determined by noting the time required for a light spot associated with it to traverse a fixed path between two photomultipliers rotating, together with a scale, in synchronism with the beaker. A detailed description of this apparatus, as well as of the theory of the method, has been given in reference 5. Calibration of the system was carried out using classical liquids (water, helium I), for the viscosity coefficients of which good agreement was obtained with tabulated data. In both cases the damping remained

constant over the whole velocity range investigated, to within the limits of experimental error.

In the case of helium II, the damping decrement has a clearly-expressed dependence upon the rotational velocity, while the curve showing the dependence of the relative increase in the damping arising as a result of the rotation upon the rotational frequency passes through a maximum (Fig. 1), both in the case of the roughened disk (curve a) and of the smooth disk (curve b). Our attention is drawn to the fact that the ordinate of curve a exceeds that of curve b by a factor of not less than two over the whole range of rotational velocities. The character of the fall of the curve beyond the maximum is quite different for the rough and smooth disks, as is the sign of the curvature.

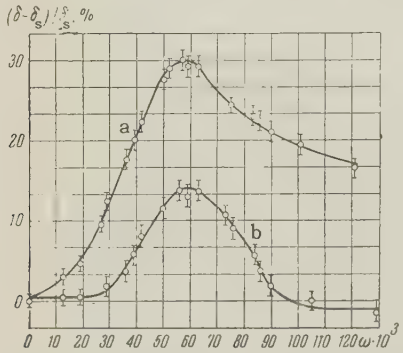

FIG. 1. Relative increase in the disk damping decrement as a function of angular velocity of rotation: a – for disk with roughened surface, b – with smooth surface; δ_s – damping in stationary helium II, δ – damping in rotating helium II; temperature 1.78°K.

In the smooth disk case the curve, near the origin, runs parallel to the x axis, which indicates, evidently, that under these conditions a slippage of the vortices is observed relative to the polished surface (i.e., the vortices are not fixed on the surface).

The temperature dependence of the maximum increase in the relative damping (at $\omega = 55 \times 10^{-3}$ sec^{-1}) for the roughened disk is shown in Fig. 2. It is characteristic that over the whole temperature interval the increase in the damping arising from entrainment of the superfluid component does not exceed 65 – 70% of the damping due to friction with the normal component.

To explain the features of the behavior of the curves presented in Fig. 1, Yu. G. Mamaladze, has suggested that the linear dependence of $(\delta - \delta_S)/\delta_S$ upon ω found at the beginning of the curve gives place to a more complex dependence when the distance between neighboring vortices becomes equal to their effective diameter. On this hypothesis the parameter $\nu = \epsilon/\rho_S\Gamma$ of

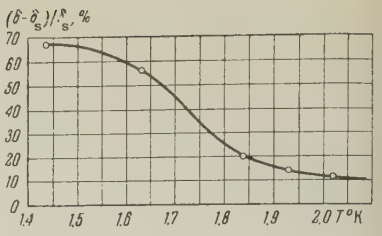

FIG. 2. Temperature dependence of the maximum value of the relative increase in the damping of the disk with roughened surface.

Hall and Vinen, where ϵ is the vortex energy per unit length and Γ is the circulation, was computed from the data of the present experiment. It was found that $\nu = 6$ to 8×10^{-4} cm^2 sec^{-1}, which agrees well with the value found by Hall himself.

The authors thank Yu. G. Mamaladze and S. G. Matinyan for their valued counsel, and L. A. Zamtaradze, T. G. Shults, and I. M. Chkheidze for their aid in performing the experiment.

*Presented at the All-Union Conference on Low Temperature Physics, Tbilisi, October, 1958.

[1] D. S. Tsakadze and É. L. Andronikashvili, paper presented to the Fourth All-Union Conference on Low Temperature Physics, Moscow, 1957.

[2] D. S. Tsakadze and É. L. Andronikashvili, Сообщения Академии наук Грузинской ССР (Commun. Acad. Sci. Georgian S.S.R.) **20**, 667 (1958).

[3] H. E. Hall, paper presented to the Fourth All-Union Conference on Low Temperature Physics, Moscow, 1957.

[4] H. E. Hall, Proc. Roy. Soc. **A245**, 546 (1958).

[5] Andronikashvili, Mamaladze, and Tsakadze, Тр. ин-та физики Академии наук Грузинской ССР (Trans. Inst. Phys. Acad. Sci. Georgian S.S.R.) **7**, 3 (1959).

Translated by S. D. Elliott
104

LOCALIZATION OF A HIGH-FREQUENCY INDUCTION DISCHARGE

M. D. RAĬZER and S. E. GREBENSHCHIKOV

P. N. Lebedev Physics Institute, Academy of Sciences, U.S.S.R.

Submitted to JETP editor April 30, 1959

J. Exptl. Theoret. Phys. (U.S.S.R.) **37**, 564-565 (August, 1959)

WE have investigated a high-frequency induction discharge in an axially symmetric magnetic field in the pressure range 1 – 100 mm Hg in various gases (air, hydrogen, and helium).

The discharge was produced by a self-excited pulsed 150 kw oscillator using GU-12A tubes. The pulse-length was one microsecond, the frequency 15 Mcs, and the anode voltage 15 kv. The coil used to produce the high-frequency magnetic field had an inductance of 0.2 μh and constituted the entire plate circuit of the oscillator. Two coils were used; the magnetic field produced by one was such as to satisfy the stability condition for a pinch in an equilibrium orbit,[1,2] (i.e., the field at the orbit $H_0 = \overline{H}/3$, where $\overline{H}$ is the mean value of the magnetic field inside the orbit); the field produced by the second coil was essentially uniform. The discharge was excited in the cylindrical vacuum chamber (diameter = 28 cm, height = 3 cm).

In the figure are shown typical streak photographs of discharges in various gases taken with an SFR-2 camera. The slit in the objective of the camera was parallel to the radius of the vacuum chamber. The radius R = 14 cm corresponds to the wall of the vacuum chamber. The equilibrium orbit is at a distance of approximately 4 cm from the side wall of the vacuum chamber. In air or hydrogen (Fig. 1, a and b) at a pressure of 10 mm Hg the breakdown occurs at 2 — 3 cm from the side wall and clearly defined plasma loops are formed; the small radii of these loops are approximately 5 mm. The large radius of the loop in air expands at a velocity of 3×10^4 cm/sec; the radius of the loop in hydrogen contracts at a velocity of 10^4 cm/sec. The loops exist for the duration of the oscillator pulse. In helium (cf. figure) the plasma loop which is formed at breakdown separates into two separate loops, which exist simultaneously.

With all other conditions being approximately the same the oscillation frequency of the plasma loops is inversely proportional to the mass of the gas: in air — 16 kcs, in helium — 6 kcs, and in hydrogen — 4 kcs. The loop current, measured by changing the oscillator frequency, is approximately 200 amp; the intensity of the induced electric field is approximately 1,000 v/cm. The current in the loop is determined by measuring the loop inductance.[3]

Spectroscopic measurements of the discharge in hydrogen at a pressure of 10 mm Hg (ISP-50 spectrometer) indicate that the current channel contains only atomic hydrogen ions. The electron temperature, as determined from the relative intensities of the H_α, H_β, and H_γ lines, is approximately 5000°, corresponding to a plasma conductivity of 2×10^{13}.

The nature of the discharge changes in a uniform magnetic field; in discharges in helium and air the current flows in a localized region at the sidewall of the chamber and does not form plasma loops. In the discharge in hydrogen there is a clearly defined loop, the small radius of which is approximately 5 mm; the oscillations of the large radius fall off much more rapidly than in the cases cited above.

A plasma loop in a uniform magnetic field

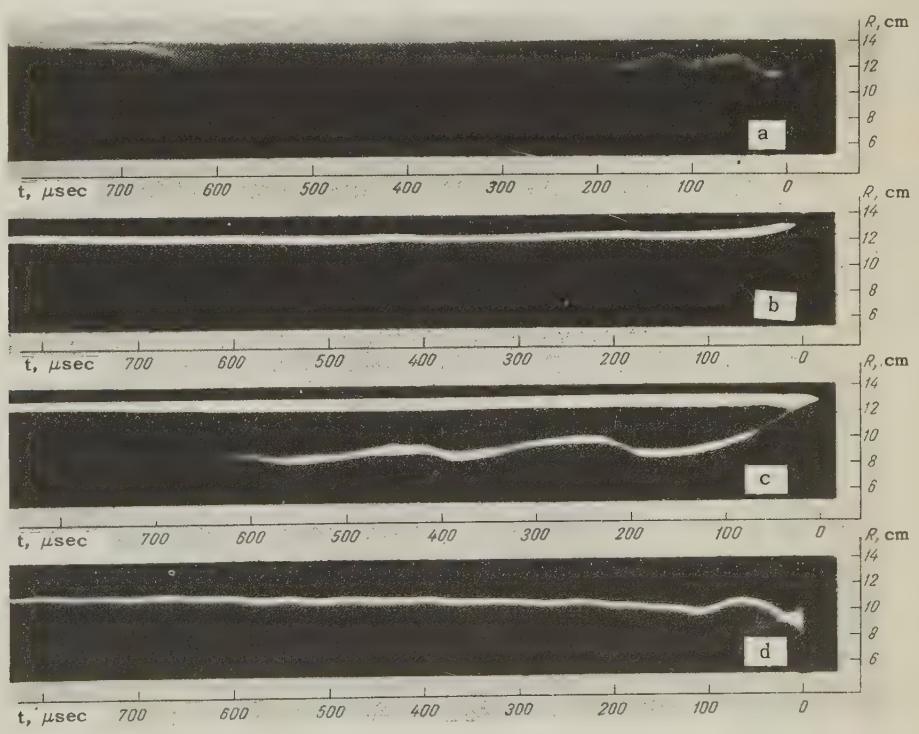

Streak photographs of the discharges: a) air, p = 7 mm Hg; J = 200 amp; b) hydrogen, p — 10 mm Hg, J = 200 amp; c) helium, p — 10 mm Hg, J = 260 amp; d) helium, p — 60 mm Hg, J = 220 amp.

which is subject to electrodynamic forces tends to reduce its large radius, contracting to the center of the vacuum chamber.[2] However no essential difference was observed in the behavior of the plasma loops in the two series of experiments indicated above. This may be due to the fact that the electrodynamic forces, which are proportional to the square of the current, are small or to the presence of strong dissipative forces due to the high gas density.

Thus, it has been established that in a high-frequency induction discharge at pressures above 1 mm Hg sharply defined plasma loops are formed; these remain separated from the walls of the vacuum chamber and exist for the duration of the high-frequency magnetic field pulse.

The authors are indebted to R. A. Latypov for assistance in the construction of the apparatus and for help in carrying out the experiments, V. A. Kiselev for carrying out the spectroscopic measurements, and L. M. Kovrizhnykh, M. S. Rabinovich and I. S. Shpigel' for a discussion of the results which have been obtained.

[1] L. M. Kovrizhnykh, J. Exptl. Theoret. Phys. (U.S.S.R.) **36**, 1834 (1959), Soviet Phys. JETP **9**, 1308 (1959).

[2] S. M. Osovets, Физика плазмы и проблема управляемых термоядерных реакций (Plasma Physics and the Problem of a Controlled Thermonuclear Reaction), Vol. II, 1958, p. 238.

[3] M. D. Raĭzer and S. E. Grebenshchikov, Отчет ФИАН (Reports, Institute of Physics, Acad. Sci.) 1958.

Translated by H. Lashinsky
105

MAGNETOSTRICTION OF ANTIFERROMAGNETIC NICKEL MONOXIDE

K. P. BELOV and R. Z. LEVITIN

Moscow State University

Submitted to JETP editor May 5, 1959

J. Exptl. Theoret. Phys. (U.S.S.R.) **37**, 565-566 (August, 1959)

DATA on the magnetostriction of antiferromagnets are at present lacking in the literature. On the basis of general considerations, however (the presence of domain structure), the magnetostriction of antiferromagnets should have an appreciable magnitude, at any rate larger than that of ordinary paramagnets.

We have measured the magnetostriction of polycrystalline nickel monoxide, NiO, prepared by the standard ceramic technique. Before the magnetostriction measurements, the room-temperature mass susceptibility and the Curie point of the specimens were measured by way of control. The measurements showed that in fields up to 7000 oe, the susceptibility is slightly field-dependent and equal to 6×10^{-6}; the Curie point was determined by the jump in Young's modulus and was 251°C. These data agree with results obtained for NiO by other authors.[1]

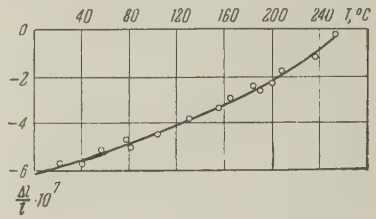

FIG. 1. Temperature dependence of the magnetostriction of NiO in a field of 14,200 oe.

The magnetostriction measurements were made by the wire-probe method by use of a photoelectro-optical amplifier. Figure 1 shows the temperature dependence of the transverse magnetostriction, measured in a field of 14,200 oe. The magnetostriction has a negative sign and decreases monotonically on approach to the Curie point. Figure 2 shows the field dependence of the transverse magnetostriction at various temperatures, and also the longitudinal magnetostriction at room temperature; the latter has a positive sign. What attracts attention is the fact that there is a certain "critical" field ($H_c \approx 5000$ oe) below which the magnetostriction is practically zero. Only after attainment of this field does the increase of magnetostriction begin.

In our opinion the magnetostriction in antiferro-

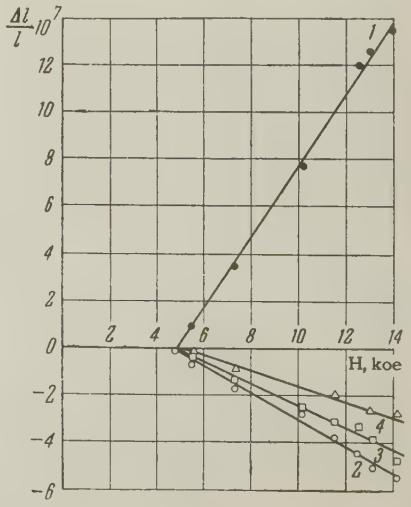

FIG. 2. Longitudinal and transverse magnetostriction of NiO. 1, longitudinal magnetostriction at 21°C; 2, transverse magnetostriction at 21°C; 3, at 53°C; 4, at 74°C.

magnetic nickel monoxide is dependent on the presence of a domain structure. This is indicated by the decrease of magnetostriction with increasing temperature, and also by the opposite signs of the longitudinal and transverse magnetostriction. The presence of a critical field is connected, in our opinion, with the existence of a coercive force, which is of order 10^4 oe for antiferromagnets according to an estimate given by Néel[2] and by Labhart.[3]

We also observed, in the specimens studied, a decrease of Young's modulus on application of a strong magnetic field (the antiferromagnetic ΔE-effect); this also indicates the existence of magnetostriction in antiferromagnetic nickel monoxide.

[1] R. Street and B. Lewis, Nature **168**, 1036 (1951); F. Trombe, J. phys. et radium **12**, 170 (1951).

[2] L. Néel, Ann. phys. **3**, 137 (1948).

[3] H. Labhart, Z. angew. Math. Phys. **4**, 1 (1953).

Translated by W. F. Brown, Jr.
106

SPACE ASYMMETRY OF LOW ENERGY POSITRONS FROM π^+-μ^+-e^+ DECAY

A. O. VAĬSENBERG

Submitted to JETP editor May 7, 1959

J. Exptl. Theoret. Phys. (U.S.S.R.) **37**, 566-568 (August, 1959)

THE aim of this note is to discuss the totality of the data obtained in this laboratory and given in the literature on the asymmetry in the space distribution of low energy positrons from the π^+-μ^+-e^+ decay.

We shall be interested in the asymmetry coefficient $a_{0-\epsilon}$ averaged over the spectrum from $\epsilon = 0$ up to the energy ϵ. The two component neutrino theory[1] gives for this coefficient the following expression

$$a_{0-\epsilon} = a(-2\varepsilon^3 + 3\varepsilon^4)/(2\varepsilon^3 - \varepsilon^4). \qquad (1)$$

Here a is the asymmetry coefficient averaged over the entire spectrum and it is, as is well known, negative; ϵ is expressed in units of the maximum positron energy in the μ-e decay. It follows from this expression that for small energies the asymmetry coefficient $a_{0-\epsilon}$ should decrease from the positive value of $-a$, at the very beginning of the spectrum, to zero at $\epsilon = 2/3$. Until now this prediction of the theory has not been verified with sufficient accuracy because the number of low energy particles in the spectrum of the decay positrons is small. Radiative corrections to the spectrum (Kinoshita and Sirlin[2] and also V. P. Kuznetsov, private communication) and the dispersion in the energy measurement in photoemulsion[3] result in a decrease of $a_{0-\epsilon}$ by approximately 40% in comparison with (1), and in a shift of the energy at which $a_{0-\epsilon}$ goes through zero from $\epsilon = 2/3$ to $\epsilon = 0.55 - 0.60$.

The following measurements were carried out in our laboratory: 1) a measurement of the entire spectrum for 1102 particles with $a = 0.077$;[4] 2) a measurement of the spectrum of slow electrons in which 345 particles were selected with energy $\epsilon < 0.6$ with $a = 0.077$;[4*] 3) a measurement of the entire spectrum for 565 positrons with $a = 0.28$.[3] Measurements 1) and 2) were performed in the usual emulsion NIKFI-R and measurement 3) in the same emulsion but placed in a magnetic field of 17 kgauss.

It is convenient to discuss the resultant experimental data in terms of the relative difference of the number of positrons emitted forwards and backwards

$$\delta = (N_F - N_B)/(N_F + N_B).$$

In the graph and in Table I are shown values of N_F, N_B, and the excess δ in the energy intervals $0 - 0.3$, $0.3 - 0.6$, $0.6 - 0.8$, $0.8 - 1.0$, and > 1.0. These results were obtained by combining data from all three above-mentioned spectra. These data show that the asymmetry falls sharply

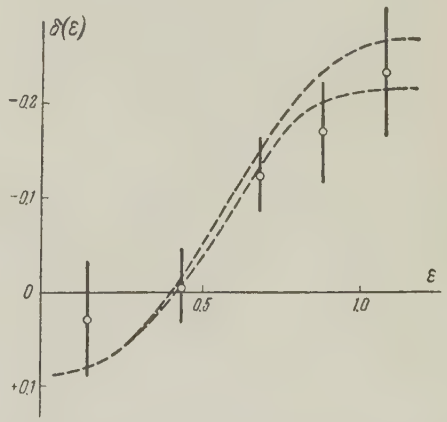

The dependence of the excess $\delta = (N_F - N_B)/(N_F + N_B)$ on the positron energy ε. The dashed line shows the dependence $\delta(\varepsilon)$ predicted by the two-component theory under the conditions of small (upper curve) and large (lower curve) dispersion of measurements. Eighty percent of the positrons were measured with intermediate values of dispersion.

TABLE I

N_F	149	352	211	134	79
N_B	140	361	270	189	124
N	289	713	481	323	206
δ	$+0.03\pm0.06$	-0.01 ± 0.04	-0.12 ± 0.04	-0.17 ± 0.05	-0.25 ± 0.07

TABLE II

Reference	$\varepsilon = 0-0.3$			$\varepsilon = 0-0.6$			a_l	k_l
	N_i	N_{iF}	N_{iB}	N_i	N_{iF}	N_{iB}		
4	245	130	115	784	398	386	0.08	0.64
3	42	19	23	218	103	115	0.28	0.90
5	74	41	33	373	184	189	0.14	0.64
6	24	15	9	209	105	104	0.14	0.64
7	32	12	20	205	89	116	0.14	0.64
8	183	103	80	—	—	—	0.19	0.50
Totals	600	320	280	1179	879	910		
Excess δ		$+0.07\pm0.04$ (observed)			-0.02 ± 0.02 (observed)			
		$+0.04$ (expected)			0.0 (expected)			

as one goes from the high end of the spectrum towards low energies and is practically absent for $\epsilon < 0.5$.

The statistical accuracy of the low-energy results will be significantly improved if one considers not only these data but also all other known data on the asymmetry at low energies obtained by the photoemulsion method. These are given in Table II (N_i stands for the number of particles in the energy interval indicated). All these measurements were carried out under quite similar conditions by the same method and with approximately the same experimental accuracy. They form a group of data which are in good agreement with each other. Table II also contains data obtained with a propane bubble chamber since the method of measurement and selection used by the author is analogous to the photoemulsion methods.[8] In the last two lines of Table II we give the observed and expected values of the excess δ. For the interval $0-0.3$ the expected value of δ was found from the formula $\delta = \alpha\Sigma N_i a_i k_i / \Sigma N_i$ where k_i is a coefficient determined by the geometry of the experiment, and $\alpha = 0.6$ serves to approximate the decrease of the expected excess due to averaging over the interval $0-0.3$, due to radiative corrections and due to the dispersion in the measurements. In the interval $0-0.6$ the expected excess equals zero. A comparison of the values of the excess δ in the last two lines of Table II shows that the observed values do not contradict the values expected on the basis of the two component theory.

Measurements of the asymmetry at low energies have also been performed by the magnetic spectrometer method.[9] The results so obtained are in agreement with those given here.

*The data as given here differ somewhat from the values given in reference 4. This is due in the first place to the fact that an analysis of the data showed that the scattering constant had to be changed from K = 25 used in reference 4 to K = 23.5/100 μ used in this work. In the second place, three newly measured particles were added to spectrum 1, which in reference 4 consisted of 1099 particles.

[1] L. Landau, Nucl. Phys. **3**, 127 (1957).

[2] T. Kinoshita and A. Sirlin, Phys. Rev. **107**, 593 (1957).

[3] Vaĭsenberg, Smirnit-skiĭ, Kolganova and Rabin, J. Exptl. Theoret. Phys. (U.S.S.R.) **37**, 326 (1959), Soviet Phys. JETP **10**, 231 (1960).

[4] Vaĭsenberg, Smirnit-skiĭ, Kolganova, Minervina, Pesotskaya, and Rabin, J. Exptl. Theoret. Phys. (U.S.S.R.) **35**, 645 (1958), Soviet Phys. JETP **8**, 448 (1959).

[5] C. Besson and V. Brisson-Fouche, Nuovo cimento **10**, 1143 (1958).

[6] Babayan, Marutyan, Matevosyan, and Sarinyan, J. Exptl. Theoret. Phys. (U.S.S.R.) **35**, 561 (1958), Soviet Phys. JETP **8**, 387 (1959).

[7] C. Costagnoli and Mandredini, preprint.

[8] Barmin, Pershin, Kanavets, and Morozov, J. Exptl. Theoret. Phys. (U.S.S.R.) **35**, 542 (1958), Soviet Phys. JETP **8**, 374 (1959).

[9] H. Kruger and M. Crowe, preprint.

Translated by A. M. Bincer
107

THE NUMBER OF ELEMENTARY BARYONS AND THE UNIVERSAL BARYON REPULSION HYPOTHESIS

Ya. B. ZEL'DOVICH

Submitted to JETP editor May 11, 1959

J. Exptl. Theoret. Phys. (U.S.S.R.) **37**, 569-570 (August, 1959)

CONSIDER a hypothetical experiment in which neutrons are compressed to a density such that the energy at the Fermi surface exceeds a few Mc^2. In that case a partial transformation of neutrons into other baryons — protons and hyperons — will be thermodynamically favored, and it will be necessary to consider as many independent Fermi distributions as there are elementary particles. The problem of the number of elementary particles may be approached in this way since if some particle is in reality not elementary it would not give rise to a separate Fermi distribution. If, for example, the Σ^+ is a bound p and K^0 complex, then at high densities it will turn out that "inside" the Σ^+ there is a p identical to other free protons (the Σ^+ will be "crushed").

In the asymptotic expression for the energy of a relativistic Fermi gas $\epsilon = AN^{4/3}$, where N is the total density of all baryons, the coefficient A is given by

$$A = [3(3\pi^2)^{1/3}/4]\,\nu^{-1/3}hc = a\nu^{-1/3},$$

where ν is the number of the kinds of truly elementary particles and a is the coefficient for $\nu = 1$. Thus there exists in principle, a possibility of determining ν; it was assumed in the above that in the limit of large densities all interactions are small compared to the Fermi energy.

If one were to insist on designating as different particles (index 1 and 2) that are actually made up of identical fermions with different surrounding boson clouds, then the increase in the total energy of a system consisting of N_1 particles of one type and N_2 particles of the second type, in comparison with the Fermi energy of each group separately, will give the appearance of a repulsion of these particles:

$$\varepsilon = a(N_1 + N_2)^{4/3} = aN_1^{4/3} + aN_2^{4/3} + V,$$

where V is the energy of the apparent interaction.

The question arises whether the experimentally observed nucleon repulsion ("hard core") at small distances is not precisely such an "apparent" interaction, due to the fact that all baryons contain "inside" them one common fermion — the carrier of the conserved baryon charge. Such a repulsion may be investigated in an elementary example.* Let us consider the collision between a proton p and a mesic atom H consisting of p and π^-. We may treat p and H as two different spin $\frac{1}{2}$ particles. Then the ^3S state of the system with parallel spins and zero orbital angular momentum is allowed. The wave function ψ for the system, after separating out the center of mass motion and the spin function, may be written as

$$\psi(\mathbf{R}, \boldsymbol{\rho}) = \Phi(\mathbf{R})\chi(\mathbf{R}, \boldsymbol{\rho}), \qquad \mathbf{R} = \mathbf{r}_1 - \mathbf{r}_2.$$
$$\boldsymbol{\rho} = \mathbf{r}_\pi - (\mathbf{r}_1 + \mathbf{r}_2)/2.$$

For the ^3S state χ should be an odd function and may be written approximately as

$$\chi = B[\varphi(\boldsymbol{\rho} - \mathbf{R}/2) - \varphi(\boldsymbol{\rho} + \mathbf{R}/2)],$$

where φ stands for the ground state function of the π^- in the atom:

$$\varphi(\boldsymbol{\rho} - \mathbf{R}/2) \sim \varphi(\mathbf{r}_\pi - \mathbf{r}_1), \qquad \varphi(\boldsymbol{\rho} + \mathbf{R}/2) = \varphi(\mathbf{r}_\pi - \mathbf{r}_2).$$

As the protons approach each other χ goes over into the function describing a P-state meson ($l_\pi = 1$) in the field of the two protons with a projection of the angular momentum onto the direction $\mathbf{R}$ equal to $l_{\mathbf{R}} = 0$. In deriving the Schrödinger equation for Φ it is customary to add to $V(\mathbf{r}_1 - \mathbf{r}_2) = V(\mathbf{R})$ the meson energy $E_\pi(R)$ calculated from the function χ as $\langle \chi^* H_\pi \chi \rangle$ where

$$H_\pi = -(\hbar^2/2m_\pi)\Delta_\rho + V(|\mathbf{r}_\pi - \mathbf{r}_1|) + V(|\mathbf{r}_\pi - \mathbf{r}_2|).$$

Actually it is also necessary to consider the effect of the operator $(-\hbar/2\mu)\Delta_R$ on $\chi(\mathbf{R}, \boldsymbol{\rho})$ (μ is reduced mass of the two protons). For small R the contribution of this term is (due to the angular part of Δ_R)

$$E_1 = \langle \chi^* | -(\hbar^2/2\mu)\Delta_R | \chi \rangle = (\hbar^2/2\mu)2R^{-2}.$$

The Schrödinger equation for Φ

$$-(\hbar^2/2\mu)\Delta_R\Phi + [V(R) + E_\pi(R) + \hbar^2/\mu R^2]\Phi = E\Phi,$$

insures the vanishing for $R = 0$ of a spherically symmetric function Φ only if the term E_1 is included. Such a result is self-explanatory: two protons with parallel spins must at small distances be in a state† $L = 1$ and E_1 is the centrifugal potential. However E_1 appears as the effective potential in the equation for the function Φ describing the spherically symmetric (S) state.

In the study of the scattering of p on H after elimination of the ^3S component the contribution fo E_1 will manifest itself as a strong repulsion at small distances. In contrast to the usual term E_π the expression for E_1 does not depend on the properties (mass, charge) of the meson.

The appearance of E_1 is entirely due to the fact that the "interiors" of the two different particles p and H are identical. If the meson cloud surrounding the proton in the H atom is in a state with $l_\pi = 1$ then a repulsion will appear not only in the ^3S but also in the ^1S state. The average value of the coefficient of the term $\hbar^2/2\mu R^2$ should be of the order of unity.

In the study of two identical particles (e.g., two atoms H) with meson clouds having $l_\pi = 1$ there also appears a repulsion in the ^1S state. However the average Fermi energy in this case remains unchanged; that is, the repulsion in the ^1S state is compensated for by an attraction in the ^3P state (reduced centrifugal potential in that state).

Let us return from models to baryons. The hypothesis of one common "core" leads to the conclusion that in the interaction of different or identical baryons in S states there should appear a strong repulsion at small distances with a potential $\sim \hbar^2/2\mu R^2$. The present-day data[1] on the p-p and p-n interactions at small distances are in agreement with this estimate. No such repulsion should be observed in the interaction of any baryons with any antibaryons.

In the interaction of identical particles the short range interaction, averaged appropriately over the various angular momentum states, vanishes. The study of short range forces between different particles in various spin and angular momentum states could replace the "gedanken" experiment on the determination of the number ν of elementary particles from the density dependence of the energy considered at the beginning of this note, and would make it possible to establish whether or not the different pairs of particles under study have a common "interior."

I take this opportunity to express my gratitude to A. D. Sakharov; a discussion with him on the state of matter in superdense stars served as the origin of this work.

*This example was discussed by S. S. Gershteĭn in connection with the theory of hydrogen mesic molecules.

†The total orbital angular momentum of the system equals zero, however the meson also carries one unit of angular momentum.

[1] P. S. Signell and R. E. Marshak, Phys. Rev. 109, 1229 (1958).

Translated by A. M. Bincer
108

POLARIZATION EFFECTS IN THE DIRECT TRANSITION OF $\mu^+\mu^-$ INTO AN ELECTRON-POSITRON PAIR

B. A. LYSOV

Moscow State University

Submitted to JETP editor May 13, 1959

J. Exptl. Theoret. Phys. (U.S.S.R.) 37, 571-572 (August, 1959)

RECENTLY Zel'dovich[1] called attention to the possibility of a direct transition of a $\mu^+\mu^-$ pair through a virtual photon into an electron-positron pair. It is of interest to study this process in more detail, in particular using not only the nonrelativistic approximation employed by Zel'dovich.

The matrix element describing this process can be obtained directly from the exchange part of the matrix element for Bhabha scattering (see, e.g., reference 2, formula 49,49) by replacing the initial state electron and positron wave functions in it by μ-meson wave functions. Keeping this remark in mind it is easy to write down the expression for the probability of the transition $\mu^+\mu^- \to e^+e^-$. In the center-of-mass system, neglecting the rest masses of the electron and positron in comparison to their energies, we obtain

$$dw = (e^4 d\Omega / 8c\hbar^2 L^3 K_\mu^2)\, S^+ S, \tag{1}$$

where the spin part of the matrix element is

$$S = b_\mu'^{+}\alpha_\nu b_\mu b_e'^{+}\alpha_\nu b_e. \tag{2}$$

Here α_ν is a four-vector composed of Dirac matrices and the b's are the spinor amplitudes of the wave functions of the corresponding particles. Further calculations dealing with the spin states of the particles are considerably simplified if use is made of a table given in the monograph by Sokolov[2] (formulas 21,17 and 21,18). Applying these formulas to Eq. (1) and summing over the electron and positron spins we find

$$dw(s_\mu, s_\mu') = \frac{e^4 d\Omega}{8c\hbar^2 L^3 K_\mu^2}\left(1 - s_\mu s_\mu' \frac{k_\mu^2}{K_\mu^2} + \frac{k_{0\mu}^2}{K_\mu^2}\right)(1 - s_\mu s_\mu' \cos^2\theta). \tag{3}$$

Here $\hbar\mathbf{k}$ is the momentum of the particle, $c\hbar K = c\hbar\sqrt{k^2 + k_0^2}$ is its energy, s is the projection of the particle's spin onto its direction of motion, and θ is the angle between the meson and electron momenta. In Eq. (3) $s_\mu s_\mu'$ can take on the values ± 1, where the value -1 corresponds to the ortho-state of $\mu^+\mu^-$ with total spin parallel or antipar-

allel to the direction of motion of the mesons. Setting $s_\mu s'_\mu = -1$ in Eq. (3) we find

$$dw_1^s = dw_{-1}^s = (e^4 d\Omega / 4c\hbar^2 L^3 K_\mu^2)(1 + \cos^2\theta). \quad (4)$$

In order to find the transition probability $\mu^+\mu^- \rightarrow e^+e^-$ in the third ortho-state where the projection of the total spin of the mesons onto their direction of motion is zero, we introduce the appropriate symmetric combination of the spinor amplitudes directly into Eq. (1) and write it in the form

$$dw_0^s = (e^4 d\Omega / 8c\hbar^2 L^3 K_\mu^2)(b_e^+ \alpha_{1\nu} b'^+_e \alpha_{2\nu} b_e) \cdot 2^{-1/2}\{b_\mu^+(1)\alpha_{1\nu} b'_\mu(1) + b_\mu^+(-1)\alpha_{1\nu} b'_\mu(-1)\} \cdot 2^{-1/2}\{b'^+_\mu(1)\alpha_{2\nu} b_\mu(1) + b'^+_\mu(-1)\alpha_{2\nu} b_\mu(-1)\}. \quad (5)$$

For simplicity let us choose the z axis along the direction of motion of the mesons. One can then show that $b(s) = \rho_3\sigma_1 b(-s)$. With this fact in mind we obtain from Eq. (5), after summing over the electron and positron spins, the following expression for the transition probability in the third ortho-state:

$$dw_0^s = (e^4 d\Omega / 4c\hbar^2 L^3 K_\mu^2) \times (1 - k_\mu^2 / K_\mu + k_{0\mu}^2 / K_\mu^2)(1 - \cos^2\theta). \quad (6)$$

A comparison of Eqs. (4) and (6) shows that the transition probability in the orthostate depends strongly on the value of the projection of the total spin of the mesons onto their direction of motion. When this projection equals ± 1 the electrons are emitted mainly along the direction of motion of the mesons, whereas when this projection equals 0 the electrons are emitted mainly in a direction perpendicular to the line of motion of the mesons.

In the nonrelativistic approximation ($k_\mu \rightarrow 0$, $\cos^2\theta \rightarrow 1/3$) the $\mu^+\mu^- \rightarrow e^+e^-$ transition probability is the same in all three ortho-states and is equal to

$$w^s = 4\pi e^4 / 3c\hbar^2 L^3 k_{0\mu}, \quad (7)$$

which agrees with the result of Zel'dovich. However as the meson energy increases w_0^S decreases much faster then w_1^S, w_{-1}^S and in the extreme relativistic limit (when $K_\mu \gg k_{0\mu}$) the probability w_0^S vanishes.

As can be seen from Eqs. (3), (4), and (6) the $\mu^+\mu^- \rightarrow e^+e^-$ transition probability in the para-state is zero not only in the nonrelativistic approximation but in general.

I am indebted to Prof. A. A. Sokolov for his help and advice.

[1] Ya. Zel'dovich, J. Exptl. Theoret. Phys. (U.S.S.R.) **36**, 646 (1959), Soviet Phys. JETP **9**, 450 (1959).

[2] A. A. Sokolov, Введение в квантовую электродинамику (Introduction to Quantum Electrodynamics), M., Fizmatgiz, 1958, Ch. 4.

Translated by A. M. Bincer
109

AN INVESTIGATION OF THE QUANTIZED OSCILLATIONS IN THE MAGNETIC SUSCEPTIBILITY OF BISMUTH AT EXTREMELY LOW TEMPERATURES

N. B. BRANDT, A. E. DUBROVSKAYA, and G. A. KYTIN

Moscow State University

Submitted to JETP editor May 14, 1959

J. Exptl. Theoret. Phys. (U.S.S.R.) **37**, 572-575 (August, 1959)

IT can be deduced from galvanomagnetic measurements that bismuth belongs to the group of metals having equal numbers of electrons and holes. We can now regard it as established that a portion of the Fermi surface for groups of electrons is well described by Shoenberg's three-ellipsoid model,[1] proposed on the basis of the measurement of quantized oscillations of the magnetic susceptibility of bismuth at helium temperatures.

Experiments by other authors on oscillations of magnetic susceptibility,[2,3] electrical resistance and Hall emf[4,5,6] in high magnetic fields, related to another part of the Fermi surface, have not until now yielded positive results. We thought that these oscillations were not observed at helium temperatures because of their small amplitude, which would be sufficiently enhanced for observation at much lower temperatures. For this purpose we developed the apparatus[7] and measured the anisotropy of magnetic susceptibility of bismuth at extremely low temperatures. These experiments are of interest in themselves since, as far as we know, the magnetic susceptibility of metals and semiconductors has not before been studied at these low temperatures.

The apparatus, which is a torsion balance, is shown in Fig. 1. The salt pill, 1, with the heat link,[8] 2, and the sample holder, 3, are fixed to the balance suspension system. The glass sleeve for the balance, 4, consists of two tubes separated

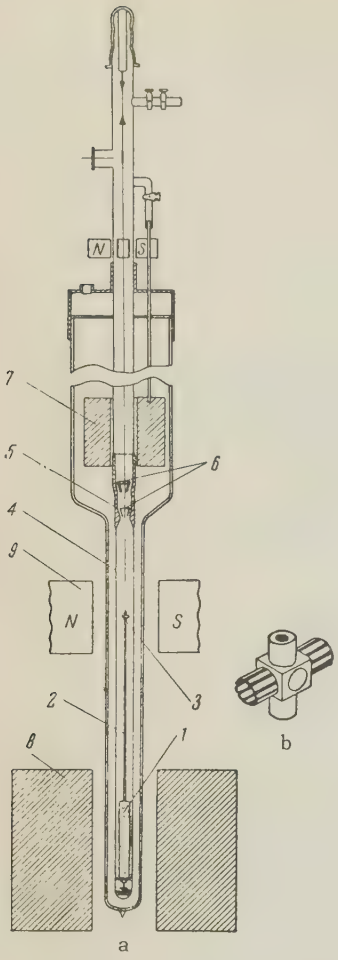

FIG. 1. a – Schematic drawing of the apparatus. b – Specimen holder.

by the copper connector, 5, inside which two copper pieces are freely fixed, with holes in their centers, to shield the specimen and salt from radiation. The sleeve, 4, is in the liquid helium bath and can be evacuated by the charcoal pump, 7. After adiabatic demagnetization of the salt the balance was lowered until the pill was in the center of the magnetic shield, 8, while the specimen was in the center of the pole pieces, 9, of the electromagnet. In a single-run adiabatic demagnetization of the salt and cooling of the specimen could be repeated 6 or 7 times. The temperature was deduced from the susceptibility of the salt. The apparatus heated up from 0.06° to 0.1° K in 60 to 70 minutes, so that curves could be plotted of the dependence of the moment of the forces, Δ, due to the anisotropy of the specimen, acting in the plane perpendicular to the balance axis, on the direction of the uniform magnetic field H, within a temperature interval of about 0.02° K.

We used a cylindrical single crystal of bismuth of diameter 3.6 mm and length 7 – 8 mm, grown from Hilger bismuth, purified by thirty vacuum recrystallizations. The trigonal axis was perpendicular to the axis of the balance and the binary

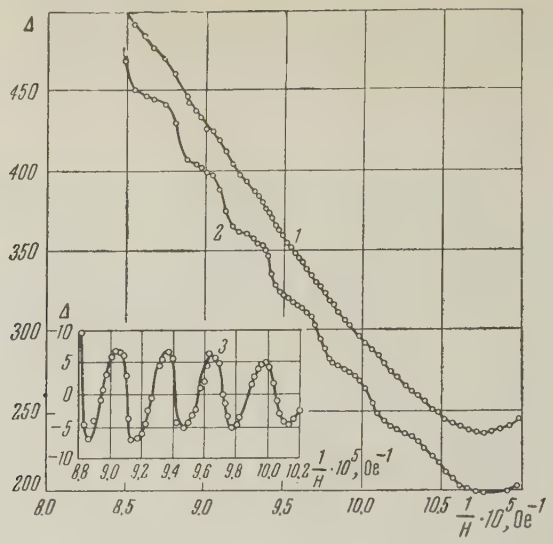

FIG. 2. Dependence of the moment of the forces, Δ, (in arbitrary units) acting on the specimen, on the magnetic field strength for $\psi = 81.5°$. Curve 1 is for T = 1.6° K, curve 2 for T = 0.07° K. Curve 3 represents the high frequency component deduced, at T = 0.07° K.

axis parallel to it. The error in orientation of the axes was not more than 0.3 – 0.4°.

At the lowest temperatures high frequency oscillations can be seen, superimposed on the curves of the low frequency oscillations. Figure 2 shows the dependence of Δ on H for a particular value of ψ, the angle between the direction of H and the trigonal axis of the specimen.

The frequency of oscillation of the susceptibility (or of Δ) with changing H is proportional to the area of the corresponding extreme cross-section, S_m, of the Fermi surface perpendicular to H.[9] The angular dependence of S_m for the

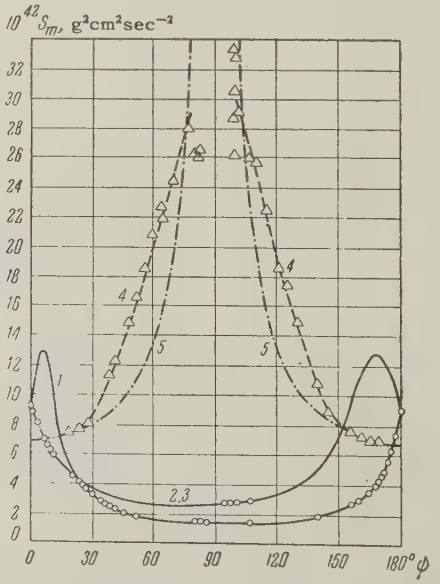

FIG. 3. Angular dependence of S_m for the new oscillations (curve 4) and for the oscillations connected with Shoenberg's three-ellipsoid model (curves 1, 2, 3).

new oscillations is shown in Fig. 3 by the dashed curve. It appears that these oscillations correspond to a group of holes which have a Fermi surface in the form of a surface of revolution, stretched out along the trigonal axis.* On the assumption that this surface is closed, a rough calculation leads to a value of the "hole" concentration $n \approx 0.5 \times 10^{18}$ cm^{-3} and an effective mass along the trigonal axis $m_3^* = (\frac{1}{2}\pi)(\partial S_m/\partial E) \approx 0.06\, m_0$ (m_0 is the free electron mass). It is most probable that the high frequency oscillations in the angular range $105° > \psi > 75°$ belong to another group of charge carriers. (Measurements in much greater magnetic fields are necessary for studying this question.) This is in agreement with the suggestion that there must be at least three charge carrier groups in bismuth.[10]

We are most grateful to A. M. Kosevich for discussion of the results, to A. I. Shal'nikov for his interest in the work and to M. V. Volkova for assistance with the measurements.

*More exact measurements show that the part of this surface, corresponding to the angular range $180° \geq \psi \geq 105°$ and $75° \geq \psi \geq 0°$, approximates an ellipsoid.

[1] D. Shoenberg, Proc. Roy. Soc. **A170**, 341 (1939).

[2] D. Shoenberg, Phil. Trans. Roy. Soc. **A245**, 1 (1952).

[3] J. S. Dhillon and D. Shoenberg, Phil. Trans. Roy. Soc. **A248**, 1 (1955).

[4] M. C. Steele and J. Babiskin, Phys. Rev. **98**, 359 (1955).

[5] R. A. Connell and J. A. Marcus, Phys. Rev. **107**, 940 (1957).

[6] J. Babiskin, Phys. Rev. **107**, 981 (1957).

[7] N. B. Brandt, Приборы и техника эксперимента (Instrum. and Meas. Engg.), in press.

[8] N. E. Alekseevskiĭ and Yu. P. Gaĭdukov, J. Exptl. Theoret. Phys. (U.S.S.R.) **25**, 383 (1953); ibid. **31**, 947 (1956), Soviet Phys. JETP **4**, 807 (1957).

[9] I. M. Lifshitz and A. M. Kosevich, Dokl. Akad. Nauk SSSR **96**, 963 (1954); J. Exptl. Theoret. Phys. (U.S.S.R.) **29**, 730 (1955), Soviet Phys. JETP **2**, 636 (1956).

[10] N. B. Brandt and V. A. Venttsel', J. Exptl. Theoret. Phys. (U.S.S.R.) **35**, 1083 (1958), Soviet Phys. JETP **8**, 757 (1959).

Translated by R. Berman
110

POLARIZATION EFFECTS IN THE $\pi^0 \to e^- + e^+ + \gamma$ *DECAY*

B. K. KERIMOV, A. I. MUKHTAROV, and S. A. GADZHIEV

Moscow State University

Submitted to JETP editor May 16, 1959

J. Exptl. Theoret. Phys. (U.S.S.R.) **37**, 575-576 (August, 1959)

A number of events were recently observed[1,2] which corresponded to a charge exchange scattering of π^- mesons on hydrogen ($\pi^- + p \to \pi^0 + n$) followed by the decay of the π^0 meson into a Dalitz pair and a photon:

$$\pi^0 \to e^- + e^+ + \gamma. \qquad (1)$$

The probability for the decay (1), summed over the polarizations of the particles in the final state, was calculated by Dalitz[3] and Kroll and Wada.[4] In this paper we give the results of a calculation of the probability for the π^0 meson to decay according to the mode (1), taking into account the spin states (longitudinal polarizations) of the electron-positron pair and of the photon.

The direct interaction Hamiltonian for process (1) is given by

$$H_{\text{int}} = eg\,\psi_{\pi^0}\{\psi_{e^-}^{\pm} O_i D^{-1}(\boldsymbol{\alpha}\mathbf{A}^+)\,\psi_{e^+} + (\psi_{e^-}^{\pm}\boldsymbol{\alpha}\mathbf{A}^+ D^{-1})\,O_i\psi_{e^+}\}. \qquad (2)$$

Here ψ_{π^0}, $\psi_{e^-}^{*}$, ψ_{e^+} and A^+ are the wave functions of the π^0 meson, electron, positron and photon respectively; D is the Dirac operator; $\boldsymbol{\alpha} = \rho_1\sigma$ is a Dirac matrix; if the π^0 meson is pseudoscalar $O_i = \rho_2$ and if it is scalar $O_i = \rho_3$.

The field amplitude of a circularly polarized photon is given by the formula[5]

$$\mathbf{a}_l^+ = (\beta - il[\mathbf{n}\times\beta])/\sqrt{2}, \qquad \mathbf{n} = \boldsymbol{\varkappa}/\varkappa, \qquad (3)$$

where $\boldsymbol{\varkappa}$ is the photon wave vector and $\boldsymbol{\beta} \perp \mathbf{n}$ is an arbitrary unit vector. For a right-circularly polarized photon $l = 1$ (spin parallel to $\boldsymbol{\varkappa}$) and for a left-circularly polarized photon $l = -1$ (spin antiparallel to $\boldsymbol{\varkappa}$). We made use of formula (21.15) in Sokolov's[5] book to calculate the matrix elements of the decay (1) with longitudinal polarization of the pair taken into account. We obtain the following expression, in the rest system of the π^0 meson (pseudoscalar), for the probability for the decay (1) with prescribed polarizations of the particles:

$$dW(s_-, s_+, l, \theta) = \frac{e^2 g^2}{\hbar^2 c^4 (2\pi)^3}\,\frac{k_+^2\, d\Omega_+\, (dk_-)}{k_{0\pi}k_+K_-(k_{0\pi} - K_-) + k_{0\pi}K_-k_-K_+\cos\theta}$$

$$\times\{\Phi_1 + s_-s_+\Phi_2 + ls_-\Phi_3 + ls_+\Phi_4\}, \qquad (4)$$

where

$$\Phi_1 = k_{0\pi}^2 q^{-2} k_-^2 k_+^2 \sin^2\theta + 2\,[K_-(k_{0\pi} - K_-)\,q^2 - (k_-^2 + \mathbf{k}_-\mathbf{k}_+)(k_-^2 + \mathbf{k}_-\mathbf{k}_+ + (2K_- - k_{0\pi})\,q)],$$

$$\Phi_2 = q^{-2} k_- k_+ \sin^2\theta\,[k_{0\pi}^2 (K_- K_+ - k_0^2) + 2k_0^2 q^2] + (2/k_+)\{q^2 k_- (K_+ (k_{0\pi} - K_-) - k_0^2) - K_+ \times (k_- + k_+ \cos\theta)\,[K_-(k_-^2 + \mathbf{k}_-\mathbf{k}_+) + (2k_-^2 - k_{0\pi} K_-)\,q]\},$$

$$\Phi_3 = 2q^{-2} k_-^2 k_+^2 \sin^2\theta k_{0\pi} K_- q + 2k_- (k_{0\pi} - K_-)\,q^2 - 2(k_- + k_+\cos\theta)\,[K_-(k_-^2 + \mathbf{k}_-\mathbf{k}_+ + (2K_- - k_{0\pi})\,q) - k_0^2 q],$$

$$\Phi_4 = 2q^{-2} k_-^2 k_+ \sin^2\theta k_{0\pi} K_+ q + 2(K_-/k_+)\,q^2\,[K_+(k_{0\pi} - K_-) - k_0^2] - (2/k_+)(k_-^2 + \mathbf{k}_-\mathbf{k}_+)\,[K_+(k_-^2 + \mathbf{k}_-\mathbf{k}_+ + (2K_- - k_{0\pi})\,q) + k_0^2 q],$$

$$\mathbf{q} \equiv -\varkappa = \mathbf{k}_- + \mathbf{k}_+, \qquad \cos\theta = \mathbf{k}_-\mathbf{k}_+ / k_- k_+, \quad k_{0\pi} = m_{\pi^0} c/\hbar,$$

$$k_+ = \frac{-2bk_-\cos\theta \pm a\sqrt{b^2 - k_0^2(a^2 - 4k_-^2\cos^2\theta)}}{a^2 - 4k_-^2\cos^2\theta},$$

$$a = 2(k_{0\pi} - K_-), \qquad b = k_{0\pi}(k_{0\pi} - 2K_-) + 2k_0^2,$$

$$K_\pm = \sqrt{k_0^2 + k_\pm^2}. \qquad (5)$$

Here $E_\pm = c\hbar K_\pm$, $p_\pm = \hbar \mathbf{k}_\pm$ stand for the total energy and momentum of the electron and positron; $k_0 = m_0 c/\hbar$ is the rest mass; $d\Omega_+$ is the solid angle of positron emission; s_+, $s_- = \pm 1$ are the eigenvalues of the projection operator $\sigma \cdot \mathbf{k}_\pm / k_\pm$. For $s_- = 1$ ($s_+ = 1$) the electron (positron) has right polarization and for $s_- = -1$ ($s_+ = -1$) left polarization. The corresponding expressions for Φ_i ($i = 1, 2, 3, 4$) are also easy to obtain for the case of a scalar π^0 meson. Formula (4) gives the angle and energy dependence of the degree of longitudinal polarization of the created pairs and the correlation between polarizations (the terms proportional to $s_- s_+$, $l s_-$, $l s_+$) in the decay (1); this could be of value in the determination of the properties of the π^0 meson. It follows from (4) and (5) that for extremely relativistic electrons and positrons (when $k_-, k_+ \gg k_0$ and $\Phi_1 = \Phi_2$, $\Phi_3 = \Phi_4$) the probability for the decay (1) will differ from zero only if both the electron and positron of a pair are right polarized ($s_- = s_+ = 1$) or left polarized ($s_- = s_+ = -1$). In that case the π^0-decay with the emission of a left polarized electron ($s_- = -1$) and right polarized positron ($s_+ = +1$) or vice versa ($s_- = +1$, $s_+ = -1$) is forbidden since the probability (4) vanishes.

In conclusion we express gratitude to Prof. A. A. Sokolov for his interest in this work.

[1] Budagov, Viktor, Dzhelepov, Ermolov, and Moskalev, J. Exptl. Theoret. Phys. (U.S.S.R.) **35**, 1575 (1958), Soviet Phys. JETP **8**, 1101 (1959).

[2] Sargent, Cornelius, Rinehart, Lederman, and Rogers, Phys. Rev. **98**, 1349 (1955).

[3] R. H. Dalitz, Proc. Phys. Soc. **A64**, 667 (1951).

[4] N. M. Kroll and W. Wada, Phys. Rev. **98**, 1355 (1955).

[5] A. A. Sokolov, Введение в квантовую электродинамику (Introduction to Quantum Electrodynamics), M., Fizmatgiz, 1958.

Translated by A. M. Bincer
111

ATTRACTION OF SMALL PARTICLES SUSPENDED IN A LIQUID AT LARGE DISTANCES

L. P. PITAEVSKIĬ

Institute of Terrestrial Magnetism, Ionosphere, and Radio Wave Propagation, Academy of Sciences, U.S.S.R.

Submitted to JETP editor May 15, 1959

J. Exptl. Theoret. Phys. (U.S.S.R.) **37**, 577-578 (August, 1959)

In the present note we derive formulas for the interaction energy connected with the Van-der-Waals forces of interaction between uncharged particles suspended in a liquid. The distance between the particles will be assumed large compared with their dimensions.

In principle this problem can be solved on the basis of the general theory of Van-der-Waals forces in dielectrics.[1] However, as shown earlier,[2] the expression for the interaction forces of arbitrary bodies in a medium can be derived by simple transformation from the corresponding expression for the interaction forces in vacuum. Indeed, the expression for the additional pressure in a medium of dielectric constant ϵ can be obtained from the expression for the pressure in vacuum by multiplying the integrand in the integral with respect to frequency* (this integral determines the pressure) by $\epsilon^{3/2}$, by replacing the dielectric constant of the interacting bodies ϵ_1 by ϵ_1/ϵ, and by increasing all the linear dimensions by a factor of $\sqrt{\epsilon}$. In accordance with this, the energy U of the interaction of the particles in the medium can be obtained from the energy of interaction in vacuum U_0 by replacing the dielectric constant of the particles ϵ_1 by ϵ_1/ϵ, their volume V by

$\epsilon^{3/2}V$, and the distance R between them by $\sqrt{\epsilon}R$.

On the other hand, the energy of interaction of small particles in vacuum is given directly by the formulas of London or Casimir-Polder (at distances which are respectively smaller or larger than the characteristic wavelengths λ_0 in the spectrum), because only the smallness of the dimensions of the interacting systems is used in the derivation of these equations. We shall find it convenient to rewrite these equations in the following form:[3]

$$U_0 = (3\hbar/\pi R^6)\int_0^\infty \alpha^2(i\xi)\,d\xi, \quad \text{for } R \ll \lambda_0,$$
$$U_0 = (23\hbar c/4\pi R^7)\alpha^2(0), \quad \text{for } R \gg \lambda_0, \qquad (1)$$

where $\alpha(\omega)$ is the complex polarizability of the particles. Considering that the polarizability of spherical particles of volume V with dielectric constant ϵ_1 is given by

$$\alpha(\omega) = \frac{3}{4\pi}\frac{\varepsilon_1(\omega)-1}{\varepsilon_1(\omega)+2}V, \qquad (2)$$

and performing the transformation indicated in the beginning of the article, we obtain a final equation for the interaction energy in the liquid

$$U = \frac{27\hbar V^2}{16\pi^3 R^6}\int_0^\infty \left[\frac{\varepsilon_1(i\xi)-\varepsilon(i\xi)}{\varepsilon_1(i\xi)+2\varepsilon(i\xi)}\right]^2 d\xi, \quad \text{for } R \ll \lambda_0,$$
$$U = \frac{207}{64\pi^3}\frac{V^2}{R^7}\frac{\hbar c}{\sqrt{\varepsilon(0)}}\left[\frac{\varepsilon_1(0)-\varepsilon(0)}{\varepsilon_1(0)+2\varepsilon(0)}\right]^2, \quad \text{for } R \gg \lambda_0. \qquad (3)$$

We note that for the second equation in (3) to be applicable it is enough that the dimensions of the particles be small only compared with the distance between them (and not compared with λ_0).

Equations (3) can be also rewritten in a different form, taking into account the fact that the change in the dielectric constant of a liquid, due to the presence of N particles per unit volume, is equal to

$$\delta\varepsilon = 3NV(\varepsilon_1-\varepsilon)\varepsilon/(\varepsilon_1+2\varepsilon). \qquad (4)$$

(where $NV \ll 1$; see, for example, reference 3, problems of Sec. 9).

Using (4), we rewrite (3) in the form

$$U = \frac{3\hbar}{16\pi^3 R^6}\int_0^\infty \left(\frac{\partial\varepsilon(i\xi)}{\partial N}\right)^2 \frac{d\xi}{\varepsilon^2(i\xi)}, \quad \text{for } R \ll \lambda_0,$$
$$U = \frac{23\hbar c}{64\pi^3 R^7 \varepsilon^{5/2}(0)}\left(\frac{\partial\varepsilon(0)}{\partial N}\right)^2, \quad \text{for } R \gg \lambda_0 \qquad (5)$$

[$\epsilon(\omega)$ is the dielectric constant of the mixture and N is the number of particles per unit volume].

We note that in this form Eqs. (5) describe not only the interaction of macroscopic particles suspended in a liquid, but also the interaction of particles with dimensions on the order of interatomic distances, as well as the interaction between molecules of a dissolved substance in a solution. Here, however, the value of the quantity $\partial\epsilon(\omega)/\partial N$ — the derivative of the dielectric constant of the solution with respect to the concentration — can naturally no longer be calculated from Eq. (4), but must be obtained directly from experiment.

*We use the equations for the absolute temperature zero, and the influence of the temperature on the interaction forces under ordinary conditions is very small.

[1] I. E. Dzyaloshinskiĭ and L. P. Pitaevskiĭ, J. Exptl. Theoret. Phys. (U.S.S.R.) **36**, 1797 (1959), Soviet Phys. JETP **9**, 1282 (1959).

[2] Dzyaloshinskiĭ, Lifshitz, and Pitaevskiĭ, J. Exptl. Theoret. Phys. (U.S.S.R.) **37**, 229 (1959), Soviet Phys. JETP **10**, 161 (1960).

[3] L. D. Landau and E. M. Lifshitz, Электродинамика сплошных сред, (Electrodynamics of Continuous Media), Gostekhizdat, 1957.

Translated by J. G. Adashko
112

A SIMPLE MODEL IN THE THEORY OF SUPERCONDUCTIVITY

Yu. B. RUMER

Institute of Radiophysics and Electronics, Siberian Branch, Academy of Sciences, U.S.S.R.

Submitted to JETP editor May 16, 1959

J. Exptl. Theoret. Phys. (U.S.S.R.) **37**, 578-580 (August, 1959)

THE key to the understanding of superconductivity lies in the Cooper phenomenon, i.e., in the fact that two electrons with opposite momenta and spins near the Fermi surface can form bound states. These states obviously represent bosons, which form a condensate at low temperatures.

In constructing a theory of superconductivity it is then natural to take the Bose condensation of these bosons explicitly into account. In analogy to the theory of superfluidity of Bogolyubov we therefore introduce the boson creation and annihilation operators $c^+(q)$ and $c(q)$.

The Hamiltonian which takes account of the

creation and the decay of the bosons is written in the form

$$H = \sum_k \varepsilon(k)\,(a^+(k)\,a(k) + b^+(-k)\,b(-k)) + \sum_q \omega(q)\,c^+(q)\,c(q) + \sum_{k,q} f(q)\,(c^+(q)\,a(k)\,b(q-k) + c(q)\,b^+(q-k)\,a^+(k)), \quad (1)$$

where $a^+(k)$ and $a(k)$ ($b^+(k)$ and $b(k)$) are the Fermion operators for electrons with "right" ("left") spin; $\epsilon(k) = k^2/2m$; $\omega(q)$ is the energy of the bosons; it is important that $\omega(0) \neq 0$, i.e., that the bosons have a non-vanishing rest energy.

We shall further assume that the overwhelming majority of the bosons lies in the condensate. We therefore neglect all terms with $q \neq 0$ in the Hamiltonian (1). This leads to the approximate Hamiltonian

$$H' = \sum_k \varepsilon(k)\,(a^+(k)\,a(k) + b^+(-k)\,b(-k)) + \omega(0)\,c^+(0)\,c(0) + f(0)\sum_k (c^+(0)\,a(k)\,b(-k) + c(0)\,b^+(-k)\,a^+(k)). \quad (2)$$

As in the theory of superfluidity, we disregard the non-commutativity of the operators $c^+(0)$ and $c(0)$, i.e., we regard these operators as numbers. Without loss of generality we may regard

$$c^+(0) = c(0) = \Delta / f(0) \quad (3)$$

as a real number. In this approximation we obtain the model Hamiltonian

$$H_R = \sum_k \varepsilon(k)\,[a^+(k)\,a(k) + b^+(-k)\,b(-k)] + \Delta \sum_k [a(k)\,b(-k) + b^+(-k)\,a^+(k)] + \omega(0)\,\Delta^2 / f^2(0). \quad (4)$$

It can be easily verified that the Hamiltonian H commutes with the operator of the total number of electrons:

$$N = \sum_k [a^+(k)\,a(k) + b^+(-k)\,b(-k)] + \sum_q 2c^+(q)\,c(q). \quad (5)$$

Denoting the chemical potential by μ, we see that the operator $H_R - \mu N$ can at once be diagonalized by the canonical transformation of Bogolyubov:

$$a(k) = \xi_k \cos\varphi_k + \eta_k^+ \sin\varphi_k,$$
$$b(-k) = -\xi_k^+ \sin\varphi_k + \eta_k \cos\varphi_k, \quad (6)$$

where

$$\tan 2\varphi_k = \Delta / [\varepsilon(k) - \mu].$$

In terms of the new coordinates ξ_k, η_k we have

$$H_R - \mu N = \sum_k \Big\{[\varepsilon(k) - \mu] - \sqrt{[\varepsilon(k) - \mu]^2 + \Delta^2}\,(1 - \xi_k^+\xi_k - \eta_k^+\eta_k)\Big\} + (\omega(0) - 2\mu)\,\Delta^2 / f^2(0). \quad (7)$$

We average the operator (7) over the state with an energy E corresponding to the given temperature T:

$$\langle H_R - \mu N\rangle_E = \sum_k \{[\varepsilon(k) - \mu] - \sqrt{[\varepsilon(k) - \mu]^2 + \Delta^2}\,(1 - 2n(k))\} + [\omega(0) - 2\mu]\,\Delta^2 / f^2(0), \quad (8)$$

where

$$n(k) = \langle \xi_k^+\xi_k\rangle_E = \langle \eta_k^+\eta_k\rangle_E = [\exp\{\sqrt{[\varepsilon(k) - \mu]^2 + \Delta^2}\,/\,T\} + 1]^{-1}.$$

To find Δ we minimize $\langle H_R - \mu N\rangle_E$ with constant $n(k)$. We have

$$\frac{\partial}{\partial\Delta}\langle H_R - \mu N\rangle = -\sum_k \frac{\Delta}{\sqrt{[\varepsilon(k) - \mu]^2 + \Delta^2}} \tanh\frac{\sqrt{[\varepsilon(k) - \mu]^2 + \Delta^2}}{2T} + \frac{2[\omega(0) - 2\mu]}{f^2(0)}\Delta = 0, \quad (9)$$

which leads to the following equation for the determination of Δ:

$$1 = \frac{f^2(0)}{2[\omega(0) - 2\mu]} \sum_k \frac{\tanh\{\sqrt{[\varepsilon(k) - \mu]^2 + \Delta^2}\,/\,2T\}}{\sqrt{[\varepsilon(k) - \mu]^2 + \Delta^2}}. \quad (10)$$

Comparing (10) with the corresponding formula of the usual theory, we see that our model leads to superconductivity if $\omega(0) - 2\mu > 0$. At first sight it seems reasonable to set $\omega(0) - 2\mu \approx -2\Delta < 0$, since $\omega(0) - 2\mu$ is just the binding energy of the pair. It should be noted, however, that the Hamiltonian (1) does not take account of the direct interaction of the unpaired electrons with one another. The amplitudes $c^+(0)$ and $c(0)$ and the energy $\omega(0)$ are therefore the renormalized amplitudes and energy of the pair. As our calculations show, we can neglect the four-fermion terms in the Hamiltonian and at the same time renormalize the pair energy such that the inequality $\omega_0 - 2\mu > 0$ is satisfied.

We see that the quantity $f^2(0)/[\omega(0) - 2\mu] = g > 0$ is the same as the interaction constant in the Bardeen-Cooper-Schrieffer theory.

Translated by R. Lipperheide
113

RESIDUAL IONIZATION OF A GAS EXPANDING IN VACUUM

Yu. P. RAĬZER

Submitted to JETP editor April 1, 1959

J. Exptl. Theoret. Phys. (U.S.S.R.) **37**, 580-582 (August, 1959)

IN many processes, rapid heating of a substance to a high temperature, on the order of several tens of thousands of degrees, produces a gas cloud which then scatters in vacuum.*

During the stage of sufficiently large expansion, the scattering of the gas occurs with an almost constant average velocity, u, corresponding to the total conversion of the initial internal energy ϵ_0 into kinetic energy, ($u = \sqrt{2\epsilon_0}$ if the process is adiabatic). The dimensions of the cloud are in this case on the order of $r = ut$ and the mean density (the number of atoms per cubic centimeter) is

$$n = n_0 (r_0 / r)^3 = n_0 (t_0 / t), \quad t_0 = r_0 / u, \tag{1}$$

where n_0 and r_0 are the initial density and dimension of the heated body. The gas cools adiabatically

$$T = (Ae^{S/R})^{\gamma-1} n^{\gamma-1} \sim t^{-3(\gamma-1)}. \tag{2}$$

Here γ is the adiabatic exponent, S the specific entropy, and A is a constant determined from the known equations of statistical mechanics.

At high temperature the gas is strongly ionized. In thermodynamic equilibrium, the degree of ionization would rapidly tend to zero upon cooling. Actually, however, if the expansion obeys Eq. (1), the number of particle collisions, even after an infinite time interval, is limited and the recombination is never completed at $t \to \infty$ ($T \to 0$): a so-called "quenching" occurs (unlike the plane case, when $n \sim 1/t$, see reference 2).

To estimate the residual ionization, let us consider the kinetic equations (for simplicity we restrict ourselves to the case of a monatomic gas made up of atoms of a single element, incapable of producing negative ions). If x is the actual degree of ionization, x_{eq} the equilibrium degree of ionization, and $\alpha(x, n, T)$ is the coefficient of recombination, then the kinetic equation can be written in the following form, which will be found convenient later on:

$$dx / dt = \alpha n [x_{eq}^2 - x^2], \tag{3}$$

where the quantity $\alpha n x_{eq}^2$ represents the rate of ionization, transformed with the aid of the principle of detailed balance, and $\alpha n x^2$ is the recombination rate. Using Saha's equation for $x_{eq} \ll 1$ we get

$$x_{eq}^2 = 2 (g_+ / g_0) (2\pi m_e kT / h^2)^{3/2} n^{-1} e^{-I/kT} = B (T^{3/2} / n) e^{-I/kT} \tag{4}$$

Let the ionization at first, at high temperatures, be almost in equilibrium and let it "follow" the cooling: $x \approx x_{eq}(t)$, $x^2 - x_{eq}^2 \approx x_{eq}^2$. Quenching begins when the difference between the recombination and ionization rates increases to a value on the order of the rates themselves. This instant t_1 and the corresponding quantities T_1, n_1, and $x_1 \approx x_{eq1}$ can be estimated by inserting into (3) $dx/dt = dx_{eq}/dt$ and putting $x^2 - x_{eq}^2 \approx x_{eq}^2$. We obtain an approximate equation which is solved together with (1) and (2):

$$\alpha_1 n_1 x_{eq1} t_1 = {}^3/_2 (\gamma - 1) I / kT_1. \tag{5}$$

The recombination consists of photorecombination and recombination in triple collisions with participation of electrons.† Expressing the coefficient of the latter with the aid of the principle of detailed balance we obtain

$$\alpha = \bar{v}_e \sigma_{ph} + x (n \bar{v}_e \sigma_e / BT^{3/2}) I / kT, \tag{6}$$

where $\bar{v}_e$ is the velocity of the electrons, $\sigma_{ph} = \text{const}/T$ is the cross section for photorecombination, and σ_e is the average cross section for ionization by electrons of energies greater than I.

Starting with the instant t_1, it is possible to neglect in Eq. (3) the rate of ionization, i.e., the term proportional to x_{eq}^2. If we put approximately $\gamma = {}^5/_3$ ($T \sim n^{2/3} \sim t^{-2}$), which does not lead to a large error, the integration reduces to elementary quadrature.

The expressions are particularly simple if one of the recombination mechanisms predominates. Thus, if the quenching begins early, at relatively large densities and at high ionization (the initial dimension r_0 and the time scale t_0 are small), the recombination proceeds principally via triple collisions and the residual ionization is $x_\infty \approx x_1 (kT_1/2I)^{1/2}$. In the case of large time scales, to the contrary, the quasi-equilibrium stage is drawn out, and the principal role is played in the quenching region by photorecombination: $x_\infty \approx x_1 (kT/I)$.

By way of an example we list the calculated residual ionization of iron vapor, from initially heated solid iron of normal density, at $T_0 = 116{,}000°$.‡ An estimate of the energy and entropy, with allowance for the electronic specific heat, yields $\epsilon_0 = 72$ ev/atom, S = 61 cal/mole-degree, u = 15.5 km/sec. If the initial radius is $r_0 = 10$ m

(large iron meteorite), then $x_1 = 4.2 \times 10^{-3}$, $T_1 = 4550°$, $n_1 = 1.4 \times 10^{17}$ cm^{-3}, and $x_\infty = 2.1 \times 10^{-4}$. If $r_0 = 1$ cm, which is closer to the laboratory scale, then $x_1 = 0.58$, $T_1 = 9300°$, $n_1 = 6.6 \times 10^{17}$ cm^{-3}, $r_1 = 50$ cm, and $x_\infty = 0.13$.

The smaller the mass of the evaporated substance and the greater the initial heating, the greater the residual ionization.

I express deep gratitude to Ya. B. Zel'dovich for interest in the work and for valuable comments.

*For example, when high-energy meteorites strike the surface of a planet that has no atmosphere, during explosions of wire by electric currents in evacuated apparatus, during evaporation of anode points in pulsed X-ray tubes,[1] etc.

†Triple collisions in which heavy particles participate are important only if $x \lesssim 10^{-4}$ and do not play any role under our conditions.

‡In view of the absence of experimental data we assume the following likely values for the cross sections:

$$\sigma_e = 3 \cdot 10^{-17} \text{ cm}^2, \quad \sigma_{ph} = 2 \cdot 10^{-21} T^{-1} \text{ cm}^2 \text{ (T is in ev).}$$

[1] V. A. Tsukerman and M. A. Manakova, J. Tech. Phys. (U.S.S.R.) **27**, 391 (1957), Soviet Phys.–Tech. Phys. **2**, 353 (1957).

[2] Ya. B. Zel'dovich and Yu. P. Raĭzer, J. Exptl. Theoret. Phys. (U.S.S.R.) **35**, 1402 (1958), Soviet Phys. JETP **8**, 980 (1959).

Translated by J. G. Adashko
114

MEASUREMENTS OF NUCLEAR MAGNETIC MOMENTS IN THE ALKALI EARTHS BY MOLECULAR BEAM MAGNETIC RESONANCE

A. G. KUCHERYAEV, Yu. K. SZHENOV, and Sh. M. GOGICHAĬSHVILI

Physico-Technical Institute, Academy of Sciences, Georgian S.S.R.

Submitted to JETP editor May 19, 1959

J. Exptl. Theoret. Phys. (U.S.S.R.) **37**, 582-583 (August, 1959)

THE molecular beam magnetic resonance method (MBMR) has a number of advantages as compared with other methods of measuring nuclear magnetic moments in those cases in which the molecular beam consists of atoms in the S_0 state. The interaction of such atoms with an external magnetic field depends solely on the orientation of the nuclear magnetic moment. The magnetic resonance spectrum consists of one line and the shape of the line is not distorted by other interactions. Moreover, the position of the resonance is not subject to chemical shifts. Thus, the diamagnetic correction, which has been calculated accurately only for atomic and molecular hydrogen,[1] can be examined carefully.

The MBMR method (using atoms in the S_0 state) has been used to measure the magnetic moments of Ba^{135} and Ba^{137},[2] Ne^{21},[3] and Sr^{87}.[4] The application of this technique to other nuclei has been limited by the possibility of producing and detecting the appropriate atomic beams. It has been found possible to carry out these measurements in atomic beams of all the alkali earth metals using apparatus developed for this purpose.[5] This apparatus has been described by us earlier.[4]

Atomic beams of strontium, barium, and magnesium have been obtained by heating these metals (natural isotopic composition) in an oven source. A calcium atomic beam with sufficient intensity for detection of the Ca^{43} isotope was obtained by heating a mixture of CaO with 6% of the Ca^{43} isotope and mischmetal. The atomic beam was detected by a mass-spectrometer detector, using surface ionization of the atoms on tungsten, cleansed by oxygen under the optium conditions for each element.[5] The detectable intensities of narrow beams (I), the corresponding source temperatures (t), and the surface ionization coefficients (β) for the optimum detection conditions are given in Table I.

TABLE I

Isotope	t, °C	I, counts/sec	β
Mg^{25}	600	200	$2 \cdot 10^{-4}$
Ca^{43}	1070	300	0.02
Sr^{87}	750	10^4	0.2
Ba^{135}	800	500	0.6
Ba^{137}		850	

The measurements, carried out by the techniques which have been described,[5] were made at fixed field. The field was measured by the magnetic resonance of protons in water and the magnetic resonance of the Sr^{87} in the atomic beam; in the latter case the source was loaded with the necessary amount of metallic strontium in addition to the material being investigated. The values of the magnetic moment μ (with the diamagnetic correction) thus obtained are given in nuclear magnetons in Table II. In these calculations the magnetic moment of the proton has been taken as 2.79275[6] while the magnetic moment of Sr^{87}

TABLE II

Nucleus	μ
Mg^{25}	-0.855 ± 0.002
Ca^{43}	1.317 ± 0.003
Sr^{87}	-0.0924 ± 0.0009
Ba^{135}	$+1.8370\pm0.0008$
Ba^{137}	$+0.9364\pm0.0009$

has been taken from the value obtained in the present work. The spins of the nuclei investigated in the present work have been taken from reference 7. The ratio of the resonance frequencies in Ba^{137} and Ba^{135} is found to be 1.1187 = 0.0003. The sign of the magnetic moments is determined from the Millman effect.[8] The sign of the magnetic moment of Ca^{43} was not determined. The chief source of error in these measurements is the instability in the detected intensity of the atomic beams and the spread of values of the magnetic field which arises in the remagnetization of the magnet which produces the homogeneous field.

The value of the Sr^{87} magnetic moment, which we have obtained earlier,[4] has been refined in the present work by virtue of the more exact calibration of the uniform magnetic field. In order to exclude systematic errors use was made of two electromagnets, each of which was calibrated independently. The results obtained with each magnet are the same.

All values of the magnetic moments obtained by the MBMR method in the present work agree with the values obtained by nuclear induction (within the limits of the quoted errors).[9-12]

In conclusion the authors with to thank T. S. Bokuchav, K. G. Mirzoev, and I. N. Leont'eva for help in carrying out the measurements and M. I. Guseva, V. M. Gusev, and D. V. Chkuaseli for preparing the enriched Ca^{43} samples.

[1] W. C. Dickinson, Phys. Rev. **80**, 563 (1950).

[2] R. H. Hay, Phys. Rev. **60**, 75 (1941).

[3] La Tourrette, Quinn, and Ramsey, Phys. Rev. **107**, 1202 (1957).

[4] Kucheryaev, Szhenov, Gogichaĭshvili, Leont'eva, and Vasil'ev, J. Exptl. Theoret. Phys. (U.S.S.R.) **34**, 774 (1958), Soviet Phys. JETP **7**, 533 (1958).

[5] Kucheryaev, Szhenov, Gogichaĭshvili, Leont'eva, and Vasil'ev, Приборы и техника эксперимента (Instruments and Meas. Engg.) in press.

[6] Cohen, DuMond, Layton, and Rollet, Revs. Modern Phys. **27**, 363 (1955).

[7] Kyul'ts, Kunts, and Hartman, Usp. Fiz. Nauk **55**, 537 (1955).

[8] S. Millman, Phys. Rev. **55**, 628 (1939).

[9] F. Alder and F. C. Yu., Phys. Rev. **82**, 105 (1951).

[10] C. D. Jeffries, Phys. Rev. **90**, 1130 (1953).

[11] C. D. Jeffries and P. B. Sogo, Phys. Rev. **91**, 1286 (1953).

[12] H. E. Walchli and T. J. Rowland, Phys. Rev. **102**, 1334 (1956).

Translated by H. Lashinsky
115

ON THE CROSS SECTION FOR COMPOUND-NUCLEUS FORMATION BY CHARGED PARTICLES

A. D. PILIYA

Leningrad Physico-Technical Institute, Academy of Sciences, U.S.S.R.

Submitted to JETP editor May 21, 1959

J. Exptl. Theoret. Phys. (U.S.S.R.) **37**, 583-585 (August, 1959)

IN considering nuclear reactions it is often necessary to evaluate the cross section for the formation of a compound nucleus. In the nonresonance region at comparatively large energies, this cross section is satisfactorily determined by the well known formula[1]

$$\sigma_c = \frac{\pi}{k^2}\sum_{l=0}^{\infty}(2l+1)\,\frac{4s_l KR}{\Delta_l^2 + (KR+s_l)^2}, \qquad (1)$$

where k and K are the wave numbers of the particles inside and outside the nucleus; R is the radius of the nucleus;

$$s_l = kR/(G_l^2 + F_l^2),$$

$$\Delta_l = kR\,(G_l G_l' + F_l F_l')/(G_l^2 + F_l^2) \text{ with } r = R,$$

where $F_l(r)$ denotes the regular solution of the radial equation, while $G_l(r)$ is the irregular solution at zero.

The use of Eq. (1) is inconvenient for charged particles at large values of the Coulomb parameter $\eta = Z_1 Z_2 e^2/\hbar v \gg 1$. In the present communication we obtain for σ_c a closed expression, valid under the condition that the particle energy is lower than or very little higher than the Coulomb barrier.

In this case the following expressions[2] hold for the radial Coulomb functions

$$F_l(r) = (2\eta)^{4/3} v\,[(2\eta)^{-1/3}(\eta + \sqrt{\eta^2 + (l+1/2)^2} - kr)],$$
$$G_l(r) = (2\eta)^{1/3} u\,[(2\eta)^{-1/3}(\eta + \sqrt{\eta^2 + (l+1/2)^2} - kr)], \quad (2)$$

where v and u are Airy[3] functions. These functions are related to Bessel functions of order $1/3$ in the following manner:

$$\left.\begin{matrix} u(t) \\ v(t) \end{matrix}\right\} = \sqrt{\frac{\pi}{3}\,t}\left\{I_{-1/3}\left(\frac{2}{3}\,t^{3/2}\right) \pm I_{1/3}\left(\frac{2}{3}\,t^{3/2}\right)\right\}, \quad t > 0,$$
$$\left.\begin{matrix} u(t) \\ v(t) \end{matrix}\right\} = \sqrt{\frac{\pi}{3}\,|t|}\left\{J_{-1/3}\left(\frac{2}{3}\,|t|^{3/2}\right) \mp J_{1/3}\left(\frac{2}{3}\,|t|^{3/2}\right)\right\}, \quad t < 0.$$

Since the Airy functions vary substantially when the magnitude of their argument changes by an amount on the order of unity, the root in the arguments of the functions (2) can be expanded in powers of $(l+\frac{1}{2})^2\eta^{-2}$, retaining only the linear term. Furthermore, it is permissible to change in (1) from summation with respect to l to integration with respect to the variable t:

$$t = (l+1/2)(2\eta)^{-4/3} + z_0, \qquad z_0 = (2\eta)^{-1/3}(2\eta - kr),$$
$$\sum_{l=0}^{\infty}(2l+1)\ldots \to (2\eta)^{4/3}\int_{z_0}^{\infty} dt\ldots$$

For the evaluation of the integral thus obtained, we note that the quantities $u'(t)/u(t)$, $v'(t)/v(t)$, and $u(t)v(t)$ vary very slowly with t in comparison with $u^{-2}(t)$, [indeed, $u^{-2}(t)$ determines a substantial range of t] and they can be regarded as constants, with $t = z_0$. Now, changing to a new variable of integration, $x = v(t)/u(t)$, and noting that

$$v'(t)\,u(t) - v(t)\,u'(t) = 1, \qquad u^{-2}dt = dx,$$

we get

$$\sigma_c = \frac{8\pi\eta}{k^2}\left(\frac{k}{K}\right)\int_0^{x_0}\frac{dx}{(1+x^2)}\left[\left(1+\frac{\alpha x}{1+x^2}\right)^2 + \left(\frac{\beta+\gamma x^2}{1+x^2}\right)^2\right]^{-1},$$

where

$$\alpha = k/(2\eta)^{1/3}Ku(z_0)\,v(z_0), \qquad \beta = u'(z_0)\,k/u(z_0)(2\eta)^{1/3}K;$$
$$\gamma = v'(z_0)/v(z_0)(2\eta)^{1/3}K.$$

Expanding the integrand in powers of $k/(2\eta)^{1/3}K$ and retaining only the first two terms, we have finally

$$\sigma_c = \frac{8\pi\eta}{k^2}\left(\frac{k}{K}\right)\left\{\tan^{-1}\frac{v(z_0)}{u(z_0)} - \frac{k}{(2\eta)^{1/3}K}\,\frac{v(z_0)}{u(z_0)\,|u^2(z_0)+v^2(z_0)|}\right\}.$$

[1] J. M. Blatt and V. F. Weisskopf, Theoretical Nuclear Physics, Wiley 1952, Russ. Transl. IIL, M. 1954.

[2] Biedenhorn, Gluckstern, Hull, and Breit, Phys. Rev. **97**, 542 (1955).

[3] V. A. Fock, Таблицы функций Эйри (Tables of Airy Functions), M. 1946.

Translated by J. E. Viscardi
116

THE ENERGY OF A COMPRESSED IMPERFECT FERMI GAS

D. A. KIRZHNITS

P. N. Lebedev Physics Institute, Academy of Sciences, U.S.S.R.

Submitted to JETP editor May 25, 1959

J. Exptl. Theoret. Phys. (U.S.S.R.) **37**, 585-587 (August, 1959)

We consider a uniform degenerate Fermi gas whose particles interact according to a short-range law [two-body potential $V(r_{12})$, range of the forces a]. The mean distance between the particles is assumed small compared to a. There are no restrictions imposed upon the magnitude of the interaction, and we assume only that the Fourier transform of the potential $\nu(q)$ exists. The properties of such a simple model are of interest for the problem of nuclear matter where $\xi \sim 3$ or 4 (see below) and also for some astrophysical problems.

We evaluate in the following the energy ϵ per single fermion, which depends on the dimensionless "compression parameter"* $\xi = ap_0 \gg 1$ and "coupling constant" $\alpha = \nu(0)/a$. Here $p_0 = (3\pi^2\rho)^{1/3}$ is the Fermi momentum, and ρ the number density of the particles.

It is well known that the kinetic energy of the nonrelativistic gas is equal to $\epsilon_0 = 3p_0^2/10$. In the Hartree-Fock approximation the interaction energy corresponds to the first order of perturbation theory in α. Its non-exchange part is equal to

$$\varepsilon_1 = (\rho/2)\int V d\mathbf{r} \sim \alpha\xi p_0^2. \quad (1)$$

The magnitude of the exchange term

$$\varepsilon_2 = -(8\pi^3\rho)^{-1}\int d\mathbf{p}_1 d\mathbf{p}_2 \nu(\mathbf{p}_1 - \mathbf{p}_2), \quad p_{1,2} < p_0,$$

depends on the behavior of V at small r. If $V(0)$ is finite,

$$\varepsilon_2 = -V(0)/2 \sim \alpha p_0^2/\xi^2 \ll \varepsilon_1. \quad (2)$$

To estimate the correlation energy (i.e., the higher terms of perturbation theory) we consider that the transition from the n-th to the n+1-st

order in α occurs either through the addition of another interaction vertex between those particles which are already present in the n-th term, or through the increase by unity of the number of particles which are correlated. In the first case there occurs in the expression for the energy a superfluous integration over the momentum transfer $q \sim a^{-1}$, and in the second case over the momentum of the new particle $p \sim p_0$.

If $ap_0 \gg 1$, the ratio of the corresponding integrals is small and the main part is played by that chain where in each (n-th) order of perturbation theory the maximum number (equal to n) of particles is connected. The energy of such many-particle correlations was found by Gell-Mann and Brueckner[1] and can for $\xi \gg 1$ be put in the form†

$$\varepsilon_3 = (5/8\,\pi p_0^2) \int_{-\infty}^{\infty} dv \int_0^{p_0} dq q^3 (A + \ln(1 - A)),$$

$$A(q, v) = 8\pi p_0 \nu(q)(1 - v \tan^{-1}(v^{-1})) \sim \alpha\xi. \qquad (3)$$

If α is so small that $\alpha\xi \ll 1$,

$$\varepsilon_3 = -8\pi^2 (1 - \ln 2) \int_0^{p_0} dq q^3 \nu^2(q). \qquad (4)$$

For the most important kinds of interaction $\nu^2(q) \approx Cq^{-4}$ when $aq \gg 1$ [for a rectangular well, for instance, $C = V(0)^2 a^2/8\pi^4$]. The integral in (4) is thus equal to $C \ln \xi$.

A much more important case is $\alpha\xi \gg 1$ (but $\alpha/\xi \ll 1$). We introduce a momentum $q_0 \sim (\alpha\xi)^{1/2}/a$ by the condition $A(q_0, 1) \sim 1$. The main, logarithmic contribution to the integral over q in (3) gives a term of second order in A in the range from q_0 to p_0 (the range from 0 to q_0 gives a non-logarithmic contribution since $A \sim 1$). We therefore return to (4) but with the limits of integration from q_0 to p_0.

$$\varepsilon_3 = -4(1 - \ln 2)\pi^2 C \ln(\xi/\alpha) \sim \alpha^2 (p_0/\xi)^2 \ln \xi. \qquad (5)$$

We now proceed to discuss the results.

a) Even for a strongly imperfect compressed gas the correlation energy is small and the Hartree-Fock approximation is permissible.‡

b) The equation of state of a compressed gas is of the form

$$P = \rho^2 \partial\varepsilon/\partial\rho = (\rho^2/2) \int V d\mathbf{r} + \tfrac{1}{5}(3\pi^2)^{2/3}\rho^{5/3} + \ldots \qquad (6)$$

and is determined not by the kinetic energy but by the interaction. Making the gas relativistic makes this conclusion stronger. The more the gas is compressed, the further it will thus be from being perfect. This property is quite clearly pronounced: even when $\xi \simeq 1$, the first term in (6) will be an order of magnitude larger than the second one (for $\alpha \sim 1$). In a neutral electron-nuclear gas (Coulomb interaction) the first term in (6) falls out and the opposite situation occurs.

c) If $\int V d\mathbf{r} < 0$, i.e., if attractive forces predominate, $P < 0$ and the gas tends to an unbounded compression. It is thus necessary to require that $\int V d\mathbf{r} > 0$. This condition makes the well known considerations about the change in sign of the potential, which refers to the problem of the saturation of the nuclear forces, more precise.

To extend the results obtained to real systems one must bear in mind the inevitability of the occurrence in a strongly compressed gas of many-particle forces which depend moreover on the state of the interacting particles (momenta, spins, and so on).

One may, on the other hand, think that these results have a not too limited range of applicability. The smallness of the correlation energy is thus apparently a general property of compressed Fermi systems: because of the Pauli principle there is only a narrow range of momenta of the intermediate states over which one must integrate and it decreases with increasing compression. Moreover, conclusions based upon Eq. (6) are valid also for not too strong compressions, as was noted. In that region, however, the experimental data on the interaction of nucleons can be described by a two-particle potential with a not very sharp dependence on the state.**

The model under consideration does not enable us to describe a "hard core" corresponding to nuclear interactions. This problem will be considered separately.

*We use units where $\hbar = M = 1$.

†In that paper a compressed electron gas was considered. The condition $\xi \gg 1$ (large range of the forces) brings that case nearer to the one investigated in the present paper. We note that in quantum field theory language the approximation under consideration corresponds to the lowest approximation in α for the polarization operator.

‡The opposite situation occurs in a well known sense for a rarefied gas: although the interaction is small in that case compared with the kinetic energy, all terms in an expansion in α (for $\alpha \gtrsim 1$) are equally important.

**It is easy to take this dependence into account in the formulas given above. For a system of particles of two kinds which are coupled by Serber forces, it is then necessary to use a coefficient 3/8 in (1) and (5) and –3/2 in (2).

[1] M. Gell-Mann and K. A. Brueckner, Phys. Rev. **106**, 364 (1957).

Translated by D. ter Haar
117

*QUANTUM-MECHANICAL SEMICONDUCTOR GENERATORS AND AMPLIFIERS OF ELECTROMAGNETIC OSCILLATIONS**

N. G. BASOV, B. M. VUL, and Yu. M. POPOV

P. N. Lebedev Physics Institute, Academy of Sciences, U.S.S.R.

Submitted to JETP editor May 18, 1959

J. Exptl. Theoret. Phys. (U.S.S.R.) **37**, 587-588 (August, 1959)

IN the present note we consider the possibility of using the electronic transitions between the conduction band (valence band) and the donor (acceptor) impurity levels of a semiconductor to obtain electromagnetic radiation assisted by the phenomenon of stimulated emission in a fashion similar to that which takes place in the molecular generator.[1]

To make semiconductor generators and amplifiers, one needs to obtain such a distribution of electrons (holes) in the conduction (valence) band as would exist if the effective temperature of the conduction electrons (holes) relative to the ionized donors (acceptors) were negative. Such a semiconductor has negative losses at the frequency corresponding to transitions of electrons (holes) from the conduction (valence) band to the impurity level. Therefore, on irradiating a semiconductor in the condition described above with an electromagnetic wave, it is possible to obtain amplification of this wave due to the quanta of stimulated emission. Further, on fulfilling certain conditions (the conditions of self-excitation), such a device can function as a generator.

To obtain negative temperatures it is proposed to use the impurity ionization mechanism which operates in a semiconductor specimen at a low temperature when an electric field pulse is applied.

The peak voltage of the pulse is chosen so that impact ionization of the impurity atoms or direct field-extraction results. Thus, the number of electrons (holes) in the conduction (valence) band increases sharply, so that practically all the impurity atoms are ionized. Provided the decay of the voltage pulse is sufficiently rapid, all the electrons (holes) fall to the lowest energy levels of the corresponding band. The electron (hole) density and the crystal temperature should be chosen so that in the conduction (valence) band a state is thus created which is almost degenerate and which is equivalent to a negative temperature relative to the donor (acceptor) levels.

The state of negative temperature will be preserved for the relaxation time of the electrons (holes) with the vacant impurity levels. For impurity contents sufficiently small compared with the number of atoms in the crystalline lattice, the lifetime τ_2 of conduction electrons (holes) will be much larger than the time τ_1 between collisions of the electrons (holes) with the lattice. The time τ_2 can be controlled by the impurity concentration. During the interval τ_2 the system may be used as a generator or amplifier of electromagnetic oscillations. The oscillation frequency is determined by the position of the impurity energy levels relative to the bands. The original spectral line breadth is determined by the energy spread of the occupied levels in the main bands.

For the system to work as a generator it is necessary to satisfy the conditions of self-excitation, which involve the choice of the transmission and reflection coefficients of the waves at the specimen boundary.[2,3] Reducing the surface reflection coefficients or the dimensions of the specimen can change the system from a generator into an amplifier.

Every pulse of the external voltage will be accompanied by the formation of a state of negative temperature; thus such a system will function in a pulsed manner.

The operating principle in quantum-mechanical semiconductor generators and amplifiers using electronic transitions between two different bands will not differ from that discussed above, since in this case also two characteristic times, τ_1 and τ_2, exist.

---

*The present work was registered with the Committee on Discoveries and Inventions of the Council of Ministers of the U.S.S.R., with priority date July 7, 1958.

---

[1] N. G. Basov and A. M. Prokhorov, Usp. Fiz. Nauk **57**, 485 (1955).

[2] N. G. Basov, Радиотехника и электроника (Radio Engineering and Electronics) **3**, 297 (1958).

[3] A. M. Prokhorov, J. Exptl. Theoret. Phys. (U.S.S.R.) **34**, 1658 (1958), Soviet Phys. JETP **7**, 1140 (1958).

Translated by K. F. Hulme
118